Curso 2011/12
CIENCIAS Y TECNOLOGÍAS/40
I.S.B.N.: 978-84-15910-42-8

JONATHAN BARROSO GONZÁLEZ

Mecanismos moleculares implicados en la infección por el VIH-1

Director
AGUSTÍN VALENZUELA FERNÁNDEZ

SERVICIO DE PUBLICACIONES
UNIVERSIDAD DE LA LAGUNA

SOPORTES AUDIOVISUALES E INFORMÁTICOS
Serie Tesis Doctorales

A MI FAMILIA

Agradecimientos:

En primer lugar, quiero agradecer muchas cosas a mi director de tesis, Agustín Valenzuela. En primer lugar por confiar en mí como el primer miembro de su grupo de investigación, por transmitir su entusiasmo por la ciencia a todo lo que hago, por luchar intensamente para que nunca me faltara nada personal y profesionalmente, por sus consejos, por su absoluta disposición a aceptar nuevas ideas, y sobre todo, aunque no siempre lo merezca, por darme libertad en el trabajo diario. Además, quiero agradecer la gran ayuda recibida por parte de los compañeros del laboratorio, Laura de Armas, Serena y Soledad, por su buen humor, su compañerismo, y en gran parte por aceptar la tarea de encargarse de aquellos trabajos que no he podido terminar.

Al catedrático D. Manuel Feria por ayudarnos a conseguir un espacio en la Universidad de La Laguna donde poder trabajar, por estar pendiente de cualquiera de nuestras necesidades y por su gran sentido del humor capaz de alegrarnos cada mañana.

Al Dr. Federico Díaz y a las “chicas”, Chus, Mayte, Ada y Elsa, por ser los primeros en ayudarnos en nuestra vuelta a Tenerife y por estar siempre pendiente de todo lo que necesitase. Hay que ver la de viajes que me daba antes a la 5ª planta, el autoclave era un espectáculo, por cierto ¿aún funciona? y sobre todo, ¿cuántos minutos había que dejarlo antes de apagarlo? y así con todo, por lo que es de agradecer su paciencia. Aún me queda la pena de no saber como poner a funcionar la campana de flujo. Además, a Anita y Ricardo (el de Ada) con quienes también compartimos algunos buenos momentos.

Al Dr. Francisco Sánchez Madrid del Hospital de La Princesa por permitirme pasar unos meses trabajando en Madrid, y a todos los integrantes de su laboratorio. También a todo el grupo del Dr. Manuel Landazuri y del Dr. Manuel López, quienes siempre nos permitieron utilizar todos sus recursos. Igualmente al grupo de la Dra. María Ángeles Muñoz del Gregorio Marañón, por su necesaria contribución a este trabajo. Al Dr. Julia Blanco y su laboratorio, en especial a Isabel Puigdomenech, por su acogida y ayuda el tiempo que pasé con ellos.

Al Dr. Ricardo Borges y al Dr. José David Machado por su gran acogida en la Unidad de Farmacología, y su continua predisposición a la colaboración. Por supuesto, no puedo olvidarme de la compañía durante este tiempo de Bea, Dani, Jésica, José Francisco, Marcial, Marta, Miriam, Mónica, Natalia, Yezer y “el quillo”, además de la nueva oleada, Carmen, Judith, José y Josué, con los que he compartido grandes momentos divertidos. Creo que sólo me queda ver como Dani se baña en una playa

de Santander. También tengo mucho que agradecer a JuanRamón por su dedicación y empeño.

A los doctores Diego Álvarez y Teresa Giraldez, porque sus consejos me han ayudado a mejorar en algunas técnicas del laboratorio. Sin su colaboración, algunas cosas habrían sido más difíciles. También a Alberto, Cristina, Diana, Fabián e Iván, por ser muy buenos compañeros de laboratorio, y porque uno nunca se aburre si los tiene a su lado. También a todos los miembros del grupo del Dr. Tomás González, sobre todo a Nacho que nos "alumbra" de vez en cuando con su presencia.

A los doctores Ángel Gutiérrez, Ana Estévez y Rafael Zárate por su colaboración durante la realización de una parte importante de esta Tesis Doctoral, y por supuesto, a Nabil y a Fátima por su entusiasmo y motivación.

A mis primeros "jefes", los doctores Celedonio González y Nélida Brito, por introducirme en este mundillo de la investigación, dándome la oportunidad de cacharrear en su laboratorio. Ahora miro hacia atrás y veo que el tiempo que pasé allí ha sido muy bueno para mi evolución como investigador. También, por supuesto, a José, Judith, Belén y Nabil, por considerarme su "*padawan*", por su compañerismo, y porque sin sus "truquillos" nunca habría podido aprender nada de nada. Nunca olvidaré cómo Chuck Norris contó, dos veces, las colonias de un césped de *E.coli*.

También quiero acordarme de Marina, Margarita y Rosa porque siempre estuvieron dispuestas a ayudarme en la medida de lo posible.

Quiero agradecer a mi familia, por todo el apoyo que he recibido desde que decidí estudiar esa carrera llamada Biología. Sobre todo a mi padre, que se dejó la piel cada día para que pudiésemos recibir una educación con fundamento, y también a mi madre porque siempre ha estado pendiente de que no nos faltase de nada, aunque las cosas hayan sido muy difíciles.

Además quiero agradecer especialmente el trabajo de mi compañera, mi amiga y mi esposa Laura García, sin su ayuda esto no habría sido posible. Ha sido mi mejor apoyo en los malos momentos y con quien he podido compartir los buenos momentos, que los ha habido y muchos. Es mi complemento perfecto y siempre ha sido una fuente de motivación en lo personal y en lo profesional.

Por último, quiero agradecerle a Dios su ayuda, con la que he podido llegar hasta aquí a pesar de las dificultades, por ser un punto de apoyo, y porque en él nunca me ha faltado nada, ni me faltará.

FINANCIACIÓN:

La realización de esta Tesis Doctoral ha sido posible gracias a la financiación obtenida por el Ministerio de Sanidad y Consumo a través de la Fundación de Investigación y Salud del Instituto de Salud Carlos III (FIS-ISCIII, PI050995), por la Fundación Canaria de Investigación y Salud (FUNCIS, PI56/07) y por la Fundación para la Investigación y Prevención del SIDA en España (FIPSE, FIPSE-24-0740-09).

ABREVIATURAS:

ABP	Proteína de unión a actina
ADCC	Citotoxicidad celular dependiente de anticuerpos
ADN	Ácido desoxirribonucleico
AMPc	Adenosín monofosfato cíclico
AP-2	Proteína adaptadora 2
APOBEC3G	"*Apoplipoprotein B mRNA-editing, enzyme-catalytic, polypeptide-like 3G*"
ARN	Ácido ribonucleico
ARNi	ARN interferente
ARNm	ARN mensajero
ARN pol II	ARN polimerasa II
ARNt	ARN transferente
BA	Ácido betulínico
CA	Cápside del VIH-1
CCP	Invaginaciones cubiertas de clatrina
CCS	Estructuras cubiertas de clatrina
CCV	Vesículas cubiertas de clatrina
CME	Endocitosis mediada por clatrina
CTL	Células T citotóxicas
DAG	Diacilglicerol
DC	Células dendríticas
EBP50	Fosfoproteína de 50KDa de unión a ezrina
Env	Complejo de envuelta del VIH
ERM	Ezrina/radixina/moesina
FAK	Quinasa de las adhesiones focales
FDA	"*Food and drug administration*"
Gag	Antígeno específico de grupo
GAG	Glicosaminoglicanos
GALT	Tejido linfoide asociado al intestino
GFP	Proteína verde fluorescente
GPCR	Receptores acoplados a proteína G
HLA	Antígeno leucocitario humano
HSC	Células madre hematopoyéticas
IFN	Interferón
IL	Interleucina
IN	Integrasa del VIH-1
IP3	Inositol-1,4,5-trifosfato
LFA-1	Antígeno 1 asociado a la función de los linfocitos
LIMK	Proteína quinasa conteniendo un motivo LIM
LTR	Repeticiones largas terminales
LTS	Supervivientes a largo plazo
MA	Matriz del VIH-1
MCP	Proteína quimioatrayente de monocitos
MHC	Complejo principal de histocompatibilidad
MIP	Proteína inflamatoria de macrófagos
MLCK	Quinasa de la cadena ligera de miosina
NC	Nucleocápside del VIH-1
Nef	Factor Negativo del VIH-1
PBL	Linfocitos de sangre periférica
PBMC	Células mononucleares de sangre periférica
Pak	Quinasa activada por p21
pDC	Células dendríticas plasmacitoides

PDZ	Dominio tipo PSD-95/DlgA/ZO-1
PIC	Complejo de preintegración
PI3K	Fosfatidilinositol-3-quinasa
PI4P5-K	Fosfatidilinositol-4-fosfato-5-quinasa
PIP_2	Fosfatidilinositol-4,5-bifosfato
PLC	Fosfolipasa C
PKA	Proteína quinasa A
PKC	Proteína quinasa C
PR	Proteasa del VIH-1
PTX	Toxina pertúsica
Pyk2	Tirosín quinasa 2 rica en prolina
RANTES	Regulado tras activación, normalmente expresado y presumiblemente secretado en células T
RE	Retículo endoplasmático
Rev	Regulador de la expresión viral
ROCK	Quinasa dependiente de Rho
RT	Transcriptasa reversa
SDF-1α	Factor 1α derivado de las células estromales
SIDA	Síndrome de inmunodeficiencia adquirida
TARc	Terapia antirretroviral combinada
Tat	Transactivador de la transcripción
TcR	Receptor de la célula T
Tf	Transferrina
TfR	Receptor de transferrina
TIRFM	Microscopia de fluorescencia por reflexión interna total
TNF	Factor de necrosis tumoral
Tsg101	Gen 101 susceptible a tumor
UNAIDS	Programa de las Naciones Unidas sobre VIH/SIDA
VIH	Virus de la Inmunodeficiencia Humana
Vif	Factor de infectividad viral
VIS	Virus de la Inmunodeficiencia en Simios
Vpr	Proteína viral R del VIH-1
Vpu	Proteína viral U del VIH-1
VSV	Virus de la estomatitis vesicular
ZAP-70	Proteína quinasa de 70KDa asociada a la cadena zeta de CD3

ÍNDICE

ÍNDICE:

1. INTRODUCCIÓN

1.1. EPIDEMIA DEL VIH/SIDA

Desde el descubrimiento, hace más de 25 años, del Virus de la Inmunodeficiencia Humana (VIH) como el agente etiológico causante del Síndrome de Inmunodeficiencia Adquirida (SIDA), éste ha representado uno de los problemas de salud pública más significativos de todos los tiempos. El VIH fue identificado por primera vez por el grupo del Dr. Luc Montagnier y Françoise Barré-Sinoussi del Instituto Pasteur de París, en Francia (Barre-Sinoussi et al., 1983), quienes recibieron por ello el premio Nobel de Medicina en el año 2008. Al mismo tiempo, el equipo del Dr. Robert Gallo determinó la existencia de cepas virales T linfotrópicas, consiguiendo la replicación viral *in vitro* (Gallo et al., 1983).

El virus VIH originalmente se denominó virus asociado a linfadenopatía (LAV: "*lymphadenopathy-associated virus*") (Barre-Sinoussi et al., 1983), y de forma incorrecta virus linfotrópico de células T humanas de tipo III (HTLV-III: "*human T-lymphotropic virus type III*") (Gallo et al., 1983). El nombre fue definitivamente sustituido por el de VIH (Coffin et al., 1986), y la confirmación del VIH como el agente etiológico causante del SIDA tuvo lugar en el año 2000 en Durban (Sudáfrica), en una reunión científica mundial sobre SIDA (The Durban Declaration, 2000).

Con una estimación de individuos infectados por el VIH cercana a los 34 (30,9-36,9) millones de personas en 2010 (UNAIDS, "*United Nations Programme on HIV/AIDS*", 2010), en comparación a los 33 millones en el año 2009 (UNAIDS, 2009) **(Figura 1)**, la búsqueda de un tratamiento efectivo contra la infección por el VIH constituye uno de los objetivos más urgentes de la salud pública mundial.

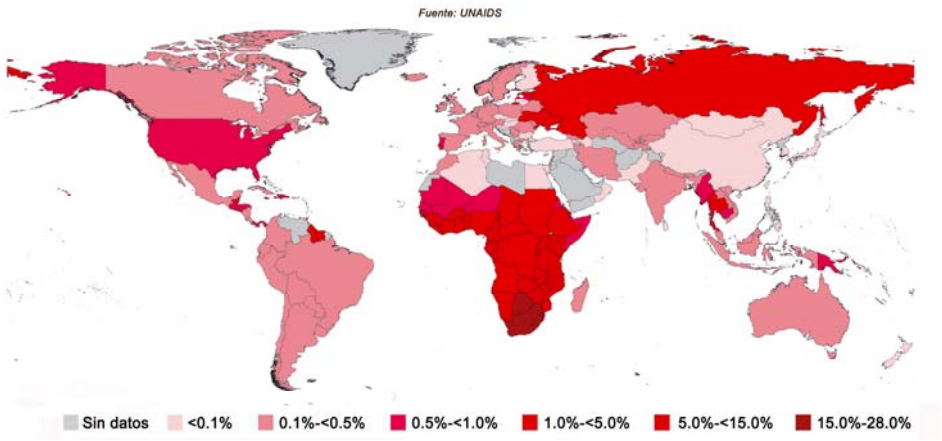

Figura 1: Prevalencia de individuos con SIDA en 2009 (UNAIDS 2009)

1.2. ESTRUCTURA Y ORGANIZACIÓN GENÓMICA DEL VIRUS VIH-1.

El VIH es un Retrovirus (de la familia *Retroviridae*) perteneciente al género *Lentivirus*. La principal propiedad de los Lentivirus consiste en su capacidad de infectar células que no están en división causando efectos citopáticos en ellas. Se han identificado dos tipos de VIH, el de tipo 1 (VIH-1) y el de tipo 2 (VIH-2). El VIH-2 se encuentra más relacionado con el Virus de la Inmunodeficiencia en Simios (VIS) que con el VIH-1, con quien comparte sólo un 40% de homología (Chakrabarti et al., 1987).

El tipo viral VIH-1 es muy diverso genéticamente, encontrándose dividido en tres grupos principales, el M (principal, "*main*"), el N (nueva, "*new*") y el O (periféricos, "*outer*"). Los virus de VIH-1 del grupo M son los que se encuentran más ampliamente distribuidos y son los causantes del 99% de las infecciones por VIH-1 a nivel global. Los grupos difieren entre sí un 30% en la secuencia, mientras que los subtipos varían alrededor de un 15-20%. El grupo M se encuentra dividido en 9 diferentes subtipos (A-K), de los cuales el subtipo B es el dominante en Europa, América y Australia, el subtipo C es el dominante en Sudáfrica, China e India, y son los responsables de la mayoría de las infecciones por el VIH-1 a nivel mundial (McCutchan, 2000), y los subtipos A y D son comunes en Asia Central y del Este. Está clasificación se realiza actualmente en base a la totalidad de la secuencia de nucleótidos del virus (Robertson et al., 2000). Sin embargo, resulta complicado clasificar cada virus dentro de un subtipo específico, debido a las formas recombinantes generadas entre cepas virales de VIH de diferentes grupos y subtipos. Las recombinaciones tienen lugar con mayor frecuencia durante la fase aguda de la infección, y pueden ocurrir a partir de co-infecciones o superinfección de células diana con dos o más virus antes del establecimiento de una infección crónica (Smith et al., 2005).

La partícula viral madura del VIH-1 tiene un diámetro aproximado de 100 nm y se encuentra rodeado de una bicapa lipídica procedente de la célula hospedorada que ha infectado. El genoma viral encapsidado del VIH-1 está compuesto de dos copias homólogas pero no idénticas de ácido ribonucleico (ARN) monocatenario con polaridad positiva de unas 9 Kilobases, y que codifica para una serie de proteínas reguladoras, accesorias, estructurales y enzimáticas **(Figura 2).** Las proteínas accesorias determinan la extensión de sus características patogénicas y replicativas, que a su vez varían entre grupos y subtipos.

Gen	splicing ARNm	Proteína(s)
Genes reguladores		
tat	multiple	Tat (16KDa)
rev	multiple	Rev (19KDa)
Genes accesorios		
vif	único	Vif (23KDa)
vpr	único	Vpr (14KDa)
vpu	único	Vpu (15-20KDa)
nef	multiple	Nef (25-27KDa)
Genes estructurales y enzimáticos		
gag	sin splicing	$Pr55^{gag}$: MA (p17), CA (p24), NC (p7), p6
pol	sin splicing	$Pr160^{gag\text{-}pol}$: PR (p10), RT (p61/p52), IN (p31)
env	único	gp160: gp120, gp41

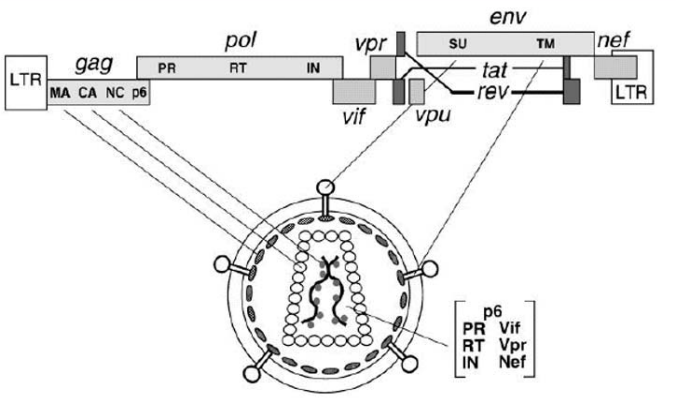

Figura 2: A la izquierda se muestran los genes del VIH-1, su procesamiento y las proteínas codificadas, y a la derecha se muestra la organización estructural y genómica del VIH-1.

1.2.1. Genes estructurales y enzimáticos

A este grupo pertenecen los genes estructurales comunes a todos los retrovirus como son: *gag* ("*group-specific antigen*", antígeno específico de grupo), *pol* (polimerasa) y *env* (envuelta). Estos genes codifican para distintas poliproteínas que, tras su procesamiento proteolítico, dan lugar a las proteínas individuales maduras con funciones específicas morfológicas y funcionales durante el ciclo de vida viral.

La poliproteína Gag ($Pr55^{Gag}$) está formada por la proteína MA (matriz, p17), la CA (cápside, p24), la NC (nucleocápside, p7), p6 y los péptidos espaciadores sp1 y sp2, que junto con las dos proteínas de la envuelta del virus, gp120 (la subunidad superficial, SU) y gp41 (la subunidad transmembrana, TM), conforman las proteínas estructurales.

La MA se encuentra localizada justo debajo de la bicapa lipídica viral estabilizándola. En el interior se encuentra la CA que presenta una morfología cónica-truncada **(Figura 2)**, y protege al complejo de ribonucleoproteínas (formado por el ARN viral y otras proteínas accesorias) estabilizado a su vez por la NC. Por último, p6 participa en el empaquetamiento y liberación de las nuevas partículas de VIH-1 de la célula infectada (Freed, 1998; Turner and Summers, 1999).

El gen *env* codifica para las proteínas de la envuelta viral (gp120 y gp41), y es el gen más variable de todo el genoma del VIH-1. Posee un 35% de diversidad entre distintos subtipos, 20% de diversidad dentro de un mismo subtipo y hasta un 10% de diversidad de secuencia en un mismo individuo infectado (Shankarappa et al., 1999). Las proteínas de la envuelta, gp120 y gp41 se encuentran ancladas en la bicapa lipídica viral, unidas entre sí de manera no covalente formando trímeros, siendo de

gran importancia en los primeros estadios de anclaje e infección eficaz de la célula diana. La proteína gp120 del virus determina la especificidad del tipo celular a infectar por unión específica a receptores presentes en la superficie de la célula diana, mientras que la subunidad transmembrana gp41 es la responsable de la fusión entre las membranas viral y celular (Wyatt and Sodroski, 1998).

Las tres proteínas con actividad enzimática del gen *pol*, la proteasa (PR), la retro-transcriptasa (RT) y la integrasa (IN), son esenciales para completar el ciclo de vida del VIH-1 y se encuentran incorporadas en el interior viral. La PR es la encargada del procesamiento proteolítico de las poliproteínas del VIH para dar lugar a las subunidades maduras funcionales. El ARN viral del VIH es retrotranscrito a ácido desoxirribonucleico (ADN) de doble cadena mediante la acción de la RT, y es integrado en el genoma de la célula hospedadora mediante la acción de la IN (Freed, 1998; Turner and Summers, 1999).

1.2.2. Genes reguladores

Los genes reguladores del VIH son *tat* ("*trans-activator of transcription*", transactivador de la transcripción) y *rev* ("*regulator of virion expression*", regulador de la expresión génica viral). Estos genes son los primeros que se expresan tras la infección e integración del genoma viral en el hospedador. El gen *tat* codifica para una proteína de localización nuclear que se une a las regiones LTR ("*long-term repeat*", repeticiones largas terminales) del ADN proviral integrado, potenciando la iniciación y la elongación de la transcripción de los genes del VIH-1 (Ruben et al., 1989). El producto del gen *rev* participa en el transporte específico de distintos grupos de ARN mensajeros (ARNm) virales, sin procesar o procesados parcialmente, desde el núcleo al citoplasma celular, para ser posteriormente traducidos en las proteínas virales, o ser integrado en la nueva partícula viral (Freed, 1998; Turner and Summers, 1999).

1.2.3. Genes accesorios

Los genes accesorios del VIH son *nef* ("*negative factor*", factor negativo), *vif* ("*viral infectivity factor*", factor de infectividad viral), *vpu* ("*viral protein U*", proteína viral U) y *vpr* ("*viral protein R*", proteína viral R). Todas ellas son empaquetadas dentro de las partículas virales nacientes.

El producto del gen *nef* se expresa de manera abundante en los primeros estadios de infección, y es un elemento clave en la progresión de la infección por el VIH-1 hacia la fase SIDA, facilitando la replicación viral y potenciando la infectividad de las partículas virales, al incrementar la incorporación de proteínas de la envuelta (Chowers et al., 1994; Miller et al., 1995; Spina et al., 1994). Además, Nef tiene otras funciones que permiten la progresión del ciclo de vida viral, como la disminución de la expresión en la superficie celular de los receptores para el virus VIH-1, CD4, CXCR4 y CCR5, del receptor de transferrina (TfR) y del complejo principal de histocompatibilidad (MHC, "*major histocompatibility complex class*") de tipo I y II, también denominado HLA ("*human leukocite antigen*"). Estas funciones permiten al virus evitar el reconocimiento y destrucción de la célula infectada por el sistema inmunológico, evitar la superinfección celular y dificultar la sinapsis inmunológica (Geleziunas et al., 1994; Thoulouze et al., 2006).

El producto del gen *vif* es importante para mantener la infectividad de las partículas virales libres del VIH-1 actuando sobre el factor de restricción intracelular APOBEC3G ("*apoplipoprotein B mRNA-editing, enzyme-catalytic, polypeptide-like 3G*"), con actividad citidina desaminasa, evitando la expresión de su ARNm (Mercenne et al., 2010; Stopak et al., 2003) o degradando la proteína vía proteasoma (Conticello et al., 2003; Stopak et al., 2003). APOBEC3G es capaz de incorporarse en la partícula viral, por unión directa al ARN genómico viral, e inhibir la infección por partículas virales de VIH-1 defectivas en Vif, mediante la generación de hipermutaciones invalidantes C-U/T en el genoma proviral (proceso de "*editing*" genómico) durante el siguiente ciclo viral (revisado en (Chiu and Greene, 2009)). Sin embargo, recientemente, se ha descrito que APOBEC3G también puede generar hipermutaciones en el genoma viral, no invalidantes, sino que confieren, por el contrario, resistencia del virus a ciertos fármacos antirretrovirales, como al análogo nucleosídico lamivudina (3TC) ((Kim et al., 2010).

El producto del gen *vpr* participa en la formación del complejo de pre-integración (PIC, "*pre-integration complex*") del virus y en su transporte hacia el interior del núcleo (Freed, 1998; Turner and Summers, 1999). La unión de la proteína Vpr a la proteína p6 del precursor $Pr55^{Gag}$ permite su incorporación en las nuevas partículas virales, y con ello la infección de células que no están en división, como los macrófagos (Connor et al., 1995; Paxton et al., 1993). En este sentido, se ha descrito recientemente que *vpx*, el gen auxiliar homólogo a *vpr* que se encuentra exclusivamente en el virus VIH-2 y en algunos VIS, regula positivamente el contenido intracelular de deoxinucleótidos (dNTP) en monocitos/macrófagos y células dendríticas

permitiendo un estado metabólico favorable para la replicación viral, tras la degradación selectiva vía proteasoma, por formación de un complejo ubiquitín ligasa Cul4A-DDB1-DCAF1, de la enzima trifosfatohidrolasa de dNTP SAMHD1 *("SAM domain and HD domain-containing protein 1")* (Goldstone et al., 2011; Powell et al., 2011). Asimismo, la presencia de Vpr en estas células, permite detener el ciclo celular en la fase G2, lo que favorece la expresión de las proteínas virales. Por otro lado, Vpr parece ser secretado por las células infectadas e inducir apoptosis en células no infectadas, principalmente, a través de la permeabilización de la membrana mitocondrial y pérdida del potencial de membrana, actuando sobre un complejo dinámico poliproteico de poro (PTPC, "*permeability transition pore complex*") (Deniaud et al., 2004; Moon and Yang, 2006). Además, Vpr es responsable de la formación de canales iónicos que dan lugar a despolarización de la membrana plasmática y muerte celular en neuronas (Piller et al., 1999).

El producto del gen *vpu* codifica para una proteína integral de membrana que tiene la función de inducir la degradación del principal receptor para el virus VIH-1, el antígeno de superficie CD4, a través de la interacción de Vpu con CD4 a nivel del retículo endoplasmático (RE) y de manera dependiente del proteasoma (Magadan et al., 2010; Willey et al., 1992). Además, la proteína de la envuelta viral gp160 también es capaz de retener a CD4 en el RE, formando agregados. Ambos mecanismos, evitan el transporte de CD4 a la superficie celular, favoreciendo la infectividad de las partículas virales salientes, además de evitar la superinfección celular (revisado en (Nethe et al., 2005)).

1.3. INTERACCIÓN VIRUS-CÉLULA

El VIH-1 tiene como diana células del sistema inmunitario que expresan en su superficie celular el antígeno CD4, como linfocitos T $CD4^+$ (en reposo, activados y de memoria), monocitos, macrófagos y células dendríticas (DCs, "*dendritic cells*"), que expresan además alguno de los correceptores para el virus, principalmente CXCR4 y/o CCR5. La infección por el VIH-1 va a generar en el organismo hospedador una respuesta inmune, compuesta por la inmunidad innata y la inmunidad adaptativa. Esta respuesta (ver apartado 1.3.3) que limita en principio la replicación viral, a largo plazo no consigue evitar el establecimiento de reservorios de latencia viral ni la erradicación del virus del organismo (Wen et al., 2005).

1.3.1. Ciclo de vida del VIH

El ciclo de vida del VIH-1 **(Figura 3)**, comienza con la unión inespecífica a componentes de la superficie de la célula diana, con la posterior unión específica del virus a los receptores CD4 y CXCR4 o CCR5. Esta unión permite los posteriores eventos de fusión, entrada e infección viral. A continuación, tiene lugar la entrada y desestructuración de la CA viral, con la liberación del material genético y de las proteínas accesorias al citoplasma de la célula diana. El ARN es retrotranscrito por la RT viral a ADN de doble cadena que es transportado al núcleo por el PIC (Arhel et al., 2007), e integrado en el genoma del hospedador por la IN viral. Por último, tiene lugar la transcripción y traducción del genoma viral dando lugar a las proteínas que van a constituir la nueva progenie del VIH-1. Estas proteínas junto con las hebras de ARN genómico viral, sin traducir ni procesar, se ensamblan en la membrana plasmática. El proceso termina con el empaquetamiento, liberación y maduración de las nuevas partículas virales (revisión en (Freed, 1998; Turner and Summers, 1999) **(Figura 3).**

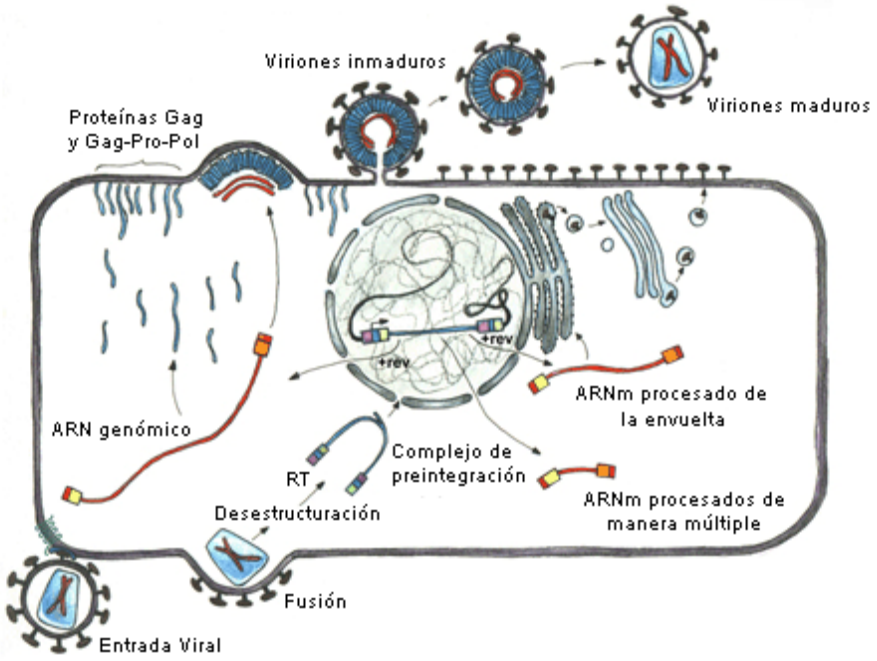

Figura 3: Representación esquemática del ciclo de vida completo del VIH-1.

1.3.1.1. Glicoproteínas de la envuelta del virus: gp120 y gp41.

La síntesis del precursor del complejo glicoproteíco de la envuelta, la glicoproteína gp160, ocurre en el RE, y su procesamiento tiene lugar en los compartimentos *cis* y medios del aparato de Golgi. El procesamiento proteolítico de gp160 que da lugar a las proteínas maduras, ocurre por corte preferencial en una

secuencia localizada en la región C-terminal de la glicoproteína (Arg^{508}-Gln-Lys-Arg^{511}). Cabe resaltar que el corte proteolítico de gp160 por una proteasa celular (endoproteasa furina o del tipo de la furina) es altamente dependiente de su conformación (mediada por puentes disulfuro) y oligomerización (mediada por formación de dímeros e incluso tetrámero a nivel del RE), que son importantes para el transporte de gp160 al lugar de proteolisis en el Golgi (Bour et al., 1995). Por último, en el aparato de Golgi (en la región *trans*) tiene lugar la adición de cadenas oligosacarídicas. La proteína gp120 presenta una mezcla de cadenas complejas oligosacarídicas (principalmente glucosa y ácido siálico, y oligomanosídicas)), representando aproximadamente el 50% del peso molecular de la proteína (Bour et al., 1995). Sin embargo, no parecen tener funciones importantes sobre la interacción de gp120 con CD4, ni con el correceptor viral (revisado en (Poignard et al., 2001)).

Tras el procesamiento proteolítico en el Golgi, las proteínas maduras gp120 y gp41 son transportadas hacia la superficie celular, donde forman una estructura compleja de tipo estaca, constituida por complejos triméricos de gp120 y gp41 unidos no covalentemente. Esta estructura se encuentra estabilizada por puentes disulfuro entre residuos Cys conservados (revisado en (Poignard et al., 2001)).

Gp120 presenta 5 regiones con secuencias variables de aminoácidos (aa) (V1-V5) entre las que se encuentran intercaladas otras tantas secuencias constantes de aa (C1-C5) **(Figura 4 y 5).**

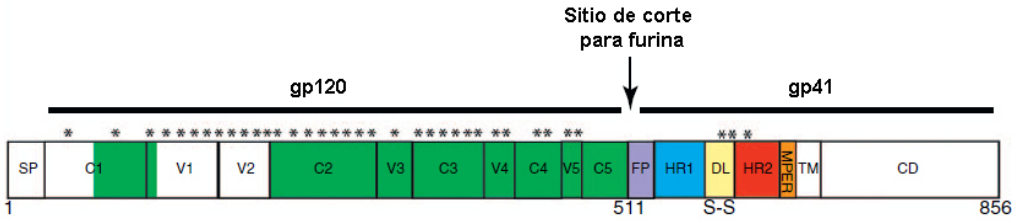

Figura 4: Secuencias variables y constantes en gp120, junto con los dominios de gp41. Además, se muestra el lugar de procesamiento post-traduccional por la endoproteasa furina.

El dominio de unión a CD4 en la proteína viral gp120 está constituido por un bolsillo conformacional, siendo su región constante C4 **(Figura 5),** y particularmente, el bolsillo hidrofóbico formado por el Trp^{427} rodeado de los aa Asp y Glu, cargados negativamente, los que participan en la interacción directa con los residuos hidrofílicos de la región CDR2 (del dominio D1) de CD4 (Bour et al., 1995).

Por otro lado, el principal determinante de la especificidad del VIH-1 por un determinado correceptor se encuentra en el tercer dominio variable (V3) de gp120

(Dragic, 2001), y en menor extensión en las regiones variables V1/V2, que también participan en el contacto directo con el correceptor durante el proceso de entrada viral (Bieniasz and Cullen, 1998). **(Figura 5).**

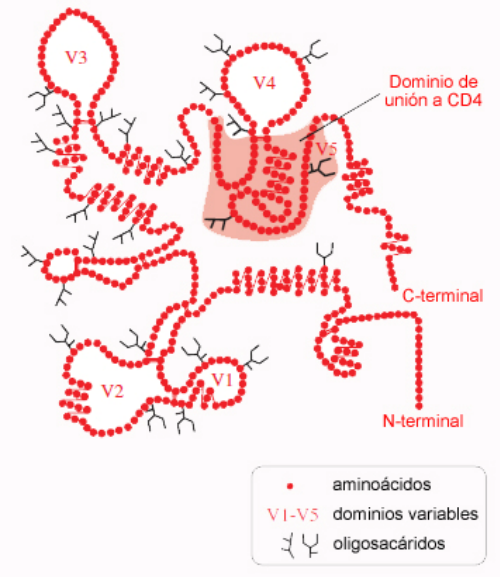

Figura 5: Estructura de la proteína de la envuelta gp120 con la disposición de los 5 dominios variables, entre los cuales se encuentran intercalados los 5 dominios constantes.

Por otro lado, la superficie más larga de unión al correceptor se encuentra en otra región altamente conservada de gp120 denominada "*bridging sheet*", que se encuentra entre los dominios variables V3 y V1/V2 (Rizzuto et al., 1998). Esta región presenta una estructura de cuatro láminas β antiparalelas que conectan los dos principales dominios de gp120, el interior y el exterior. En la superficie de esta región están los determinantes comunes para la unión al correceptor, mientras que la estructura y carga del dominio V3 y de los dominios V1/V2 dictan la especificidad por un determinado correceptor, CCR5 o CXCR4 (Lusso, 2006).

Desde el punto de vista del tropismo viral, existen tres variantes virales del VIH-1: las cepas R5 trópicas que utilizan CCR5 como correceptor, las cepas X4 trópicas que utilizan CXCR4 y las cepas virales dual trópicas que utilizan indistintamente CCR5 o CXCR4 como correceptor (Moore et al., 1997). En cuanto a la carga del dominio V3, las envueltas X4 trópicas presentan una carga más positiva en comparación con las envueltas R5 trópicas. Esta característica está relacionada directamente con su unión a la superficie extracelular del correceptor adecuado, que presenta una carga más negativa en CXCR4 que en CCR5 (Berson and Doms, 1998). Por último, dado que el bloqueo de la región variable V3 inhibe la unión a CD4 y a los correceptores del VIH

(Valenzuela et al., 1997), inhibiendo así la infección, a esta región de la proteína gp120 se le ha denominado, **dominio principal de neutralización**.

Por último, estudios centrados en la estructura y función del bucle V3, como determinante del tropismo viral, han llevado a determinar qué mutaciones puntuales (generalmente una o dos) en la proteína de la envuelta viral puede provocar un cambio en la utilización del correceptor (Berson and Doms, 1998). A pesar de la cristalización de gp120 en su conformación unida a CD4 (Huang et al., 2005), aún quedan por resolver los determinantes estructurales de gp120 importantes para la unión al co-receptor.

La glicoproteína gp41 está compuesta por siete dominios: el péptido de fusión N-terminal, la hepta repetición 1 (HR1), un bucle disulfuro, la hepta repetición 2 (HR2), una región con un ectodominio proximal de membrana (MPER), el dominio transmembrana y el dominio citoplasmático **(Figura 4).** El ectodominio N-terminal altamente hidrofóbico de gp41, que contiene el conocido péptido de fusión, forma junto a los motivos HR1 y HR2 (también conocidos como hélice-N y hélice-C) una estructura trimérica, determinante de la reacción de fusión entre las membranas celular y viral (Turner and Summers, 1999). El mecanismo completo de la fusión será descrito en el apartado 1.3.1.3.

1.3.1.2. Receptores para el VIH-1 y tropismo viral: CD4 y receptores de quimiocinas (CXCR4/CCR5).

CD4 es una glicoproteína integral de membrana, de 55-58 kDa, con funciones en la diferenciación de timocitos y en la activación de células T periféricas. La proteína madura contiene 433 aa, con un ectodominio de 371 aa unidos al dominio transmembrana de 24 aa hidrofóbicos y 38 aa básicos en el dominio citoplasmático **(Figura 6)**. La región extracelular de CD4 está plegada en 4 dominios (D1-D4). El dominio D1 presenta una extensa homología estructural con la región variable de la cadena ligera de las inmunoglobulinas (Ig). Los otros tres dominios, aunque con menor homología en su estructura primaria, el patrón de plegamiento es similar, lo que hace que CD4 se clasifique dentro de la superfamilia de las inmunoglobulinas. El dominio D1 de CD4 es el responsable de la unión de la envuelta gp120 (Bour et al., 1995).

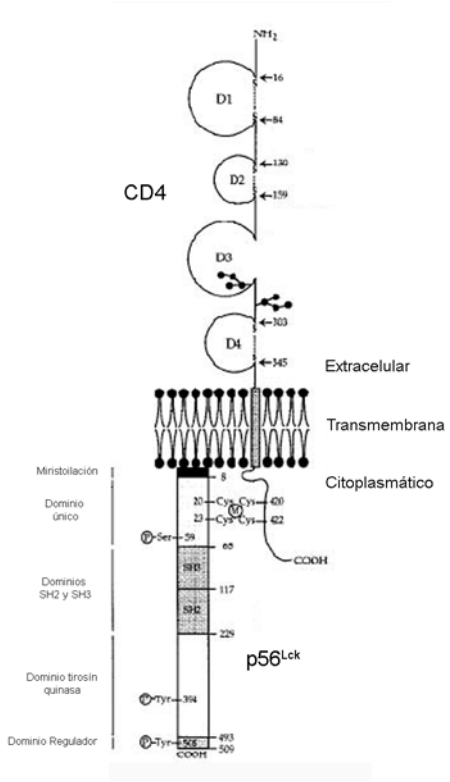

Figura 6: Representación esquemática del antígeno CD4 y la quinasa intracelular asociada $p56^{Lck}$. Se muestran los cuatro dominios tipo inmunoglobulina de CD4, los puentes disulfuro y los sitios de glicosilación (Bour et al., 1995).

CD4 se expresa en la superficie de los timocitos en desarrollo, linfocitos T primarios, activados y de memoria, en monocito/macrófago y células dendríticas (Este and Telenti, 2007). CD4 se encuentra asociado al receptor de la célula T (TcR, "*T-cell receptor*"), y a través de su dominio de unión a MHC-II transmite señales de activación celular durante la sinapsis inmunológica. La activación de las células T $CD4^+$ por contacto entre el complejo TcR/CD3 y CD4 con el complejo MHC-II/antígeno tiene lugar gracias a la asociación de CD4 con una proteína tirosín quinasa denominada $p56^{Lck}$. La activación de ésta permite la fosforilación de la cadena ζ de CD3, que permite a su vez la unión de ZAP-70 ("*Zeta-chain-associated protein kinase 70*") al complejo TcR/CD3, siendo posteriormente fosforilada también por $p56^{Lck}$. ZAP-70 activada fosforilada va a activar a su vez a otros efectores como LAT ("*linker of activated T cells*"), una proteína transmembrana que permite la activación de otras proteínas, principalmente a la quinasa PI3K ("*phosphatidilinositol-3-kinase*") y a la fosfolipasa C (PLC, "*phospholipase C*"). El producto final de esta activación consiste en la producción, a partir de factores de transcripción como NF-κB, NF-AT y AP-1, de citocinas como interleucina-2 (IL-2) que promueven la proliferación y diferenciación de los linfocitos activados de manera específica de antígeno (Bour et al., 1995). CD4

también puede actuar como una molécula de adhesión, reforzando la interacción entre las células presentadoras de antígenos y las células T durante la sinapsis inmune. La unión entre CD4 y MHC-II favorecería la sinapsis inmune en aquellos casos en los que existe una interacción de baja afinidad entre el TcR y el complejo antígeno/MHC-II presente en la célula presentadora de antígenos (Bowers et al., 1997). En función de la afinidad de unión entre estos componentes, se va a producir la diferenciación y proliferación de distintas poblaciones de células T. $P56^{Lck}$ es específica de líneas celulares del linaje linfoide, y es esencial para activar la ruta de señalización que controla la activación y proliferación de los timocitos. Además de su función como tirosín quinasa, $p56^{Lck}$ contiene dominios SH2 y SH3 **(Figura 6)** que le permiten actuar como una proteína adaptadora que recluta otros efectores de señalización. Por otro lado, $p56^{Lck}$ actúa evitando la endocitosis constitutiva de CD4, que tendría lugar en ausencia de ésta (Yoshida et al., 1992), como podría ocurrir en la estirpe monocítica desprovista de esta quinasa, y donde la escasa estabilidad de CD4 en la superficie celular dificulta su infección por el VIH-1 (Pelchen-Matthews et al., 1991; Pelchen-Matthews et al., 1995). La activación de $p56^{Lck}$ dependiente de CD4 provoca que este complejo se localize en las fracciones insolubles de la célula, la asociada al citoesqueleto celular general (Ha-Lee et al., 2000). Además, $p56^{Lck}$ ancla CD4 a las microvellosidades (Foti et al., 2002), que son zonas de adsorción viral (Singer et al., 2001).

CD4 representa el receptor principal para la infección por el VIH-1 (Dalgleish et al., 1984; Klatzmann et al., 1984). Esto determina que la infección esté restringida a la población de los linfocitos T (naïve, no proliferativos, activados y de memoria), monocitos, macrófagos y células dendríticas, que presentan expresión superficial del antígeno CD4. Asimismo, CD4 también es el receptor principal para la entrada del VIH-2 y el VIS. Aún así, es importante notar que la presencia de CD4 es un factor necesario pero no suficiente para que tenga lugar una entrada productiva del VIH-1, por lo que es necesario que las mismas células también presenten en superficie un receptor de quimiocinas que actúe como correceptor durante la entrada viral.

El domino D1 de CD4, con su puente disulfuro, es el implicado en la unión a la proteína gp120. Concretamente, parece ser particularmente importante el bolsillo hidrofóbico, formado por el plegamiento de cuatro residuos cargados (Lys^{29}, Lys^{35}, Lys^{46} y Arg^{59}) alrededor de un residuo Phe^{43} hidrofóbico, en el contacto y unión entre CD4 y gp120. (Bour et al., 1995).

Se ha propuesto, que el VIH-1 puede utilizar receptores alternativos a CD4 con el fin de lograr entrar en células que no expresan este receptor en superficie. Este es el caso del esfingolípido galactosil-ceramida (Gal-Cer), que parece mediar la infección por el VIH-1, con una eficiencia muy baja pero proporcional al nivel de Gal-Cer en la superficie celular, en líneas celulares de origen epitelial y neuronal, por unión directa con la proteína gp120, en una región diferente a la región implicada en la unión de gp120 a CD4 (Fantini et al., 1993; Harouse et al., 1991).

Los receptores de quimiocinas representan un subconjunto especializado de la superfamilia de receptores acoplados a proteína G (GPCR). La superfamilia de GPCR constituye el grupo más amplio de receptores de superficie celular. Estos receptores son activados por citocinas quimioatrayentes, denominadas quimiocinas. Los GPCR comparten una serie de características comunes, como un segmento N-terminal extracelular, siete segmentos α-hélice transmembrana, tres bucles extracelulares (ECL, "*extracellular loop*"), tres bucles intracelulares (ICL, *"intracellular loop"*) y un segmento C-terminal citoplasmático. Presentan además dos residuos conservados de Cys, en ECL1 y ECL2, que forman un puente disulfuro importante para el mantenimiento de la integridad funcional del receptor y para el acceso de la quimiocina al bolsillo generado por la estructura extracelular del receptor (Perlman et al., 1995). Asímismo, varios receptores de quimiocinas contienen otro puente disulfuro entre dos residuos de Cys localizados en el segmento N-terminal y en ECL3, que parece contribuir al mantenimiento de la conformación y estabilidad del receptor (Baggiolini et al., 1997). Otra característica común a los GPCR es su capacidad de activar proteínas G heterotriméricas, tras la unión de su ligando natural. Esta unión induce alteraciones en la orientación de las α-hélices transmembrana, seguido por cambios conformacionales en los ICL. Cambios que permiten la unión de las proteínas G heterotriméricas ($G\alpha\beta\gamma$) en su forma unida a GDP. A continuación, el receptor va a actuar como un GEF ("*guanine exchange factor*", factor de intercambio del nucleótido guanina) que va a provocar la disociación del GDP del complejo heterotrimérico $G\alpha\beta\gamma$ permitiendo la asociación de GTP. La unión de GTP va a disociar las subunidades GTP-$G\alpha$ y $G\beta\gamma$ del GPCR, dando lugar diversas funciones efectoras. La hidrólisis del GTP de la proteína G finaliza la señalización (ciclo GTPasa) (Hamm, 1998).

Se han identificado cuatro clases principales de proteínas $G\alpha$: $G\alpha i$, $G\alpha s$, $G\alpha q$ y $G\alpha 12/13$. Cada clase de proteínas $G\alpha$ se encuentra asociada a un patrón de

señalización característico que va a influir en una respuesta celular diferencial **(Figura 7)** (Wu and Yoder, 2009).

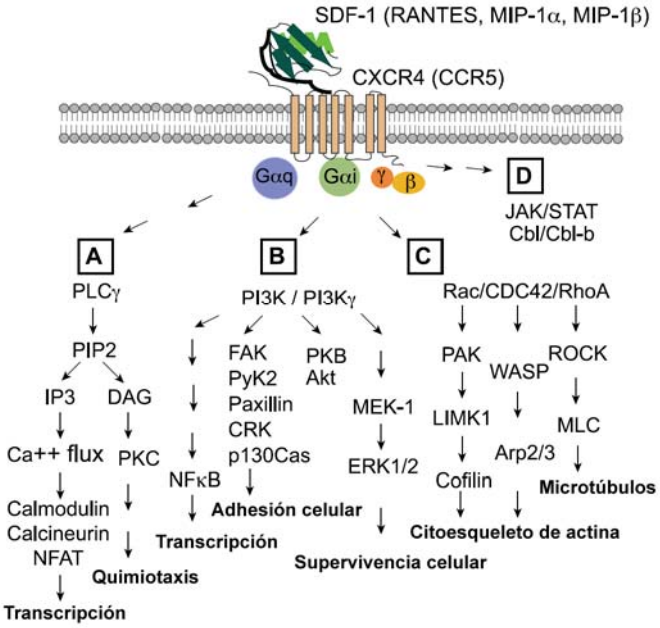

Figura 7: Rutas de señalización activadas a partir de subunidades Gαi, Gαq y Gβγ de los receptores de quimiocinas CXCR4 y CCR5 (Wu and Yoder, 2009).

En principio, parece que los receptores de quimiocinas se encuentran acoplados a proteínas G de las familias Gαi y Gαq (Arai and Charo, 1996; Wu and Yoder, 2009) **(Figura 7)**. La señalización a través de proteína Gαi es inhibida por toxina pertúsica (PTX), mientras que la señalización a través de proteína Gαq, Gαs y Gα12/13 no se ve afectada (Simon et al., 1991). Aún así, se ha mostrado que los receptores acoplados a proteína G pueden señalizar a través de la interacción con otras proteínas celulares, no sólo a través de proteína G (Hall et al., 1999). Los receptores de quimiocinas se encuentran agrupados, de manera general, en las clases CC, CXC, CX3C y C, en función del tipo de agonista afín a cada clase (Murphy et al., 2000). Asimismo, es importante resaltar que múltiples GPCR pueden señalizar a través de un único tipo de proteína G, y en muchos casos, un único receptor puede activar más de un tipo de proteína G (Hamm, 1998).

CXCR4 y CCR5 forman parte de la familia de receptores de quimiocinas de siete dominios transmembrana de unión a proteína G que son, como se ha descrito anteriormente, los dos correceptores principales en células primarias para la infección por virus VIH-1, tanto de cepas X4 como R5 trópicas, respectivamente (Berger et al., 1999). Asimismo, se han descrito toda una serie de receptores de siete dominios

transmembrana, de la familia de las quimiocinas o no, capaces de ejercer una función correceptora para la infección por un número muy limitado de variantes del virus VIH, como son los receptores de quimiocinas CCR2b, CCR3, CCR8, CCR9, CCR1, CCR4, CX3CR1, CXCR6, CXCR7, STRL33, D6 y RDC1, los receptores huérfanos V28, APJ, GPR1 y GPR15, y el receptor de quimiocinas US28 codificado por el citomegalovirus (CMV) humano (Berson and Doms, 1998; Dimitrov et al., 1998).

En general, como se ha indicado anteriormente, se pueden distinguir tres variantes virales del VIH-1 en base a su habilidad de utilizar selectivamente CCR5, CXCR4 o ambos como correceptores de la entrada viral. Las cepas virales R5 trópicas van a utilizar CCR5 como correceptor, las cepas virales X4 trópicas van a utilizar CXCR4 y las cepas virales dual trópicas ("*dual mixed*") van a utilizar indistintamente CCR5 o CXCR4 (Moore et al., 1997). Estas variantes virales además se distinguen en función de su prevalencia durante el estadio clínico de la infección. Así, las cepas virales dual trópicas son consideradas como los intermediarios en la evolución de una cepa viral R5 trópica, predominante en los primeros estadios de infección y responsable de la transmisión viral (Doms, 2000; Schuitemaker et al., 1992), a una cepa viral X4 trópica, predominante en los últimos estadios de la infección e implicadas directamente en la progresión hacia la fase SIDA (Singh and Collman, 2000). Se ha encontrado que esta preferencia inicial en el uso de CCR5 como correceptor, cambia durante el transcurso de la enfermedad sólo en aproximadamente el 50% de los pacientes infectados por el subtipo B del VIH-1 (Schuitemaker et al., 2011). Este cambio en el uso del correceptor está asociado con la pérdida masiva de células T $CD4^+$, y con ello, una mayor velocidad en la progresión de la enfermedad (Koot et al., 1993). Aún así, los virus R5 trópicos pueden ser responsables de estos efectos en aquellos individuos donde no tiene lugar el cambio de tropismo (Agrawal et al., 2006; Quakkelaar et al., 2007). Por último, parece que el cambio de tropismo viral tiene lugar, principalmente, debido a la evolución hacia cepas X4 trópicas a partir de cepas R5 trópicas, con un intermediario dual trópico, por mutaciones dependientes de la RT viral en aa clave dentro de la proteína de la envuelta gp120 (generalmente en la región V3, determinante principal de neutralización) (Schuitemaker et al., 2011).

La importancia de CCR5 en la transmisión del VIH-1 resalta del hecho de que individuos que presentan una deleción de 32 pares de bases, en el ORF ("*open ready frame*") del gen que codifica para CCR5 (CCR5Δ32), son altamente resistentes a la infección por el VIH-1 (Samson et al., 1996). Aún así, el efecto protector de esta mutación no es total y por ello se han detectado, en individuos homocigóticos Δ32, cepas virales X4 trópicas y/o dual trópicas que utilizan CXCR4 (Alkhatib, 2009). Por

otro lado, parece que la resistencia a la infección en estos individuos homocigóticos Δ32, también depende de una disminución de la expresión superficial de CXCR4 por causa de la proteína mutante CCR5Δ32 (Agrawal et al., 2004). Por ultimo, recientemente se ha informado del éxito del primer transplante de células madre de un individuo homocigótico CCR5Δ32 hacia un individuo infectado por el VIH-1. El seguimiento posterior de este paciente indicó la restauración de su sistema inmune, sobre todo de las células T. Aún así, las posibles consecuencias a largo plazo, si es que las hay, aún son desconocidas (Alkhatib, 2009). Aunque la ausencia de CCR5 no parece tener consecuencias inmunológicas, se ha descrito que estos individuos presentan mayor susceptibilidad a sufrir infecciones por el flavivirus "*West Nile*", un virus encefalítico de origen africano que se transmite en humanos por picaduras de mosquitos, y que se encuentra en expansión en los países desarrollados (revisado en (Lim et al., 2006)).

El receptor de quimiocinas CCR5 ha sido identificado como el correceptor para la entrada de cepas virales R5 trópicas y dual trópicas (R5/X4) del VIH-1 (Alkhatib et al., 1996; Choe et al., 1996; Deng et al., 1996; Doranz et al., 1996; Dragic et al., 1996). CCR5 es además el receptor para las quimiocinas MIP-1α ("*Macrophage inflammatory protein 1α*", CCL3), MIP-1β ("*macrophage inflammatory protein 1β*", CCL4), RANTES ("*Regulated upon Activation, Normal T cell Expressed and presumably Secreted*", CCL5), MCP-1 ("*monocyte chemotactic protein-1*", CCL2), MCP-2 ("*monocyte chemotactic protein-2",* CCL8), MCP-3 ("*monocyte chemotactic protein-3",* CCL7), MCP-4 ("*monocyte chemotactic protein-4",* CCL13) y eotaxina (CCL11) (Alkhatib, 2009).

CCR5 **(Figura 8)** se expresa en la superficie de células dendríticas (plasmacitoides y de Langerhans), monocitos/macrófagos y en un subconjunto de células $CD4^+$ (15-35%) previamente activadas/memoria $CD45R0^+$, CD26 alto CD45RA bajo) (Bleul et al., 1997). Diversos estudios utilizando mutantes y quimeras de receptores de quimiocinas que permiten o no la infección por el VIH-1, han permitido mostrar que el dominio N-terminal extracelular de CCR5 representa la región más importante y suficiente para conferir actividad correceptora (con menor eficiencia que el receptor entero) a receptores de quimiocinas que no permiten la fusión y entrada viral (Alkhatib et al., 1997a; Atchison et al., 1996; Bieniasz et al., 1997; Doranz et al., 1997a; Doranz et al., 1997b; Dragic et al., 1998; Lu et al., 1997; Picard et al., 1997b; Rabut et al., 1998; Rucker et al., 1996). Este dominio N-terminal, es modificado post-

traduccionalmente mediante la adición de motivos sulfato sobre residuos de Tyr, favoreciendo las interacciones electroestáticas entre esta región y la región de aa positivos localizada en el*"bridging sheet*" y en la región V3 de gp120 (Farzan et al., 1999). En cuanto a los ECL de CCR5, todos pueden contribuir a la actividad correceptora como segundo punto de unión, y el requerimiento o contribución de cada una de ellas al proceso de fusión, depende de la sensibilidad de unión de la cepa viral empleada (Alkhatib et al., 1997b; Atchison et al., 1996; Bieniasz et al., 1997; Doranz et al., 1997b; Picard et al., 1997a; Rucker et al., 1996). Así, las cepas virales dual trópicas que infectan células $CCR5^+$ son más sensibles a modificaciones en la región N-terminal de CCR5 que las cepas R5 trópicas (Doranz et al., 1997b). Por último, se ha determinado que el bucle ECL2 de CCR5 parecen ser crítico en la unión al complejo gp120/CD4, favoreciendo los eventos posteriores de fusión e infección (Xiao et al., 1999).

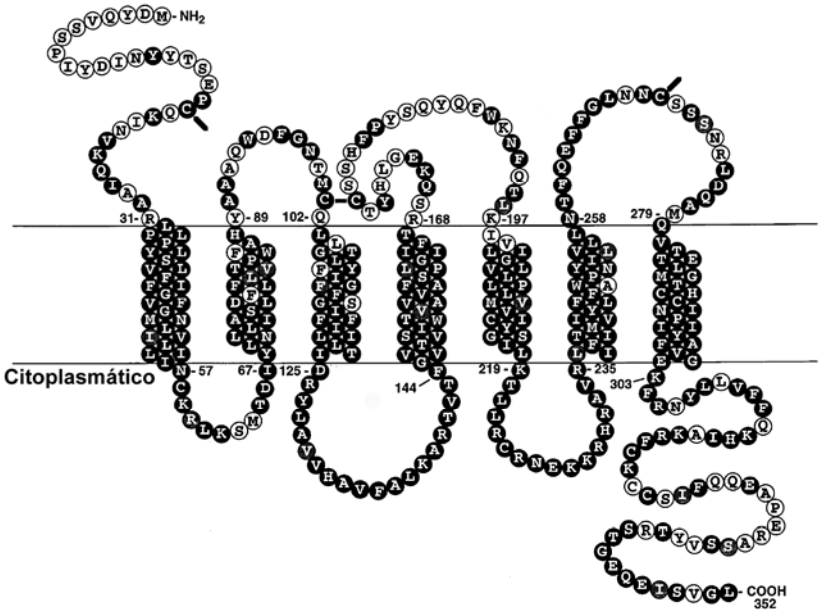

Figura 8: Orientación en membrana de los dominios del correceptor CCR5, con la secuencia de aminoácidos. Las barras indican los residuos Cys extracelulares que forman los puentes disulfuro. Se marcan en negro los residuos idénticos entre CCR5 y CCR2b, otro receptor de quimiocinas que permite la infección por cepas dual trópicas del VIH-1, y que comparte un 76% de homología con CCR5 (Rucker et al., 1996).

CXCR4 **(Figura 9)** es el correceptor implicado en la entrada de cepas virales X4 trópicas y dual trópicas (X4/R5) del VIH-1 (Feng et al., 1996). Además es el receptor de la quimiocina SDF-1α ("*stromal cell-derived factor-1*α"/CXCL12) (Oberlin et al., 1996). CXCR4 se encuentra expresado constitutivamente en la superficie de

algunas células como los macrófagos, las células T neoplásicas y los linfocitos T de sangre periférica, predominantemente naïve (CD45RA)/quiescentes (CD45RO)/no proliferativas (CD69) (Bleul et al., 1997). Los dominios de CXCR4 implicados en la actividad correceptora han sido determinados mediante la utilización de homólogos no humanos de CXCR4, receptores quiméricos, mutantes puntuales o delecionados en diversos dominios. A partir de estos estudios se ha determinado que la región N-terminal de CXCR4 no es crítica para su actividad correceptora, mostrando distinto grado de actividad correceptora en función de la proteína de envuelta utilizada (Brelot et al., 1997; Lu et al., 1997; Picard et al., 1997b). Así, mientras unas envueltas son capaces de tolerar cambios (mutaciones o deleciones) en esta región, otras envueltas son más sensibles a estos cambios y no pueden mediar la fusión con la célula diana de manera eficiente. Datos similares, obtenidos tras el procesamiento de la región N-terminal de CXCR4 por la enzima humana leucocitaria elastasa (HLE, "*human leukocyte elastase*") en un contexto proinflamatorio, confirman la importancia de esta región extracelular de CXCR4 para la unión, función antiviral y agonista de su ligando CXCL12, siendo aún el CXCR4 truncado en su región N-terminal correceptor para el VIH-1 (Valenzuela-Fernandez et al., 2002).

Por otro lado, se ha demostrado que el bucle ECL2 de CXCR4, y en menor medida el bucle ECL1, sí que juega un papel crítico en la infección, ya que su sustitución afecta a todas las cepas X4 trópicas testadas (Lu et al., 1997), siendo además suficiente para conferir actividad correceptora a receptores de quimiocinas que no permiten la infección por el VIH-1 (Brelot et al., 1997). Estos resultados indicarían que la envuelta del VIH-1 podría utilizar como punto de unión un estructura compleja conformacional formada por todos los ECL del correceptor (Doranz et al., 1999). Además, el ECL2 de CXCR4 presenta una alta carga negativa, a diferencia de la misma región en CCR5, lo que le permite interacción con envueltas X4 trópicas cargadas positivamente (básicas) en el dominio V3 (revisado en (Berson and Doms, 1998)). En general, de todos estos estudios se puede concluir que la unión entre la proteína viral de superficie gp120 con CXCR4, al igual que con CCR5, es bastante compleja y varía en función de la envuelta X4 trópica utilizada.

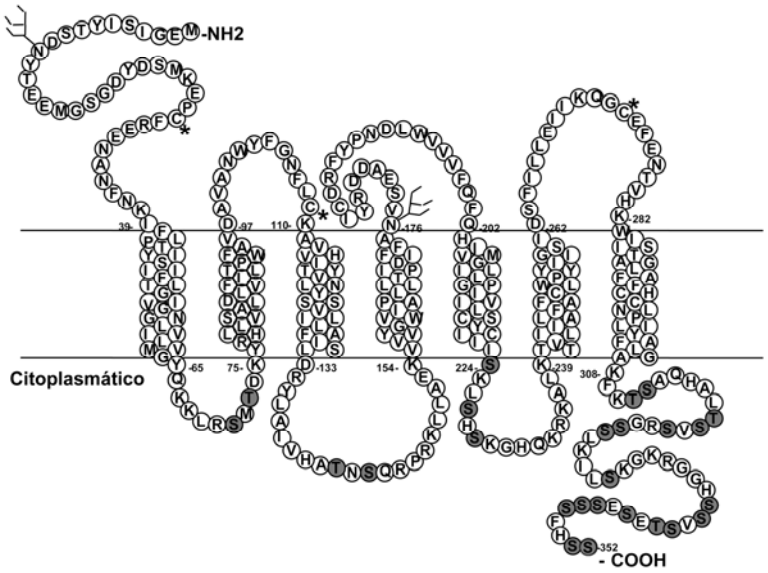

Figura 9: Orientación en membrana de los dominios del correceptor CXCR4, con la secuencia de aminoácidos. Los residuos sombreados en los dominios intracelulares representan los sitios potenciales de fosforilación. Los asteriscos representan los residuos Cys involucrados en los puentes disulfuro (Alkhatib, 2009).

De manera poco frecuente se pueden detectar cepas virales de VIH-1 y VIH-2 capaces de infectar células que expresan el correceptor pero de manera independiente de CD4 (Endres et al., 1996). Esto ha llevado a postular la existencia de un virus ancestral de VIH cuya entrada depende de su unión directa al correceptor (Lusso, 2006). Sin embargo, todos los aislados clínicamente relevantes del VIH-1 dependen, para infectar, críticamente de su unión a CD4 y a uno de los correceptores CCR5 y/o CXCR4.

3.1.3. Mecanismo de fusión y entrada del virus

Se pueden diferenciar varios estadios en el proceso que lleva al virus a entrar en la célula diana. El primer estadio puede estar mediado por la unión no productiva del VIH-1 a lectinas, glicosaminoglicanos (GAG) o a través de interacciones ligando-receptor dependiente de proteínas de la superficie celular, incorporadas en la membrana del virión, y cuya función principal es la de concentrar partículas virales en la superficie de la célula hospedadora, favoreciendo las interacciones específicas posteriores y potenciando la infección (revisado en (Ott, 2008)). Por otro lado, el VIH-1 puede ser capturado, en su conformación infecciosa, por una proteína transmembrana de tipo II que contiene un dominio lectina de tipo C de unión a manosa (DC-SIGN, "*dendritic cell-specific intercellular adhesion molecule-3-grabbing non-integrin*"),

presente en la superficie celular de algunos tipos de DC, y ser transmitido a células T $CD4^+$ en los nodos linfoides (Lore et al., 2005). Además, se ha identificado la integrina $\alpha4\beta7$ como sitio de unión para el VIH-1 en células T $CD4^+$ de memoria (Arthos et al., 2008).

Una vez el virus se encuentra en la superficie de la célula diana **(Figura 10, paso 1)**, tiene lugar la unión de la glicoproteína gp120 a su receptor principal CD4 **(Figura 10, paso 2).** Esta unión provoca un cambio conformacional en la proteína gp120, que tiene como consecuencia la exposición de los dominios de unión al correceptor, CCR5 o CXCR4, permitiendo unirse a ellos **(Figura 10, paso 3)** (Berger et al., 1999; Doms and Trono, 2000).

La unión de gp120 al correceptor da lugar a otro cambio conformacional fundamental en el proceso de fusión entre las membranas celular y viral, y que va a estar mediado por la glicoproteína gp41 **(Figura 10, paso 4)** (Berger et al., 1999; Doms and Trono, 2000). Este segundo cambio conformacional en gp120 permite la exposición del péptido de fusión hidrofóbico HR1 de gp41, que va a interaccionar con la membrana plasmática de la célula hospedadora dando lugar a una estructura en espiral enrollada de triple hebra α-hélice, formada por los tres segmentos HR1 de cada una de las subunidades gp41 del trímero. Esta estructura crea un surco hidrofóbico altamente conservado, expuesto de manera transitoria durante el proceso de fusión (revisado en (Doms and Trono, 2000)), y puede ser inhibida por péptidos basados en el dominio helicoidal C-terminal de gp41, bloqueando la formación del haz de seis hélices (Wild et al., 1994). A continuación, las regiones α-hélice HR2 C-terminales de gp41 van a unirse a este surco hidrofóbico de HR1, dando lugar al haz de seis α-hélices (revisado en (Doms and Trono, 2000)), responsable final de la fusión entre la membrana celular y viral (Melikyan et al., 2000) **(Figura 10)**.

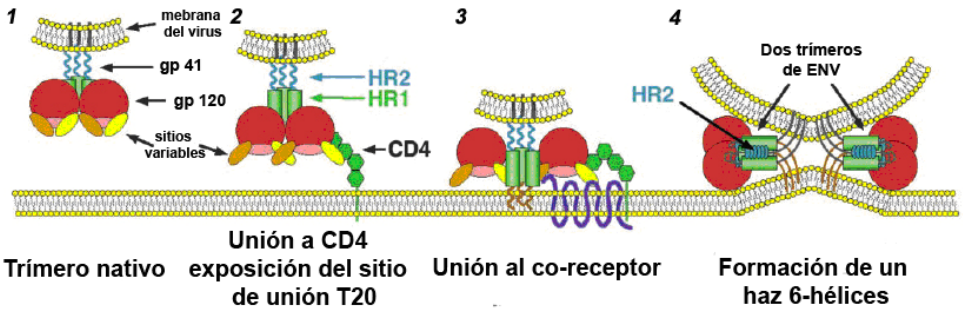

Figura 10: Esquema representativo de los diferentes estadios del proceso de fusión entre el VIH-1 y la célula diana: 1) Representación superficial de los trímeros de gp120 unidos no covalentemente a gp41; 2) unión de la glicoproteína de la envuelta viral gp120 a CD4; 3) tras la

unión de gp120 a CD4, tiene lugar un cambio conformacional que permite la unión de gp120 al correceptor adecuado; 4) la unión al correceptor permite la activación de la función de la proteína gp41 en la fusión entre las membranas celular y viral (Doms and Trono, 2000).

De hecho, parece que la energía libre liberada tras la transición al haz de seis hélices debería ser suficiente para la formación del poro de fusión (Melikyan et al., 2000). Asimismo, como el proceso de fusión es independiente de pH y altamente cooperativo que depende de la densidad y afinidad de unión de múltiples proteínas de la envuelta del VIH-1 con múltiples proteínas receptoras (Doms, 2000), se trata de un proceso más lento que requiere de una fase inicial lenta a 37ºC de 15 a 20 minutos o incluso menos (Frey et al., 1995; Melar et al., 2007; Melikyan et al., 2000), que parece depender de la interacción entre CD4 y gp120 (Frey et al., 1995; Melikyan et al., 2000), a diferencia de aquellos virus con proteínas de envuelta activadas a pH ácido donde la fusión ocurre rápidamente (Melikyan et al., 2000). Por último, la fusión mediada por la envuelta del VIH-1 depende de la temperatura, bloqueándose totalmente la misma a temperaturas inferiores a 25ºC (Frey et al., 1995).

Para la formación eficiente del poro de fusión es necesario el cambio conformacional de varios trímeros de la envuelta del VIH (revisado en (Moore and Doms, 2003)), por lo que hace falta el agrupamiento de un cierto número de moléculas de CD4 y correceptores en las zonas de contacto virus-célula. En este sentido, se ha mostrado que se necesitan múltiples eventos de unión a CD4 para activar los trímeros de la envuelta del VIH-1 (Layne et al., 1990) y de 4 a 6 moléculas de CCR5 para la formación final del poro de fusión (Kuhmann et al., 2000). La fusión entre las membranas lipídicas resulta en la liberación de la nucleocápside viral en el citoplasma de la célula hospedadora.

1.3.1.4. Transcripción reversa e integración proviral

El VIH-1, como cualquier retrovirus, es capaz de convertir el ARN de su genoma en ADN de doble cadena una vez a entrado en la célula diana **(Figura 11)**. Después de la entrada de la nucleocápside viral en el citoplasma, tiene lugar su desestructuración y la liberación del material genético (el ARN genómico), junto con diversas proteínas virales (entre ellas la IN y RT) y celulares empaquetadas en la partícula viral. La RT viral comienza la síntesis de la hebra de ADN negativo ("*minus*"), a partir de un cebador de ARN transferente (ARNt) incorporado en la partícula viral. El primer fragmento sintetizado se conoce como ADN MSSS ("*minus-strand strong stop*"), cuyo extremo 3´ va a ser utilizado posteriormente como cebador para completar la

síntesis de la hebra "*minus*" de ADN **(Figura 11)** (revisado en (Abbink and Berkhout, 2008). Durante el proceso, la actividad ARNasaH de la RT va a degradar la hebra de ARN viral molde y el cebador de ARNt. La síntesis de la hebra positiva ("*plus"*) tiene lugar mediante la utilización, como cebadores, de pequeños fragmentos de ARN que quedan después de la síntesis de la hebra "*minus"* de ADN y que la ARNasaH no ha eliminado. Una característica final de la transcripción reversa del ARN viral, consiste en la presencia de un plegamiento en la zona central del ADN de doble cadena (denominada "*central flap*") debido al desplazamiento de la hebra de ADN *plus* unos 100 nucleótidos respecto a la hebra de ADN *minus* **(Figura 11)**. Este plegamiento parece tener una función en el transporte al núcleo del PIC (Zennou et al., 2000). Además la interacción entre el ARN y la RT es de baja afinidad, por lo que el proceso de transcripción reversa incorpora mutaciones en el genoma del virus, generando poblaciones de virus VIH-1 altamente heterogéneas en secuencia (en su conjunto denominadas cuasiespecies) que son capaces de evadir fácilmente la respuesta inmune y los tratamientos antirretrovirales.

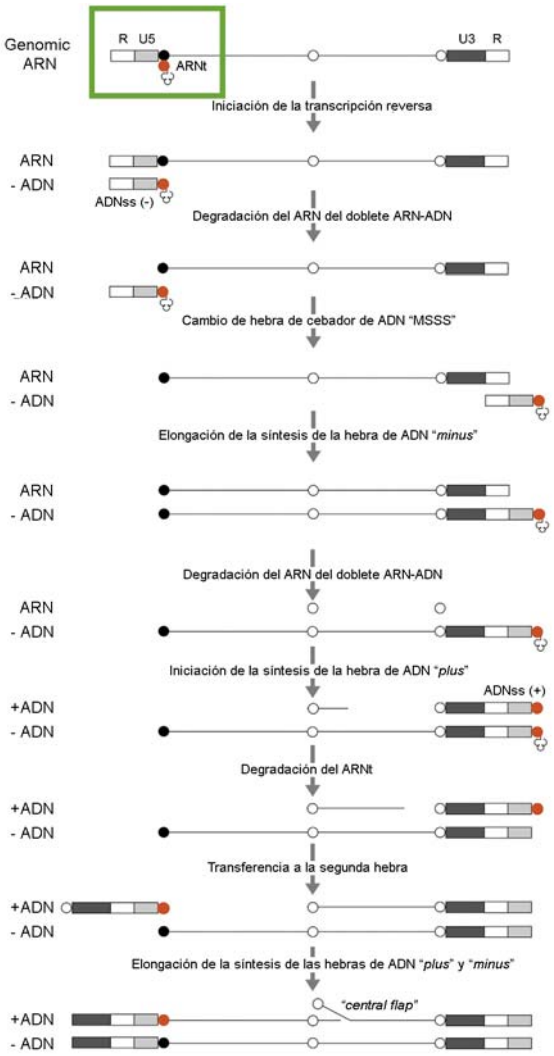

Figura 11: Esquema del proceso de transcripción reversa mediado por la RT del VIH-1 (Abbink and Berkhout, 2008).

El complejo PIC, formado por el ADN complementario (ADNc) de doble cadena junto con varias proteínas virales (MA, NC, IN y Vpr) y celulares (Farnet and Haseltine, 1991), se trasladaría al núcleo, ayudado por el citoesqueleto de actina y/o tubulina, atravesando los poros nucleares. Este proceso parece ser mediado por la interacción de las proteínas virales (IN, MA y Vpr) con la maquinaria celular de importe nuclear (Trono, 1995). Dentro del núcleo, la integración del ADN viral de doble cadena ocurre, en principio, de manera inespecífica pero preferencialmente en regiones del genoma del hospedador transcripcionalmente activas (Schroder et al., 2002). La IN es la encargada de cortar el ADN viral en la región LTR y el ADN cromosómico, seguido por la ligación de ambas secuencias (Bushman and Craigie, 1991). El proceso de integración finaliza gracias a la acción de las enzimas celulares de reparación del ADN, que terminan de sellar las uniones entre el ADN viral y celular. Cuando el genoma del VIH está integrado en el hospedador se denomina "provirus" aunque también puede permanecer en el núcleo como ADN no integrado, en forma de ADN lineal, y de ADN episomal 2-LTR o 1-LTR (por recombinación y pérdida de un LTR) **(Figura 12)** (Meyerhans A, 2003).

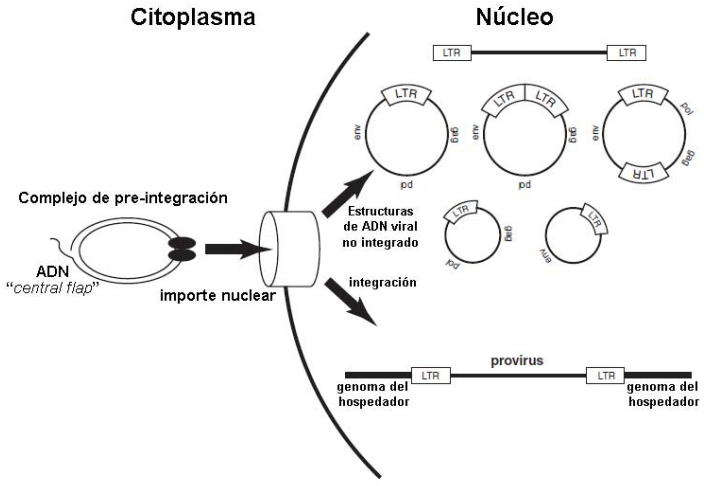

Figura 12: Esquema de las múltiples variantes del ADN viral en núcleo de las células diana. El ADN viral de doble cadena con la región central de triple hebra ("*central flap*"), para a través de los poros nucleares y puede ser integrado en el cromosoma del hospedador, pasando a llamarse provirus. El ADN viral también puede permanecer en el núcleo de manera lineal no integrada o recircularizarse dando lugar a las formas 2LTR o 1LTR (Meyerhans A, 2003).

1.3.1.5. Expresión génica viral

La transcripción del ADN proviral integrado en el cromosoma del hospedador va a generar los ARNm virales que, en último término, van a codificar las proteínas estructurales, reguladoras y accesorias necesarias para completar el ciclo de vida del virus. El sitio de iniciación de la transcripción se encuentra en la región LTR presente en el extremo 5´ del ADN proviral. La región LTR está compuesta de tres regiones: U3 (para extremo 3´), R (repetida) y U5 (para extremo 5´) **(Figura 13)**.

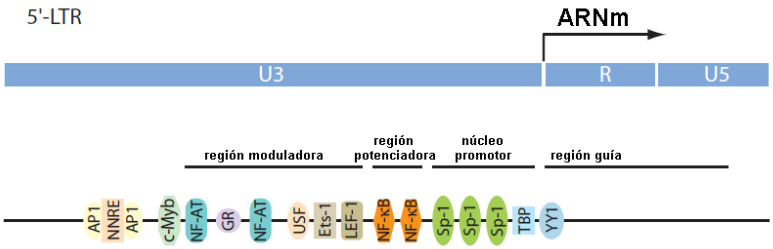

Figura 13: Organización del LTR viral 5´ del VIH-1. Regiones U3, R, U5 y la localización de los sitios de unión para factores de transcripción celulares.

La transcripción se inicia en la unión U3/R mediante la unión de la maquinaria de transcripción celular dependiente de la ARN polimerasa II (ARN pol II). En la región U3, corriente arriba del sitio de iniciación de la transcripción (caracterizado por la presencia de un motivo TATA), se encuentran una serie de regiones moduladoras de unión a diversos factores de transcripción (**Figura 13**) (Stevens et al., 2006). La expresión inicial a partir del LTR del VIH es muy baja, incrementándose significativamente gracias a la proteína viral Tat (Ruben et al., 1989). Esta transcripción basal inicial produce cortos ARNm procesados que van a codificar para las proteínas virales Tat, Rev y Nef (Yankulov et al., 1994). Esta expresión inicial provoca la acumulación de Tat, que interacciona con la región de respuesta a transactivación (TAR, "*transactivation response region*"), reclutando varios factores como el heterodímero CycT1/CDK9 ("*cyclin T1/cyclin-dependent kinase 9*"), que permiten la elongación transcripcional por hiperfosforilación de la ARN pol II (Zhou et al., 2000). Esta respuesta origina los distintos ARNm virales, no procesados (ARN genómico, Gag y Gag-Pol), parcialmente procesados (Env, Vif, Vpu y Vpr) y procesados de manera múltiple (Rev, Tat y Nef) (Purcell and Martin, 1993). Los ARNm no procesados o parcialmente procesados, que codifican las proteínas estructurales, y el ARN genómico viral son transportados fuera del núcleo por la interacción de la proteína viral Rev y del elemento de respuesta a Rev (RRE, "*Rev responsive element*")

con la maquinaria de exporte nuclear, culminando con su transporte al citoplasma celular.

1.3.1.6. Ensamblaje viral, liberación y maduración.

La generación de las nuevas partículas virales tiene lugar mediante el ensamblaje del ARN genómico y las proteínas virales en la membrana plasmática o en los endosomas tardíos/cuerpos multivesiculares. El principal componente que dirige el ensamblaje de las nuevas partículas virales en la membrana plasmática de las células infectadas es la proteína precursora $Pr55^{Gag}$, compuesta por tres polipéptidos plegados (MA, CA, y NC), dos péptidos espaciadores más pequeños sp1 y sp2, y el péptido p6 (revisión en (Ganser-Pornillos et al., 2008)) (**Figura 14**).

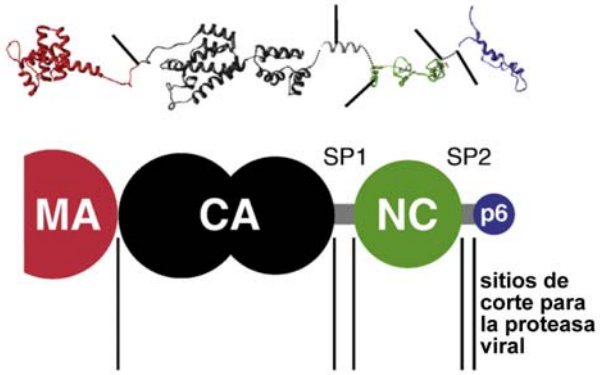

Figura 14: Regiones y estructura proteína del precursor $Pr55^{Gag}$ y los sitios de corte por la PR del VIH-1 (Briggs and Krausslich, 2011).

Las funciones de esta proteína consisten en su unión a la membrana plasmática (principalmente a regiones raft), el reclutamiento y multimerización de proteínas precursoras Gag en el lugar de liberación viral, empaquetamiento del ARN viral, formación de complejos Gag/Gag-Pol, asociación con las glicoproteínas de la envuelta, formación de complejos de pre-ensamblaje conteniendo Vif, Vpr y proteínas del huésped, y estimulación final de la liberación de las nuevas partículas virales en la membrana plasmática (revisado en (Bukrinskaya, 2004; Freed, 1998; Freed, 2001). El proceso de plegamiento adecuado y encapsidación del ARN viral tiene lugar mediante la interacción entre la señal de empaquetamiento (sitio Ψ) del ARN con la región NC de Gag (revisado en (Freed, 2001). Aparte del ARN genómico no procesado, también se va a incorporar el cebador celular de ARNt que va a tener una función importante en la transcripción reversa de ARN viral durante el siguiente ciclo de infección {Tritel, 2001 #280).

La región NC, el ARN viral y el dominio C-terminal de CA también participan en la generación de complejos Gag/Gag y Gag/Gag-Pol. Además, el transporte de estos complejos a la membrana plasmática tiene lugar gracias a la miristoilación de la proteína MA (revisión en (Ganser-Pornillos et al., 2008)). El proceso de liberación es controlado por secuencias específicas dentro de la proteína precursora $Pr55^{Gag}$, en concreto, por el dominio "L" ("*late domain*") de p6, que interacciona con la proteína Tsg101 ("*tumor susceptibility gene 101*") del complejo ESCRT-I ("*endosomal sorting complexes required for transport*"), y con la proteína celular ALIX, para facilitar y completar la reacción de ensamblaje y liberación de las partículas virales (Bukrinskaya, 2004).

La ubiquitinación de Gag y/o de los péptidos virales estructurales derivados constituye una modificación postraduccional importante en el proceso de ensamblaje del VIH-1 (Gottwein et al., 2006; Gottwein and Krausslich, 2005), de hecho, la inhibición del proteasoma dificulta la producción de partículas virales nacientes de VIH-1, afectando, de algún modo, al procesamiento correcto del Gag ubiquitinado (Schubert et al., 2000). HIV-$1_{NL4.3}$-Gag contiene 38 residuos de Lys potencialmente ubiquitinables, 13 localizados en MA (6 de ellos importantes para la localización en membrana de Gag), 11 en CA, 10 en NC, 2 en sp2 y 2 en p6**.** En este sentido, la monoubiquitinación de la proteína p6 favorece *in vitro* su interacción con Tsg101 (Morita and Sundquist, 2004). Sin embargo, mutaciones de los residuos de Lys ubiquitinables en p6, parecen no afectar a la producción y capacidad infecciosa de los viriones (Gottwein et al., 2006), ni a la ubiquitinación en otras regiones de la proteína $Pr55^{Gag}$ del VIH-1 (Gottwein and Krausslich, 2005). Sin embargo, datos recientes indican que la ubiquitinación en la región C-terminal de $Pr55^{Gag}$, a partir de CA y en p6 principalmente, es importante para el procesamiento correcto de $Pr55^{Gag}$ y la liberación de las partículas virales nacientes (Gottwein et al., 2006).

El proceso final del ciclo de vida viral consiste en la liberación de los viriones de la superficie celular en principio como partículas inmaduras, no infecciosas **(Figura 15)**. Parece que la liberación tiene lugar en regiones de la membrana plasmática ricas en colesterol, glicoesfingolípidos y esfingolípidos, y ricas en PIP_2 conocidos como "*lípid rafts*" (Nguyen and Hildreth, 2000; Ono et al., 2004).

La liberación de las partículas activa la PR viral, que va a ser la encargada del corte proteolítico secuencial de las poliproteínas precursoras $Pr55^{Gag}$. Este procesamiento permite la reorganización de la estructura del virión y en último término la generación de partículas virales infecciosas maduras **(Figura 15)** (revisión en

(Ganser-Pornillos et al., 2008)). El procesamiento y liberación adecuada de cada fragmento estructural de la poliproteína $Pr55^{Gag}$, representa un requisito indispensable para la generación de viriones infecciosos. El primer sitio de corte se encuentra en la región de unión entre sp1 y NC, lo que conduce a la división intermedia entre la secuencia MA-CA-sp1 y la secuencia NC-p6, con el posterior procesamiento en MA y CA-sp1 de la primera secuencia liberada **(Figura 15)**. La división de la secuencia CA-sp1 es un evento tardío, siendo la liberación de sp1 muy importante en la formación de la cápside troncocónica en los viriones maduros **(Figura 15)**. Además, durante el ensamblaje de los virus, el dominio N-terminal de CA del VIH-1, no del VIH-2 ni del VIS, interacciona con la proteína ciclofilina A favoreciendo su empaquetamiento, que parece potenciar la infectividad de las nuevas partículas virales (revisión en (Briggs and Krausslich, 2011; Ganser-Pornillos et al., 2008)).

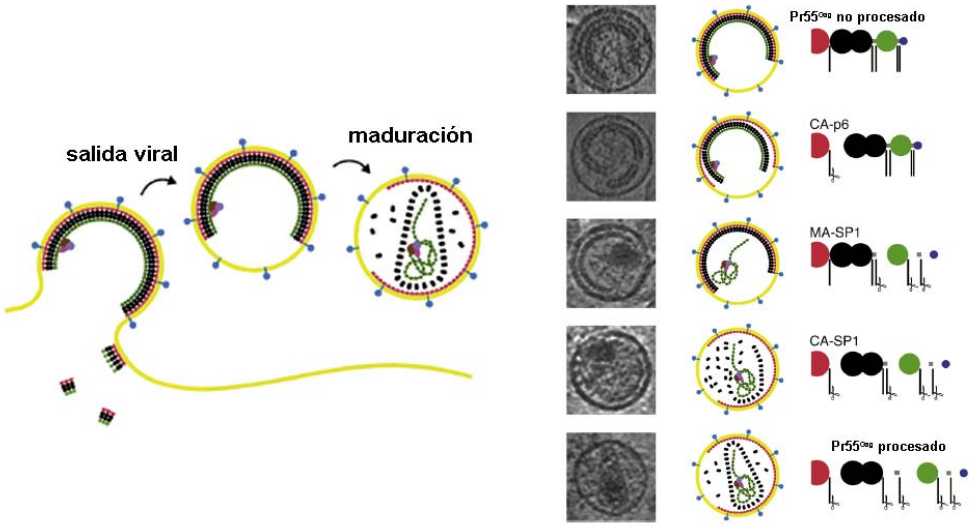

Figura 15: Esquema del proceso de maduración de las partículas de VIH-1. ***Izquierda*:** Estadio final de liberación de las partículas virales de la membrana plasmática de la célula huésped con posterior maduración de la poliproteína $Pr55^{Gag}$. ***Derecha*:** Secuencia de procesamiento y maduración de $Pr55^{Gag}$ por la PR viral tras la liberación de las partículas virales. Se muestra un esquema y una imagen de microscopía electrónica de cada estadio hasta la obtención de la partícula madura con forma tronco cónica (Briggs and Krausslich, 2011).

1.3.2. Curso natural de la infección por el VIH-1

La transmisión e infección horizontal por el VIH tiene lugar principalmente por contacto sexual, a través del tracto genital o la mucosa rectal, por transfusión sanguínea, por compartir agujas con individuos infectados o mediante el transplante de tejidos de individuos infectados (Levy, 2009). Además, en el caso de la transmisión vertical, de madre a hijo, ésta tiene lugar perinatalmente, durante el parto o durante el periodo postparto de lactancia (Scarlatti, 2004). La transmisión del VIH depende de la

naturaleza biológica del virus transmitido, de su concentración en los fluidos corporales expuestos y la susceptibilidad del hospedador a la infección. El virus puede conseguir establecer una infección productiva atravesando la mucosa del epitelio por trancitosis, mediante el contacto directo con DC intraepiteliales, o puede moverse a través de los espacios intercelulares del epitelio y contactar con las células de Langerhans y las células T $CD4^+$ presentes en el epitelio (McMichael et al., 2010).

El curso clínico de la enfermedad en humanos en ausencia de tratamiento está caracterizado por tres etapas **(Figura 16).** La primera etapa, denominada primoinfección o fase aguda de la infección, ocurre inmediatamente después de la infección y está caracterizado por un incremento de la viremia y diseminación viral generalizada. En esta fase, el VIH-1 ha llegado desde el lugar de entrada a los órganos linfoides, y ha establecido los reservorios virales por todo el cuerpo, a partir de poblaciones celulares que mantienen integrado el VIH-1, de manera latente, durante largos periodos de tiempo (Alexaki et al., 2008). Estudios de secuencia de los virus asociados a una infección productiva, parecen indicar que la infección inicial por el VIH-1 ocurre a partir de un "único virus", llamado "virus primario fundador" y principalmente R5 trópico (revisado en (McMichael et al., 2010)). Este virus infectaría células T $CD4^+$ con mayor eficiencia que monocitos y macrófagos, como células T $CD4^+CCR5^+$ residentes en la mucosa (revisado en (McMichael et al., 2010)). La replicación del virus en esta región activa el sistema inmune innato, que provoca el reclutamiento de más células T susceptibles a la infección. A continuación, el virus o las células infectadas se diseminan al órgano linfoide de drenaje y al tejido linfoide asociado al intestino (GALT, "*gut-associated lymphoid tissue*"), donde infecta gran cantidad de células T $CD4^+CCR5^+$ activadas, incrementando su tasa de replicación de manera exponencial hasta alcanzar un pico en sangre (generalmente > $1x10^6$ copias de ARN viral por mL de sangre) **(Figura 16)** (Brenchley et al., 2004). Este incremento en la viremia está asociado con un descenso en el número de células T $CD4^+$ (Levy, 2009).

Esta primera etapa provoca la estimulación del sistema inmunológico innato y adaptativo, que responde de varias maneras, incrementando la expansión de células T $CD8^+$ citotóxicas (CTL, "*cytotoxic T cells*") específicas para el virus, activando células NK, estimulando la producción de altos niveles de anticuerpos contra proteínas del VIH, y mediante la participación de otros factores como el sistema del complemento (Levy, 2009). Esta respuesta rápida del sistema inmunológico lleva a una disminución de la carga viral en el plasma sanguíneo (generalmente por debajo de 20.000 copias de ARN por mL de sangre) **(Figura 16)**, hasta alcanzar un nivel más estable, conocido

como punto de ajuste viral ("*viral set point*"). La disminución de la carga viral está asociada con la finalización de la sintomatología asociada a la primoinfección (fiebre, linfadenopatía, faringitis, erupciones cutáneas, mialgia, y úlceras en boca y esófago), pero sin erradicar completamente el virus. Así, durante este descenso de la carga viral por la presión selectiva del sistema inmune adaptativo, tiene lugar la diversificación viral, seleccionándose múltiples variantes virales de escape (McMichael et al., 2010).

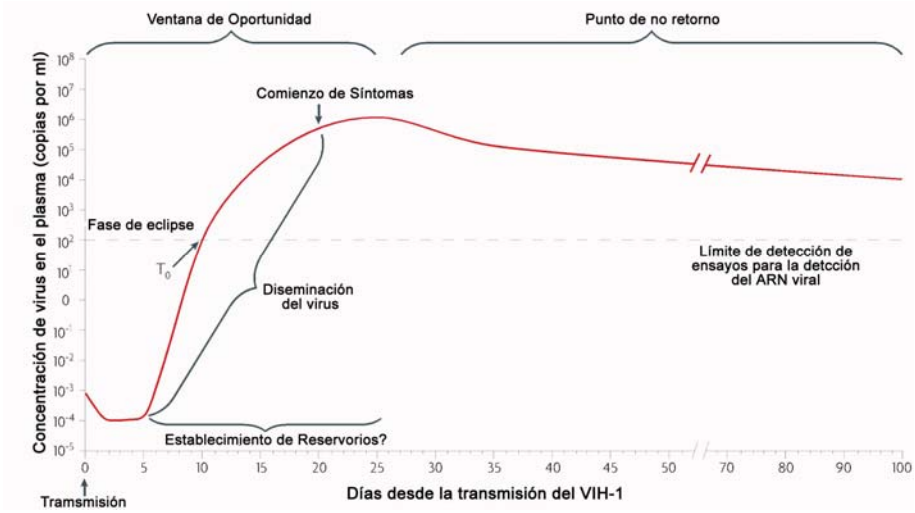

Figura 16: Eventos durante la fase aguda de la infección. La primera fase se caracteriza por una replicación viral en la mucosa y posteriormente en los órganos linfoides de drenaje. La fase de eclipse es el periodo de tiempo que tiene lugar hasta la primera detección del ARN viral en plasma (T_0). Coincidiendo con el pico de viremia comienzan los síntomas y los reservorios de latencia ya se han generado. La ventana de oportunidad constituye un periodo de tiempo crucial para controlar la replicación viral, porque ocurre antes de la destrucción masiva de las poblaciones de células T $CD4^+$ y posiblemente antes del establecimiento de los reservorios virales (McMichael et al., 2010).

A continuación comienza el periodo de latencia clínica, definida como estadio crónico de la enfermedad. En esta etapa los niveles de la carga viral permanecen bajos y estables, en función del punto de ajuste viral. La disminución de la carga viral coincide con un ligero aumento en el número de células T $CD4^+$, que seguidamente se van reduciendo de manera gradual durante la etapa crónica de la infección. Esta etapa se caracteriza por una replicación viral muy baja, durante un largo periodo de tiempo, gracias a la eficacia inicial de la respuesta inmune de cada hospedador. En esta etapa, las partículas virales se encuentran en los órganos linfoides atrapados por las células dendríticas foliculares, y rodeadas por tejidos ricos en células T $CD4^+$ que también pueden llegar a ser infectadas. La duración de este periodo de latencia es diferente en cada individuo infectado, en relación al punto de ajuste viral (revisado en (De Biasi, 2011; McMichael et al., 2010)).

En algunos individuos, la ausencia de una viremia detectable (< 50 copias de ARN viral por mL de sangre) indica el control eficiente del VIH, este grupo inusual de individuos han sido denominados como controladores de élite. Estos individuos tienen células T $CD8^+$ con una alta capacidad proliferativa y de producción de citocinas, y baja tendencia a sufrir apoptosis (Saez-Cirion et al., 2007).

La última etapa es la fase sintomática, también conocida como fase SIDA. Esta fase está caracterizada por un descenso dramático del número de células T $CD4^+$ (por debajo de 350 células por μL de sangre) y aumento de la carga viral. Este hecho lleva al colapso del sistema inmune (específicamente de las respuestas inmunes asociadas a las células T $CD4^+$), reflejado además por la destrucción del tejido linfoide, que va a permitir la aparición de tumores e infecciones oportunistas, que en último término pueden provocar la muerte del individuo (revisado en (Appay et al., 2007)) **(Figura 17).**

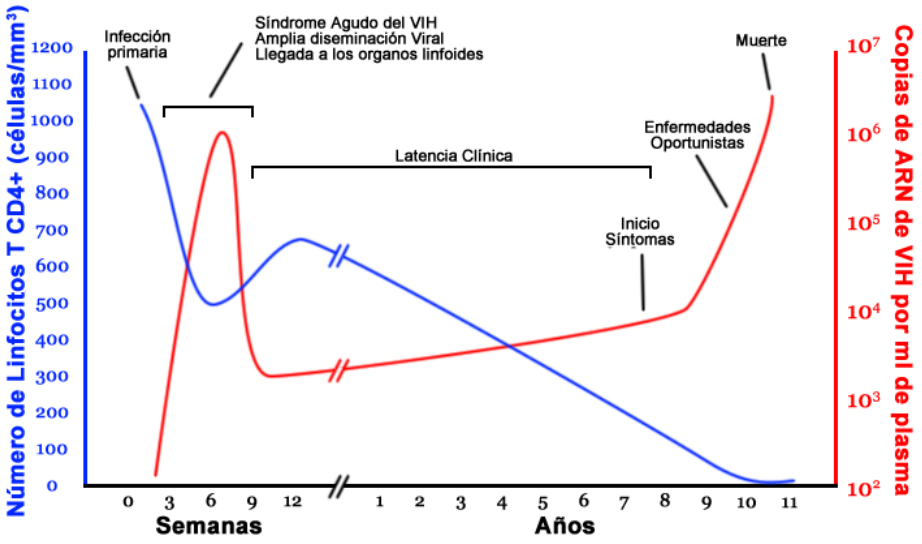

Figura 17: Curso clínico de infección por el VIH-1. La línea azul y la línea roja representan la evolución del número de células T $CD4^+$ y de la carga viral durante el curso de la infección, respectivamente.

1.3.3. Respuesta inmune contra el VIH-1

El sistema de defensa del hospedador contra las infecciones presenta tres niveles: las barreras físicas superficiales, el sistema de defensa inmunológico innato y el adaptativo. Mediante la respuesta inmune innata y adaptativa, el organismo tiene la habilidad de reconocer y eliminar cualquier agente extraño de manera inespecífica y específica, respectivamente. Por ello, el nivel de activación y efectividad del sistema inmunológico determina el curso clínico de la enfermedad.

Tras la infección por un patógeno (por ejemplo, el VIH-1), tiene lugar una activación rápida de la respuesta inmune innata, que va a reconocer un patrón conformacional del patógeno. Este reconocimiento va a dar lugar a la secreción de citocinas necesarias para el reclutamiento y activación en el lugar de la infección de otros componentes del sistema inmune, por ejemplo, las células NK. Esta población celular responde a una infección viral mediante la citolisis celular y la producción de citocinas/quimiocinas (revisado en (Borrow and Bhardwaj, 2008). La activación de la inmunidad innata va a favorecer la posterior activación de la respuesta inmune adaptativa que actúa a través de mecanismos mediados por células B (respuesta inmune humoral) y por células T (respuesta inmune celular). Las células T $CD4^+$ son los principales componentes del sistema inmune adaptativo, pero también son las principales dianas del VIH-1, y por ello el descenso continuado del número y función de estas células provoca una pérdida dramática de la función del sistema inmune del hospedador (McMichael et al., 2010).

1.3.3.1. Respuesta inmune humoral

La respuesta inmune humoral es aquella que tiene lugar mediante la generación, por activación de las células B, de anticuerpos específicos contra proteínas extrañas. Durante la etapa aguda de la infección por el VIH, tiene lugar la generación de anticuerpos no neutralizantes contra las proteínas de la envuelta gp41 y gp120 (Binley et al., 1997), sin embargo, tienen poca efectividad en las primeras etapas de la infección por el VIH-1 y son capaces de seleccionar variantes virales de escape. A continuación, tiene lugar la generación de ciertos anticuerpos neutralizantes, que pueden controlar la diversidad de partículas virales presentes en el momento de la generación de estos anticuerpos, aunque esta respuesta es escasa y permite una rápida aparición de cepas virales de escape (Richman et al., 2003). Por último, raramente se generan anticuerpos neutralizantes de alto título durante la infección por el VIH, en ese caso se generan por un mecanismo de maduración de la afinidad de los anticuerpos y después de 20-30 meses de la infección. Estos anticuerpos estarían dirigidos contra motivos carbohidrato de la envuelta gp120, contra el sitio de unión a CD4 y contra la región proximal de membrana de gp41. Este mecanismo de maduración de la afinidad, que depende de células T $CD4^+$ y células B, en la mayoría de los individuos infectados por el VIH-1, se ve perjudicado debido a la pérdida masiva de ambas poblaciones celulares (revisado en (McMichael et al., 2010)). En resumen, el efecto global y la eficiencia de este conjunto de anticuerpos

neutralizantes *in vivo* no está clara, puesto que el virus siempre es capaz de adquirir resistencia, lo que provoca que la respuesta inmune necesite de una continua adaptación a estos nuevos mutantes (Richman et al., 2003).

Por otro lado, los anticuerpos no neutralizantes de unión al VIH pueden contribuir al aclaramiento del VIH *in vivo* mediante la inducción de funciones efectoras como la lisis celular dependiente del complemento, la citotoxicidad mediada por células dependiente de anticuerpos (ADCC, "*antibody dependent cellular cytotoxicity*") o la fagocitosis. La lisis del VIH-1, mediada por el complemento, tiene lugar mediante el recubrimiento de los viriones con anticuerpos y fragmentos del complemento, los cuales son reconocidos por otros miembros del sistema del complemento, desencadenando la formación del complejo de ataque a la membrana sobre la superficie del virión, y que en último término van a desintegrar la partícula viral mediante la creación de poros (Blue et al., 2004). La respuesta ADCC es mediada a través de receptores Fc, presente en las células NK, que van a reconocer células infectadas recubiertas de anticuerpos dirigidos contra la proteína de la envuelta del VIH-1. Este reconocimiento, va a desencadenar la destrucción de la célula infectada por liberación de gránulos citotóxicos (perforinas, granzimas), citocinas (factor de necrosis tumoral o TNF, "*tumor necrosis factor*"), quimiocinas, proteasas, óxido nítrico, radicales de oxígeno radiactivos o apoptosis dependiente de Fas/FasL (Russell and Ley, 2002), aunque su relevancia *in vivo* aún no ha sido determinada. Por último, los virus o células opsonizadas, por unión del complemento o anticuerpos a su superficie, son fagocitadas, internalizadas y destruidas por células mononucleares (macrófagos y monocitos), neutrófilos y células dendríticas (Rabinovitch, 1995).

A pesar de estas respuestas anti-virales mediadas por anticuerpos, en la mayoría de los pacientes seropositivos, estos mecanismos de respuesta inmune humoral frente al VIH se han revelado poco eficaces.

1.3.3.2. Respuesta inmune celular

Como se ha descrito anteriormente, la infección por el VIH-1 se caracteriza por una fase inicial con un pico de viremia (la fase aguda), seguida por una fase crónica de larga duración. Tras la primera etapa aguda de la infección, la respuesta CTL se desarrolla rápidamente por expansión masiva de células T $CD8^+$ naïve, y cuya consecuencia consiste en la disminución del pico de viremia inicial (McMichael et al., 2010). La disminución de la viremia está asociada al reconocimiento y bloqueo, por acción citotóxica, de epitopos virales presentados en MHC-I en las células infectadas

por el VIH-1. Sin embargo, esta respuesta CTL genera una presión selectiva sobre el virus que va a generar cambios dramáticos en la secuencia de los virus, dando lugar a la aparición de mutantes de escape viral durante el descenso de la viremia hasta el punto de ajuste viral (revisado en (McMichael et al., 2010)). La aparición de variantes virales a partir de ese punto es menor, pero lo suficientemente alta para lograr escapar a la respuesta inmunológica. La respuesta citotóxica es mediada a través de la secreción de perforinas y granzimas, que terminan lisando la célula productora de virus.

Los diferentes alelos de MHC-I (HLA) tienen diferentes especificidades por los péptidos virales. En este sentido, algunos alelos de HLA han sido asociados con un buen control de la enfermedad y una progresión más lenta hacia la fase SIDA, tal como HLA-B∗5701, HLA-B∗5703, HLA-B∗5801, HLA-B27 y HLA-B51 (Carrington and O'Brien, 2003). Por el contrario, existe un polimorfismo, HLA-B35, que está asociado a una progresión más rápida de la enfermedad (Gao et al., 2001).

La respuesta CTL puede disminuir la replicación del VIH-1 mediante la producción de factores solubles, que influyen directamente sobre la célula infectada sin matarla, esta respuesta se denomina respuesta anti-viral no citotóxica de las CTL (CNAR, "*$CD8^+$ cell noncytotoxic antiviral response*") (revisado en (Levy, 2009)). Las citocinas producidas incluyen interferon-γ (IFN-γ) y las quimiocinas MIP-1α, MIP-1β y RANTES como inhibidores de la replicación viral, y TNF-α, que parece aumentarla (Levy, 2003). Esta respuesta se ha detectado que es mayor en individuos no progresores a largo plazo (LTS, "*long-term survivors*").

Por otro lado, el VIH-1 es capaz de evadir la respuesta CTL y de células NK a través de la disminución de la expresión superficial de HLA en las células infectadas, de manera dependiente de la unión de Nef a un motivo citoplasmático de este complejo (Blagoveshchenskaya et al., 2002; Le Gall et al., 1998). Mientras que HLA-A y HLA-B tienen este motivo y pueden ser degradadas de la superficie, HLA-C y HLA-E no posee este motivo y, por tanto, su nivel de expresión superficial se mantiene durante la infección (Cohen et al., 1999).

Otros tipos celulares implicados en el control de la infección por el VIH-1 son las células dendríticas plasmacitoides (pDC, "*plasmacitoid dendritic cells*") y las células NK. Durante la fase aguda de la infección por el VIH-1, el número de pDC se reduce, por muerte celular inducida por activación o por migración a nódulos linfoides. De manera destacable, individuos LTS tienen menores índices de pérdida de pDC que individuos sanos (Soumelis et al., 2001). Una de las citocinas secretadas por pDC

cuando entran en contacto con el virus es el IFNα, que estimula la respuesta inmune adaptativa (Siegal et al., 1999). Otro factor soluble producido por las pDC en contacto con el virus es IDO ("*indolenamine 2,3-dioxygenase*"), factor que induce la diferenciación de células T en T reguladoras (Tregs) cuya función principal es suprimir la respuesta inmune específica contra el VIH (Manches et al., 2008). Por otro lado, las células NK también son activadas durante la respuesta inmune, y se encargan de lisar células infectadas por el VIH-1 que carecen de expresión superficial de MHC-I (HLA-A/B). Sin embargo, la expresión de receptores inhibidores de actividad NK (KIR) en estas células, en presencia del VIH-1, y su unión a motivos HLA-C/E pueden evitar esta actividad (Borrow and Bhardwaj, 2008). Aún así, parece que el balance de señales activadoras de la función NK son predominantes debido, en parte, a la sobreexpresión en las células infectadas por el VIH-1, de otros ligando para receptores activadores de citotoxicidad expresados en la superficie de las células NK (revisado en (Borrow and Bhardwaj, 2008)).

En resumen, la respuesta inmune contra el VIH depende de una compleja red de componentes inmunológicos, muchos de los cuales son dañados durante el progreso de la infección viral y la evolución de la enfermedad hacia la fase SIDA, principalmente las células T $CD4^+$. El papel de los anticuerpos neutralizantes *in vivo* también es incierto, debido a que el virus siempre es capaz de escapar a su acción. Además, aunque la respuesta de las células T $CD8^+$ es intensa durante los primeros estadios de la infección, el papel de estas poblaciones celulares durante la fase crónica de la enfermedad parece ser subóptimo, debido al escape continuo de las nuevas variantes virales generadas. Una estrategia óptima para el control de la enfermedad consistiría en la estimulación de las respuestas inmunológicas humoral y celular en los primeros estadios de la infección (en una región temporal conocida como "ventana de oportunidad"), antes del establecimiento de los reservorios virales y de la generación de daños irreversibles en el sistema inmune, sobre todo los ejercidos sobre las poblaciones de células T $CD4^+$.

1.3.3.3. Tratamientos antirretrovirales, reservorios de latencia viral e inmuno senescencia.

Desde el descubrimiento del VIH-1 como el agente causante del SIDA, se han realizado grandes esfuerzos destinados a la búsqueda de compuestos destinados al bloqueo de alguna de las etapas del ciclo de vida del VIH. La comprensión de los diferentes estadios del ciclo de vida viral, junto con la detección de los elementos

celulares que utiliza el virus para completar su ciclo, han ayudado en la identificación de diferentes inhibidores, algunos de ellos con resultados prometedores. Todas las etapas del ciclo de vida viral han sido consideradas como potenciales dianas para su intervención en una posible terapia anti-VIH-1 (Clercq, 2009). Asimismo, la complejidad en el tratamiento contra el VIH-1 incrementa a medida que aumenta el número de nuevos agentes anti-virales disponibles y la información asociada a su uso (Lundgren et al., 2008). A continuación vamos a describir el funcionamiento de estos inhibidores, clasificados en función de la diana hacia la que están dirigidos.

Inhibidores de la fase de transcripción reversa

La RT viral es una polimerasa de ADN dependiente de ARN y ADN, que va a retrotranscribir el ARN monocatenario viral en el ADN viral de doble cadena. Existen tres clases de inhibidores: los inhibidores de RT análogos nucleosídicos (NRTIs), los inhibidores de RT análogos nucleotídicos (NtRTI) y los inhibidores de RT análogos no nucleosídicos (NNRTI). El mecanismo de acción de NRTI y NtRTI depende de su unión al sitio activo de la RT, para ello necesitan ser fosforilados por la célula a trifosfato y difosfato, respectivamente. Los NNTRI interaccionan en un sitio alostérico localizado próximo al sitio catalítico de la RT, interfiriendo con el normal funcionamiento del sitio activo.

Los **NRTI** aprobados para el tratamiento de infecciones por el VIH-1 son siete: zidovudina (AZT), didanosina (ddI), zalcitabina (ddC), stavudina (d4T), lamivudina (3TC), abacavir (ABC) y emtricitabina ((-)FTC) **(Figura 18)**. Estos compuestos actuarían como inhibidores competitivos, cuyo mecanismo de bloqueo depende de la carencia de un grupo 3´ hidroxilo, necesario para la elongación de la cadena de ADN. El primer fármaco activo fue el 3´-ácido-3´-deoxitimidina (AZT) (Mitsuya et al., 1985), aprobado en 1987. Generalmente, se combinan dos medicamentos de esta clase como cuerpo central de la terapia combinada o triple terapia (Clercq, 2009). Sin embargo, no reducen la replicación viral a largo plazo, debido a la aparición de cepas resistentes y muchos de ellos presentan además alta toxicidad en monoterapia.

Los **NtRTI** contienen un grupo fosfonato y por tanto no pueden ser inactivados por hidrolasas (esterasas), una vez se hayan incorporado a la cadena de ADN. El NtRTI más conocido es el tenofovir *("(R)-9-(2-phosphonomethoxypropyl)adenine*"), y el más utilizado para el tratamiento de infecciones de VIH es la variante de administración oral de tenofovir, el TDF ("*tenofovir disoproxil fumarate*" o comercialmente denominado Viread®) **(Figura 18)** (Clercq, 2009).

Inhibidores Nucleosídicos (NRTIs) y Nucleotídicos (NtRTIs) de la Transcriptasa Reversa

Nombre Comercial	Nombre Genérico	Nombre del Fabricante	Fecha Aprobación
Combivir	lamivudine and zidovudine	GlaxoSmithKline	27-Sep-97
Emtriva	emtricitabine, FTC	Gilead Sciences	02-Jul-03
Epivir	lamivudine, 3TC	GlaxoSmithKline	17-Nov-95
Epzicom	abacavir and lamivudine	GlaxoSmithKline	02-Aug-04
Hivid	zalcitabine, dideoxycytidine, ddC (no longer marketed)	Hoffmann-La Roche	19-Jun-92
Retrovir	zidovudine, azidothymidine, AZT, ZDV	GlaxoSmithKline	19-Mar-87
Trizivir	abacavir, zidovudine, and lamivudine	GlaxoSmithKline	14-Nov-00
Truvada	tenofovir disoproxil fumarate and emtricitabine	Gilead Sciences, Inc.	02-Aug-04
Videx EC	enteric coated didanosine, ddI EC	Bristol Myers-Squibb	31-Oct-00
Videx	didanosine, dideoxyinosine, ddI	Bristol Myers-Squibb	9-Oct-91
Viread	tenofovir disoproxil fumarate, TDF	Gilead	26-Oct-01
Zerit	stavudine, d4T	Bristol Myers-Squibb	24-Jun-94
Ziagen	abacavir sulfate, ABC	GlaxoSmithKline	17-Dec-98

Figura 18: Inhibidores nucleosídicos y nucleotídicos con licencia de la FDA ("*food and drug administration*").

Los **NNRTI** interaccionan con un bolsillo de unión cercano al sitio activo de la RT. Esta unión interfiere con el sitio catalítico impidiendo el funcionamiento normal de la enzima. Son moléculas pequeñas con alta diseminación y con una vida media larga. El problema de estos compuestos es que los aa colocados en el bolsillo de unión a los NNRTI son muy propensos a la mutación por la RT. Los más prometedores, aprobados por la FDA ("*Food and Drug Administration*"), son etravirina (enero de 2008), nevirapinaXR (marzo de 2011) y particularmente rilpivirina (mayo de 2011) **(Figura 19)** (Clercq, 2009).

Inhibidores No-Nucleosídicos (NNRTIs)

Nombre Comercial	Nombre Genérico	Nombre del Fabricante	Fecha Aprobación
Edurant	rilpivirine	Tibotec Therapeutics	20-May-11
Intelence	etravirine	Tibotec Therapeutics	18-Jan-08
Rescriptor	delavirdine, DLV	Pfizer	4-Apr-97
Sustiva	efavirenz, EFV	Bristol Myers-Squibb	17-Sep-98
Viramune (Liberación Inmediata)	nevirapine, NVP	Boehringer Ingelheim	21-Jun-96
Viramune XR (Liberación Larga)	nevirapine, NVP	Boehringer Ingelheim	25-Mar-11

Figura 19: Inhibidores no nucleosídicos con licencia de la FDA.

Inhibidores de la Proteasa

La PR es una aspartil proteasa que actúa en forma dimérica, y su función es el procesamiento proteolítico de las proteínas virales precursoras, para dar lugar a las

proteínas virales maduras (Flexner, 1998). Los inhibidores de la PR son moléculas peptidomiméticas que actúan imitando el sitio de corte por la PR viral, impidiendo su funcionamiento. Los fármacos peptidomiméticos eficaces son selectivos y eficaces contra la PR viral dimérica, sin actuar sobre las aspartil proteasas celulares y monoméricas. Hay actualmente diez inhibidores o combinaciones de inhibidores de la PR viral (PIs) aprobados para el tratamiento de infecciones por el VIH **(Figura 20)**. El ritonavir es el inhibidor más fuerte, y el saquinavir es probablemente el más débil

Inhibidores Proteasa (PIs)

Nombre Comercial	Nombre Genérico	Nombre del Fabricante	Fecha Aprobación
Agenerase	amprenavir, APV	GlaxoSmithKline	15-Apr-99
Aptivus	tipranavir, TPV	Boehringer Ingelheim	22-Jun-05
Crixivan	indinavir, IDV,	Merck	13-Mar-96
Fortovase	saquinavir (no longer marketed)	Hoffmann-La Roche	7-Nov-97
Invirase	saquinavir mesylate, SQV	Hoffmann-La Roche	6-Dec-95
Kaletra	lopinavir and ritonavir, LPV/RTV	Abbott Laboratories	15-Sep-00
Lexiva	Fosamprenavir Calcium, FOS-APV	GlaxoSmithKline	20-Oct-03
Norvir	ritonavir, RTV	Abbott Laboratories	1-Mar-96
Prezista	darunavir	Tibotec, Inc.	23-Jun-06
Reyataz	atazanavir sulfate, ATV	Bristol-Myers Squibb	20-Jun-03
Viracept	nelfinavir mesylate, NFV	Agouron Pharmaceuticals	14-Mar-97

Figura 20: Inhibidores dirigidos contra la PR viral aprobados por la FDA para su uso en individuos infectados por el VIH-1.

Como muchos inhibidores utilizados contra el VIH-1, los PIs también tienen efectos tóxicos a largo plazo, como la lipodistrofia y la dislipidemia. Por ejemplo el ritonavir es un potente inhibidor del citocromo P450, permitiéndo que los niveles en sangre de los antirretrovirales se mantengan por más tiempo en concentraciones óptimas, aunque también resulta en un incremento en la toxicidad y severidad de los efectos adversos asociados a estos inhibidores.

Inhibidores de la entrada y fusión

Desde el descubrimiento del VIH, las glicoproteínas de la envuelta viral (gp120/gp41) siempre han sido consideradas para el desarrollo de inhibidores contra la entrada viral. Además, se trata de la diana más atractiva puesto que impediría la entrada del virus en la célula y la generación de los reservorios virales. Aun así, el descubrimiento de compuestos dirigidos contra la envuelta del VIH tiene una serie de inconvenientes. En primer lugar, la RT viral es propensa a cometer errores dando lugar a mutaciones en las proteínas virales (Gaschen et al., 2002). En segundo lugar, aunque el 50% de la envuelta contenga regiones conservadas, parece difícil dirigir compuestos inhibidores contra estas regiones debido a la alta glicosilación de las

regiones variables que se encuentran alrededor (Reitter et al., 1998). Por todo ello, las estrategias de inhibición dirigidas contra la envuelta del VIH (gp120/gp41) están dirigidas contra regiones altamente conservadas que son expuestas transitoriamente durante el proceso de entrada viral. En este sentido, se han desarrollado péptidos sintéticos miméticos de la región C-terminal de gp41, tales como el C-34, el T-20 y el T-1249, que se unen a la región N-terminal de esta glicoproteína expuesta durante la formación del intermediario de fusión, inhibiendo la infección por el VIH-1 (Chan and Kim, 1998; Judice et al., 1997).

El único inhibidor de fusión con licencia de la FDA, para terapia en humanos, es enfuvirtide (Fuzeon, T-20 o DP-178, aprobado el 13 de Marzo de 1993 y comercializado por Hoffmann-La Roche & Trimeris), con una potente actividad contra un amplio espectro de aislados del VIH-1 *in vitro* (Wild et al., 1994).

Inhibidores de unión a correceptor

Este grupo de inhibidores, dirigidos a evitar la unión del virus a los correceptores, tiene la desventaja de una posible interferencia con las funciones normales de estas proteínas humanas contra las que se dirige la inhibición, dando lugar a posibles efectos secundarios. Hasta ahora sólo hay un inhibidor aprobado para su administración que bloquea la unión de cepas de VIH-1 R5 trópicas a CCR5, el agonista inverso Maraviroc (“Selzentry”, aprobado en 6 de Agosto de 2007 y comercializado por Pfizer) (Garcia-Perez et al., 2011). Sin embargo, ya se están detectando cepas resistentes a Maraviroc, y a los otros inhibidores de unión a CCR5, Vicriviros y Aplaviroc (revisado en (Gorry and Ancuta, 2011)).

Inhibidores de la Integrasa

Las funciones catalíticas de la IN se pueden dividir en: procesamiento de extremos 3´ del ADN de doble cadena viral y la transferencia de hebras. El primer y único inhibidor de la IN con licencia es raltegravir (“Isentress”, aprobado el 12 de octubre de 2007, y comercializado por Merck & Co., Inc.) (Gazzard et al., 2008). Este inhibidor está dirigido contra la reacción de transferencia de la hebra, y se ha mostrado eficiente reduciendo la carga viral en pacientes infectados por el VIH-1.

Terapia antirretroviral de gran actividad (TARGA) o terapia antirretroviral combinada (TARc).

La replicación continuada del VIH lleva al daño irreversible del sistema inmune y progresión a la fase SIDA. Los niveles de ARN viral reflejan la magnitud de la replicación del VIH, y el número de células T $CD4^+$ indica el nivel de eficiencia del sistema inmune. Estos valores son distintos en cada individuo y, por tanto, los tratamientos deben ser individualizados. El objetivo de la terapia consiste en la máxima supresión de la replicación viral junto con el bloqueo de la emergencia de cepas virales resistentes, con los menores efectos secundarios sobre el individuo. La estrategia terapéutica más efectiva consiste en la combinación simultánea de varios fármacos anti-VIH **(Figura 21)**. Esta terapia previene la aparición de mutaciones específicas, que llevan a la aparición de resistencias, y ayuda a lograr una supresión viral estable. La combinación de 2 ó 3 medicamentos anti-VIH, de 2 o más clases diferentes, se denomina terapia antirretroviral de gran actividad (TARGA) o tratamiento antirretroviral combinado de alta eficiencia (TARc) (en inglés "*Highly Active Anti-Retroviral Therapy*" (HAART)). Este tratamiento es considerado cuando el número de células T $CD4^+$ cae por debajo de 350 células por μL de sangre. La aplicación de esta terapia ha llevado a una reducción drástica de la mortalidad y la morbilidad relacionada con el SIDA (Clercq, 2009).

Combinación de Productos de Varias Clases

Nombre Comercial	Nombre Genérico	Nombre del Fabricante	Fecha Aprobación
Atripla	efavirenz, emtricitabine and tenofovir disoproxil fumarate	Bristol-Myers Squibb and Gilead Sciences	12-July-06
Complera	emtricitabine, rilpivirine, and tenofovir disoproxil fumarate	Gilead Sciences	10-August-11

Figura 21: Algunas de las combinaciones de productos antirretrovirales, de varias clases, aprobados por la FDA para el tratamiento de individuos infectados por el VIH-1.

Los combinados antirretrovirales más utilizados son Atripla (efavirenz, emtricitabine y tenofovir disoproxil fumarato, comercializado por Bristol-Myers Squibb y Gilead Science), Truvada (tenofovir disoproxil fumarato y emtricitabine, comercializado por Gilead Science, Inc) y Kaletra (lopinavir y ritonavir, comercializado por GlaxoSmithKline). Existe otra combinación pendiente de aprobación por parte de la FDA, se combina: tenofovir + emtricitabina+ elvitegravir + cobicistat, se llama QUAD y está siendo desarrollado por Gilead Sciences.

En muchos casos, sobre todo en individuos sometidos a terapia antirretroviral combinada (TARc), la viremia en plasma se reduce a niveles casi indetectables (< 50

copias de ARN viral por mL de sangre). Sin embargo, la supresión de esta terapia da lugar a una rápida replicación viral, lo que indica la existencia de reservorios virales de latencia de larga duración (Wong et al., 1997).

La latencia viral se caracteriza por la ausencia de expresión génica del patógeno en la célula hospedadora, asegurando la supervivencia del mismo durante un largo periodo de tiempo. La latencia puede dar lugar a reservorios virales, y su establecimiento depende del sitio de integración del provirus, del estado metabólico y de activación del hospedador después de la integración, y de la ausencia de niveles de expresión suficientes de las proteínas virales Tat, Rev y de otros factores de transcripción del hospedador (Siliciano and Siliciano, 2000). Existen varios reservorios de latencia en un individuo infectado por el VIH-1. Los principales parecen ser las células T $CD4^+$ de memoria en un estado de reposo, los monocitos y células dendríticas foliculares, células madre hematopoyéticas ($CD34^+$) e incluso el GALT (Alexaki et al., 2008). Las células T $CD4^+$ de memoria en reposo tienen un papel importante en la latencia del VIH-1 (Alexaki et al., 2008), gracias en parte a su persistencia en el organismos durante largos periodos de tiempo como parte de la memoria inmunológica. Una de las características más notables que determina la latencia en células T $CD4^+$ en reposo, consiste en la ausencia de señales de activación celular, como los factores de transcripción NF-AT y NF-κB que actúan sinérgicamente con la proteína Tat viral en la expresión génica viral (Stevens et al., 2006). Otro mecanismo de generación de latencia, en células T $CD4^+$ en reposo, es mediado por los miR (microARN, reguladores de la expresión génica mediante la inhibición de la traducción de los ARNm contra los que están dirigidos) (Huang et al., 2007).

Los monocitos también se han propuesto como reservorios virales de latencia a largo plazo, sobre todo un grupo reducido de monocitos que expresan el marcador $CD16^+$, y que representan un 5% del total de monocitos. Este grupo de monocitos son más susceptibles a la infección por el VIH-1 y permiten la expresión génica viral y la replicación cuando se diferencian en macrófagos (Dong et al., 2009).

Las células dendríticas foliculares son capaces de retener partículas de VIH-1 en su superficie y transferirlas posteriormente a las células T $CD4^+$ durante la sinapsis virológica que tiene lugar en los nódulos linfoides (Alexaki et al., 2008). Otros reservorios del VIH-1 pueden encontrarse en las células progenitoras hematopoyéticas (HSC, *"hematopoietic stem cells"*, $CD34^+$) (Alexaki et al., 2008). Estas células parece

que se infectan por el VIH-1, *in vivo* e *in vitro* con baja eficiencia, dando lugar a una infección latente que puede activarse mediante el tratamiento con citocinas y posterior diferenciación celular (Carter et al., 2010). La infección de HSC podría permitir la presencia del genoma del VIH-1 en múltiples linajes hematopoyéticos, como los monocitos/macrófagos del linaje mieloide y las células T del linaje linfoide. Por último, parece que el tejido linfoide asociado a la mucosa (MALT, "*Mucosal-Associated Lymphoid Tissue"*) constituye un reservorio viral fuera de la sangre periférica, por su importancia en los primeros estadios de la replicación del VIH-1 (Veazey et al., 1998).

Estos reservorios celulares de latencia pueden reactivarse y dar lugar a una infección productiva, y con ello a la transmisión viral. En este sentido, las terapias antirretrovirales deben bloquear la generación de reservorios de latencia y/o reactivar estos reservorios, en individuos crónicamente infectados, para asegurar la completa erradicación del virus del organismo. Por todo ello, y considerando el modo de acción de los fármacos antirretrovirales, que no inhiben la infección ni la instalación de los reservorios (fracaso terapéutico y cepas resistentes a la terapia), y las características de los reservorios virales, se estima que los pacientes crónicamente infectados necesitarían estar sujetos a las terapias antirretrovirales actuales durante al menos 60 años, para una potencial erradicación total del virus del organismo (Finzi et al., 1999).

Toxicidad de terapia antirretroviral y envejecimiento del sistema inmune.

A pesar de los beneficios de la terapia antirretroviral de alta eficacia, los distintos fármacos antirretrovirales que la componen presentan múltiples efectos secundarios, algunos de los cuales pueden comprometer el éxito terapéutico, llegando a amenazar la vida del paciente (Quirk et al., 2004). Por otro lado, la terapia antirretroviral, aunque es capaz de mantener controlada la replicación del VIH-1, no es capaz de restaurar totalmente el estatus inmunológico y de salud de un individuo infectado. Por ello, los individuos infectados por el VIH-1, sometidos a tratamientos antirretrovirales de larga duración, tienen una expectativa de vida más corta que los individuos no infectados. Este acortamiento de la vida, se debe a un aumento del riesgo de sufrir complicaciones no SIDA (Bhaskaran et al., 2008) como, enfermedades relacionadas con el corazón (arterioesclerosis, infarto de miocardio, hipertensión, diabetes o dislipidemia), el hígado, el riñón y los huesos (fracturas, osteopenia y osteoporosis), cáncer (de hígado, de pulmón, colorrectal, melanomas y enfermedad de Hodgkin), debilitamiento neurocognitivo (demencia), aumento de la fragilidad muscular (sarcopenia y debilitamiento muscular) y síndrome metabólico (obesidad visceral y

lipodistrofia) (revisado en (Deeks, 2011)). Curiosamente, la mayoría de estas complicaciones son comunes en individuos ancianos, por lo que parece que las personas infectadas por VIH-1, sufren un envejecimiento prematuro, a nivel metabólico y de diferentes componentes del sistema inmune. Actualmente, se sabe que estos cambios son consecuencia de la toxicidad de la terapia antirretroviral unida a la activación inmune e inflamación persistente debida a la infección y replicación por el VIH-1, y que tiene como consecuencia final el deterioramiento de la funcionalidad del sistema inmune, y en último término inmunosenescencia (envejecimiento prematuro del sistema inmune), que será descrita a continuación.

Al igual que lo que ocurre con cualquier órgano del cuerpo humano, el sistema inmune exhibe cambios significativos con el envejecimiento natural de una persona. Este envejecimiento o inmunosenescencia, parece ser consecuencia de una continua activación inmune e inflamación (revisado en (Desai and Landay, 2010)), y está caracterizado por el reducido número y función de las células madre hematopoyéticas, involución tímica, descenso en el número de células T $CD4^+$ *naïve* circulantes, descenso en el ratio CD4/CD8, mayor número de células T de memoria $CD28^-$ ($CD4^+$ o $CD8^+$) en estado altamente diferenciado e incremento en la secreción de citocinas pro-inflamatorias (IL-6, IL-1β y TNFα). Así mismo, muchas de estas alteraciones inmunológicas encontradas en individuos de avanzada edad también pueden ser encontradas en individuos infectados por el VIH-1. Estas alteraciones se caracterizan por la continua activación del sistema inmune (innato y adaptativo) e inflamación, que tiene lugar por la presencia continua de viriones de VIH-1 circulantes (infecciosos y no infecciosos). La alta tasa de mutaciones del VIH-1 también tiene su efecto potenciador de la activación del sistema inmune, mediante la activación y proliferación de nuevos repertorios celulares para el reconocimiento de los nuevos antígenos virales expuestos que van a cambiar con rapidez, dirigiendo estos repertorios celulares anérgicos a la apoptosis (De Biasi, 2011). Por otro lado, estas alteraciones inmunológicas junto con la activación de células T, el incremento en la susceptibilidad a la muerte celular inducida por activación y una baja restauración de esta población celular (Kelley et al., 2009), llevan a una pérdida progresiva (senescencia o apoptosis) de células naïve, de memoria y reguladoras. Los factores que influyen en la pérdida de regeneración de las células T son varios, entre ellos están la continua renovación de células T, la disfunción tímica (o infección directa de timocitos o sus precursores), el estrés oxidativo y la acumulación de alteraciones genéticas (revisado en (Deeks, 2011)).

La ausencia de una respuesta anti-inflamatoria por parte de las células Tregs tiene lugar por la contínua activación inmune, y por la acumulación excesiva de

mediadores de la inflamación (IL-6, IL-1β y TNFα), secretados por células del sistema inmune innato (Eggena et al., 2005), aún en presencia de terapia antirretroviral. La persistencia de esta inflamación puede ser favorecida por otros factores como la replicación del VIH, la presencia de otros patógenos (CMV y herpesvirus) y la translocación de lipopolisacáridos (LPS) a través de daños en GALT (Brenchley et al., 2006; Naeger et al., 2010). Además, los individuos infectados por el VIH-1 presentan niveles reducidos de células T $CD4^+$ y $CD8^+$ naïve y de memoria central, y mayores niveles de células T $CD4^+$ y $CD8^+$ efectoras terminalmente diferenciadas. Estos datos confirman la pérdida de la homeostasis de las células T, la activación inmune y la senescencia en individuos infectados por el VIH-1.

Por otra parte, la inmunosenescencia del sistema inmune por la infección del VIH-1 también afecta a la función de las células B y a la respuesta inmune innata (monocitos/macrófagos y células dendríticas). Por un lado, el repertorio de células B naïve y de memoria también desciende, y por otro lado, la infección por el VIH-1 parece disminuir la funcionalidad de las células NK, monocitos, macrófagos, pDC y neutrófilos (De Biasi, 2011). En este sentido las estrategias para controlar la inmunosenescencia pasan por la aplicación de la TARc con compuestos encargados de bloquear la activación inmune e inflamación (revisado en (Deeks, 2011)).

Sin embargo, a pesar de que el acceso a las TARc ha disminuido la patología y la mortalidad asociada a la infección por el VIH-1 (Clercq, 2009), la epidemia asociada al VIH-SIDA sigue en continua expansión, a consecuencia de la incapacidad de los tratamientos de eliminar por completo el virus del organismo de los individuos infectados (reservorios virales) (Alexaki et al., 2008), debido a la rápida aparición de resistencias y a los efectos secundarios asociados a los tratamientos en uso (Carr, 2003). Por otro lado, la infección por el VIH, junto con las infecciones oportunistas asociadas al SIDA, están constantemente activando respuestas inmunológicas innatas y adaptativas, que tiene como consecuencia la liberación continuada de mediadores de inflamación. La combinación de ambos procesos, probablemente, termina con un rápido envejecimiento temprano de las células T, que junto a la destrucción masiva de las células T $CD4^+$ de memoria contribuyen a la generación de inmunodeficiencia en el individuo infectado.

En resumen, la aparición de resistencias frente a los fármacos antirretrovirales, que constituye la causa más frecuente del fracaso de los tratamientos, y la existencia de santuarios de latencia, replicación y propagación para el VIH-1 en el organismo, que impiden la eliminación de los provirus integrados, plantean un obstáculo enorme

para la erradicación del virus en la lucha contra el SIDA. Es por esto, que urge encontrar nuevas dianas moleculares y celulares anti-VIH-1, necesarias para el desarrollo de nuevas estrategias terapéuticas, y que, por otra parte, resultaría en el esclarecimiento de los procesos moleculares y celulares que subyacen a la infección de las células del sistema inmune y a los procesos de escape inmunológico del VIH-1.

1.4. SEÑALIZACIÓN CELULAR Y REORGANIZACIÓN DEL CITOESQUELETO DE ACTINA EN LA INFECCIÓN POR EL VIH-1.

1.4.1. Interacciones no productivas virus-célula independientes de CD4 y correceptor (CCR5/CXCR4).

El primer estadio en la interacción del VIH-1 con la célula hospedadora puede estar mediado por la unión inespecífica a lectinas, GAG o a través de interacciones ligando-receptor dependiente de proteínas de la superficie celular, como la molécula de adhesión LFA-1 (*"lymphocyte function-associated antigen 1"*) y moléculas de adhesión inter-celular (ICAM, "*inter-cellular adhesion molecule*"), complejos HLA y otros antígenos específicos de cada tipo celular, incorporadas selectivamente o no en la membrana del virión durante el empaquetamiento y salida de las nuevas partículas virales (revisado en (Ott, 2008)). La interacción de estas moléculas con sus parejas específicas presentes en la célula diana, parecen potenciar la infectividad (Ott, 2008), y podrían activar rutas, aún desconocidas, de señalización cuyo resultado final estaría relacionado con un cambio del estado de activación de la célula que favoreciera la entrada viral.

Entre las proteínas incorporadas en la superficie del virión, podemos encontrar a los antígenos CD55 y CD59 que parecen proteger al VIH-1 de su destrucción por el sistema del complemento, evitando la unión y formación del complejo de ataque a la membrana (Saifuddin et al., 1995). Otros componentes celulares incorporados en las partículas de VIH-1 son CD28, CD152, CD80 y CD86, su presencia incrementa la unión del virus con la célula diana, la internalización viral, y la replicación mediante la activación, en sinergia con TcR/CD3, del factor de transcripción NF-κB (Giguere et al., 2004; Giguere et al., 2005). También se ha descrito que el VIH-1 incorpora grandes cantidades de MHC-II (HLA-DR) cargadas con antígenos, que pueden inducir la activación y proliferación de células T $CD4^+$ específicas de antígeno (Roy et al., 2005). Por otra parte, la unión de la proteína gp120 del VIH-1 a la integrina $\alpha4\beta7$, de manera independiente de CD4, parece favorecer la estabilización de la sinapsis viral

permitiendo la transmisión viral célula a célula (Arthos et al., 2008). Esta integrina está asociada a CD4 y a CCR5, se expresa preferencialmente en células T $CD4^+$ activadas localizadas en el MALT y son altamente susceptibles a la infección por el VIH-1 (revisado en (Cicala et al., 2011)). Además, la proteína de envoltura viral gp120 del VIH-1 puede interaccionar con proteoglicanos heparán sulfato (HS) de la superficie celular, interfiriendo en la interacción entre gp120-CXCR4 (Roderiquez et al., 1995). En este sentido, recientemente se ha desarrollado la síntesis de conjugados entre compuestos miméticos de CD4 unidos a HS, que se unen a la envuelta viral gp120 inhibiendo la entrada e infección de ambos tropismos virales (Baleux et al., 2009).

Por otro lado, otras proteínas que modulan la infección por el VIH-1 son las tetraspaninas (de 4 dominios de transmembrana, TM4). Por un lado, estas TM4 son reclutadas a los sitios de salida viral durante la sinapsis viral (Jolly and Sattentau, 2007). En este sentido, la sobreexpresión de las tetraspaninas CD63, CD9 y CD81, en la célula productora de virus, reduce la infectividad, la transmisión y la fusión viral (Krementsov et al., 2009; Weng et al., 2009). Por otro lado, la interferencia específica, mediante un ARN interferente (ARNi), de la expresión de CD9 y CD81 en la célula diana, potencia la entrada viral y la formación de sincitios, mientras que la sobreexpresión de CD9 y CD81 tiene el efecto contrario (Gordon-Alonso et al., 2006).

La fusión y entrada del VIH-1 se ha visto que también ocurre en áreas específicas de la superficie celular enriquecidas en los receptores virales y en actina, tales como "*ruffles*", microvellosidades y microdominios de membrana (denominados "*lipid rafts*") (Singer et al., 2001; Steffens and Hope, 2003), necesarios para que tenga lugar la fusión entre las membranas celular y viral de manera eficiente (Hug et al., 2000; Nguyen and Taub, 2002; Viard et al., 2002). Uno de los componentes de los "*lipid rafts*", el colesterol, también es necesario durante el estadio de entrada viral. En este sentido, la reducción del contenido en colesterol de la membrana plasmática de linfocitos y macrófagos afecta negativamente al agrupamiento de los receptores virales inducido por la proteína viral gp120 (Manes et al., 2000; Popik et al., 2002), e inhibe la fusión de las membranas celular y viral (Viard et al., 2002). Por último, otro mecanismo descrito, previo a la entrada del virus en la célula, es el movimiento del VIH-1 a lo largo de los filopodios de manera dependiente de actina y miosina II, hasta llegar a un lugar favorable para la entrada viral (Lehmann et al., 2005). En resumen, como veremos más adelante, el comportamiento y remodelación dinámica de estas estructuras depende del citoesqueleto de actina cortical y de la activación o inhibición de las diversas proteínas de unión a actina, como aquellas responsables del corte o

crecimiento de los filamentos de actina, el recubrimiento de actina y formación de estructuras complejas de actina (Mangeat et al., 1999).

1.4.2. Señalización a través de CD4.

La unión de la proteína viral gp120 a CD4 activa rutas de señalización que, aunque en principio descritas como innecesarias para la entrada del VIH-1 (Salzwedel et al., 2000), son capaces de facilitar la integración del genoma viral en la célula diana y modular la replicación viral (Cicala et al., 2006a; Cicala et al., 2002; Kinter et al., 2003). De manera global, se pueden clasificar dos conjuntos de señales inducidas a través de CD4, aquellas que favorecen la supervivencia de la célula infectada impidiendo su muerte y asegurando la replicación viral, y las señales de defensa contra la infección que tratarían de inhibir la replicación viral en la célula infectada mediante señales de muerte celular.

La primera señal "positiva" descrita que favorece el ciclo de vida del VIH-1, e inducida por la unión entre gp120 con CD4 en células T, fue la fosforilación de la tirosín quinasa $p56^{Lck}$, que parece disociarse posteriormente de la cola citoplasmática de CD4, permitiendo la endocitosis del receptor (Goldman et al., 1994; Juszczak et al., 1991; Trushin et al., 2010). Este proceso de endocitosis y "down"-regulación de CD4 podría ser clave para asegurar el proceso infectivo y la supervivencia de las partículas de VIH-1 incorporadas en primera instancia, al evitar la lisis de la célula diana por superinfección (Nethe et al., 2005). La activación de $p56^{Lck}$, por unión de gp120 a CD4, estimula la actividad de las quinasas PI3K y PI4K ("*phosphatidylinositol 4-kinase*") (Briand et al., 1997; Prasad et al., 1993; Schmid-Antomarchi et al., 1996). La activación de PI3K y posteriormente de la proteína quinasa B (PKB/Akt) por el VIH-1, parece ser importante para prolongar la supervivencia de las células infectadas (Ji and Liu, 2008). Igualmente, $p56^{Lck}$ se asocia, fosforila y activa la quinasa Ser/Thr Raf-1, de manera independiente de Ras (Popik and Pitha, 1996). La activación de Raf-1, da lugar a la activación de la ruta MEK/ERK (*"mitogen-activated protein kinase\ERK kinase"/"extracellular-signal-regulated kinase"*), con posterior activación de los factores de transcripción NF-κB y AP-1, que van a incrementar la actividad del promotor del VIH-1 (de manera dependiente o independiente de Tat), además de activar el promotor de genes codificantes para diversas citocinas (por ejemplo, IFNγ, TNF-α, IL-1, IL-6 e IL10) capaces a su vez de incrementar la transcripción del provirus del VIH-1 integrado (Benkirane et al., 1994; Briant et al., 1998; Chirmule et al., 1995; Oyaizu et al., 1991; Popik et al., 1998; Popik and Pitha, 1996; Tamma et al., 1997). La unión de gp120 a

CD4, también puede activar Ras que promueve la replicación viral a través de la producción de TNF-α, y activación posterior de NF-κB (Tamma et al., 1997). Además, la activación de la ruta MEK/ERK depende del dominio citoplasmático de CD4, por lo que parece que la interacción de CD4 con $p56^{Lck}$ es necesaria para activar estas señales (Popik et al., 1998). A parte del factor de transcripción NF-κB, también se ha mostrado un efecto sinérgico en la unión de gp120 con CD4 y con CXCR4 o CCR5, en la activación de la replicación del VIH-1 a partir del factor de transcripción NF-AT (Cicala et al., 2006a; Cicala et al., 2002). Por tanto, la activación parcial de la célula T $CD4^+$ por unión de gp120 a CD4, independientemente de TcR, favorecería su disfuncionalidad, evitando la posterior activación y proliferación de estas células a través de señales que si dependen del complejo TcR/CD3 e inducción de IL-2 (Cefai et al., 1990; Chirmule et al., 1999; Hubert et al., 1995; Tamma et al., 1997).

Otra señal, dependiente de la unión entre gp120 y CD4, que favorece la entrada viral e infección consiste en una activación intracelular, de origen aún desconocido, que da lugar a un incremento de la tubulina acetilada (en Lys^{40}) total celular, localizada y acumulada en las zonas de contacto virus-célula (Valenzuela-Fernandez et al., 2005). Una de las proteínas citoplasmáticas que une y regula el estado de acetilación de tubulina es la histona desacetilasa 6 (HDAC6) (Matsuyama et al., 2002). Así, la sobreexpresión de HDAC6 provoca una disminución de la cantidad de tubulina acetilada total célular disminuyendo la susceptibilidad celular a la infección y replicación por el VIH-1 (Valenzuela-Fernandez et al., 2005), un efecto también generado por la expresión de la cola citoplamática de gp41 (Malinowsky et al., 2008) y por la expresión de un dominante activo de RhoA (RhoV14) (Wang et al., 2000). Además, se ha descrito recientemente la necesidad de la activación de RhoA y su efector, la quinasa dependiente de Rho (ROCK), de manera dependiente de Filamina A y de la unión de gp120 con CD4 y un correceptor, para la entrada viral (Jimenez-Baranda et al., 2007). ROCK activaría a LIMK1 (*"LIM Motif-containing Protein Kinase")* que a su vez inactiva a cofilina por fosforilación, permitiendo un estadio temprano de polimerización de actina. Esta polimerización también está asociada a un incremento de la unión constituida entre Filamina A con CD4 y CXCR4, agrupándose en la zona de contacto virus-célula, lo que favorece la entrada viral e infección (Jimenez-Baranda et al., 2007).

Asimismo, recientemente se ha descrito que el incremento en la F-actina debido a la unión de gp120 a CD4, inhibe la migración de células T $CD4^+$ en respuesta a SDF-1α, favoreciendo la diseminación viral por acumulación de células T $CD4^+$ en los nodos linfoides (Vasiliver-Shamis et al., 2008). La inhibición de la migración celular

parece que depende de la inhibición de la dinámica del córtex de F-actina por fosforilación e inactivación de cofilina, de manera dependiente de la activación de $p56^{Lck}$ por unión entre gp120 y CD4 (Trushin et al., 2010), en contraste al efecto inhibidor de la migración celular descrito debido a la reducción de la expresión superficial de CXCR4, por fosforilación e internalización, mediado por la unión entre gp120 con CD4 y posterior activación de $p56^{Lck}$ en células T $CD4^+$ (Su et al., 1999), o proteín quinasa C (PKC) en monocitos (que carecen de $p56^{Lck}$) (Wang et al., 1998). Aún así, el intermediario que actúa entre la activación de la tirosín quinasa $p56^{Lck}$ y la fosforilación de cofilina (en Ser-3), y de la cola citoplasmática de CXCR4 (en Ser/Thr), aún está por determinar.

Por último, recientemente se ha descrito que la unión de gp120 a CD4 activa las células Tregs $CD4^+/CD25^+$, por estimulación dependiente de $p56^{Lck}$ de la producción de adenosín monofosfato cíclico (AMPc) inducida por proteína Gαs. Este AMPc difunde posteriormente a través de uniones en hendidura desde la célula Treg hacia la célula T efectora donde inhibe la actividad de $p56^{Lck}$ por activación de la proteín quinasa A (PKA) a través del AMPc difundido. Este efecto provoca la incapacidad de la célula T efectora de responder a estímulos específicos contra el VIH-1 mediados por el complejo TcR/CD3 (Becker et al., 2009).

Con respecto a las señales "negativas" que impiden el correcto desarrollo del ciclo de vida del VIH-1, las más importantes son las que tienen lugar mediante la muerte celular programada (apoptosis) de la célula infectada. Por ejemplo, las citocinas TNF-α e IFN-γ, aún potenciando la replicación viral, tienen la capacidad de desencadenar un programa de apoptosis de las células T por sobreexpresión del antígeno Fas (CD95) (Oyaizu et al., 1994), aunque el papel de Fas en el proceso de apoptosis inducido por el VIH-1 parece controvertido (Ohnimus et al., 1997). Por otro lado, las caspasas implicadas en el proceso de muerte celular programada pueden ser activadas por la proteína de la envuelta del VIH-1 (Ohnimus et al., 1997). Además, la activación, por cepas de VIH-1 X4 y R5 trópicas, de las caspasas 3 y 6 en linfocitos es dependiente de la unión de la envuelta viral a CD4 (Cicala et al., 2000). La activación de estas caspasas provoca el corte de uno de sus sustratos, la quinasa de las adhesiones focales (FAK, "*focal adhesion kinase*"), que también es activada por la interacción con el VIH-1, junto a otro miembro de la familia FAK, la tirosín quinasa 2 rica en Pro (Pyk2, "*proline-rich tyrosine kinase 2*") (Cicala et al., 1999). En este sentido, parece que mientras Pyk2 induce apoptosis, FAK activa fosforilada presenta actividad protectora de apoptosis y su corte por caspasa-3 parece estar asociado con los

estadios iniciales de la muerte celular programada (Levkau et al., 1998; Xiong and Parsons, 1997).

Diversos estudios han determinado que la infección productiva por el VIH-1 desencadena un proceso de apoptosis celular que parece ser independiente de la región citoplasmática de CD4 (Guillerm et al., 1998) y, por tanto, independiente de la unión entre $p56^{Lck}$ y CD4 (Moutouh et al., 1998), aunque, sin embargo, la unión entre ambas puede acelerar la transmisión de una señal de muerte celular, al parecer en un estadio posterior a la expresión génica del VIH-1 post-entrada (Corbeil et al., 1996; Guillerm et al., 1998).

Por otro lado, se ha descrito *in vitro* la activación de un programa de muerte de células T $CD4^+$ "*bystander*", que depende de la unión superficial entre CD4 y gp120, y la posterior inducción de activación inmune de esas células a través del complejo TcR/CD3, por patógenos que coinfectan con el VIH-1, por superantígenos expresados por los patógenos o por la propia respuesta inmune inducida contra el VIH-1 (Banda et al., 1992; Groux et al., 1992). Además, se ha implicado a la fosfatasa CD45 en la apoptosis de células T $CD4^+$ inducida por gp120 y en presencia de señal estimuladora dependiente del TcR como se ha descrito anteriormente (por un antígeno activador u otro agente infeccioso), mediante la sobreexpresión y activación de la ruta FasL/Fas e inhibición de las rutas de supervivencia dependientes de la activación de PI3K/Akt (Anand and Ganju, 2006).

En la mayoría de los casos, la unión de la proteína de la envuelta viral gp120 a CD4, desencadena una señalización celular que depende de la activación de $p56^{Lck}$, una tirosín quinasa ausente en células del linaje mieloide, una población de células diana de la infección por el VIH-1. La ausencia de $p56^{Lck}$, protegería a los monocitos/macrófagos de la inducción de mecanismos de apoptosis, lo que explicaría, la mayor persistencia de los monocitos/macrófagos, en comparación a las células T $CD4^+$, durante el curso de la infección por el VIH-1 y progresión hacia fase SIDA, representando importantes reservorios virales (Crowe and Sonza, 2000). Asimismo, la expresión de $p56^{Lck}$, en células T $CD4^+$, evita la endocitosis constitutiva de CD4, que ocurriría en ausencia de ésta (Pelchen-Matthews et al., 1995). El bloqueo de esta endocitosis constitutiva, alarga la presencia de CD4 en la superficie celular favoreciendo los contactos con la envuelta del virus aumentando la eficiencia de la infección viral. Por tanto, en el caso de monocitos/macrófagos, la probabilidad de

contactos entre CD4 con la envuelta es menor, por lo que se reduciría la eficiencia de la infección por el VIH-1.

1.4.3. Señalización a través de receptores de quimiocinas CCR5/CXCR4.

El descubrimiento del requerimiento necesario de los receptores de quimiocinas, CCR5 y CXCR4, como correceptores para la infección por el VIH-1, permitió estudiar la posible señalización celular inducida por la unión del VIH-1 a estos receptores, y la importancia o no de esta señalización durante el proceso de fusión, infección y replicación viral. Estos estudios determinaron que la unión de gp120 a los correceptores activa rutas de señalización similares, aunque no idénticas, a las generadas por la unión de sus ligandos naturales, RANTES y SDF-1α respectivamente. Las señales activadas por la interacción de la proteína de la envuelta viral con los correceptores CCR5 y CXCR4 comprenden la liberación de Ca^{2+} citoplasmático (Alfano et al., 1999; Arthos et al., 2000; Balabanian et al., 2004; Harmon and Ratner, 2008; Lee et al., 2003; Liu et al., 2000; Melar et al., 2007), la activación de canales iónicos (Liu et al., 2000), la activación de la tirosín quinasa Pyk2 (Cicala et al., 1999; Davis et al., 1997; Del Corno et al., 2001; Harmon and Ratner, 2008; Lee et al., 2003; Misse et al., 1999), la fosforilación y activación de FAK (Cicala et al., 1999; Kinter et al., 2003), la fosforilación de ZAP70 (Cicala et al., 1999; Kinter et al., 2003), la activación de PKC (Harmon and Ratner, 2008), la activación de PI3K/Akt (Balabanian et al., 2004; Francois and Klotman, 2003; Lee et al., 2003), la disminución del AMPc (Guntermann et al., 1999), la activación de la ruta MAPK ERK1/2 (Balabanian et al., 2004; Kinet et al., 2002; Popik et al., 1998; Popik and Pitha, 1998), la activación de la ruta MAPK p38 (Del Corno et al., 2001; Lee et al., 2003; Misse et al., 2001; Popik and Pitha, 1998), la activación de la ruta MAPK JNK (Del Corno et al., 2001; Lee et al., 2003; Misse et al., 2001; Popik and Pitha, 1998), la secreción de metaloproteasas (Misse et al., 2001), quimiotaxis celular (Iyengar et al., 1999; Lin et al., 2000; Misse et al., 1999), inducción de la secreción de β-quimiocinas (Del Corno et al., 2001; Fantuzzi et al., 2001; Lee et al., 2003) y la remodelación del citoesqueleto de actina (Balabanian et al., 2004; Harmon and Ratner, 2008; Pontow et al., 2004; Yoder et al., 2008).

En cuanto a la señal de liberación de calcio y quimiotaxis detectada en células T $CD4^+$ activadas, células dendríticas inmaduras y macrófagos, ésta es más intensa con envueltas R5 trópicas que con envueltas X4 trópicas (Lee et al., 2003; Lin et al., 2000; Liu et al., 2000), posiblemente por una menor expresión de CXCR4. Algunas de

estas señales, han mostrado ser activadas a través de proteína Gαi sensible a PTX ("*Pertussis toxin*") en líneas celulares T $CD4^+$ transformadas (Davis et al., 1997), y también ser insensibles a PTX en células T $CD4^+$ primarias y macrófagos y, por tanto, activadas a través de una subunidad distinta de la proteína G (Cicala et al., 1999; Del Corno et al., 2001; Lee et al., 2003), o dependientes de la entrada de Ca^{2+} desde el medio extracelular a través de canales CRAC ("*Ca^{2+} release-activated Ca^{2+}*") en macrófagos (Del Corno et al., 2001).

Por último, cabe destacar que la mayoría de los eventos de señalización celular inducidos por la proteína gp120 tienen lugar independientemente del tropismo pero con distinta intensidad, lo que podría indicar un patrón diferencial en el resultado final de la señalización, por ejemplo, sobre la inducción de diferentes factores de transcripción (Cicala et al., 2006b). Estas diferencias en la intensidad de la activación de señales intracelulares por las envueltas X4 y R5 trópicas del VIH-1, por ejemplo, por diferencias en la amplitud, frecuencia y longitud de la señal de elevación de Ca^{2+} intracelular, indicaría diferencias en la capacidad de activar toda una serie de moléculas dentro de una determinada ruta de señalización. En este sentido, se ha determinado que aproximadamente 10 pM de gp120 recombinante soluble es suficiente para iniciar la señalización (por liberación de Ca^{2+} citoplasmático) a través de los correceptores CXCR4 y CCR5 en células T $CD4^+$ primarias no estimuladas, una cantidad de gp120 presente en el suero de pacientes infectados por el VIH-1. Asimismo, esta señalización puede ser iniciada por una cantidad de viriones que oscila entre dos y cuatro (Melar et al., 2007).

Aunque parece claro que la envuelta del VIH-1 estimula la activación de rutas de señalización en la célula diana, no existe un claro consenso sobre si esta señalización es necesaria para la infección por el VIH-1.

Por un lado, diversos estudios han sugerido que la señalización mediada por el correceptor es dispensable para la entrada del VIH-1 en la célula diana. Esta conclusión deriva de estudios realizados en líneas celulares transformadas, bloqueando la señalización a través de proteína Gαi con PTX, estudios utilizando deleciones de la cola C-terminal citoplasmática de los correceptores, infecciones en condiciones de desensibilización del correceptor, o mediante la utilización de mutantes en el dominio DRY (Arp-Arg-Tyr) de unión a proteína Gαi y Gαq, presente en el ICL2 del receptor y que es importante para la activación de la señalización celular dependiente de ligando. Se observó que mutantes del dominio DRY (Arp^{125}-Arg-Tyr^{127}) y la deleción de la cola C-terminal citoplasmática de CCR5, que impiden la

movilización de Ca^{2+} y la desensibilización e internalización del receptor, respectivamente, no alteran la capacidad de CCR5 de actuar como correceptor para la infección por el VIH-1 (Alkhatib et al., 1997a; Gosling et al., 1997). En este sentido, otro estudio realizado con un mutante $Tyr^{297}Ala$ del septimo dominio transmembrana de CCR5, incapaz de movilizar Ca^{2+} y de permitir la internalización del receptor, mostró que la señalización a través de CCR5, su fosforilación, desensibilización e internalización, son dispensables para la entrada del VIH-1 (Aramori et al., 1997). Por otro lado, otros mutantes de CCR5, $Asp^{76}Asn$ (en el segundo dominio transmembrana), $Arg^{126}Asn$ y $Asp^{125}Asn/Arg^{126}Asn$ (ambos del dominio DRY presente en el ICL2 de CCR5), incapaces de movilizar Ca^{2+} en respuesta a agonistas, favorecen la entrada viral de manera tan eficiente como el correceptor CCR5 funcional (Farzan et al., 1997). Por último, un receptor quimérico de CCR5 que contiene la mitad N-terminal de CCR2b (que sólo permite la entrada de cepas virales dual trópicas, y no de cepas virales R5 trópicas de VIH-1) y la mitad C-terminal de CCR5 (desde el ECL2), es capaz de señalizar por unión de los ligandos MIP-1α, MIP-1β, RANTES y MCP-1, pero no es capaz de permitir la infección por cepas virales R5 trópicas del VIH-1. Estos resultados indicarían que la actividad correceptora para el VIH-1 puede disociarse de la respuesta del receptor a su ligando natural (Atchison et al., 1996).

En cuanto a CXCR4, se ha visto que los mutantes $Asp^{187}Ala$ (presente en el ECL2) y Δi3Ala (que carece de los cuatro residuos Ser^{227}-His-Ser-Lys^{230} del ICL3, necesarios para la activación de eventos de señalización intracelular mediados por β-arrestina) que aún siendo defectivos en la señalización mediada por SDF-1α (Brelot et al., 2000), siguen permitiendo la entrada de cepas virales X4 trópicas del VIH-1 (Brelot et al., 2000; Tokunaga et al., 2001). Además, mutantes de CXCR4 en el dominio DRY (Asn^{133}-Ala-Ala^{135}) y mutantes de CXCR4 que carecen de la cola C-terminal citoplasmática (desde el residuo Ser^{319}, además de contener mutaciones en los residuos Ser^{312} y Thr^{318}), que evitan la señalización a través de proteína G e impiden la endocitosis del receptor, también permiten la fusión dependiente del VIH-1 (Lu et al., 1997). Otro trabajo mostró que una construcción de CXCR4 sin el dominio citoplasmático (CXCR4 ΔCyt, que no permite su internalización inducida por SDF-1α), no se encuentra afectado en su capacidad de actuar como correceptor para la entrada del VIH-1, sin embargo, afecta a la supresión de la infectividad que tendría lugar mediante la internalización del receptor inducida por ligando (Amara et al., 1997).

Estas conclusiones fueron obtenidas en líneas celulares transformadas donde la necesidad de esta señalización, puede ser diferente a los requerimientos de dicha

señalización durante la infección de células primarias. Por ello, se determinó en células primarias (PBMC, "*Peripheral blood mononuclear cells*", células mononucleares de sangre periférica) naïve, activadas y macrófagos, aisladas de individuos homocigóticos CCR5Δ32, la no implicación de la señalización a través de proteína Gαi o Gαq de CCR5 en la infección y replicación del VIH-1 (Amara et al., 2003). Estos resultados fueron obtenidos mediante la expresión, en células primarias y macrófagos, de mutantes de CCR5 en el dominio DRY ($Arg^{126}Asn$ y $Asp^{125}Asn/Arg^{126}Asn$) deficientes en cuanto a la señalización a través de proteína G, con respecto a la proteína salvaje. Se mostró que ninguna de las construcciones afectó a la infección por cepas virales R5 trópicas, por lo que la señalización y la infección parecen estar disociadas en el contexto del VIH-1 (Amara et al., 2003). Sin embargo, en otro trabajo se observó que la transfección del mismo mutante en el dominio DRY de CCR5 ($Arg^{126}Asn$), en PBMC no activados ($CD25^-/CD69^-$) de distintos donantes, bloqueó la infección por cepas virales R5 trópicas de VIH-1, sin afectar a la infección por cepas virales X4 trópicas (Lin et al., 2005).

Por otro lado, aunque los trabajos descritos anteriormente parecen indicar que la señalización de los correceptores por unión a la envuelta del VIH-1, es una función innecesaria para la entrada y replicación viral, también hay estudios contrarios que proponen que la activación de estas señales son necesarias para una infección eficiente por el VIH-1, o que al menos podrían contribuir a la patogénesis del VIH-1 afectando a eventos post-entrada como la replicación viral. En primer lugar, como hemos visto anteriormente, parece que la señalización a través de proteína Gαi (sensible a PTX) asociada al dominio DRY del bucle ICL2 de CCR5 es necesaria para una replicación eficiente del VIH-1 en PBMC no estimuladas (Lin et al., 2005), y estimuladas con PHA/IL-2 (Guntermann et al., 1999). Sin embargo, el tratamiento de PBMC (activados con PHA/IL-2) con el oligomero B de PTX (que modula la señalización independiente de proteína Gαi), también bloquea la entrada de cepas virales R5 trópicas evitando la transcripción reversa del ARN viral (Alfano et al., 1999), e inhibiendo la replicación de cepas virales X4 trópicas en varios estadios posteriores a la transcripción reversa (Alfano et al., 2000). Por otra parte, parece que sólo aquellas cepas virales R5 trópicas que activan señales a través de CCR5, con un cierto umbral (medido por incremento de Ca^{2+} citoplasmático), en macrófagos, son capaces de completar la transcripción reversa y replicar de manera eficiente (Arthos et al., 2000). Incluso, la señalización a través de CCR5 por sus ligandos naturales, puede favorecer, en macrófagos y en células T, la replicación de cepas virales X4 trópicas, mientras que bloquean la replicación de cepas R5 trópicas de VIH-1 (Arthos et al., 2000; Kinter et

al., 1998; Popik and Pitha, 2000). Este bloqueo de la replicación de cepas R5 trópicas de VIH-1, por la señalización derivada de los ligandos naturales de CCR5, parece revertirse con el tratamiento con PTX (Kinter et al., 1998), mientras que también se ha descrito lo contrario (Cocchi et al., 1996). A parte de las rutas de señalización dependientes de proteína Gαi (sensibles a PTX), también se ha descrito la activación, por parte del VIH-1, de rutas de activación insensibles a PTX dependientes de Gαq, Gαs e independientes de proteína G (Del Corno et al., 2001; Kanmogne et al., 2007; Lee et al., 2003; Masci et al., 2003). En este sentido, recientemente se ha descrito la participación de la señalización dependiente de la subunidad Gαq asociada a CCR5 en el proceso de entrada viral, descartando la participación de la ruta de señalización dependiente de proteína Gαi y proteína Gαs (Harmon and Ratner, 2008).

Igualmente, estudios realizados en células primarias T $CD4^+$ no estimuladas indican que la unión entre la proteína viral gp120 y CXCR4 es necesaria para la activación de diversas rutas de supervivencia celular, dependientes de PI3K/Akt y Erk-1/2 MAPK, requeridas para el correcto desarrollo del ciclo de vida del virus (Balabanian et al., 2004). Del mismo modo, la infección por cepas X4 trópicas del VIH-1 en células T no proliferativas puede ser bloqueada por el tratamiento con PTX, en estadios posteriores a la fusión entre la membrana celular y viral (Yoder et al., 2008). Esta inhibición sólo ocurre en células T no proliferativas, porque como se ha descrito anteriormente, el tratamiento con PTX en células T primarias activadas o transformadas no inhibe la infección y/o replicación del VIH-1 (Alkhatib et al., 1997a; Cocchi et al., 1996; Harmon and Ratner, 2008). Aún así, la inhibición de la infección y replicación por PTX también ha sido descrita para la infección de virus R5 trópicos en células T primarias no estimulas (Lin et al., 2005), y estimuladas (Guntermann et al., 1999), por lo que la relación entre la señalización a través de proteína Gαi con el estado de activación celular necesita más investigación. Además, la regulación de la internalización y del reciclaje de los correceptores virales puede, a su vez, condicionar la propagación viral, al afectar a la actividad anti-viral ejercida por los ligandos naturales de estos correceptores. En este sentido, la actividad anti-viral de SDF-1α (CXCL12) frente a cepas X4 trópicas del virus VIH-1 depende de la correcta ocupación e internalización de CXCR4 (Amara et al., 1997), esta última, mediada por la molécula motora miosina IIA no muscular, y de forma dependiente de SDF-1α (Rey et al., 2007).

Por último, cabe resaltar la asociación constitutiva entre CD4 y CCR5 en la membrana plasmática, incluso en ausencia de la proteína viral gp120, importante para una rápida infección de las células diana por cepas virales R5 trópicas (Xiao et al.,

1999), de manera dependiente de la activación de gp120 por CD4 previa a la unión al correceptor CCR5 (Trkola et al., 1996; Wu et al., 1996). Por otro lado, la asociación entre CD4 y CXCR4 es muy baja, incrementándose significativamente de manera inducible por la unión entre gp120 y CD4 (Lapham et al., 1999; Ugolini et al., 1997; Wang et al., 2004; Xiao et al., 1999), un proceso directamente relacionado con una mayor eficiencia de la fusión e infección viral (Lapham et al., 1996; Lee et al., 2000; Singer et al., 2001). Estos datos indicarían diferencias, entre ambos tropismos, en relación al patrón de señalización inicial y al curso temporal de la entrada e infección de la célula diana. De hecho, como se ha indicado anteriormente, la señalización ejercida por envueltas R5 y X4 trópicas del VIH-1 sobre el estado metabólico y transcripcional de PBMC en reposo es diferente y parece ser independiente de la unión del VIH-1 a CD4 (Cicala et al., 2006b).

Las diferencias en las conclusiones obtenidas por los diferentes grupos de investigación dependen, en gran medida, de la diversidad de líneas celulares utilizadas, del estado de activación y diferenciación de estas líneas celulares, y la metodología empleada. Pero sin lugar a dudas, en su conjunto, son clara prueba de la complejidad de la señalización celular inducida por el virus VIH-1 en las primeras etapas del ciclo de vida viral, y de su importancia para asegurar la fusión y entrada viral de manera eficaz, necesario para el establecimiento de los reservorios de latencia viral y para la diseminación sistémica del virus, siempre evitando las respuestas anti-virales de los diferentes componentes del sistema inmune.

1.4.4. Remodelación del citoesqueleto de actina en la invasión por microorganismos.

La actina es una de las proteínas más abundantes en la mayoría de tipos celulares. Se trata de una proteína de 43KDa globular con una hendidura central ocupada por un nucleótido, adenosín trifosfato (ATP) o adenosín difosfato (ADP). La actina puede encontrarse en dos estados, monomérica (G-actina) o formando filamentos (F-actina). Los filamentos de actina son fibras de 7-9 nm de diámetro formados a partir de la unión no covalente entre subunidades de G-actina. La transición de la actina de un estado a otro le aporta una dinámica que le permite participar de manera precisa en una gran cantidad de procesos celulares, determinando la formación de estructuras celulares como lamelas, filopodios, fibras de estrés y adhesiones focales (Bailly and Condeelis, 2002). La actina es esencial para la supervivencia de la mayoría de las células por varios motivos: los filamentos de actina

ofrecen un soporte mecánico para la estructuración intracelular, proporciona pistas para el movimiento de estructuras intracelulares y representa la principal fuerza para el movimiento celular.

Los filamentos de actina son estructuras polarizadas, es decir, presentan dos extremos diferenciados, el positivo ("(+)") y el negativo ("(-)"). El extremo (+) es el más dinámico y se encuentra favorecido para la adición rápida de nuevos monómeros de actina que van a encontrarse unidos al nucleótido ATP, y el extremo (-) es el extremo del que se van a separar las subunidades de actina unidos al nucleótido ADP (con un intermediario ADP + Pi), que se incorporan luego en el extremo (+) una vez recuperen el ATP en el citoplasma celular. Este fenómeno de continua renovación de los filamentos de actina por entrada de monómeros en el extremo (+) y salida desde el extremo (-) se conoce como "*actin threadmilling*" de filamentos de actina (Pollard and Borisy, 2003).

La organización y polimerización de la actina se encuentran reguladas espacial y temporalmente de manera precisa en respuesta a una amplia variedad de estímulos externos, como citocinas, factores de crecimiento y hormonas. Estos estímulos inician en la célula una serie de eventos de señalización cuyo resultado consistirá en la remodelación dinámica del citoesqueleto de actina, una característica fundamental para la vida celular. Uno los aspectos más interesantes de la dinámica de actina consiste en la regulación del ensamblaje y desensamblaje de los filamentos de actina, mediante el control del balance homeostático entre las dos formas de actina en respuesta a estos estímulos (Ridley and Hall, 1992; Ridley et al., 1992). Esta regulación tiene lugar mediante la estimulación o la inhibición de la actividad de las proteínas accesorias de unión a actina (ABP, "*actin binding protein*").

Las ABP que van a regular todos estos procesos a nivel de la superficie celular se van a diferenciar en: Proteínas capaces de iniciar la polimerización y elongación de filamentos de actina *(como RhoGTPasas, el complejo Arp2/3, la familia de proteínas WASP/WAVE, profilina y las forminas)*; Proteínas de recubrimiento y corte de filamentos de actina *(como las encargadas de unirse a los extremos de crecimiento positivo evitando la elongación de estos filamentos como gelsolina, CapG, Eps8 y twinfilina; las proteínas encargadas de cortar los filamentos de actina como gelsolina y ADF/cofilina; las encargadas de disociar monómeros de actina de los extremos (-) de los filamentos como ADF/cofilina; y las encargadas de evitar el intercambio ADP-ATP en los monómeros de actina liberados en el citoplasma como ADF/cofilina)*; Proteínas encargadas de la formación de estructuras paralelas o entrelazadas de filamentos de

actina *(mediante la formación de uniones cruzadas como filamina y α-actinina, o paralelas entre filamentos de actina como fimbrina, valina y fascina, o conectando estos filamentos de actina a la membrana plasmática celular como las ERM*; y proteínas encargadas de unirse y secuestrar monómeros de actina *(como profilina y timosina β-4)* (Pollard and Borisy, 2003).

Para el VIH-1, igual que para otros muchos virus ("*murine leukemia virus*", "*vesicular stomatitis virus*", "*human papilloma virus*", "*vaccinia virus*", "*coxsackie virus*", "*adenovirus*", "*herpesvirus*", "*Ebola virus*", "*poliovirus*" y "*human respiratory syncytial virus*") (revisado en (Taylor et al., 2011)) y microorganismos patógenos (como las bacterias *Listeria*, *Salmonella*, *Shigella y Rickettsia*, y los parásitos *Plasmodium* y *Toxoplasma*) (Bamburg, 2011; Baum et al., 2008; Frischknecht and Way, 2001), el citoesqueleto de actina cortical representa una barrera física previa a la entrada e infección de la célula diana. Por tanto, la entrada de estos patógenos, depende de su capacidad de secuestrar, en su favor, la maquinaria celular de remodelación del citoesqueleto de actina, que le permita atravesar dicha barrera. El VIH-1 parece cumplir este propósito a través de la inducción de complejos de señalización de manera superficial e intracelular en la célula hospedadora que dependen de la interacción entre la proteína de la envuelta viral gp120 con el receptor CD4 y los correceptores CXCR4 o CCR5. Además, el mecanismo de fusión entre membranas biológicas no ocurre de manera espontánea, debido a las fuerzas electroestáticas contrapuestas entre las dos bicapas lipídicas. En este sentido, el citoesqueleto de actina cortical puede actuar de dos formas no excluyentes y cooperativas: por un lado, puede actuar concentrando espacialmente complejos activos de fusión, y por otro lado, puede actuar aplicando la fuerza o la tensión de membrana necesaria para que el proceso de fusión entre las membranas viral y celular tenga lugar de forma eficaz y/o con mayor probabilidad.

La primera evidencia de la participación del citoesqueleto de actina en la entrada del VIH-1 demostró la inducción de una región polarizada, en la célula T expuesta a la proteína viral gp120, enriquecida en actina y en los receptores virales CD4 y CXCR4 (Iyengar et al., 1998). Esta intensa aglomeración de receptores/correceptores en una región de la célula promueve el primer estadio de infección, que implica múltiples interacciones cooperativas de unión entre el virus y la célula diana (Doms, 2000; Kuhmann et al., 2000; Moore et al., 1991), y que en último término favorecen la formación del complejo proceso de fusión e infección del VIH-1, que ocurre en la membrana plasmática (Marsh and Helenius, 2006; Sougrat et al., 2007). Así, el bloqueo de esta polarización de la F-actina en respuesta a la envuelta

del VIH-1 inhibe la entrada e infección por el VIH-1 (Iyengar et al., 1998). De hecho, en un sistema de transmisión viral célula a célula de VIH-1, se observó que el reclutamiento de CD4 y CXCR4 dependiente de gp120 a la zona de contacto virus-célula es además dependiente de la actina (Jolly et al., 2004). Igualmente, fármacos que afectan a la dinámica de actina (como latrunculina, "*jasplakinolide"* y citocalasina) parecen inhibir la fusión mediada por la envuelta viral del VIH-1 (Eitzen, 2003; Frey et al., 1995; Gallo et al., 2001; Iyengar et al., 1998; Pontow et al., 2004). Lo que no está claro es si estos fármacos afectan a la actividad de la envuelta del VIH-1 (Campbell et al., 2004; Yonezawa et al., 2005), o a la estabilidad de los microtúbulos o de los filamentos intermedios, necesarios para el correcto funcionamiento del ciclo celular y, por tanto, del ciclo de vida viral intracelular. Por último, aunque la interacción entre CD4 con actina (Kinch et al., 1993) y de CXCR4 con actina (Rey et al., 2002) ya ha sido descrita, y existe una clara correlación entre el reclutamiento y polarización de grupos de receptores/correceptores, mediado por el VIH-1 y por la F-actina cortical, con una eficiente fusión viral e infección (Iyengar et al., 1998; Jimenez-Baranda et al., 2007; Jolly et al., 2004; Manes et al., 2000; Ugolini et al., 1997), poco se sabe acerca de los mecanismos moleculares que relacionan el enriquecimiento e interacción entre CD4 y los correceptores con aquellos mecanismos que regulan la remodelación y/o polarización de la F-actina en las células expuestas a la envuelta del VIH-1. Esta polarización y agrupamiento de complejos receptor/correceptor parece tener dos funciones, por un lado alcanzar la densidad suficiente de heterodímeros CD4/correceptor que permitan la unión y activación de una cantidad suficiente de trímeros del complejo de envuelta viral, que permitan el correcto desarrollo del proceso de fusión, y por otro lado puede permitir la activación de señales celulares importantes para la infección y/o replicación viral.

De esta forma, la activación por el VIH-1 de señales en la célula diana, podría resultar en la formación de complejos de señalización con potencial para reorganizar las estructuras asociadas al citoesqueleto de actina cortical. Así, se ha observado que la proteína de envuelta gp120 del VIH-1 puede inducir un proceso de polimerización de actina en células primarias T $CD4^+$ no estimuladas, dando lugar a la formación de "*ruffles*" de membrana (Balabanian et al., 2004). Este fenómeno transitorio de polimerización rápida de filamentos de actina (Balabanian et al., 2004; Yoder et al., 2008) puede ser importante para el agrupamiento de altas concentraciones de los receptores CD4/CXCR4 o CD4/CCR5, que van a facilitar la infección viral (Iyengar et al., 1998; Jimenez-Baranda et al., 2007; Liu et al., 2009), la síntesis eficiente del ADN viral post-entrada (Bukrinskaya et al., 1998; Yoder et al., 2008) y la migración

intracelular hacia el núcleo de manera dependiente de actina (McDonald et al., 2002). Además, la actina también interacciona con otros componentes del VIH-1 como la NC, la RT y la IN (Hottiger et al., 1995; Turlure et al., 2004; Wilk et al., 1999), por lo que, el citoesqueleto de actina participa en varios estadios del ciclo de vida del VIH-1.

En cuanto a las ABP activadas por el VIH-1 que favorecen la entrada viral, se ha descrito que la unión de envueltas R5 trópicas de VIH-1 a CCR5 media la activación de la pequeña GTPasa Rac-1 (Rac-GTP) (Pontow et al., 2004), de manera dependiente de Trio y Tiam-1 (dos factores de intercambio de nucleótido guanina que activan esta GTPasa) (Pontow et al., 2007). Así, un dominante negativo de Rac-1 (RacN17), pero no de RhoA (RhoN19) ni de Cdc42 (Cdc42N17), inhibe la fusión de membranas dependiente de células y virus, independientemente del tropismo de la envuelta viral (Pontow et al., 2004). Esta inhibición fue superada por la sobreexpresión de un mutante de Rac-1 constitutivamente activo (RacV12), por lo que la activación de Rac-1 parece ser esencial en los procesos iniciales de infección por el VIH-1 (Pontow et al., 2007). Sin embargo, no se observó ningún efecto inhibidor en presencia de inhibidores contra otros efectores de Rac-1 como NADPH oxidasa, MEK, PI3K, la quinasa de la cadena ligera de miosina (MLCK, "*Myosin Light Chain Kinase*"), o dominantes negativos de las quinasas Pak-2 ("*p21 activated kinase-2")* y PI3K (Pontow et al., 2007). Aún así, parece que la fosforilación de la cadena ligera de miosina por MLCK parece ser necesaria, en parte, para el agrupamiento de complejos CD4/correceptor durante la transmisión viral célula a célula (Jolly et al., 2004). Mediante la utilización de pequeñas moléculas inhibidoras, se determinó que la activación de Rac-1, por envueltas virales X4 y R5 trópicas, depende de la activación de PLCβ, liberación de Ca^{2+} de los reservorios intracelulares, activación de PKCα/β, activación de Pyk2, de Ras y finalmente de Rac-1 por Tiam-1 (Harmon and Ratner, 2008). Esta activación final de Rac-1 en la célula diana podría estar implicada en la remodelación del citoesqueleto de actina necesario para una eficiente fusión, entrada e infección por el VIH-1 (Harmon and Ratner, 2008; Pontow et al., 2007; Pontow et al., 2004). De manera interesante, la liberación de Ca^{2+} citoplasmático y la activación de Ras pueden tener también funciones en otros procesos celulares, de manera independiente a la activación de Rac-1 (Harmon and Ratner, 2008). Por otro lado, estos inhibidores, a excepción del inhibidor de PLCβ, parecen ser específicos para la entrada de partículas virales pseudotipadas con la envuelta del VIH-1, sin observar ningún efecto sobre la entrada endocítica de partículas virales pseudotipadas con las envueltas VSV-G o A-MLV ("*amphotropic murine leucemia virus*") (Harmon and Ratner, 2008). Por último, recientemente se ha determinado que la función remodeladora de

actina dependiente de Rac-1 se consigue a través de la activación del complejo nucleador de actina Arp2/3, por la quinasa Abl y el complejo Wave2 ("*WASP family verprolin-homologous protein 2*") a través de IRSp53 (*"insulin receptor substrate (IRS) p53*"), un proteína adaptadora que une Rac-1 y Wave2 (Harmon et al., 2010) a la membrana plasmática en regiones ricas en PIP_2 y PIP_3 (Kurisu and Takenawa, 2010). Así, estos componentes favorecen la remodelación de actina necesaria para la formación y alargamiento del poro de fusión, y posterior entrada del VIH-1. A pesar de estos resultados, ninguno de los componentes de esta ruta de activación ha sido visualizado en el contexto del agrupamiento de los receptores/correceptores con F-actina en las zonas de entrada viral, inducidos por la proteína viral gp120 del VIH-1.

Por otro lado, se ha implicado a la proteína de unión a actina filamina A en la entrada del VIH-1. Esta proteína tiene la propiedad de unirse a las colas citoplasmáticas de los receptores de VIH-1 (CD4, CXCR4 y CCR5) y a su vez al citoesqueleto de actina, permitiendo su agrupamiento mediado por la proteína de la envuelta viral gp120 (Jimenez-Baranda et al., 2007). Se observó que la relocalización de complejos receptor/correceptor, F-actina y filamina A depende de la interacción entre gp120 con CD4 y CXCR4, y de éstos con filamina A. Esta estructura estable permitiría subsecuentes cambios conformacionales en la proteína viral gp120 que favorecerían la posterior fusión entre las membranas celular y viral, dependiente de la activación de la proteína de fusión gp41. Además, observaron que la utilización del mutante RhoN19, pero no de RacN17, bloqueaba la fusión célula-célula mediada por envueltas X4 trópicas del VIH-1 (del Real et al., 2004; Jimenez-Baranda et al., 2007). Igualmente, se observó la activación de RhoA (RhoGTP) por gp120, en linfocitos T primarios activados, de manera dependiente de filamina A (Jimenez-Baranda et al., 2007) y en linfocitos T transformados (del Real et al., 2004). Datos contradictorios con respecto a los obtenidos por otros grupos de investigación donde RhoN19 no afecta (Pontow et al., 2004) y la expresión de una construcción dominante activa de RhoA bloquea la replicación del VIH-1 (Wang et al., 2000). Asimismo, parece que RhoA activa la quinasa ROCK que a su vez actúa sobre LIMK1, que en último término inactiva por fosforilación a cofilina (Arber et al., 1998; Yang et al., 1998), una proteína relacionada directamente con el recambio de filamentos de actina por corte y despolimerización (Lappalainen and Drubin, 1997), permitiendo el estadio inicial de polimerización de actina mediado por la proteína viral gp120 (Jimenez-Baranda et al., 2007), y necesario para la entrada e infección viral eficiente del VIH-1.

En contraposición con los resultados anteriores obtenidos mediante la utilización de líneas celulares transformadas o primarias activadas, la unión de gp120

a CXCR4 en células T no proliferativas genera una señal necesaria para la activación de cofilina, requerida para que el virus pueda atravesar la barrera de actina cortical post-fusión, permitir la entrada de la nucleocápside en la célula diana y la posterior localización nuclear del ADN viral (Yoder et al., 2008). Además, el citoesqueleto de actina cortical es importante para dirigir el movimiento de la NC desde la superficie celular hacia la red microtubular, donde tiene lugar la formación del complejo de retrotranscripción y posterior migración del ADN viral hacia el núcleo celular (Bukrinskaya et al., 1998; McDonald et al., 2002; Naghavi et al., 2007). Esta activación de cofilina parece ser importante para la generación de una infección latente de virus X4 trópicos en células T no activadas y no proliferativas (Yu et al., 2009). Al mismo tiempo, se describió la implicación de las quimiocinas CCL19 y CCL21, en la permisividad de células T $CD4^+$ no proliferativas de memoria a la infección por virus X4 y R5 trópicos del VIH-1, dando lugar a la generación de un reservorio viral latente (Saleh et al., 2007). Así, la interacción de CCL19/CCL21 con su receptor CCR7 también provoca cambios en la dinámica de actina por activación de cofilina (Cameron et al., 2010). Otras quimiocinas que favorecen la migración nuclear e integración del ADN viral, sin afectar a la replicación viral productiva, son CXCL19, CXCL20 y CCL20. Estos resultados indican que la generación del reservorio viral latente no sólo puede depender de una interacción de gp120 con CXCR4 sino también de la interacción de diversas quimiocinas con los receptores CCR7, CCR6 y CXCR3 (Cameron et al., 2010). Aún así, queda por determinar si existe un mecanismo similar en la generación de latencia en células T $CD4^+$ no proliferativas, como se ha descrito ejercida por virus R5 trópicos a través del correceptor CCR5 (Chun et al., 2005; Chun et al., 2008; Pierson et al., 2000).

Del mismo modo, se ha descrito que la proteína viral Nef incorporada en los viriones nacientes, puede favorecer la remodelación del citoesqueleto de actina cortical en la célula diana, durante la etapa temprana de infección, incrementando la eficiencia de la infección por el VIH-1 (Campbell et al., 2004). Nef es capaz de interaccionar con el factor RhoGEF Vav y con miembros de la familia de las serín/treonín quinasas Pak induciendo cambios en el citoesqueleto de actina (Fackler et al., 1999; Manninen et al., 1998; Renkema et al., 2001). Curiosamente, recientemente se ha descrito que Nef provoca la hiperfosforilación de cofilina de manera dependiente de Pak-2, inhibiendo la capacidad de las células a migrar en respuesta a gradientes quimiotácticos (Stolp et al., 2009). Asimismo, la inhibición de la quimiotaxis celular por fosforilación de cofilina puede tener lugar a partir de la unión de gp120 a CD4, de manera dependiente de $p56^{Lck}$ (Trushin et al., 2010). Esta inhibición

de la respuesta quimiotáctica, también ha sido atribuida a una internalización por fosforilación de CXCR4 dependiente de la unión entre gp120 y CD4 (Badr et al., 2005; Su et al., 1999; Wang et al., 1998). Por otro lado, la presencia de Nef parece ser necesaria para la síntesis del ADN viral (Aiken and Trono, 1995; Schwartz et al., 1995), un proceso que parece ser dependiente del citoesqueleto de actina (Campbell et al., 2004), por lo que sería interesante determinar, en distintos modelos celulares, la relación entre Nef, F-actina y cofilina durante la entrada viral, y en estadios post-entrada previos a la transcripción reversa.

El proceso de polimerización inicial de F-actina, mediado por la unión de gp120, parece depender de la activación por fosforilación de LIMK1, y posterior fosforilación e inactivación de cofilina (Vorster et al., 2011). La incubación de células T no proliferativas, células T primarias activadas y macrófagos con la envuelta del VIH-1, genera dos picos de activación de LIMK1, con un estadio intermedio inactivo (Vorster et al., 2011). Esta activación parece ser dependiente de la unión al correceptor, aunque el mismo perfil de activación se observó a partir de la unión del VIH-1 a CD4 (Vorster et al., 2011). Esto indicaría que pueden activarse rutas de señalización similares a través de CD4 y correceptor, permitiendo un mecanismo compensador entre los dos componentes (Cicala et al., 1999; Graziani-Bowering et al., 2002; Stantchev and Broder, 2001). La activación de LIMK1 puede tener lugar a partir a las quinasas ROCK (activada por RhoA) o Pak (activada por Rac o Cdc42). En este sentido, el VIH-1 parece que induce la activación de LIMK1 a través de Pak-1 y Pak-2 (Vorster et al., 2011). Sin embargo, otros grupos de investigación han descartado la participación de Pak-1 (Jimenez-Baranda et al., 2007) y Pak-2 (Pontow et al., 2007) en su capacidad de bloquear la fusión célula-célula dependiente de la envuelta del virus. Además, también se ha descartado la participación de Pak1 en la activación de LIMK1 inducida por el VIH-1, siendo ésta al parecer activada por la vía RhoA/ROCK (Jimenez-Baranda et al., 2007). Por otro lado, la activación de Pak parece depender de una activación previa de Rac-1 (Vorster et al., 2011), resultados que coinciden con aquellos que también muestran la activación de Rac-1 por el VIH-1, de manera dependiente de correceptor e insensible a PTX, aunque con diferentes efectores implicados (Harmon et al., 2010; Harmon and Ratner, 2008; Pontow et al., 2007; Pontow et al., 2004). Asimismo, parece que el VIH-1 no activa RhoA ni Cdc42 (Vorster et al., 2011), aunque la activación de RhoA, dependiente de la unión del VIH-1 a CD4, ha sido detectada previamente durante la infección por el VIH-1 (del Real et al., 2004; Jimenez-Baranda et al., 2007). Igualmente, parece que esta polimerización de actina dependiente de LIMK1 parece ser crítica para la síntesis del ADN viral post-entrada y,

por tanto, para la generación de una infección latente en células T no proliferativas (Vorster et al., 2011). Aún así, el papel de LIMK1 sobre cofilina en células T no proliferativas, en donde cofilina se encuentra constitutivamente inactiva fosforilada (Yoder et al., 2008), está aún por esclarecer. Además, aún no se han identificado las fosfatasas implicadas en la activación de cofilina, necesaria para que el VIH-1 pueda atravesar la barrera compuesta por el citoesqueleto de actina cortical. Por todo ello, es posible que la polimerización de actina dependiente del VIH-1 no sólo dependa de la inactivación de cofilina por LIMK1 (Vorster et al., 2011), sino de la activación de otros efectores, por ejemplo, de Rac-1, como el complejo Arp2/3 (Harmon et al., 2010). En definitiva, los mecanismos que controlan la remodelación de actina cortical que tienen lugar durante la interacción del VIH-1 no se conocen bien, sobre todo en el contexto de las diferentes líneas celulares diana de la infección, y en relación a las proteínas implicadas en función del estado de activación y/o diferenciación de estas líneas celulares.

Recientemente se ha descrito la participación, en eventos posteriores a la fusión del virus VIH-1 con la célula diana pero antes de la transcripción reversa, de las proteínas adaptadoras de F-actina moesina y ezrina como determinantes de la susceptibilidad celular a la infección retroviral (Haedicke et al., 2008; Naghavi et al., 2007). Estas proteínas afectarían a la estabilidad del citoesqueleto de tubulina, al parecer necesario para la formación correcta del complejo de retrotranscripción viral. Se observó que la expresión de las proteínas funcionales moesina y ezrina, y sus respectivos dominantes negativos (N-moesina y N-ezrina) disminuye la formación de microtúbulos estables (de-tirosinados), disminuyendo la transcripción reversa viral y, por tanto, la infección retroviral (Haedicke et al., 2008; Naghavi et al., 2007). Por el contrario, otro estudio sobre el efecto de las proteínas ERM (ezrina/radixina/moesina) en la infección por el VIH-1, mostró un bloqueo de la infección X4 trópica del VIH-1 mediante el uso de un dominante negativo de ezrina y por la interferencia específica de ezrina, moesina y radixina (Kubo et al., 2008). En relación a las infecciones por envueltas R5 trópicas, el interferente de ezrina no afecta a la infección, el interferente de radixina la bloquea y el interferente de moesina la aumenta, aunque en modelos de fusión célula-célula se observa un bloqueo significativo por los tres interferentes. Estos datos indicarían que las ERM participarían de manera diferencial en la infección por el VIH-1 en función del tropismo viral, quizás relacionado con la asociación constitutiva de CD4 y CCR5 en la superfice celular (Steffens and Hope, 2003) y no de CD4 con CXCR4 (Kozak et al., 2002), lo que podría indicar una posible función de las ERM en la regulación de la remodelación del citoesqueleto de actina y en el agrupamiento de

los receptores virales inducido por el VIH-1. Aún así, las discrepancias en los resultados obtenidos sobre el papel ejercido por las proteínas ERM en los primeros estadios de infección, indican la necesidad de seguir explorando la función de estas proteínas en la infección por el VIH-1.

Por último, el VIH-1 es capaz de activar componentes de adhesiones focales (Cicala et al., 1999; Garron et al., 2008), y utilizarlas para favorecer la transmisión viral célula-célula, como es el caso de talina y LFA-1 (Jolly et al., 2004). En relación a estos resultados, recientemente se ha descrito la participación de proteínas presentes en adhesiones focales en la infección por el VIH-1 (Brown et al., 2011), y que añaden más complejidad al proceso de entrada viral. Estas observaciones indican que talina-1 y vinculina, parecen mediar en el estado de fosforilación de paxilina por FAK, que en último término va a influir en la infección retroviral (Brown et al., 2011). Estas proteínas bloquean la infección en un estadio post-entrada y previa a la transcripción reversa, sin afectar al citoesqueleto de actina y/o tubulina (Brown et al., 2011). De manera interesante, células PBMC de individuos infectados por el VIH-1 presentan niveles superiores de las proteínas vinculina, filamina-A y talina-1 (Zhang et al., 2010). Por último, la actividad de las proteínas de la familia Rho parecen ser necesarias para el ensamblaje y mantenimiento de las adhesiones focales, por lo que su activación por el VIH-1 (del Real et al., 2004; Jimenez-Baranda et al., 2007; Pontow et al., 2007; Pontow et al., 2004; Vorster et al., 2011) puede favorecer el mantenimiento estructural y espacial de las proteínas asociadas a las adhesiones focales, y su posterior función en los eventos de entrada viral eficiente.

Como se ha descrito hasta ahora, a pesar del incremento en el número de factores celulares que participan en los primeros estadios de infección por el VIH-1, aún quedan por determinar las diferencias entre los factores celulares que influyen en la infección por los distintos tropismos virales, y en las distintas líneas celulares susceptibles de infección.

Por todo ello, el objetivo central de la presente Tesis Doctoral consiste en aportar conocimiento sobre el ciclo de vida viral, en concreto referido a la identificación y caracterización de nuevas rutas de señalización, así como los componentes celulares activados e inducidos por el VIH-1, durante las primeras etapas de contacto virus-célula. Estos componentes celulares controlarían los mecanismos iniciales de reclutamiento y concentración de receptores, de manera dependiente del citoesqueleto de actina, las posteriores interacciones múltiples entre las glicoproteínas del virus con

los receptores y correceptores, y finalmente la formación del poro de fusión e infección viral productiva.

Además, sería interesante la caracterización de posibles moléculas cabeza de serie con actividad anti-fusogénica viral, para el desarrollo de estrategias anti-VIH alternativas a los tratamientos actuales contra el SIDA, inhibiendo la infección por VIH-1 en las etapas tempranas de adhesión, fusión y entrada viral.

2. HIPÓTESIS Y OBJETIVOS

2.1. HIPÓTESIS:

1. El VIH-1 infecta eficazmente células diana mediante la reorganización del citoesqueleto de actina cortical, que daría lugar a un estado dinámico de tensión y fluidez de membrana plasmática, adecuado para la interacción estable entre la proteína gp120 con los receptores virales, dirigiendo su redistribución e interacción directa en las zonas de contacto virus-célula, y favoreciendo el anclaje de la proteína gp41 a la membrana plasmática y la consiguiente formación del poro de fusión. La alteración de la tensión de la membrana plasmática depende directamente de su asociación con el citoesqueleto de actina cortical y del estado de activación de diversas proteínas de unión a actina. Esta asociación, podría ser modificada por el VIH-1, durante las primeras etapas de contacto virus-célula. En este sentido las proteínas ERM, son capaces de organizar el córtex celular mediante el anclaje inducible y reversible de la membrana plasmática al citoesqueleto de actina cortical. Esta función permite a estas proteínas estructurar de manera dinámica la membrana plasmática, de manera dependiente del citoesqueleto de actina, en respuesta a estímulos externos. Además, el principal activador de estas proteínas es el PIP_2 presente en la membrana plasmática, producido por la quinasa PI4P5-K de tipo I, que también modifica el reclutamiento y el estado de activación de proteínas de unión a actina en la membrana plasmática, además de participar en la fusión entre membranas biológicas. Por tanto, estudiaremos estos componentes en el contexto de los cambios dinámicos y de tensión de la membrana plasmática que tienen lugar durante los primeros estadios de fusión, entrada e infección por el VIH-1.

2. La endocitosis dependiente de clatrina (CME) es un proceso clave en la internalización de un gran número de receptores de la superficie celular. Recientemente se ha descrito que la ruta principal de entrada del VIH-1 depende de una ruta endocítica mediada por clatrina y posterior fusión en endosomas. Como existe una asociación cercana entre CME y el citoesqueleto de actina, estudiaremos el papel de las ERM, que postulamos clave en las etapas tempranas de fusión y entrada por el VIH-1, durante la formación, internalización y reciclaje de estructuras de clatrina y su relación con la entrada del VIH-1 a través de esta ruta endocítica.

3. Una de las estrategias terapéuticas menos utilizadas para el tratamiento del SIDA, es el uso de bloqueantes dirigidos contra las primeras etapas de fusión y entrada del VIH. Por lo tanto, no son muchas las moléculas anti-virales descritas que puedan evitar la propagación eficaz del virus interfiriendo en las etapas de fusión y

entrada viral. En este marco, este trabajo trata de identificar y caracterizar nuevas moléculas, naturales o semisintéticas, dirigidas a los correceptores del VIH-1, CCR5 y CXCR4, a partir de un banco de biomóleculas triterpenoides de origen vegetal, para, además, caracterizar su mecanismo de acción.

2.2. OBJETIVOS:

Los objetivos principales se enumeran a continuación:

1. Análisis de la activación por fosforilación de los adaptadores del citoesqueleto moesina y ezrina, en la infección viral y en la fusión inducida por gp120, y estudio de la posible ruta de activación mediada por la envuelta del VIH-1. Estudio de la interacción y redistribución de los receptores virales CD4 y CXCR4 por construcciones activas, dominantes negativos y ARNi específicos de las ERM, en relación a la reorganización del citoesqueleto de actina cortical inducido por la proteína viral gp120.

2. Estudio de la participación de la quinasa PI4P5-K de tipo I en la posible producción de PIP_2, mediada por la envuelta viral, durante el proceso de infección por el VIH-1, y su posible relación con la activación de las proteínas moesina y ezrina. Estudiar la localización de los receptores virales en los procesos de fusión y entrada viral, mediada por la inhibición y/o sobreexpresión de diferentes construcciones de la quinasa PI4P5-K de tipo I.

3. Estudio de la participación del adaptador de actina moesina durante el proceso de formación, internalización y reciclaje de las estructuras de clatrina en la membrana plasmática, y su participación durante la posible entrada endocítica del VIH-1.

4. Identificación y caracterización de una serie de triterpenos de tipo lupano no ácidos, naturales o derivados semisintéticos, en su capacidad de bloquear la unión, entrada e infección por el VIH-1, mediante el uso de un modelo de fusión e infección viral, que evalua y cuantifica la actividad fusogénica de las envueltas virales X4 y R5 trópicas del VIH-1.

3. RESULTADOS

3.1. LA ACTIVACIÓN DE MOESINA POR EL VIH-1 ES NECESARIA PARA LA INTERACCIÓN ENTRE CD4 Y CXCR4, Y LA REDISTRIBUCIÓN DE LA F-ACTINA CORTICAL, PROCESOS CLAVE PARA LA FUSIÓN, ENTRADA E INFECCIÓN EFICIENTE POR EL VIH-1 EN LINFOCITOS T

El citoesqueleto de actina cortical juega un papel importante y necesario durante los primeros estadios de entrada e infección por el VIH-1, mediante la organización de complejos estructurales de unión y señalización viral en regiones específicas de la membrana plasmática. Las proteínas ezrina-radixina-moesina (ERM) constituyen una familia de organizadores del citoesqueleto de actina cortical, gracias a su capacidad de unir los filamentos de actina a la membrana celular. Las proteínas ERM pueden unirse de manera inducible y reversible a la membrana plasmática, ya sea directa o indirectamente, y al citoesqueleto de actina cortical, regulando la formación superficial de dominios complejos y estructuras de membrana como las microvellosidades (Bretscher, 1999; Mangeat et al., 1999).

Las propiedades funcionales de las proteínas ERM dependen de sus dos estados, el inactivo y el activo. Estos estados dependen de la presencia de una región N-terminal de unos 300 aminoácidos de longitud denominado dominio FERM (N-ERMAD: "*N-ERM associated domain"*) asociado a la membrana plasmática, seguido por una larga región de α-hélices, un región rica en el aminoácido Pro y un dominio C-terminal (C-ERMAD: "*C-ERM associated domain"*) capaz de unirse a F-actina (revisado en (Chishti et al., 1998; Mangeat et al., 1999)). Las proteínas ERM en su estado inactivo en el citoplasma no presentan capacidad de unirse a la membrana plasmática y a la actina debido a una asociación intramolecular, entre su dominio N-ERMAD y el dominio de unión a actina C-ERMAD (Chishti et al., 1998). La activación de las formas solubles de las proteínas ERM requiere la disociación de estos dominios, para así facilitar otras interacciones intermoleculares (Hirao et al., 1996), principalmente conectando la F-actina cortical con la membrana plasmática. El principal indicador de activación de las proteínas ERM consiste en la detección de la fosforilación de un residuo de Thr C-terminal (Thr^{576} en ezrina, Thr^{564} en radixina, y Thr^{558} en moesina) (Fievet et al., 2004). Se han identificado una gran cantidad de quinasas implicadas en la fosforilación de las proteínas ERM en su residuo Thr C-terminal, que incluyen ROCK, PKCα, PKCθ, NIK ("*Nck-interacting kinase*"), Mst4 ("*Mammalian Ste20-like* Kinase*")* y LOK ("*Lymphocyte-oriented kinase")*, ésta última

responsable de la mayoría de la fosforilación de las ERM en la membrana plasmática de los linfocitos (revisado en (Fehon et al., 2010)). Aunque la fosforilación C-terminal de ERM indica la activación de la molécula, ésta sólo tiene lugar tras la liberación de la interacción intramolecular. Así, se ha propuesto un modelo de activación, en el cual las proteínas ERM son reclutadas a regiones de la membrana plasmática ricas en fosfatidilinositol-(4,5)-bifosfato (PIP_2), provocando cambios conformacionales que permiten la posterior fosforilación del residuo conservado de Thr C-terminal (Fehon et al., 2010). La inactivación de las proteínas ERM tiene lugar por defosforilación del residuo Thr C-terminal mediante la acción de fosfatasas, como la fosfatasa de la cadena ligara de miosina, o mediante su degradación por corte proteolítico mediado por calpaina (revisado en (Louvet-Vallee, 2000)).

El dominio N-ERMAD de las proteínas ERM, en su conformación activa, puede interaccionar directamente con un región de aminoácidos cargados positivamente presente en las colas citoplasmáticas de varias proteínas integrales de membrana como CD43, CD44, ICAM1, ICAM2 e ICAM3, determinando su localización y concentración en la superficie celular de manera dependiente del citoesqueleto de actina (revisado en (Mangeat et al., 1999)).

Por otro lado, las proteínas ERM pueden unirse a la membrana plasmática de manera indirecta a través de la unión de su domino N-ERMAD a otras proteínas adaptadoras como EBP50 ("*ezrin binding phosphoprotein 50*", también conocida como NHERF1) y E3KARP (también conocida como NHERF2), cada una de las cuales tiene dos dominios PDZ ("*PSD-95/DlgA/ZO-1-like domain*") seguido por un dominio de unión a ERM (revisado en (Fehon et al., 2010)). Los sitios de unión a estos dominios PDZ están presentes en la región citoplasmática de un gran número de proteínas integrales de membrana (Weinman et al., 2006).

A parte de su función como organizadores del córtex celular apical, las proteínas ERM también presentan funciones como coordinadores superficiales de eventos de señalización intracelular (Neisch and Fehon, 2011), gracias a su capacidad de acercar receptores de la superficie celular a efectores de diversas rutas de señalización. Por ejemplo, las ERM también funcionan como reguladores de la activación de las células T (en sinapsis inmunológica), en desarrollo y diferenciación, en la regulación de la señalización dependiente de AMPc/PKA, en la activación de la GTPasa RhoA, en la supresión de la apoptosis, en metástasis y en la ruta secretora de insulina (revisado en (Fehon et al., 2010; Louvet-Vallee, 2000; Neisch and Fehon, 2011)).

En cuanto a la infección por el VIH-1, se han detectado fragmentos cortados de ezrina y moesina en preparaciones de partículas virales de VIH-1, así como otros componentes del citoesqueleto de actina (Ott et al., 1996). Además, ezrina y moesina se unen a la proteína de la envuelta gp120, al parecer favoreciendo su transporte hacia la membrana plasmática donde tiene lugar la salida viral (Hecker et al., 1997). Asimismo, una de las principales estructuras generadas por la activación de las ERM, son las microvellosidades (Yonemura et al., 1999), regiones donde existe una mayor concentración de receptores virales necesarios para la entrada viral (Singer et al., 2001; Steffens and Hope, 2003). Así, se ha descrito que la activación de la GTPasa RhoA, también activada por gp120 (Jimenez-Baranda et al., 2007), es capaz de activar las proteínas ERM induciendo la formación de microvellosidades en linfocitos, favoreciendo su interacción con proteínas integrales de la membrana plasmática. En este sentido, recientemente se ha mostrado el papel que ejercen las proteínas ezrina y moesina en la infección retroviral, pero a través de su acción sobre el citoesqueleto de tubulina (Haedicke et al., 2008; Naghavi et al., 2007). Sin embargo, otro estudio mostró que las proteínas ERM ejercen efectos pleiotrópicos sobre la infección por el VIH-1, que dependen del tropismo de la cepa viral empleada (Kubo et al., 2008).

Aunque todos estos datos sugieren un papel de las proteínas ERM en el empaquetamieto viral o infección, no existen evidencias que indiquen el papel funcional de las proteínas ERM dependiente de su actividad de unión a membrana y a F-actina en los primeros estadios del ciclo viral, ni el papel que podrían desempeñar estas proteínas en el agrupamiento de complejos de receptores/correceptores de manera dependiente del citoesqueleto de actina e inducido por el VIH-1.

RESULTADOS

Los resultados obtenidos indican que la reorganización del citoesqueleto de actina dependiente de la proteína adaptadora moesina es necesaria para la redistribución y asociación de los receptores CD4/CXCR4, dependiente de la interacción de la envuelta del VIH-1 con la célula diana. Además, la actividad de moesina dirigida a unir la membrana plasmática a la actina cortical es fundamental para una fusión e infección eficiente por el VIH-1.

En primer lugar observamos que la proteína de envuelta gp120 del VIH-1 recombinante soluble (rs-gp120$_{IIIB}$) induce la fosforilación de las proteínas ERM, principalmente moesina y en menor extensión ezrina. Además, mediante microscopía confocal, en linfocitos T CD4$^+$, se observó que la envuelta X4 trópica del VIH-1

provoca la relocalización de formas fosforiladas de moesina hacia un polo de la célula junto con F-actina y los receptores virales CD4 y CXCR4. Esta fosforilación inducida por la envuelta del VIH-1 es independiente de PKC y ROCK. Además, la fosforilación depende de la unión de la envuelta del VIH-1 a CD4 y no al correceptor CXCR4. A continuación, observamos que la sobreexpresión de una construcción funcional de moesina (FL-moesina), que puede unirse a la membrana plasmática y a F-actina, favorece la redistribución de F-actina y la fosforilación de moesina endógena inducida por la envuelta del VIH-1, favoreciendo la entrada e infección por el VIH-1. Por el contrario, la supresión de la actividad funcional de moesina, por una construcción dominante negativa de moesina (N-moesina) o mediante un ARNi específico contra moesina endógena, evita tanto la relocalización de la F-actina como la fosforilación de la proteína moesina endógena en respuesta al VIH-1, inhibiendo la entrada e infección por el VIH-1. Sin embargo, ninguna de las construcciones de moesina alteró el nivel de F-actina total inicial ni el nivel de expresión en superficie de los receptores para el VIH-1, CD4 y CXCR4, en la célula diana. Además, la interferencia específica del ARNm de moesina no afectó a la entrada e infección, a través de una ruta endocítica de clatrina, de virus pseudotipados con la envuelta VSV-G. Por último, la sobreexpresión de la proteína FL-moesina promueve la formación del poro de fusión incrementando el nivel de fusión virus-célula y célula Env^+-célula, mientras que la proteína N-moesina y la interferencia específica de moesina endógena bloquean el nivel de fusión por inhibición de la formación del poro de fusión. Por último, se observó que la redistribución y asociación entre CD4 y CXCR4, dependiente de la proteína de envuelta gp120, es favorecida por la redistribución de la F-actina dependiente de la proteína moesina funcional, mientras que la proteína N-moesina y la interferencia específica de moesina evitaron esta asociación aún en presencia de la envuelta viral. Por lo tanto, la activación de moesina, inducida tras el contacto gp120/CD4, promueve la redistribución de la F-actina junto con el agrupamiento de CD4/CXCR4, en las zonas de contacto virus-célula, necesario para la fusión, entrada e infección eficiente de linfocitos T $CD4^+$ por cepas de VIH-1 X4 trópicas.

MATERIALES Y MÉTODOS

Los tipos celulares utilizados durante el estudio fueron: líneas celulares T CEM (células linfoblásticas T de leucemia) $CD4^+/CXCR4^+$; linfocitos de sangre periférica (PBL, "*Peripheral blood lymphocytes*") activados con PHA/IL-2 aislados de donantes sanos mediante centrifugación en un gradiente de Ficoll; líneas celulares Jurkat que

expresan la envuelta X4 trópica del VIH-1 Hxbc2; y líneas HeLa P4 ($CD4^+$/$CXCR4^+$/LTR-β-Gal) y HeLa 243 (X4 Env^+/Tat^+). Para los ensayos funcionales se utilizaron anticuerpos específicos contra CD4 neutralizantes y no-neutralizantes de la unión de gp120, bloqueantes de CXCR4 (AMD3100) y anticuerpos específicos para detectar las proteínas ERM y sus formas fosforiladas, y para la detección de CD4 y CXCR4, tanto por "*western blot"* como por inmunofluorescencia. En algunos ensayos se utilizó una proteína de envuelta X4 trópica gp120 recombinante soluble (rs-$gp120_{IIIB}$), para la estimulación de células T diana $CD4^+$. Se utilizaron las construcciones de la proteína funcional de moesina (FL-moesina), el dominante negativo (N-moesina), que sólo se une a membrana y ha perdido la capacidad de unir F-actina al carecer de éste dominio C-terminal, y el mutante que sólo presenta el dominio C-terminal de unión a actina y que no se une a membrana (C-moesina). Además, se utilizaron secuencias de ARNi específicas para la proteína moesina. Se utilizó la nucleofección como la técnica para la introducción de las construcciones de ADN plasmídico y los ARNi en la célula diana. La microscopía de fluorescencia confocal se utilizó para monitorizar la localización de moesina, de F-actina, y de los receptores CD4 y CXCR4, durante la formación del poro de fusión. La técnica de "*western blot*" nos permite detectar la sobreexpresión de las proteínas ERM en comparación con los niveles endógenos, el grado de fosforilación de ERM y el nivel de interferencia específica de las proteínas ERM endógenas. Por citometría de flujo se determinó el nivel de expresión superficial de CD4, CXCR4 y CCR5, y el nivel de F-actina en las células diana en cada condición experimental. Las células 293T se utilizaron para la producción de virus defectivos en replicación. Se utilizaron partículas virales infecciosas de VIH-1 para estudios de entrada y replicación, y partículas virales de un único ciclo de infección deficientes en replicación, que contienen el gen que codifica para la enzima luciferasa (vector HIV/Δ*nef*/Δ*env*/Luc^+ pseudotipado con una envuelta X4 trópica Hxbc2), o partículas virales que contienen la proteína quimérica BlaM-Vpr, para comparar el nivel de fusión y entrada viral en las células diana en cada condición experimental. Por último, se utilizó la co-inmunoprecipitación para detectar la asociación entre CD4 y CXCR4 en cada condición experimental.

Research Article 103

Moesin is required for HIV-1-induced CD4-CXCR4 interaction, F-actin redistribution, membrane fusion and viral infection in lymphocytes

Marta Barrero-Villar[1,*], José Román Cabrero[1,*], Mónica Gordón-Alonso[1], Jonathan Barroso-González[2], Susana Álvarez-Losada[3], M. Ángeles Muñoz-Fernández[3], Francisco Sánchez-Madrid[1,‡] and Agustín Valenzuela-Fernández[1,2]

[1]Servicio de Inmunología, Hospital Universitario de La Princesa, 28006 Madrid, Spain
[2]Departamento de Medicina Física y Farmacología, Facultad de Medicina, Universidad de La Laguna, 38071 Tenerife, Spain
[3]Servicio de Inmuno-Biología Molecular, Hospital General Universitario Gregorio Marañón, 28007 Madrid, Spain
*These authors contributed equally to this work
‡Author for correspondence (e-mail: fsanchez.hlpr@salud.madrid.org)

Accepted 6 October 2008
Journal of Cell Science 122, 103-113 Published by The Company of Biologists 2009
doi:10.1242/jcs.035873

Summary

The human immunodeficiency virus 1 (HIV-1) envelope regulates the initial attachment of viral particles to target cells through its association with CD4 and either CXCR4 or CCR5. Although F-actin is required for CD4 and CXCR4 redistribution, little is known about the molecular mechanisms underlying this fundamental process in HIV infection. Using $CD4^+$ $CXCR4^+$ permissive human leukemic CEM T cells and primary lymphocytes, we have investigated whether HIV-1 Env might promote viral entry and infection by activating ERM (ezrin-radixin-moesin) proteins to regulate F-actin reorganization and CD4/CXCR4 co-clustering. The interaction of the X4-tropic protein HIV-1 gp120 with CD4 augments ezrin and moesin phosphorylation in human permissive T cells, thereby regulating ezrin-moesin activation. Moreover, the association and clustering of CD4-CXCR4 induced by HIV-1 gp120 requires moesin-mediated anchoring of actin in the plasma membrane. Suppression of moesin expression with dominant-negative N-moesin or specific moesin silencing impedes reorganization of F-actin and HIV-1 entry and infection mediated by the HIV-1 envelope protein complex. Therefore, we propose that activated moesin promotes F-actin redistribution and CD4-CXCR4 clustering and is also required for efficient X4-tropic HIV-1 infection in permissive lymphocytes.

Supplementary material available online at
http://jcs.biologists.org/cgi/content/full/122/1/103/DC1

Key words: ERM, Ezrin-radixin-moesin, F-actin redistribution, CD4-CXCR4 interaction, HIV-1 infection and entry

Introduction

The entry of HIV into a target cell requires the interaction of multiple receptor and co-receptor molecules with each viral envelope (Env) trimer to promote the formation of fusion pores (Doms, 2000; Kuhmann et al., 2000). F-actin reassembly appears to be involved in Env-induced CD4, CXCR4 and LFA-1 redistribution to cell-cell junctions during viral spreading (Jolly et al., 2004), and drugs that affect actin dynamics appear to inhibit Env-mediated fusion (Eitzen, 2003; Pontow et al., 2004); but it is unclear whether these drugs affect HIV-1 Env activity (Campbell et al., 2004; Yonezawa et al., 2005). Although there is a clear correlation between HIV-1-mediated recruitment, CD4 and co-receptor polarization, and efficient viral fusion and infection (Iyengar et al., 1998; Jolly et al., 2004; Manes et al., 2000), little is known about the molecular mechanisms regulating the CD4–co-receptor interaction. Recently, it has been reported that filamin A links HIV-1 receptors to the actin cytoskeleton to allow their clustering (Jimenez-Baranda et al., 2007).

HIV-1 viral entry occurs at specific cell-surface areas enriched in viral receptors, such as ruffles and microvilli (Singer et al., 2001; Steffens and Hope, 2003). The behavior of these structures is governed by cortical actin dynamics, which in turn depend on the activity of several actin cytoskeleton associated proteins such as those responsible for actin filament growth and capping (Mangeat et al., 1999). Ezrin-radixin-moesin (ERM) proteins provide an inducible and reversible link between membrane-associated proteins and the actin cytoskeleton (Bretscher, 1999; Mangeat et al., 1999), thereby regulating microvilli formation (Takeuchi et al., 1994). Soluble ERM proteins in the cytoplasm do not display plasma membrane and actin crosslinking capacity. This inactive state of ERM proteins is controlled by intramolecular associations between the N-terminal FERM domain (band 4.1-ezrin-radixin-moesin) and the C-terminal domain (Chishti et al., 1998; Pearson et al., 2000). ERM activation requires dissociation of these domains to facilitate other intermolecular interactions (Gary and Bretscher, 1995; Hirao et al., 1996; Matsui et al., 1998). Phosphorylation of C-terminal threonine residues in ERM (moesin Thr558 and ezrin Thr567) is indicative of the activation of the ERM molecules (Fievet et al., 2004), which in their active conformation connect cortical F-actin to the plasma membrane. The FERM domain also interacts with the cytoplasmic tails of several integral membrane proteins such as CD43, CD44, VCAM1, and ICAM1, ICAM2 and ICAM3, and mediates their cell-surface clustering (Barreiro et al., 2002; Heiska et al., 1998; Helander et al., 1996; Hirao et al., 1996; Matsui et al., 1998; Serrador et al., 1997; Takeuchi et al., 1994; Yonemura et al., 1993). The C-terminal domain of ERM molecules binds to actin filaments (Algrain et al., 1993).

Journal of Cell Science

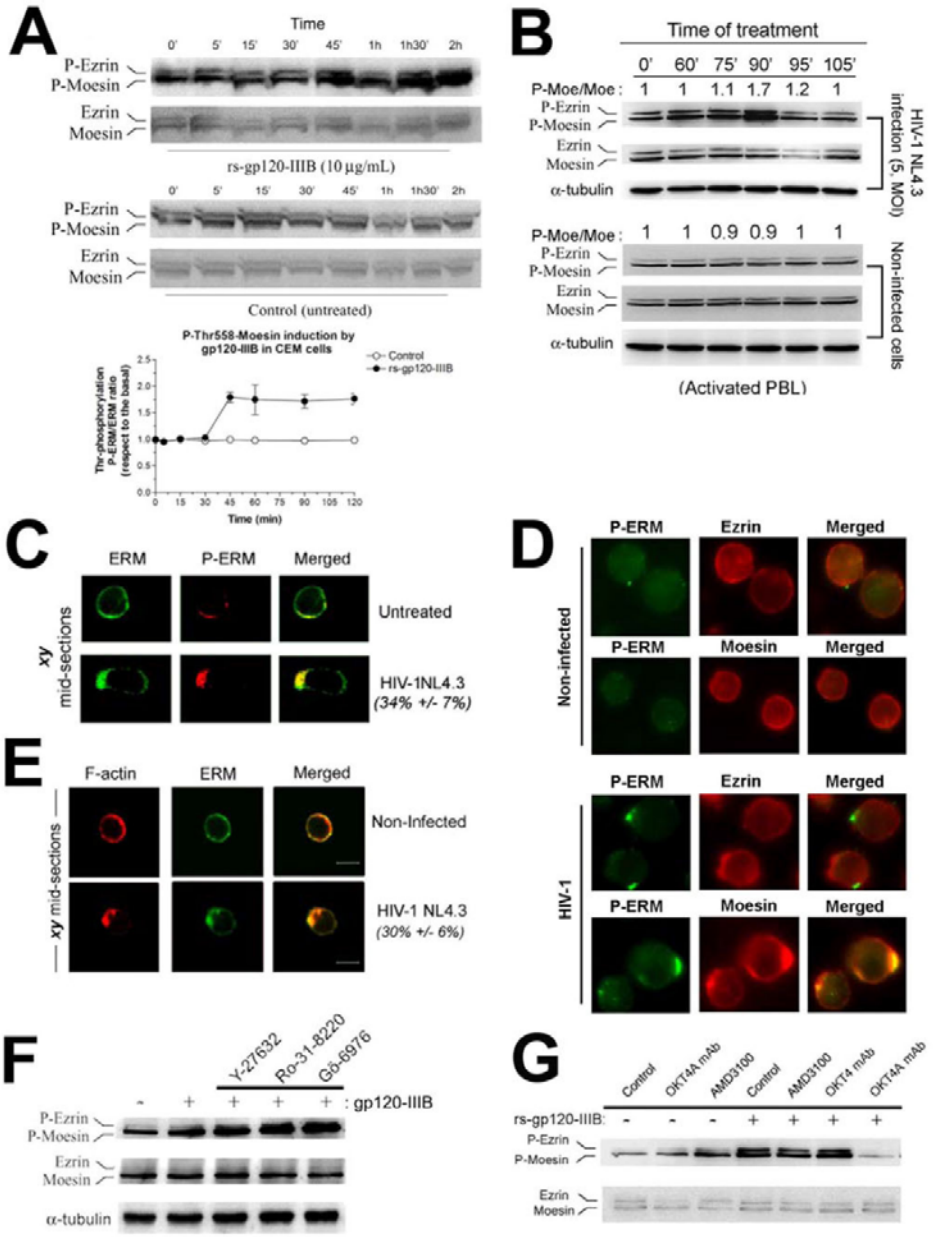

Fig. 1. HIV-1 phosphorylates endogenous ERM and redistributes F-actin. (A) Western blot analysis of rs-gp120-induced phosphorylation of C-terminal Thr residues of ERM proteins (P-ezrin and P-moesin). Results from untreated control CEM cells are shown in the blot below. Total ERM (ezrin and moesin) is shown for all experimental conditions. A representative experiment of three is shown. The graph shows quantification of Thr phosphorylation of ERMs from three independent experiments. (B) Time course of ERM Thr phosphorylation in PHA-activated PBL, during early infection with the X4-tropic HIV-$1_{NL4.3}$ viral strain (MOI, 5) compared with non-infected cells. Basal phosphorylation of endogenous ERM-Thr, total ERM and total α-tubulin expression are shown for all experimental conditions. (C) Confocal microscopy shows polarized distribution (*xy* mid-sections) of activated endogenous ERM in CEM cells, 1 hour after HIV-1 infection (MOI, 1; HIV-1NL4.3). Untreated, non-infected cells. Quantification of HIV-1-induced ERM or ERM-*P* capping is indicated ± s.d. (D) Confocal analysis of ERM-*P* and endogenous ezrin and moesin localization and redistribution in non-infected or HIV-1-infected CEM cells (1 hour; MOI, 1). (E) Confocal analysis of F-actin and endogenous ERM localization and redistribution in non-infected or HIV-1-infected CEM cells (1 hour; MOI, 1). Quantification of HIV-1-induced ERM actin capping is indicated ± s.d. (F) Western blot analysis of ezrin and moesin phosphorylation induced by rs-$gp120_{IIIB}$ (1 hour exposure) in CEM cells. Blots of total expression of ezrin, moesin and α-tubulin are also shown. Rho-K (ROCK) and PKC inhibitors failed to prevent rs-$gp120_{IIIB}$-induced Thr phosphorylation of ezrin and moesin. A representative of three independent experiments is shown. (G) Blockade of rs-$gp120_{IIIB}$ (5 µg/ml)-induced ERM Thr phosphorylation in CEM cells with neutralizing or non-neutralizing anti-CD4 mAbs (OKT4A or OKT4, respectively), or with the CXCR4 antagonist AMD3100. Blots of total ezrin and moesin proteins are shown. A representative example of three independent experiments is shown.

Analyses of HIV-1 viral preparations indicate that cleaved ezrin and moesin fragments, as well as other cytoskeletal components, are found inside the virions (Lapham et al., 1996). Recently, ezrin has been shown to have a tubulin-dependent role in HIV-1 infection (Haedicke et al., 2008). ERM proteins seem to exert pleiotropic effects on HIV-1 infection, which are dependent of the tropism of the HIV-1 viral strain (Kubo et al., 2008). Although all these data suggest a role for ERM proteins during virus budding or infection, there has been no published evidence indicating an actin-dependent role of ERM in the first steps of the viral cycle.

The data presented here show that moesin-dependent reorganization of the actin cytoskeleton is a critical feature of HIV-1 Env-mediated CXCR4-CD4 colocalization and association. Moreover, moesin activity linking the plasma membrane to actin is required for efficient HIV-1 Env-mediated membrane fusion and infection.

Results

HIV-1 Env induces ERM phosphorylation and F-actin redistribution in $CD4^+$ $CXCR4^+$ lymphocytes

It has recently been proposed that ERM proteins require phosphorylation to maintain their active state (Bretscher, 1999; Yonemura et al., 2002). To study the involvement of ERM proteins and F-actin redistribution in HIV-1 infection, we first investigated whether the HIV-1 envelope (Env) gp120 viral protein and/or HIV-1 viral particles activate ERM proteins in permissive primary lymphocytes or human leukemic CEM T cells. When CEM cells were incubated with the X4-tropic recombinant soluble (rs)-$gp120_{IIIB}$ protein, the phosphorylation of moesin, and to a lesser extent ezrin, increased (Fig. 1A, top panel), whereas total moesin and ezrin expression was unaffected (Fig. 1A, bottom panel). Remarkably, ERM proteins were also phosphorylated during early viral infection of PHA-activated primary T lymphocytes, with a

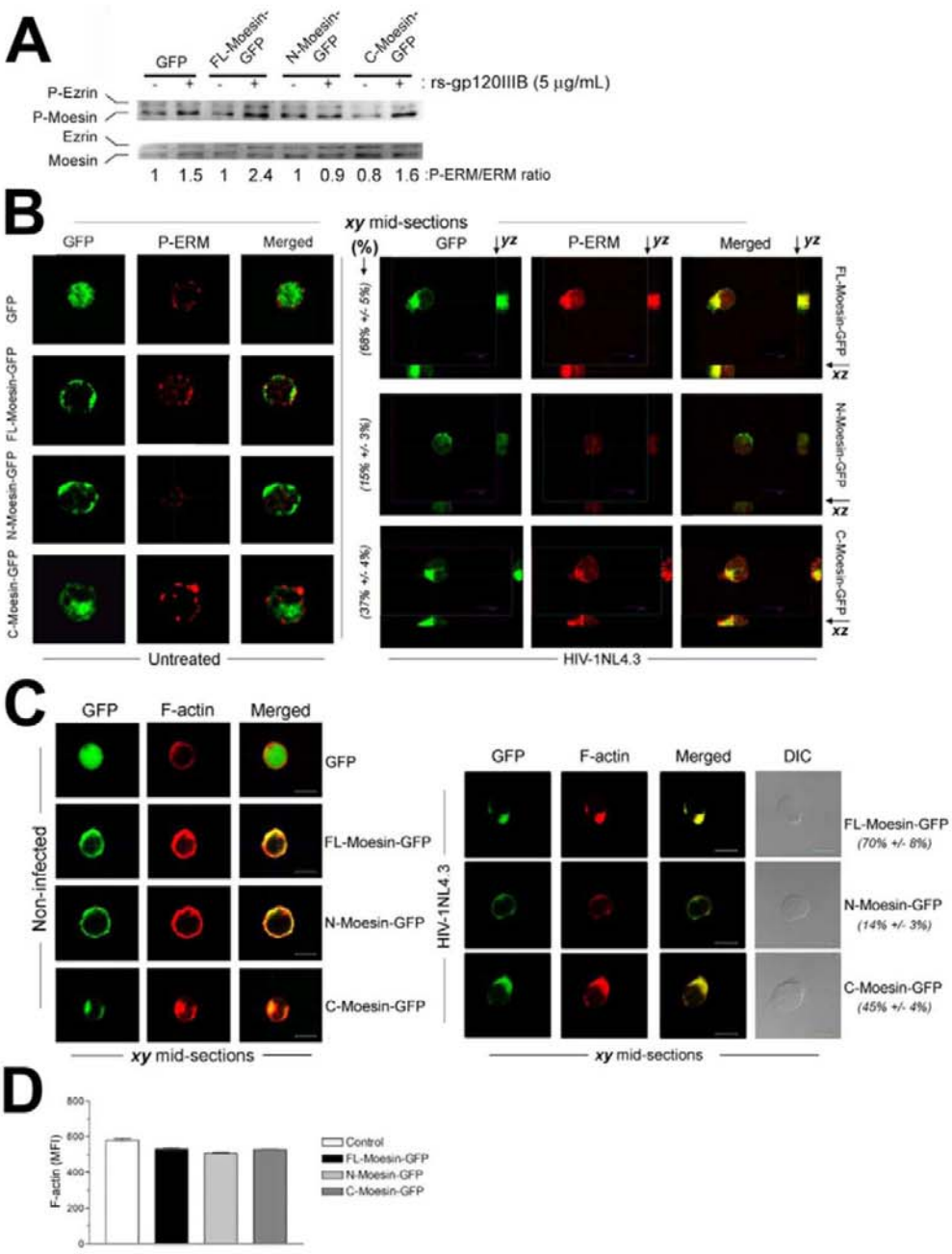

Fig. 2. F-actin and activated exogenous moesin polarize during early HIV-1 infection. (A) Western blot analysis of HIV-1 Env-induced phosphorylation of endogenous moesin in CEM cells overexpressing GFP fusions of full-length moesin (FL-moesin), the N-terminal FERM domain (N-moesin), or the C-terminal domain (C-moesin). A representative experiment is shown. ERM-*P*/ERM band density ratios from three independent experiments are shown beneath lanes. (B) ERM phosphorylation and subcellular localization of nucleofected moesin-GFP proteins in CEM cells either without infection (untreated, left panels) or 1 hour after HIV-1 infection (MOI, 1; right panels). Localization of exogenous moesin-GFP fusions was tracked by GFP fluorescence (GFP). Active ERM-*P* (Thr-*P*) was monitored with a specific Thr-*P* antibody and Alexa Fluor 568-labeled secondary antibody. The *yz* and *xz* planes are shown for each *xy* mid-section presented (arrows in the right panel). Data are from three independent experiments, presented as means ± s.e.m. Quantification of basal (untreated) and HIV-1 Env-mediated co-distribution of ERM-*P* and ERM is shown in parentheses; the percentages represent the number of cells showing co-distribution per 200 cells counted. (C) Distribution of F-actin and nucleofected moesin-GFP proteins in non-infected or HIV-1-infected (1 hour; MOI, 1) CEM cells. Quantification of HIV-1 Env-mediated co-distribution of endogenous moesin, nucleofected moesin-GFP constructs and F-actin are shown in parentheses. Scale bars: 10 μm. (D) Quantified flow cytometry of F-actin in non-infected CEM T cells that were either untransfected (Control) or nucleofected with GFP or FL-, N- or C-moesin-GFP. Data are from three independent experiments, presented as mean ± s.e.m.

peak 90 minutes after infection, which then later declined to basal levels (Fig. 1B). Confocal analysis during early HIV-1 viral exposure showed that the X4-tropic HIV-$1_{NL4.3}$ strain induces Thr phosphorylation of ERM proteins (Fig. 1C). Endogenously phosphorylated ERM displayed a polarized distribution within 1 hour of viral infection (Fig. 1C). This polarized distribution and Thr phosphorylation is mainly due to moesin, not ezrin, as indicated by the specific colocalization of moesin protein and phosphorylated threonine (Thr-*P*) (Fig. 1D). Analysis of F-actin organization showed that F-actin and endogenous moesin are cortically distributed in non-infected cells, with no capping observed (Fig. 1E), and that during early HIV-1 infection or after exposure to rs-gp120, F-actin redistributes to a pole in about 30% of cells (Fig. 1E and data not shown).

ERM C-terminal Thr residues are targets for phosphorylation in vitro by Rho kinase (ROCK) and PKC (Nakamura et al., 1999). We therefore assessed whether these kinases were responsible for the HIV-1-induced ERM phosphorylation. Phosphorylation of moesin and ezrin in response to treatment with rs-$gp120_{IIIB}$ or rs-$gp120_{SF2}$ was not affected by the specific ROCK inhibitor Y-27632 or by the PKC inhibitors Ro-31-8220 and Gö-6976 (Fig. 1F), demonstrating that HIV-1 Env-induced moesin and ezrin phosphorylation is not mediated by ROCK or PKC in lymphocytes. Moreover, neither the CXCR4 antagonist AMD3100 nor a non-neutralizing anti-CD4 OKT4 mAb affected rs-$gp120_{IIIB}$-induced moesin and ezrin phosphorylation (Fig. 1G). By contrast, pretreatment of cells with a neutralizing anti-CD4 mAb (OKT4A) abolished rs-$gp120_{IIIB}$-mediated ERM activation (Fig. 1G).

Therefore, it appears that HIV-1 Env induces moesin and ezrin phosphorylation and activation through specific CD4 engagement, ruling out the involvement of CXCR4.

Active moesin drives F-actin redistribution during initial HIV-1 to cell contacts

To further investigate the role of moesin in HIV-1 Env-mediated F-actin reorganization, we transiently nucleofected CEM cells with one of three C-terminally GFP-tagged moesin constructs: FL-moesin (full-length moesin), N-moesin (the N-terminal FERM domain), or C-moesin (the C-terminal actin-binding region) (Amieva et al., 1999). These cells were then incubated with HIV-1 viral particles. Remarkably, overexpression of functional FL-moesin increased HIV-1 Env-mediated phosphorylation of endogenous ERM (Fig. 2A), thus suggesting a cooperative effect during moesin activation (Simons et al., 1998), which could reflect enhanced anchoring of cortical F-actin filaments to plasma membrane. In non-infected cells, endogenous moesin was restricted to the cell cortex (Fig. 1E; Fig. 2B), as were exogenous FL- and N-moesin-GFP proteins (Fig. 2B, left panel). By contrast, C-moesin-GFP was detected in the cytoplasm (Fig. 2B, left panel). Interestingly, HIV-1 viral particles induced the formation of a prominent pseudopod in cells overexpressing FL-moesin or C-moesin, in which the active phosphorylated forms of moesin presented a polarized distribution (Fig. 2B, right panel). HIV-1-induced moesin redistribution and activation was not observed in CEM cells overexpressing N-moesin-GFP (Fig. 2B, right panel), which has been previously described as a dominant-negative moesin construct that lacks the capacity to bind F-actin, thereby disconnecting plasma membrane from cortical actin (Amieva et al., 1999). Moreover, the dominant-negative N-moesin construct inhibited HIV-1 Env-induced phosphorylation of endogenous moesin (Fig. 2A). These results indicate that moesin protein is activated and phosphorylated early during HIV-1 infection.

In cells overexpressing FL-moesin-GFP or C-moesin-GFP, F-actin redistribution was readily observed during HIV-1 infection or treatment with rs-gp120 viral protein (Fig. 2C, and data not shown). By contrast, N-moesin abolished HIV-1-induced F-actin redistribution (Fig. 2C). However, F-actin levels, as determined by flow cytometry (Vicente-Manzanares et al., 2004), were not altered significantly by overexpression of any of the moesin constructs (Fig. 2D). Therefore, it seems that active moesin drives F-actin redistribution during the first HIV-1 to cell contacts.

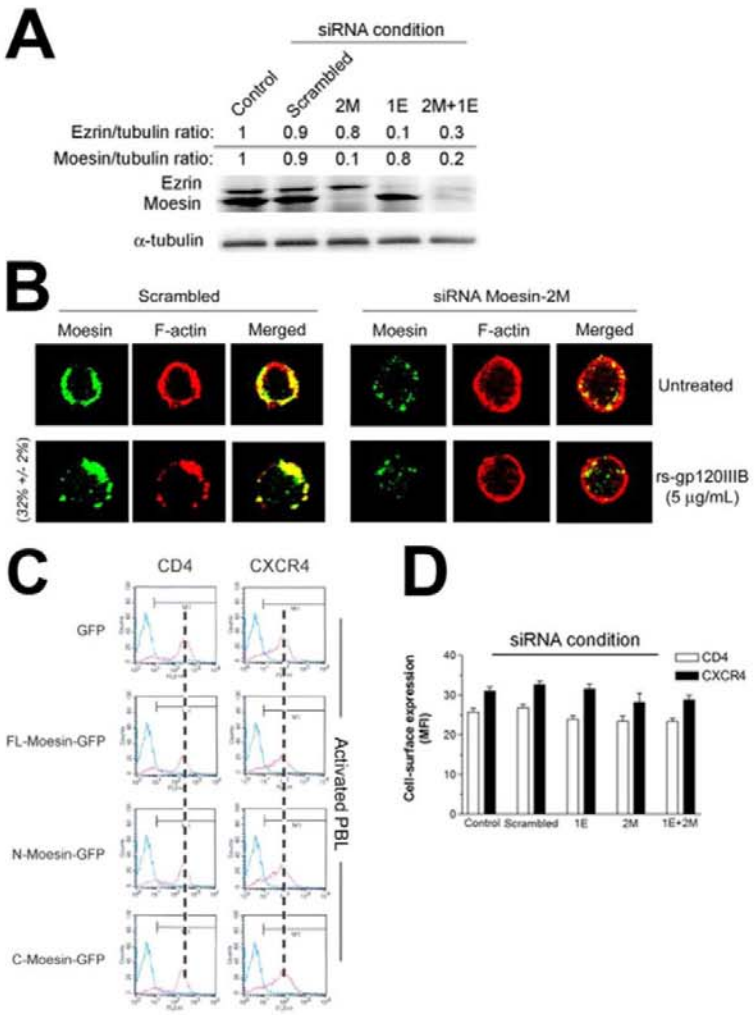

Fig. 3. Effect of overexpressed moesin-GFP proteins and moesin knockdown on CD4 and CXCR4 cell-surface levels and F-actin distribution in primary lymphocytes. (A) Western blot analysis of specific silencing of endogenous expression of ezrin (oligo 1E) and/or moesin (oligo 2M) 72 hours after siRNA nucleofection of CEM cells. Silencing of endogenous ezrin and/or moesin expression is quantified as the band intensity ratios to α-tubulin. A representative experiment of four is shown. (B) Confocal analysis of HIV-1 Env-induced F-actin redistribution in CEM cells in which endogenous moesin is suppressed by knockdown (siRNA moesin-2M). Scrambled indicates the control. *xy* mid-sections are shown. Quantification of HIV-1-induced moesin or Actin capping is indicated ± s.d. (C) CD4 and CXCR4 cell-surface expression levels (red histograms) in PHA-activated PBLs overexpressing GFP or FL-, N- or C-moesin-GFP fusion proteins. A representative flow cytometry analysis of three is shown. Blue histograms indicate IgG negative control. (D) Flow cytometry analysis of the effect of specific moesin-silencing on CD4 and CXCR4 cell surface expression in primary lymphocytes. Data are the means ± s.e.m. of four independent experiments carried out in triplicate.

Moesin regulates X4-tropic HIV-1 infection in permissive T cells

We next assessed the involvement of moesin in HIV-1 infection. We first confirmed the effect of moesin on F-actin distribution by suppressing endogenous moesin expression. Expression of ezrin, moesin or both proteins was suppressed with specific short-interfering RNAs (siRNAs) (Fig. 3A) (oligonucleotides 1E, 2M or 2M+1E; an alternative oligo for moesin was also used) (see supplementary material Fig. S1A). Knockdown of moesin expression blocked HIV-1 Env-induced F-actin redistribution (Fig. 3B). Neither overexpression of the GFP-tagged moesin constructs nor knockdown of ezrin, moesin, or both proteins affected the cell-surface expression of CD4 and CXCR4 receptors by primary lymphocytes (Fig. 3C,D).

To determine whether moesin is involved in X4-tropic HIV-1 infection, we nucleofected CEM cells or PHA-activated peripheral blood lymphocytes (PBLs) with one of the three C-terminal GFP-tagged moesin constructs and infected the cells with the X4-tropic

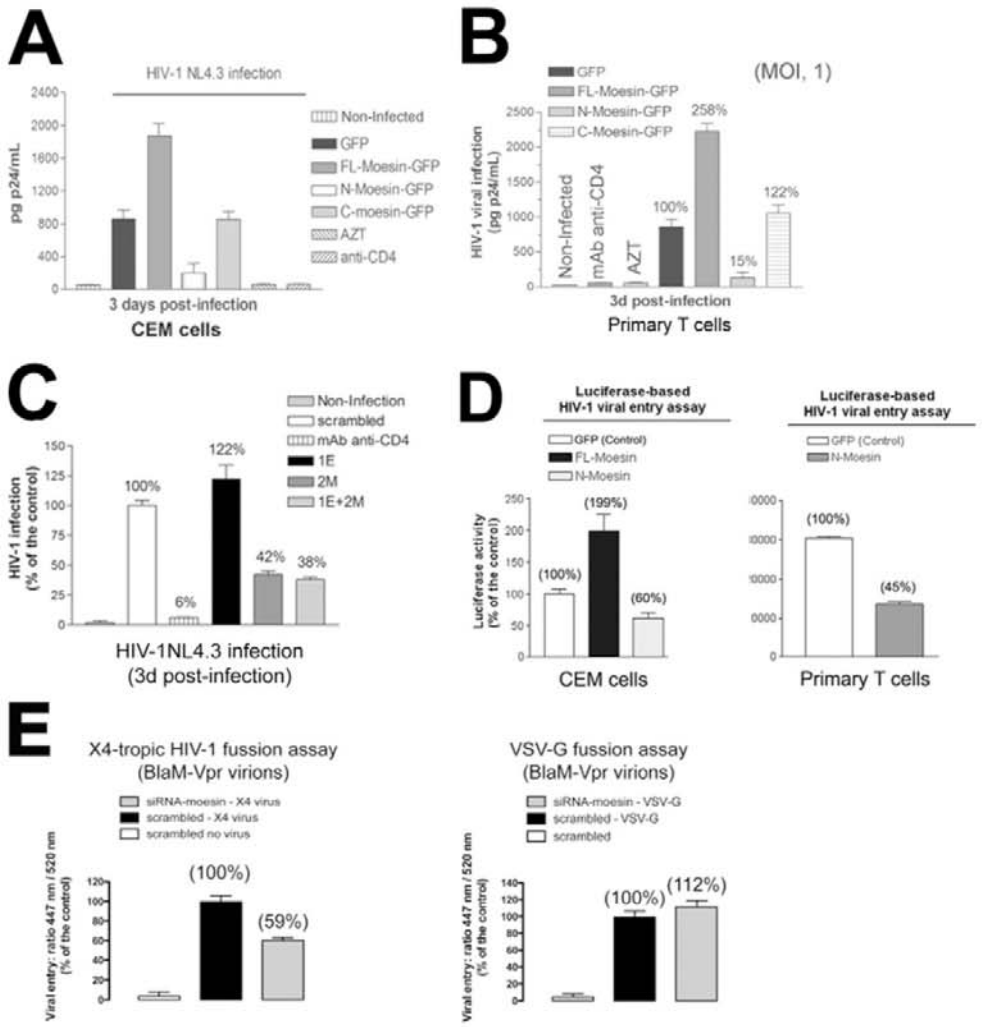

Fig. 4. Effect of overexpressed moesin-GFP proteins and moesin knockdown on HIV-1 infection and entry. (A) Effect of FL-, N- and C-moesin-GFP fusions on HIV-1 infection (MOI, 1) in CEM cells. GFP indicates transfection control for virus infection. As further controls, non-transfected cells were either not infected (non-infected) or infection was blocked with neutralizing anti-CD4 Ab (1 μg/ml) or AZT (5 μM). Data are the means ± s.e.m. of four independent experiments carried out in triplicate. (B) Effect of moesin-GFP fusions on HIV-1 infection of PHA-activated PBL (MOI, 1). GFP indicates transfection control for virus infection (defined as 100% infection). Data are the means ± s.e.m. of three independent experiments carried out in triplicate. (C) Effect of silencing endogenous ezrin and/or moesin expression on HIV-1 viral infection in CEM cells. Data are from three independent experiments carried out in triplicate, presented as means ± s.e.m. Scrambled indicates the control. When indicated, infection was inhibited with neutralizing anti-CD4 mAb. (D) Luciferase-based assay of viral entry by non-replicative HIV-1 particles in CEM T cells (left) or primary T cell blasts (right) overexpressing GFP (control, defined as 100% viral entry) or FL- or N-moesin-GFP fusions as indicated. Data are means ± s.e.m. of three independent experiments carried out in triplicate. (E) β-lactamase-based assay of viral entry by non-replicative HIV-1 particles in CEM T cells silenced for moesin (control, defined as 100% viral entry) with X4-tropic HIV-1 envelope (left panel) or VSV-G envelope (right panel). Data are means ± s.e.m. of three independent experiments carried out in triplicate.

HIV-$1_{NL4.3}$ strain. Whereas overexpression of FL-moesin strongly enhanced HIV-1 infection, the level of infection with C-moesin was similar to non-transfected or GFP-transfected permissive cells (Fig. 4A,B). CEM cells or primary T cells overexpressing the N-moesin product were less infected than controls (Fig. 4A,B). This finding was confirmed by infection of permissive moesin-silenced CEM cells; suppression of endogenous moesin, but not ezrin, inhibited HIV-1 infection (Fig. 4C; supplementary material Fig. S1B). The fact that the ezrin protein appears not to be involved in HIV-1-mediated viral infection might be explained by the low expression of this actin adaptor in T cells (Serrador et al., 1997) (and data not shown).

We next studied the involvement of moesin in the early steps of HIV-1 infection. To exclude any influence of possible effects at late steps in the infection cycle, we infected cells with a single-cycle virus bearing either the reporter gene Luciferase (Luc-HIV-1) (Gummuluru et al., 2002) or the reporter enzyme β-lactamase (Blam-HIV-1) (Cavrois et al., 2002). Non-replicative Luc-HIV-1 particles were incubated with CEM permissive cells or primary T lymphoblasts. Overexpression of FL-moesin potentiated the Luc-HIV-1 signal, whereas it was inhibited by overexpression of dominant-negative N-moesin (Fig. 4D). Therefore, the early steps of HIV-1 infection are regulated by moesin. Non-replicative Blam-HIV-1 virions were incubated with CEM permissive cells silenced

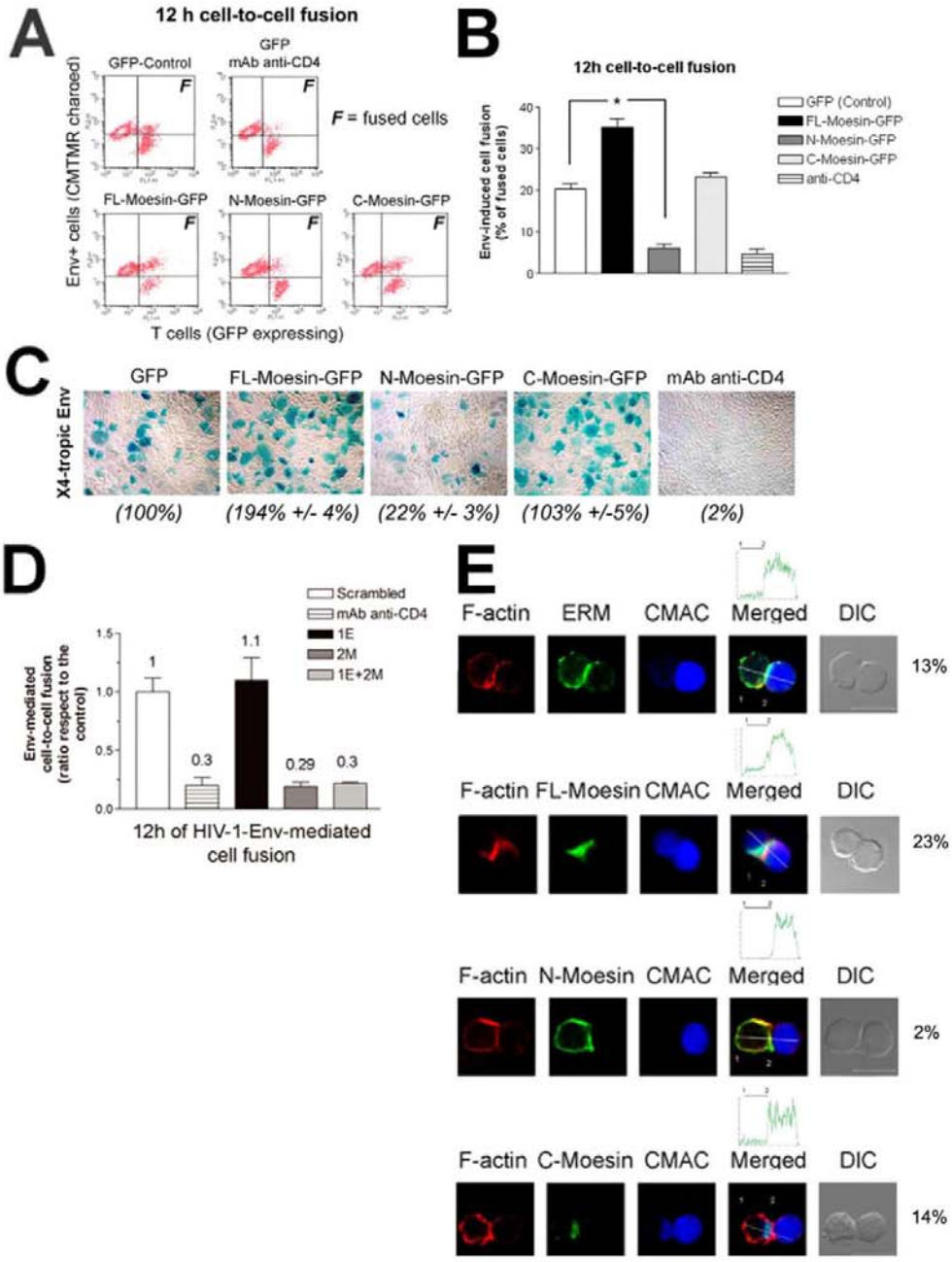

Fig. 5. Effect of moesin-GFP fusions on HIV-1 infection and HIV-1 Env-mediated cell-to-cell fusion. (A) Flow cytometry histograms show fusion (*F*) after 12 hours co-culture of Env+Jurkat-Hxbc2 cells and CEM cells overexpressing GFP (control) or FL-, N- or C-moesin-GFP fusions. A representative experiment of six is shown. (B) Quantification of six independent cell-to-cell fusion experiments as shown in A; bars show means ± s.e.m. **P*<0.01 using the Mann-Whitney U test. (C) A series of X-Gal staining showing Env-mediated membrane fusion of HeLa P4 cells, 24 hours after their lipotransfection with moesin-GFP constructs, and X4-tropic Env-HeLa 243 cells. A representative experiment of four is shown. GFP indicates transfection control for Env-induced cell fusion (100%). Quantification of three independent experiments (mean ± s.e.m., *n*=3) is shown in parentheses. (D) Effect of silencing endogenous ezrin and/or moesin on HIV-1 Env-mediated CEM-Hxbc2 cell fusion. When indicated, cell-to-cell fusion was inhibited by a neutralizing anti-CD4 mAb. Values are means ± s.e.m., *n*=4. Oligos are as indicated in Fig. 3; scrambled, non-specific RNA control sequence. (E) Confocal microscopy and quantification of Hxbc2-Env-mediated membrane fusion after 30 minutes. Localization of F-actin and endogenous ERM, and CMAC diffusion from Jurkat-derived Hxbc2 cells (blue cell to right) to the target CEM T cell (left); FL-moesin-GFP concentrates at cell-cell contacts where there is a strong accumulation of F-actin and CMAC diffuses better; N-moesin does not localize to cell contacts, impairing the redistribution of F-actin and cell-cell diffusion of CMAC; C-moesin-GFP concentrates at cell-cell contacts along with F-actin and CMAC cell-diffusion was observed. Histograms show quantification of CMAC fluorescence along the white lines (see merged pictures); segments between points 1 and 2 correspond to the cytoplasm of the target cell. The percentages represent the number of contacting cells showing redistribution per 200 cell-cell contacts counted.

for moesin to analyze the specific role of moesin in HIV-1 entry. Moesin knockdown rendered cells less susceptible to Blam-HIV-1 entry (Fig. 4E), indicating that moesin is necessary for the efficient entry of HIV-1. This process is mediated by the HIV-1 envelope because VSV-G virions penetrated equally in untreated and moesin-silenced target cells (Fig. 4E).

Moesin regulates X4-tropic HIV-1-mediated cell fusion and promotes fusion pore formation

The effect of the different moesin constructs on HIV-1-Env-dependent cell fusion was assessed in a quantitative T fusion assay, in which CEM T cells are the target for infection by Jurkat-Hxbc2 cells expressing functional X4-tropic Env. Overexpression of the N-moesin in CEM cells blocked cell fusion similarly to the neutralizing anti-CD4 mAb. By contrast, FL-moesin increased syncytia formation two- to threefold; overexpression of C-moesin did not significantly affect Env-mediated membrane fusion (Fig. 5A,B). Similar results were obtained in a HeLa-cell-based X4-tropic Env-induced fusion model (Fig. 5C).

We also assessed the involvement of ERM proteins in HIV-1 Env-mediated cell fusion by specific knockdown of lymphocyte ezrin and/or moesin protein expression. Suppression of endogenous moesin expression, but not ezrin, inhibited HIV-1 Env-mediated cell fusion (Fig. 5D).

To define the mechanism of moesin in fusion pore formation, we quantitatively assayed F-actin and moesin redistribution, as well

as dye diffusion from charged-Hxbc2-Env$^+$ cells to fused target cells. After 30 minutes, F-actin was recruited to the Env$^+$ cell-target cell contact area (Fig. 5E). ERM-*P* also accumulated in this region. Overexpression of functional FL-moesin accelerated dye diffusion from Env$^+$ cells to fused target cells, indicating enhanced membrane fusion. Moreover, F-actin recruitment to cell-cell contact areas was enhanced in cells expressing FL-moesin. By contrast, overexpression of N-moesin blocked F-actin redistribution and moesin phosphorylation at cell-cell contact areas. Moreover, N-moesin abrogated dye diffusion from Env$^+$ cells to associated T cells, indicating failure of membrane fusion. C-moesin did not affect F-actin redistribution or fusion pore formation. These results indicate that virus-activated moesin regulates an early step in HIV-1 infection by controlling fusion-pore formation, which is related to the capacity to reorganize F-actin and to promote HIV-1-Env-mediated CD4-CXCR4 interaction.

HIV-1 Env-mediated moesin activation promotes CD4-CXCR4 clustering and direct interaction

We next determined whether active moesin is involved in the HIV-1 Env-induced association of CD4-CXCR4, a process directly related to efficient viral fusion and infection (Lapham et al., 1996; Lee et al., 2000; Singer et al., 2001). The constitutive CD4-CXCR4 association (Lapham et al., 1999; Wang et al., 2004) was enhanced after gp120/CD4 engagement in CEM T cells (Fig. 6A; supplementary material Fig. S2). This gp120-induced CD4-CXCR4 association was further enhanced in cells overexpressing FL-moesin, but was blocked in cells overexpressing the dominant-negative N-moesin (Fig. 6A). CD4-CXCR4 association was also diminished in moesin-knockdown CEM T cells (Fig. 6B).

Clustering of CD4 and CXCR4 receptors during the first HIV-1 to cell contacts was assessed by confocal microscopy. HIV-1 induced an early co-distribution of CD4-CXCR4 (Fig. 6C). To further analyze how HIV-1 induces this polarization and clustering, the capping of the redistributed molecules was quantified over time by microscopy. ERMs and F-actin were the first to be recruited to the capping area, followed by CD4 and CXCR4 (Fig. 6D). Enhanced co-distribution of CD4-CXCR4 was observed in cells overexpressing FL-moesin construct (Fig. 6F), whereas the clustering in GFP-transfected cells was the same as in untransfected controls (Fig. 6E). The effect of C-moesin on receptor clustering varied in different experiments, inducing a slight enhancement of clustering (mean average 27% in C-moesin-transfected cells compared with 20% in control cells). However, no other functional effects were exerted by C-moesin in any other assays. Consistently, overexpression of N-moesin (Fig. 6E,F) or moesin mRNA silencing (Fig. 6G) impaired CD4 and CXCR4 redistribution at capping domains. Therefore, moesin regulates HIV-1-induced CD4 and CXCR4 clustering in permissive lymphocytes during the first virus-cell contacts, and this event correlates with the requirement of moesin activation for HIV-1 membrane fusion and infection.

Discussion

We have shown that HIV-1 activates endogenous ERM proteins during early viral infection. The rs-gp120 viral envelope proteins activate moesin and ezrin through interaction with CD4, but not with the CXCR4 co-receptor. Moesin phosphorylation in response to HIV-1 to T cell contact is required for cell fusion, and this is related to the capacity of phosphorylated moesin to promote CD4-CXCR4 interaction and the redistribution of F-actin and CD4-CXCR4 to sites of T-cell–virus contact. Jimenez-Baranda et al. have recently described a role for Filamin A, another actin binding protein, in the clustering of CD4-CXCR4 facilitated by the actin cytoskeleton. It is conceivable that several actin-binding proteins contribute to the regulation of transmembrane protein clustering through the actin cytoskeleton to provide the cell with the plasticity needed to respond to the environment.

The identity of the kinase responsible for moesin phosphorylation is not known. ROCK and PKC can phosphorylate ERM Thr residues in vitro (Bretscher, 1999; Nakamura et al., 1999), but the in vivo relevance of this has been controversial (Bretscher, 1999; Matsui et al., 1999; Yonemura et al., 2002). Results of the present study suggest that these kinases are not involved in HIV-1-mediated ERM phosphorylation. Increased moesin phosphorylation has been correlated with enhanced association of moesin with the cortical actin cytoskeleton (Simons et al., 1998). Moesin may thus potentiate HIV-1 Env-mediated F-actin to plasma membrane anchoring events at sites of virus to cell contact. Further studies are needed to identify the kinase or kinases that phosphorylate the C-terminal ERM-Thr in vivo in this Env-triggered CD4-signaling pathway.

Viral receptors on the surface of non-infected T cells rapidly polarize after contact with HIV-1-infected cells (Piguet and Sattentau, 2004), but the molecular signaling pathway that triggers this recruitment remains to be elucidated. The constitutive association between CD4 and CXCR4 (Lapham et al., 1999; Wang et al., 2004) is augmented after gp120-CD4 engagement. Remarkably, functional FL-moesin strongly enhanced the HIV-1 gp120-induced CD4-CXCR4 interaction and co-clustering at one pole of the lymphocyte, whereas dominant-negative N-moesin or moesin knockdown impaired this association. An important finding was that N-moesin overexpression inhibits HIV-1 Env-induced phosphorylation of endogenous moesin, thereby blocking rs-gp120- or HIV-1-induced F-actin reorganization and CD4-CXCR4 capping and interaction. Silencing of moesin impairs HIV-1 Env-mediated CD4-CXCR4 interaction, and inhibits HIV-1 viral entry and infection. By contrast, in T cells overexpressing FL-moesin, HIV-1 particles and rs-gp120 viral protein induce the formation of prominent pseudopodia, to which F-actin and CD4 and CXCR4 viral receptors redistributed. These FL-moesin-overexpressing cells were readily infected by HIV-1 replicative and non-replicative viral particles. It is thus conceivable that moesin controls the interaction of Env with CD4-CXCR4 by increasing the density of CD4-CXCR4 clusters at one pole of the cell. In turn, this would favor viral synapse and fusion-pore formation and therefore HIV-1 entry and infection.

F-actin disorganization negatively affects CD4-CXCR4 clustering and infection by X4-tropic viruses (Iyengar et al., 1998), and efficient HIV-1 viral spreading requires an intact F-actin skeleton (Jolly et al., 2007). It has recently been described that moesin and ezrin limit HIV-1 viral replication by affecting tubulin cytoskeleton at a post-entry step (Haedicke et al., 2008; Naghavi et al., 2007). Strikingly, in that study, dominant-negative N-moesin was equally as effective as the functional full-length protein at blocking viral replication, which apparently contradicts previous knowledge about how these proteins exert their function. Although the mechanism of inhibition by N-moesin, acting as a dominant negative, is not completely known, it is thought that the inhibitory activity of constructs containing only the FERM domain relies on the capacity of this domain to interact with the C-terminal regions of active endogenous ERM, thereby preventing their interaction with F-actin (reviewed by Bretscher, 1999). Therefore, when HIV-1 Env triggers moesin activation, a large fraction of the C-terminal exposed regions of endogenous moesin would be sequestered by the overexpressed

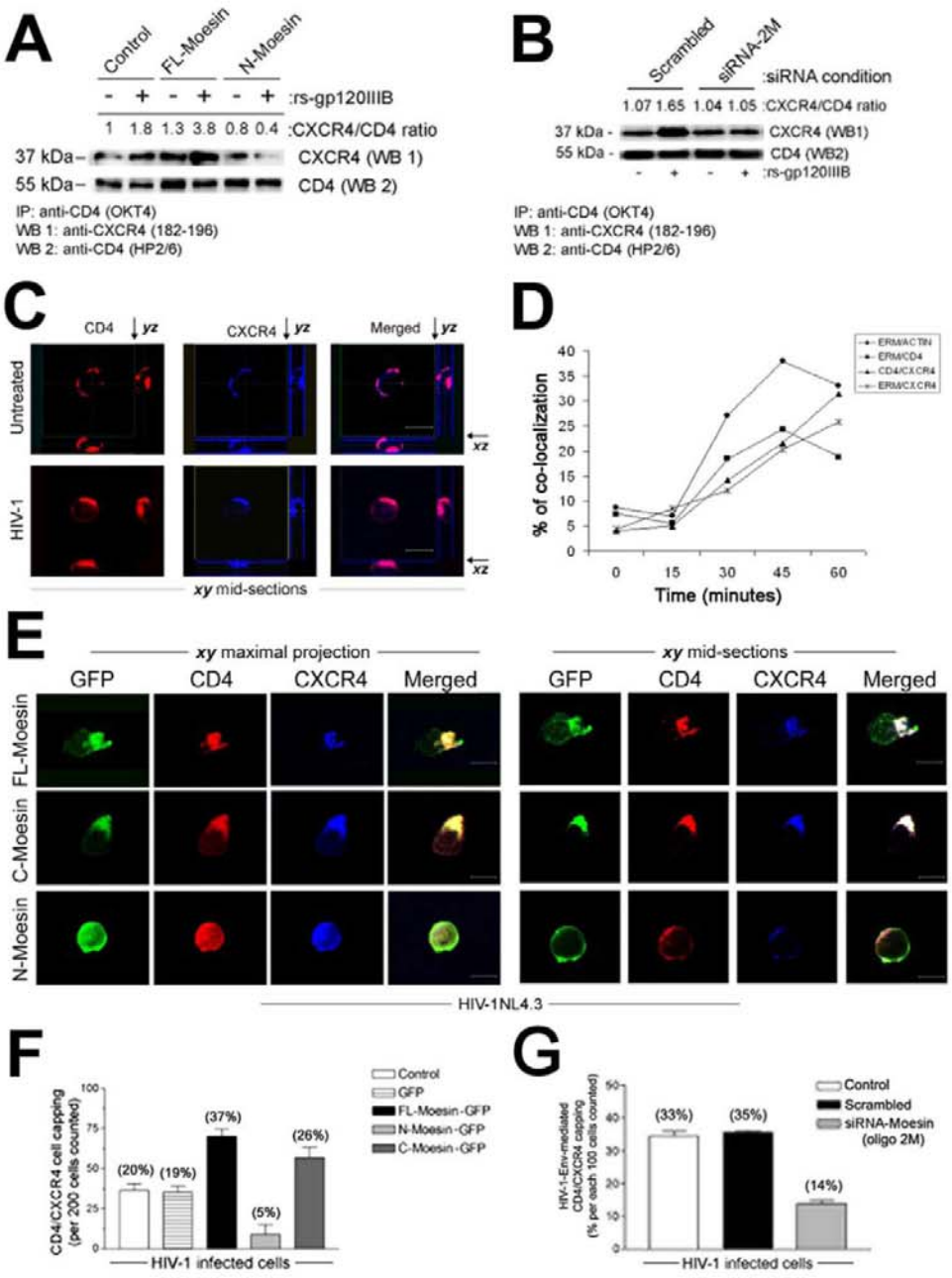

Fig. 6. Moesin drives HIV-1 Env-mediated CD4-CXCR4 interaction and polarized redistribution, during early viral infection. (A) Effect of FL- and N-moesin constructs on rs-gp120$_{IIIB}$ (10 μg/mL)-induced CD4/CXCR4 direct association. Immunoprecipitation assays were performed with anti-CD4 OKT4 mAb. Inducible co-immunoprecipitation of both receptors was measured as the ratio between the intensities of CXCR4 and CD4 immunoblotted bands. A representative experiment of three is shown. (B) Effect of the silencing of endogenous moesin on HIV-1 Env-induced direct CD4-CXCR4 interaction, in CEM cells. One representative experiment of three is shown. (C) Confocal microscopy of CD4 (anti-CD4 mAb HP2/6) and CXCR4 (biotin-conjugated mAb anti-CXCR4 12G5) in non-infected (Untreated) or 1 hour HIV-1-infected CEM cells (MOI, 1). The *yz* and *xz* planes are shown for each *xy* mid-section presented (arrows). Scale bars: 10 μm. (D) Percentage of colocalization of ERM and CD4, Actin or CXCR4, and of CD4 and CXCR4 in the presence of HIV-1 (MOI, 3) during a tim-course assay. (E) CD4 and CXCR4 redistribution in 1 hour HIV-1-infected cells overexpressing the different moesin-GFP proteins. *xy* maximal projections (left) and *xy* mid-sections (right) are shown. Scale bars: 10 μm. (F) Quantification of HIV-1-induced CD4-CXCR4 co-distribution in CEM T cells overexpressing FL-moesin-GFP and N-moesin-GFP constructs. (G) Quantification of HIV-1-induced CD4-CXCR4 capping in untransfected cells (Control), cells overexpressing the scrambled siRNA or lacking endogenous moesin (siRNA-moesin oligo 2). In F and G, quantification of HIV-1-induced CD4-CXCR4 capping is indicated as a percentage of each 200 and 100 cells counted, respectively, under each experimental condition.

FERM domain of the N-moesin construct. In agreement with our data, ERM proteins have very recently been identified as positive regulators of X4-tropic HIV-1 infection in non-lymphoid cell lines (Kubo et al., 2008). However, the molecular mechanism of the effects on HIV infection described in the study was not explored. Here, our study provides compelling evidence that ERM proteins regulate HIV-1-mediated membrane fusion and infection through the promotion of F-actin redistribution and the molecular association

and clustering of CD4 and CXCR4. Our results obtained from infection with single-cycle, non-replicative HIV-1 particles exclude effects that require late gene expression, and confirm the involvement of moesin in HIV-1 viral entry.

Our work suggests a model of moesin involvement in X4-tropic HIV-1 membrane fusion and infection of lymphocytes. In this model, HIV-1 virus activates lymphocyte moesin, as monitored by phosphorylation of Thr558. Activated moesin stabilizes and reorganizes F-actin, which may be necessary for CD4-CXCR4 colocalization at one pole of the cell. Activated moesin thus drives the HIV-1 Env-induced CD4-CXCR4 interaction. This process increases the probability of HIV-1 Env-CD4-CXCR4 interactions, potentiating fusion pore formation and thus HIV-1 viral fusion and infection. It is also conceivable that moesin-directed F-actin reorganization might drive the final steps of lipid mixing, perhaps by producing mechanical strain on the lipid bilayer (Eitzen, 2003), thus favoring viral fusion. In this regard, open-activated moesin allows F-actin anchoring in the plasma membrane, which is enhanced by FL-moesin and prevented by N-moesin. Interfering with this process inhibits HIV-1 viral fusion and infection. Therefore, the function of lymphocyte moesin is required for efficient HIV-1 viral fusion and infection.

Materials and Methods

Cells

The human $CD4^+$ $CXCR4^+$ CEM cell line was cultured in RPMI 1640 culture medium with 10% FCS. The Jurkat cell line expressing X4-tropic HIV-1-Hxbc2 Env under tetracycline-off regulation was kindly provided by the NIH-AIDS Reagent Program. Human peripheral blood lymphocytes (PBLs) were isolated from healthy donors using Ficoll-Hypaque density gradient centrifugation (GE Healthcare, Little Chalfont, UK). The PBLs were activated over 3 days with 1 μg/ml phytohemagglutinin (Murex Diagnostics, Norcross, GA), and then cultured with interleukin-2 (6 U/ml) as described (Valenzuela-Fernandez et al., 2005). The HeLa P4 cell clone, stably transfected with human CD4 cDNA and an HIV-LTR-driven β-gal reporter gene, were kindly provided by Marc Alizon (Hôpital Cochin, Paris, France). HeLa 243, also provided by M. Alizon, co-express Tat and X4-tropic Env HIV-1 proteins.

Antibodies and reagents

The anti-CD4 monoclonal antibody (mAb) HP2/6 and the non-neutralizing anti-CD4 v4-phycoerythrin mAb (PE) were previously described (Valenzuela-Fernandez et al., 2005). The neutralizing (OKT4A) and non-neutralizing (OKT4) anti-CD4 mAbs were from Ortho Diagnostic (Raritan, New Jersey). The biotin-conjugated mAb against human CXCR4 (12G5) was from Becton Dickinson Pharmingen (San Jose, CA), and anti-CXCR4 used for blots was Fusin 182-196 from Sigma (St Louis, MO). Anti-ezrin (C-19) sc-6407 is a goat polyclonal antibody (pAb) against human moesin and ezrin; and P-moesin (Thr 558) sc-12895 is a goat pAb against human moesin-*P* and ezrin-*P* at Thr558 and Thr567, respectively (Santa Cruz Biotechnology, Santa Cruz, CA). The specific anti-ezrin (4A5) sc-32759 is a mouse monoclonal antibody from Santa Cruz Biotechnology (Santa Cruz, CA). Specifc anti-moesin (38/87) ab3196 is a mouse monoclonal antibody from Abcam (Cambridge, UK). F-actin was detected with Alexa Fluor 568-labeled Phalloidin (Invitrogen, Carlsbad, CA). The anti-α-tubulin B-5-1-2 mAb and the anti-GFP pAb were from Sigma. The kinase inhibitors Ro-31-8220 (10 μM), Gö-6976 (1 μM) and Y-27632 (10 μM) were from Calbiochem (San Diego, CA). The inhibitory activity of these reagents has been tested appropriately.

Western blotting

Treated cells were resuspended in 60 μl MES buffer (10 mM MES at pH 7.4, 150 mM NaCl, 5 mM EGTA, 5 mM $MgCl_2$, 1 mM Na_3VO_4, 1 mM NaF, and a protease inhibitor cocktail (Roche Diagnostics, Mannheim, Germany), boiled for 5 minutes and immunoblotted with specific antibodies. Protein bands were analyzed using the LAS-1000 CCD system and Image Gauge 3.4 software (Fuji Photo Film Co., Tokyo, Japan).

Actin polymerization assay

Actin polymerization was analyzed as described previously (Vicente-Manzanares et al., 2004). Briefly, 24 hours after transfection, CEM T cells were fixed to stop intracellular actin polymerization with a solution containing 4% formaldehyde in PBS, 1% Triton X-100, and 5 μg/ml Alexa Fluor 647-phalloidin from Molecular Probes (Eugene, OR). Cells were incubated for 15 minutes at 37°C and washed once in PBS, and the intracellular polymerized actin was then determined with a FACScan flow cytometer (BD Biosciences, Mountain View, CA) using CellQuest software.

Immunofluorescence

Cells were fixed and permeabilized for 3 minutes in 2% formaldehyde, 0.5% Triton X-100 in PBS, and then immunostained for total ERM, P-ERM, CD4, CXCR4 or F-actin.

Moesin recombinant DNA constructs and cell transfection

Human FL-moesin-GFP, GFP-FL-moesin, N-moesin-GFP and C-moesin-GFP constructs were kindly provided by Heinz Furthmayr (Stanford University, CA) (Amieva et al., 1999). Plasmids were nucleofected into cells with Amaxa kits V (for CEM T cells) and T (for primary T cells) (Amaxa, Koeln, Germany) and transfected cells were used 24 hours after transfection. Percentages of positive nucleofected cells ranged between 40% and 70%.

HIV-1 viral preparation and infection

Preparation of $HIV\text{-}1_{NL4.3}$ and measurement of viral replication were performed as described (Valenzuela-Fernandez et al., 2005). Highly infectious preparations of $HIV\text{-}1_{NL4.3}$ viral strain were generated by several consecutive passages of the original HIV-1 isolates in peripheral blood mononuclear cells (PBMCs). Briefly, PBMCs were infected with one synchronous dose of $HIV\text{-}1_{NL4.3}$, and culture supernatants were recovered 3 days later and stored at −70°C. Freshly thawed aliquots were filtered through 0.22 μm filters before use. $HIV\text{-}1_{NL4.3}$ entry at multiplicity of infection (MOI=1) was assayed in phytohemagglutinin (PHA; 1 μg/ml)-activated PBLs or CEM T cells for 90 minutes. Cells were then trypsinized and extensively washed with fresh medium to remove viral input. Infected cells were kept in culture, and viral entry and infection was monitored every 48 hours by measuring the concentration of p24 in the culture supernatant by enzyme-linked immunosorbent assay (Innotest HIV-1 antigen mAb; Innogenetic, Ghent, Belgium). When indicated, permissive cells were pretreated with anti-CD4 mAbs (5 μg/ml) or 3′-azido-2′,3′-dideoxythymidine (AZT) (5 μg/ml) before addition of virus.

Luciferase virus assay

Luciferase-HIV-1 viral particles deficient for replication were kindly provided by Suryaram Gummuluru (Boston University, Boston, MA). Replication-deficient viral particles were produced by transfecting a luciferase-expressing reporter virus, $HIV/\Delta nef/\Delta env/luc^+$, which contains the luciferase gene inserted into the *nef* ORF and does not express *env* glycoprotein (Yamashita and Emerman, 2004), with a CXCR4-tropic (Lai) *env* glycoprotein. Virus stocks were generated by PolyFect transient transfection of HEK293T cells (Gummuluru and Emerman, 2002). Two days after transfection, cell-free virus-containing supernatants were clarified of cell debris and concentrated by centrifugation (16,000 ***g*** 1 hour at 4°C) and stored at −80°C until required. HIV-1 virus preparations were titrated by ELISA and determination of the $p24^{Gag}$ content. Untreated or nucleofected CEM or PBLs activated over 2 days with PHA (1 μg/ml), were infected with a synchronous dose of luciferase-based virus for 2 hours. Virus was removed by washing infected cells. After 32 hours of infection, luciferase activity was determined with a luciferase assay kit (Promega Corporation, Madison, WI) and a 1450 Microbeta Luminescence Counter (Walax, Trilux). Protein contents were measured by the bicinchoninic acid method (BCA protein assay kit from Pierce, Rockford, IL) according to the manufacturer's instructions.

Production of non-replicative viral particles containing BlaM-Vpr

X4-tropic HIV-1 viral particles deficient for replication and containing the BlaM-Vpr chimera were produced by co-transfecting HEK293T cells with the following vectors: pNL4-3.Luc.R-E (20 μg; NIH-AIDS Reagent Program); CXCR4-tropic (HXB2-env; NIH-AIDS Reagent Program) env glycoprotein vector (10 μg) and the pCMV-BlaM-Vpr vector (10 μg). The BlaM-Vpr chimera was kindly provided by Warner C. Greene (University of California, San Francisco, CA). Co-transduction of the pNL4-3.Luc.R-E- (20 μg) vector with the pHEF-VSV-G (10 μg; NIH-AIDS Reagent Program) and pCMV-BlaM-Vpr (10 μg) vectors was used to generate non-replicative viral particles that fuse with cells in a VSV-G-dependent manner. Viral plasmids were transduced in HEK293T cells by using linear polyethylenimine with an average molecular mass of 25 kDa (PEI25k) (Polyscience, Warrington, PA). The PEI25k was prepared as a 1 mg/ml solution in water and adjusted to neutral pH. After addition of PEI25k to the viral plasmids (at a plasmid: PEI25k ratio of 1:5 w/w), the solution was mixed immediately, incubated for 20-30 minutes at room temperature and then added to HEK293T cells in culture. Viruses were harvested 40 hours after transfection. The supernatant was clarified by centrifugation at 3000 rpm for 30 minutes. Viral stocks were normalized by p24-Gag content measured by ELISA (Innogenetics, Gent, Belgium).

Virion-based fusion assay

1×10^6 CEM T permissive cells were incubated for 3 hours with equivalent viral inputs of BlaM-Vpr-containing virions (500 ng of p24) in 500 μl RPMI-1640 medium. Cells were then extensively washed to remove free virions and incubated (1 hour, room temperature) with CCF2-AM loading mix, as recommended by the manufacturer (GeneBLAzer™ detection kit; Invitrogen, Carlsbad, CA). Next, excess dye was

washed off and cells were incubated for 16 hours at room temperature prior to fixation with 4% paraformaldehyde. The percentages of cells infected were determined by measuring the fluorescence intensities of intact and cleaved CCF2 probe in virus-infected CCF2-loaded target cells in a fluorescence spectrophotometer (Cary Eclipse, Varian; Melbourne, Australia). An increase in the ratio of blue (447 nm; cleaved CCF2) to green (520 nm; intact CCF2) fluorescent signals indicates more virions fused to target cells. The background blue and green fluorescence was determined in non-infected CCF2-loaded cells (without β-lactamase activity).

CXCR4-CD4 capping assay

For capping assays, cells were co-cultured with the HIV-$1_{NL4.3}$ strain (MOI, 1) or with rs-$gp120_{IIIB}$ (5 μg/ml) for 1 hour at 37°C as described previously (Gordon-Alonso et al., 2006). Viral particles were then washed out and the cells were fixed with 2% paraformaldehyde. CD4 and CXCR4 were detected by immunofluorescence, and molecule distribution was analyzed with a Leica TCS-SP confocal microscope (Leica. Heidelberg, Germany).

CD4-CXCR4 co-immunoprecipitation

Parental or moesin-nucleofected cells were treated with rs-$gp120_{IIIB}$ (5 μg/ml) for 1 hour at 37°C. Cells were lysed at 4°C (1% CHAPS and a protease inhibitor cocktail), precleared, and incubated overnight at 4°C with anti-CD4 OKT4 mAb non-covalently complexed to protein-G-Sepharose. Co-immunoprecipitated proteins were blotted with anti-CXCR4 rabbit pAb, and reprobed after membrane stripping with HP2/6 anti-CD4 mAb.

mRNA silencing

Double-stranded siRNAs were generated against the following mRNA sequences: 5′-uccacuauguggauaauaa-3′ (1E; ezrin) 5′-agaucgaggaacagacuaa-3′ (2M; moesin) (Pust et al., 2005), (Eurogentec, Seraing, Belgium). Oligo 1M was purchased from Santa Cruz Biotechnology (moesin siRNA Ref: sc-35955). Cells were nucleofected with 1 μM siRNA and assayed 24 hours later. Irrelevant scrambled siRNA (Eurogentec) served as a control. Interference in ERM protein expression was sustained for at least 96 hours.

HIV-1 Env-mediated cell-cell fusion assays

A dual-fluorescence cell-fusion assay was also performed as described previously (Gordon-Alonso et al., 2006). Briefly, CMTMR-loaded Env+Jurkat-Hxbc2 cells were mixed with Calcein-AM-loaded parental or transfected CEM cells. The double-labeled cells were detected 6 or 12 hours later by flow cytometry. The target cells were then washed extensively to remove the drugs before co-culturing with Env-expressing cells. Anti-CD4 mAb (5 μg/ml for 30 minutes at 37°C) was used as a control for the blockage of cell fusion. The extent of fusion was calculated as the percentage fusion=(number of bound cells positive for both dyes/number of bound cells positive for calcein-labeled target cells) × 100. The β-Galactosidase and X-Gal staining cell fusion assays in the HeLa system were performed as described (Gordon-Alonso et al., 2006).

We thank M. López-Cabrera for helpful comments on the manuscript and Rafael Samaniego for confocal microscopy analyses. Editorial support was provided by S. Bartlett. This work was supported by grants BFU2005-08435/BMC, FIPSE 36289/02 (Fundación para la Investigación y Prevención del SIDA en España), Ayuda a la Investigación Básica 2002 (Fundación Juan March) and Fundación Lilly (to F.S-M.). A.V-F. was supported by grants FIPSE 24508/05, FMM (Fundación Mutua Madrileña, Spain), FIS-PI050995 from the Instituto de Salud Carlos III, Ministerio de Sanidad y Consumo, Spain, and IDT-TF-06/066 and IDT-TF-06/063 from Gobierno Autónomo de Canarias, Spain and Fondo Social Europeo (FSE; RYC2002-3018). We also thank J.M. Serrador and M. Pérez-Martinez for their support.

References

Algrain, M., Turunen, O., Vaheri, A., Louvard, D. and Arpin, M. (1993). ezrin contains cytoskeleton and membrane binding domains accounting for its proposed role as a membrane-cytoskeletal linker. *J. Cell Biol.* **120**, 129-139.

Amieva, M. R., Litman, P., Huang, L., Ichimaru, E. and Furthmayr, H. (1999). Disruption of dynamic cell surface architecture of NIH3T3 fibroblasts by the N-terminal domains of moesin and ezrin: *in vivo* imaging with GFP fusion proteins. *J. Cell Sci.* **112**, 111-125.

Barreiro, O., Yanez-Mo, M., Serrador, J. M., Montoya, M. C., Vicente-Manzanares, M., Tejedor, R., Furthmayr, H. and Sanchez-Madrid, F. (2002). Dynamic interaction of VCAM-1 and ICAM-1 with moesin and ezrin in a novel endothelial docking structure for adherent leukocytes. *J. Cell Biol.* **157**, 1233-1245.

Bretscher, A. (1999). Regulation of cortical structure by the ezrin-radixin-moesin protein family. *Curr. Opin. Cell Biol.* **11**, 109-116.

Campbell, E. M., Nunez, R. and Hope, T. J. (2004). Disruption of the actin cytoskeleton can complement the ability of Nef to enhance human immunodeficiency virus type 1 infectivity. *J. Virol.* **78**, 5745-5755.

Cavrois, M., De Noronha, C. and Greene, W. C. (2002). A sensitive and specific enzyme-based assay detecting HIV-1 virion fusion in primary T lymphocytes. *Nat. Biotechnol.* **20**, 1151-1154.

Chishti, A. H., Kim, A. C., Marfatia, S. M., Lutchman, M., Hanspal, M., Jindal, H., Liu, S. C., Low, P. S., Rouleau, G. A., Mohandas, N. et al. (1998). The FERM domain: a unique module involved in the linkage of cytoplasmic proteins to the membrane. *Trends Biochem. Sci.* **23**, 281-282.

Doms, R. W. (2000). Beyond receptor expression: the influence of receptor conformation, density, and affinity in HIV-1 infection. *Virology* **276**, 229-237.

Eitzen, G. (2003). Actin remodeling to facilitate membrane fusion. *Biochim. Biophys. Acta* **1641**, 175-181.

Fievet, B. T., Gautreau, A., Roy, C., Del Maestro, L., Mangeat, P., Louvard, D. and Arpin, M. (2004). Phosphoinositide binding and phosphorylation act sequentially in the activation mechanism of ezrin. *J. Cell Biol.* **164**, 653-659.

Gary, R. and Bretscher, A. (1995). ezrin self-association involves binding of an N-terminal domain to a normally masked C-terminal domain that includes the F-actin binding site. *Mol. Biol. Cell* **6**, 1061-1075.

Gordon-Alonso, M., Yanez-Mo, M., Barreiro, O., Alvarez, S., Munoz-Fernandez, M. A., Valenzuela-Fernandez, A. and Sanchez-Madrid, F. (2006). Tetraspanins CD9 and CD81 modulate HIV-1-induced membrane fusion. *J. Immunol.* **177**, 5129-5137.

Gummuluru, S. and Emerman, M. (2002). Advances in HIV molecular biology. *AIDS* **16 Suppl. 4**, S17-S23.

Gummuluru, S., KewalRamani, V. N. and Emerman, M. (2002). Dendritic cell-mediated viral transfer to T cells is required for human immunodeficiency virus type 1 persistence in the face of rapid cell turnover. *J. Virol.* **76**, 10692-10701.

Haedicke, J., de Los Santos, K., Goff, S. P. and Naghavi, M. H. (2008). The ERM family member ezrin regulates stable microtubule formation and retroviral infection. *J. Virol.* **82**, 4665-4670.

Heiska, L., Alfthan, K., Gronholm, M., Vilja, P., Vaheri, A. and Carpen, O. (1998). Association of ezrin with intercellular adhesion molecule-1 and -2 (ICAM-1 and ICAM-2). Regulation by phosphatidylinositol 4, 5-bisphosphate. *J. Biol. Chem.* **273**, 21893-21900.

Helander, T. S., Carpen, O., Turunen, O., Kovanen, P. E., Vaheri, A. and Timonen, T. (1996). ICAM-2 redistributed by ezrin as a target for killer cells. *Nature* **382**, 265-268.

Hirao, M., Sato, N., Kondo, T., Yonemura, S., Monden, M., Sasaki, T., Takai, Y., Tsukita, S. and Tsukita, S. (1996). Regulation mechanism of ERM (ezrin/radixin/moesin) protein/plasma membrane association: possible involvement of phosphatidylinositol turnover and Rho-dependent signaling pathway. *J. Cell Biol.* **135**, 37-51.

Iyengar, S., Hildreth, J. E. and Schwartz, D. H. (1998). Actin-dependent receptor colocalization required for human immunodeficiency virus entry into host cells. *J. Virol.* **72**, 5251-5255.

Jimenez-Baranda, S., Gomez-Mouton, C., Rojas, A., Martinez-Prats, L., Mira, E., Ana Lacalle, R., Valencia, A., Dimitrov, D. S., Viola, A., Delgado, R. et al. (2007). Filamin-A regulates actin-dependent clustering of HIV receptors. *Nat. Cell Biol.* **9**, 838-846.

Jolly, C., Kashefi, K., Hollinshead, M. and Sattentau, Q. J. (2004). HIV-1 cell to cell transfer across an Env-induced, actin-dependent synapse. *J. Exp. Med.* **199**, 283-293.

Jolly, C., Mitar, I. and Sattentau, Q. J. (2007). Requirement for an intact T-cell actin and tubulin cytoskeleton for efficient assembly and spread of human immunodeficiency virus type 1. *J. Virol.* **81**, 5547-5560.

Kubo, Y., Yoshii, H., Kamiyama, H., Tominaga, C., Tanaka, Y., Sato, H. and Yamamoto, N. (2008). ezrin, Radixin, and moesin (ERM) proteins function as pleiotropic regulators of human immunodeficiency virus type 1 infection. *Virology* **375**, 130-140.

Kuhmann, S. E., Platt, E. J., Kozak, S. L. and Kabat, D. (2000). Cooperation of multiple CCR5 coreceptors is required for infections by human immunodeficiency virus type 1. *J. Virol.* **74**, 7005-7015.

Lapham, C. K., Ouyang, J., Chandrasekhar, B., Nguyen, N. Y., Dimitrov, D. S. and Golding, H. (1996). Evidence for cell-surface association between fusin and the CD4-gp120 complex in human cell lines. *Science* **274**, 602-605.

Lapham, C. K., Zaitseva, M. B., Lee, S., Romanstseva, T. and Golding, H. (1999). Fusion of monocytes and macrophages with HIV-1 correlates with biochemical properties of CXCR4 and CCR5. *Nat. Med.* **5**, 303-308.

Lee, S., Lapham, C. K., Chen, H., King, L., Manischewitz, J., Romantseva, T., Mostowski, H., Stantchev, T. S., Broder, C. C. and Golding, H. (2000). Coreceptor competition for association with CD4 may change the susceptibility of human cells to infection with T-tropic and macrophagetropic isolates of human immunodeficiency virus type 1. *J. Virol.* **74**, 5016-5023.

Manes, S., del Real, G., Lacalle, R. A., Lucas, P., Gomez-Mouton, C., Sanchez-Palomino, S., Delgado, R., Alcami, J., Mira, E. and Martinez, A. C. (2000). Membrane raft microdomains mediate lateral assemblies required for HIV-1 infection. *EMBO Rep.* **1**, 190-196.

Mangeat, P., Roy, C. and Martin, M. (1999). ERM proteins in cell adhesion and membrane dynamics. *Trends Cell Biol.* **9**, 187-192.

Matsui, T., Maeda, M., Doi, Y., Yonemura, S., Amano, M., Kaibuchi, K., Tsukita, S. and Tsukita, S. (1998). Rho-kinase phosphorylates COOH-terminal threonines of ezrin/radixin/moesin (ERM) proteins and regulates their head-to-tail association. *J. Cell Biol.* **140**, 647-657.

Matsui, T., Yonemura, S., Tsukita, S. and Tsukita, S. (1999). Activation of ERM proteins in vivo by Rho involves phosphatidyl-inositol 4-phosphate 5-kinase and not ROCK kinases. *Curr. Biol.* **9**, 1259-1262.

Naghavi, M. H., Valente, S., Hatzioannou, T., de Los Santos, K., Wen, Y., Mott, C., Gundersen, G. G. and Goff, S. P. (2007). moesin regulates stable microtubule formation and limits retroviral infection in cultured cells. *EMBO J.* **26**, 41-52.

Nakamura, F., Huang, L., Pestonjamasp, K., Luna, E. J. and Furthmayr, H. (1999). Regulation of F-actin binding to platelet moesin *in vitro* by both phosphorylation of threonine 558 and polyphosphatidylinositides. *Mol. Biol. Cell* **10**, 2669-2685.

Pearson, M. A., Reczek, D., Bretscher, A. and Karplus, P. A. (2000). Structure of the ERM protein moesin reveals the FERM domain fold masked by an extended actin binding tail domain. *Cell* **101**, 259-270.

Piguet, V. and Sattentau, Q. (2004). Dangerous liaisons at the virological synapse. *J. Clin. Invest.* **114**, 605-610.

Pontow, S. E., Heyden, N. V., Wei, S. and Ratner, L. (2004). Actin cytoskeletal reorganizations and coreceptor-mediated activation of rac during human immunodeficiency virus-induced cell fusion. *J. Virol.* **78**, 7138-7147.

Pust, S., Morrison, H., Wehland, J., Sechi, A. S. and Herrlich, P. (2005). Listeria monocytogenes exploits ERM protein functions to efficiently spread from cell to cell. *EMBO J.* **24**, 1287-1300.

Serrador, J. M., Alonso-Lebrero, J. L., del Pozo, M. A., Furthmayr, H., Schwartz-Albiez, R., Calvo, J., Lozano, F. and Sanchez-Madrid, F. (1997). moesin interacts with the cytoplasmic region of intercellular adhesion molecule-3 and is redistributed to the uropod of T lymphocytes during cell polarization. *J. Cell Biol.* **138**, 1409-1423.

Simons, P. C., Pietromonaco, S. F., Reczek, D., Bretscher, A. and Elias, L. (1998). C-terminal threonine phosphorylation activates ERM proteins to link the cell's cortical lipid bilayer to the cytoskeleton. *Biochem. Biophys. Res. Commun.* **253**, 561-565.

Singer, II, Scott, S., Kawka, D. W., Chin, J., Daugherty, B. L., DeMartino, J. A., DiSalvo, J., Gould, S. L., Lineberger, J. F., Malkowitz, L. et al. (2001). CCR5, CXCR4, and CD4 are clustered and closely apposed on microvilli of human macrophages and T cells. *J. Virol.* **75**, 3779-3790.

Steffens, C. M. and Hope, T. J. (2003). Localization of CD4 and CCR5 in living cells. *J. Virol.* 77, 4985-4991.

Takeuchi, K., Sato, N., Kasahara, H., Funayama, N., Nagafuchi, A., Yonemura, S., Tsukita, S. and Tsukita, S. (1994). Perturbation of cell adhesion and microvilli formation by antisense oligonucleotides to ERM family members. *J. Cell Biol.* **125**, 1371-1384.

Valenzuela-Fernandez, A., Alvarez, S., Gordon-Alonso, M., Barrero, M., Ursa, A., Cabrero, J. R., Fernandez, G., Naranjo-Suarez, S., Yanez-Mo, M., Serrador, J. M. et al. (2005). Histone deacetylase 6 regulates human immunodeficiency virus type 1 infection. *Mol. Biol. Cell* **16**, 5445-5454.

Vicente-Manzanares, M., Viton, M. and Sanchez-Madrid, F. (2004). Measurement of the levels of polymerized actin (F-actin) in chemokine-stimulated lymphocytes and GFP-coupled cDNA transfected lymphoid cells by flow cytometry. *Methods Mol. Biol.* **239**, 53-68.

Wang, J., Alvarez, R., Roderiquez, G., Guan, E. and Norcross, M. A. (2004). Constitutive association of cell surface CCR5 and CXCR4 in the presence of CD4. *J. Cell Biochem.* **93**, 753-760.

Yamashita, M. and Emerman, M. (2004). Capsid is a dominant determinant of retrovirus infectivity in nondividing cells. *J. Virol.* **78**, 5670-5678.

Yonemura, S., Nagafuchi, A., Sato, N. and Tsukita, S. (1993). Concentration of an integral membrane protein, CD43 (leukosialin, sialophorin), in the cleavage furrow through the interaction of its cytoplasmic domain with actin-based cytoskeletons. *J. Cell Biol.* **120**, 437-449.

Yonemura, S., Matsui, T., Tsukita, S. and Tsukita, S. (2002). Rho-dependent and -independent activation mechanisms of ezrin/radixin/moesin proteins: an essential role for polyphosphoinositides *in vivo*. *J. Cell Sci.* **115**, 2569-2580.

Yonezawa, A., Cavrois, M. and Greene, W. C. (2005). Studies of ebola virus glycoprotein-mediated entry and fusion by using pseudotyped human immunodeficiency virus type 1 virions: involvement of cytoskeletal proteins and enhancement by tumor necrosis factor alpha. *J. Virol.* **79**, 918-926.

Journal of Cell Science

SUPPLEMENTAL DATA

Legend to supplemental Figure S1 – Two different siRNA oligonucleotide sequences against Moesin impaired HIV-1 infection. (A) Western blot analysis of specific silencing of endogenous expression of Moesin with two different siRNA sequences (Oligos 1M and 2M) 48 hours after siRNA-oligo nucleofection of CEM cells. Silencing of Moesin expression is quantified as the band intensity ratios to α-tubulin. Scrambled indicates the siRNA-oligo control. (B) Effect of silencing endogenous Moesin expression on HIV-1 viral infection in CEM cells by using two independent and different siRNA oligonucleotides (Oligo 1M and Oligo 2M). Data are from one representative experiment carried out in duplicate. Scrambled indicates the siRNA oligo control.

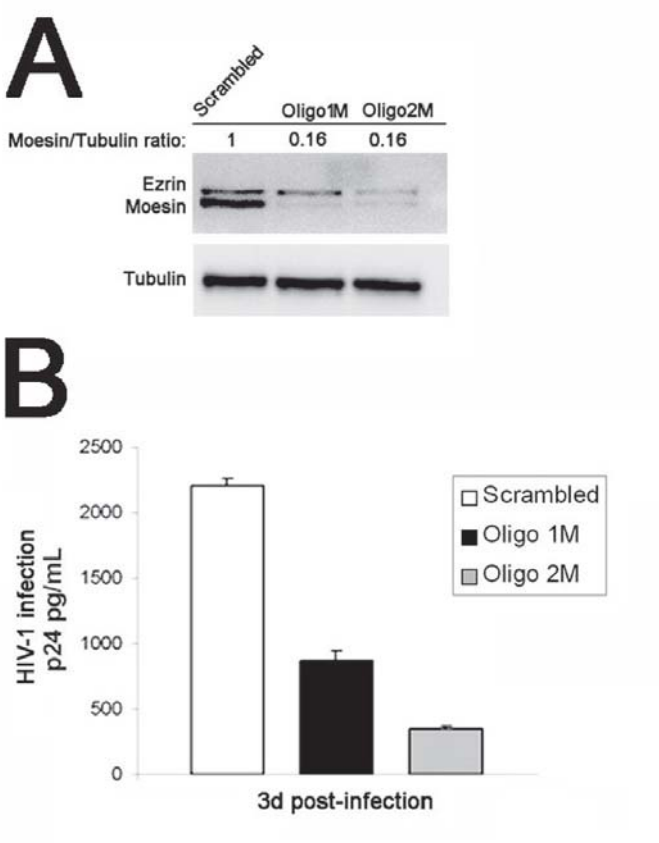

Supplemental Figure S1

Legend to supplemental Figure S2 – Time-course analysis for gp120-induced CD4/CXCR4 interaction in CEM cells. The CD4-CXCR4 association was enhanced after gp120/CD4 engagement, peaking at 60 minutes after gp120 (10 µg/ml) exposure. One representative experiment out of three is shown.

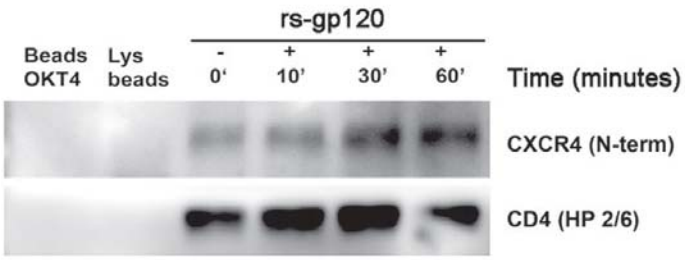

Supplemental Figure S2

3.2. LA ACTIVACIÓN DE LA QUINASA PI4P5-K Iα ES NECESARIA PARA LA ENTRADA E INFECCIÓN EFICIENTE DE CÉLULAS T $CD4^+$ POR EL VIH-1

Además de la remodelación del citoesqueleto de actina en sí mismo mediante la acción directa de las proteínas de unión a actina en respuesta a señales externas, cabe destacar que la transmisión de estas señales se produce precisamente a través de la membrana plasmática hacia el citoesqueleto de actina. Las moléculas reguladoras más importantes y versátiles presentes en la membrana plasmática que participan en la transmisión de señales al citoesqueleto de actina son el fosfatidilinositol y sus derivados fosforilados. Estas moléculas tienen diversas funciones en la modulación de eventos celulares como el tráfico de membrana, señalización intracelular, organización del citoesqueleto celular y apoptosis (Niggli, 2005).

El derivado forforilado más importante es el $PI(4,5)P_2$ (PIP_2), constituyendo entre un 0,3-1,5% de los fosfolípidos presentes en la membrana plasmática y más del 99% de los fosfoinositoles di-fosforilados. La cantidad de PIP_2 parece ser relativamente constante en una célula, pero se han detectado cambios dinámicos en la concentración de PIP_2 presente en regiones de fagocitosis y en "*ruffles"* de membrana (Botelho et al., 2000; Ling et al., 2006).

Las funciones específicas asociadas al PIP_2 constituyen el agrupamiento de complejos de señalización, mantenimiento de la adhesión entre la membrana plasmática y el citoesqueleto de actina, remodelación del citoesqueleto de actina, generación de segundos mensajeros intracelulares, regulación de canales iónicos, endocitosis y exocitosis, señalización a través de integrinas, citocinesis, morfología y movilidad celular, apoptosis y fagocitosis (revisado en (Saarikangas et al., 2010)).

El PIP_2 se une, a partir de su grupo principal fosforilado, a una amplia variedad de proteínas de unión a actina regulando su localización y actividad subcelular (revisado en (Saarikangas et al., 2010; Yin and Janmey, 2003)), sugiriéndose que éste podría controlar la unión o comunicación entre la membrana plasmática y el citoesqueleto de actina cortical (Raucher et al., 2000). La interacción del PIP_2 con varias de estas proteínas puede provocar el agrupamiento del PIP_2, que a su vez resulta en la formación de microdominios de membrana donde se concentran el PIP_2 y otras proteínas específicas necesarias para el ensamblaje de complejos multimoleculares de activación y señalización celular (revisado en (Saarikangas et al.,

2010; Yin and Janmey, 2003)). De manera general, el PIP_2 inhibe la acción de aquellas proteínas encargadas de romper los filamentos de actina y activa a proteínas encargadas de la polimerización de actina (revisado en (Yin and Janmey, 2003)), mientras que el secuestro del PIP_2 lleva a un defecto en la adhesión entre la membrana plasmática con el citoesqueleto de actina cortical (Raucher et al., 2000). Además, el PIP_2 también es considerado como un marcador que distingue la membrana plasmática de otras organelas intracelulares más enriquecidas en otros fosfolípidos (revisado en (Saarikangas et al., 2010)).

Además de ser el principal segundo mensajero intracelular, el PIP_2 también es el precursor, a través de su hidrólisis por la PLC, de otros importantes segundos mensajeros como el diacilglicerol (DAG) y el inositol-1,4,5-trifosfato (IP3), y de fosfatidilinositol-3,4,5-trifosfato (PIP_3), generado a partir de la acción de PI3K, los cuales van a activar otras rutas de señalización que van a terminar en la remodelación del citoesqueleto de actina. El IP3 va a dar lugar a la liberación de Ca^{2+} de los reservorios intracelulares, o en algunos casos de los canales de Ca^{2+} presentes en la membrana plasmática y que dependen del Ca^{2+} intracelular. Por otro lado, el DAG va a activar, junto con el Ca^{2+} liberado, a la PKC. El DAG puede ser también ser convertido ácido fosfatídico (PA) a partir de la acción de la enzima DAG quinasa, activando otros efectores como la propia quinasa generadora de PIP_2, la PI4P5-K, y otros efectores celulares. Por último, otros mecanismos de disipación del PIP_2 consisten en su conversión a PI(4)P por la acción de synaptojanina y Ocrl, o la disipación del PIP_2 generado por difusión (revisado en (Huang and Sauer, 2010; Mao and Yin, 2007)).

El nivel celular de PIP_2 depende de un balance entre su síntesis y su disipación, regulado espacial y temporalmente. El PIP_2 es generado, principalmente, a partir de la acción de la quinasa PI4P5-K (tipo I: α, β, γ), utilizando como sustrato el PI(4)P. La quinasa PI4P5-K de tipo I se encuentra localizada principalmente en la membrana plasmática. Existen tres isoformas de la quinasa PI4P5-K de tipo I (Iα, Iβ y Iγ), cada una de las cuales con variantes de procesamiento (Mao and Yin, 2007). Esta amplia variedad sugiere que la regulación diferencial de las diferentes isoformas de la quinasa PI4P5-K de tipo I, podría permitir a las células dirigir específicamente la producción de PIP_2 en procesos y localizaciones celulares específicas. Los linfocitos humanos expresan dos isoformas de la quinasa PI4P5-K de tipo I, Iα y Iβ (Oude Weernink et al., 2004). La isoforma Iα se ha mostrado localizada específicamente en "*ruffles*" de membrana, mientras que la isoforma Iβ parece localizarse principalmente en estructuras vesiculares citoplasmáticas (revisado en (Kwiatkowska, 2010)). Así, por

lo tanto, parece que la quinasa PI4P5-K Iα es la principal isoforma implicada en la producción del PIP_2 asociado a la membrana plasmática.

Varios grupos de investigación han demostrado que el PIP_2 asociado a la membrana plasmática es crucial para el ensamblaje del virus VIH-1 (Chukkapalli et al., 2008; Ono et al., 2004). El anclaje del VIH-1 a la membrana plasmática es mediado por la localización en membrana de la proteína precursora de Gag, $Pr55^{Gag}$, de manera dependiente de PIP_2 (Chukkapalli et al., 2008). La rotura de este PIP_2 por medio de la sobreexpresión de la enzima polifosfoinositidol (polyphosphoinositide) 5-fosfatasa IV (5ptasaIV) induce la redistribución de la proteína Gag madura desde la membrana plasmática hacia compartimentos positivos para el marcador CD63, reduciéndose la producción viral de VIH-1 (Chukkapalli et al., 2008).

A pesar de la función de la membrana plasmática como la barrera inicial de la entrada viral, poco se sabe sobre el papel que puede desempeñar el PIP_2 de membrana durante los primeros estadios de unión y entrada viral. De manera destacable, recientemente nuestro laboratorio ha mostrado que el tráfico funcional de vesículas de PIP_2 dependiente de la GTPasa Arf6 es necesario para la entrada eficiente del VIH-1 en la célula diana, afectando de manera crítica a la dinámica de la membrana plasmática en las zonas de entrada viral, controlando la fusión virus-célula entre la membrana inerte viral y la bioregeneradora celular ((Garcia-Exposito et al., 2011), y ANEXO 2).

RESULTADOS

Los resultados indican que la producción de PIP_2 inducida por la envuelta del VIH-1 y dependiente de la quinasa PI4P5-K Iα es necesaria para la regulación de la infección por partículas virales X4 y R5 trópicas del VIH-1 durante los primeros estadios del ciclo viral, concretamente la fusión y entrada del VIH-1.

Las partículas virales de VIH-1, a través de la acción de la proteína viral de envuelta gp120, estimula la producción de PIP_2 durante los primeros contactos entre el virus y los linfocitos T permisivos $CD4^+/CXCR4^+$. Se observó un pico máximo de producción de PIP_2 a los 30 minutos, seguido de un rápido descenso de los niveles detectados. Además, la producción de PIP_2 inducida por la proteína de la envuelta viral depende de su unión a CD4 y no a CXCR4, confirmado por el bloqueo efectivo en la producción de PIP_2 mediante la utilización de un anticuerpo neutralizante anti-CD4 (OKT4A), y no por empleo de un anticuerpo no neutralizante anti-CD4 (OKT4) o por el

bloqueo funcional de CXCR4 con el antagonista AMD3100. De acuerdo con estos resultados, se observó que el PIP_2 producido se acumulaba en la zona de contacto entre células permisibles con células que expresan la envuelta del VIH-1. Esta relocalización del PIP_2 (detectado mediante la sonda GFP-PHD) coincidió con el reclutamiento de F-actina y de la enzima PI4P5-K Iα dependiente de la envuelta del VIH-1. A continuación, se observó que la producción de PIP_2 inducida por gp120 era potenciada por la quinasa PI4P5-K Iα y por la quinasa PI4P5-K Iβ, mientras que la sobreexpresión de la construcción mutante inactiva D227-(D/A)-PI4P5-K Iα, pero no la construcción mutante inactiva D268-(D/A)-PI4P5-K Iβ, bloqueó la producción de PIP_2 mediada por rs-$gp120_{IIIB}$. Además, la expresión superficial de los receptores para el VIH-1 (CD4, CXCR4 y CCR5) no se vio afectada en ninguna de las condiciones experimentales. Por otro lado, se observó un incremento en la producción de VIH-1 determinada tres días post-infección en linfocitos primarios que sobreexpresan la construcción activa de la PI4P5-K Iα, mientras que se observó una inhibición en células que sobreexpresan el mutante inactivo de la quinasa. Estudios con partículas de VIH-1 de un solo ciclo de infección, que contienen el gen reportero *luciferasa* o la proteína quimérica BlaM-Vpr, indican que la sobreexpresión de la construcción activa de PI4P5-K Iα incrementó la fusión y la entrada viral, en comparación con las células control, mientras que el dominante negativo la disminuyó. Por último, la interferencia específica de la enzima PI4P5-K Iα generó una inhibición significativa de la infección por el VIH-1 en células T. Estos datos experimentales indican que la producción de PIP_2 mediada por PI4P5-K Iα, en las zonas de contacto virus-célula, está involucrada directamente en la regulación la infección por el VIH-1 en los primeros estadios del ciclo de vida viral, antes del ensamblaje y liberación de nuevas partículas virales, quizás por modificación de la fluidez de membrana plasmática.

MATERIALES Y MÉTODOS

Los tipos celulares utilizados durante el estudio fueron: líneas celulares T CEM (células linfoblásticas T de leucemia, $CD4^+/CXCR4^+$); líneas celulares T CEM.NKR-CCR5 ($CD4^+/CXCR4^+/CCR5^+$); PBL aislados de donantes sanos mediante centrifugación en un gradiente de Ficoll; y líneas celulares Jurkat que expresa la envuelta X4 trópica del VIH-1 Hxbc2 o la línea celular inactiva para la fusión Jurkat ΔKS que expresa únicamente la proteína Rev viral y sin Env. Para los ensayos funcionales se utilizaron anticuerpos específicos de CD4 neutralizantes y no neutralizantes, un anticuerpo señalizador a través de CD3 (OKT3), bloqueates de

CXCR4 (AMD3100) y anticuerpos específicos para detectar las isoformas de las quinasas PI4P5-K Iα/Iβ y el PIP_2 celular. Además se utilizó el colorante vital CMAC para observar su difusión como consecuencia de la formación del poro de fusión dependiente de la envuelta del VIH-1. En algunos ensayos se utilizó una proteína de envuelta X4 trópica gp120 recombinante soluble (rs-$gp120_{IIIB}$) para la estimulación de las células diana $CD4^+$. Se utilizaron las construcciones de las proteínas funcionales de PI4P5-K Iα y PI4P5-K Iβ, y sus respectivos mutantes D227A-(D/A)-PI4P5-K Iα y D268A-PI4P5-K Iβ. Además, se emplearon secuencias de ARN interferentes específicas para la PI4P5-K Iα. Se utilizó la nucleofección como la técnica para la introducción de las construcciones de ADN plasmídico y los ARNi en la célula diana. Se utilizó un sistema "*dot-blot*" junto con anticuerpos anti-PIP_2 para detectar el PIP_2 generado en la célula en cada condición experimental. La microscopía de fluorescencia confocal se utilizó para monitorizar la localización del PIP_2, de la F-actina, de la PI4P5-K Iα y la difusión del colorante CMAC durante la formación del poro de fusión. La técnica de "*western blot*" nos permite detectar la sobreexpresión de las quinasas PI4P5-K en comparación con los niveles endógenos, y el nivel de interferencia específica de PI4P5-K Iα endógena. Por citometría de flujo se determinó el nivel de expresión superficial de CD4, CXCR4 y CCR5 en las células diana en cada condición experimental. Por último, las células 293T se utilizaron para la producción de partículas virales de un único ciclo de infección, deficientes en replicación, que contienen el gen luciferasa (vector HIV/Δ*nef*/Δ*env*/Luc^+ pseudotipado con envueltas X4, R5 y VSV-G), o partículas virales con la proteína quimérica BlaM-Vpr, utilizadas para comparar el nivel de fusión y entrada viral en las células diana en cada condición experimental.

The Journal of Immunology

PI4P5-Kinase Iα Is Required for Efficient HIV-1 Entry and Infection of T Cells[1]

Marta Barrero-Villar,* Jonathan Barroso-González,† J. R. Cabrero,* Mónica Gordón-Alonso,* Susana Álvarez-Losada,‡ M. A. Muñoz-Fernández,‡ Francisco Sánchez-Madrid,[2]* and Agustín Valenzuela-Fernández[2]*†

HIV-1 envelope (Env) triggers membrane fusion between the virus and the target cell. The cellular mechanism underlying this process is not well known. Phosphatidylinositol 4,5-bisphosphate (PIP_2) is known to be important for the late steps of the HIV-1 infection cycle by promoting Gag localization to the plasma membrane during viral assembly, but it has not been implicated in early stages of HIV-1 membrane-related events. In this study, we show that binding of the initial HIV-1 Env-gp120 protein induces PIP_2 production in permissive lymphocytes through the activation of phosphatidylinositol-4-phosphate 5-kinase (PI4P5-K) Iα. Overexpression of wild-type PI4P5-K Iα increased HIV-1 Env-mediated PIP_2 production and enhanced viral replication in primary lymphocytes and CEM T cells, whereas PIP_2 production and HIV-1 infection were both severely reduced in cells overexpressing the kinase-dead mutant D227A (D/A)-PI4P5-K Iα. Similar results were obtained with replicative and single-cycle HIV-1 particles. HIV-1 infection was also inhibited by knockdown of endogenous expression of PI4P5-K Iα. These data indicate that PI4P5-K Iα-mediated PIP_2 production is crucial for HIV-1 entry and the early steps of infection in permissive lymphocytes. *The Journal of Immunology,* **2008, 181: 6882–6888.**

Phosphatidylinositol (4, 5)-bisphosphate (PIP_2)[3] is a second messenger that binds, through its phosphorylated headgroup, to a variety of effector molecules and regulates their function and cellular localization. Several highly conserved phosphoinositide-binding sequences have been characterized, among which are the pleckstrin homology domain (PHD) and band four-point-one ezrin-radixin-moesin domain (1, 2). PIP_2 has also been reported to bind to a plethora of actin-binding proteins (3, 4), suggesting that it may control the link between the plasma membrane and cortical actin cytoskeleton (5, 6).

The major route for PIP_2 synthesis is the phosphorylation of phosphatidylinositol 4-phosphate (PI4P) by type I phosphatidylinositol 4-phosphate 5-kinases (PI4P5-K I) (7–9). Three PI4P5-K I isoforms (Iα, Iβ, and Iγ) have been reported, each having alternative splice variants (10, 11). This variety suggests that differential regulation of PI4P5-K I isoforms may enable cells to direct PIP_2 production for specific processes and to specific locations. Lymphocytes express two PI4P5-K I isoforms, PI4P5-K Iα and Iβ (7). Human PI4P5-K Iα has been shown to specifically localize to Rac1-induced membrane ruffles, whereas PI4P5-K Iβ is excluded from these structures and is detected primarily in cytosolic vesicular structures (12, 13). It therefore appears that PI4P5-K Iα is primarily involved in the production of PIP_2 related to the plasma membrane.

Plasma membrane-associated PIP_2 has been shown to be crucial for HIV-1 viral assembly (14–16). Anchorage of HIV-1 assembly to the plasma membrane is mediated by the PIP_2-dependent membrane localization of the Gag precursor protein $Pr55_{Gag}$ (14). Disruption of PIP_2 by overexpression of polyphosphoinositide 5-phosphatase IV (5ptaseIV) induces a redistribution of mature Gag from the plasma membrane to CD63-positive compartments and markedly reduces HIV-1 viral production (15, 17).

As the initial barrier to viral entry, the plasma membrane is also of fundamental importance in the initial stages of the viral cycle; however, little is known about the potential role of PIP_2 during viral attachment and entry to the target cell. In this study, we examine whether PI4P5-K Iα and associated PIP_2 production affect the early steps of the HIV-1 cycle. Our results suggest that HIV-1 viral particles, through the action of envelope (Env)-gp120 viral protein, trigger PIP_2 production in a PI4P5-K Iα-dependent manner during viral contact. Overexpression of wild-type (wt) PI4P5-K Iα enhances Env-induced PIP_2 production and HIV-1 infection, whereas these events are impaired by overexpression of an inactive mutant or PI4P5-K Iα silencing. These findings indicate that PI4P5-K Iα-mediated PIP_2 production is involved in the regulation of HIV-1 viral infection during the first steps of the viral cycle, before viral assembly and egress.

*Servicio de Inmunología, Hospital Universitario de La Princesa, Madrid, †Departamento de Medicina Física y Farmacología. Facultad de Medicina, Universidad de La Laguna, Tenerife, and ‡Servicio de Inmuno-Biología Molecular, Hospital General Universitario Gregorio Marañón, Madrid, Spain

Received for publication May 16, 2008. Accepted for publication September 5, 2008.

The costs of publication of this article were defrayed in part by the payment of page charges. This article must therefore be hereby marked *advertisement* in accordance with 18 U.S.C. Section 1734 solely to indicate this fact.

[1] This work was supported by Grants BFU2005-08435/BMC, FIPSE 36289/02 and 36658/07 (Fundación para la Investigación y Prevención del SIDA en España), "Ayuda a la Investigación Básica 2002" (Fundación Juan March), and "Fundación Lilly" (to F.S.-M.). A.V.-F. was supported by Grants FIPSE 24508/05, Fundación Mutua Madrileña, Spain, FIS-PI050995 from the "Instituto de Salud Carlos III, Ministerio de Sanidad y Consumo," Spain, and IDT-TF-06/066 and IDT-TF-06/063 from the "Consejería de Industria, Comercio y Nuevas Tecnologías del Gobierno Autónomo de Canarias," Spain, and "Fondo Social Europeo (RYC2002-3018)."

[2] Address correspondence and reprint requests to Francisco Sánchez-Madrid and Agustín Valenzuela-Fernández, Servicio de Inmunología, Hospital Universitario de La Princesa, Madrid, Spain. E-mail addresses: fsanchez.hlpr@salud.madrid.org and avalenzu@ull.es

[3] Abbreviations used in this paper: PIP_2, phosphatidylinositol 4,5-biphosphate; PI4P5-K type Iα, phosphatidylinositol 4-phosphate 5-kinase type Iα; PHD, pleckstrin homology domain; Env, envelope; wt, wild type; HA, hemagglutinin; MOI, multiplicity of infection; siRNA, short interference RNA.

Materials and Methods

Cells

The human $CD4^+/CXCR4^+$ CEM (acute lymphoblastic T cell leukemia) cell line was cultured in RPMI 1640 culture medium-10% FCS. The Jurkat cell line expressing X4-tropic HIV-1-Hxbc2 Env under tetracycline-off regulation, the fusion-inactive control Jurkat ΔKS cells expressing only the Rev viral protein, and CEM.NKR-CCR5 permissive cells were kindly provided by National Institutes of Health-AIDS Reagent Program. Human PBLs were isolated from healthy donor blood by Ficoll-Hypaque density gradient centrifugation (GE Healthcare). The PBLs were activated over 3 days with 1 μg/ml PHA (Murex Diagnostics) and then cultured with IL-2 (6 U/ml) as described (18).

Abs and reagents

The anti-CD4 HP2/6 mAb and non-neutralizing Ab were as described (18). Neutralizing anti-CD4 (OKT4A) was purchased from Ortho Diagnostic. The anti-CD3 OKT3 mAb was a gift from B. Alarcón (Centro de Biología Molecular, Madrid, Spain). The HRP-labeled anti-PIP_2 mAb Z-H045 was from Echelon Biosciences. The anti-PI4P5-K I (E-16, sc-11783), the anti-PI4P5-K Iα (C-17, sc-11774), and the anti-influenza hemagglutinin (HA) mAb (F-7, sc-7392) were from Santa Cruz Biotechnology. The cell tracker CMAC was from Molecular Probes. Recombinant soluble X4-tropic (rs)-HIV-1 gp120 viral protein (rs-gp120)-IIIB was obtained from either National Institutes of Health AIDS Research and Reference Reagent Program or Innogenetics, and was produced in either baculovirus or *Escherichia coli*, respectively. Both viral proteins similarly induced the production of PIP_2 at a dose of 5 μg/ml. AMD3100 was purchased from Sigma-Aldrich.

Type I PI4P5-K recombinant DNA constructs and cell transfection

Constructs encoding HA-tagged wt-PI4P5-K Iα, HA-tagged wt-PI4P5-K Iβ, and the HA-tagged kinase-dead mutants D227A (D/A)-PI4P5-K Iα and D268A-PI4P5-K Iβ were kindly provided by Dr. C. Lewis Cantley (Harvard Institute of Medicine, Boston, MA). The N-terminally GFP-tagged PHD from phosphatidylinositol-specific-phospholipase $C\gamma_1$ (GFP-PHD) was kindly provided by Dr. T. Balla (National Institutes of Health, Bethesda, MA). The PI4P5-K Iα and GFP-PHD constructs were nucleofected into cells using AMAXA kits (Amaxa), and cells were used 24 h posttransfection.

PIP_2 production

Cells (1×10^6) were equilibrated in RMPI 1640 complete medium containing 10 mM LiCl and then exposed to 5 μg/ml rs-$gp120_{IIIB}$. For the blocking experiments, cells were pretreated with neutralizing anti-CD4 or AMD3100 for 30 min at 37°C. Cells were lysed in MES buffer (10 mM MES (pH 7.4), 150 mM NaCl, 5 mM EGTA, 5 mM $MgCl_2$, 1 mM Na_3VO_4, 1 mM NaF, and a protease inhibitor mixture (Roche Diagnostics)) containing 1% SDS and 10 mM LiCl at different point times (from 0 to 2 h). Lysates were spotted onto nitrocellulose membranes with a dot-blot apparatus (Bio-Rad), and PIP_2 bands were probed with the anti-PIP_2 Ab Z-H045.

Luciferase viral entry assay

Luciferase-HIV-1 viral particles deficient for replication were kindly provided by Dr. Gummuluru (Boston University, Boston, MA). Replication-deficient viral particles were derived by the luciferase expressing reporter virus HIV/Δnef/Δenv/luc+ (which contains the *luciferase* gene inserted into the *nef* ORF and does not express *env* glycoprotein (19)) with a CXCR4-tropic (Lai) *env* glycoprotein. Virus stocks were generated by PolyFect transient transfection of 293T cells (20) Two days posttransfection, cell-free virus-containing supernatants were clarified of cell debris, concentrated by centrifugation (16,000 × *g*, 1 h at 4°C), and stored at −80°C until required. HIV-1 virus preparations were titrated by ELISA and determination of the $p24_{Gag}$ content. Untreated or nucleofected CEM or PBLs (activated over 2 days with PHA (1 μg/ml)) were infected with a synchronous dose of luciferase-based virus for 2 h. Virus was removed by washing infected cells. After 32 h of infection, luciferase activity was determined with a luciferase assay kit (Promega) and a 1450 MicroBeta Luminiscence Counter (Walax, Trilux). Protein contents were measured by the bicinchoninic acid method (BCA protein assay kit; Pierce) according to the manufacturer's instructions.

HIV-1 preparation and infection

Preparation of $HIV\text{-}1_{NL4.3}$ and measurement of viral replication were performed as described (18) Highly infectious preparations of $HIV\text{-}1_{NL4.3}$ viral strain were generated by several consecutive passages of the original HIV-1 isolates in PBMC. Briefly, PBMCs were infected with one synchronous dose of $HIV\text{-}1_{NL4.3}$, and culture supernatants were recovered 3 days later and stored at −70°C. Freshly thawed aliquots were filtered through 0.22-μm filters before use. $HIV\text{-}1_{NL4.3}$ entry and multiplicity of infection (MOI, 1) was assayed in PHA (1 μg/ml)-activated PBLs or CEM T cells over 90 min. Cells were then trypsinized and extensively washed with fresh medium to remove viral input. Next, infected cells were kept in culture and viral entry and infection was monitored every 48 h by measuring the concentration of p24 in the culture supernatant by enzyme-linked immunosorbent assay (INNOTEST HIV-1 Ag mAb; Innogenetic). When indicated, permissive cells were pretreated with neutralizing anti-CD4 mAb (5 μg/ml) or 3′-azido-2′,3′-dideoxythymidine (5 μM) before addition of virus.

Production of nonreplicative viral particles containing BlaM-Vpr

X4- or R5-tropic HIV-1 viral particles deficient for replication and containing the BlaM-Vpr chimera were produced by cotransfecting 293T cells (70% confluence) in 75 cm^2 flasks the following vectors: pNL4–3.Luc.R-E- (20 μg; National Institutes of Health-AIDS Reagent Program); a CXCR4-tropic (HXB2-env; National Institutes of Health-AIDS Reagent Program) or CCR5-tropic (pCAGGS SF162 gp160; National Institutes of Health-AIDS Reagent Program) *env* glycoprotein vector(10 μg); and the pCMV-BlaM-Vpr vector (10 μg). The BlaM-Vpr chimera was kindly provided by Dr. Warner C. Greene (University of California, San Francisco, CA). Cotransduction of the pNL4–3.Luc.R-E- (20 μg) vector with the pHEF-VSV-G (10 μg; National Institutes of Health-AIDS Reagent Program) and pCMV-BlaM-Vpr (10 μg) vectors was used to generate nonreplicative viral particles that fuse with cells in a VSV-G-dependent manner. Viral plasmids were transduced in 293T cells by using linear polyethylenimine with an average molecular mass of 25kDa (PEI25k) (Polyscience). For this, viral plasmids were first dissolved in 1/10 of the final tissue culture volume of DMEM, free of serum and antibiotics. The PEI25k was prepared as a 1-mg/ml solution in water and adjusted to neutral pH. After addition of PEI25k to the viral plasmids (at a plasmid: PEI25k ratio of 1:5 (w/w)), the solution was mixed immediately, incubated for 20–30 min at room temperature, and then added to 293T cells in culture. After 4 h, the medium was changed to RPMI 1640, supplemented with 10% FCS and antibiotics, and the cells were cultivated to allow viral production. Viruses were harvested 40 h posttransfection. The supernatant was clarified by centrifugation at 3000 rpm for 30 min. Virions were then stored at −80°C. Viral stocks were normalized by p24-Gag content measured by ELISA (Innogenetics).

Virion-based fusion assay

A total of 1×10^6 CEM.NKR-CCR5 permissive cells were incubated 3 h with equivalent viral inputs of BlaM-Vpr-containing virions (500 ng of p24) in 500 μl RPMI 1640 medium. Cells were then extensively washed to remove free virions and incubated (1 h, room temperature) with CCF2-AM loading mix, as recommended by the manufacturer (GeneBLAzer detection kit; Invitrogen). Next, excess dye was washed off and cells were incubated for 16 h at room temperature before fixation with 4% paraformaldehyde. Then, 8×10^5 cells were placed in a 96-well plate per each experimental condition. The associated emission light to cleaved CCF2 (blue; 447 nm) and intact CCF2 probe (green; 520 nm) was measured. The entry of Blam-Vpr containing virions was measured as the ratio of the maximum fluorescence intensity between cleaved and intact CCF2. Thereby, an increase in this ratio indicates more fused viruses with target cells. The percentage of 100% of infection was determined by measuring the fluorescence intensities of intact and cleaved CCF2 probe in control infected cells (scrambled or pCDNA.3 transfected cells) and subtracting the background blue and green fluorescecence ratio determined in noninfected cells (without β-lactamase activity), as proposed by the manufacturer virus-infected (GeneBLAzer detection kit; Invitrogen).

Western blot

Treated cells were resuspended in 60 μl MES buffer, boiled for 5 min, and immunoblotted with anti-HA specific Ab. Protein bands were analyzed using the LAS-1000 CCD system and Image Gauge 3.4 software (Fuji Photo Film).

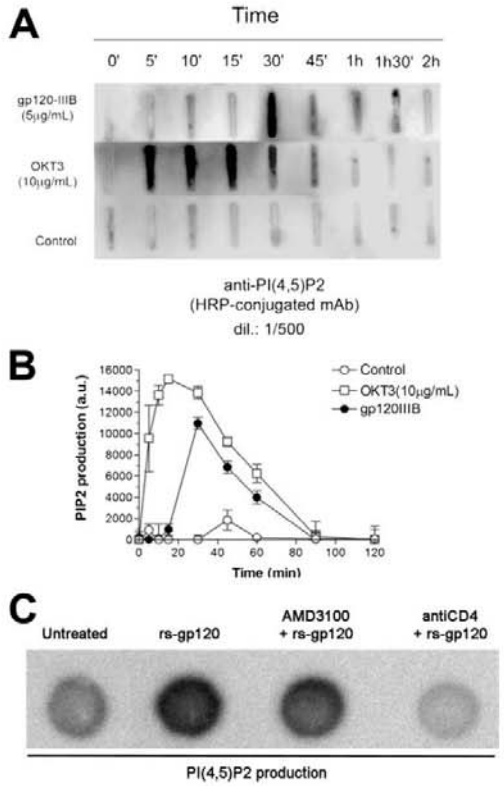

FIGURE 1. HIV-1-Env gp120 viral protein triggers PIP_2 production through CD4. *A*, Dot-blot analysis of rs-$gp120_{IIIB}$-induced PIP_2 production (*gp120-IIIB*), PIP_2 production after CD3 engagement (*OKT3*), and basal PIP_2 (untreated cells; *Control*) in CEM cells; a representative experiment of three is shown. CEM T cells were treated with 5 μg/ml rs-gp120 during the time-course. *B*, Quantification of PIP_2 production in three independent experiments. Data are means ± SEM. *C*, Dot-blot analysis of rs-$gp120_{IIIB}$-induced PIP_2 production in CEM T cells in the presence or absence of a neutralizing anti-CD4 mAb (OKT4A) or the CXCR4 antagonist AMD3100. A representative experiment of three is shown.

Immunofluorescence monitoring of PIP_2 during fusion-pore formation

For HIV-1 Env-mediated PIP_2 accumulation during fusion-pore formation, CMAC-charged Hxbc2-Env+ cells and nucleofected CEM cells were cocultured for 30 min (1:1 ratio) at 37°C. PIP_2-enriched plasma membranes during Env-mediated membrane fusion were monitored with the GFP-PHD biosensor (21). CMAC diffusion from Hxbc2-Env+ cells toward contacting cells was quantified by confocal microscopy.

mRNA silencing

Double-stranded short interference RNAs (siRNA) were generated against the following mRNA sequences of PI4P5-K Iα: 5′-uaggccaua gaaguguuga-3′ (*siRNA-1*; PI4P5-K Iα) and 5′-acacaguacucaguugaua-3′ (*siRNA-2*; PI4P5-K Iα) (Eurogentec). siRNA (1 μM) was nucleofected into cells, and assays were performed 24 h later. Irrelevant scrambled siRNA (Eurogentec) served as a control. Interference of PI4P-5K Iα expression was sustained for at least 96 h.

Results

HIV-1 Env-gp120 viral protein specifically triggers PIP_2 production in target cells

To assess the ability of HIV-1 to activate PIP_2 production in T cells, we incubated permissive $CD4^+/CXCR4^+$ CEM T cells with recombinant soluble X4-tropic (rs)-HIV-1 gp120 viral protein (rs-gp120). Cells were harvested over a time course (0–2 h), and cell lysates were analyzed for PIP_2 production (Fig. 1). Although untreated control cells did not accumulate PIP_2, treatment with rs-$gp120_{IIIB}$ specifically triggered PIP_2 production, with a peak at 30 min followed by a rapid decline (Fig. 1*A* and quantified in *B*). Correct metabolism of PIP_2 was confirmed in parallel positive control experiments with CD3; specific CD3 engagement with OKT3 Ab induced a strong peak of PIP_2 production after 10–15 min, as described (22), which thereafter declined (Fig. 1, *A* and *B*).

To further analyze gp120 induction of PIP_2 production, we performed the experiment in the presence of either a neutralizing anti-CD4 mAb or the CXCR4 antagonist AMD3100, to specifically block gp120 signal through CD4 or CXCR4. Although AMD3100 was functionally inhibiting CXCR4 signaling (data not shown), there was no significant effect in PIP_2 production after of rs-gp120 incubation. However, exposure to the neutralizing anti-CD4 mAb (OKT4A) effectively blocked gp120-induced PIP_2 production (Fig. 1*C*).

We next analyzed whether PIP_2 is produced during HIV-1 Env-mediated membrane fusion. To address this point, we used a cell-to-cell fusion system in which target T cells (CEM) are coincubated with Env+ cells (Hxbc2 Jurkat). To monitor PIP_2 localization during cell-to-cell contacts, target cells were transfected with GFP-PHD, which acts as a PIP_2 biosensor (21) (Fig. 2*A*). We also analyzed Env-induced membrane fusion by monitoring the diffusion of the cytoplasmic probe CMAC from charged-Hxbc2-Env+ cells to fused target cells. After 30 min of cell-to-cell contact, PIP_2 in the target cell was concentrated at the contact area with the Env+ cell, to where F-actin was also recruited (Fig. 2*A*). A similar redistribution to the cell membrane area in contact with Env+ cells was observed for endogenous PI4P5-K Iα (Fig. 2*C*). The specificity of these results was demonstrated by substituting the Hxbc2 cells with ΔKS cells, which lack a functional viral Env protein. Neither PIP_2 nor F-actin accumulated at heterotypic non-fused cell-cell contacts (Fig. 2*B*). These data suggest that HIV-1 Env specifically produces PIP_2 in permissive cells during the first contacts.

PI4P5-K Iα mediates HIV-1 Env-mediated PIP_2 production

In mammalian cells, PIP_2 is synthesized by type I PI4P5-K enzymes (7, 23). We therefore examined the involvement of PI4P5-K I in HIV-1-gp120-mediated PIP_2 production in permissive T cells. CEM cells were transfected with N-terminally HA-tagged versions of either the catalytically active wt PI4P5-K Iα, (wt) PI4P5-K Iβ, or the dominant-negative kinase-dead mutants D227A (D/A)-PI4P5-K Iα and D268A (D/A)-PI4P5-K Iβ (Fig. 3*A* and data not shown). Overexpression of wt-PI4P5-K Iα increased the amounts of PIP_2 produced upon exposure to rs-$gp120_{IIIB}$, 30 min (Fig. 3*B*). In contrast, overexpression of D/A-PI4P5-K Iα strongly impaired rs-$gp120_{IIIB}$-mediated PIP_2 production (Fig. 3*B*). Neither construct affected the production of PIP_2 by untreated cells (Fig. 3*B*). Although overexpression of wt-PI4P5-K Iβ also promoted HIV-1 Env-mediated PIP_2 production, its dead-mutant D/A-PI4P5-K Iβ had no effect on phosphoinositide production (Fig. 3*C*). The membrane expression of CD4 and CXCR4/CCR5 was unaffected by transfection with the PI4P5-K Iα constructs (Fig. 3*D*). These data therefore indicate the specific involvement of PI4P5-K Iα in HIV-1 Env-induced PIP_2 production.

HIV-1 infection of permissive lymphocytes requires the presence of functional PI4P5-K Iα

We next assessed the functional involvement of PI4P5-K Iα in HIV-1 infection. Primary lymphocytes overexpressing the active PI4P5-K Iα construct showed enhanced HIV-1 viral production at

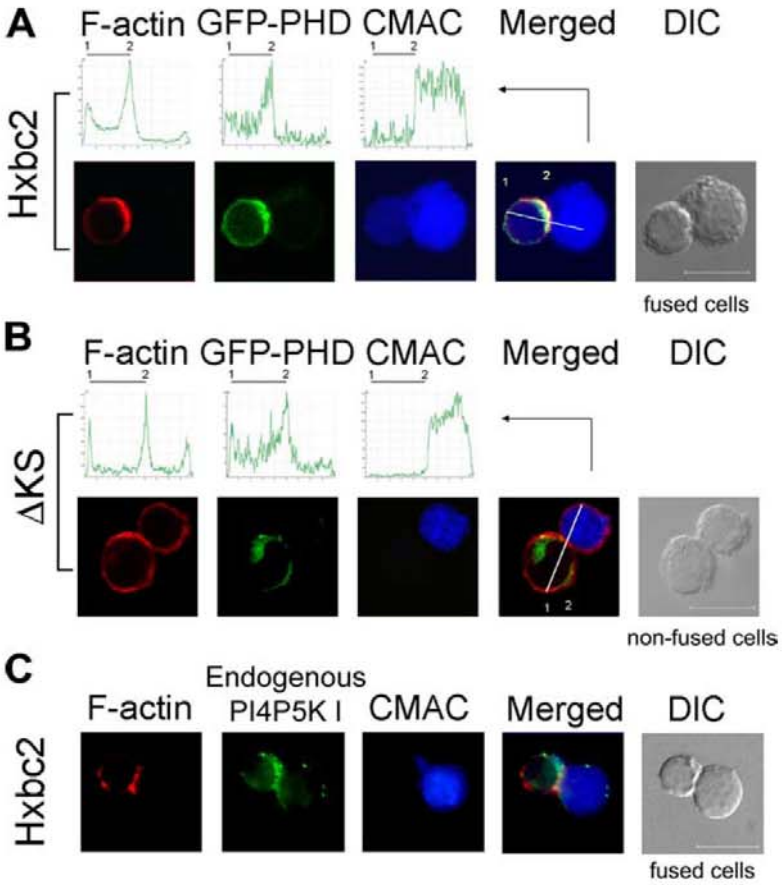

FIGURE 2. PIP_2 is produced in an Env-dependent manner during HIV-1 Env-mediated membrane fusion. *A*, Confocal microscopy and quantification of Hxbc2-Env-mediated PIP_2 production during membrane fusion after 30-min coculture. Accumulation of PIP_2 was determined from the fluorescence of GFP-PHD biosonde. Images show localization of F-actin and GFP-PHD at cell-cell contacts and diffusion of the cytoplasmic probe CMAC from Jurkat-derived Hxbc2 cells (blue cell to *right*) to the target CEM T cell (*left*). CMAC diffusion from Env+ Hxbc2 cells to target cells and F-actin and GFP-PHD accumulation were quantified along lines (see *Merged* pictures) drawn through the region of cell-cell contact. Points 1 and 2 indicate target-cell measurement points and cell diameters. *B*, Confocal microscopy showing the same analysis for heterotypic nonfused cell-cell contacts between CEM T cells and ΔKS (Env-) cells after 30-min coculture. Images show the absence of F-actin and GFP-PHD localization at cell-cell contacts and of CMAC diffusion from Jurkat-derived ΔKS cells (blue cell to *right*) to the target T cell (*left*). *xy* mid-sections are shown. Bar, 10 μm. *C*, Immunofluorescence microscopy images of F-actin and PI4P5-K Iα localization at cell-cell contacts and CMAC diffusion from Jurkat-derived Hxbc2 cells (blue *right-hand cell*) to the target CEM T cell (*left cell*) are shown.

3 days postinfection, whereas infection was inhibited in cells overexpressing the D/A-PI4P5-K Iα construct (Fig. 4*A*). These observations could be due to the action of PIP_2 during viral assembly and budding, so to explore the role of PI4P5-K Iα in the early steps of viral entry we conducted experiments with a single-cycle virus. Nonreplicative HIV-1 viral particles bearing the *Luc* reporter gene were incubated with CEM permissive cells (Fig. 4*B*) or primary T cells (Fig. 4*C*) overexpressing wt- or D/A-PI4P5-K Iα. Remarkably, over-expression of active PI4P5-K Iα clearly enhanced HIV-1 viral entry compared with control GFP-transfected cells in

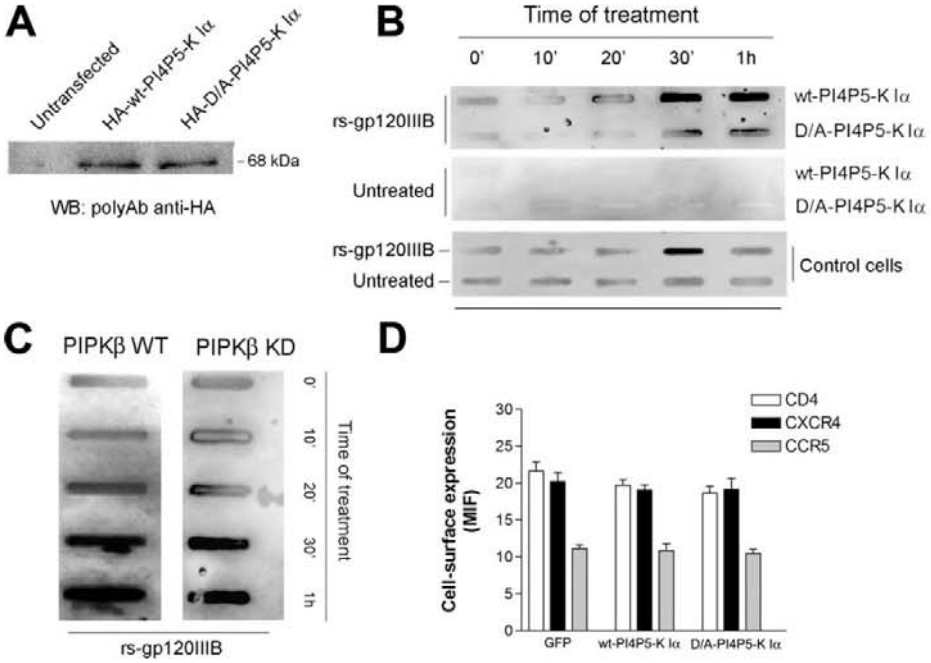

FIGURE 3. PI4P5-kinase Iα mediates specific HIV-1-Env-induced PIP_2 production. *A*, Western blot analysis of overexpressed HA-tagged wt-PI4P5-K Iα and dominant negative kinase-inactive D/A-PI4P5-K Iα in CEM cells. *B*, Dot-blot analysis of rs-$gp120_{IIIB}$-mediated PIP_2 production in CEM T cells nucleofected with wt- or D/A-PI4P5-K Iα, and compared with untransfected (control) cells. Cells were treated with 5 μg/ml rs-gp120 during the time course. Basal PIP_2 is shown for nucleofected and non-nucleofected cells (*Untreated*). A representative experiment of three is shown. *C*, Dot-blot analysis of rs-$gp120_{IIIB}$-mediated PIP_2 production in cells nucleofected with wt-PI4P5K Iβ or D/A-PI4P5-K Iβ (KD). *D*, Flow cytometry analysis of CD4, CXCR4, and CCR5 cell surface expression in PI4P5-K Iα overexpressing cells. GFP = nucleofection control.

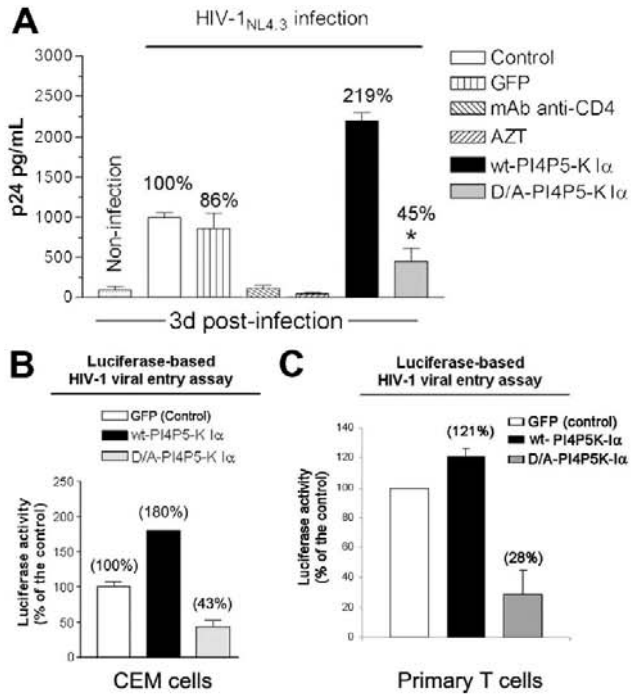

FIGURE 4. PI4P5-K Iα is required for viral entry and infection of HIV-1 particles. *A*, HIV-1 infection (MOI, 1) in primary T cells overexpressing wt-PI4P5-K Iα or D/A-PI4P5-K Iα (* indicates $p < 0.05$). The infection levels for non-nucleofected (Control) and GFP-nucleofected (GFP) cells are shown, and where indicated infection was inhibited with anti-CD4 mAb or 3′-azido-2′,3′-dideoxythymidine. Data are the means ± SEM of three independent experiments conducted in triplicate. *B*, Luciferase-based HIV-1 viral entry assay in CEM T cells overexpressing wt- or D/A-PI4P5-K Iα. Data are means ± SEM of three independent experiments. *C*, Luciferase-based HIV-1 viral entry assay in primary T cell blasts overexpressing wt- or D/A-PI4P5-K Iα, compared with cells transfected with GFP protein (Control). Data are means ± SEM of three independent experiments, conducted in triplicate.

CEM and primary T cells (Fig. 4, *B* and *C*). In contrast, overexpression of the dead-mutant D/A-PI4P5-K Iα strongly inhibited viral entry (Fig. 4, *B* and *C*).

PI4P5-K Iα regulates HIV-1 viral entry into target cells

To further analyze the role of PI4P5-K Iα during HIV-1 infection, we have performed viral fusion and entry experiments by using R5- and X4-tropic HIV-1 viral particles containing the BlaM-Vpr chimera (24). These chimera virions have been designed to specifically study the first steps of viral infection, since β-lactamase activity directly correlates with viral entry. Control, wt-, or dm-PI4P5-K Iα-transfected CEM.NKR-CCR5 cells were incubated (3 h) with equivalent viral inputs of X4-tropic or R5-tropic virions containing BlaM-Vpr fusion protein (Fig. 5*A*). Concurring with previous data, cells overexpressing wt- PI4P5-K Iα were more susceptible to viral entry, whereas in cells overexpressing D/A-PI4P5-K Iα viral entry was strongly reduced. These data indicate that functional PI4P5-K Iα is required for efficient HIV-1 viral fusion and entry, independently of the viral tropism.

As a control of the specificity of PI4P5-K Iα regulation of HIV-1-induced membrane fusion, we repeated the experiment this time using BlaM-Vpr virions pseudotyped with VSV-G Env, which allows viruses to enter the target cell using the endocytic lower pH pathway. As expected, VSV-G viral entry was independent of PI4P5-K Iα kinase activity (Fig. 5*B*).

PI4P5-K Iα knockdown impairs HIV-1 viral infection and entry

To confirm the involvement of PI4P5-K Iα in HIV-1-mediated viral infection, we suppressed expression of the endogenous enzyme by overexpressing a specific siRNA. Two different siRNA oligonucleotides were tested and yielded knockdown of 30–70% (Fig. 6*A*). The basal cell surface expression levels of the CD4 and CXCR4 cell receptors for HIV-1 infection were not affected in PI4P5-K Iα-silenced cells (Fig. 6*B*). Using the siRNA-2 oligonucleotide, we observed that the lack of endogenous PI4P5-K Iα significantly inhibited HIV-1 infection in CEM cells (Fig. 6*C*).

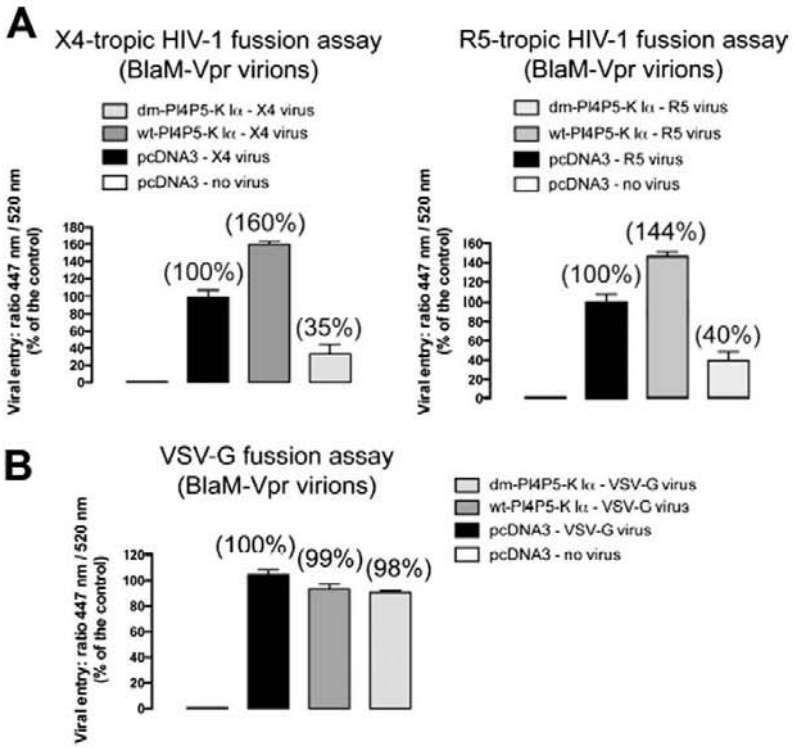

FIGURE 5. PI4P5-K Iα regulates HIV-1 viral entry into target cells. *A*, PI4P5-K Iα specifically affects the early steps of viral infection. Control, wt-, or dm-PI4P5-K Iα-transfected CEM. NKR-CCR5 cells were incubated for 3 h with equivalent viral inputs (determined by standard p24-ELISA) of X4-tropic (*left panel*) or R5-tropic (*right panel*) pNL4–3.Luc.R-E- virions containing BlaM-Vpr fusion protein. After adsorption for 3 h, a fraction of cells were treated with CCF2-AM and analyzed by fluorescence spectrophotometry after 16 h. *B*, VSV-G-mediated viral fusion is independent of PI4P5-K Iα. VSV-G virions containing the BlaM-Vpr fusion protein were used to control for the specificity of wt- or dm-PI4P5-K Iα-mediated effects on HIV-1 viral fusion. The percentages of HIV-1-fused cells were determined by measuring the ratio of blue (447 nm; cleaved CCF2) to green (520 nm; intact CCF2) fluorescent signals in target cells. Each assay was done in triplicate and results are representative of three independent experiments.

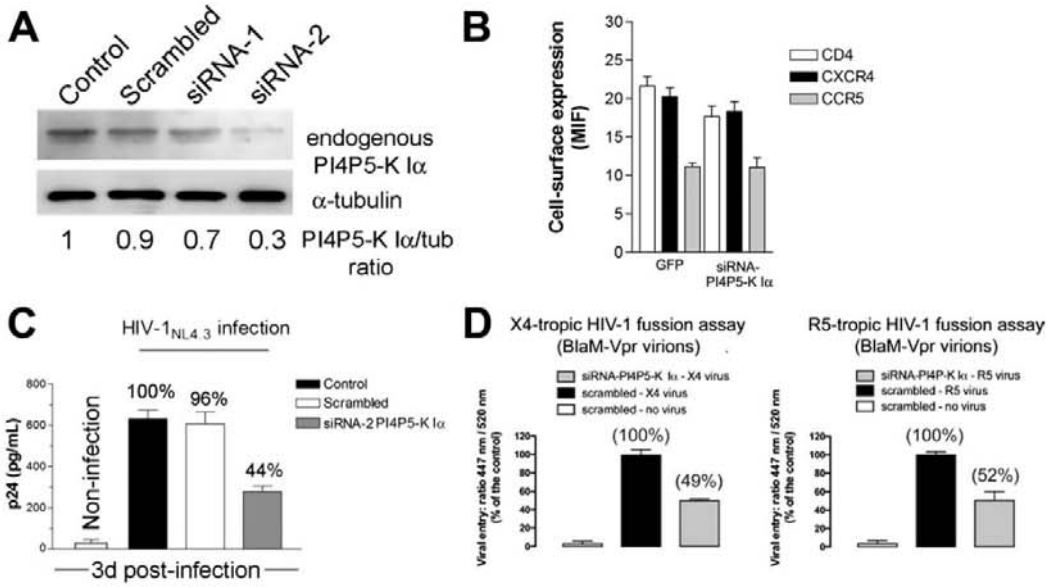

FIGURE 6. PI4P5-kinase Iα regulates HIV-1 infection at the step of viral entry, confirmed by specific mRNA silencing. *A*, Western blot analysis of specific silencing of endogenous PI4P5-K Iα (oligonucleotides *siRNA-1* and *siRNA-2*) 24 h after siRNA-oligonucleotide nucleofection of CEM cells. Silencing is quantified as the band-intensity ratio of PI4P5-K Iα to α-tubulin. A representative experiment of three is shown. *B*, Flow cytometry analysis of CD4, CXCR4, and CCR5 cell surface expression in PI4P5-K Iα-silenced cells. GFP = nucleofection control. Data are means ± SEM of three independent experiments, conducted in triplicate. *C*, HIV-1 viral infection (MOI, 1) in CEM cells in which PI4P5-K α is silenced with siRNA-2. Control, untransfected cells; scrambled, nucleofection with an unrelated scrambled siRNA oligonucleotide. Data are means ± SEM of two independent experiments, conducted in triplicate. *D*, Specific PI4P5-K Iα knock-down decreases entry into target cells of X4- or R5-tropic BlaM-Vpr-virion proteins. CEM.NKR-CCR5 cells were incubated for 3 h with equivalent viral inputs, as determined by standard p24-ELISA. After adsorption for 3 h, a fraction of cells were treated with CCF2-AM and analyzed by fluorescence spectrophotometry after 16 h. The percentages of HIV-1-fused cells were determined by measuring the ratio of blue (447 nm; cleaved CCF2) to green (520 nm; intact CCF2) fluorescent signals in target cells. Each assay was done in triplicate and results are representative of three independent experiments.

These data suggest that functional PI4P5-K Iα is required for efficient viral infection. Using the BlaM-Vpr tool to infect CEM T cells silenced for PI4P5-K Iα, we confirmed that PI4P5-K Iα is required for HIV-1-specific entry (Fig. 6*D*). This effect is independent of HIV-1 Env tropism, which suggests that PI4P5-K Iα regulates a process in target cells that is generally required during the entry stage of HIV-1 infection.

Discussion

The results presented in this study provide the first demonstration that efficient early HIV-1 infection requires T lymphocyte expression of PI4P5-K Iα and associated synthesis of PIP_2. Overexpression of functional wt-PI4P5-K Iα favors an increased production of PIP_2 in response to HIV-1 Env that is concomitant with an increase in viral entry, as observed with single-cycle HIV-1 particles (both luciferase and β-lactamase reporter systems). Conversely, overexpression of the kinase-dead mutant D/A-PI4P5-K Iα or knockdown of endogenous PI4P5-K Iα impairs viral-induced PIP_2 production and HIV-1 entry. An important role has previously been established for PIP_2 metabolism in HIV-1 assembly and egress through the localization of the Gag precursor protein $Pr55_{Gag}$ to the plasma membrane (15, 16). The current results show that PI4P5-K Iα regulates viral entry, therefore indicating that PIP_2 regulates HIV-1 infection throughout the viral cycle.

Three different isoforms of PI4P5-K I have been cloned and described; both α and β isoforms have similar molecular masses (68 kDa) (7). Nevertheless, little is known about differences in their function and regulation. The regulatory mechanism operating in specific processes could be due to different subcellular localizations of these isoforms. It has been described that human PI4P5-K Iα was found preferentially in membrane ruffles, whereas PI4P5-K Iβ isoform was localized in vesicular structures in the cellular cytoplasm (12), where it is implicated in regulation of endocytic vesicles formation. This could represent a coordinate mechanism to regulate PIP_2 production by the cell.

PI4P5-K I has been implicated in regulation of actin dynamics through the interaction of PIP_2 with cytoskeletal molecules such as gelsolin, profilin, filamin A, and ERM proteins (4, 7, 25). The PIP_2 pool at the inner leaflet of the plasma membrane is thought to promote the recruitment of these actin-related proteins to specific membrane domains or to induce activating or inhibitory conformational changes within target proteins. PI4P5K I has been shown to be involved in several processes related to this cortical actin redistribution, including cell polarity (25) cytokinesis (26), phagocytosis (27), and cell migration and the formation of membrane protrusions (28). In this regard, HIV-1 viral entry occurs at specific cell surface areas enriched in actin and viral receptors, such as ruffles and microvilli (29, 30). The behavior of these structures is governed by cortical actin dynamics, which in turn depend on the activity of actin cytoskeleton associated proteins. It is therefore possible that PI4P5-K I might regulate the formation of these structures and promote HIV-1 entry.

PIP_2 has important regulatory roles in many cellular processes (31, 32) and affects protein organization and acts as a precursor for second messengers such as DAG, IP3, and PIP3 (33). It is thought that specificity of PIP_2 action may in part be achieved through spatial confinement in pools in the plasma membrane (34, 35), where it could affect plasma membrane fluidity and protein organization (36). HIV-1 Env-mediated PIP_2 production during viral

entry might therefore alter plasma membrane fluidity or viral receptor organization to favor initial HIV-1/cell interactions and promote subsequent fusion.

PIP_2 has also been found to protect against cell apoptosis, alone or in a complex with gelsolin, by directly inhibiting the initiator caspases 8 and 9, as well as by binding and inhibiting their common effector, caspase 3 (37, 38). Therefore it is plausible that HIV-1-triggered synthesis of PIP_2 during the first steps of the viral cycle may serve to ensure cell viability and, therefore, efficient viral infection and propagation. Moreover, it is conceivable that the efficiency and/or kinetics of CD4/gp120-mediated PIP_2 production may affect the fusion process established between HIV-1 viral particles and target cells. In this way, cell signals that regulate viral activation of PI4P5-K Iα and subsequent PIP_2 production could be crucial for the control of HIV-1 viral entry and infection.

In sum, we propose that signals that regulate PI4P5-K Iα-dependent PIP_2 production and related cellular processes may control HIV-1 viral infection by regulating the first steps of viral cycle and may represent new targets for the blockade of HIV-1 infection.

Acknowledgments

We thank Dr. M. López-Cabrera for helpful comments on the manuscript and Rafael Samaniego for confocal microscopy analyses. Editorial support was provided by S. Bartlett. We thank the AIDS Research and Reagent Program, Division of AIDS, National Institute of Allergy and Infectious Diseases, National Institutes of Health, for kindly providing cells and reagents.

Disclosures

The authors have no financial conflict of interest.

References

1. Cozier, G. E., J. Carlton, D. Bouyoucef, and P. J. Cullen. 2004. Membrane targeting by pleckstrin homology domains. *Curr. Top. Microbiol. Immunol.* 282: 49–88.
2. Itoh, T., and T. Takenawa. 2002. Phosphoinositide-binding domains: Functional units for temporal and spatial regulation of intracellular signaling. *Cell. Signal.* 14: 733–743.
3. Hilpela, P., M. K. Vartiainen, and P. Lappalainen. 2004. Regulation of the actin cytoskeleton by PI(4,5)P2 and PI(3,4,5)P3. *Curr. Top. Microbiol. Immunol.* 282: 117–163.
4. Yin, H. L., and P. A. Janmey. 2003. Phosphoinositide regulation of the actin cytoskeleton. *Annu. Rev. Physiol.* 65: 761–789.
5. Raucher, D., T. Stauffer, W. Chen, K. Shen, S. Guo, J. D. York, M. P. Sheetz, and T. Meyer. 2000. Phosphatidylinositol 4,5-bisphosphate functions as a second messenger that regulates cytoskeleton-plasma membrane adhesion. *Cell* 100: 221–228.
6. Weernink, P. A., K. Meletiadis, S. Hommeltenberg, M. Hinz, H. Ishihara, M. Schmidt, and K. H. Jakobs. 2004. Activation of type I phosphatidylinositol 4-phosphate 5-kinase isoforms by the Rho GTPases, RhoA, Rac1, and Cdc42. *J. Biol. Chem.* 279: 7840–7849.
7. Oude Weernink, P. A., M. Schmidt, and K. H. Jakobs. 2004. Regulation and cellular roles of phosphoinositide 5-kinases. *Eur. J. Pharmacol.* 500: 87–99.
8. Stephens, L. R., K. T. Hughes, and R. F. Irvine. 1991. Pathway of phosphatidylinositol(3,4,5)-trisphosphate synthesis in activated neutrophils. *Nature* 351: 33–39.
9. Whiteford, C. C., C. A. Brearley, and E. T. Ulug. 1997. Phosphatidylinositol 3,5-bisphosphate defines a novel PI 3-kinase pathway in resting mouse fibroblasts. *Biochem. J.* 323: 597–601.
10. Ishihara, H., Y. Shibasaki, N. Kizuki, H. Katagiri, Y. Yazaki, T. Asano, and Y. Oka. 1996. Cloning of cDNAs encoding two isoforms of 68-kDa type I phosphatidylinositol-4-phosphate 5-kinase. *J. Biol. Chem.* 271: 23611–23614.
11. Loijens, J. C., and R. A. Anderson. 1996. Type I phosphatidylinositol-4-phosphate 5-kinases are distinct members of this novel lipid kinase family. *J. Biol. Chem.* 271: 32937–32943.
12. Doughman, R. L., A. J. Firestone, M. L. Wojtasiak, M. W. Bunce, and R. A. Anderson. 2003. Membrane ruffling requires coordination between type Iα phosphatidylinositol phosphate kinase and Rac signaling. *J. Biol. Chem.* 278: 23036–23045.
13. Padron, D., Y. J. Wang, M. Yamamoto, H. Yin, and M. G. Roth. 2003. Phosphatidylinositol phosphate 5-kinase Iβ recruits AP-2 to the plasma membrane and regulates rates of constitutive endocytosis. *J. Cell Biol.* 162: 693–701.
14. Adamson, C. S., and I. M. Jones. 2004. The molecular basis of HIV capsid assembly: five years of progress. *Rev. Med. Virol.* 14: 107–121.
15. Chukkapalli, V., I. B. Hogue, V. Boyko, W. S. Hu, and A. Ono. 2008. Interaction between the human immunodeficiency virus type 1 Gag matrix domain and phosphatidylinositol-(4,5)-bisphosphate is essential for efficient gag membrane binding. *J. Virol.* 82: 2405–2417.
16. Ono, A., S. D. Ablan, S. J. Lockett, K. Nagashima, and E. O. Freed. 2004. Phosphatidylinositol (4,5) bisphosphate regulates HIV-1 Gag targeting to the plasma membrane. *Proc. Natl. Acad. Sci. USA* 101: 14889–14894.
17. Kisseleva, M. V., M. P. Wilson, and P. W. Majerus. 2000. The isolation and characterization of a cDNA encoding phospholipid-specific inositol polyphosphate 5-phosphatase. *J. Biol. Chem.* 275: 20110–20116.
18. Valenzuela-Fernandez, A., S. Alvarez, M. Gordon-Alonso, M. Barrero, A. Ursa, J. R. Cabrero, G. Fernandez, S. Naranjo-Suarez, M. Yanez-Mo, J. M. Serrador, et al. 2005. Histone deacetylase 6 regulates human immunodeficiency virus type 1 infection. *Mol. Biol. Cell* 16: 5445–5454.
19. Yamashita, M., and M. Emerman. 2004. Capsid is a dominant determinant of retrovirus infectivity in nondividing cells. *J. Virol.* 78: 5670–5678.
20. Gummuluru, S., and M. Emerman. 2002. Advances in HIV molecular biology. *AIDS* 16 (*Suppl.* 4): S17–S23.
21. Varnai, P., and T. Balla. 1998. Visualization of phosphoinositides that bind pleckstrin homology domains: calcium- and agonist-induced dynamic changes and relationship to myo-[3H]inositol-labeled phosphoinositide pools. *J. Cell Biol.* 143: 501–510.
22. Budd, R. C., G. Winslow, S. Inokuchi, and J. B. Imboden. 1990. Intact antigen receptor-mediated generation of inositol phosphates and increased intracellular calcium in CD4 CD8 T lymphocytes from MRL lpr mice. *J. Immunol.* 145: 2862–2872.
23. Doughman, R. L., A. J. Firestone, and R. A. Anderson. 2003. Phosphatidylinositol phosphate kinases put PI4,5P(2) in its place. *J. Membr. Biol.* 194: 77–89.
24. Cavrois, M., C. De Noronha, and W. C. Greene. 2002. A sensitive and specific enzyme-based assay detecting HIV-1 virion fusion in primary T lymphocytes. *Nat. Biotechnol.* 20: 1151–1154.
25. Jimenez-Baranda, S., C. Gomez-Mouton, A. Rojas, L. Martinez-Prats, E. Mira, R. Ana Lacalle, A. Valencia, D. S. Dimitrov, A. Viola, R. Delgado, et al. 2007. Filamin-A regulates actin-dependent clustering of HIV receptors. *Nat. Cell. Biol.* 9: 838–846.
26. Logan, M. R., and C. A. Mandato. 2006. Regulation of the actin cytoskeleton by PIP2 in cytokinesis. *Biol. Cell* 98: 377–388.
27. Coppolino, M. G., R. Dierckman, J. Loijens, R. F. Collins, M. Pouladi, J. Jongstra-Bilen, A. D. Schreiber, W. S. Trimble, R. Anderson, and S. Grinstein. 2002. Inhibition of phosphatidylinositol-4-phosphate 5-kinase Iα impairs localized actin remodeling and suppresses phagocytosis. *J. Biol. Chem.* 277: 43849–43857.
28. Ling, K., N. J. Schill, M. P. Wagoner, Y. Sun, and R. A. Anderson. 2006. Movin' on up: the role of PtdIns(4,5)P(2) in cell migration. *Trends Cell Biol.* 16: 276–284.
29. Singer, I. I., S. Scott, D. W. Kawka, J. Chin, B. L. Daugherty, J. A. DeMartino, J. DiSalvo, S. L. Gould, J. E. Lineberger, L. Malkowitz, et al. 2001. CCR5, CXCR4, and CD4 are clustered and closely apposed on microvilli of human macrophages and T cells. *J. Virol.* 75: 3779–3790.
30. Steffens, C. M., and T. J. Hope. 2004. Mobility of the human immunodeficiency virus (HIV) receptor CD4 and coreceptor CCR5 in living cells: implications for HIV fusion and entry events. *J. Virol.* 78: 9573–9578.
31. Caroni, P. 2001. New EMBO members' review: actin cytoskeleton regulation through modulation of PI(4,5)P(2) rafts. *EMBO J.* 20: 4332–4336.
32. Yamamoto, M., D. H. Hilgemann, S. Feng, H. Bito, H. Ishihara, Y. Shibasaki, and H. L. Yin. 2001. Phosphatidylinositol 4,5-bisphosphate induces actin stress-fiber formation and inhibits membrane ruffling in CV1 cells. *J. Cell Biol.* 152: 867–876.
33. Rameh, L. E., and L. C. Cantley. 1999. The role of phosphoinositide 3-kinase lipid products in cell function. *J. Biol. Chem.* 274: 8347–8350.
34. Janmey, P. A., and U. Lindberg. 2004. Cytoskeletal regulation: rich in lipids. *Nat. Rev. Mol. Cell Biol.* 5: 658–666.
35. Martin, T. F. 2001. PI(4,5)P(2) regulation of surface membrane traffic. *Curr. Opin. Cell Biol.* 13: 493–499.
36. Engelman, D. M. 2005. Membranes are more mosaic than fluid. *Nature* 438: 578–580.
37. Azuma, T., K. Koths, L. Flanagan, and D. Kwiatkowski. 2000. Gelsolin in complex with phosphatidylinositol 4,5-bisphosphate inhibits caspase-3 and −9 to retard apoptotic progression. *J. Biol. Chem.* 275: 3761–3766.
38. Mejillano, M., M. Yamamoto, A. L. Rozelle, H. Q. Sun, X. Wang, and H. L. Yin. 2001. Regulation of apoptosis by phosphatidylinositol 4,5-bisphosphate inhibition of caspases, and caspase inactivation of phosphatidylinositol phosphate 5-kinases. *J. Biol. Chem.* 276: 1865–1872.

3.3. MOESINA REGULA EL TRÁFICO DE VESÍCULAS NACIENTES RECUBIERTAS DE CLATRINA.

La endocitosis es el mecanismo celular fundamental por el cual la célula internaliza material exterior o presente en la membrana plasmática (receptores de la superficie celular y proteínas integrales de membrana), regula rutas de señalización y otros procesos morfológicos. El mecanismo de endocitosis mejor estudiado es aquel que depende del recubrimiento por la proteína clatrina (CME, "*Clathrin-mediated endocytosis*"). La CME puede ser dividida en varios tipos (constitutiva o inducible por ligando) y a su vez en varias etapas, en cada una de las cuales participa un grupo específico de moléculas adaptadoras y accesorias encargadas de dirigir los mecanismos que van a terminar con la internalización de dicho cargo, y es esencial para controlar la integridad, la división y la señalización celular (revisado en (McMahon and Boucrot, 2011)). La dinámica de las estructuras de clatrina (CCS, "*clathrin-coated structures*") en superficie, se encuentra controlada mediante la participación coordinada de proteínas y componentes lipídicos que regulan la formación de invaginaciones de clatrina (CCP, "*clathrin-coated pits*") en superficie, y posterior escisión de estas estructuras de la membrana plasmática formando las vesículas de clatrina (CCV, "*clathrin-coated vesicles*") libres en el citoplasma (revisado en (McMahon and Boucrot, 2011)). Dentro de las proteínas adaptadoras que participan en la endocitosis dependiente de clatrina, el complejo AP-2 ("*adaptor protein 2*") es el más abundante, y su función es la de reclutar proteínas en las regiones de formación de CCP (Schmid et al., 2006). Además, muchos de los elementos reguladores y accesorios que participan en la formación de CCP en superficie, son reclutados a regiones de la membrana plasmática enriquecidas en PIP_2, importante para la localización y progresión adecuada de la endocitosis (Zoncu et al., 2007).

Por último, en CME de mamíferos parece que los eventos de movimiento lateral de estructuras de clatrina, su separación, liberación y el movimiento de las vesículas en el citoplasma se encuentran relacionados espacial y temporalmente con el citoesquelto de actina (Aghamohammadzadeh and Ayscough, 2009; Cao et al., 2003; Merrifield et al., 2002; Merrifield et al., 2005; Schafer, 2002). Además, parece que la actina no está implicada en la formación de las invaginaciones de clatrina sino que participa en los últimos estadios de liberación de las vesículas en el citoplasma celular (Yarar et al., 2005). La actina de encuentra unida a CCP mediante la proteína adaptadora HIP1R (Engqvist-Goldstein et al., 2001), y la polimerización de actina

necesaria para la CME parece ser dependiente de cortactina, N-WASP y Arp2/3 (revisado en (McMahon and Boucrot, 2011)).

En el contexto del VIH-1, el mecanismo de entrada viral siempre ha sido tema de debate entre los investigadores. Por un lado, la mayoría de los trabajos indican que la entrada e infección productiva del VIH-1 ocurre principalmente mediante un mecanismo de fusión entre la membrana plasmática celular y la membrana viral de manera independiente de pH (Doms and Trono, 2000). Por el contrario, recientemente se ha descrito que la ruta principal de entrada del VIH-1 en la célula diana depende de un mecanismo de endocitosis mediada por clatrina y posterior fusión en endosomas (Miyauchi et al., 2009). Sin embargo, existen evidencias que indican que la entrada endocítica del VIH-1, aunque ocurre a gran escala, no lleva a una infección productiva (Fredericksen et al., 2002; Maddon et al., 1988; McClure et al., 1988; Pelchen-Matthews et al., 1995; Stein et al., 1987; Wei et al., 2005). Por otro lado, se ha visto que el bloqueo de la endocitosis de los receptores para el VIH-1, así como su índice de endocitosis, no afecta a la entrada o replicación del VIH-1 (Alkhatib et al., 1997b; Amara et al., 1997; Aramori et al., 1997; Brandt et al., 2002; Gosling et al., 1997; Lu et al., 1997; Maddon et al., 1988; Pelchen-Matthews et al., 1995). Por todo ello, el estudio de las proteínas implicadas en los primeros estadios de infección por el VIH-1, deben además ser estudiadas en el contexto de la CME, con el objetivo último de clarificar el mecanismo principal de entrada del VIH-1 en la célula diana.

Las proteínas ERM (ezrina-radixina-moesina) son capaces de coordinar rutas de señalización con el transporte de membrana, gracias a su capacidad de unirse de manera regulada y reversible a proteínas de la membrana plasmática y al citoesqueleto de actina (Mangeat et al., 1999). Las proteínas ERM, concretamente ezrina, se ha mostrado que regula el tráfico de receptores y transportadores celulares, como el reciclaje hacia la membrana plasmática del receptor $\alpha 1\beta$-adrenérgico (Stanasila et al., 2006), implicadas en la respuesta secretora y redistribución de H,K-ATPase en membrana (Zhou et al., 2005) y el reclutamiento del intercambiador Na^+-H^+ NHE3 en la membrana apical de células intestinales, necesario para el co-transporte Na^+/glucosa intestinal (Zhao et al., 2004), al parecer a través de una interacción directa entre ezrina y un grupo de residuos básicos en NHE3 (Cha et al., 2006). Además, el tráfico de varios receptores del tipo GPCR parece estar regulado por el adaptador EBP50 de las proteínas ERM, también conocido como NHEFR1 (Li et al., 2002). Estos datos parecen indicar que la interacción entre las ERM con EBP50 puede ser necesaria para el reciclaje y traslocación en membrana del receptor, aunque el mecanismo de reciclaje dependiente del complejo receptor/EBP50/ERM/F-actina aún

no se conoce bien. De manera interesante, las proteínas ERM han sido localizadas, además de en la membrana plasmática, en compartimentos internos asociados a endosomas tempranos y de reciclaje de manera dependiente de anexina II (Morel et al., 2009; Stanasila et al., 2006), y en compartimentos de la ruta degradativa como lisosomas (Poupon et al., 2003) y fagosomas (Defacque et al., 2000). Por último, recientemente se ha descrito que las proteínas ERM parecen favorecer la maduración endosomal del EGFR ("*epidermal grow factor receptor*"), dependiente de F-actina, hacia lisosomas, regulando el reclutamiento de Rab7 y la disociación de Rab5 (Chirivino et al., 2011).

Sin embargo, a pesar de la gran cantidad de evidencias que apoyan la participación de las proteínas ERM en el tráfico vesicular, no existen evidencias de la participación de moesina durante la formación, internalización o reciclaje de CCV.

RESULTADOS

Como uno de los principales activadores de las proteínas ERM es el PIP_2 y éste está relacionado directamente con la localización y progresión adecuada de la endocitosis, y recientemente se ha descrito que la entrada del VIH-1 ocurre de manera endocítica dependiente de clatrina, quisimos estudiar la implicación del adaptador de F-actina moesina durante el tráfico de estructuras de clatrina.

Para determinar la posible participación de moesina durante la formación, internalización o reciclaje de vesículas de clatrina, se realizaron marcajes de microscopía confocal con componentes constitutivos de las estructuras de clatrina en membrana plasmática. Se observó una colocalización parcial de moesina endógena con clatrina y AP-2, pero no con AP-1. La interferencia específica de moesina endógena alteró el movimiento lateral de las estructuras de clatrina de superficie, además de provocar su agregación en comparación a la condición control. De estos agregados surgen vesículas de clatrina individuales, lo que parece indicar la participación de moesina en el tráfico de estructuras de clatrina. Mediante la utilización de una serie de construcciones de dominios de moesina, determinamos que el dominio de unión a PIP_2 presente en la región N-terminal de moesina (carente en el mutante 4K/4N-moesina, desarrollado por nosotros y que no une PIP_2) participa en su co-distribución con estas estructuras de clatrina. Además, la sobreexpresión de la construcción N-moesina también provocó cierta agregación de estructuras de clatrina. Los agregados generados por la interferencia específica de moesina, mediante estudios de microscopía de fluorescencia por reflexión interna total (TIRFM, "*total*

internal reflexion fluorescence microscopy"), estaban compuestos por clatrina, AP-2, el receptor de transferrina (TfR) y el marcador de endosoma temprano Rab5. Estos agregados parecen corresponder con vesículas de clatrina endocíticas nacientes, positivas para Rab5, intracelulares, y no con estructuras de membrana, debido a su ausencia en el análisis de preparaciones de membrana plasmática ("*membrane sheets*"). La ausencia de colocalización significativa con Rab7 y Rab11, refuerzan que son vesículas endocíticas de Rab5. Además, se describe por primera vez la localización de Rab5 en CCP, antes incluso de la formación de la vesícula endocítica naciente. La interferencia específica de moesina provocó una disminución de la expresión en superficie celular del TfR como se detectó por citometría de flujo, el cual internaliza y recicla independientemente de la unión de transferrina (Tf), de manera dependiente de clatrina y AP-2. Además, observamos que la interferencia específica de moesina no afecta a la endocitosis e internalización de Tf. Por tanto, si moesina no afecta a la formación ni a la internalización de estructuras de clatrina y, aún así, existe una menor expresión superficial del TfR en superficie, entonces podría afectar al reciclaje temprano del receptor internalizado de vuelta a la membrana plasmática. Así, se determinó que el silenciamiento de moesina provocó el secuestro del TfR en compartimentos endosomales, disminuyendo su tasa de reciclaje a membrana plasmática. Esta función de moesina sobre el reciclaje del TfR depende de su unión simultánea a estructuras de clatrina y a F-actina, quizás necesario para redirigir el movimiento adecuado de estas vesículas hacia la membrana plasmática para comenzar un nuevo ciclo de internalización.

Estos resultados indican que aunque moesina tiene un papel clave durante la fusión y entrada del VIH-1 en la célula diana, parece ser que la endocitosis dependiente de clatrina no está implicada en el proceso de entrada viral, por dos motivos: en primer lugar, la interferencia específica de moesina no modifica la entrada de virus pseudotipados con la envuelta VSV-G que entran en la célula de manera endocítica dependiente de clatrina; y en segundo lugar la interferencia de moesina no afecta a la tasa de endocitosis de vesículas de clatrina sino a su reciclaje de vuelta a la membrana plasmática una vez han internalizado. Por esto, la activación de moesina por el VIH-1 en los primeros contactos puede favorecer la dinámica de reciclaje del TfR permitiéndo un mayor índice de captación de Tf-hierro, favoreciendo la supervivencia de la célula infectada, quizás lo suficiente para completar su ciclo viral. Además, datos de nuestro grupo recientemente publicados, indican que la dinámica de membrana asociada a PIP_2 y regulada por la GTPasa Arf6 sí es importante para la

fusión, entrada e infección viral eficiente en células T $CD4^+$ ((Garcia-Exposito et al., 2011) y ANEXO 2).

MATERIALES Y MÉTODOS

Estos estudios fueron realizados en la línea celular HeLa, una línea celular ampliamente utilizada en el estudio de la endocitosis dependiente de clatrina. Se utilizaron anticuerpos específicos para detectar moesina, AP-2, AP-1, clatrina, tubulina, Rab5, Rab7, receptor de transferrina (TfR), PIP_2 y contra la proteína verde fluorescente (GFP, "*green fluorescente protein*"). Las construcciones de ADN utilizadas fueron las construcciones FL-moesina-GFP, FL-4K/4N-moesina-GFP (mutante de unión a PIP_2), N-moesina-GFP (mutante dominante negativo de unión a membrana) y C-moesina-GFP (mutante de unión a F-actina), ECFP-Rab5 (marcador de endosomas tempranos), clatrina-DsRed, EGFP-Rab7 (marcador de endosomas tardíos), EYFP-Rab11 (marcador de vesículas perinucleares que reciclan desde el Golgi a la membrana plasmática), GFP-α-adaptina y ECFP-PH como la sonda de detección de PIP_2. Además, se utilizaron oligos de ARNi-Alexa-546 contra moesina para detectar aquellas células que están siendo específicamente interferidas. Se analizó mediante "*dot-blot*" la unión a PIP_2 de las construcciones FL-moesina-GFP y FL-4K/4N-moesina-GFP en células HeLa transfectadas con estas construcciones. Se utilizó la microscopía de fluorescencia confocal para monitorizar la localización de moesina endógena con respecto a las proteínas endógenas de clatrina (cadena pesada de clatrina), AP-2 (α-adaptina) y AP-1 (γ-adaptina). El "*western blot*" nos permitió detectar la extensión de la expresión de las distintas proteínas de interés, además del nivel de silenciamiento específico por ARNi de la proteína moesina endógena. Mediante citometría de flujo se analizó el nivel de expresión en superficie del TfR, además de su índice de internalización y reciclaje, monitorizado mediante la detección del ligando transferrina (Tf) marcado con un fluorocromo Alexa-488. Se realizó un fraccionamiento subcelular por ultracentifugación en gradiente de densidad (Optiprep^{TM} 5–20%), para determinar la distribución endosomal del TfR, Rab5 y Rab7 en células interferidas en moesina con respecto a células control. Por último, se utilizó la microscopía de fluorescencia por reflexión interna total (TIRFM) para el análisis de la formación, tamaño y dinámica de las estructuras de clatrina en la membrana celular en células vivas y en preparaciones de membrana plasmática, y su grado de colocalización con otros componentes como α-adaptina, TfR, Tf-488, Rab5, Rab7 y Rab11 en células interferidas en moesina con respecto a células control. También se analizó por microscopía TIRF la endocitosis de

vesículas de clatrina y el grado de exocitosis *de novo* del receptor de transferrina (TfR).

THE JOURNAL OF BIOLOGICAL CHEMISTRY VOL. 284, NO. 4, pp. 2419–2434, January 23, 2009

Moesin Regulates the Trafficking of Nascent Clathrin-coated Vesicles*[S]

Received for publication, July 11, 2008, and in revised form, November 18, 2008 Published, JBC Papers in Press, November 30, 2008, DOI 10.1074/jbc.M805311200

Jonathan Barroso-González[‡§1], José-David Machado[§¶2], Laura García-Expósito[‡§3], and Agustín Valenzuela-Fernández[‡§4]

From the [‡]Laboratorio de Inmunología Celular y Viral, [¶]Laboratorio de Neurosecreción, [§]Unidad de Farmacología, Departamento de Medicina Física y Farmacología, Facultad de Medicina, Universidad de La Laguna, Instituto de Tecnologías Biomédicas, Campus de Ofra s/n, Tenerife 38071, Spain

Clathrin-coated vesicles are responsible for the trafficking of several internalized biological cargos. We have observed that the endogenous F-actin-linker moesin co-distributes with constitutive components of clathrin-coated structures. Total internal reflection fluorescence microscopy studies have shown that short interference RNA of moesin enhances the lateral movement of clathrin-coated structures and provokes their abnormal clustering. The aggregation of clathrin-coated structures has also been observed in cells overexpressing N-moesin, a dominant-negative construct unable to bind to F-actin. Only overexpressed moesin constructs with an intact phosphatidylinositol 4,5-bisphosphate-binding domain co-distribute with clathrin-coated structures. Hence, this N-terminal domain is mostly responsible for moesin/clathrin-coated structure association. Biochemical endosome fractioning together with total internal reflection fluorescence microscopy comparative studies, between intact cells and plasma-membrane sheets, indicate that moesin knockdown provokes the accumulation of endocytic rab5-clathrin-coated vesicles carrying the transferrin receptor. The altered trafficking of these endocytic rab5-clathrin-coated vesicles accounts for a transferrin receptor recycling defect that reduces cell-surface expression of the transferrin receptor and increases the amount of sequestered transferrin ligand. Therefore, we propose that moesin is a clathrin-coated vesicle linker that drives cargo trafficking and acts on nascent rab5-clathrin-coated vesicles by simultaneously binding to clathrin-coated vesicle-associated phosphatidylinositol 4,5-bisphosphate and actin cytoskeleton. Hence, functional alterations of moesin may be involved in pathological disorders associated with clathrin-mediated internalization or receptor recycling.

Clathrin-mediated endocytosis is a key process that governs the internalization of a plethora of cell-surface receptors in metazoans, such as G-protein-coupled receptors and epithelial growth factor receptors, and is essential for controlling cell integrity, division, and signaling (1–6). The dynamic process that enables clathrin-coated pits (CCPs)[5] to turn into clathrin-coated vesicles (CCVs) requires spatial coordination of several protein and lipid components working together to drive the formation and invagination of CCPs, and the subsequent scission and uncoating of CCVs (7, 8). Similarly, several lines of evidence have suggested a close association between the endocytic machinery in mammalian cells and the actin cytoskeleton (9–14).

Cortical actin dynamics is affected by cytoskeleton-associated proteins, such as those responsible for the growth and capping of actin filaments (15). Therefore, the ezrin-radixin-moesin (ERM) proteins from the band 4.1 superfamily are fundamental in determining signaling-induced cell shape, membrane-protein localization, cell adhesion, motility, cytokinesis, phagocytosis, and the integration of membrane transport with signaling pathways (15, 16). These ERM functions rely directly on their regulated and reversible link between membrane-associated proteins and the actin cytoskeleton (15). Remarkably, the F-actin-linker ezrin has recently been related to clathrin-mediated endocytosis of the $\alpha 1\beta$-adrenergic receptor, thereby contributing to receptor recycling to the plasma membrane (17). Moreover, the trafficking of some G-protein-coupled receptors seems to be regulated by the ERM linker EBP50, also known as NHERF1 (17–19). These data suggest that the interaction of EBP50 and ERM proteins is necessary for receptor recycling, although the mechanism that relates EBP50/ERM/F-actin linking and the receptor membrane traffic pathway is still unknown. It is interesting that ezrin and moesin proteins have been found to be associated with endosomes in an annexin-II-dependent manner (20). However, there were no reports indicating functional evidence for moesin involvement during CCV formation, internalization, or recycling.

* This work was supported in part by the Instituto de Salud Carlos III, Ministerio de Sanidad y Consumo, Spain (Grant FIS-PI050995), by the Fundación para la Investigación y Prevención del SIDA en España (Grants FIPSE-24508/05 and FIPSE-24661/07), by the Consejería de Industria, Comercio y Nuevas Tecnologías del Gobierno Autónomo de Canarias, Spain (Grant IDT-TF-06/066), and by the Universidad de La Laguna, Tenerife, Spain (Grant ULL-06-1500). The authors declare that they have no competing financial interests. The costs of publication of this article were defrayed in part by the payment of page charges. This article must therefore be hereby marked "*advertisement*" in accordance with 18 U.S.C. Section 1734 solely to indicate this fact.

[S] The on-line version of this article (available at http://www.jbc.org) contains supplemental Figs. S1–S5 and Movies S1–S4.

[1] Supported by an FIS-PI050995-associated fellowship.

[2] Supported by Fondo Social Europeo (FSE) (Grant JCI2005-1042).

[3] Supported by an FIPSE-24661/07-associated fellowship.

[4] Supported by the FSE (Grant RYC2002-3018). To whom correspondence should be addressed. Tel.: 34-922-319351; Fax: 34-922-655995; E-mail: avalenzu@ull.es.

[5] The abbreviations used are: CCP, clathrin-coated pit; CCV, clathrin-coated vesicle; ERM, ezrin-radixin-moesin; LCa-DsRed, clathrin light-chain a DsRed fusion protein; TIRFM, total internal reflection fluorescence microscopy; PIP_2, phosphatidylinositol 4,5-bisphosphate; siRNA, short interference RNA; Tf, transferrin ligand; TfR, Tf receptor; mAb, monoclonal antibody; polyAb, polyclonal antibody; GFP, green fluorescent protein; PBS, phosphate-buffered saline; CHC, clathrin heavy chain; EGFP, enhanced GFP; TfR-phl, TfR-phluorin; ECFP-PH, ECFP-tagged pleckstrin homology domain.

In the present work, we have studied the functional involvement of the F-actin-linker moesin in the trafficking of CCVs. Total internal reflection fluorescence microscopy (TIRFM) using the clathrin light-chain a DsRed fusion protein (LCa-DsRed) (21), as well as biochemical approaches, indicates that moesin is a component of the complex molecular machinery involved in the control of the trafficking of nascent moesin-associated CCVs.

EXPERIMENTAL PROCEDURES

Antibodies and Reagents—The monoclonal antibody (mAb) moesin (38/87)-sc-58806 recognizes moesin, the goat polyclonal antibody (polyAb) ezrin (C-19)-sc-6407 that recognizes ezrin and moesin, rabbit polyAb α-adaptin (M-300)-sc-10761, goat polyAb anti-rab5 (FL-205)-sc-28570, rabbit polyAb anti-rab7 (H-50)-sc-10767, mAb CD71 (3B82A1)-sc-32272 against transferrin receptor (TfR), and anti-phosphatidylinositol 4,5-bisphosphate (PIP_2) mAb (sc-53412), and anti-GFP rabbit polyAb (sc-8334) came from Santa Cruz Biotechnology Inc. (Santa Cruz, CA). Anti-clathrin heavy chain (CHC), anti-γ-adaptin and anti-α-tubulin mAbs, and PIP_2 were from Sigma-Aldrich. Secondary horseradish peroxidise-conjugated anti-mAb was from Immunotools (Friesoythe, Germany), and secondary horseradish peroxidise-conjugated anti-goat Ab was from Dako (Glostrup, Denmark). Alexa 488-conjugated transferrin (Tf), Alexa 568-labeled phalloïdin, and secondary antibodies Alexa 488- and/or Alexa 568-conjugated were from Invitrogen.

DNA Constructs—Human FL, N- and C-moesin-GFP constructs were kindly provided by Dr. Francisco Sánchez-Madrid (Universidad Autónoma de Madrid, Spain) and Dr. Furthmayr (Stanford University, CA) (22). LCa-DsRed, TfR-EGFP, and TfR-phluorin (TfR-phl) were provided by Dr. Wolfhard Almers (21) (Vollum Institute, Oregon Health & Science University, OR). ECFP-rab5, EGFP-rab7, and EYFP-rab11 were provided by Dr. Marino Zerial (Max Planck Institute of Molecular Cell Biology and Genetics, Dresden, Germany). GFP-α-adaptin construct was provided by Dr. Alexandre Benmerah (Institute Cochin, Paris, France). N-terminal ECFP-tagged pleckstrin homology domain of the phosphatidylinositol-specific phospholipase $C\delta_1$ (ECFP-PH) was provided by Dr. Senena Corbalán-García (Universidad de Murcia, Spain), and was used as a PIP_2 biosensor in the plasma membrane (23–25). All constructs were verified by digestion with restriction enzymes and automated dideoxynucleotide sequencing. The 4K/4N-moesin-GFP construct was prepared by using the QuikChange site-directed mutagenesis kit from Stratagene (Cedar Creek, TX). The oligonucleotides (sense, (5′-3′)) used for introducing the K253N/K254N and the K262N/K263N mutations in the FL-moesin-GFP-(1–578) molecule were (the changed bases are underlined) GGAACATCTCTTTCAATGATAACAACTTTGTGATCAAGCCC and GTCATCAAGCCCATCGATAACAACGCCCCGGACTTCGTC, respectively. Both oligonucleotides were used as follows: 18 cycles, 95 °C, 50 s; 60 °C, 50 s; and 68 °C, 10 min.

Cells and Transfection—The human HeLa cell line was grown at 37 °C in a humidified atmosphere with 5% CO_2 in Dulbecco's modified Eagle's medium (Lonza, Verviers, Belgium) supplemented with 10% fetal calf serum (Lonza), 1% of L-glutamine and 1% of the penicillin-streptomycin antibiotics. Cells were harvested and resuspended at a density of 50–70% in fresh supplemented Dulbecco's modified Eagle's medium, 24 h before cell transfection with siRNA and/or DNA construct. Specific Amaxa-kits (Amaxa GmbH, Koeln, Germany) were used for delivery of DNA constructs and/or siRNA into HeLa cells. Cells were nucleofected with 1 μM siRNA and/or 2 μg of each used DNA construct and assayed 24 h or 48 h later. None of the nucleofected protein constructs or siRNA oligonucleotides were toxic to the cells.

Immunofluorescence—Immunofluorescent HeLa cells were grown on glass coverslips. The cells were washed three times with phosphate-buffered saline (PBS) and fixed for 3 min in 2% formaldehyde in PBS. Cells were washed three times with PBS after fixation and then permeabilized with 0.5% Triton X-100 in PBS. The cells were washed with PBS after permeabilization and immunostained for 1 h at room temperature for primary antibodies diluted in PBS. The fluorophore-conjugated secondary antibody was also diluted in PBS for 1 h at room temperature. Finally, several washings with PBS were performed at room temperature. Coverslips were mounted in Mowiol-antifade (Dako, Glostrup, Denmark) and imaged in *xy* mid-sections in a FluoView™ FV1000 confocal microscope (Olympus, Center Valley, PA), for high-resolution imaging of fixed cells. The final images were analyzed with Metamorph software (Universal Imaging Corp., Downington, PA).

Western Blotting—The extent of protein expression or gene silencing was assessed by Western blot of cell lysates. Cells nucleofected with scrambled oligonucleotides or short interference RNA (siRNA) oligonucleotides against moesin (siRNA-moesin or -moesin2) or with the different DNA constructs were lysed 24 h later at +4 °C in 1% SDS sample buffer with a protease inhibitor mixture (Roche Diagnostics GmbH, Mannheim, Germany) and homogenized by sonication. Equivalent amounts of proteins, measured using the bicinchoninic acid method (BCA protein assay kit from Pierce), were separated by SDS-PAGE, using 12% gradient gels and electroblotted onto nitrocellulose membrane (Sigma-Aldrich). Cell lysates were immunoblotted with specific antibodies, and protein bands were detected by luminescence using an ECL System (Pierce).

Messenger RNA Silencing—Alexa 546-conjugated or non-fluorescence siRNA oligonucleotides, scrambled or siRNA-moesin, were from Qiagen. siRNA-moesin was generated against the following mRNA sequence of moesin: 5′-agaucgaggaacagacuaa-3′. siRNA-moesin2 was generated against the following mRNA sequence of moesin: 5′-acuaacucccaagauaggcuuc-3′. Irrelevant scrambled siRNA served as a control. The siRNAs for moesin sustained specific interference of moesin protein expression for at least 72 h.

Tf Uptake and Recycling Assays—Tf internalization assay: HeLa cells nucleofected with scrambled or siRNA-moesin oligonucleotides (1.5 μM) were detached with PBS/5 mM EDTA, washed three times with PBS, and balanced for 1 h at 37 °C in Tf uptake buffer (Krebs-Hepes buffer with 2 mM of Ca^{2+}), before starting the experiment. Then, equivalent amounts of cells (1×10^6 cells·ml^{-1}) were kept on ice-cold Tf uptake buffer, and

incubated with 200 nM of Alexa 488-labeled Tf ligand at +4 °C for 30 min. Cells were washed in cold Tf uptake buffer to remove unbound ligand, and surface-bound fluorescent Tf was measured at +4 °C, under any experimental condition. This prebound Alexa 488-labeled Tf ligand was internalized at 37 °C for the indicated early times. Returning the samples to ice stopped the internalization of fluorescent Tf. Cells were washed with ice-cold PBS, and the remaining surface-bound Tf was removed by acid washing (PBS-glycine 150 mM, pH 2.3) for 3 min. Alexa 488-associated fluorescence Tf uptake was measured in cells by flow cytometry, and normalized by the total amount of Tf ligand prebound at +4 °C, as described (26).

Tf Recycling Assay—HeLa cells nucleofected with scrambled or siRNA-moesin oligonucleotides (1.5 μM) were detached as described for Tf uptake. Cells (1×10^6 cells·ml^{-1}) were then incubated with Alexa 488-labeled Tf (200 nM in Tf uptake buffer) at 37 °C for 30 min. Cells were put in ice-cold buffer to stop the uptake and recycling processes and washed in acidic buffer (PBS-glycine 150 mM, pH 2.3) to remove recycled surface-Tf ligand. Cells were then reincubated to 37 °C to allow the recycling of the internalized fluorescent Tf for the indicated time points. At these time points, cells were put on ice, washed with acidic buffer to remove recycled Tf from the cell surface, and fixed (in PBS/2% paraformaldehyde). The amount of the fluorescent Tf ligand remained (non-released) in cells was measured by flow cytometry and expressed as the percentage of the initial intracellular Tf amount detected in cells (100%, time 0 of recycling), in each experimental condition.

Cell Surface Expression of the TfR—To detect cell-surface TfR, cells were labeled for 1 h at +4 °C with mouse monoclonal anti-CD71 primary antibody diluted in PBS buffer, washed, and incubated 1 h at +4 °C with goat anti-mouse Alexa 568-conjugated secondary antibody. The cells were washed, fixed for 3 min in 2% paraformaldehyde, and fluorescence intensity was analyzed using FACScan (BD Biosciences, San José, CA). Data were analyzed using WinMDI 2.9 application software (1993–2000 Joseph Trotter).

TIRFM—Cells were imaged with an inverted microscope Zeiss 200 M (Zeiss, Germany) through a 1.45-numerical aperture objective (alpha Fluar, 100×/1.45, Zeiss) in a Krebs-Hepes buffer containing 2 mM Ca^{2+}. The objective was coupled to the coverslip using an immersion fluid (n_{488} = 1.518, Zeiss). The expanded beam of an argon ion laser (Lasos, Lasertechnik GmbH, Germany) was band-pass filtered and used to selectively excite different fluorescent proteins, for evanescent field illumination. Different filters were used for each analyzed fluorophor. The beam was focused at an off-axis position in the back focal plane of the objective. Light, after entering the coverslip, underwent total internal reflection as it struck the interface between the glass and the solution or cell at a glancing angle.

Total internal reflection generates an evanescent field that declines exponentially with increasing distance from the interface, depending on the angle at which light strikes the interface. The angle was measured using a hemicylinder, as described previously (21). The images were projected onto a back-illuminated charge-coupled device camera (AxioCam MRm, Zeiss) through a dichoric and specific band-pass filter for each fluorophor. Each cell was imaged using Axiovision (Zeiss) for up to 2 min with 0.25-s exposures at 1 Hz when illuminated under the evanescent field.

Tracking Analysis of CCSs Movement by TIRFM Imaging—Tracking analysis of single LCa-DsRed-labeled structures was performed by using Metamorph. CCSs were excluded if they were larger than 0.5 μm or if they became oblong at any time. We marked the position of each tagged pit and tracked their x-y position as a function of time. The average radius for the x-y lateral trajectories of tracked CCSs were determined in single cells, as described (27), and calculated from the total number of cells analyzed by Metamorph.

TIRFM or Confocal Co-distribution Analysis—The overlap between different fluorescence molecules was determined by taking evanescent field and confocal images. The images were low-pass filtered using Metamorph. We plotted a small circle of 0.9-μm diameter around each analyzed spot and five circles outside these spots. These circles were used to calculate the local background. We drew 0.9-μm diameter circles around clathrin spots, duplicated the circles into the image of the pair molecule at identical pixel locations, and then determined whether the new circle contained a fluorescent point concentric to within 0.15 μm to quantify the degree of co-distribution of endogenous moesin with endogenous clathrin or α-adaptin molecules (by confocal), or the overexpressed fluorescent rab5, rab7, rab11, TfR, or α-adaptin molecules with LCa-DsRed-labeled CCSs (by TIRFM). Circles were scored as positive if they contained a fluorescent spot and negative if they did not. Moreover, co-localization was scored positive when the fluorescence intensity average was at least three times the standard deviation of the background. The percentage of co-distribution was determined in single cells after random co-distribution subtraction, and the average values were calculated from the total number of cells analyzed. Images were rotated 90 degrees and molecule co-distribution was calculated again, as described above, to determine that the observed correlation was not due to random signal overlap. If the observed co-localization was random, rotation of the image would not change the degree of signal overlap obtained before the rotation of the image.

TIRFM-based Analysis of the Tf Binding to Cell-surface TfR—To study the binding of the Tf ligand to TfR at the cell surface by TIRFM, Alexa 568-labeled Tf (50 nM in Tf uptake buffer (Krebs-Hepes with 2 mM of Ca^{2+})) was added at +4 °C for 30 min to control (scrambled) or moesin-silenced cells. Both of these cells transiently expressed the TfR-phl receptor. Cells were kept in starvation medium before Tf incubation, incubated on ice in Tf uptake buffer for 30 min, and washed with cold-Tf uptake buffer. After binding of Alexa 568-labeled Tf to TfR-phl, the cell-surface-associated fluorescence was analyzed by TIRFM, as described above for TIRFM co-distribution analysis.

Imaging TfR Exocytosis by TIRFM—Exocytosis of the TfR-phl receptor was monitored by TIRFM in control (scrambled) and moesin-silenced cells, both transiently overexpressing the fluorescent TfR-phl molecule. The frequency of TfR-phl exocytosis was calculated as the number of events recorded per cell for 60 s (3 frames/s), and comparing the frequency average between control and moesin-silenced cells (total events analyzed from 12 cells per each experimental condition).

Preparation of Plasma-membrane Sheets—Freshly nucleofected cells were grown on glass coverslips (ø, 12 mm) overnight. The coverslip was then rinsed in HEPES buffer (25 mM, pH 7.4), and put in contact with poly-L-Lysine (0.2 mg·ml-1)-precoated glass coverslip (ø, 18 mm) for 30 min at room temperature. Afterward, this coverslip sandwich was placed onto moist filter paper for 10 min without applying pressure. The sandwich was transferred to a Petri dish and filled with HEPES buffer, and the large coverslip (ø, 18 mm) was positioned on top. The coverslips were spontaneously separated while floating, thereby ripping off the cells to obtain plasma-membrane sheets on the poly-L-lysine-coated glass coverslip (ø, 18 mm), as described (28). These preparations were analyzed by TIRFM to visualize the different fluorescent nucleofected proteins at the cell surface.

PIP_2 Binding Assay and Dot-blot Analysis—Binding assay of FL-moesin-GFP or 4K/4N-moesin-GFP to soluble PIP_2 was performed with purified moesin molecules from lysates of respective nucleofected cells. Cells were lysed at +4 °C (PBS-1% Triton X-100, completed with a protease inhibitor mixture), and sonicated for 10 s. These lysates were precleared, and then incubated (500 μg of total protein) overnight at +4 °C with anti-GFP polyAb (40 μg), non-covalently complexed to protein G-Sepharose beads (100 μl). Co-immunoprecipitated proteins were washed with PBS buffer and incubated with 100 μl of soluble PIP_2 (0.5 mg·ml^{-1} in chloroform:methanol:1 N HCl: H_2O; at a volume ratio of 20:10:1:1) for 2 h at room temperature. The samples were washed with PBS and boiled in β-mercaptoethanol-Laemmli sample buffer for 1 min at 90 °C. Protein G-Sepharose beads were removed by centrifugation, and the supernatants were spotted in polyvinylidene fluoride membranes using a dot-blot apparatus (Slotblot, GE Healthcare). PIP_2 bands were probed with a specific anti-PIP_2 mAb (1:200). The dot blots were then reprobed, after membrane stripping with anti-GFP polyAb (1:200). PIP_2 and GFP fusion protein bands were detected by luminescence using the ECL system (Pierce).

Subcellular Fractionation and Protein Precipitation—Scrambled (control) or siRNA-moesin-treated HeLa cells (1×10^7 cells) were washed twice with PBS at +4 °C. Cells were gently scraped from culture plates and collected by centrifugation. They were then homogenized in 200 μl of buffer (78 mM KCl, 4 mM $MgCl_2$, 8.37 mM $CaCl_2$, 10 mM EGTA, 50 mM HEPES/KOH, pH 7.0) containing 250 mM sucrose and centrifuged at 1000 × *g* for 5 min. The supernatants (from scrambled or siRNA-moesin cells) were placed on a 5–20% linear Optiprep™ (Nycomed, Amersham Biosciences) gradient, formed in 12 ml of the above buffer, and centrifuged at +4 °C, for 20 h at 100,000 × *g*, in an SW28 rotor (Beckman, Germany). Following the centrifugation, the total volume gradient was separated into 1-ml fractions, collected from top to bottom (from 5% to 20% Optiprep™ concentration, respectively). The protein precipitation was as follows: the volume of each collected fraction (1 ml) was duplicated with cool acetone (1 ml, −20 °C) in acetone-compatible tubes. The samples were then vortexed and incubated for 1 h at −20 °C, and further centrifuged for 10 min at 13,000 × *g*. Samples were decanted, and the protein pellets were resuspended in Laemmli buffer to be resolved by SDS-PAGE (12%) and Western blot techniques using specific antibodies.

Statistics—Data were compared using Student's *t* test. *Asterisks* indicate $p < 0.05$.

RESULTS

Moesin Co-distributes with Constitutive Components of CCSs—To study the involvement of moesin in CCV trafficking, we first analyzed the distribution of endogenous moesin with constitutive components of CCSs by using fluorescence confocal microscopy. We observed that endogenous moesin presented a punctated pattern of distribution in HeLa cells (Fig. 1), partially co-distributing with the endogenous CHC (Fig. 1*A*; quantified in Fig. 1*D*), a main component of the clathrin triskelion that forms CCPs and CCVs (29–31). We also observed a partial co-distribution of moesin with endogenous α-adaptin (Fig. 1*B*; quantified in Fig. 1*D*), a key component of the AP2 complex for CCV formation and clathrin-mediated endocytosis (32, 33). However, endogenous moesin slightly co-distributed with the γ-adaptin protein (Fig. 1*C*; quantified in Fig. 1*D*), a component of the heterotetrameric adaptor protein complex AP-1, which has been involved in mediating cargo sorting from the *trans*-Golgi network to the endosome compartment (reviewed in Refs. 34–38), as well as in promoting retrograde endosome to *trans*-Golgi network transport (39). The quantification of moesin co-distribution with these molecules was performed as indicated under "Experimental Procedures." These data indicate that a pool of endogenous moesin mostly co-distributes with specific components of CCSs that are associated with plasma membrane-derived CCSs.

Moesin Silencing Alters Movement and Causes Clustering of CCSs—To investigate the functional involvement of moesin in CCV trafficking, we first performed TIRFM experiments tracking LCa-DsRed-labeled structures in cells where endogenous moesin was silenced by siRNA (Fig. 2, *A* and *B*). We observed that overexpressed LCa-DsRed displayed a diffraction-limited punctated pattern in transfected cells (Fig. 2*C*, *white arrows* in scrambled and siRNA-moesin images), which is characteristic of CCSs (8, 21, 27, 40), as was observed with the endogenous CHC-monitored structures (Fig. 1*A*).

Moesin silencing provoked an alteration of the lateral movement of single LCa-DsRed-labeled CCSs (Fig. 2, *D–F*), without affecting the number and size of CCSs (Fig. 2*C*, see *white arrows*, and average line scans, for 200 CCSs sized < 0.5 μm, in scrambled or siRNA-moesin condition). Hence, the trajectories obtained for the lateral movement of LCa-DsRed-labeled CCSs, calculated as previously described (27), were larger in cells lacking moesin than those observed in control cells (Fig. 2, *D–F*, and supplemental Movies S1 and S2, from Fig. 2*F*). In control conditions, >60% of analyzed LCa-DsRed-labeled CCSs moved in trajectories from 0.5 μm to <1 μm (Fig. 2*D*, *scrambled bars*, and supplemental Movie S1, from Fig. 2*F*, *scrambled images*), whereas ~40% of analyzed structures moved in trajectories between 1 and 3.5 μm (Fig. 2*D*, *scrambled bars*).

As regards the cells without endogenous moesin, ~30% of analyzed CCSs moved in trajectories from 0.5 μm to <1 μm, whereas CCSs moving in trajectories from 1 μm to 6 μm accounted for ~70% of total analyzed CCSs (Fig. 2*D*, *siRNA-*

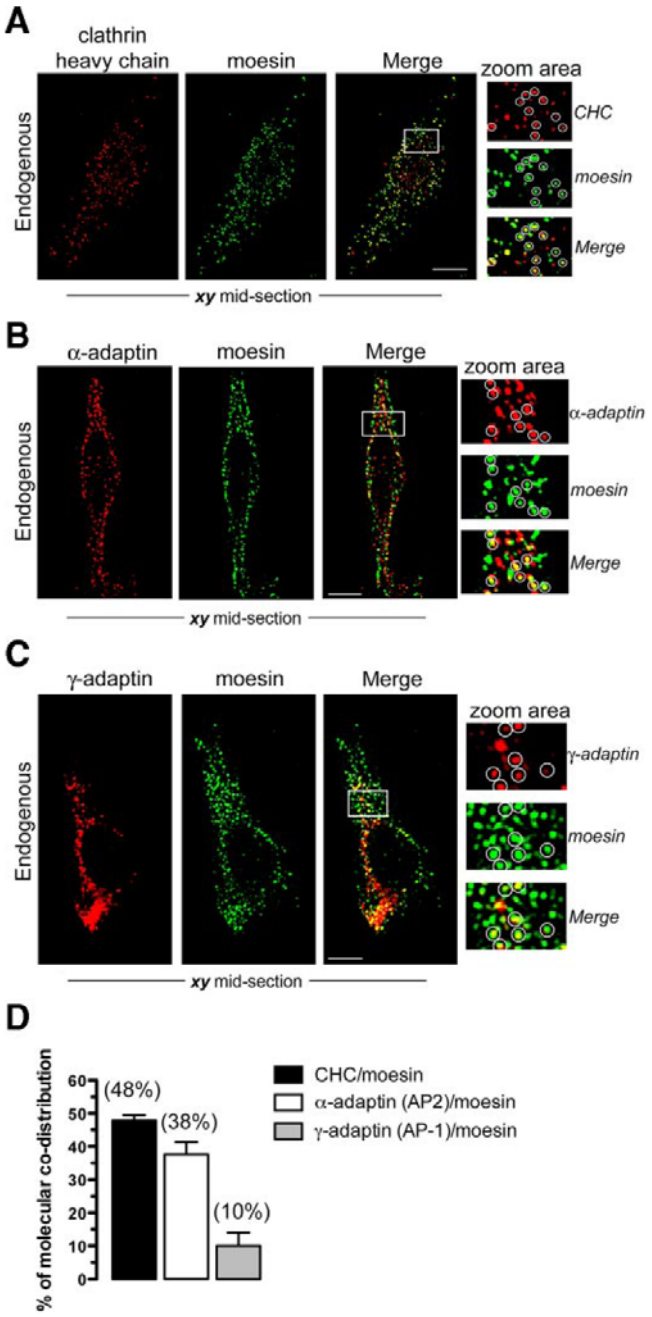

FIGURE 1. **Endogenous moesin co-distributes with components of CCSs.** *A*, confocal microscopy analysis of cellular co-distribution of endogenous CHC and moesin molecules. *B*, confocal microscopy analysis of cellular co-distribution of endogenous α-adaptin and moesin molecules. *C*, confocal microscopy analysis of cellular co-distribution of endogenous γ-adaptin and moesin molecules. From *A* to *C*, the *zoom area* shows CHC-, α-adaptin-, and γ-adaptin-labeled structures where molecule co-distribution was analyzed (*encircled vesicles* in *A*, *B*, and *C*, respectively). *D*, *bar histograms* show the quantification of the co-distribution of endogenous moesin with CHC, α-adaptin, or γ-adaptin. Data are mean ± S.E., (n = 500 spots from 5 different cells). The quantification was performed as described under "Experimental Procedures." *Bar*, 10 μm.

moesin bars, and supplemental Movie S2, from Fig. 2*F*, *siRNA-moesin images*). Similar results were obtained in moesin-silenced cells by using the siRNA-moesin2 oligo (supplemental Fig. S1, *A*, *Western blot* and *B*, *images*). Hence, the large trajectories observed for the movement of single CCSs were from 0.5 μm to <1 μm in scrambled cells (53% of CCSs analyzed), whereas single CCSs from siRNA-moesin2-treated cells mainly moved in lateral trajectories from 1 μm to <6 μm (79% of analyzed CCSs) (supplemental Fig. S1*C*). Therefore, the average area of movement for the analyzed CCSs showed the following values for the trajectory radius: 0.7 ± 0.084 μm in control (scrambled) cells and 1.4 ± 0.142 μm in moesin-silenced cells (Fig. 2*E*). Therefore, the results obtained were not conditioned by the siRNA oligonucleotide used to interfere with moesin protein expression, and depended on the specific silencing of the endogenous moesin protein.

We also observed an unusual aggregation of single LCa-DsRed-labeled CCSs in moesin-silenced cells in the evanescent field (Fig. 2*C*, *white arrowheads*, and Fig. 2*G*, see representative *clusters 1* and *2*). These clusters of CCSs were also observed in cells lacking moesin after treatment with the siRNA-moesin2 oligonucleotide (supplemental Fig. S1*B*). It appears that LCa-DsRed-labeled clusters are not formed by abnormal fusion of CCSs, because they progressively dissociate in single LCa-DsRed-labeled structures (Fig. 2*G*, time-lapse of frames and line-scan analysis, and supplemental Movie S3, disaggregation of *cluster 1*). Fluorescence intensities of these sorted CCSs rapidly dimmed in the evanescent field suggesting that these CCSs either moved out from the evanescent field or lost the clathrin coat (supplemental Movie S3).

Therefore, we propose that the formation of these clusters may be due to the accumulation of individual CCVs that were not correctly trafficked in the absence of the F-actin-linker moesin (supplemental Movie S2 from moesin-silenced cells in Fig. 2*F*, tracked CCS joining aggregates of CCSs, at the *bottom* of the *movie*). These data indicate that moesin is a CCS linker that could regulate vesicle trafficking.

The N-terminal-PIP$_2$ Binding Domain of Moesin Mediates Its Co-distribution with CCSs—We performed TIRFM-based analysis of LCa-DsRed-labeled CCSs with different moesin-GFP constructs (22), expressed in HeLa cells (Fig. 3), to explore the structural features of moesin that are responsible for its co-distribution with CCSs. Three C-terminal GFP-tagged moesin constructs were used first: FL-moesin-GFP (full-length moesin), N-moesin-GFP (N-terminal domain), or C-moesin-GFP (the C-terminal actin binding region) (22). FL-moesin-GFP, which entirely conserves functional N-terminal and C-terminal F-actin-binding domains, anchors membrane structures to F-actin filaments. On the other hand, the N-moesin product, without the F-actin-binding domain, works as a dominant negative form by disconnecting endogenous moesin from both membrane structures and cortical actin. However, C-moesin protein product binds to F-actin filaments and lacks the ability to associate with membrane structures without any negative dominant effect on endogenous moesin (22).

We observed that overexpressed FL- and N-moesin-GFP molecules mainly distributed on plasma membrane-associated structures and also showed some diffuse intracellular distribution and a punctated expression pattern (Fig. 3, *A* and *B*), as described (22, 41). Hence, FL- or N-moesin-GFP molecules that presented a punctated pattern of expression co-distributed with LCa-DsRed-labeled CCSs (Fig. 3, *A* and *B*, *white arrows*, and quantified in Fig.

3*E*). However, the C-moesin-GFP protein product, which binds to F-actin (supplemental Fig. S4*C*, C-moesin-GFP and related *images*), presented a diffused expression pattern and did not co-distribute with LCa-DsRed-labeled CCSs as observed in the evanescent field (Fig. 3, *C* and *E*).

On the other hand, we observed certain aggregates of LCa-DsRed-labeled CCSs in cell regions where the dominant negative N-moesin-GFP molecule co-distributed (Fig. 3*B*, see *white arrowheads*). These clusters of CCSs were similar to those which appeared in moesin-silenced cells (Fig. 2*C*, see *white arrowheads* in the *siRNA-moesin image*, Fig. 2*G*, and supplemental Movie S3).

It is thought that the dominant negative effect exerted by the N-moesin construct, which anchors to membrane structures, lies in its capacity to bind to the C-terminal half of the endogenous moesin molecule, thereby disconnecting moesin from actin cytoskeleton (22). Therefore, N-moesin-GFP could alter the cellular distribution of CCSs by disrupting the anchoring of moesin-associated CCSs to F-actin, as was observed in moesin-silenced cells (Fig. 2). Thus, it appears that the N-terminal part of moesin is responsible for its co-distribution with CCSs, while the C-terminal part of moesin would help to link moesin-bearing CCSs to F-actin. FL-moesin-GFP molecules distributed with preformed LCa-DsRed-labeled CCSs on plasma membrane, and their associated fluorescence intensities rapidly dimmed together in the evanescent field (supplemental Fig. S2, *A* and *B*, respectively). These data indicate that FL-moesin-GFP/LCa-DsRed-labeled CCSs moved out in the *z* axis direction, which could represent nascent moesin-positive CCVs.

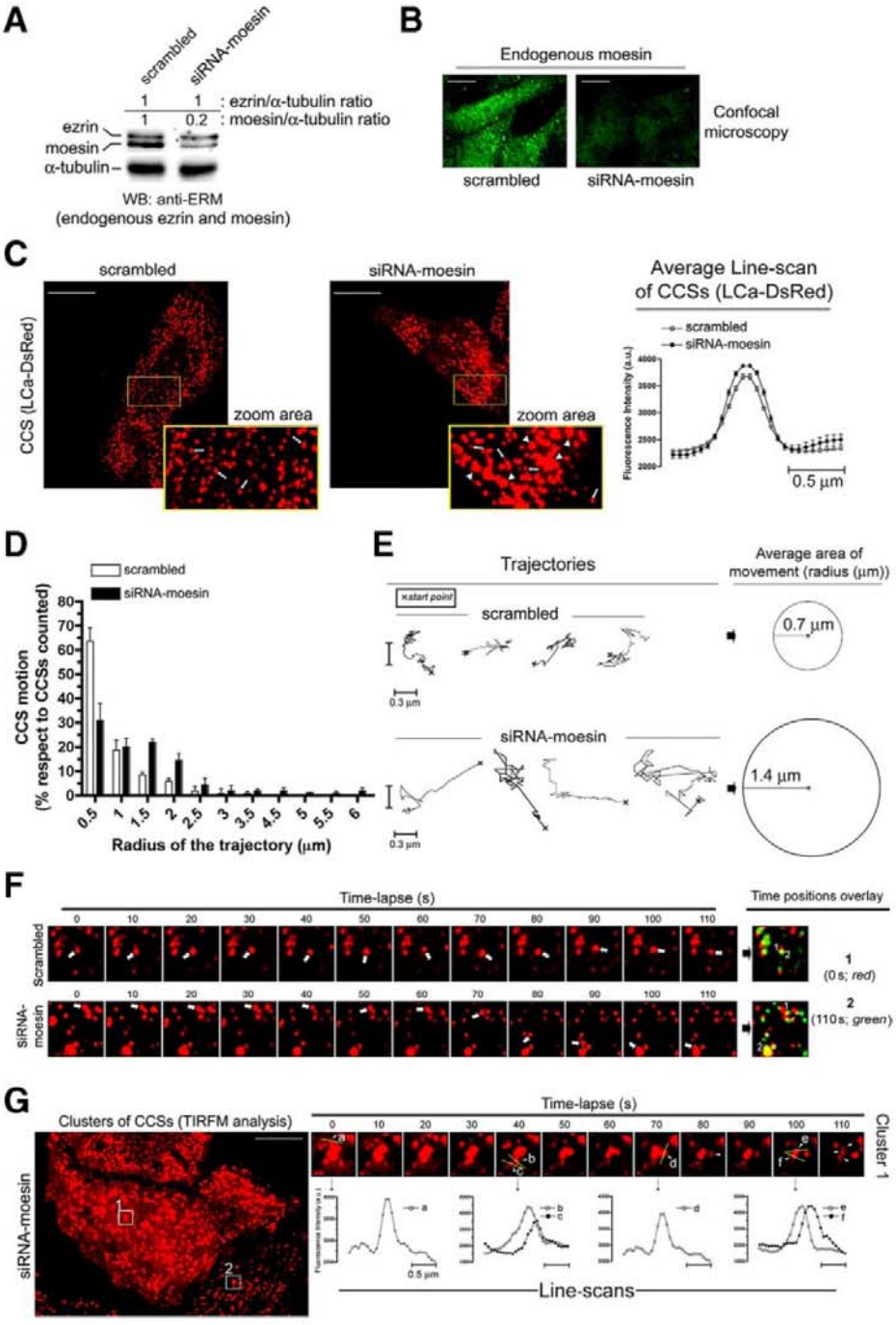

over, PIP_2 is required for the conformational activation of ERM proteins (43, 44). Therefore, we studied whether moesin associates to CCSs through its consensus PIP_2-binding domain. Combined K/N mutations of the Lys residues 253 and 254, and 262 and 263, are responsible for the loss of the interaction of ERM mutants with PIP_2 (16, 45). A similar effect is achieved in ezrin by combining the double mutation of residues K63N and K64N with the double K253N,K254N mutation (45). Then, the mutation of four N-terminal Lys residues, within the $KK(X)_n(K/R)K$ motifs, eliminates the

The term "endocytic adaptor" is generally reserved for proteins that bind to PIP_2 and also to clathrin, both of which are present in the CCSs (1). These adaptors affect the cargo-induced sorting signals during endocytosis, by interacting with the cytoplasmic tails of the CCV-associated cargos (1). The moesin protein, like other F-actin-linkers from the ERM family, presents the $KK(X)_n(K/R)K$ consensus binding site for PIP_2 at the N-terminal part of the molecule (42). More-

capacity of ERM proteins to bind to PIP_2, which redistribute to the cytoplasm (16, 45).

Therefore, and based on previous inactivating mutations reported for ezrin (16, 45), we have created a new construct by changing the N-terminal Lys residues 253, 254, 262, and 263 into Asn, thereby generating the K253N,K254N,K262N,K263N-moesin-GFP (4K/4N-moesin-GFP) mutant (Fig. 3*D*). As compared with the FL-moesin-GFP molecule (Fig. 3, *A* and *F*, and supplemental Fig. S3*A*), the inert 4K/4N-moesin-GFP mutant mainly presented a diffused and altered cytoplasmic distribution (Fig. 3*D*), which did not bind soluble PIP_2 (Fig. 3*F*) and did not distribute to PIP_2-enriched plasma membrane domains (supplemental Fig. S3*B*), as monitored by the fused ECFP-tagged pleckstrin homology domain of the phosphatidylinositol-specific phospholipase $C\delta_1$ (ECFP-PH) (23–25). In fact, the 4K/4N-moesin-GFP molecule no longer co-localized with LCa-DsRed-labeled CCSs, and mainly presented a cellular distribution pattern similar to the C-moesin-GFP construct (Fig. 3*D*, *TIRFM images*, and quantified in Fig. 3*E*). This inert mutant did not have any effect on the distribution and organization of LCa-DsRed-labeled CCSs (Fig. 3*D*).

Moreover, moesin knockdown (supplemental Fig. S4, *A* and *B*) or overexpression of FL-moesin-GFP or 4K/4N-moesin-GFP molecules (supplemental Fig. S4*C*) affected neither cell morphology nor actin cytoskeleton. Therefore, we propose that the N-terminal-PIP_2-binding domain of moesin is responsible for its co-distribution with the different CCSs, and that the moesin molecules associated with CCSs could be involved in the trafficking of nascent endocytic CCVs.

Moesin Is Involved in the Trafficking of Nascent rab5-CCVs—We tracked LCa-DsRed-labeled CCSs in cells overexpressing fluorescent rab5 (Fig. 4), rab7, or rab11 (supplemental Fig. S5, *A* or *B*, respectively) small GTPases to analyze whether moesin silencing-mediated effects on the motility of CCSs occurred at a particular endocytic intermediate. These rab GTPases are considered to be specific markers for early endosomes, late endosomes, or for perinuclear vesicles that recycle from Golgi to plasma membrane, respectively (46, 47). We used fluorescent scrambled or siRNA-moesin oligonucleotides to identify, by epifluorescence, both intact control cells and cells without endogenous moesin (Fig. 4, *A* and *B*, respectively). We further analyzed, by TIRFM, the cellular distribution of the different rab GTPases under this experimental condition. Fluorescent siRNA-moesin or -moesin2 oligonucleotides specifically silenced the expression of the endogenous moesin protein (Fig. 4*E* and supplemental Fig. S1*A*, *moesin Western blot bands*), and provoked an altered accumulation and aggregation of the CCSs, as observed in the evanescent field (Fig. 4*B* and supplemental Fig. S1*B*, *white arrowheads* indicate aggregates of CCSs).

We observed that moesin interference provoked the accumulation of ECFP-rab5/LCa-DsRed-labeled CCSs (Fig. 4*C*, *TIRFM images*, and quantified in Fig. 4*D*, ~30% of increase), when compared with control cells. The observed basal level of rab7- or rab11-labeled CCSs was not significantly affected in moesin-silenced cells (supplemental Fig. S5, *A* or *B*, respectively, and quantified in bar histograms). The transfected ECFP-rab5 protein was equally expressed in both control and moesin-silenced cells (Fig. 4*E*, ECFP-rab5 Western blot bands), as occurred with fluorescent rab7 and rab11 molecules (data not shown). Furthermore, the overexpressed amount of ECFP-rab5 did not alter the cell-surface expression level of TfR and did not affect the uptake of the Tf ligand (Fig. 4, *F* and *G*, respectively). Hence, it seems that CCSs were not perturbed by the overexpressed amount of the ECFP-rab5 molecule. Taking all these data together, we suggest that moesin knockdown induces the accumulation of CCSs carrying the rab5 molecule.

Similar results were obtained in moesin-silenced cells overexpressing the ECFP-rab5, LCa-DsRed, and GFP-α-adaptin molecules (Fig. 5*A*). First of all, we observed that LCa-DsRed and GFP-α-adaptin molecules showed a high degree of co-distribution (Fig. 5*A*, and quantified in Fig. 5*B*) indicating that the LCa-DsRed-labeled structures could be considered as functional CCSs, as previously described (48–51). Moreover, specific moesin knockdown provoked the increase of ECFP-rab5/GFP-α-adaptin/LCa-DsRed-colabeled structures in intact moesin-silenced cells (Fig. 5*A*, and quantified in Fig. 5*C*). The ECFP-rab5 molecule was equally expressed both in control and moesin-silenced cells (Fig. 5*A*, and quantified in Fig. 5*D*, Western blot). We propose that these accumulated structures represent nascent endocytic CCVs, containing the rab5 GTPase, as was further confirmed by comparative studies on plasma-membrane sheets (Fig. 5*E*).

Plasma-membrane sheets were prepared from scrambled (control) or moesin-silenced cells, expressing ECFP-rab5, TfR-EGFP, and LCa-DsRed molecules (Fig. 5*E*). It is worth mentioning that the basal level of co-distribution of TfR-EGFP/ECFP-

FIGURE 2. **Silencing of endogenous moesin alters normal trafficking of CCSs and provokes their clustering.** *A*, Western blot analysis of specific moesin knockdown (siRNA-moesin) in HeLa cells compared with control (scrambled) cells. Silencing of endogenous moesin is quantified as the ratio of moesin and α-tubulin band intensities, compared with the values for ezrin molecule. A representative experiment of three is shown. *B*, confocal microscopy images (maximal projections) for endogenous moesin silencing (siRNA-moesin), compared with control (scrambled) HeLa cells. *C*, TIRFM analysis of LCa-DsRed-associated CCSs in scrambled or moesin-silenced (siRNA-moesin) HeLa cells. In the *zoom area* of scrambled or moesin-silenced (siRNA-moesin) cells, CCSs (<0.5 μm; see "Experimental Procedures") are indicated by *white arrows*. *Right*, average CCS-diameter size for CCSs, analyzed by line scan, under any experimental condition. Data are mean ± S.E. (n = 200 CCSs from six different cells). *White arrowheads* indicate abnormal clustering of LCa-DsRed-labeled CCSs in the *zoom area* of moesin-silenced (siRNA-moesin) cells. *D*, analysis of the movement (radius of the trajectories) of LCa-DsRed-labeled CCSs in control (scrambled) or moesin-silenced (siRNA-moesin) HeLa cells. Data are from 120 CCSs counted in 10 different cells per experimental condition. *E*, *left*, four different and representative movement trajectories for LCa-DsRed-labeled CCSs are shown for control (scrambled) or moesin-silenced (siRNA-moesin) cells. The *x* symbol indicates the starting point for each trajectory indicated. *Right*, average area of movement for CCSs in cells without moesin (siRNA-moesin), compared with control cells (scrambled). The *average radius* indicates the maximum trajectories observed, under any experimental condition. Data are mean ± S.E. from three independent experiments: in each experiment, 120 CCSs were counted in 10 different cells per experimental condition. *F*, TIRFM-based time-lapse study of CCS movement for 110 s, in control (scrambled) or moesin-silenced (siRNA-moesin) HeLa cells (see *white arrow-labeled vesicles*). The *time position overlay panel* shows initial (0 s, *red*) and final (110 s, *green*) positions (*1* and *2*, respectively) for the tracked CCSs, in the same image. *G*, time-lapse analysis of the decay of the fluorescence intensity of single CCSs sorted from CCS aggregates, observed in the evanescent field of moesin-silenced cells. *Line scans* show the fluorescent intensity profiles for any of the sorted individual CCSs (*cluster 1* from the *cellular square area*), indicated with *a–f* symbols, and analyzed at times 0 s, 40 s, 70 s, and 100 s, respectively. *Bar*, 10 μm.

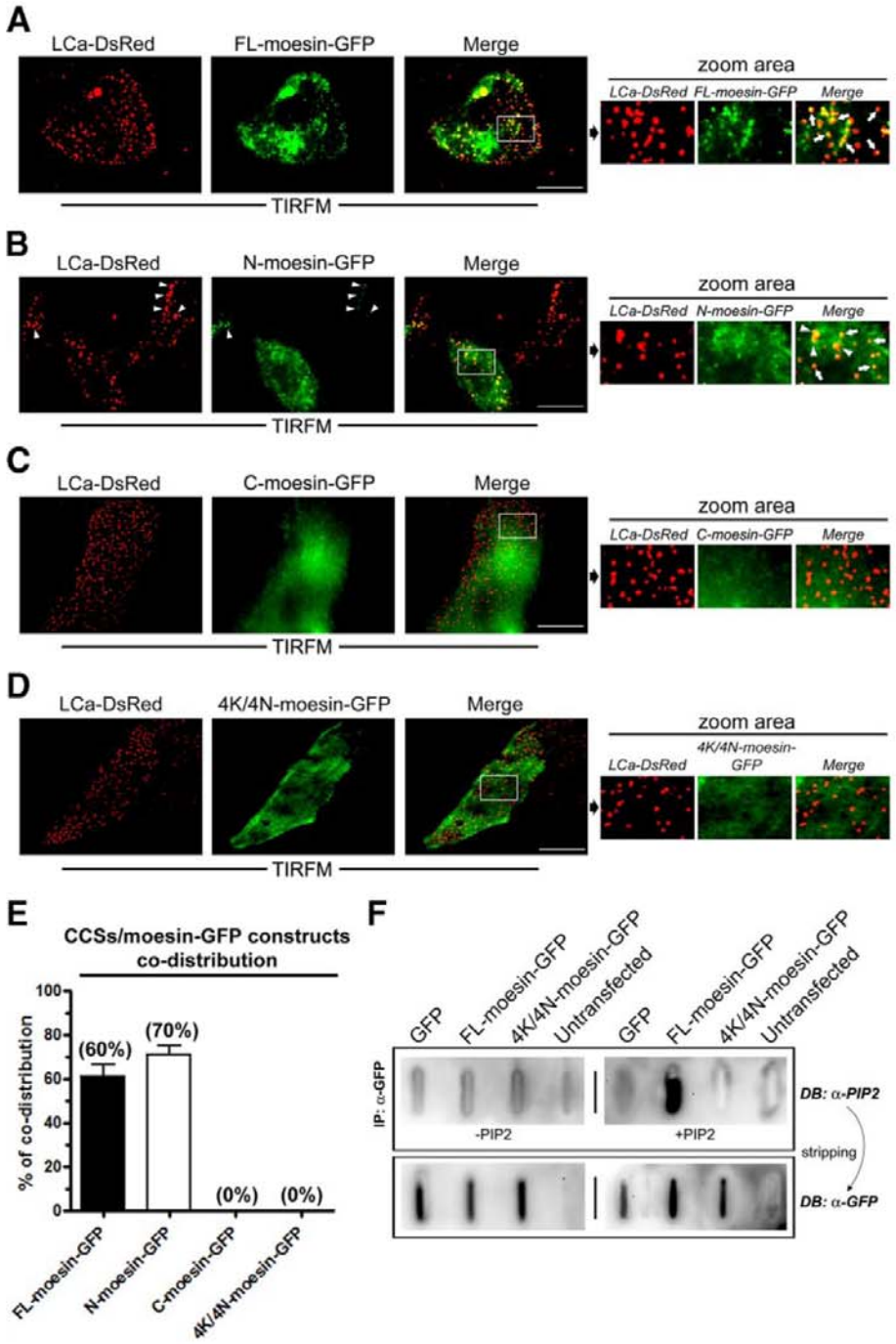

FIGURE 3. **The PIP_2-binding domain of moesin is responsible for its association with CCSs.** *A–D*, TIRFM images for the analysis of co-distribution of LCa-DsRed-labeled CCSs with FL-, N-, C-, or 4K/4N-moesin-GFP constructs, respectively, in HeLa cells. In the *zoom areas*, *white arrows* indicate representative CCS, where LCa-DsRed molecules co-distributed with FL- or N-moesin-GFP products, whereas *white arrowheads* indicate abnormal clustering of LCa-DsRed-labeled CCS co-distributed with N-moesin-GFP. *Bar*, 10 μm. *E*, *bar histograms* show the quantification of the co-distribution of FL-, N-, C-, and 4K/4N-moesin-GFP molecules with LCa-DsRed-labeled CCSs. Data are mean ± S.E. (n = 500 spots from 5 different cells). The quantification was performed as described under "Experimental Prodecures." *F*, *top dot blots*, dot-blot analysis of PIP_2 bound to purified FL-moesin-GFP and 4K/4N-moesin-GFP molecules (*DB*: α-PIP_2) from lysates of respective nucleofected cells, previously immunoprecipitated by using a specific antibody against GFP (*IP*: α-GFP). *Bottom dot blots*, dot-blot analysis of the presence of the nucleofected and immunoprecipitated GFP, FL-moesin-GFP, and 4K/4N-moesin-GFP molecules (*DB*: α-GFP), after membrane stripping of the *top dot blots*. This experiment was performed in lysates from cells nucleofected by GFP, FL-moesin-GFP, or 4K/4N-moesin-GFP, and compared with lysates from untransfected cells. A representative experiment of three performed experiments is shown.

rab5/LCa-DsRed-labeled structures did not change after moesin knockdown (Fig. 5*E*, ~10% of total observed CCSs, as shown in the *zoom areas*). These structures could correspond to deeply invaginated CCSs that have been described as containing the rab5 GTPase to promote the formation of functional transport vesicles (52). In fact, aggregates of ECFP-rab5/LCa-DsRed-labeled structures, shown in intact moesin-silenced cells (Figs. 4*C*, 6*B*, and 6*C*), were not detected in plasma-membrane sheets (Fig. 5*E*). Thereby, this indicated that these accumulated structures correspond to nascent endocytic rab5-CCVs (Figs. 4*C*, 6*B*, and 6*C*), which were removed during the cell rip-off (Fig. 5*E*). The majority of the CCSs detected in control or moesin-silenced plasma-membrane sheets were rab5-negative, and therefore represent CCPs. Patches of CCPs were not observed in moesin-silenced plasma-membrane sheets (Fig. 5*E*). These data support the fact that moesin knockdown affects cellular location and trafficking of nascent endocytic CCVs, but not CCP and CCV formation (or the TfR uptake process). Therefore, the impaired link of rab5-CCVs to F-actin filaments, after moesin silencing, perturbs the trafficking of these endocytic vesicles.

Moesin Silencing Provokes the Accumulation of TfR in Nascent rab5-CCVs, Affecting Its Cell-surface Expression and Recycling Process—TfR is constitutively associated to CCPs (8) and follows internalization, via CCVs, regardless of Tf-ligand engagement (53). Therefore, we studied the functional consequences of specific moesin knockdown in the accumulation of the TfR in nascent rab5-CCVs.

This is why we silenced endogenous moesin (Fig. 6*A*, *left Western blot panel*) in cells overexpressing TfR-EGFP, ECFP-rab5, and LCa-DsRed constructs (Fig. 6). The ECFP-rab5 molecule was equally overexpressed both in moesin-silenced and scrambled-control cells (Fig. 6*A*, *right Western blot panel*).

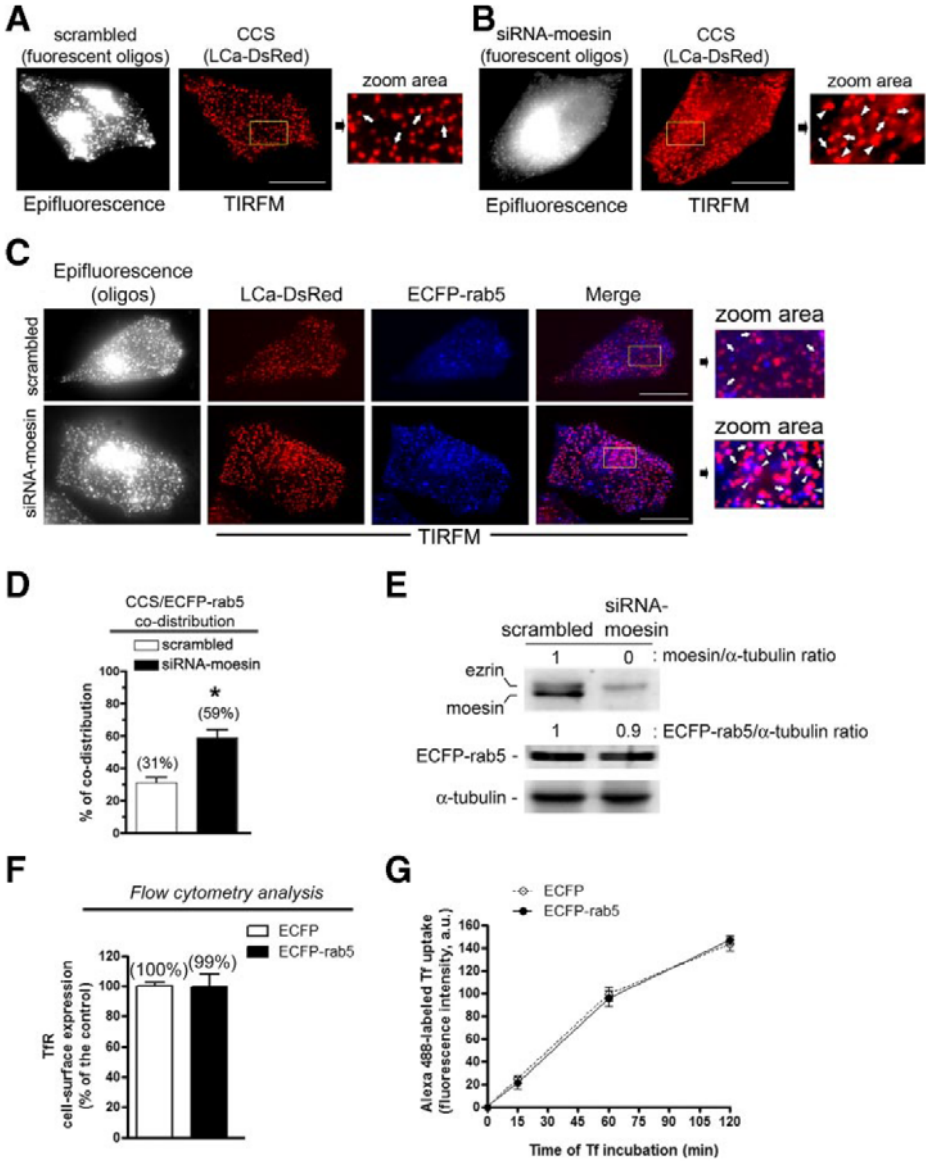

FIGURE 4. **Silencing of endogenous moesin provokes the accumulation of rab5-CCSs.** *A* and *B*, TIRFM analysis of LCa-labeled CCSs in HeLa cells treated with fluorescent-scrambled and siRNA-moesin oligonucleotides, monitored by epifluorescence. In the *zoom area*, *white arrows* indicate single representative CCSs (<0.5 μm, see "Experimental Procedures"), whereas *white arrowheads* indicate clusters of CCSs (*siRNA-moesin panel*). *C*, moesin silencing effect on LCa-DsRed-labeled CCSs in HeLa cells overexpressing ECFP-rab5, compared with control cells (scrambled). In the *zoom area*, *white arrows* indicate CCSs carrying the fluorescent rab5 marker, under any experimental condition. *White arrowheads* indicate clusters of CCSs in the *zoom area* of siRNA-moesin cells. *D*, *bar histograms* show the percentage of ECFP-rab5/LCa-DsRed co-distribution. Data indicated in *bar histograms* are mean ± S.E. (n = 1000 spots from 5 different cells). *, $p < 0.05$, t test. *E*, Western blot analysis of ECFP-rab5 expression and moesin knockdown, by using fluorescence siRNA-moesin oligonucleotides, compared with fluorescent control (scrambled) oligonucleotides. Silencing of endogenous moesin is quantified as the ratio of moesin and α-tubulin band intensities, under any experimental condition, and compared with the ezrin molecule. The total level of expression of the transfected ECFP-rab5 molecule was quantified as the ratio of ECFP-rab5 and α-tubulin band intensities, both in control and moesin-silenced cells. A representative experiment is shown. *F*, flow cytometry analysis for the quantification of TfR (CD71) cell-surface expression in control cells (overexpressing the ECFP protein, *open histograms*) or cells overexpressing the ECFP-rab5 small GTPase (*solid histograms*) cells. Data were corrected by subtracting the nonspecific adsorption of antibodies, determined by using an IgG-isotype negative control. Data are mean ± S.E. (n = 9, from three independent experiments). *G*, Alexa 488-labeled Tf uptake, determined at 15 min, 1 h, and 2 h, and analyzed by flow cytometry, in control (overexpressing the ECFP protein) or cells overexpressing the ECFP-rab5 molecule. Data are mean ± S.E. (n = 9, from three independent experiments). In *A–C* the presence of the fluorescent scrambled or siRNA-moesin oligonucleotides is monitored by epifluorescence. *Bar*, 10 μm.

Cells without endogenous moesin accumulated endocytic rab5-CCVs, as monitored by ECFP-rab5/LCa-DsRed co-distribution (Fig. 6, *B* and *C*, and quantified in Fig. 6*D*). The specific silencing of moesin did not alter the constitutive association of TfR with CCSs (Fig. 6, *B–E*, and quantified in Fig. 6*F*). Furthermore, it was observed that the TfR-EGFP, ECFP-rab5, and LCa-DsRed molecules co-distributed in these nascent CCVs (rab5-CCVs), in scrambled and in moesin-silenced cells (Fig. 6*E*). However, only moesin knockdown favors the retention of the TfR in rab5-CCVs as was detected by an increase in the TfR-EGFP/ECFP-rab5/LCa-DsRed structures (Fig. 6*B*, *siRNA-moesin images*, and quantified in Fig. 6*D*). It is conceivable that these altered endocytic rab5-CCVs containing the TfR may represent, in part, a compartment of clathrin-containing endosomes that have been previously described as being highly motile and as accumulating the Tf ligand (50).

Flow cytometry analysis of moesin-silenced cells showed reduced expression levels of the TfR at the cell surface (Fig. 7*A*, ~40% reduction), when compared with control (scrambled) cells. We then examined the ability of these cells to uptake Alexa 488-labeled Tf ligand (see "Experimental Procedures"). We observed that the rate of early internalization of Tf was similar in control and moesin-silenced cells (Fig. 7*B*), indicating that moesin did not affect Tf uptake. Therefore, the reduced cell-surface expression of TfR, in cells lacking moesin, could be due to its retention in the altered nascent rab5-CCVs rather than a defect in TfR internalization.

We analyzed the endosomal distribution of endogenous TfR, by a biochemical approach in moesin-silenced cells, and compared this to control (scrambled) cells (Fig. 7, *C* and *D*) to further confirm that moesin knockdown provokes the accumulation of the TfR in endocytic rab5-CCVs. To do this, we centrifuged postnuclear supernatants of moesin-silenced or control (scrambled) cells, on shallower 5–20% Optiprep™ gradients (see "Experimental Procedures"), and the distributions of moesin, ezrin, TfR, rab5, and rab7 proteins were determined in each subcellular fraction collected by Western blot and by using specific anti-

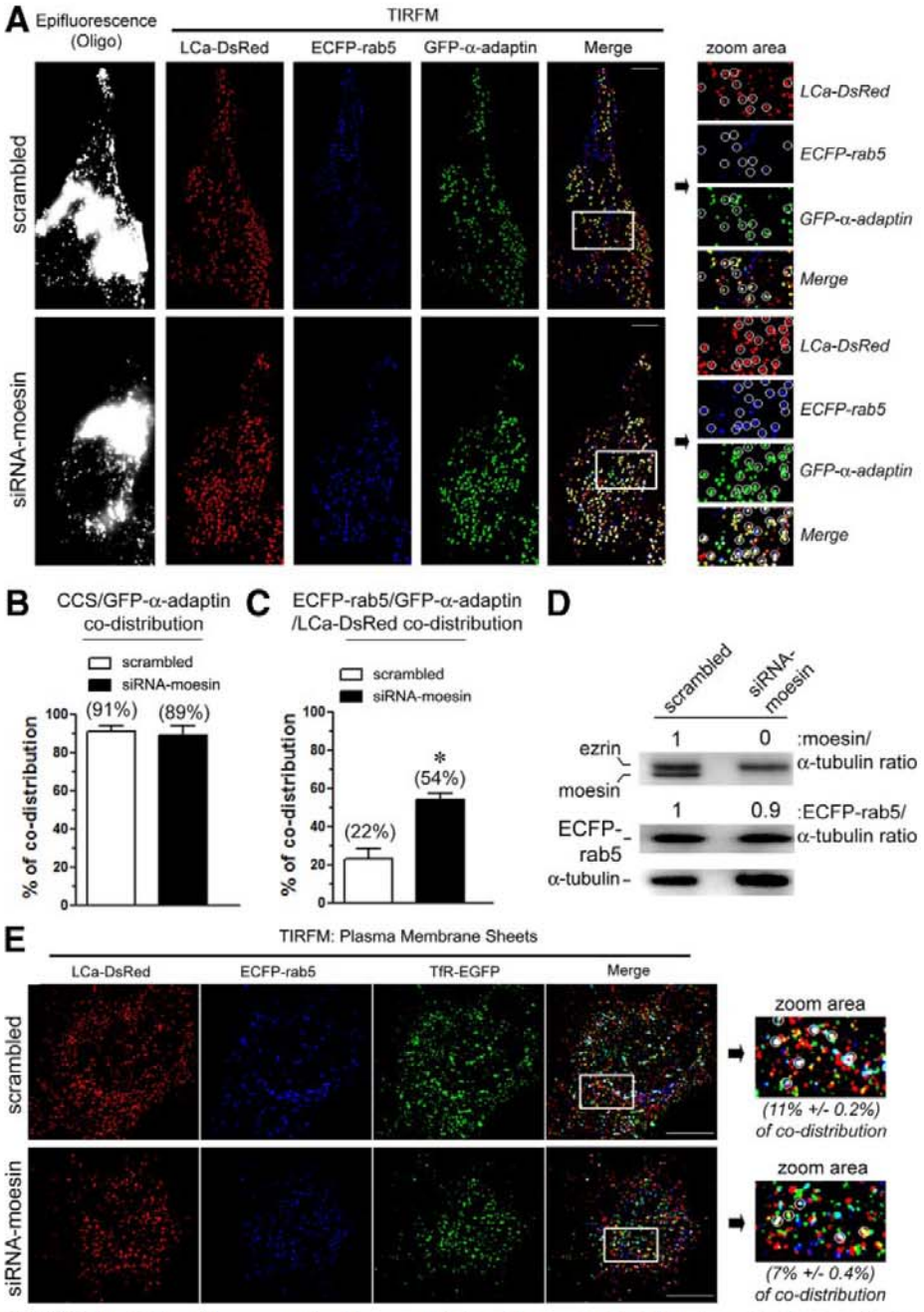

FIGURE 5. **Moesin knockdown provokes the accumulation of nascent rab5-CCVs.** *A*, moesin silencing effect on cellular distribution of ECFP-rab5/GFP-α-adaptin/LCa-DsRed-labeled CCSs, compared with control cells (scrambled). Accumulated rab5-CCSs were monitored by the ECFP-rab5/GFP-α-adaptin/LCa-DsRed labeling (*Merge images*). The presence of the fluorescent scrambled or siRNA-moesin oligonucleotides is monitored by epifluorescence. *Zoom areas*, *circles* in scrambled and siRNA-moesin cells indicate ECFP-rab5/LCa-DsRed-CCSs co-distributing with the GFP-α-adaptin molecule. *Bar*, 5 μm. *B*, *bar histograms* show the quantification of LCa-DsRed/GFP-α-adaptin co-distribution in scrambled (control cells) and in moesin-silenced cells (*open* and *solid histograms*, respectively). *C*, *bar histograms* show the quantification of ECFP-rab5/LCa-DsRed/GFP-α-adaptin co-distribution in scrambled (control cells) and in moesin-silenced cells (*open* and *solid histograms*, respectively). *, $p < 0.05$, *t* test. Data in *B* and *C* are mean ± S.E. ($n = 500$ spots from 5 different cells). *D*, Western blot analysis of ECFP-rab5 expression and specific moesin knockdown (siRNA-moesin) in HeLa cells, compared with control cells (scrambled), used to prepare plasma-membrane sheets. ECFP-rab5 expression or silencing of endogenous moesin is quantified as the ratio of ECFP-rab5/or moesin/α-tubulin band intensities. A representative experiment is shown. *E*, moesin silencing effect on LCa-DsRed, ECFP-rab5, and TfR-EGFP localization and co-distribution in plasma-membrane sheets, compared with scrambled (control) sheets. *Zoom areas*, *circles* indicate TfR-EGFP/ECFP-rab5/LCa-DsRed-colabeled structures (deeply invaginated rab5-CCSs), under any experimental condition. In the *zoom areas*, the percentages indicate the quantification of TfR-EGFP/ECFP-rab5/LCa-DsRed-colabeled structures observed in scrambled (control) or moesin-silenced plasma-membrane sheets. Data are mean ± S.E. ($n = 1000$ spots from 5 different preparations of plasma membrane sheets). *Bar*, 5 μm.

bodies against each molecule. The equilibrium distribution of the TfR, in scrambled (control) cells, was probed in the different fractions collected (Fig. 7*C*, *TfR line*). The rab5- and rab7-positive fractions were separated along the collected fractions, observing rab5 in the lower density fractions and rab7 in the densest fractions of the Optiprep™ gradient (Fig. 7*C*, *rab5* and *rab7 lines*). Endogenous moesin and ezrin were homogeneously detected in the isolated cellular compartments from scrambled cells (Fig. 7*C*, *ezrin/moesin line*). This observation confirms the above data obtained by TIRFM and confocal microscopy techniques, indicating that a part of the cellular pool of moesin co-distributed with CCSs. In contrast, only ezrin was detected along the endosome fractions collected in moesin-silenced cells (Fig. 7*D*). Indeed, the TfR mainly concentrates in the lowest density fractions together with the rab5 molecule (Fig. 7*D*, *TfR* and *rab5 lines*). Hence, moesin knockdown provoked the accumulation of endogenous TfR in rab5-positive low density fractions, which could correspond to an accumulation of rab5-CCVs carrying the TfR as observed by TIRFM (Figs. 5 and 6). Rab7 distribution, a marker for the late endosomes, did not appear to be altered by the specific silencing of moesin, in the Optiprep™ gradients, when compared with scrambled cells (Fig. 7, *C* and *D*, *rab7 lines*).

We measured the amount of Tf sequestered in control and moesin-silenced cells (Fig. 7*E*), to corroborate that moesin knockdown affects Tf recycling. To do this, cells were previously loaded with fluorescent Alexa 488-labeled Tf at 37 °C for 30 min. Cells were placed on ice and washed with acidic buffer to remove recycled surface-Tf. Cells were then shifted again to 37 °C to allow the recycling of the internalized Tf ligand, which was measured for the indicate time points. We observed that moesin-silenced cells exhibited a low rate of Tf recycling when compared with the rate of Tf released in

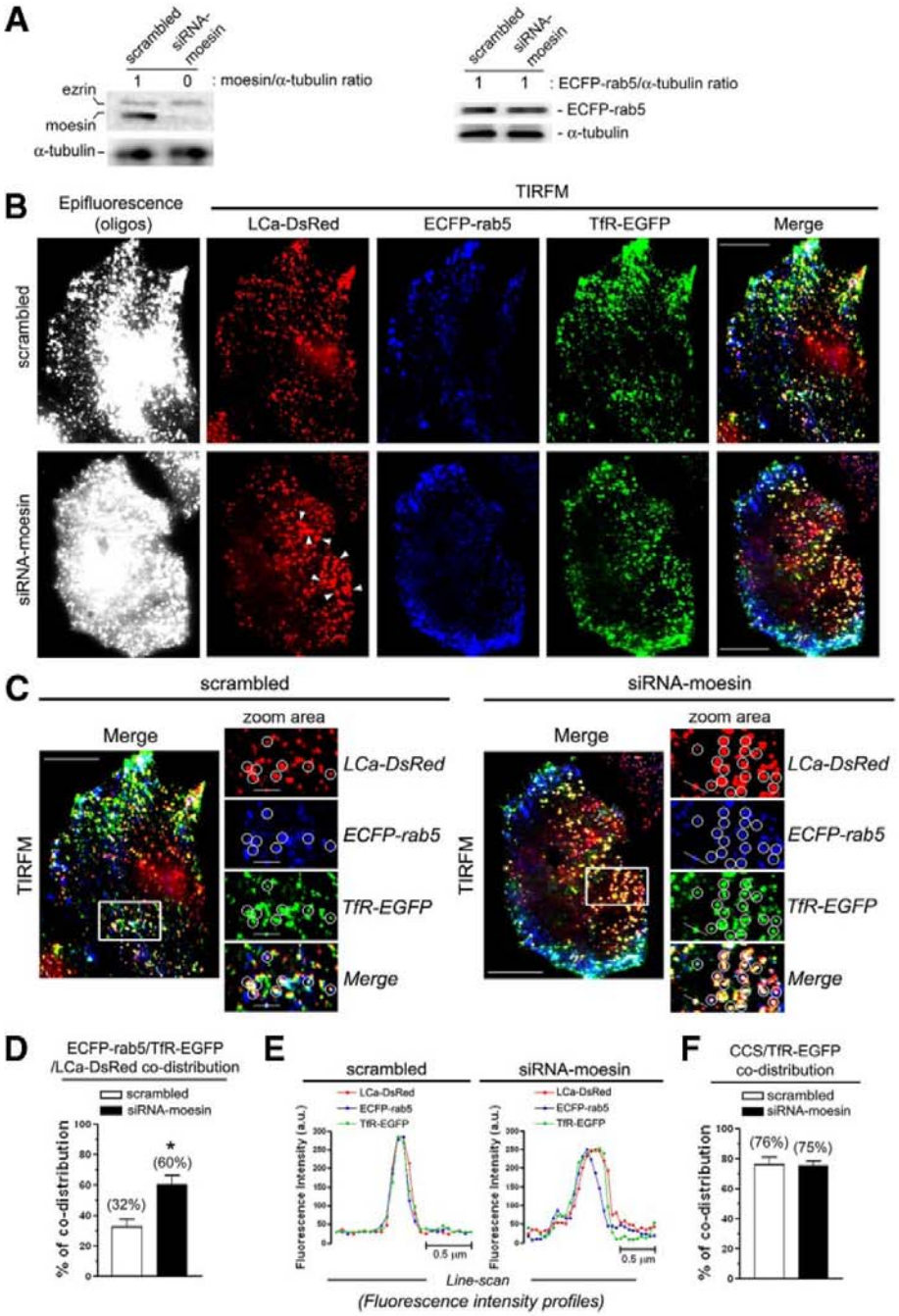

FIGURE 6. **Moesin knockdown provokes accumulation of the TfR in nascent endocytic rab5-CCVs.** *A*, Western blot analysis of specific moesin knockdown (siRNA-Moesin) (*left panel*), or overexpression of the ECFP-rab5 molecule (*right panel*), in moesin-silenced cells compared with control cells (scrambled). Silencing of endogenous moesin or expression of the ECFP-rab5 molecule is quantified as the ratio of moesin/or ECFP-rab5/α-tubulin band intensities. A representative experiment of three performed experiments is shown. *B* and *C*, moesin silencing effect on cellular distribution and trafficking of the TfR-EGFP, constitutively associated to LCa-DsRed-labeled CCVs, compared with control cells (scrambled). The accumulation (important in moesin-silenced cells) of the TfR-EGFP, in nascent rab5-CCVs, was monitored by ECFP-rab5/LCa-DsRed-CCVs/TfR-EGFP co-labeling (*Merge images* in *B* and *C*). The presence of the fluorescent scrambled or siRNA-moesin oligonucleotides is monitored by epifluorescence. The *white arrowheads* indicate clusters of LCa-DsRed-labeled CCVs in siRNA-moesin cells (*B*). In *C*, *circles* in scrambled and siRNA-moesin cells indicate ECFP-rab5/LCa-DsRed-labeled CCVs carrying the TfR-EGFP (nascent rab5-CCVs). *Bar*, 8 μm. *D*, *bar histograms* show the accumulation percentage of nascent ECFP-rab5/LCa-DsRed-labeled CCVs carrying the TfR-EGFP receptor. *, $p < 0.05$, *t* test. Data in *D* and *F* are mean ± S.E. ($n = 500$ spots from 5 different cells). *E*, line-scan analysis of LCa-DsRed, ECFP-rab5, and TfR-EGFP co-distribution in representative single nascent rab5-CCV of scrambled and moesin-silenced cells, indicated by the *line* in the *zoom areas* of *C*. *F*, *bar histograms* show the percentage of TfR-EGFP/LCa-DsRed co-distribution in scrambled (control) and moesin-silenced (siRNA-moesin) cells.

control (scrambled) cells (Fig. 7*E*). These observations could indicate a normal recycling process in control cells, which released the Tf ligand, as well as an altered process in moesin-silenced cells that retained the intracellular Tf.

On the other hand, we observed by TIRFM that the exocytosis of TfR-phl to the plasma membrane occurred with a similar frequency, both in control (scrambled) and moesin-silenced cells (Fig. 7*F*, and supplemental Movie S4). Interestingly, endogenous moesin slightly co-distributed with γ-adaptin (AP-1) (Fig. 1*C*), and moesin knockdown did not affect the number of rab11-positive CCSs detected at plasma membrane, when compared with control (scrambled) cells (supplemental Fig. S5*B*). Therefore, it seems that moesin is not involved in the *trans*-Golgi network-endosome transport and/or sorting of the TfR to the plasma membrane.

Moreover, we analyzed by TIRFM the association between the cell-surface expression level of TfR-phl and the amount of LCa-DsRed expressed per single CCS in control (scrambled) and moesin-silenced cells (Fig. 8*A*, *top histograms*). The TfR-phl molecule is a fusion construct with superecliptic phluorin attached to the extracellular domain of TfR. This phluorin molecule is a pH-sensitive variant of GFP in which fluorescence is almost completely quenched on transition from pH 7.4 to pH 5.5 (54, 55). Hence, it is thought that the TfR-phl fluorescence observed by TIRFM corresponds to TfR-phl molecules at the cell-surface associated wth CCPs or with non-endocytic CCSs (8, 56).

We observed, under this experimental condition that the average level of expression of the LCa-DsRed molecule per analyzed spot (TfR-phl/CCS) was not altered after moesin knockdown, when compared with control cells (Fig. 8*A*, *left histograms*). The fluorescence intensities of clathrin (LCa-DsRed) and TfR-phl in any analyzed CCS are proportional, which shows that CCS size influences the amount

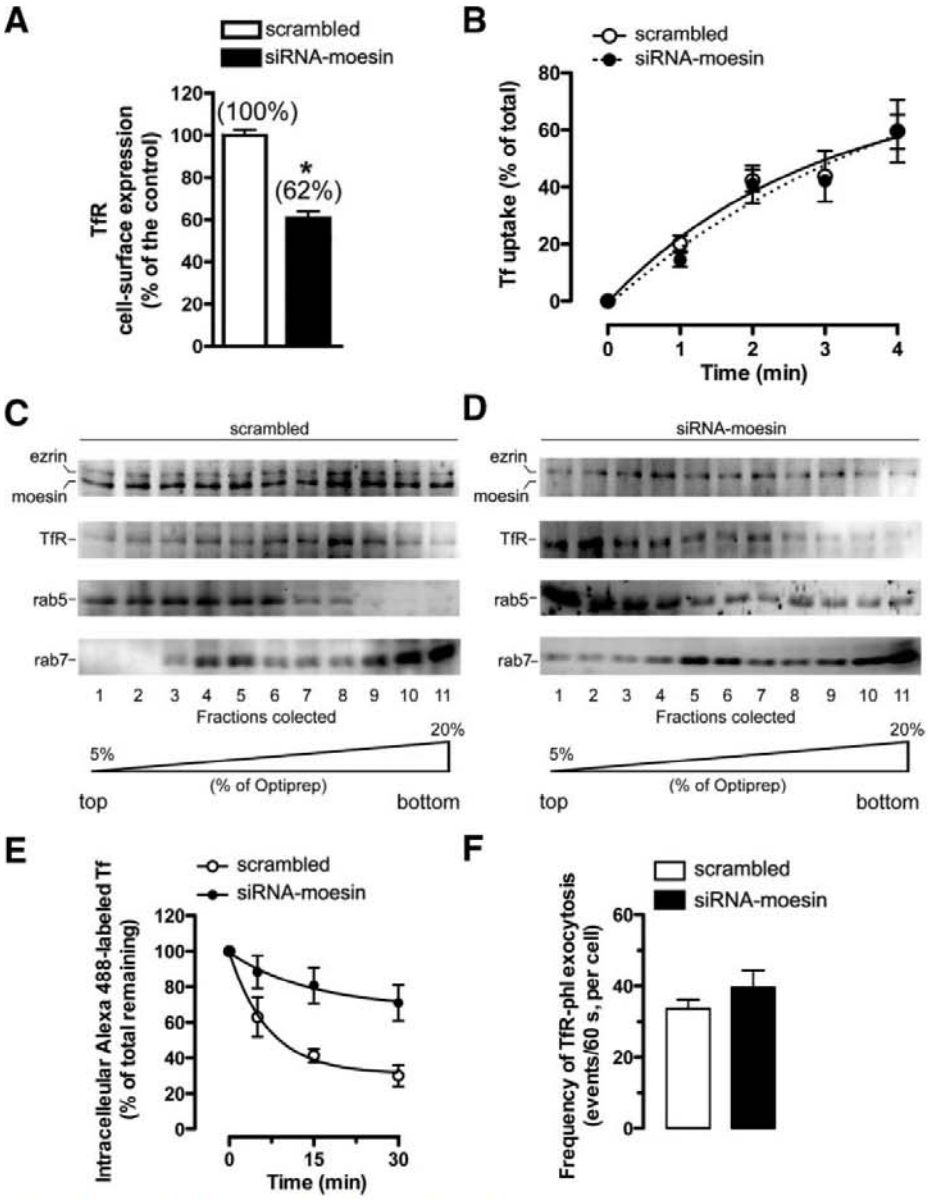

FIGURE 7. **Moesin knockdown perturbs TfR recycling, affecting TfR cell-surface expression.** *A, bar histograms* indicate specific TfR (CD71) cell-surface expression in control (scrambled) or moesin-silenced (siRNA-moesin) cells quantified by flow cytometry. Data were corrected by subtracting the nonspecific adsorption of antibodies, determined by using an IgG-isotype negative control. Data are mean ± S.E. ($n = 6$, from three independent experiments). *, $p < 0.05$, *t* test. *B*, early Tf uptake of Alexa 488-labeled Tf determined by flow cytometry in control (scrambled) or moesin-silenced (siRNA-moesin) cells for the indicated time points. Results are expressed as the percentage of internalized Tf with respect to the total prebound Tf ligand at +4 °C (100%), in each experimental condition. Data are mean ± S.E. ($n = 9$, from three independent experiments). *C* and *D*, Western blot analysis of the distribution of TfR, ezrin, and moesin molecules along the endosome, rab5-positive, and rab7-positive fractions collected (*1–11*, from *top* to *bottom*), obtained by Optiprep™ density gradient (5–20%) of cell lysates from scrambled (control) or moesin-silenced (siRNA-moesin) HeLa cells (*C* or *D panels*, respectively). Data are a representative experiment of three. *E*, quantification of Alexa 488-labeled Tf sequestered in control (scrambled) or moesin-silenced (siRNA-moesin) cells, determined by flow cytometry for the indicated time points. Results are expressed as the percentage of initial (time 0, 100%) intracellular Tf that was detected in cells during reincubation (see "Experimental Procedures"), in each experimental condition. Data are mean ± S.E. ($n = 6$, from three independent experiments). *F*, quantification of the TfR-phl frenquency of exocytosis in control (scrambled) and moesin-silenced cells (see supplemental Movie S4 for representative sequences of TfR-phl exocytosis monitored by TIRFM, in control and moesin-silenced cells). Data in the *histograms* are mean ± S.E. ($n = 12$ individual cells analyzed, from three independent experiments, under any experimental condition).

in the plasma membrane (Fig. 8*A*, *TIRFM images*). To quantify the level of expression of TfR-phl on the cell surface, under any experimental condition, we identified isolated CCSs and measured the fluorescence intensities for both LCa-DsRed and TfR-phl (Fig. 8*A*, see *zoom squares* in *TIRFM images*), as described under "Experimental Procedures." Bearing in mind that the LCa-DsRed expression is not affected after moesin knockdown (Fig. 8*A*, *left histograms* and *images*), the average ratio of TfR-phl/LCa-DsRed-associated fluorescence intensities, per analyzed spot (CCP), is indicative of the expression level of TfR-phl on the cell surface, under any experimental condition. We observed that cells lacking moesin presented a reduced TfR-phl expression at the cell surface (~51%), when compared with control cells (Fig. 8*A*, *right histograms*).

Furthermore, we observed that the Alexa 568-labeled Tf ligand was able to bind to TfR-phl at the cell surface, both in control and moesin-silenced cells (Fig. 8*B*, *TIRFM images*). To measure the Tf/TfR association at the cell surface, under any experimental condition, we identified isolated TfR-phl spots and measured the fluorescence intensities for both bound Alexa 568-labeled Tf and TfR-phl (see "Experimental Procedures"). The average fluorescence intensity Alexa 568-labeled Tf/TfR-phl ratios, per analyzed spot, were similar in the control and cells lacking moesin (Fig. 8*B*, *histograms*). Therefore, the reduced Tf uptake, observed after moesin knockdown (Fig. 7*B*), could be due to the reduced expression level of the TfR on the cell surface of moesin-silenced cells, as observed (Fig. 7*A*, *flow cytometry*, and Fig. 8*A*, *TIRFM*), and not to a change in the Tf/TfR binding ability or to an impaired TfR uptake. Taking all the above results together, we propose that moesin is key for driving the TfR recycling from endocytic rab5-CCVs to the plasma membrane.

of the TfR-phl carried per structure, as previously described (8). Hence, it seems that moesin silencing did not affect CCP formation, and TfR-phl appeared to be concentrated in CCSs

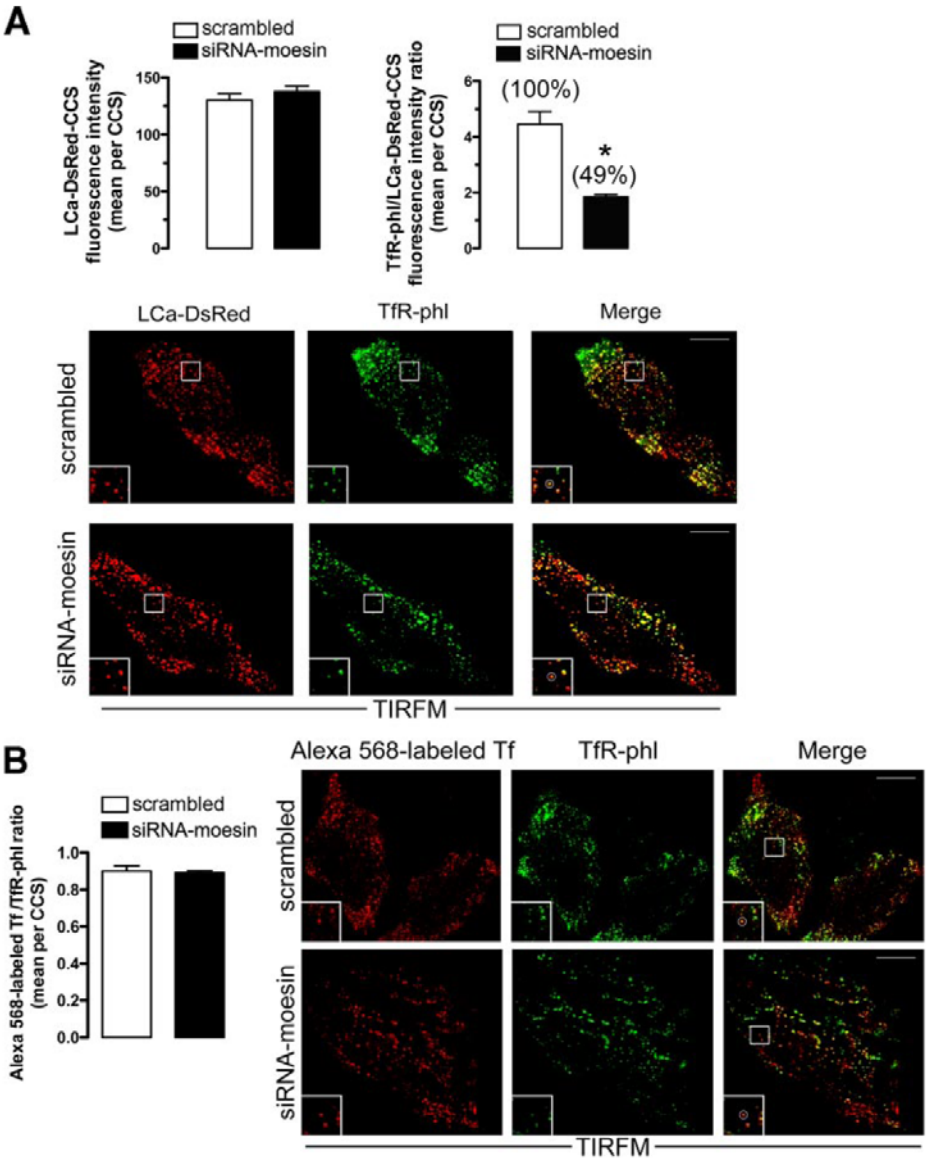

FIGURE 8. **Moesin silencing diminished the average level of expression of TfR-phl per CCS, without affecting clathrin expression and Tf/TfR ligation.** *A, left bar histograms* indicate the average LCa-DsRed-associated fluorescence intensity per single CCS (spot) analyzed, as indicated in the *zoom square* of *TIRFM images*. *Right bar histograms* indicate the average TfR-phl/LCa-DsRed-associated fluorescence intensity ratio per single CCS analyzed, as indicated in the *zoom square* of *TIRFM images*. In both *histograms*, data are mean ± S.E. ($n = 100$ independent spots analyzed from 8 different control (scrambled) or moesin-silenced cells). *, $p < 0.05$, *t* test. Images of representative cells used to measure the level of expression of LCa-DsRed and TfR-phl per CCS (spot), at cell surface of control (scrambled) or moesin-silenced cells, are shown (see "Experimental Procedures"). *Encircled* spots in the *zoom squares* represent single analyzed TfR-phl/CCS. *Bar*, 10 μm. *B*, TIRFM analysis of the binding ability of Alexa 568-labeled Tf to cell-surface TfR-phl, in control and cells without moesin (see "Experimental Procedures"). *Bar histograms* indicate the average Alexa 568-labeled Tf/TfR-phl-associated fluorescence intensity ratios per analyzed TfR-phl-spot, as indicated in the *zoom squares* of representative cells, under any experimental condition. Data are mean ± S.E. ($n = 100$ independent spots analyzed from 8 different control (scrambled) or moesin-silenced cells). *Bar*, 10 μm.

DISCUSSION

In the present work, we describe the functional involvement of the F-actin linker moesin during CCV trafficking by acting on nascent rab5-CCVs. We observe that a part of the endogenous pool of moesin co-distributes with CHC and α-adaptin molecules, constitutive key components for CCS formation and related functions (29–33). The moesin silencing-mediated effect on LCa-DsRed-labeled CCSs motility and cellular distribution suggests that moesin could be involved in the trafficking of CCVs. Lateral trajectories of CCSs were larger in moesin-silenced cells than those observed in control cells. In addition, silencing of moesin provokes the formation of CCS clusters, which progressively disaggregate into single structures. These events suggest that moesin may function as a regulatory linker for vesicle motility.

Because PIP_2 is required for the conformational activation of ERM proteins and mediates their association with F-actin (43, 44), it is plausible that moesin molecules, bound to the PIP_2 on nascent endocytic CCVs, are activated to anchor these vesicles to F-actin, thereby driving the trafficking process. However, we cannot rule out the possibility that moesin might also interact with other CCS-associated components other than PIP_2. PIP_2 facilitates the interaction of ERM with the cytoplasmic tails of several membrane proteins, such as CD43, CD44, ICAM-1, ICAM-2, and ICAM-3 (16). Moesin/CCS co-localization does not appear to be dependent on a direct moesin-clathrin interaction, because the consensus clathrin-binding domain, the LLpL(−) clathrin box motif (29), is absent in the primary structure of moesin, and the 4K/4N-moesin-GFP mutant that is unable to bind to PIP_2 does not co-distribute with CCSs. Therefore, the spatial localization of moesin within CCSs mainly depends on its N-terminal-PIP_2-binding domain that could interact with CCS-associated PIP_2.

Cells overexpressing the dominant-negative N-moesin-GFP molecule, unable to bind F-actin, presented abnormal clusters of CCSs as was similarly observed in moesin-silenced cells. In addition, the inert C-moesin-GFP molecule, which only binds to F-actin, does not co-localize with CCSs and does not affect their motility and cellular distribution. FL-moesin-GFP molecules distribute with preformed LCa-DsRed-labeled CCSs on plasma membrane, where the actin-linker moved out in the *z* axis direction associated with LCa-DsRed-labeled nascent CCVs. These data suggest that moesin regulates cellular dis-

tribution and lateral movement of a subpopulation of CCVs in an actin-dependent manner.

It has been suggested that actin plays either a structural role in clathrin-mediated endocytosis, controlling the localization of endocytic machinery on the plasma membrane, or the following mechanical roles: driving invagination, the separation of vesicles from the plasma membrane, and/or the translocation of nascent vesicles into the cytoplasm (57–59). For instance, the inhibition of actin dynamics blocks the internalization and lateral motility of a subpopulation of CCVs, which are differentially sensitive to actin disruption (60). Actin polymerization at endocytic sites is an early event that occurs during invagination of CCPs (21) and requires the cooperative contribution of several actin-associated proteins that allows the formation and endocytosis of nascent CCVs (reviewed in Refs. 21, 56–59, and 61–64). Hence, vesicle scission depends on the activity of the large GTPase dynamin that is recruited early on during CCP formation (21) and accumulates before vesicle pinching off (48, 65). A phenomenon that naturally follows vesicle scission is the recruitment of cortactin that binds to dynamin and F-actin (8, 66) and activates the Arp2/3 complex (8, 64), which is responsible for nucleation of actin polymerization (67). Therefore, it is thought that cortactin may link actin rearrangements with dynamin-mediated vesicle scission. A number of other endocytic proteins, including intersectin-1, huntingtin-interacting proteins, syndapin, the superfamily of Bin-Amphiphysin-Rvs proteins, which bind to dynamin, synaptojanin, or to the Arp2/3 activator neuronal Wiskott-Aldrich syndrome protein, and the Abi1 and neuronal Wiskott-Aldrich syndrome proteins have been shown to interact directly or indirectly with cortical actin to regulate CCV formation and related functions (5, 9, 68–77). Therefore, our data add complexity to this picture and provide evidence for the functional contribution of moesin, through binding to F-actin and CCS-associated PIP_2, in controlling lateral motility and cellular distribution of a subpopulation of moesin-associated CCVs.

It is conceivable that the hydrolisis of CCV-associated PIP_2, which could be performed by inositol-5-phosphatase synaptojanin (78–83), or its conversion to PIP_3 may represent a control mechanism for moesin-CCS association. This event may account for the partial moesin/CCS co-distribution observed in the present work. Thus, molecules that may directly or indirectly affect the ability of moesin to bind to actin or CCS-associated PIP_2 are potential candidates for the control of moesin-dependent trafficking of nascent endocytic CCVs.

Rab proteins, which constitute the largest family of monomeric small GTPases (84), have been identified as key regulators of intracellular transport at the endosome level (46, 85). We have observed that moesin knockdown provokes the accumulation of CCVs carrying the rab5 molecule, which represent nascent endocytic CCVs, and were not detected in plasma-membrane sheets.

Therefore, it appears that nascent rab5-CCVs require functional moesin to traffic correctly, after vesicle fission from plasma membrane. The functional perturbation of moesin may alter the trafficking of cargos associated with moesin-bearing CCVs as the constitutive associated TfR. TIRFM comparative studies, between intact cells and plasma-membrane sheets, together with biochemical cell fractioning indicate that moesin silencing induces the accumulation of the TfR in endocytic rab5-CCVs. These data correlate with a reduced cell-surface expression of the TfR, determined by flow cytometry analysis and TIRFM-based studies, and the increase in the amount of the sequestered Tf ligand, which are indicative of a recycling defect of the TfR. Moreover, the presence of rab5-negative CCPs and deeply invaginated rab5/CCSs, equally detected in control and moesin-silenced plasma-membrane sheets, indicates that moesin does not affect either CCP formation or CCV invagination and fission from the plasma membrane. Hence, the Tf uptake is not affected during the first TfR internalization step in cells without moesin. Because TfR turnover is a constitutive process governed by the trafficking of endocytic CCVs (86), and considering that moesin knockdown does not appear to affect the frequency of TfR exocytosis to the plasma membrane, we propose that TfR recycling could be controlled in endocytic rab5-CCVs by signals affecting the functional status of moesin.

Interestingly, some members of the newly identified family of rab11 interacting proteins (rab11-FIP) possess an ERM domain in their C-terminal half of the molecule (87), which regulates FIP molecular self-interactions or interactions with rab11 GTPase during trafficking (88). Hence, it is possible that moesin may also regulate CCV trafficking by interacting with rab11-FIP members, thus perturbing FIP self-association or rab11-FIP/rab interactions.

In conclusion, we describe for the first time that moesin co-distributes with plasma membrane-derived CCSs, mostly in a PIP_2-dependent manner. The moesin protein controls lateral motility, cellular distribution, and trafficking of a subpopulation of nascent rab5-CCVs, probably promoting CCV recycling, through its ability to simultaneously bind to CCV-associated PIP_2 and F-actin.

These data represent an important mechanistic insight regarding the complex molecular machinery associated with CCSs, which drives clathrin-mediated endocytosis, and the functional involvement of moesin in the trafficking of CCVs. The study of cell signals or genetic mutations that regulate moesin activation might be important to understand the molecular basis of several pathological processes like cancer progression, congenital disorders of the central nervous system, and viral infection, all of which are reported to be associated with altered clathrin-mediated receptor internalization or recycling (89–92).

Acknowledgments—We thank M. Feria, M. Camacho, and F. Díaz-González for their helpful comments on the manuscript. We thank R. Borges for TIRFM laboratory support. We thank the excellent work done by M. del Valle Croissier-Elías in the correction of the manuscript. We thank the Fundación Rafael Clavijo para la Investigación Biomédica from Hospital Universitario de Canarias.

REFERENCES

1. Maldonado-Baez, L., and Wendland, B. (2006) *Trends Cell Biol.* **16,** 505–513
2. Ungewickell, E. J., and Hinrichsen, L. (2007) *Curr. Opin. Cell Biol.* **19,** 417–425

3. Le Borgne, R., Bardin, A., and Schweisguth, F. (2005) *Development* **132,** 1751–1762
4. Le Roy, C., and Wrana, J. L. (2005) *Nat. Rev. Mol. Cell. Biol.* **6,** 112–126
5. Benesch, S., Polo, S., Lai, F. P., Anderson, K. I., Stradal, T. E., Wehland, J., and Rottner, K. (2005) *J. Cell Sci.* **118,** 3103–3115
6. Scott, M. G., Benmerah, A., Muntaner, O., and Marullo, S. (2002) *J. Biol. Chem.* **277,** 3552–3559
7. Slepnev, V. I., and De Camilli, P. (2000) *Nat. Rev. Neurosci.* **1,** 161–172
8. Merrifield, C. J., Perrais, D., and Zenisek, D. (2005) *Cell* **121,** 593–606
9. Schafer, D. A. (2002) *Curr. Opin. Cell Biol.* **14,** 76–81
10. Laroche, G., Rochdi, M. D., Laporte, S. A., and Parent, J. L. (2005) *J. Biol. Chem.* **280,** 23215–23224
11. Hirasawa, A., Awaji, T., Sugawara, T., Tsujimoto, A., and Tsujimoto, G. (1998) *Br. J. Pharmacol.* **124,** 55–62
12. Lunn, J. A., Wong, H., Rozengurt, E., and Walsh, J. H. (2000) *Am. J. Physiol. Cell Physiol.* **279,** C2019–2027
13. Zaslaver, A., Feniger-Barish, R., and Ben-Baruch, A. (2001) *J. Immunol.* **166,** 1272–1284
14. Cao, H., Orth, J. D., Chen, J., Weller, S. G., Heuser, J. E., and McNiven, M. A. (2003) *Mol. Cell. Biol.* **23,** 2162–2170
15. Mangeat, P., Roy, C., and Martin, M. (1999) *Trends Cell Biol.* **9,** 187–192
16. Bretscher, A., Edwards, K., and Fehon, R. G. (2002) *Nat. Rev. Mol. Cell. Biol.* **3,** 586–599
17. Stanasila, L., Abuin, L., Diviani, D., and Cotecchia, S. (2006) *J. Biol. Chem.* **281,** 4354–4363
18. Cao, T. T., Deacon, H. W., Reczek, D., Bretscher, A., and von Zastrow, M. (1999) *Nature* **401,** 286–290
19. Li, J. G., Chen, C., and Liu-Chen, L. Y. (2002) *J. Biol. Chem.* **277,** 27545–27552
20. Harder, T., Kellner, R., Parton, R. G., and Gruenberg, J. (1997) *Mol. Biol. Cell* **8,** 533–545
21. Merrifield, C. J., Feldman, M. E., Wan, L., and Almers, W. (2002) *Nat. Cell Biol.* **4,** 691–698
22. Amieva, M. R., Litman, P., Huang, L., Ichimaru, E., and Furthmayr, H. (1999) *J. Cell Sci.* **112,** 111–125
23. Stauffer, T. P., Ahn, S., and Meyer, T. (1998) *Curr. Biol.* **8,** 343–346
24. Varnai, P., and Balla, T. (1998) *J. Cell Biol.* **143,** 501–510
25. Marin-Vicente, C., Gomez-Fernandez, J. C., and Corbalan-Garcia, S. (2005) *Mol. Biol. Cell* **16,** 2848–2861
26. Sever, S., Damke, H., and Schmid, S. L. (2000) *J. Cell Biol.* **150,** 1137–1148
27. Gaidarov, I., Santini, F., Warren, R. A., and Keen, J. H. (1999) *Nat. Cell Biol.* **1,** 1–7
28. Burns, A. R., Oliver, J. M., Pfeiffer, J. R., and Wilson, B. S. (2008) *Methods Mol. Biol.* **440,** 235–245
29. Kirchhausen, T. (2000) *Annu. Rev. Biochem.* **69,** 699–727
30. Musacchio, A., Smith, C. J., Roseman, A. M., Harrison, S. C., Kirchhausen, T., and Pearse, B. M. (1999) *Mol. Cell* **3,** 761–770
31. Ybe, J. A., Brodsky, F. M., Hofmann, K., Lin, K., Liu, S. H., Chen, L., Earnest, T. N., Fletterick, R. J., and Hwang, P. K. (1999) *Nature* **399,** 371–375
32. Brodsky, F. M., Chen, C. Y., Knuehl, C., Towler, M. C., and Wakeham, D. E. (2001) *Annu. Rev. Cell Dev. Biol.* **17,** 517–568
33. Conner, S. D., and Schmid, S. L. (2003) *Nature* **422,** 37–44
34. Schmid, S. L. (1997) *Annu. Rev. Biochem.* **66,** 511–548
35. Knuehl, C., Chen, C. Y., Manalo, V., Hwang, P. K., Ota, N., and Brodsky, F. M. (2006) *Traffic* **7,** 1688–1700
36. Robinson, M. S. (2004) *Trends Cell Biol.* **14,** 167–174
37. Kirchhausen, T. (2002) *Cell* **109,** 413–416
38. Boehm, M., and Bonifacino, J. S. (2001) *Mol. Biol. Cell* **12,** 2907–2920
39. Meyer, C., Zizioli, D., Lausmann, S., Eskelinen, E. L., Hamann, J., Saftig, P., von Figura, K., and Schu, P. (2000) *EMBO J.* **19,** 2193–2203
40. Engqvist-Goldstein, A. E., Warren, R. A., Kessels, M. M., Keen, J. H., Heuser, J., and Drubin, D. G. (2001) *J. Cell Biol.* **154,** 1209–1223
41. Franck, Z., Gary, R., and Bretscher, A. (1993) *J. Cell Sci.* **105,** 219–231
42. Ivetic, A., and Ridley, A. J. (2004) *Immunology* **112,** 165–176
43. Fievet, B. T., Gautreau, A., Roy, C., Del Maestro, L., Mangeat, P., Louvard, D., and Arpin, M. (2004) *J. Cell Biol.* **164,** 653–659
44. Nakamura, F., Huang, L., Pestonjamasp, K., Luna, E. J., and Furthmayr, H. (1999) *Mol. Biol. Cell* **10,** 2669–2685
45. Barret, C., Roy, C., Montcourrier, P., Mangeat, P., and Niggli, V. (2000) *J. Cell Biol.* **151,** 1067–1080
46. Zerial, M., and McBride, H. (2001) *Nat. Rev. Mol. Cell. Biol.* **2,** 107–117
47. Ullrich, O., Reinsch, S., Urbe, S., Zerial, M., and Parton, R. G. (1996) *J. Cell Biol.* **135,** 913–924
48. Ehrlich, M., Boll, W., Van Oijen, A., Hariharan, R., Chandran, K., Nibert, M. L., and Kirchhausen, T. (2004) *Cell* **118,** 591–605
49. Rappoport, J. Z., Simon, S. M., and Benmerah, A. (2004) *Traffic* **5,** 327–337
50. Keyel, P. A., Watkins, S. C., and Traub, L. M. (2004) *J. Biol. Chem.* **279,** 13190–13204
51. Rappoport, J. Z., Benmerah, A., and Simon, S. M. (2005) *Traffic* **6,** 539–547
52. McLauchlan, H., Newell, J., Morrice, N., Osborne, A., West, M., and Smythe, E. (1998) *Curr. Biol.* **8,** 34–45
53. Aisen, P. (2004) *Int. J. Biochem. Cell. Biol.* **36,** 2137–2143
54. Miesenbock, G., De Angelis, D. A., and Rothman, J. E. (1998) *Nature* **394,** 192–195
55. Sankaranarayanan, S., De Angelis, D., Rothman, J. E., and Ryan, T. A. (2000) *Biophys. J.* **79,** 2199–2208
56. Perrais, D., and Merrifield, C. J. (2005) *Dev. Cell* **9,** 581–592
57. Qualmann, B., Kessels, M. M., and Kelly, R. B. (2000) *J. Cell Biol.* **150,** F111–F116
58. Engqvist-Goldstein, A. E., and Drubin, D. G. (2003) *Annu. Rev. Cell Dev. Biol.* **19,** 287–332
59. Merrifield, C. J. (2004) *Trends Cell Biol.* **14,** 352–358
60. Yarar, D., Waterman-Storer, C. M., and Schmid, S. L. (2005) *Mol. Biol. Cell* **16,** 964–975
61. Girao, H., Geli, M. I., and Idrissi, F. Z. (2008) *FEBS Lett.* **582,** 2112–2119
62. Lanzetti, L. (2007) *Curr. Opin. Cell Biol.* **19,** 453–458
63. Kaksonen, M., Toret, C. P., and Drubin, D. G. (2006) *Nat. Rev. Mol. Cell. Biol.* **7,** 404–414
64. Merrifield, C. J., Qualmann, B., Kessels, M. M., and Almers, W. (2004) *Eur. J. Cell Biol.* **83,** 13–18
65. Zoncu, R., Perera, R. M., Sebastian, R., Nakatsu, F., Chen, H., Balla, T., Ayala, G., Toomre, D., and De Camilli, P. V. (2007) *Proc. Natl. Acad. Sci. U. S. A.* **104,** 3793–3798
66. Daly, R. J. (2004) *Biochem. J.* **382,** 13–25
67. Takenawa, T., and Miki, H. (2001) *J. Cell Sci.* **114,** 1801–1809
68. McPherson, P. S. (2002) *Trends Cell Biol.* **12,** 312–315
69. Itoh, T., Erdmann, K. S., Roux, A., Habermann, B., Werner, H., and De Camilli, P. (2005) *Dev. Cell* **9,** 791–804
70. Tsujita, K., Suetsugu, S., Sasaki, N., Furutani, M., Oikawa, T., and Takenawa, T. (2006) *J. Cell Biol.* **172,** 269–279
71. Dawson, J. C., Legg, J. A., and Machesky, L. M. (2006) *Trends Cell Biol.* **16,** 493–498
72. Takenawa, T., and Suetsugu, S. (2007) *Nat. Rev. Mol. Cell. Biol.* **8,** 37–48
73. Innocenti, M., Gerboth, S., Rottner, K., Lai, F. P., Hertzog, M., Stradal, T. E., Frittoli, E., Didry, D., Polo, S., Disanza, A., Benesch, S., Di Fiore, P. P., Carlier, M. F., and Scita, G. (2005) *Nat. Cell Biol.* **7,** 969–976
74. Chen, C. Y., and Brodsky, F. M. (2005) *J. Biol. Chem.* **280,** 6109–6117
75. Le Clainche, C., Pauly, B. S., Zhang, C. X., Engqvist-Goldstein, A. E., Cunningham, K., and Drubin, D. G. (2007) *EMBO J.* **26,** 1199–1210
76. Wilbur, J. D., Chen, C. Y., Manalo, V., Hwang, P. K., Fletterick, R. J., and Brodsky, F. M. (2008) *J. Biol. Chem.* **283,** 32870–32879
77. Qualmann, B., and Kelly, R. B. (2000) *J. Cell Biol.* **148,** 1047–1062
78. McPherson, P. S., Garcia, E. P., Slepnev, V. I., David, C., Zhang, X., Grabs, D., Sossin, W. S., Bauerfeind, R., Nemoto, Y., and De Camilli, P. (1996) *Nature* **379,** 353–357
79. Cremona, O., Di Paolo, G., Wenk, M. R., Luthi, A., Kim, W. T., Takei, K., Daniell, L., Nemoto, Y., Shears, S. B., Flavell, R. A., McCormick, D. A., and De Camilli, P. (1999) *Cell* **99,** 179–188
80. Haffner, C., Takei, K., Chen, H., Ringstad, N., Hudson, A., Butler, M. H., Salcini, A. E., Di Fiore, P. P., and De Camilli, P. (1997) *FEBS Lett.* **419,** 175–180
81. Harris, T. W., Hartwieg, E., Horvitz, H. R., and Jorgensen, E. M. (2000) *J. Cell Biol.* **150,** 589–600
82. Verstreken, P., Koh, T. W., Schulze, K. L., Zhai, R. G., Hiesinger, P. R., Zhou, Y., Mehta, S. Q., Cao, Y., Roos, J., and Bellen, H. J. (2003) *Neuron* **40,**

733–748
83. Gad, H., Ringstad, N., Low, P., Kjaerulff, O., Gustafsson, J., Wenk, M., Di Paolo, G., Nemoto, Y., Crun, J., Ellisman, M. H., De Camilli, P., Shupliakov, O., and Brodin, L. (2000) *Neuron* **27,** 301–312
84. Bock, J. B., Matern, H. T., Peden, A. A., and Scheller, R. H. (2001) *Nature* **409,** 839–841
85. Rink, J., Ghigo, E., Kalaidzidis, Y., and Zerial, M. (2005) *Cell* **122,** 735–749
86. Daniels, T. R., Delgado, T., Rodriguez, J. A., Helguera, G., and Penichet, M. L. (2006) *Clin. Immunol.* **121,** 144–158
87. Lindsay, A. J., and McCaffrey, M. W. (2004) *J. Cell Sci.* **117,** 4365–4375
88. Wallace, D. M., Lindsay, A. J., Hendrick, A. G., and McCaffrey, M. W. (2002) *Biochem. Biophys. Res. Commun.* **299,** 770–779
89. Polo, S., Pece, S., and Di Fiore, P. P. (2004) *Curr. Opin. Cell Biol.* **16,** 156–161
90. Cataldo, A. M., Peterhoff, C. M., Troncoso, J. C., Gomez-Isla, T., Hyman, B. T., and Nixon, R. A. (2000) *Am. J. Pathol.* **157,** 277–286
91. Venkatesan, S., Rose, J. J., Lodge, R., Murphy, P. M., and Foley, J. F. (2003) *Mol. Biol. Cell* **14,** 3305–3324
92. Connor, J. R., Wang, X. S., Patton, S. M., Menzies, S. L., Troncoso, J. C., Earley, C. J., and Allen, R. P. (2004) *Neurology* **62,** 1563–1567

SUPPLEMENTAL DATA

Legend to supplemental Figure 1. Silencing of endogenous moesin by using the siRNA-moesin2 oligo also alters the normal trafficking of CCSs and provokes their clustering.
A, western-blot analysis of specific moesin knock-down by using the siRNA-moesin or siRNA-moesin2 oligo in HeLa cells, and compared with control (scrambled) cells. Silencing of endogenous moesin is quantified as the ratio of moesin and α-tubulin band intensities. A representative experiment of three is shown. *B*, TIRFM analysis of LCa-DsRed-labeled CCSs in scrambled or moesin-silenced (siRNA-moesin2) HeLa cells. White arrowheads indicate abnormal clustering of LCa-DsRed-labeled CCSs in moesin-silenced (siRNA-moesin2) cells. *C*, histograms indicate the quantitative analysis of the movement (average radius of the large trajectories observed) of single LCa-DsRed-labeled CCSs in control (scrambled) or moesin-silenced (siRNA-moesin2) HeLa cells. Data are mean ± SEM from three independent experiments: 120 single CCSs counted in 10 different cells per each experimental condition. Bar, 10 μm.

Legend to supplemental Figure 2. TIRFM-based studies of FL-moesin-GFP molecule and LCa-DsRed-labeled CCSs dynamics.
A, Time-lapse (s) dynamics of FL-moesin-GFP molecules approaching a preformed LCa-DsRed-labeled CCS. Line-scans indicate the fluorescent intensity profiles of FL-moesin-GFP and LCa-DsRed molecules co-distributed at the same CCS, marked by a line, and tracked at times 0 s, 20 s, 35 s, and 55 s. The asterisk indicates a preformed LCa-DsRed-labeled CCS without the FL-moesin-GFP molecule. *B*, Time-lapse (from 0 s to 55 s) dynamics of the internalization of FL-moesin-GFP/LCa-DsRed-labeled nascent CCV. LCa-DsRed-labeled CCV, indicated by (a), is tracked for FL-moesin-GFP and LCa-DsRed internalization, whereas LCa-DsRed-labeled CCS (b) represents a control, non-internalized CCS.

Legend to supplemental Fig. 3. Analysis of the ability of purified FL-moesin-GFP and 4K/4N-moesin-GFP molecules to distribute to PIP_2-enriched regions on plasma membrane.
A and *B*, TIRFM-based analysis of distribution of the FL-moesin-GFP and 4K/4N-moesin-GFP molecules, respectively, to PIP_2-enriched domains at plasma membrane of intact cells, monitored by ECFP-PH. White arrowheads, in the inserted zoom areas of Merge images, show FL-moesin-GFP molecules distributing in ECFP-PH-labeled plasma membrane regions, whereas the 4K/4N-moesin-GFP mutant is absent on plasma membrane. Representative cells are shown. Bar, 5 μm.

Legend to supplemental Fig. 4. Effect of endogenous moesin knock-down, and over-expression of FL-moesin-GFP, 4K/4N-moesin-GFP mutant or C-moesin-GFP on cell shape and actin cytoskeleton.
A, western-blot analysis of specific moesin silencing (siRNA-moesin) in HeLa cells, compared with control cells (scrambled). Silencing of endogenous moesin is quantified as the ratio of moesin and α-tubulin band intensities, under any experimental condition. A representative experiment of three performed experiments is shown. *B*, confocal microscopy **x-y** mid-sections showing endogenous moesin (green) and F-actin filament (red, Alexa 568-phalloïdin) distribution in scrambled (control) and moesin-silenced (siRNA-moesin) cells. A representative experiment is shown. *C*, confocal microscopy **x-y** mid-sections showing cellular distribution of over-expressed FL-moesin-GFP, 4K/4N-moesin-GFP or C-moesin-GFP molecules (green), and F-actin filaments (red, Alexa 568-phalloïdin). A representative experiment is shown. In *B* and *C*, the nucleus is monitored by DAPI labeling in Merge images. Bar, 5 μm.

Legend to supplemental Fig. 5. Co-distribution of EGFP-rab7 and EYFG-rab11 molecules within CCSs.
A and *B*, moesin silencing effect on cellular distribution of EGFP-rab7- and EYFP-rab11/LCa-DsRed-labeled CCSs, compared to control cells (scrambled). The presence of the fluorescent scrambled or siRNA-moesin oligos is monitored by epifluorescence. In zoom areas, white arrows indicate EGFP-rab7- or EYFP-rab11/LCa-DsRed-labeled CCSs, in both scrambled and siRNA-moesin cells, whereas white arrowheads indicate clusters of CCSs in moesin-silenced cells. Bar, 5 μm. Bar histograms show the quantification of molecule co-distribution analyzed in scrambled (control cells) or in moesin-silenced cells (open and solid histograms, respectively). Data are mean ± SEM, (n = 500 spots from 5 different cells).

SUPPLEMENTAL MOVIES

Legend to supplemental movie 1. Movement of a representative CCS in control cells. Movie of a representative CCS, tracked by TIRFM in a control (scrambled) live cell, which corresponds to the time-lapse sequence shown in Fig. 2*F* (*scrambled* images).

Legend to supplemental movie 2. Movement of a representative CCS in moesin-silenced cells. Movie of a representative CCS, tracked by TIRFM in a moesin-silenced live cell, which corresponds to the time-lapse sequence shown in Fig. 2*F* (*siRNA-moesin* images).

Legend to supplemental movie 3. Disaggregation of a cluster of CCSs in moesin-silenced cell. Movie of a representative cluster of CCSs disaggregating in individual vesicles, tracked by TIRFM in a moesin-silenced live cell, which corresponds to the time-lapse sequence shown in Fig. 2*G* (cluster 1, *siRNA-moesin* images). Fluorescence intensities of sorted CCSs rapidly dimmed in the evanescent field suggesting that these single CCSs either moved out from the evanescent field or lost the clathrin coat.

Legend to supplemental movie 4. TfR-phl frequency of export to cell-surface in control (scrambled) and moesin-silenced cells. *Top* and *bottom* movies showing the export of the transiently expressed TfR-phl molecule to the plasma membrane, in representative control (scrambled) or moesin-silenced (siRNA-moesin) cells, respectively. Fluorescence intensities of exported TfR-phl rapidly dimmed on the plasma membrane due to the rapid lateral difusion of the exocytosed TfR-phl molecules on plasma membrane. Recording conditions: exocytosis events during 60 s, at 3 frames/s. A representative sequence of exocytosis during 5 s is shown for control and cells lacking moesin. Bar, 10 μm. The quantification of the average of TfR-phl frequency of export per cell is shown in Fig. 7*F*, for each experimental condition (from 12 different cells during 60 s, at 3 frames /s).

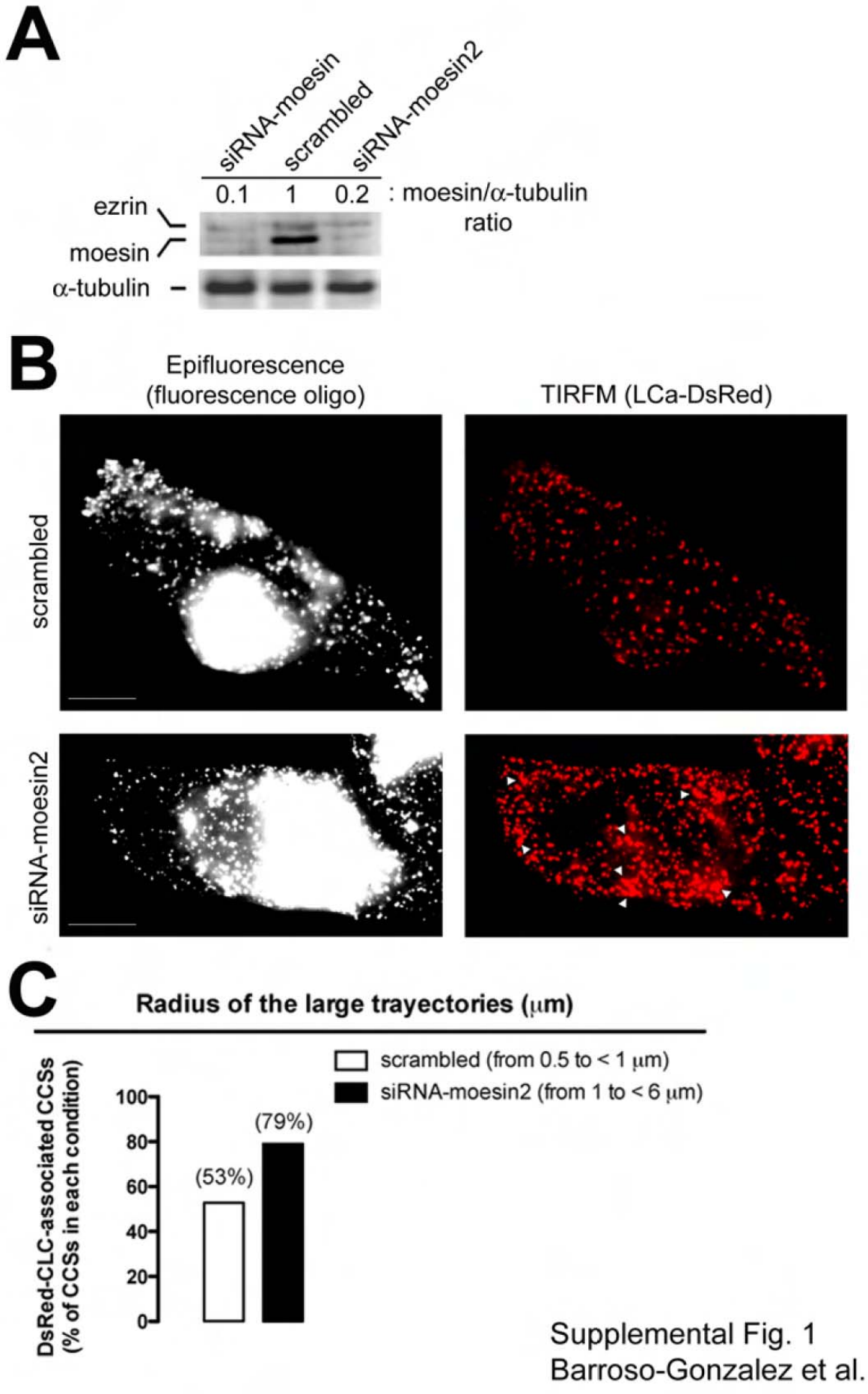

Supplemental Fig. 1
Barroso-Gonzalez et al.

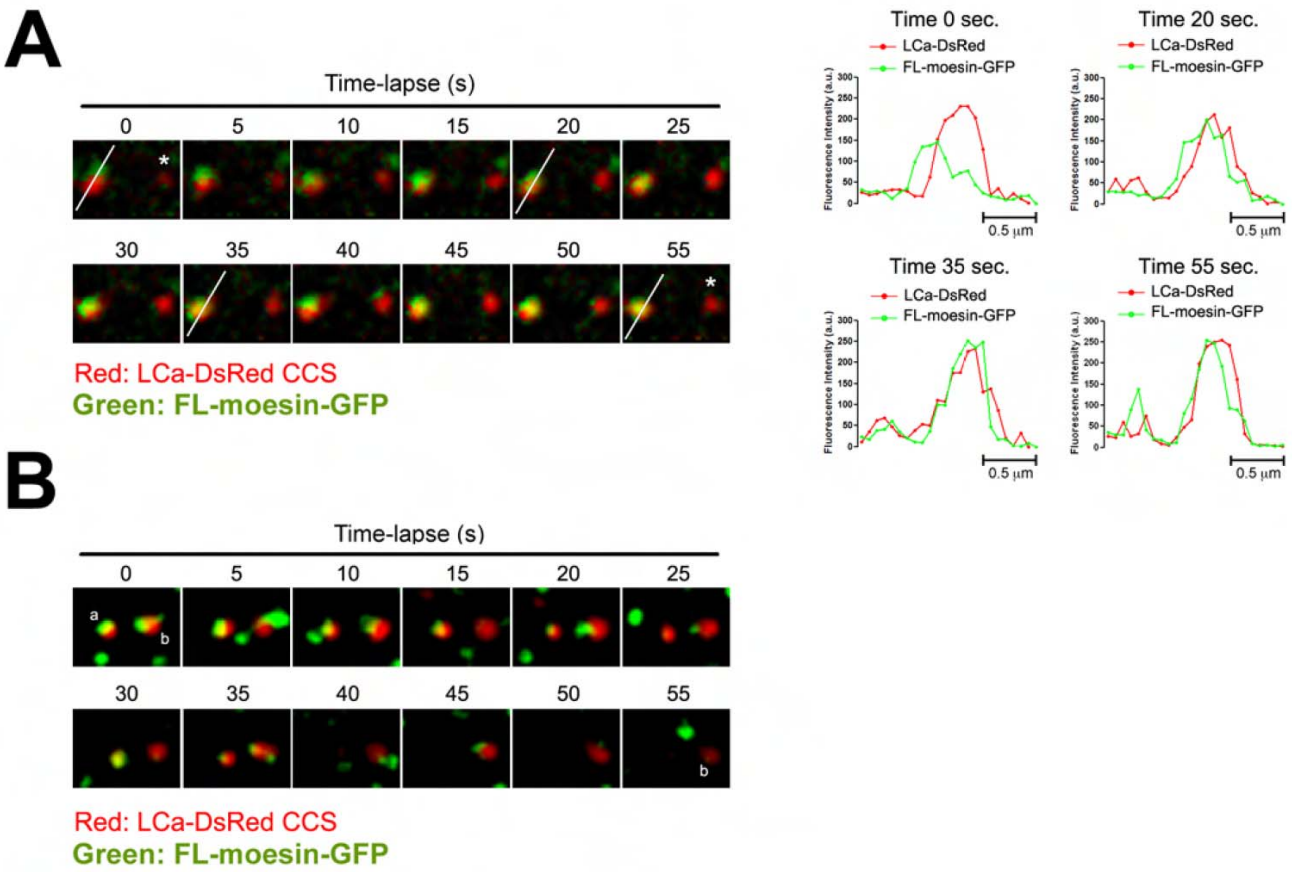

Supplemental Figure 2
Barroso-González et al.

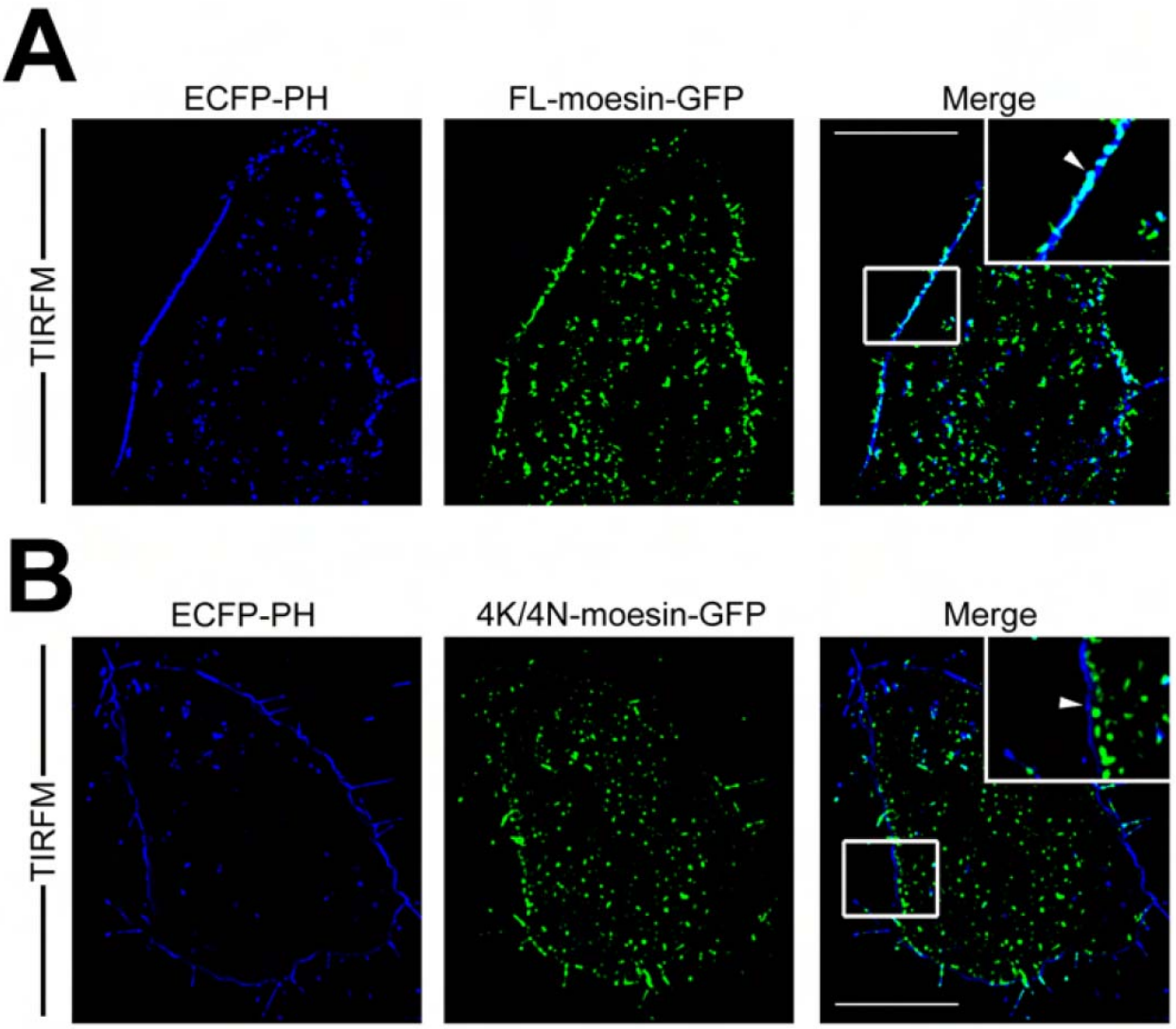

Supplemental Figure 3.
Barroso-González et al.

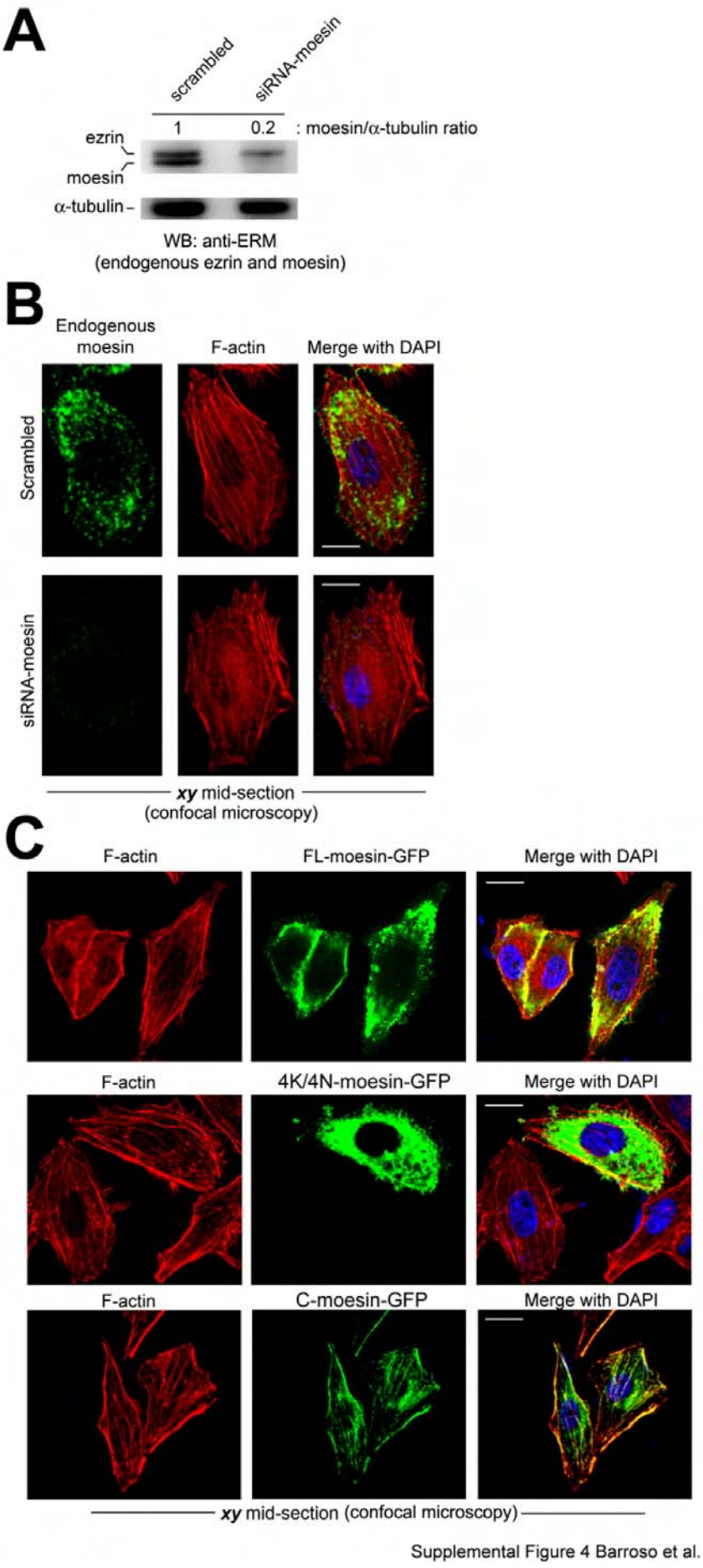

Supplemental Figure 4 Barroso et al.

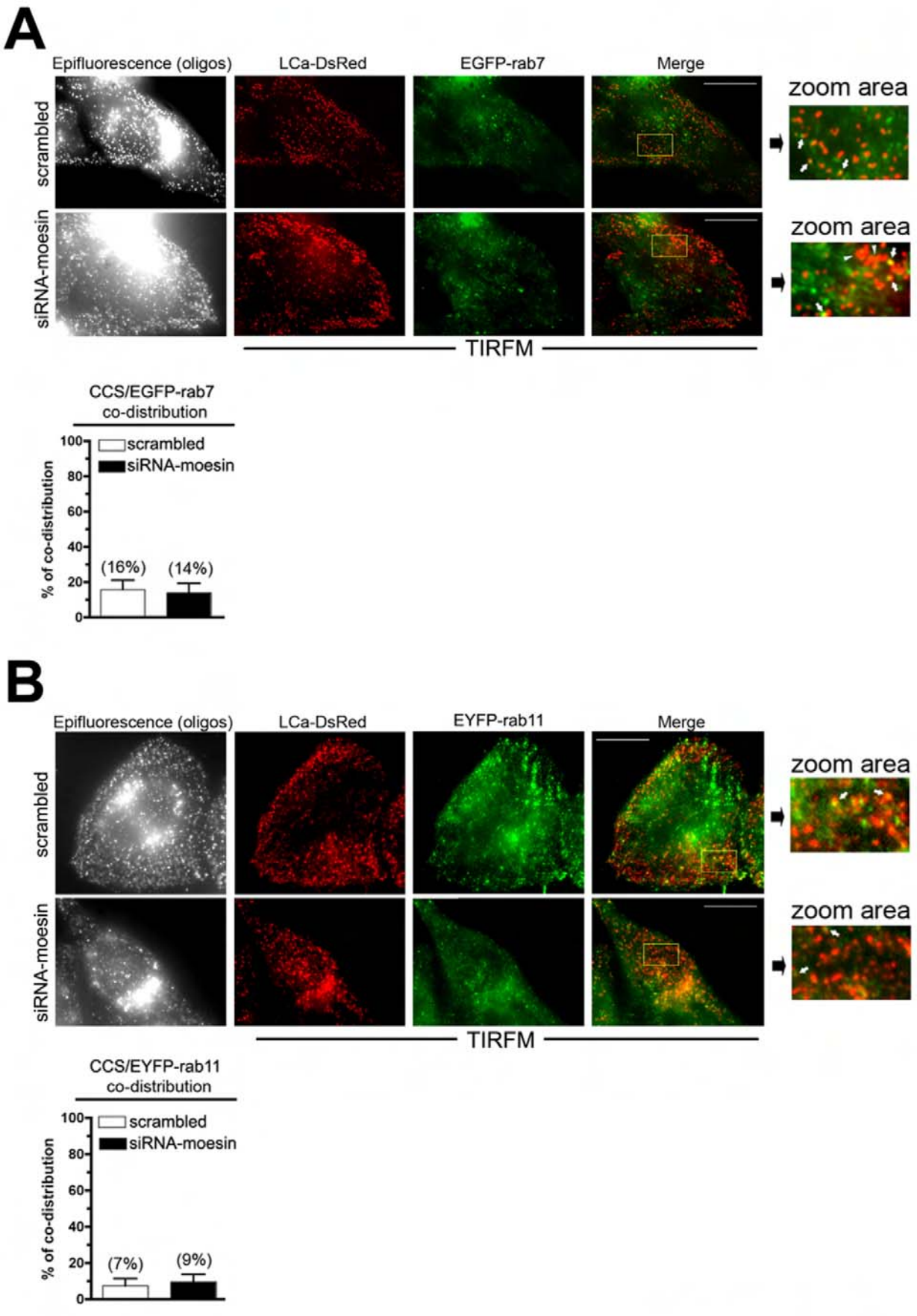

Supplemental Figure 5
Barroso et al.

3.4. EL TRITERPENO SEMISINTÉTICO 30-OXO-CALENDULADIOL ES UN ANTAGONISTA DE CCR5, CON ACTIVIDADES ANTI-VIH-1 Y ANTI-QUIMIOTÁCTICAS.

A pesar de que la introducción de la terapia antirretroviral ha mostrado ser efectiva en reducir la carga viral en plasma a niveles casi indetectables, la emergencia de cepas de VIH-1 resistentes frente a estos fármacos antirretrovirales junto con la toxicidad de los mismos, constituye la causa más frecuente del fracaso de los tratamientos. Además, la existencia de santuarios de latencia, replicación y propagación del VIH-1 en el organismo, impiden la eliminación de los provirus integrados y plantean un obstáculo enorme para la erradicación total del virus en la lucha contra el SIDA. Por tanto, es urgente la identificación y el desarrollo de nuevas moléculas antirretrovirales, necesarias para el desarrollo de nuevas estrategias terapéuticas dirigidas a inhibir las cepas virales resistentes, y con ello a evitar la propagación del virus. Estas nuevas moléculas antirretrovirales estarían dirigidas a cepas virales resistentes a los tratamientos actuales presentes en individuos infectados durante las últimas décadas (Simon et al., 2006).

Dentro de los posibles nuevos agentes antirretrovirales, los triterpenos pentacíclicos representan una clase variada y prometedora de productos naturales con actividades anti-virales y anti-tumorales (Aiken and Chen, 2005; Cichewicz and Kouzi, 2004). Uno de los triterpenos de tipo lupano pentacíclicos mejor estudiado es el ácido betulínico (BA, "*betulinic acid*"), que presenta actividades anti-inflamatorias y anti-VIH-1 en experimentos *in vitro* (Aiken and Chen, 2005; Cichewicz and Kouzi, 2004). Existen dos tipos de derivados de BA con potentes actividades anti-VIH, por un lado, los de clase I interfieren con el proceso de maduración de las partículas virales al nivel del procesamiento proteolítico de p25 (CA/SP1) (Keller et al., 2011; Li et al., 2003; Zhou et al., 2004), mientras que derivados de BA de clase II pueden actuar como inhibidores de la fusión entre las membranas celular y viral, mediante el bloqueo de la unión de la envuelta del VIH-1 a la célula diana (Lai et al., 2008; Soler et al., 1996).

En este trabajo, estudiamos la capacidad de una serie de triterpenos de tipo lupano no ácidos, naturales o derivados, en su capacidad de bloquear la infección por el VIH-1, y en ese caso determinar el mecanismo de acción.

RESULTADOS

Teniendo en cuenta que los tratamientos antirretrovirales actuales no consiguen erradicar completamente el virus del organismo, el presente trabajo constituye un esfuerzo dirigido a la identificación de nuevas moléculas inhibidoras de la entrada del VIH-1 con nuevos modos de acción que impidan, por tanto, el establecimiento de los reservorios virales latentes tan difíciles de erradicar y responsables de la propagación viral.

Se estudiaron una serie de triterpenos tipo lupano naturales y semisintéticos con una estructura química similar, para identificar nuevas moléculas pequeñas capaces de inhibir la infección por VIH-1. Ninguna de las moléculas ensayadas presentó toxicidad celular en las concentraciones de ensayo (en un rango desde 1 nM a 10 μM). Entre ellos, se observó que el compuesto semisintético triterpenoide 30-oxo-calenduladiol perturbó la fusión célula-célula, mediada por envueltas R5 trópicas, sin afectar a la fusión celular mediada por las envueltas X4 trópica. En ensayos de infección utilizando partículas virales de un único ciclo de infección, deficientes en replicación conteniendo el gen *luciferasa*, se observó que el 30-oxo-calenduladiol inhibió la entrada e infección de viriones R5 trópicos, en células permisivas CEM.NKR-CCR5 ($CD4^+/CXCR4^+/CCR5^+$). Sin embargo, este compuesto no afectó a la entrada e infección por partículas virales X4 trópicas, ni pseudotipadas con la proteína viral de envoltura VSV-G de fusión endocítica dependiente de clatrina. Experimentos de infección a distintas dosis del compuesto, mostraron que el 30-oxo-calenduladiol fue menos efectivo que la quimiocina RANTES (CCL5), ligando natural de CCR5, en inhibir la infección por VIH-1 de cepas R5 trópicas, pero, aún así, mostrando una buena potencia anti-viral, en experimentos dosis-respuesta. Estos resultados indican que esta estructura química podría ser de interés para el desarrollo de nuevas moléculas anti-VIH-1. La inhibición observada sobre la infección de virus R5 trópicos es debida a la interacción directa, con una afinidad cercana a la de RANTES, y reversible del 30-oxo-calenduladiol con CCR5, y no con CD4 ni con CXCR4. Esta unión compite con la unión entre RANTES y CCR5. Estos datos coinciden con la actividad neutralizante específica mostrada frente a cepas de VIH-1 con envueltas R5 trópicas. Este compuesto no internaliza el receptor de quimiocinas, incluso a concentraciones de 1 μM, e inhibe la internalización de CCR5 inducida por RANTES, como se observó por citometría de flujo y microscopía dinámica TIRF. Este hecho podría explicar la menor potencia anti-viral del 30-oxo-calenduladiol respecto de RANTES, ya que la competición frente a gp120 por la ocupación de CCR5 es un componente importante de la actividad anti-viral de los agonistas y/o antagonistas de

CCR5, pero la internalización de CCR5, que induce RANTES pero no así 30-oxo-calenduladiol, es otro componente clave en la actividad y eficacia anti-viral de RANTES. A continuación, y relacionado con esta activación endocítica de CCR5, se determinó el papel del 30-oxo-calenduladiol sobre la capacidad señalizadora de CCR5. Se observó que la pre-incubación de células $CCR5^+$ con 30-oxo-calenduladiol bloqueó la movilización de Ca^{2+} intracelular y la quimiotaxis dependiente de CCR5, mediada por la quimiocina natural RANTES. Por lo tanto, parece que el 30-oxo-calenduladiol compite no sólo la unión de la proteína de envuelta viral gp120 y del ligando de CCR5 RANTES, sino que también compite con la señalización de RANTES a través de su receptor CCR5. Por último, se observó que el 30-oxo-calenduladiol no afecta a la capacidad de diversos anticuerpos monoclonales de reconocer sus receptores humanos específicos, CCR1, CCR2b, CCR3 o CCR4. Además no tiene ningún efecto sobre la unión de RANTES a CCR1 o CCR2b, Eotaxina a CCR3, y TARC ("*Thymus-and activation-regulated chemokine*") a CCR4, lo que indica la especificidad de acción del 30-oxo-calenduladiol sobre el receptor CCR5, sin afectar a otros CC quimiorreceptores, y que explicaría así su actividad anti-VIH y anti-quimiotáctica como antagonista específico de CCR5.

MATERIALES Y MÉTODOS

Se utilizaron para los ensayos seis lupanos naturales o semisintéticos. Los compuestos fueron proporcionados por el grupo de investigación del Dr. Ángel Gutiérrez Ravelo, del Instituto Universitario de Bio-orgánica (IUBO) Antonio González. Se utilizaron anticuerpos monoclonales ficoeritrinados (PE) para CD4, CXCR4, CCR5, CCR1, CCR2b, CCR3 y CCR4. Además, se utilizó la sonda Fura2-AM para los ensayos funcionales de medición de calcio, y las quimiocinas RANTES, MCP-1, Eotaxina y TARC biotinilados para los ensayos de competición de su unión a sus respectivos receptores. Los vectores de expresión codificantes para los receptores de β-quimiocinas CCR1, CCR2b, CCR3 y CCR4 se obtuvieron de OriGene (Origene Technology, Inc., Rockville, MD). Los plásmidos utilizados para la producción de partículas virales fueron, pNL4-3.Luc.R-E- (Cuerpo viral Δ*Env*/Δ*nef*/*Luc*$^+$), pHXB2-env (envuelta X4 trópica), pCAGGS SF162 (envuelta R5 trópica) y pHEF-VSV-G (proteína G del virus de estomatitis vesicular). Se utilizaron las líneas celulares permisivas humanas CEM.NKR-CCR5 para las infecciones y análisis de niveles de expresión superficial de receptores. Las células 293T se utilizaron para la producción de virus defectivos en replicación, y para los ensayos de competición con los receptores

CCR1, CCR2b, CCR3 y CCR4. Las células HeLa P5, que expresan CCR5-GFP en superficie, se utilizaron para los estudios de internalización del receptor por microscopía de fluorescencia confocal y de manera dinámica mediante microscopía TIRF. Esta técnica de microscopía TIRF nos permite visualizar, en un contexto dinámico, moléculas presentes en la membrana plasmática con una profundidad hacia el citoplasma inferior a 200 nm, por lo que se pueden estudiar, por ejemplo, eventos de endocitosis de receptor inducido por ligando. Las células HeLa P5 ($CD4^+/CXCR4^+/CCR5^+$ y LTR-β-Gal) se utilizaron junto a las células HeLa 243 (Env^+/X4 trópica y Tat^+) y HeLa ADA (Env^+/R5 trópica y Tat^+) para los estudios de fusión célula-célula. Por citometría de flujo se analizó el nivel de expresión en superficie de los distintos receptores, y el nivel de expresión de los receptores durante los ensayos de competición de unión de ligando. La movilización de Ca^{2+} intracelular se midió en un espectrofotómetro de fluorescencia, utilizando la sonda de Ca^{2+} Fura 2-AM (5 μM) cargada en las células CEM.NKR-CCR5. La migración de células CEM.NKR-CCR5 en respuesta a quimiocina se determinó en cámaras de 48 pocillos. Estas cámaras contienen dos partes separadas por una membrana de policarbonato (tamaño de poro de 8 μm), en la parte de arriba se encuentran las células y en la parte de abajo se encuentra el medio quimiotáctico. Esta membrana puede ser atravesada por células CEM.NKR-CCR5 en respuesta a un gradiente quimiotáctico.

THE JOURNAL OF BIOLOGICAL CHEMISTRY VOL. 284, NO. 24, pp. 16609–16620, June 12, 2009

The Lupane-type Triterpene 30-Oxo-calenduladiol Is a CCR5 Antagonist with Anti-HIV-1 and Anti-chemotactic Activities*[S]

Received for publication, January 8, 2009, and in revised form, April 8, 2009 Published, JBC Papers in Press, April 22, 2009, DOI 10.1074/jbc.M109.005835

Jonathan Barroso-González[‡§¶1], Nabil El Jaber-Vazdekis[§¶2], Laura García-Expósito[‡¶3], José-David Machado[‡], Rafael Zárate[§¶4], Ángel G. Ravelo[§¶], Ana Estévez-Braun[§¶5], and Agustín Valenzuela-Fernández[‡¶6]

From the [‡]Laboratorio de Inmunología Celular y Viral, Unidad de Farmacología, Departamento de Medicina Física y Farmacología, Facultad de Medicina, Instituto de Tecnologías Biomédicas, Universidad de La Laguna, 38071 Tenerife, the [§]Instituto Universitario de Bio-Orgánica, Universidad de La Laguna, La Laguna, 38206 Tenerife, and the [¶]Instituto Canario de Investigación del Cáncer (ICIC), c/o Hospital Universitario La Candelaria, Carr. El Rosario, 38010 Tenerife, Spain

The existence of drug-resistant human immunodeficiency virus (HIV) viruses in patients receiving antiretroviral treatment urgently requires the characterization and development of new antiretroviral drugs designed to inhibit resistant viruses and to complement the existing antiretroviral strategies against AIDS. We assayed several natural or semi-synthetic lupane-type pentacyclic triterpenes in their ability to inhibit HIV-1 infection in permissive cells. We observed that the 30-oxo-calenduladiol triterpene, compound 1, specifically impaired R5-tropic HIV-1 envelope-mediated viral infection and cell fusion in permissive cells, without affecting X4-tropic virus. This lupane derivative competed for the binding of a specific anti-CCR5 monoclonal antibody or the natural CCL5 chemokine to the CCR5 viral coreceptor with high affinity. 30-Oxo-calenduladiol seems not to interact with the CD4 antigen, the main HIV receptor, or the CXCR4 viral coreceptor. Our results suggest that compound 1 is a specific CCR5 antagonist, because it binds to the CCR5 receptor without triggering cell signaling or receptor internalization, and inhibits RANTES (regulated on activation normal T cell expressed and secreted)-mediated CCR5 internalization, intracellular calcium mobilization, and cell chemotaxis. Furthermore, compound 1 appeared not to interact with β-chemokine receptors CCR1, CCR2b, CCR3, or CCR4. Thereby, the 30-oxo-calenduladiol-associated anti-HIV-1 activity against R5-tropic virus appears to rely on the selective occupancy of the CCR5 receptor to inhibit CCR5-mediated HIV-1 infection. Therefore, it is plausible that the chemical structure of 30-oxo-calenduladiol or other related dihydroxylated lupane-type triterpenes could represent a good model to develop more potent anti-HIV-1 molecules to inhibit viral infection by interfering with early fusion and entry steps in the HIV life cycle.

The human immunodeficiency virus (HIV)[7] pandemic is a medical challenge and represents the public health crisis of our time (1–5). Antiretroviral treatment achieves long-lasting viral suppression and, subsequently, reduces the morbidity and mortality of HIV-infected individuals. However, current drugs do not eradicate HIV infection and lifelong treatment might be needed (2).

Emerging drug-resistant HIV viruses, in patients receiving high active antiretroviral treatment, urgently needs the development of new antiretroviral molecules designed to inhibit resistant viruses, because many patients treated during the past decades harbor viral strains with reduced susceptibilities to many if not all available drugs (2, 6). In this matter, pentacyclic triterpenes represent a varied class of natural products presenting antitumor and antiviral activities (7–9). A well studied pentacyclic lupane-type triterpene is the betulinic acid (3β-hydroxy-lup-20(29)-en-28-oic acid), widely distributed throughout the plant kingdom, which presents anti-inflammatory, anti-malarial, and anti-HIV-1 effects *in vitro* (7, 9, 10). Although its mechanism of action has not been fully determined, it has been reported that some lupane-type triterpene derivatives impair HIV-1 fusion through interacting with the viral glycoprotein gp41, or disrupting the assembly and budding of emerging viral particles in infected target cells (reviewed in Ref. 9).

In the present work, we aimed to test the ability of several non-acid lupane-type triterpene, natural or derivative compounds, to inhibit HIV-1 viral infection and to determine the mechanism of action. Our results indicate that the semi-synthetic 30-oxo-calenduladiol, compound **1**, specifically interacts

* This work was supported in part by Ministerio de Ciencia e Innovación, Spain, Grant SAF2008-01729, Fundación para la Investigación y Prevención del SIDA en España Grants Fundación para la Investigación y Prevención del SIDA en España (FIPSE)-24508/05 and FIPSE-24661/07, Consejería de Industria, Comercio y Nuevas Tecnologías del Gobierno Autónomo de Canarias, Spain, Grant IDT-TF-06/066, and the Fundación Mutua Madrileña, Spain. This work was also supported by the Canary Islands Cancer Research Institute (ICIC), and project SAF 2006-06720 from the Spanish Ministry of Education and Science (MEC).

[S] The on-line version of this article (available at http://www.jbc.org) contains supplemental Fig. S1.

[1] Supported by associated Fellowship Fundación Canaria de Investigación y Salud (FUNCIS)-PI56/07.

[2] Supported by a predoctoral fellowship from CajaCanarias.

[3] Supported by associated Fellowship FIPSE-24661/07.

[4] Supported Fondo Social Europeo Grant RYC2002-694.

[5] To whom correspondence may be addressed. Tel.: 34-922-318576; Fax: 34-922-318571; E-mail: aestebra@ull.es.

[6] Supported by Fondo Social Europeo (FSE) Grant RYC2002-3018. To whom correspondence may be addressed: Laboratorio de Inmunología Celular y Viral, Unidad de Farmacología, Facultad de Medicina, Universidad de La Laguna, Campus de Ofra s/n, La Laguna, 38071 Tenerife, Spain. Tel.: 34-922-319351; Fax: 34-922-655995; E-mail: avalenzu@ull.es.

[7] The abbreviations used are: HIV-1, human immunodeficiency virus type 1; VSV-G, vesicular stomatitis virus G protein; RANTES, regulated on activation normal T expressed and secreted; TIRFM, total internal reflection fluorescence microscopy; PE, phycoerythrin; MCP-1, monocyte chemotactic protein 1; TARC, thymus- and activation-regulated chemokine; EGFP, enhanced green fluorescent protein; EF, evanescent field; IR, infrared; mAb, monoclonal antibody; PBS, phosphate-buffered saline; Env, envelope.

with the G protein-coupled CCR5 chemokine receptor, acting as an antagonist, inhibiting R5-tropic HIV-1 viral infection and CCL5 (regulated on activation normal T expressed and secreted (RANTES) chemokine)-mediated CCR5 internalization, cell signaling, and chemotaxis.

EXPERIMENTAL PROCEDURES

Chemistry

General—All solvents and reagents were purified by Standard techniques, as previously described (11). All reactions were monitored by thin layer chromatography (TLC) (on silica gel POLYGRAM® SIL G/UV$_{254}$ foils). Pre-coated SIL G-100 UV$_{254}$ (Machery-Nagel, Düren, Germany) TLC plates were used for preparative TLC purification. ^{1}H nuclear magnetic resonance spectra were recorded in $CDCl_3$ or C_6D_6 at 300 and 400 MHz, using Bruker AMX300 and AMX400 instruments. For ^{1}H spectra, chemical shifts are given in parts per million (ppm) and are referenced to the residual solvent peak. The following abbreviations are used: s, singlet; d, doublet; t, triplet; q, quartet; m, multiplet; br, broad.

Proton assignments and stereochemistry were supported by ^{1}H-^{1}H COSY and ROESY where necessary. Data are reported in the following manner with chemical shift (integration, multiplicity, and coupling constant, if appropriate). Coupling constants (J) are given in Hertz (Hz) to the nearest 0.5 Hz. ^{13}C NMR spectra were recorded at 75 and 100 MHz using Bruker AMX300 and AMX400 instruments. Carbon spectra assignments were supported by DEPT-135 spectra, ^{13}C-^{1}H (HMQC), and ^{13}C-^{1}H (HMBC) correlations where necessary. Chemical shifts are quoted in ppm and are referenced to the appropriate residual solvent peak. MS and HRMS were recorded at VG Micromass ZAB-2F. IR spectra were taken on a Bruker IFS28/55 spectrophotometer.

Molecules Assayed—Six natural or derivative lupanes were assayed (**1–6**). Compounds **1–3** and **5** were semi-synthesized as described below, whereas natural compounds **4** and **6** were isolated from *Maytenus apurimacensis*, using a previously described method (12–16). The degree of purity of the tested compounds was estimated higher than 99% by NMR spectroscopy.

*Preparation of 30-Oxo-calenduladiol (**1**)*—10 mg (0.023 mmol) of calenduladiol in 2 ml of EtOH were treated with 2.6 mg (1 eq) of SeO_2. The reaction mixture was heated under reflux for 10 h. Then, the reaction mixture was cooled and EtOH was removed under reduced pressure. The crude was treated with water and extracted three times with CH_2Cl_2. The organic layer was dried and concentrated under reduced pressure. The residue was purified by preparative TLC with hexanes/EtOAc (7:3) as solvent to obtain 3.6 mg (30.4%) of **1** as amorphous pale yellow solid. Compound **1** showed identical spectroscopic data to those previously reported (16).

*Preparation of Resinone Oxime Diacetate (**2**)*—15 mg (0.035 mmol) of resinone (17) in 2 ml of EtOH were treated with 7.3 mg (3 eq) of hydroxylamine hydrochloride and a solution of 5.75 mg (2 eq) of sodium acetate in 0.5 ml of H_2O. The reaction mixture was heated under reflux for 15 h. Then, the reaction mixture was cooled and the solvent was removed under reduced pressure. The crude was treated with water and extracted three times with CH_2Cl_2. The organic layer was dried and concentrated under reduced pressure. The residue was purified by preparative TLC with hexanes/EtOAc (7:3) as solvent to obtain 13.0 mg (80%) of resinone oxime as amorphous pale yellow solid. Then 6 mg (0.013) of resinone oxime in 2 ml of CH_2Cl_2 were treated with pyridine, the catalytic amount of 4-dimethylaminopyridine, and an excess of Ac_2O (10 μl). The reaction mixture was stirred at room temperature for 10 h. Then the solvent was removed under reduced pressure and the residue was purified by TLC preparative with hexanes/EtOAc (4:1) as solvent to afford 2.6 mg (38.5%) of compound **2** as an amorphous solid: $[\alpha]_D^{20}$, +4.6 (c 0.26, $CHCl_3$); UV (EtOH) λ_{max} (log ϵ) nm, 340 (2.42); 273 (2.72); IR ($CHCl_3$) ν_{max}, 2925, 2854, 1735, 1459, 1370, 1023, 755 cm^{-1}; ^{1}H NMR($CDCl_3$) δ, 4.89 (1H, dd, J = 8.5; 3.9 Hz, H-16), 4.72 (1H, s, H-29b), 4.62 (1H, s, H-29a), 2.20 (3H, s, $OCOCH_3$), 2.04 (3H, s, $OCOCH_3$), 1.69 (3H, s, H-30), 1.14 (3H, s, H-26), 1.08 (H, s, H-23), 1.05 (3H, s, H-27), 0.94 (3H, s, H-24), 0.87 (6H, s, H-25, H-28); ^{13}C NMR ($CDCl_3$) δ, 170.0 (2xs, OCOCH3), 167.0 (s, C-3), 149.5 (s, C-20), 109.7 (t, C-29), 78.7 (d, C-16), 54.9 (d, C-5), 49.3 (d, C-9), 47.3 (d, C-18), 47.1 (d, C-19), 47.0 (s, C-17), 43.9 (s, C-14), 40.9 (s, C-4), 40.7 (s, C-8), 38.9 (t, C-1), 37.4 (t, C-22), 37.3 (d, C-13), 36.9 (s, C-10), 33.6 (t, C-15), 33.3 (t, C-7), 31.6 (t, C-2), 29.1 (t, C-21), 27.2 (c, C-23), 24.3 (t, C-12), 22.4 (2xc, C-24, C-11), 21.1 (2x c, $OCOCH_3$), 20.8 (t, C-6), 19.8 (c, C-30), 15.8 (c, C-25), 15.6 (c, C-26), 13.8 (c, C-27), and 12.4 (c, C-28); EIMS m/z (%), 481 [M^+-C_2H_5ON] (40); 466 (6); 452 (1); 422 (5); HREIMS m/z (%), 481.3688 (calculated for $C_{32}H_{49}O_3$ 481.3682), 452.3545 (M^+-$C_4H_8O_2$) (calculated for $C_{30}H_{46}O_2N$, 452.3529).

*Preparation of Compound **3** (3β,16β-Diacetyl-lup-12-ene)*—5.8 mg (0.01 mmol) of 3β,16β-dihydroxylup-12-ene were acetylated with 2.5 eq of Ac_2O (2.5 μl), following the same procedure described for compound **2**. The residue was purified by TLC preparative with hexane/EtOAc (4:1) as solvent to yield 6.8 mg (86%) of compound **3** as an amorphous white solid: $[\alpha]_D^{20}$, +36.4 (c, 0.6, $CHCl_3$); UV (EtOH) λ_{max} (log ϵ) nm, 258 (3.09); IR ($CHCl_3$) ν_{max}, 2926, 2855, 1737, 1456, 1368, 1243, and 1025 cm^{-1}; ^{1}H NMR ($CDCl_3$) δ, 5.45 (1H, dd, J = 11.3; 5.4 Hz, H-16), 5.19 (1H, t, J = 3.4 Hz, H-12), 4.50 (1H, dd, J = 5.5;9.0 Hz, H-3), 2.04 (3H, s, $OCOCH_3$), 2.02 (3H, s, $OCOCH_3$), 1.18 (3H, s, H-27), 1.02 (3H, s, H-26), 0.97 (3H, s, H-23), 0.92 (3H, s, H-25), 0.87 (3H, s, H-24), 0.86 (3H, d, J = 7.7 Hz, H-29), 0.85 (3H, s, H-28), 0.79 (3H, d, J = 6.2 Hz, H-30); ^{13}C NMR (CDCl3) δ: 170.7 (s, $OCOCH_3$), 170.5 (s, $OCOCH_3$), 137.3 (s, C-13), 124.9 (d, C-12), 80.6 (d, C-3), 70.5 (d, C-16), 60.5 (d, C-18), 54.9 (d, C-5), 46.5 (d, C-9), 43.6 (s, C-14), 39.8 (s, C-8), 39.2 (2xd, C-19, C-20), 38.1 (t, C-1), 37.4 (s, C-17), 37.3 (s, C-4), 36.4 (s, C-10), 35.1 (t, C-15), 32.5 (t, C-7), 32.0 (t, C-22), 30.3 (t, C-21), 27.8 (c, C-23), 24.8 (c, C-27), 23.3 (t, C-2), 23.1 (t, C-11), 22.4 (c, C-28), 21.0 (C-30), 20.9 (2x c, $OCOCH_3$), 17.9 (t, C-6), 17.3 (c, C-25), 16.6 (c, C-26), 16.4 (t, C-29), 15.5 (c, C-24); EIMS m/z (%), 526 [M^+] (1), 466 (16), 451 (7); HREIMS, 526.4029 (calculated for $C_{34}H_{54}O_4$, 526.4022), 466.3778 (M^+-$C_2H_4O_2$) (calculated for $C_{32}H_{50}O_2$, 466.3811).

*Preparation of Compound **5** (3α,16β-Diacetyl-lup-12-ene)*—5.9 mg (84.6%) of compound **5** as amorphous solid were obtained from 6.0 mg (0.013 mmol) of 3α,16β-dihydroxylup-12-ene under identical reaction and purification conditions as

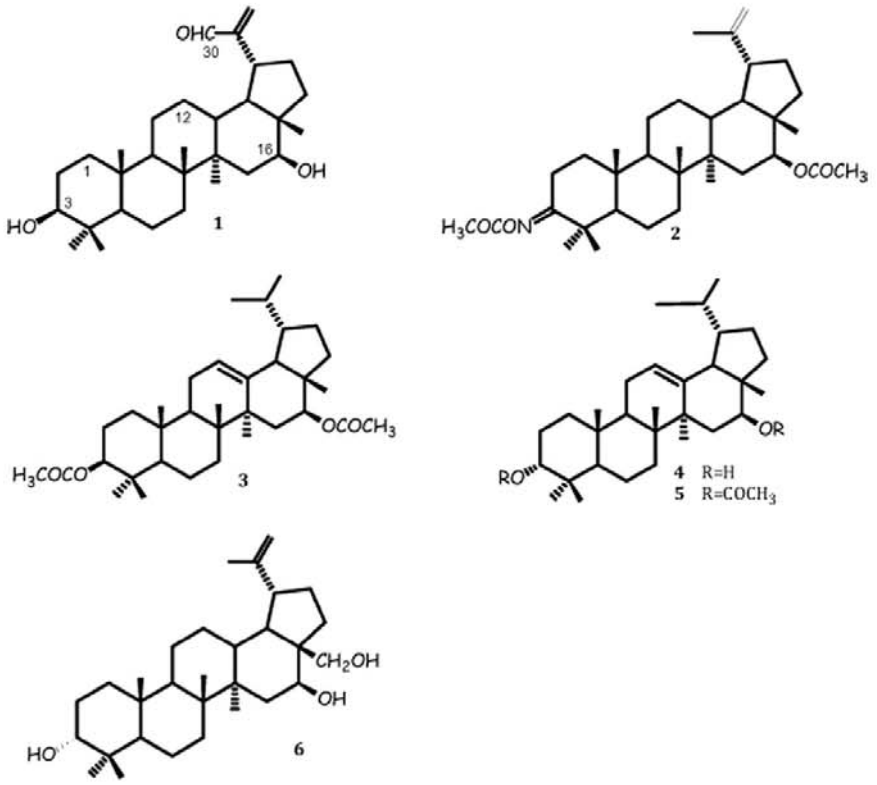

Lupane-type triterpene molecules assayed

FIGURE 1. **Chemical structures of a series of lupane-type triterpenes assayed in their capacity to inhibit HIV-1 infection.** Compounds **1**-**3** and **5** are semi-synthetic lupane triterpenes, whereas compounds **4** and **6** are natural triterpenes isolated from *M. apurimacensis*.

those used for compound **3**: $[\alpha]_D^{20}$, +11.2 (c 0.6, $CHCl_3$); UV (EtOH) λ_{max} (log ϵ), 202 (3.79) nm; IR ($CHCl_3$) ν_{max}, 2926, 2856, 1737, 1457, 1372, 1244, 1024, and 756 cm^{-1}; ^1H NMR ($CDCl_3$) δ, 5.47 (1H, dd, J = 11.4; 5.4 Hz, H-16), 5.20 (1H, t, J = 3.4, H-12), 4.63 (1H, bs, H-3), 2.08 (3H, s, $OCOCH_3$), 2.03 (3H, s, $OCOCH_3$), 1.24 (3H, s, H-27), 1.22 (3H, d, J = 7.1 Hz, H-29), 1.03 (3H, s, H-26), 0.97 (3H, s, H-25), 0.89 (3H, s, H-23), 0.87 (6H, s, H-28, H-24), and 0.80 (3H, d, J = 6.3 Hz, H-30); ^{13}C NMR ($CDCl_3$) δ, 170.6 (2xs, $OCOCH_3$), 137.2 (s, C-13), 125.1 (d, C-12), 77.8 (d, C-3), 70.5 (d, C-16), 60.5 (d, C-18), 49.7 (d, C-5), 46.4 (d, C-9), 43.6 (s, C-14), 40.0 (s, C-8), 39.2 (2xd, C-19, C-20), 37.3 (s, C-17), 36.5 (s, C-4), 36.2 (s, C-10), 35.1 (t, C-7), 33.6 (t, C-1), 32.4 (t, C-15), 32.1 (t, C-22), 30.3 (t, C-21), 27.5 (c, C-23), 24.1 (c, C-27), 23.0 (t, C-2), 22.9 (c, C-24), 22.4 (t, C-11), 21.7 (c, C-28), 21.1 (c, $OCOCH_3$), 21.0 (c, $OCOCH_3$), 20.9 (c, C-29), 17.8 (t, C-6), 17.3 (c, C-30), 16.6 (c, C-26), and 15.2 (t, C-25); EIMS m/z (%), 526 [M^+] (1), 466 (14), 451 (6); HRE-IMS: 526.4038 (calculated for $C_{34}H_{54}O_4$, 526.4022), 467.3917 (M^+-$OCOCH_3$) (calculated for $C_{32}H_{51}O_2$, 467.3889).

Antibodies and Reagents

The monoclonal antibodies (mAbs) CD184 (clone 12G5) and CD195 (clone 2D7/CCR5), used as phycoerythrin (PE) conjugates (BD Bioscience/BD Pharmingen, San Jose, CA), are directed against the second extracellular loop of CXCR4 and CCR5, respectively. The PE-labeled mAb RPT-4 is a neutralizing antibody against CD4 (eBioscience, San Diego, CA). PE-conjugated mAbs against human CCR1 (FAB145P), CCR2b (FAB151P), CCR3 (FAB155P), and CCR4 (FAB1567P) chemokine receptors were from R&D Systems (Minneapolis, MN). The Cremophor® EL emulsifying agent that is used in aqueous preparations of hydrophobic substances was from Sigma. In all experiments, 30-oxo-calenduladiol and the other assayed triterpenes were dissolved in the following working buffer solution: Cremophor EL/dimethyl sulfoxide/culture medium at a ratio of 1:1:8 (v/v/v). The Fura 2-AM probe was from Invitrogen. The Fluorokine™ human biotinylated RANTES (CCL5), monocyte chemotactic protein 1 (MCP-1), Eotaxin, or thymus- and activation-regulated chemokine (TARC) kits, and the human recombinant RANTES were from R&D Systems.

Cells

The human CEM.NKR-CCR5 permissive cell line (catalog number 4376, NIH AIDS Research and Reference Reagent Program) was grown at 37 °C in a humidified atmosphere with 5% CO_2 in RPMI 1640 medium (Lonza, Verviers, Belgium) supplemented with 10% fetal calf serum (Lonza), 1% L-glutamine, and 1% penicillin-streptomycin antibiotics. Cells were regularly passaged every 3 days. The 293T cell line was similarly cultured, in supplemented Dulbecco's modified Eagle's medium (Lonza), and were regularly passaged every 2–3 days. 24 h before cell transfection with viral or human DNA constructs, cells were harvested and resuspended at a density of 50–70% in fresh supplemented Dulbecco's modified Eagle's medium. The HeLa-P5 cells, stably transfected with human CD4 and C-terminal enhanced green fluorescent protein (EGFP)-tagged CCR5 cDNAs and with an HIV-long terminal repeat-driven β-galactosidase reporter gene (18), as well as, HeLa-243 and HeLa-ADA cells, co-expressing the Tat and X4- and R5-tropic HIV-1-Env proteins, respectively, were provided by Dr. M. Alizon (Hôpital Cochin, Paris, France) (18, 19). Human astroglia U87 cell line, stably expressing human CD4 and CCR3 receptors (U87.CD4.CCR3), was kindly provided by Dr. Guido Poli (San Raffaele Scientific Institute, Milano, Italy) and Dr. Dan R. Littman (Skirball Institute of Biomolecular Medicine, New York).

Human DNA Constructs

Human cDNAs of the β-chemokine CCR1, CCR2b, CCR3, and CCR4 receptors were from OriGene (Origene Technologies, Inc., Rockville, MD).

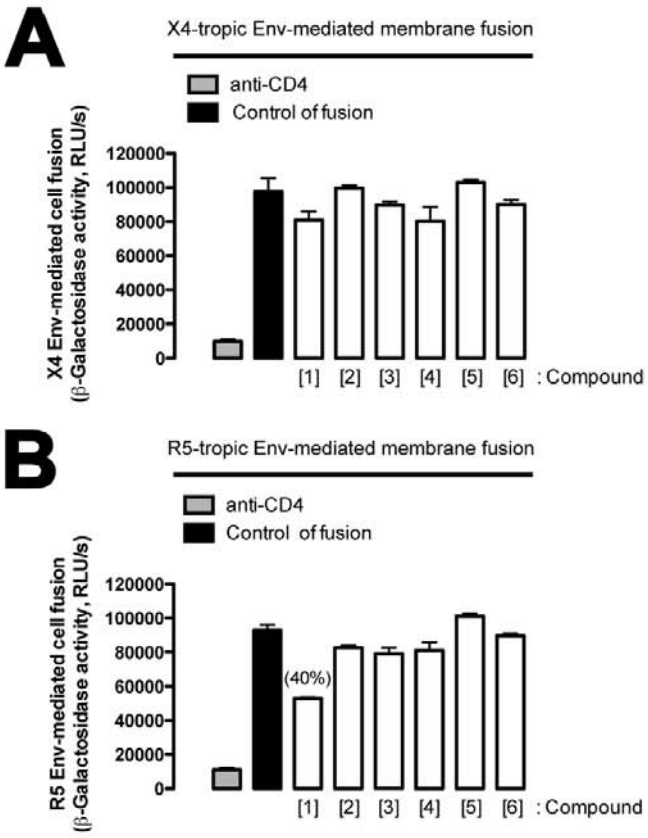

FIGURE 2. **30-Oxo-calenduladiol (1) perturbs R5-tropic HIV-1 Env-mediated membrane fusion.** In *A* and *B*, quantification (β-galactosidase production) of Env-mediated cell fusion between HeLa-243 (X4-tropic Env) or HeLa-ADA (R5-tropic Env) cells and HeLa-P5 (CD4+/CCR5+/CXCR4+) cells in the absence (control) or presence of different lupane-type pentacyclic triterpenes (compounds **1**-**6**) at 5 μM. Compound **1** inhibited about 40% of the R5-tropic Env-mediated cell fusion process. A neutralizing anti-CD4 mAb (5 μg/ml) was used to completely inhibit Env-mediated cell-to-cell fusion. The values are from three independent experiments (mean ± S.E.; $n = 9$).

Viral DNA Constructs

The pNL4-3.Luc.R-E- provirus (catalog number 6070013), the HXB2-env (catalog number 5040154), and pCAGGS-SF162-gp160-env (catalog number 3041817) glycoprotein vectors, and the pHEF-VSV-G vector (catalog number 4693), encoding the vesicular stomatitis virus G (VSV-G) protein, were obtained through the NIH AIDS Research and Reference Reagent Program.

HIV-1-Env-mediated Cell-to-cell Fusion Assay

A β-galactosidase cell fusion assay was performed as previously described (19, 20). Briefly, HeLa-243 or HeLa ADA cells were mixed with HeLa-P5 cells, in 96-well plates, in a 1:1 ratio (20,000 total cells), in the absence or presence of 5 μM of the different molecules assayed. These co-cultures were kept at fusion for 16 h at 37 °C. The fused cells were washed with Hanks' balanced salt solution, lysed, and the enzymatic activity was evaluated by chemiluminescence (β-galactosidase reporter gene assay; Roche Diagnostics, Germany). Anti-CD4 neutralizing mAb (5 μg/ml was preincubated in HeLa-P5 cells for 30 min at 37 °C before co-culture with Env+ HeLa cells) was used as a control for the blockage of cell fusion.

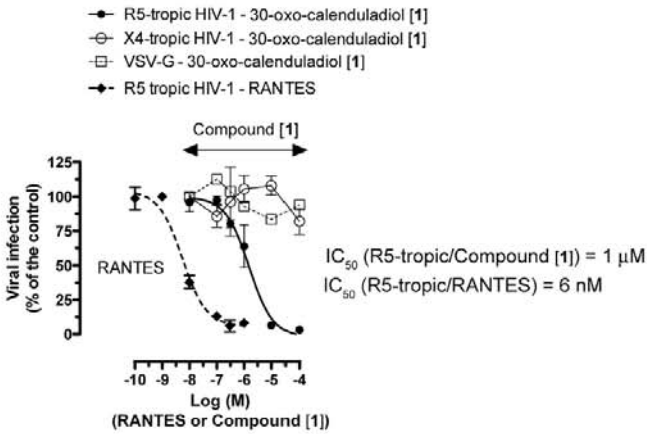

FIGURE 3. **30-Oxo-calenduladiol (1) specifically inhibits R5-tropic HIV-1 infection.** CEM.NKR-CCR5 permissive cells were incubated with equivalent viral inputs, as determined by a standard p24-enzyme-linked immunosorbent assay test, of luciferase-based X4- or R5-tropic pNL4-3.Luc.R-E- virions. Then, cells were kept in culture for 2 days at 37 °C. To control the specificity of the compound **1**-mediated effect on HIV-1 viral infection, luciferase-based VSV-G virions were used. Viral infected cells were determined by measuring the luciferase activity. Percentage inhibition of luciferase activity (of viral entry) was calculated for each dose point after subtracting the background (in the presence of a neutralizing anti-CD4 mAb at 5 μg/ml), and IC_{50} was determined. Each assay was done in triplicate and results are representative of four independent experiments (mean ± S.E.; $n = 12$).

Production of Viral Particles

X4- or R5-tropic HIV-1 viral particles were produced by co-transfecting 293T cells (70% of confluence) in 75-cm^2 flasks with pNL4-3.Luc.R-E- (20 μg) and CXCR4-tropic (HXB2-env) or CCR5-tropic (pCAGGS SF162 gp160) env glycoprotein (10 μg) vector, as previously described (21). Co-transduction of the pNL4-3.Luc.R-E- (20 μg) vector with the pHEF-VSV-G (10 μg) vector generates non-replicative viral particles that infect with cells in a VSV-G-dependent manner. Viral plasmids were transduced in 293T cells by using linear polyethylenimine, with an average molecular mass of 25 kDa (PEI25k) (Polyscience Inc., Warrington, PA). For this purpose, viral plasmids were first dissolved in 1/10th of the final tissue culture volume of Dulbecco's modified Eagle's medium, free of serum and antibiotics. The PEI25k was prepared as a 1 mg/ml solution in water and adjusted to neutral pH. After addition of PEI25k to the viral plasmids (at a plasmids:PEI25k ratio of 1:5 (w/w)), the solution was mixed immediately, incubated for 20–30 min at room temperature and then added to 293T cells in culture. After 4 h the medium was changed to RPMI 1640, supplemented with 10% fetal calf serum and antibiotics, and the cells were cultivated to allow viral production. Viruses were harvested 40 h post-transfection. The supernatant was clarified by centrifugation at 3,000 × *g* for 30 min. Virions were then stored at −80 °C. Viral stocks were normalized by p24-Gag content measured with an enzyme-linked immunosorbent assay test (Innogenetics, Gent, Belgium).

Viral Infection Assay

1×10^6 CEM.NKR-CCR5 permissive cells were incubated in the presence of different amounts of RANTES or 30-oxo-calenduladiol, with a synchronous dose of luciferase-based X4- or R5-tropic HIV-1 or VSV-G viral inputs (500 ng of p24), in 500 μl of RPMI 1640 medium for 2 h, as described (21). Cells were then

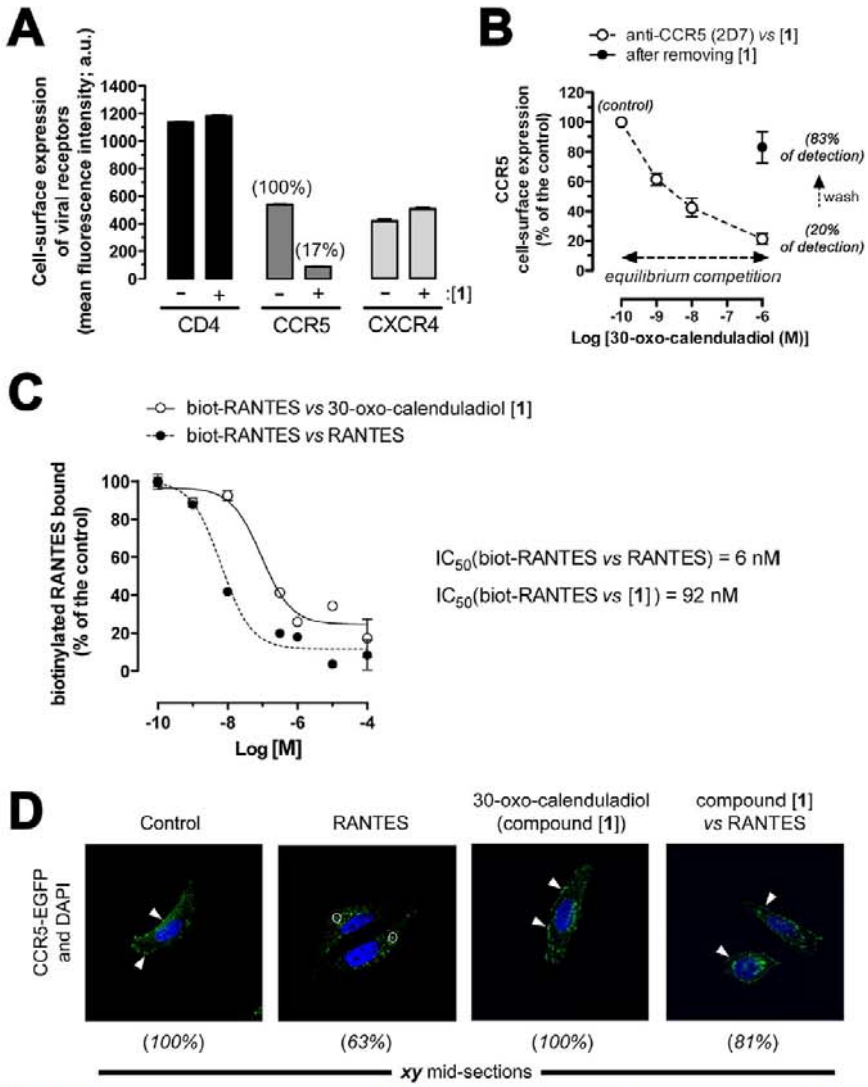

FIGURE 4. **30-Oxo-calenduladiol (1) interacts with the CCR5 receptor without promoting receptor internalization.** *A*, flow cytometry-based study of the ability of compound **1** (1 μM, for 1 h at 4 °C) to perturb the recognition of the CD4, CXCR4, and CCR5 viral receptors by their specific mAbs on the cell surface of CEM.NKR-CCR5 permissive cells. Compound **1** inhibits CCR5 recognition by a specific anti-CCR5 mAb (83% of inhibition). Data are from three independent experiments (mean ± S.E.; $n = 9$). *B*, equilibrium competition binding of the anti-CCR5 mAb 2D7 in the presence of different concentrations of compound **1** (*open circles*), for 1 h at 4 °C in CEM.NKR-CCR5 cells. The *solid circle* indicated the recovery of the ability of the mAb 2D7 to recognize the cell surface CCR5 receptor at 4 °C, after removing the pre-added compound **1** (1 μM) by extensively washing cells at 4 °C. *C*, competition binding assay. CEM.NKR-CCR5 cells were incubated with 5 nM human biotinylated RANTES and competed with different amounts of unlabeled human RANTES or 30-oxo-calenduladiol, for 1 h at 4 °C. Incubations were terminated by centrifugation at 4 °C, and cell pellets were resuspended in ice-cold PBS and the biotinylated RANTES bound was measured by flow cytometry after specific fluorescein isothiocyanate-avidin-mediated labeling. Nonspecific binding was determined in the presence of 1 μM of unlabeled RANTES. Results are from six independent experiments (mean ± S.E.; $n = 18$). Non-linear analysis of the competition curves yielded IC_{50} binding values as follows: biotinylated RANTES *versus* RANTES (*solid circles*), 6 ± 0.23 nM; biotinylated RANTES *versus* compound **1** (*open circles*), 92 ± 0.4 nM. *D*, analysis of the 30-oxo-calenduladiol (1 μM, for 1 h at 37 °C) effect on CCR5-EGFP internalization in HeLa-P5 cells by confocal microscopy. RANTES (150 nM, for 30 min at 37 °C)-mediated CCR5-EGFP internalization is shown (see *circled* CCR5-EGFP receptors in the RANTES image) and its inhibition by compound **1** (in the presence of 1 μM; see *white arrowheads* in the 30-oxo-calenduladiol *versus* RANTES image). *White arrowheads* or *circles* indicate non-internalized or internalized CCR5-EGFP receptor in *xy* midsections, respectively. The green fluorescence monitors the stably transfected CCR5-EGFP receptor. 4′,6-Diamidino-2-phenylindole-associated nuclei stain is shown. Percentages quantify the displayed pattern of CCR5-ECFP expression, RANTES-mediated internalization or compound **1**-dependent blockade from every 100 cells counted per each experimental condition. Data are from three independent experiments.

extensively washed to remove free virions. After 32 h of infection, luciferase activity was determined by using a luciferase assay kit (Promega Corporation) with a microplate reader (GeNios™, Tecan Trading AG, Switzerland). Data were analyzed using GraphPad Prism 5.0 software (GraphPad Software, Inc., San Diego, CA).

Flow Cytometry Analysis

CEM.NKR-CCR5 cells were incubated with PE-labeled specific antibodies against CD4, CXCR4, or CCR5 in the presence of different amounts of the 30-oxo-calenduladiol compound, for 1 h at 4 °C to avoid receptor internalization. Then, cells were washed by ice-cold PBS, fixed in PBS, 1% formaldehyde, and analyzed by flow cytometry (XL-MCL system, Beckman-Coulter Inc.). Cell surface expression analysis of CCR1, CCR2b, CCR3, or CCR4 receptors, transiently expressed in 293T cells, was similarly performed by using specific PE-conjugated mAbs, and their binding were equally assayed in the presence of 30-oxo-calenduladiol.

Confocal Microscopy Analysis of CCR5 Internalization

HeLa-P5 cells on coverslips at 50% confluence were starved for 30 min at 37 °C in Dulbecco's modified Eagle's medium without serum. They were then incubated in 80 μl of Dulbecco's modified Eagle's medium (with 0.5% bovine serum albumin) with RANTES (150 nM) or 30-oxo-calenduladiol (1 μM) at 37 °C for 30 min, or for 15 min at 37 °C with 30-oxo-calenduladiol (1 μM) before adding RANTES (150 nM) for a further 30 min at 37 °C. These CCR5-EGFP+ cells were rinsed three times at the end of incubation with ice-cold PBS and fixed in PBS, 2% paraformaldehyde for 3 min at room temperature. Cells were then rinsed and mounted in ProLong® Gold antifade reagent (Invitrogen) containing the 4′,6-diamidino-2-phenylindole probe to stain the nucleus of cells. The internalization of the CCR5-EGFP molecule was analyzed by fluorescence confocal microscopy (Leica DMR photomicroscope and Leica TCS-SP confocal microscope; Leica, Heidelberg, Germany).

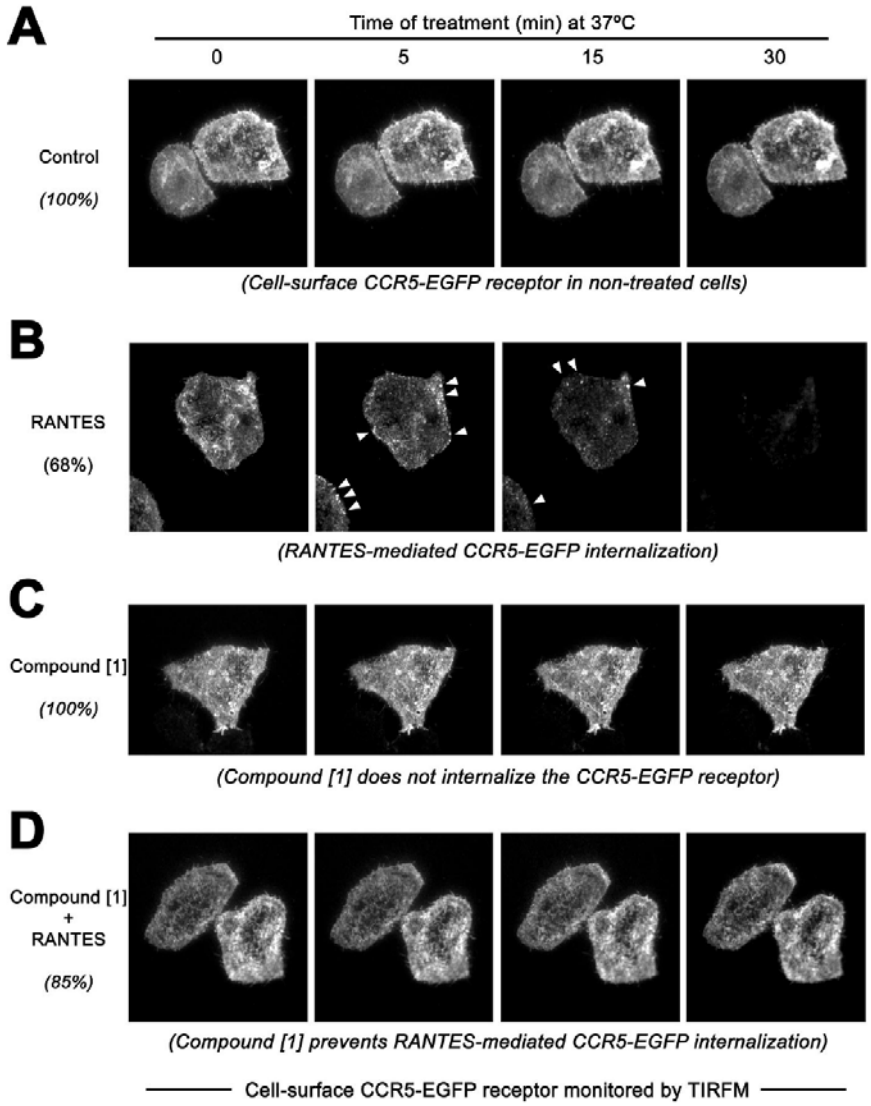

FIGURE 5. **30-Oxo-calenduladiol (1)-mediated inhibition of RANTES-induced CCR5 internalization analyzed by TIRFM.** TIRFM-based time-lapse study, in living HeLa-P5 cells at 37 °C, of CCR5-EGFP expression at plasma membrane of untreated (*control*) cells (*A*), cells treated with RANTES (150 nM) (*B*) or compound **1** (1 μM) (*C*), or previously treated with compound **1** (1 μM), for 15 min at 37 °C, before adding RANTES (150 nM) (*D*). In *B*, *white arrowheads*, in the 5- and 15-min images indicate clusters of CCR5-EGFP induced by RANTES, during receptor internalization. Percentages indicate the quantification of cells displaying the pattern of CCR5-EGFP expression (*A*, *C*, and *D*) or internalization (*B*) per each 100 cells counted, under any experimental condition. A representative experiment of three is shown.

Total Internal Reflection Fluorescence Microscopy (TIRFM) Analysis of CCR5 Internalization

HeLa-P5 cells, stably expressing the CCR5-EGFP receptor, were imaged with an inverted microscope Zeiss 200M (Zeiss, Germany) through a 1.45 NA objective (αFluar, ×100/1.45; Zeiss) in a Krebs-Hepes buffer containing 2 mM Ca^{2+} at 37 °C, in the absence or presence or RANTES (150 nM), compound **1** (1 μM), or pre-incubating compound **1** (1 μM), for 15 min at 37 °C, before adding RANTES (150 nM). RANTES-induced CCR5-EGFP internalization, or its prevention by compound **1** was analyzed by TIRFM technology, as described (22, 23). Briefly, total internal reflection generates an evanescent field (EF) that declines exponentially with increasing distance from the interface, depending on the angle at which the light strikes the interface. The angle was measured using a hemicylinder, as described (24). The images were projected onto a back-illuminated CCD camera (AxioCam MRm, Zeiss) through a dichoric and specific band-pass filter for the EGFP fluorophor. CCR5-EGFP molecules were analyzed at 37 °C, and imagined on the cell surface of HeLa-P5 cells using Axiovision (Zeiss) with 0.5-s exposures at 10 Hz, when illuminated under EF at the indicated times for any experimental condition.

Ligand Competition Assays

CEM.NKR-CCR5 cells were incubated with 5 nM human biotinylated RANTES and competed with different amounts of unlabeled human recombinant RANTES, as indicated by the manufacturer (Fluorokine™ RANTES (CCL5) kit, R&D Systems), or the 30-oxo-calenduladiol triterpene in a final volume of 300 μl for 1 h at 4 °C. Incubations were terminated by centrifugation at 4 °C. Cell pellets were resuspended in ice-cold PBS and fluorescein isothiocyanate-labeled avidin (The Fluorokine™ biotinylated RANTES (CCL5) kit, R&D Systems) was added to detect bound biotinylated RANTES. The CCR5-associated biotinylated RANTES was quantified by flow cytometry. Binding assays for human CCR1, CCR2b, CCR3, or CCR4 receptor (OriGene), transiently transfected in 293T cells, were carried out in a similar way, by analyzing the ability of 30-oxo-calenduladiol to compete the specific binding of their respective biotinylated natural ligands (RANTES, MCP-1, Eotaxin, or TARC (R&D Systems), respectively). The nonspecific binding of each ligand assayed was measured in cells pre-treated with specific blocking anti-receptor Abs (1 μg/ml) (included in the respective Fluorokine kits (R&D Systems)), which entirely prevented specific ligand-receptor binding.

Measurement of Cytosolic Free Calcium

Intracellular calcium levels were measured in a fluorescence spectrophotometer (Eclypse Variant; Melbourne, Australia) using Fura 2-AM (5 μM)-loaded CEM.NKR-CCR5 cells (5 × 10^6 cells/ml), as similarly described (25). Briefly, cells were resuspended in Hanks' balanced salt solution buffer (140 mM NaCl, 5 mM KCl, 1 mM $MgCl_2$, 1 mM $MgSO_4$,

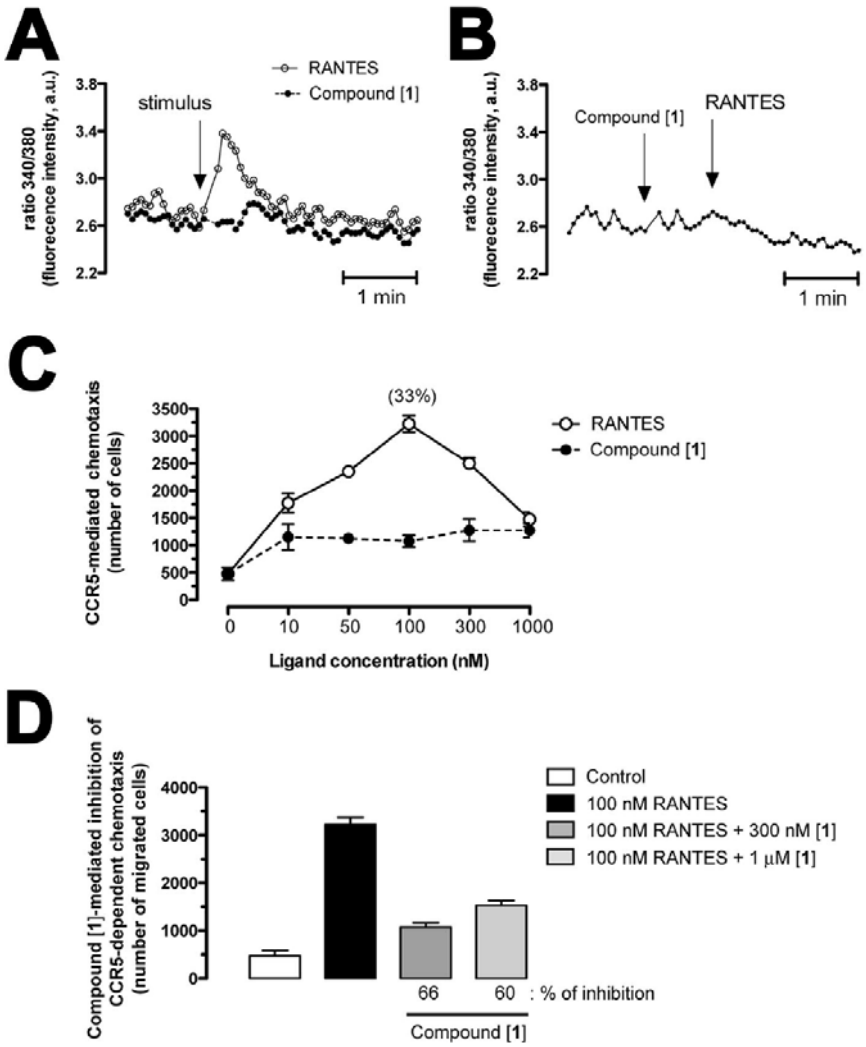

FIGURE 6. **30-Oxo-calenduladiol (1) is a CCR5 antagonist that inhibits RANTES-mediated cell signal and cell chemotaxis.** *A*, intracellular calcium mobilization, a comparative analysis of RANTES *versus* compound **1** was performed using Fura 2-loaded CEM.NKR-CCR5 cells at 37 °C in a fluorescence spectrophotometer. 30-Oxo-calenduladiol did not induce calcium mobilization at any concentration tested (ranging from 5 nM to 1 μM), and the result obtained at 1 μM is shown. RANTES-mediated calcium mobilization at 150 nM is shown. A representative experiment of three is shown. *B*, intracellular calcium mobilization, a competitive analysis of compound **1** (1 μM)-mediated inhibition of RANTES (150 nM)-dependent calcium mobilization is shown, in Fura 2-loaded CEM.NKR-CCR5 cells at 37 °C. A representative experiment of three is shown. *C*, chemotaxis assay, migration of CEM.NKR-CCR5 lymphoblastoid cells was measured following stimulation with the indicated concentrations of RANTES or compound **1** for 3 h at 37 °C, and migrated viable cells were quantitated. The percentage at 100 nM RANTES indicates cells migrated with respect to the total cellular input. Results are from four independent experiments (mean ± S.E.; $n = 12$). *D*, competitive chemotaxis assay, optimal RANTES (100 nM)-mediated migration of CEM.NKR-CCR5 cells was inhibited by compound **1** (at 300 nM and 1 μM) for 3 h at 37 °C. Results are from four independent experiments (mean ± S.E.; $n = 12$).

1.2 mM $CaCl_2$, 10 mM Hepes, 5 mM glucose, 0.3 mM KH_2PO_4, and 2 mM Na_2HPO_4), pH 7.0, for 30 min at 37 °C. For calcium measurements, aliquots of this cell suspension were preincubated in a 1-ml cuvette, in a total volume of 200 μl (1×10^6 cells/ml) in Hanks' balanced salt solution supplemented with 5% heat-inactivated fetal calf serum, pH 7.4, for 5 min at 37 °C. RANTES or the 30-oxo-calenduladiol triterpene were added at the indicated times. The intracellular calcium mobilization was estimated by the 340:380 nm fluorescence ratio, per each experimental condition.

Chemotaxis Assay

Migration of CEM.NKR-CCR5 cells was assessed in 48-well chambers (Neuro Probe Inc., Cabin John, MD), as previously described (25). Briefly, RANTES or 30-oxo-calenduladiol were added to the lower well at different concentrations, in a total volume of 30 μl in 25 mM Hepes-buffered RPMI 1640 at pH 7.4 (chemotaxis medium). The chemotaxis chamber was then assembled using polyvinylpyrrolidone-free polycarbonate membranes with 8-μm pore size (Costar, Cambridge, MA), and 50 μl of CEM.NKR-CCR5 cells (1×10^6 cells/ml), in chemotaxis medium without chemokine, was added to the upper well. After incubation in a 5% CO_2 humidified incubator at 37 °C for 3 h, the chamber was disassembled, and cells that migrated through to the lower wells were transferred to a working 96-well plate. The migrated viable cells were then quantified by flow cytometry.

RESULTS

The 30-Oxo-calenduladiol Triterpene Specifically Inhibits R5-tropic HIV-1 Infection—We have studied a series of natural and semi-synthesized lupane-type triterpenes, with a similar backbone chemical structure (Fig. 1, compounds **1–6**), to identify new small molecules able to inhibit HIV-1 infection. First, the capacity of these triterpenes to perturb X4- and R5-tropic HIV-1-envelope (Env)-mediated fusion membrane was assayed in a cell-to-cell fusion model (19, 20). It was observed that the semi-synthetic 30-oxo-calenduladiol triterpene (**1**) perturbs R5-tropic Env-mediated cell-to-cell fusion, without affecting X4-tropic Env-mediated cell fusion (Fig. 2, compound **1**). The rest of the triterpene molecules analyzed did not present any anti-fusogenic activity against X4- or R5-tropic HIV-1-Env, in this HeLa-based cellular model (Fig. 2). None of the molecules assayed were toxic (ranging from 1 nM to 10 μM), as analyzed by flow cytometry and propidium iodide cellular labeling (supplemental Fig. S1). Hence, this data could suggest that the 30-oxo-calenduladiol triterpene may act specifically against the R5-tropic HIV-1 virus.

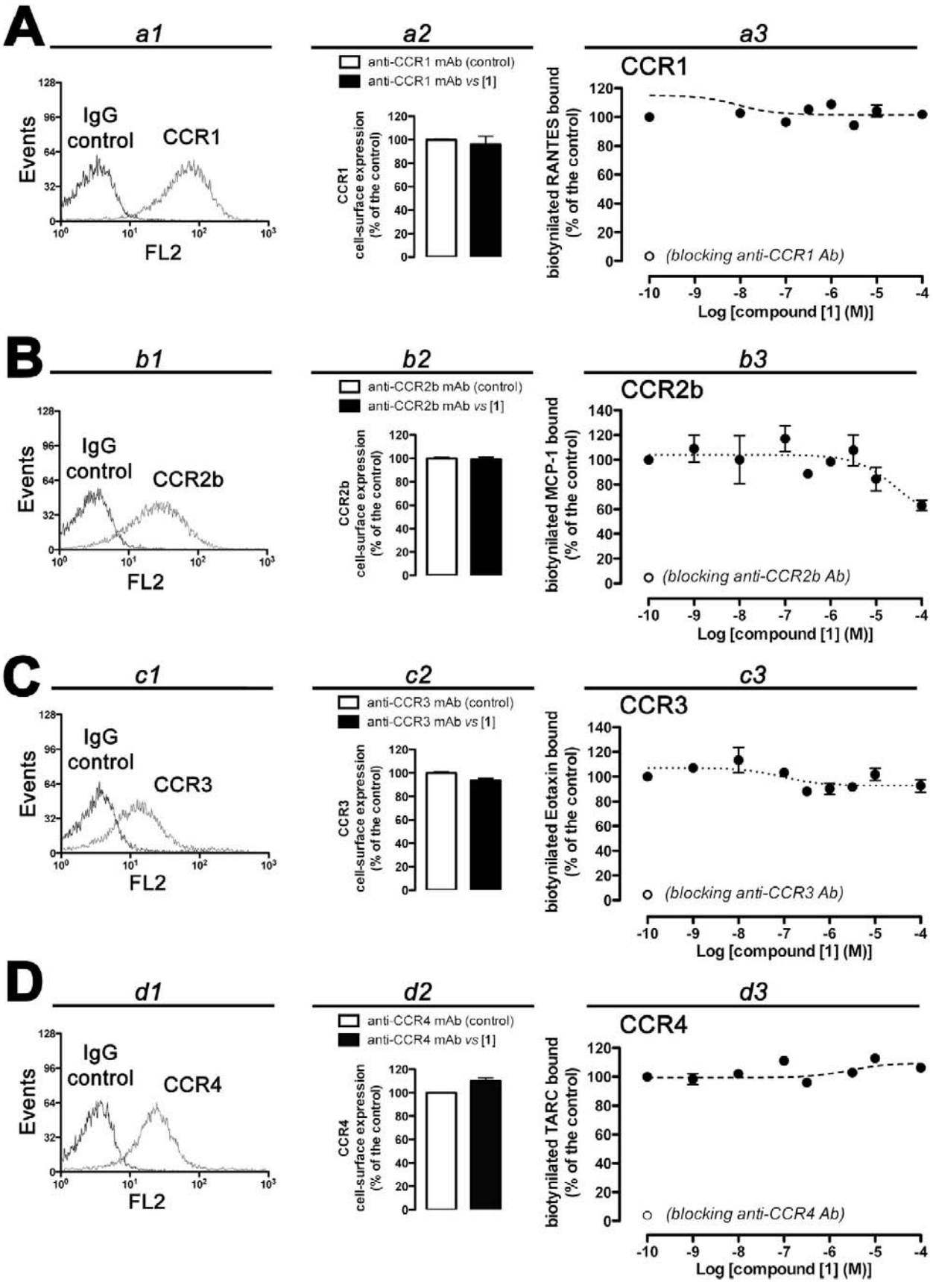
A
a1
IgG control
CCR1
Events
FL2
a2
anti-CCR1 mAb (control)
anti-CCR1 mAb vs [1]
CCR1 cell-surface expression (% of the control)
a3
CCR1
biotynilated RANTES bound (% of the control)
(blocking anti-CCR1 Ab)
Log [compound [1] (M)]
B
b1
IgG control
CCR2b
Events
FL2
b2
anti-CCR2b mAb (control)
anti-CCR2b mAb vs [1]
CCR2b cell-surface expression (% of the control)
b3
CCR2b
biotynilated MCP-1 bound (% of the control)
(blocking anti-CCR2b Ab)
Log [compound [1] (M)]
C
c1
IgG control
CCR3
Events
FL2
c2
anti-CCR3 mAb (control)
anti-CCR3 mAb vs [1]
CCR3 cell-surface expression (% of the control)
c3
CCR3
biotynilated Eotaxin bound (% of the control)
(blocking anti-CCR3 Ab)
Log [compound [1] (M)]
D
d1
IgG control
CCR4
Events
FL2
d2
anti-CCR4 mAb (control)
anti-CCR4 mAb vs [1]
CCR4 cell-surface expression (% of the control)
d3
CCR4
biotynilated TARC bound (% of the control)
(blocking anti-CCR4 Ab)
Log [compound [1] (M)]

Subsequently, the ability of 30-oxo-calenduladiol, and the others lupane-type triterpenes (Fig. 1) to inhibit HIV-1 viral infection was analyzed. We observed that 30-oxo-calenduladiol inhibited the infection of luciferase-based R5-tropic HIV-1 virions, in CCR5+/CXCR4+/CD4+ permissive cells (Fig. 3, IC_{50} = 1 μM). However, this compound (**1**) did not inhibit cell infection by luciferase-based X4-tropic HIV-1 viral particles or by luciferase-based VSV-G fusogenic virions (Fig. 3). In this regard, the rest of triterpenes assayed (Fig. 1, *compounds* **2–6**) did not present any antiviral activity against HIV-1 or VSV-G virions (data not shown). These data correlate with the results obtained in HIV-1-Env-mediated cell-to-cell fusion assays with the R5- and X4-tropic viral Envs (Fig. 2).

Thereby, it appears that 30-oxo-calenduladiol has specific antiviral activity, as the natural CCR5-ligand CCL5 (RANTES) (Fig. 3, IC_{50} = 6 nM), against R5-tropic HIV-1 virus, which infects permissive cells in a CD4/CCR5-dependent manner. 30-Oxo-calenduladiol was less effective than the chemokine RANTES in inhibiting HIV-1 infection, but it shows a good antiviral potency indicating that it could be considered as an interesting chemical structure to develop new anti-HIV-1 molecules. Moreover, the absence of any effect of the triterpene (**1**) on the infection of VSV-G viral particles suggests that 30-oxo-calenduladiol does not affect general viral-induced membrane fusion events, thereby specifically acting against R5-tropic HIV-1 virus.

30-Oxo-calenduladiol Specifically Interacts with the CCR5 Chemokine Receptor—To further analyze whether 30-oxo-calenduladiol (**1**) inhibits R5-tropic HIV-1 viral infection by directly interacting with CCR5, or some of the other viral receptors, binding of specific antibodies against the CD4, CCR5, or CXCR4 molecules was performed in CD4+/CCR5+/CXCR4+ permissive cells, in the presence of 1 μM compound **1** for 1 h at 4 °C (experimental conditions that avoid receptor internalization). Flow cytometry analysis showed that compound **1** impaired the binding of the neutralizing antibody (2D7) directed to CCR5, without affecting the antibody-mediated recognition of the CD4 or CXCR4 cell-surface antigen (Fig. 4*A*). Hence, compound **1** inhibited 2D7/CCR5 binding in a dose-dependent manner at 4 °C (Fig. 4*B*, *open circles*). The CCR5/compound **1** interaction seems to be reversible, because the ability of compound **1** to compete the 2D7-CCR5 binding at 4 °C (Fig. 4*B*, about 80% of inhibition at 1 μM of **1**) was almost entirely reverted after extensively washing pre-treated cells at 4 °C (Fig. 4*B*, *solid circle* indicates about 83% of 2D7-CCR5 binding).

To further confirm the ability of compound **1** to interact with the CCR5 chemokine receptor, we competed the binding of biotinylated RANTES to the CCR5 receptor at equilibrium with different concentrations of this lupane-type triterpene. It was determined that compound **1** competed the biotinylated RANTES/CCR5 binding with an IC_{50} value of 92 nM, compared with the IC_{50} value of 6 nM for unlabeled RANTES (Fig. 4*C*). Hence, 30-oxo-calenduladiol appears to bind to CCR5 with an attractive affinity, quite similarly to RANTES. These data correlate with the specific neutralizing activity shown by this triterpene against R5-tropic HIV-1 Env (Figs. 2 and 3).

Therefore, it seems that compound **1** inhibits R5-tropic viral infection by interacting with the CCR5 viral co-receptor, without affecting cell surface CD4 or CXCR4 receptors on permissive cells. These data could explain the fact that compound **1** did not inhibit X4-tropic HIV-1 viral infection (Fig. 3).

30-Oxo-calenduladiol Prevents RANTES-mediated CCR5 Internalization—Despite the above data were obtained under experimental conditions that prevented the internalization of the CCR5 molecule, it is conceivable that compound **1** could promote the internalization of CCR5 during viral infection. Thus, the ability of this triterpene to internalize CCR5 was studied and compared with RANTES-mediated CCR5 internalization at 37 °C, in permissive HeLa-P5 cells that stably express the fluorescent C-terminal EGFP-tagged CCR5 (CCR5-EGFP) receptor (Fig. 4*D*, in the *control* image, *white arrowheads* indicate cell-surface CCR5-EGFP). It was observed by confocal microscopy that RANTES induced the internalization of the cell-surface CCR5-EGFP receptor (Fig. 4*D*, see *circled* internalized CCR5-EGFP in the RANTES image), which was not observed at the cell surface of RANTES-treated cells. On the contrary, compound **1** did not internalize the chemokine receptor, even at concentrations of 1 μM (Fig. 4*D*, see *white arrowheads* indicating CCR5-EGFP at the cell surface in the 30-oxo-calenduladiol image). Remarkably, RANTES-induced CCR5 internalization was impaired in the presence of 30-oxo-calenduladiol (Fig. 4*D*, see *white arrowheads* indicating CCR5-EGFP at cell surface in the 30-oxo-calenduladiol versus RANTES image).

To further support these data, we have analyzed by TIRFM the ability of 30-oxo-calenduladiol to impair RANTES-mediated CCR5 internalization, in living cells at 37 °C (Fig. 5). The EF generated by TIRFM selectively illuminates fluorescent molecules near the plasma membrane interface, and leaves more remote cytosolic structures in the dark. Hence, the EF reaches from the plasma membrane into the cytosol for little more than 100 nm, allowing to monitor the dynamic behavior of molecules at plasma membrane (22–24), as ligand-induced internalization of the CCR5-EGFP molecule.

First, the steady-state distribution of CCR5-EGFP receptors on the cell surface of untreated HeLa-P5 cells was monitored (Fig. 5*A*, *control*). Then, we observed that the addition of RANTES (150 nM) induced the formation of CCR5-EGFP clus-

FIGURE 7. **30-Oxo-calenduladiol (1) does not interact with the CCR1, CCR2b, CCR3, or CCR4 β-chemokine receptors.** Flow cytometry analysis of cell surface expression of human CCR1-, CCR2b-, CCR3-, or CCR4-transfected receptors in 293T cells (*A* (*a1 panel*), *B* (*b1 panel*)), *C* (*c1 panel*)), or *D* (*d1 panel*), respectively). A representative experiment of three is shown. Equilibrium competition binding of specific mAbs directed against the CCR1, CCR2b, CCR3, or CCR4 chemokine receptors in the presence of compound **1** (1 μM), for 1 h at 4 °C (*A* (*a2 panel*), *B* (*b2 panel*)), *C* (*c2 panel*)), or *D* (*d2 panel*), respectively). Data are normalized from three different experiments (n = 9). Competition binding assay, 293T cells, transiently transfected with CCR1, CCR2b, CCR3, or CCR4 receptors, were incubated with 5 nM of their respective and specific human biotinylated-natural ligands (RANTES, MCP-1, Eotaxin, or TARC, respectively) and competed with different amounts of compound **1**, for 1 h at 4 °C (*solid circle curves*, in *A* (*a3 panel*), *B* (*b3 panel*)), *C* (*c3 panel*)), or *D* (*d3 panel*), respectively). Incubations were terminated and competition data were obtained as indicated in the legend to Fig. 4*C*. Nonspecific binding was determined in the presence of 1 μg/ml of specific blocking antibodies against the related chemokine receptor (*open circles*, in *A* (*a3 panel*), *B* (*b3 panel*)), *C* (*c3 panel*)), or *D* (*d3 panel*), respectively). Results are from three independent experiments (mean ± S.E.; n = 12).

ters at the plasma membrane, during the first minutes of treatment (Fig. 5*B*, *white arrowheads*, in the 5- and 15-min images, indicate clusters of CCR5-EGFP), which then internalized as monitored by the dim of the CCR5-EGFP-associated fluorescence in the EF of HeLa-P5 cells (Fig. 5*B*, cell surface CCR5-EGFP receptors disappeared from the EF, after 30 min of treatment). However, compound **1** (1 μM) did not induce the clustering of CCR5-EGFP molecules at the plasma membrane, and did not internalize the chemokine receptor (Fig. 5*C*). Remarkably, pre-treatment of HeLa-P5 cells with compound **1** (1 μM), during 15 min at 37 °C, prevented RANTES (150 nM)-mediated clustering and further internalization of the CCR5-EGFP receptor, which did not disappear from the EF (Fig. 5*D*). Thereby, all these data suggest that compound **1** specifically interacts with cell-surface CCR5 without promoting receptor internalization, and impairing the action of its natural ligand, RANTES.

30-Oxo-calenduladiol Is a Specific CCR5 Antagonist—To further investigate the actions of compound **1** on the normal function of the CCR5 receptor, it was assayed whether this molecule acts as an antagonist of this chemokine receptor. We observed that RANTES, a natural ligand of CCR5, triggered the mobilization of intracellular calcium (Fig. 6*A*), unlike compound **1**, which was not able to mobilize intracellular calcium at any concentration assayed in CCR5+ permissive cells (Fig. 6*A*, *1* μM 30-oxo-calenduladiol is only shown). Remarkably, preincubation of CCR5+ cells with compound **1**, before adding the chemokine ligand, impaired RANTES-mediated intracellular calcium mobilization (Fig. 6*B*). Thereby, it appears that compound **1** competed the binding and signaling of RANTES via the CCR5 receptor.

Moreover, the ability of compound **1** to induce CCR5-mediated cell migration and alter the chemotactic activity of RANTES was also studied. RANTES efficiently mediated chemotaxis of CCR5-expressing lymphocytes with a peak of chemotactic activity at 100 nM (Fig. 6*C*). On the contrary, 30-oxo-calenduladiol did not promote cell migration of these CCR5-expressing cells (Fig. 6*C*), and inhibited optimal CCR5-dependent chemotaxis mediated by RANTES (Fig. 6*D*).

To determine whether the inhibitory effect of 30-oxo-calenduladiol triterpene on chemokine binding is specific to CCR5 or is promiscuous to other β-chemokine receptors (26), the activity of compound **1** was examined in CCR1, CCR2b, CCR3, or CCR4 receptors, transiently expressed in 293T cells (Fig. 7, *A* (*a1 panel*), *B* (*b1 panel*), *C* (*c1 panel*), or *D* (*d1 panel*), respectively). We first observed that compound **1** did not affect the ability of some mAbs to recognize their specific human receptors, CCR1, CCR2b, CCR3, or CCR4, (Fig. 7, *A* (*a2 panel*), *B* (*b2 panel*), *C* (*c2 panel*), or *D* (*d2 panel*), respectively). Remarkably, compound **1** did not have any effect on the binding of RANTES, Eotaxin, or TARC to CCR1, CCR3, or CCR4, respectively (Fig. 7, *A* (*a3 panel*), *B* (*b3 panel*), *C* (*c3 panel*), or *D* (*d3 panel*), respectively). Regarding the CCR2b receptor, compound **1** slightly affected the binding of MCP-1, but only at high triterpene concentrations (Fig. 7*B* (*b3 panel*), 20% reduction of the total MCP-1 binding at 100 μM compound **1**), and without signal (data not shown). Hence, our results indicate that compound **1** could not be considered as a potential ligand of CCR2b (Fig. 7*B* (*b3 panel*)). Moreover, compound **1**-mediated equilibrium binding competition for the MCP-1/CCR2b or Eotaxin/CCR3 pairs was also assayed in the THP-1 monocytic cell line or U87.CD4.CCR3 cells, respectively, obtaining similar results in all cases (data not shown). Thereby, it seems that compound **1** is a selective antagonist for CCR5 (Figs. 2–6) and appears not to have any effect on CCR1, CCR2b, CCR3, and CCR4 chemokine receptors (Fig. 7). Altogether these data suggest that 30-oxo-calenduladiol behaves as a specific CCR5 antagonist to inhibit CCR5-mediated intracellular calcium mobilization and cell migration, presenting neutralizing activity against R5-tropic HIV-1 virus *in vitro*.

DISCUSSION

In the present work we have described for the first time the anti-HIV-1 activity of 30-oxo-calenduladiol, compound **1**, a semi-synthetic dihydroxylated lupane-type triterpene. This compound specifically interfered with cellular fusion and infection mediated by R5-tropic viral Env and HIV-1 virus, respectively. Hence, compound **1** did not perturb the related processes mediated by X4-tropic HIV-1 virus or viral Env. This specific antiviral activity of compound **1** relies on its ability to interact with the HIV-1 co-receptor CCR5. This lupane-type triterpene seems not to interact with the CD4 antigen, the main viral receptor, or the CXCR4 co-receptor. Furthermore, compound **1** impaired the binding of CD195 (2D7), a specific anti-CCR5 mAb, to the CCR5 chemokine receptor, and competed with high affinity CCL5/CCR5 interaction.

The ability of compound **1** to compete the binding of the neutralizing anti-CCR5 mAb (2D7) or the natural ligand RANTES, and to inhibit R5-tropic HIV-1 infection may relay on its capacity to interact with the second extracellular loop of the CCR5 receptor. This region represents the conformational binding domain for the neutralizing antibody 2D7 (27), which has been involved in ligand/ or virus/receptor interaction (27–30). However, as occurs with other antiviral small molecules (31–34), it is also plausible that compound **1** may occupy the CCR5 pocket, inducing a conformational change that may affect the second extracellular loop of CCR5, impairing its recognition by the anti-CCR5 mAb CD195 (2D7). These potential conformational changes may also affect RANTES-CCR5 binding and CCR5/gp120-mediated R5-tropic HIV-1 viral infection.

In the course of HIV infection *in vivo*, R5-tropic HIV-1 viruses predominate in early asymptomatic stages of infection, whereas R5/X4-dual tropic and X4-tropic HIV-1 viral strains appear at later stages of HIV-1 infection (35). Furthermore, R5 viruses are responsible for transmission of HIV-1 as evidenced by the high degree of resistance to infection of individuals homozygous for a 32-bp deletion in the gene encoding CCR5, who consequently lack a functional receptor (36, 37). In this regard, it is thought that the blockade of R5-tropic HIV-1 infection could be key for preventing primary viral infection and transmission. Hence, the development of CCR5 antagonists is important to battle HIV viral infection, and to complement the existing antiretroviral strategies against AIDS in the near future. Because CCR5 Δ32/Δ32 homozygote persons exhibit no consequences of being CCR5 negative, and present a high degree of resistance against viral infection (36, 37), the discov-

ery of new CCR5 antagonists, which do not trigger cell signals or mediate immune responses, represents an emerging and important area of research (38–40).

In this regard, the 30-oxo-calenduladiol-associated IC_{50} value for the inhibition of R5-tropic HIV-1 infection was of 1 μM. This IC_{50} value could be compared with those values obtained with good anti-HIV-1 molecules recently described (reviewed in Ref. 35).

Our results suggest that the 30-oxo-calenduladiol molecule is a non-toxic, specific CCR5 antagonist, which binds to the CCR5 receptor without triggering intracellular calcium mobilization or receptor internalization, and inhibits RANTES-mediated intracellular calcium mobilization, cell chemotaxis, and CCR5 internalization. Therefore, 30-oxo-calenduladiol-mediated anti-HIV-1 activity against the R5-tropic virus appears to rely in the occupancy of the CCR5 receptor to inhibit CCR5-mediated HIV-1 infection. Moreover, compound **1** also appears not to interact with other β-chemokine receptors, such as CCR1, CCR3, and CCR4. In addition, compound **1** shows a small degree of interaction with CCR2b, only at high concentrations (100 μM) of the molecule. It is plausible that the homology existing between CCR5 and CCR2b receptors (about 72% sequence identity) (reviewed in Ref. 41), may be responsible for the small degree of competition observed against the MCP-1/CCR2b binding. Altogether these results indicate that compound **1** is not a promiscuous antagonist for the above β-chemokine receptors, presenting selectivity of action on the CCR5 receptor.

Although target specificity is desired and required for antagonist-mediated treatment of several diseases, recently much expectation has been set upon the use of promiscuous, or polypharmacology compounds (42) to develop more efficient therapeutical approaches to battle multifactorial diseases (26, 41, 43, 44). Thereby, it would be interesting to further explore the potential antagonist activity of compound **1** on other cell surface receptors, different or not from the chemokine family.

Observing the structure of the 30-oxo-calenduladiol (**1**), and the structure of the different lupane-type triterpene assayed (Fig. 1), it is plausible that the two hydroxyl residues at carbons C-3 and C-16 together with the α,β-unsaturated aldehyde function, at carbon C-30, could stabilize the 30-oxo-calenduladiol/CCR5 association by establishing hydrogen bonds with some complementary residues in the viral receptor pocket. Thereby, these functional groups may be responsible for the antiviral activity of the molecule, acting as Michael acceptors with some nucleophilic residues of the corresponding CCR5 viral receptor that would explain the specific activity against R5-tropic viral Env. Hence, compound **4** (Fig. 1), which possesses the two hydroxyl residues but not the aldehyde function, was inert against HIV-1 infection. Therefore, the chemical structure of the 30-oxo-calenduladiol triterpene could represent a good model to develop more potent anti-HIV-1 molecules. In this matter, compound **1** is a dihydroxylated (3β,16β-diol) lupane, containing a formyl group at position C-30 conjugated with a double bond. Interestingly, the betulinic acid, a pentacyclic triterpene with described anti-HIV-1 activity, is easily derived by the abundant naturally occurred betulin, a related lupane-type triterpene diol (3β,28-diol) (10). Hence, it is conceivable that other natural lupane-type triterpene diols, as the 30-oxo-calenduladiol compound characterized in the present work, may present good anti-HIV-1 activities.

Considering all the presented data, we suggest that 30-oxo-calenduladiol is a new and specific CCR5 antagonist that exhibits great promise as a bioactive agent for the development of new high active derivatives for treatment of HIV-1 infection, and against biological disorders related to CCR5-mediated cell migration, such as for instance, inflammation, immune response, and tumor cell migration (45–57).

Acknowledgments—We specially thank Dr. M. Feria for helpful reading and discussion of the manuscript. We thank M. del Valle Croissier-Elías for excellent work done for correction of this manuscript. We thank the National Institutes of Health AIDS Research and Reference Reagent Program for providing pNL4-3.Luc.R-E-provirus, HXB2-env, and pCAGGS-SF162-gp160-env glycoprotein vectors, pHEF-VSV-G vector, and the CEM.NKR-CCR5 permissive cell line.

REFERENCES

1. Inciardi, J. A., and Williams, M. L. (2005) *AIDS Care* **17,** Suppl. 1, S1–8
2. Simon, V., Ho, D. D., and Abdool Karim, Q. (2006) *Lancet* **368,** 489–504
3. Kuehn, B. M. (2006) *JAMA* **296,** 29–30
4. Kallings, L. O. (2008) *J. Intern. Med.* **263,** 218–243
5. UNAIDS (2008) *Report on the Global AIDS Epidemic,* UNAIDS, Joint United Nations Programme on HIV/AIDS, Geneva, Switzerland
6. Pöhlmann, S., and Reeves, J. D. (2006) *Curr. Pharm. Des.* **12,** 1963–1973
7. Cichewicz, R. H., and Kouzi, S. A. (2004) *Med. Res. Rev.* **24,** 90–114
8. Connolly, J. D., and Hill, R. A. (2000) *Nat. Prod. Rep.* **17,** 463–482
9. Aiken, C., and Chen, C. H. (2005) *Trends Mol. Med.* **11,** 31–36
10. Alakurtti, S., Mäkelä, T., Koskimies, S., and Yli-Kauhaluoma, J. (2006) *Eur. J. Pharm. Sci.* **29,** 1–13
11. Perrin, D. D., and Amarego, W. L. F. (eds) (1988) *Purification of Laboratory Chemicals,* 3rd Ed., Pergamon Press, New York
12. Mesa-Siverio, D., Chavez, H., Estevez-Braun, A., and Ravelo, A. G. (2005) *Tetrahedron* **61,** 429–436
13. Mesa-Siverio, D., Estevez-Braun, A., Ravelo, A. G., Murguia, J. R., and Rodriguez-Afonso, A. (2003) *Eur. J. Org. Chem.* 4243–4247
14. Gutiérrez, F., Estévez-Braun, A., Ravelo, A. G., Astudillo, L., and Zarate, R. (2007) *J. Nat. Prod.* **70,** 1049–1052
15. Delgado-Méndez, P., Herrera, N., Chávez, H., Estévez-Braun, A., Ravelo, A. G., Cortes, F., Castanys, S., and Gamarro, F. (2008) *Bioorg. Med. Chem.* **16,** 1425–1430
16. Neukirch, H., D'Ambrosio, M., Sosa, S., Altinier, G., Della Loggia, R., and Guerriero, A. (2005) *Chem. Biodivers* **2,** 657–671
17. Núñez, M. J., Reyes, C. P., Jiménez, I. A., Moujir, L., and Bazzocchi, I. L. (2005) *J. Nat. Prod.* **68,** 1018–1021
18. Pleskoff, O., Tréboute, C., Brelot, A., Heveker, N., Seman, M., and Alizon, M. (1997) *Science* **276,** 1874–1878
19. Valenzuela-Fernández, A., Alvarez, S., Gordon-Alonso, M., Barrero, M., Ursa, A., Cabrero, J. R., Fernández, G., Naranjo-Suárez, S., Yáñez-Mo, M., Serrador, J. M., Muñoz-Fernández, M. A., and Sánchez-Madrid, F. (2005) *Mol. Biol. Cell* **16,** 5445–5454
20. Valenzuela-Fernández, A., Palanche, T., Amara, A., Magerus, A., Altmeyer, R., Delaunay, T., Virelizier, J. L., Baleux, F., Galzi, J. L., and Arenzana-Seisdedos, F. (2001) *J. Biol. Chem.* **276,** 26550–26558
21. Barrero-Villar, M., Barroso-González, J., Cabrero, J. R., Gordón-Alonso, M., Alvarez-Losada, S., Muñoz-Fernández, M. A., Sánchez-Madrid, F., and Valenzuela-Fernández, A. (2008) *J. Immunol.* **181,** 6882–6888
22. Barroso-González, J., Machado, J. D., García-Expósito, L., and Valenzuela-Fernández, A. (2009) *J. Biol. Chem.* **284,** 2419–2434
23. Steyer, J. A., and Almers, W. (2001) *Nat. Rev. Mol. Cell Biol.* **2,** 268–275
24. Merrifield, C. J., Feldman, M. E., Wan, L., and Almers, W. (2002) *Nat. Cell Biol.* **4,** 691–698

25. Valenzuela-Fernández, A., Planchenault, T., Baleux, F., Staropoli, I., Le-Barillec, K., Leduc, D., Delaunay, T., Lazarini, F., Virelizier, J. L., Chignard, M., Pidard, D., and Arenzana-Seisdedos, F. (2002) *J. Biol. Chem.* **277,** 15677–15689
26. Horuk, R. (2009) *Nat. Rev. Drug Discov.* **8,** 23–33
27. Lee, B., Sharron, M., Blanpain, C., Doranz, B. J., Vakili, J., Setoh, P., Berg, E., Liu, G., Guy, H. R., Durell, S. R., Parmentier, M., Chang, C. N., Price, K., Tsang, M., and Doms, R. W. (1999) *J. Biol. Chem.* **274,** 9617–9626
28. Wu, L., Paxton, W. A., Kassam, N., Ruffing, N., Rottman, J. B., Sullivan, N., Choe, H., Sodroski, J., Newman, W., Koup, R. A., and Mackay, C. R. (1997) *J. Exp. Med.* **185,** 1681–1691
29. Wu, L., LaRosa, G., Kassam, N., Gordon, C. J., Heath, H., Ruffing, N., Chen, H., Humblias, J., Samson, M., Parmentier, M., Moore, J. P., and Mackay, C. R. (1997) *J. Exp. Med.* **186,** 1373–1381
30. Blanpain, C., Doranz, B. J., Bondue, A., Govaerts, C., De Leener, A., Vassart, G., Doms, R. W., Proudfoot, A., and Parmentier, M. (2003) *J. Biol. Chem.* **278,** 5179–5187
31. Baba, M., Nishimura, O., Kanzaki, N., Okamoto, M., Sawada, H., Iizawa, Y., Shiraishi, M., Aramaki, Y., Okonogi, K., Ogawa, Y., Meguro, K., and Fujino, M. (1999) *Proc. Natl. Acad. Sci. U. S. A.* **96,** 5698–5703
32. Condra, J. H., Miller, M. D., Hazuda, D. J., and Emini, E. A. (2002) *Annu. Rev. Med.* **53,** 541–555
33. Watson, C., Jenkinson, S., Kazmierski, W., and Kenakin, T. (2005) *Mol. Pharmacol.* **67,** 1268–1282
34. Seto, M., Aikawa, K., Miyamoto, N., Aramaki, Y., Kanzaki, N., Takashima, K., Kuze, Y., Iizawa, Y., Baba, M., and Shiraishi, M. (2006) *J. Med. Chem.* **49,** 2037–2048
35. Princen, K., and Schols, D. (2005) *Cytokine Growth Factor Rev.* **16,** 659–677
36. Liu, R., Paxton, W. A., Choe, S., Ceradini, D., Martin, S. R., Horuk, R., MacDonald, M. E., Stuhlmann, H., Koup, R. A., and Landau, N. R. (1996) *Cell* **86,** 367–377
37. Samson, M., Libert, F., Doranz, B. J., Rucker, J., Liesnard, C., Farber, C. M., Saragosti, S., Lapoumeroulie, C., Cognaux, J., Forceille, C., Muyldermans, G., Verhofstede, C., Burtonboy, G., Georges, M., Imai, T., Rana, S., Yi, Y., Smyth, R. J., Collman, R. G., Doms, R. W., Vassart, G., and Parmentier, M. (1996) *Nature* **382,** 722–725
38. Cascieri, M. A., and Springer, M. S. (2000) *Curr. Opin. Chem. Biol.* **4,** 420–427
39. Proudfoot, A. E. (2002) *Nat. Rev. Immunol.* **2,** 106–115
40. Fernandez, E. J., and Lolis, E. (2002) *Annu. Rev. Pharmacol. Toxicol.* **42,** 469–499
41. Horuk, R. (2009) *Expert Rev. Mol. Med.* **11,** e1
42. Overington, J. P., Al-Lazikani, B., and Hopkins, A. L. (2006) *Nat. Rev. Drug Discov.* **5,** 993–996
43. Frantz, S. (2005) *Nature* **437,** 942–943
44. Roth, B. L., Sheffler, D. J., and Kroeze, W. K. (2004) *Nat. Rev. Drug Discov.* **3,** 353–359
45. Luster, A. D. (1998) *N. Engl. J. Med.* **338,** 436–445
46. Sallusto, F., Schaerli, P., Loetscher, P., Schaniel, C., Lenig, D., Mackay, C. R., Qin, S., and Lanzavecchia, A. (1998) *Eur. J. Immunol.* **28,** 2760–2769
47. Sozzani, S., Allavena, P., D'Amico, G., Luini, W., Bianchi, G., Kataura, M., Imai, T., Yoshie, O., Bonecchi, R., and Mantovani, A. (1998) *J. Immunol.* **161,** 1083–1086
48. Wysocki, C. A., Jiang, Q., Panoskaltsis-Mortari, A., Taylor, P. A., McKinnon, K. P., Su, L., Blazar, B. R., and Serody, J. S. (2005) *Blood* **106,** 3300–3307
49. Charo, I. F., and Ransohoff, R. M. (2006) *N. Engl. J. Med.* **354,** 610–621
50. Zhou, Y., Kurihara, T., Ryseck, R. P., Yang, Y., Ryan, C., Loy, J., Warr, G., and Bravo, R. (1998) *J. Immunol.* **160,** 4018–4025
51. Qin, S., Rottman, J. B., Myers, P., Kassam, N., Weinblatt, M., Loetscher, M., Koch, A. E., Moser, B., and Mackay, C. R. (1998) *J. Clin. Invest.* **101,** 746–754
52. Schröder, C., Pierson, R. N., 3rd, Nguyen, B. N., Kawka, D. W., Peterson, L. B., Wu, G., Zhang, T., Springer, M. S., Siciliano, S. J., Iliff, S., Ayala, J. M., Lu, M., Mudgett, J. S., Lyons, K., Mills, S. G., Miller, G. G., Singer, I. I., Azimzadeh, A. M., and DeMartino, J. A. (2007) *J. Immunol.* **179,** 2289–2299
53. Suzaki, Y., Hamada, K., Nomi, T., Ito, T., Sho, M., Kai, Y., Nakajima, Y., and Kimura, H. (2008) *Eur. Respir. J.* **31,** 783–789
54. Azenshtein, E., Luboshits, G., Shina, S., Neumark, E., Shahbazian, D., Weil, M., Wigler, N., Keydar, I., and Ben-Baruch, A. (2002) *Cancer Res.* **62,** 1093–1102
55. van Deventer, H. W., O'Connor, W., Jr., Brickey, W. J., Aris, R. M., Ting, J. P., and Serody, J. S. (2005) *Cancer Res.* **65,** 3374–3379
56. Karnoub, A. E., Dash, A. B., Vo, A. P., Sullivan, A., Brooks, M. W., Bell, G. W., Richardson, A. L., Polyak, K., Tubo, R., and Weinberg, R. A. (2007) *Nature* **449,** 557–563
57. van Deventer, H. W., Wu, Q. P., Bergstralh, D. T., Davis, B. K., O'Connor, B. P., Ting, J. P., and Serody, J. S. (2008) *Am. J. Pathol.* **173,** 253–264

SUPPLEMENTAL DATA

Legend to Supplemental Figures.

Supplemental Figure 1. The different concentrations used of the lupane-type triterpene 30-oxo-calenduladiol [1] are not toxic for cells.
A, flow cytometry-based analysis of propidium iodide uptake in control, non-transfected 293T cells (*top left panel*) and CCR2b-transfected 293T cells (24 h post-transfection) (*top middle and right panels*, *CCR2b-transfected cells*), or CCR2b-transfected 293T cells (24 h post-transfection) further treated by different concentrations of compound [**1**] (*from 1 nM to 10 μM*), for 6 h at 37ºC. Quantification of propidium iodide uptake (*FL3*) by cells is indicated in regions 1 (*R1, in red*) of plots, per each experimental condition. The percentage of CCR2b-transfected 293T cells is indicated in regions 2 (R2, in black) of each plot. Cell-surface expressed CCR2b receptor is detected by using a specific PE-conjugated mAb (*FL2*), under any experimental condition. A representative experiment of three is shown.

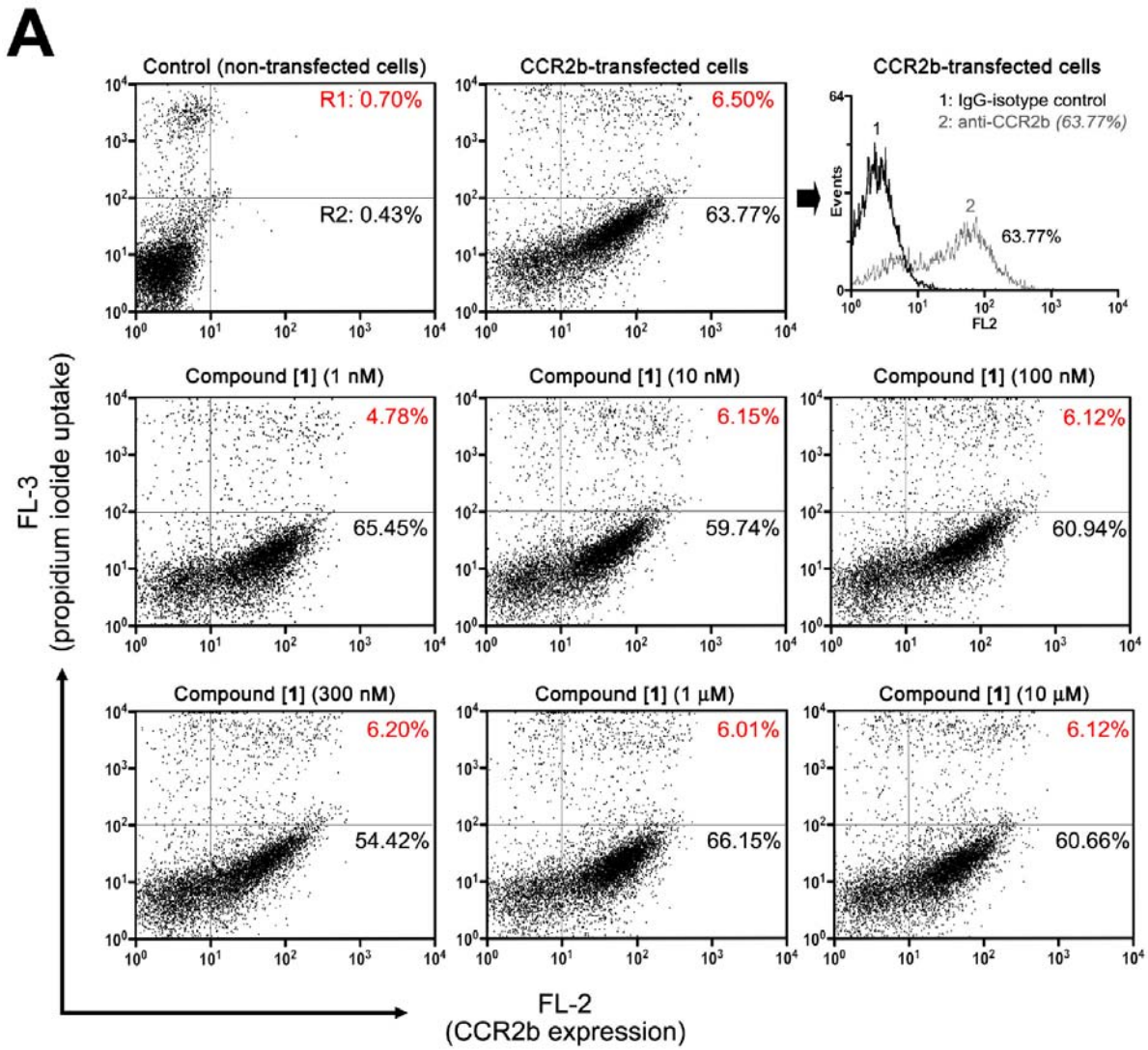

Supplemental Figure 1
Barroso-González et al.

4. DISCUSIÓN

Los resultados presentados en esta Tesis Doctoral indican que el VIH-1 transduce una señal a través de CD4 que induce la producción de PIP_2, por la quinasa PI4P5-K Iα, dando lugar a la activación de la proteína adaptadora de F-actina moesina. Esta activación parece ser necesaria para la interacción directa entre CD4 y CXCR4, y su reclutamiento en las zonas de contacto virus-célula, dependiente del citoesqueleto de actina, va a favorecer en último término la fusión de las membranas celular y viral en la membrana plasmática de la célula diana. Además, nuestros datos indican que el tráfico de clatrina no está implicado en las etapas de fusión, entrada e infección por VIH-1 (Nuestros datos y ANEXO 2, (Garcia-Exposito et al., 2011)). Por tanto, moesina no está implicada en la regulación de una posible entrada viral del VIH-1 mediada por clatrina, aunque sí cumple una función importante en el reciclaje hacia la membrana plasmática de vesículas de clatrina endocíticas nacientes, favoreciendo la supervivencia de la célula infectada a partir de un incremento en la captación del complejo hierro-Tf por el sistema Tf/TfR. Este proceso estaría favorecido en las primeras etapas de infección por el propio VIH-1, mediante la activación de moesina, lo que unido al control y regulación de la fusión y entrada viral, el VIH-1 se aseguraría la supervivencia celular durante estos eventos tempranos de infección, importantes para asegurar la integración y replicación viral. Por último, hemos caracterizado una nueva molécula antiviral que bloquea la entrada de virus R5 trópicos, por unión competitiva al receptor CCR5, pudiendo ser un prometedor agente bioactivo (posible cabeza de serie) para el desarrollo de nuevos derivados más eficaces para el tratamiento del VIH-1.

De esta manera, nuestros resultados añaden más complejidad al proceso de infección por el VIH-1, sobre todo en cuanto a la remodelación dinámica y temporal del citoesqueleto de actina cortical durante las primeras etapas del ciclo de vida viral, en donde es posible que no sólo una sino un conjunto de proteínas participen activamente en la modificación de la plasticidad celular en respuesta a la unión del VIH-1, mediante la remodelación del córtex celular y la concentración de complejos de proteínas en regiones delimitadas de la membrana plasmática.

4.1. Moesina regula la infección por cepas X4 trópicas del VIH-1.

Durante esta Tesis, hemos mostrado que el VIH-1 activa las proteínas ERM endógenas durante los primeros estadios de infección viral. La activación, o liberación de la conformación autoinhibida, tiene lugar a través de la interacción de gp120 con CD4, y se detecta por fosforilación de la región C-terminal de la proteína. Esta

activación representa un requisito fundamental para la fusión viral, evento que se encuentra relacionado directamente con la capacidad de moesina de promover, tras su activación, la reorganización e interacción entre los receptores virales CD4 y CXCR4 de manera dependiente de la F-actina. Este efecto da lugar a la relocalización de la F-actina, CD4 y CXCR4 en la zona de contacto virus-célula.

La identidad de la quinasa responsable de la fosforilación de moesina en respuesta al VIH-1 es desconocida. Aunque se ha descrito que ROCK y PKC pueden fosforilar las ERM *in vitro* (Bretscher, 1999; Nakamura et al., 1999), nuestros resultados, mediante el uso de inhibidores específicos de ROCK y PKC, indican que estas quinasas no parecen ser las responsables de la fosforilación de las proteínas ERM mediadas por el contacto del VIH-1. Asimismo, parece que la activación y fosforilación de moesina se corresponde con un incremento de su asociación con el citoesqueleto de actina cortical (Simons et al., 1998), por lo que durante los primeros estadios de infección puede favorecer el anclaje de la membrana plasmática al citoesqueleto de actina cortical, reorganizando complejos de proteínas en las zonas de contacto virus-célula, lo que incrementaría la eficiencia de la entrada viral e infección.

Aunque la redistribución de los receptores para el VIH-1, tras el contacto con partículas de VIH-1, es un evento conocido (Iyengar et al., 1998; Piguet and Sattentau, 2004), aún quedan por determinar muchos de los componentes moleculares implicados. La asociación superficial entre CD4 y CXCR4 se encuentra potenciada por la envuelta del VIH-1 (Lapham et al., 1999; Wang et al., 2004), por lo que las señales que permiten la interacción entre ambos debe ser transmitida a través de CD4. Igualmente, trabajos previos han mostrado que la desorganización del citoesqueleto de actina cortical afecta de manera negativa al agrupamiento de CD4-CXCR4 y entrada de virus X4 trópicos (Iyengar et al., 1998; Pontow et al., 2004). En nuestro estudio demostramos que la proteína funcional Fl-moesina potencia significativamente el agrupamiento e interacción entre CD4 y CXCR4, de manera dependiente de la F-actina. Esta interacción incrementa la susceptibilidad celular a la infección por el VIH-1. Por el contrario, una construcción dominante negativa N-moesina o un ARNi específico de la proteína moesina endógena bloquean este efecto, inhibiendo la entrada viral e infección. Además, la sobreexpresión de N-moesina también inhibe la fosforilación de la proteína moesina endógena en respuesta a la envuelta del VIH-1, por lo que bloquea la reorganización de la F-actina, CD4 y CXCR4. Por ello, es posible que moesina controle la asociación y agrupamiento de los receptores virales CD4 y CXCR4 en la región de formación de la sinapsis viral, formación del poro de fusión, entrada e infección por el VIH-1.

Por otro lado, se ha descrito que moesina y ezrina limitan la infección retroviral afectando a la estabilidad del citoesqueleto de tubulina en un estadio posterior a la fusión viral y previo a la transcripción reversa del ARN viral (Haedicke et al., 2008; Naghavi et al., 2007), proponiéndose que las proteínas ERM participan en la transición del genoma viral desde el citoesqueleto de actina hacia una región de microtúbulos estables donde podría tener lugar la transcripción reversa viral (McDonald et al., 2002). De manera llamativa, las construcciones N-moesina y N-ezrina se comportan de manera similar a la construcción funcional en su capacidad de conferir resistencia a infección retroviral (Haedicke et al., 2008; Naghavi et al., 2007). Estos resultados son aparentemente contradictorios teniendo en cuenta la función dominante negativa de estas construcciones, que aunque no se conozca en profundidad, parece depender de la unión del dominio FERM N-terminal a la región C-terminal de las proteínas ERM endógenas abiertas, por tanto, enmascarando el dominio de interacción con F-actina (Bretscher, 1999). Por tanto, estos dominantes negativos secuestran los extremos C-terminales de unión a actina de las proteínas ERM abiertas, por el contacto del VIH-1 con CD4, inhibiendo su función, como mostramos durante este trabajo.

De acuerdo con nuestros datos, el silenciamiento específico de moesina bloquea la infección y/o fusión célula-célula por cepas X4 trópicas del VIH-1 en líneas celulares no linfoides (Kubo et al., 2008), al parecer incrementando la infección R5 trópica, y sin afectar a la infección de virus VSV-G y E-MLV. Curiosamente, el principal bloqueo de la infección se observó con un ARNi contra la proteína radixina endógena, la cual se expresa muy poco en las células diana de la infección por el VIH-1 ((Shcherbina et al., 1999) y nuestros resultados). A pesar de estos resultados, el mecanismo molecular del efecto de las proteínas ERM sobre la infección del VIH-1 no ha sido explorado hasta ahora. Aquí, nuestros resultados proporcionan evidencias de la participación de moesina en la regulación de la fusión e infección, mediada por la envuelta del VIH-1, a través de la reorganización de los receptores CD4 y CXCR4, dependiente de la F-actina cortical.

Los resultados presentados en esta tesis doctoral muestran además que la proteína ezrina, aunque también se activa por el VIH-1, no parece tener ningún efecto sobre la fusión, entrada e infección por el VIH-1. Por un lado, puede ser debido a diferencias en el nivel de expresión de las distintas proteínas ERM en linfocitos, donde la proteína mayoritaria moesina podría compensar la ausencia de la proteína ezrina, pero quizás no al revés. Por otro lado, puede ocurrir que ambas proteínas, aunque simultáneamente activadas por fosforilación en Thr, cumplan funciones diferentes en la célula diana. Así, se ha descrito que ezrina, pero no moesina, puede regularse por

fosforilación en Tyr (Tyr^{145} e Tyr^{353}) además de en Thr. De manera interesante, la fosforilación en el residuo Tyr^{145} de ezrina puede ser mediada por $p56^{Lck}$ de manera dependiente de CD4 *in vitro*, aunque no se conoce su relevancia en células T. Además, la fosforilación en Tyr^{353} permite a ezrina unirse a la subunidad reguladora de la quinasa PI3K activando señales de supervivencia celular (revisado en (Burkhardt et al., 2008)). Igualmente, ezrina es capaz de interaccionar con la quinasa FAK y reclutarla a la membrana plasmática, donde puede activarse por auto-fosforilación, permitiendo la estimulación de rutas de supervivencia dependientes de PI3K/Akt (Poullet et al., 2001). Así, sería interesante estudiar si la activación y liberación de la conformación autoinhibida por el VIH-1 en ezrina va acompañada por una fosforilación en Tyr que determine otras funciones efectoras de la proteína. En cuanto a la supervivencia celular, ezrina (pero no moesina y radixina) interacciona directamente con Fas (CD95) inhibiendo el mecanismo de apoptosis mediado por la activación de la caspasa 8 dependiente de la interacción Fas/FasL (revisado en (Neisch and Fehon, 2011)). Estos datos podrían indicar una posible función de protección frente a la apoptosis ejercida por la proteína ezrina, que podría favorecer la replicación viral.

Por último, mostramos que la activación de moesina y ezrina, tiene lugar de manera transitoria durante el curso temporal de infección por el virus VIH-1. Estos resultados indican que la inactivación posterior de moesina, junto con la acción de otras proteínas de unión a actina como cofilina (Yoder et al., 2008), sería fundamental para la desestructuración de los complejos de actina formados en membrana en la región de contacto virus-célula, necesarios para liberar la tensión e incrementar la fluidez de la membrana plasmática que permitiría la entrada de la nucleocápside en el citoplasma de la célula diana.

4.2. La producción de PIP_2 inducido por el VIH-1 es necesaria para la fusión eficiente de las membranas celular y viral.

El PIP_2 producido, de manera dependiente del VIH-1, durante la interacción del virus con la célula diana puede tener varias funciones. Por un lado, puede afectar a la fluidez de la membrana plasmática en las zonas de contacto virus-célula fomentando el proceso de fusión y, por otro lado, puede afectar a la organización de los receptores virales favoreciendo los procesos iniciales de interacción entre la célula y el VIH-1, y la consiguiente fusión e infección. En este sentido, recientemente se ha descrito la participación necesaria del recambio de la membrana plasmática dependiente del tráfico de vesículas de PIP_2 por la GTPasa Arf6, para una eficiente fusión e infección

del virus con la célula diana ((Garcia-Exposito et al., 2011) y ANEXO 2). Por otro lado, se ha establecido el papel del PIP_2 durante los estadios de ensamblaje y salida de partículas de VIH-1, a través de la localización de la proteína precursora $Pr55^{Gag}$ en la membrana plasmática (Chukkapalli et al., 2008; Ono et al., 2004). Estos datos en su conjunto, muestran que el PIP_2 y la dinámica de membrana asociada, estaría regulando diversos estadios del ciclo de vida del VIH-1, tanto en la entrada como en la salida. En este sentido, muchos virus secuestran la maquinaria de tráfico vesicular celular para completar su ciclo de vida de manera eficiente, ya sea durante la etapa de entrada o durante el proceso de replicación viral, y así, evadir la respuesta inmune del organismo contra el patógeno (revisado en (Barroso-Gonzalez et al., 2011), ver ANEXO 3).

Nuestros resultados muestran las primeras evidencias sobre el requerimiento de la actividad de la quinasa PI4P5-K Iα y la síntesis de PIP_2 asociado para una eficiente infección por el VIH-1 en linfocitos T. La sobreexpresión de una construcción funcional de PI4P5-K Iα incrementa la producción de PIP_2 mediado por el contacto de la envuelta del virus con el receptor CD4. Este incremento en la cantidad de PIP_2 está correlacionado con un incremento en la entrada e infección del VIH-1.

La quinasa PI4P5-K puede regular diversas estructuras de la superficie celular, modificando la dinámica de actina cortical por interacción del PIP_2 con proteínas de unión a actina como gelsolina, vinculina, profilina, filamina, cofilina o las proteínas de la familia de las ERM (revisado en (Saarikangas et al., 2010; Yin and Janmey, 2003)). En este sentido, existen regiones de la superficie celular preferentes para la entrada del VIH-1, enriquecidas en actina y en los receptores virales, como "*ruffles*" y microvellosidades (Singer et al., 2001; Steffens and Hope, 2003). Estas estructuras son reguladas por la dinámica de actina cortical y por la actividad de las proteínas asociadas a ella. Datos de nuestro equipo de investigación, indican que el PIP_2 producido por la activación de la quinasa PI4P5-K Iα, mediado por la proteína gp120 del VIH-1, puede reclutar y activar las proteínas ERM en las zonas de contacto virus-célula permitiendo la apertura de su conformación autoinhibida, por unión a su dominio FERM N-terminal, favoreciendo su anclaje al citoesqueleto de actina y a la membrana plasmática, y permitiendo la reorganización del córtex celular observado durante los primeros estadios de infección por el VIH-1 (ver datos no publicados en ANEXO 1). Observamos que la sobreexpresión de una construcción funcional de la quinasa PI4P5-K Iα potencia la fosforilación de moesina mediada por la envuelta gp120 del VIH-1, mientras que la sobreexpresión de un mutante inactivo la inhibe (ANEXO 1)

Además, la actividad de la quinasa PI4P5-K Iα puede estar regulada por las proteínas de la familia de las GTPasas Rho, estimulando la síntesis de PIP_2 en membrana (Oude Weernink et al., 2004), quien a su vez puede regular la actividad de estas GTPasas (Yoshida et al., 2009). Por ello, la activación de RhoA y Rac-1 por el VIH-1 (del Real et al., 2004; Harmon and Ratner, 2008; Jimenez-Baranda et al., 2007; Pontow et al., 2007; Pontow et al., 2004; Vorster et al., 2011), podrían regular la actividad de la quinasa PI4P5-K, y la consiguiente generación de PIP_2, favoreciendo la fusión viral e infección. Por otro lado, Rac-1 parece ser crítico para la fusión de membranas biológicas (Eitzen, 2003), por lo que su actividad puede favorecer el proceso de fusión entre la membrana viral y celular, posiblemente, a través de la producción del lípido fusogénico PIP_2 en las zonas de contacto virus-célula.

Por otro lado, el PIP_2 puede tener otras funciones durante la entrada del VIH-1. En primer lugar, el PIP_2 puede unirse e inactivar la proteína despolimerizadora de actina cofilina aún cuando ésta se encuentra en su estado activo (van Rheenen et al., 2007). Esta inactivación de cofilina por el PIP_2 y por fosforilación mediada por LIMK1 dependiente de ROCK (Jimenez-Baranda et al., 2007) y Pak (Pontow et al., 2007; Vorster et al., 2011), permitiría la estabilización inicial de actina necesaria para el reclutamiento, dependiente de moesina y filamina ((Jimenez-Baranda et al., 2007) y nuestros resultados), de los receptores/correceptores en las zonas de contacto virus-célula. Además, la hidrólisis del PIP_2, como ocurre durante el curso de la infección por el VIH-1, podría estar implicada en la desestabilización del complejo de F-actina inicial, por inactivación de las ERM (Hao et al., 2009) y por reactivación de cofilina permitiendo su actividad de despolimerización y corte de filamentos de actina, lo que permitiría la entrada de la NC viral en el citoplasma celular (Yoder et al., 2008). En segundo lugar, la síntesis de PIP_2 por el VIH-1 e hidrólisis posterior por PLCβ puede permitir la progresión adecuada de la ruta de señalización que termina con la activación de Rac1 y Arp2/3, al parecer necesario para la remodelación de actina durante la entrada viral e infección (Harmon and Ratner, 2008; Vorster et al., 2011). En tercer lugar, el PIP_2 puede unirse y activar las proteínas vinculina y talina aumentando la afinidad de unión entre ellas y ayudando a la formación adecuada de las adhesiones focales (revisado en (Saarikangas et al., 2010)), también implicadas en los primeros estadios de infección retroviral (Brown et al.). La activación de la conformación autoinhibida de vinculina por el PIP_2 permite su unión a otras proteínas implicadas en la infección por el VIH-1 como talina, paxilin y el complejo Arp2/3, además de a actina (revisado en (Saarikangas et al., 2010). El PIP_2 también es un activador de la proteína talina, promoviéndo la unión, agrupamiento y activación de β-integrinas (Cluzel et al.,

2005). Por último, el PIP_2 puede incrementar la viabilidad de las células T infectadas, actuando como un protector contra la apoptosis celular inhibiendo las caspasas 8 y 9, así como su efector la caspasa 3, asegurando una eficiente infección y propagación viral (Azuma et al., 2000).

Con estos resultados, podemos sugerir un modelo de la participación de la quinasa PI4P5-K Iα, el PIP_2 y moesina en la infección de linfocitos por partículas de VIH-1 X4 trópicas **(Figura 22, paso 1)**. Así, la unión del virus a CD4 activa la proteína moesina de linfocitos pasando de su forma citoplasmática durmiente a una forma abierta activa, cuyo "*readout*" de activación es la fosforilación del residuo Thr^{558} C-terminal por una quinasa aún por determinar, por su unión al PIP_2 producido en las zonas de contacto virus-célula por la quinasa PI4P5-K Iα de manera dependiente del VIH-1 durante la entrada viral **(Figura 22, paso 2)**. Moesina en su conformación activa se encargaría de estabilizar y reorganizar el citoesqueleto de F-actina cortical, necesario para la redistribución e interacción entre los receptores CD4-CXCR4 en un polo de la célula **(Figura 22, paso 3)**. Este proceso incrementa la probabilidad de interacciones múltiples entre la envuelta del VIH-1 con CD4 y CXCR4, necesarias para la formación del poro de fusión, entrada e infección **(Figura 22, paso 4)**. Además, no podemos excluir que la redistribución de la F-actina por moesina pueda estar implicada en proporcionar la tensión superficial mecánica adecuada en el estadio final de mezcla de bicapas lipídicas (Eitzen, 2003), favoreciendo así la fusión viral. En este sentido, el anclaje de F-actina a la membrana plasmática por moesina en un estado activado abierto, es potenciado por una construcción FL-moesina e inhibido por un dominante negativo N-moesina. Interferir con este proceso inhibe la infección por el VIH-1. En el caso de los virus R5 trópicos en los que moesina no parece tener un papel crucial durante las etapas de fusión e infección viral, la actividad de la quinasa PI4P5-K Iα y el PIP_2 producido sí parecen tener un papel importante en la regulación de los mecanismos de infección viral, seguramente a través de otros mecanismos efectores como los indicados anteriormente durante la discusión.

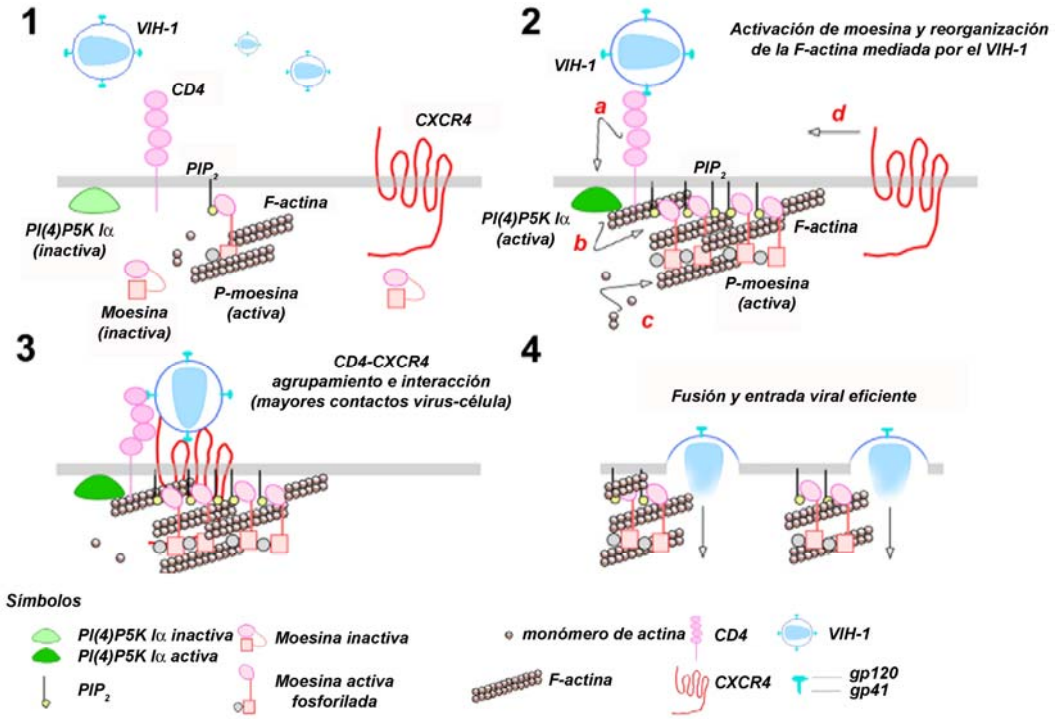

Figura 22: Modelo de la participación de la quinasa PI4P5-K Iα, el PIP_2 y moesina en la infección por cepas virales X4 trópicas del VIH-1 (Paso 1). El VIH-1 contacta con CD4 (Paso 2a) activando la producción de PIP_2 a través de la quinasa PI4P5-K Iα (Paso 2b). Este PIP_2 libera la conformación autoinhibida de moesina (ver datos no publicados en ANEXO 1), permitiendo su anclaje a membrana plasmática y a la F-actina (Paso 2c). Con ello, moesina estabiliza y reorganiza el citoesqueleto de actina favoreciendo el agrupamiento e interacción entre CD4 y CXCR4 (Paso 2d). Este efecto favorece múltiples interacciones entre la envuelta viral y la célula (Paso 3), favoreciendo la fusión, entrada e infección eficaz por VIH-1 (Paso 4).

4.3. Moesina regula el tráfico y el reciclaje de vesículas de clatrina nacientes, asegurando la infección y replicación del VIH-1.

Desde el descubrimiento del VIH-1 como el agente etiológico causante del SIDA, muchos trabajos de investigación se han centrado en determinar el mecanismo de entrada viral. Aunque los primeros estudios determinaron que la entrada e infección productiva del VIH-1 ocurría principalmente en la membrana plasmática mediante un mecanismo de fusión entre la membrana celular y la viral de manera independiente de pH (Doms and Trono, 2000), recientemente se ha descrito que la ruta principal de entrada del VIH-1 depende de un mecanismo de endocitosis mediada por clatrina/dinamina y posterior fusión en endosomas (Miyauchi et al., 2009). Aún así, existe bastante controversia sobre este último trabajo, por dos motivos. Por un lado, la proteína dinamina participa en multitud de procesos celulares aparte de la endocitosis, como el transporte vesicular, citocinesis, división de organelas, movimiento celular, señalización celular e incluso la reorganización del citoesqueleto de actina, por lo que

su inhibición puede afectar de manera inespecífica a varios procesos (revisado en (Yu et al., 2009)), y por otro lado, el inhibidor de dinamina "*dynasore*" afecta negativamente a la remodelación activa del citoesqueleto de F-actina (Yamada et al., 2009). Además, existen evidencias que indican que la entrada endocítica del VIH-1, aunque ocurre a gran escala, no lleva a una infección productiva (Fredericksen et al., 2002; McClure et al., 1988; Pelchen-Matthews et al., 1995; Wei et al., 2005). Por otro lado, se ha visto que el bloqueo de la endocitosis de los receptores para el VIH-1, así como su índice de endocitosis, no afecta a la entrada o replicación del VIH-1 (Alkhatib et al., 1997b; Amara et al., 1997; Aramori et al., 1997; Brandt et al., 2002; Gosling et al., 1997; Lu et al., 1997; Maddon et al., 1988; Pelchen-Matthews et al., 1995). Por último, se han descrito proteínas implicadas en la remodelación del citoesqueleto de actina cortical que afectando a la entrada del VIH-1, no tienen efecto sobre la entrada endocítica del virus VSV-G (del Real et al., 2004; Harmon et al., 2010; Harmon and Ratner, 2008; Jimenez-Baranda et al., 2007; Vorster et al., 2011; Yu et al., 2009).

Los resultados presentados en esta tesis doctoral muestran que, aunque la quinasa PI4P5-K Iα, el PIP_2 e incluso las proteínas ERM han sido implicadas en diversos estadios de la endocitosis dependiente de clatrina, la inhibición de la función de la quinasa PI4P5-K Iα, mediante un dominante inactivo de la enzima, o la interferencia específica de la proteína moesina endógena, no tiene ningún efecto sobre la entrada e infección de virus VIH-1 pseudotipados con la envuelta VSV-G, cuyo mecanismo de entrada es dependiente de clatrina y posterior fusión en endosomas. Estos resultados indican que el contacto de la envuelta del VIH-1 con sus receptores, presentes en la célula diana, constituye un requisito fundamental para la etapa inicial de remodelación del córtex celular, necesario para que tenga lugar la entrada productiva del virus en la célula diana, por fusión directa con la membrana plasmática.

Aún así, como se ha establecido el requerimiento del PIP_2 en los primeros estadios de la endocitosis dependiente de clatrina (Beck and Keen, 1991; Zoncu et al., 2007), y la participación de las proteínas ERM en diversos estadios del tráfico vesicular (Chirivino et al., 2011; Morel et al., 2009; Poupon et al., 2003; Stanasila et al., 2006), estudiamos el papel de moesina en los estadios de formación, internalización y reciclaje de CCV.

Los resultados presentados en esta Tesis Doctoral indican que la proteína moesina endógena colocaliza con clatrina y con α-adaptina endógenas (revisado en (McMahon and Boucrot, 2011)), y el silenciamiento específico de moesina endógena afecta a la movilidad y distribución de las estructuras de clatrina (CCS). Asimismo, el

silenciamiento de moesina generó un incremento en la movilidad lateral de CCS, y la formación de agrupamientos que se disgregan progresivamente en estructuras individuales. Por todo ello, parece que moesina podría funcionar como un adaptador que dirige el movimiento de CCS.

Como se ha descrito anteriormente, la activación de las proteínas ERM por el PIP_2 permite la activación y unión de éstas a la F-actina (Fievet et al., 2004; Nakamura et al., 1999), por lo que el control del tráfico de CCS por moesina podría estar dirigido por su unión a F-actina de manera dependiente de su unión al PIP_2 presente en CCV nacientes. La colocalización de moesina con clatrina parece depender de una interacción indirecta mediada por PIP_2, y no por una interacción directa con clatrina, debido a que un mutante de moesina de unión a PIP_2 (4K4N-moesin) no colocaliza con clatrina, al igual que una construcción de moesina que sólo se une a F-actina y carece del dominio de unión a PIP_2 (C-moesina). De manera similar a los resultados obtenidos con la interferencia específica de moesina, una construcción N-moesina incapaz de unirse a F-actina colocaliza con clatrina y provoca el agrupamiento aberrante de estas estructuras. De manera destacable, observamos que Fl-moesina colocaliza con CCV y se mueve con ellas en el plano z, datos que confirman la participación de moesina en la distribución y movimiento de una subpoblación de CCV de manera dependiente de actina.

Además de la propia actina, existe una gran cantidad de proteínas de unión a actina que participan en diversos estadios del proceso de endocitosis dependiente de clatrina, que incluyen la organización adecuada de la maquinaria endocítica, la invaginación de las estructuras de clatrina, su separación de la membrana plasmática y el movimiento de las vesículas en el citoplasma (Engqvist-Goldstein and Drubin, 2003; Merrifield, 2004). Además, de acuerdo con nuestros resultados, se ha descrito que la inhibición de la dinámica de actina bloquea la internalización y movilidad de una subpoblación de CCV (Yarar et al., 2005). Por ello, nuestros datos aportan una mayor complejidad al proceso dinámico de la endocitosis y reciclaje de estructuras vesiculares, y proporcionan evidencias de la participación del adaptador de F-actina moesina en el control de la distribución y movilidad lateral de una subpoblación de CCV asociadas a moesina.

Otras proteínas importantes en la regulación del transporte intracelular a nivel endosomal son las proteínas de la familia de las Rab GTPasas (Rink et al., 2005). Nuestros resultados indican que el silenciamiento específico de moesina endógena provoca la acumulación de Rab5 en CCV, estructuras que no fueron observadas en

preparaciones de láminas de membrana, por lo que representan una población de CCV endocíticos nacientes. Si el silenciamiento de moesina afecta al tráfico de estructuras Rab5-CCV, entonces debe afectar a la dinámica de cargos asociados a CCV como el TfR. Analizando el TfR, observamos por TIRFM y por fraccionamiento celular que el silenciamiento de moesina provoca la acumulación del TfR en estructuras Rab5-CCV. Datos que correlacionan con estudios de citometrías de flujo donde se observó una menor expresión superficial del TfR, y una mayor cantidad del ligando Tf secuestrado en el interior celular, indicativo de un defecto en el reciclaje de TfR. Además, estudios de preparaciones de membrana plasmática donde se observó una cantidad equivalente de estructuras Rab5-CCV en ambas condiciones, en condiciones control con respecto a la condición interferente de moesina endógena, indican que el silenciamiento de moesina no afecta a la formación ni a la invaginación y fisión de las vesículas de clatrina. Por tanto, como el silenciamiento específico de moesina no afecta al proceso de captación de Tf ni al proceso de exocitosis general del TfR hacia la membrana plasmática, pero si provoca el secuestro del ligando Tf en el citoplasma celular en ensayos de reciclaje, entonces proponemos que moesina estaría controlando el reciclaje de TfR a partir de una dinámica de movimiento de estructuras Rab5-CCV dependiente del citoesqueleto de actina.

En resumen, moesina controla el movimiento lateral, la distribución celular y el tráfico de una subpoblación de vesículas nacientes Rab5-CCV, probablemente promoviendo el reciclaje de CCV a través de su capacidad de unión simultánea a PIP_2 y a F-actina. Además, en relación a la infección por el VIH-1, moesina no afecta a los primeros estadios de formación e internalización de estructuras de clatrina, como se observó por su incapacidad de afectar a la entrada por endocitosis dependiente de clatrina del virus VSV-G. Lo que si ocurre es que moesina es capaz de regular el reciclaje temprano del TfR hacia la membrana plasmática tras ser internalizado. Por todo ello, la activación de moesina por el VIH-1 podría favorecer la captación de Hierro por la célula diana, mediante un incremento de la velocidad de reciclaje del TfR hacia la membrana plasmática para comenzar un nuevo ciclo de captación/internalización, lo que facilitaría la supervivencia celular, asegurando la progresión del ciclo de vida viral y la replicación del VIH-1.

4.4. Estudio de inhibidores de la infección por el VIH-1

Como ya hemos descrito anteriormente, *"in vivo"* las cepas de VIH-1 que predominan durante la fase aguda de la infección y principales responsables de la

transmisión viral son las R5 trópicas (Princen and Schols, 2005), evidenciado por el alto grado de resistencia a la infección de individuos homocigóticos CCR5Δ32, quienes carecen de un receptor CCR5 funcional (Liu et al., 1996; Samson et al., 1996). Por ello, el desarrollo de antagonistas dirigidos a bloquear la infección R5 trópica del VIH-1, podría ser fundamental para luchar contra la infección por el VIH-1, y para complementar las estrategias antirretrovirales existentes contra el SIDA en un futuro cercano. Asimismo, representa un área de investigación emergente e importante.

En este trabajo de Tesis doctoral, describimos por vez primera la actividad anti-VIH-1 del 30-oxo-calenduladiol (compuesto **1**), un triterpeno tipo lupano dihidroxilado semisintético. Este compuesto interfiere específicamente con la fusión celular y la infección mediada por las envueltas R5 trópicas del VIH-1, a concentraciones similares a otras moléculas anti-VIH-1 (Princen and Schols, 2005). Así, el compuesto **1** no perturba los procesos relacionados mediados por las envueltas X4 trópicas o VSV-G. Esta actividad anti-viral específica del compuesto **1** depende de su capacidad de interaccionar con el correceptor del VIH-1 CCR5 y así evitar la unión de la envuelta viral. Este triterpeno tipo lupano parece no interaccionar con el antígeno CD4, el principal receptor para el VIH-1, ni con el correceptor CXCR4.

La capacidad del compuesto **1** a competir la unión del anticuerpo monoclonal neutralizante anti-CCR5 (2D7) o la unión de su ligando natural RANTES, y de inhibir la infección de cepas R5 trópicas del VIH-1, puede depender de su interacción con el ECL2 del receptor CCR5. Esta región, representa el dominio de unión conformacional para el anticuerpo 2D7 (Lee et al., 1999), el cual ha sido involucrado en la interacción virus-receptor y ligando-receptor (Blanpain et al., 2003; Lee et al., 1999; Wu et al., 1997). Sin embargo, como ocurre con otras moléculas pequeñas anti-virales (Baba et al., 1999; Seto et al., 2006), es posible que el compuesto pueda ocupar el bolsillo de CCR5, induciendo un cambio conformacional que podría afectar al ECL2 de CCR5, impidiendo el reconocimiento por el anticuerpo anti-CCR5 (2D7). Estos potenciales cambios conformacionales podrían también afectar a la unión entre RANTES/CCR5 y la infección viral del VIH-1 mediada por la interacción entre la proteína gp120 y CCR5.

Nuestros resultados indican que el compuesto 1 es un antagonista específico de CCR5, que se une al receptor CCR5 sin desencadenar movilización de Ca^{2+} intracelular o internalización del receptor. Además, inhibe la movilización de Ca^{2+} intracelular, la quimiotaxis y la internalización de CCR5 mediada por RANTES, por lo que su actividad anti-viral parece depender de la ocupación del receptor CCR5. Además, el compuesto **1** parece que no interaccionar con otros receptores de β-

quimiocinas, tales como el CCR1, CCR3 y CCR4. Aunque el compuesto **1** muestra un pequeño grado de interacción con CCR2b, a altas concentraciones (100μM) de la molécula. Es posible que la alta homología existente entre los receptores CCR5 y CCR2b (un 72% de identidad de secuencia) (Horuk, 2009), puede ser responsable del pequeño grado de competición observado contra la unión MCP-1/CCR2b. Todos estos datos indican que el compuesto **1** no es un antagonista promiscuo para los receptores de β-quimiocinas arriba indicados, presentando selectividad de acción sobre el receptor CCR5.

Aunque lo deseado y requerido es la especificidad de dianas para el tratamiento mediado por antagonistas de varias enfermedades, recientemente ha cobrado mucha expectación el uso de compuestos polifarmacológicos o promiscuos para el desarrollo de aproximaciones terapéuticas más eficientes para combatir enfermedades multifactoriales (Horuk, 2009). Por lo tanto, sería interesante una mayor exploración de la potencial actividad antagonista del compuesto **1** sobre otros receptores de la superficie celular, diferentes o no de la familia de las quimiocinas.

Considerando los datos presentados en esta tesis doctoral, sugerimos que el 30-oxo-calenduladiol es un nuevo y específico antagonista de CCR5, pudiendo ser un prometedor agente bioactivo para el desarrollo de nuevos derivados más eficaces para el tratamiento de la infección por el VIH-1, y contra desordenes biológicos relacionados con la migración celular mediada por CCR5, tales como por ejemplo la inflamación, respuesta inmune y migración de células tumorales (Luster, 1998; van Deventer et al., 2008).

5. CONCLUSIONES

Conclusiones:

1. La reorganización del citoesqueleto de actina, dependiente de la activación de moesina por el virus VIH-1, es crítica para la asociación directa y colocalización de los receptores CD4 y CXCR4, en las zonas de contacto virus-células T $CD4^+$, durante las primeras etapas de infección por VIH-1, e inducida por la envoltura del virus, lo que favorece el número de interacciones virus-célula. Además, la actividad adaptadora de moesina, permitiéndo la unión de la membrana plasmática al citoesqueleto de actina cortical, predispone la dinámica y tensión de membrana adecuadas para que tenga lugar una fusión, entrada e infección viral eficiente mediada por la envuelta del VIH-1.

2. La producción de PIP_2 dependiente de la envuelta del VIH-1 y mediada por la actividad de la quinasa PI4P5-K Iα es necesaria en la regulación de los primeros estadios de la infección por el VIH-1, antes del ensamblaje y liberación viral, promoviendo la formación del poro de fusión, entrada e infección viral, al aumentar la fluidez de la membrana celular mediante el incremento del lípido fusogénico PIP_2 en las zonas de contacto virus-células T $CD4^+$.

3. Moesina es un componente de la compleja maquinaria molecular que controla el tráfico de CCVs nacientes asociados a moesina, de manera dependiente a su anclaje simultáneo, tanto al citoesqueleto de actina (por el dominio C-terminal) como al PIP_2 (por su dominio N-terminal) asociado a la membrana de las vesículas CCV. De esta forma, moesina regula el tráfico y reciclaje vesicular de vesículas endocíticas nacientes de clatrina, por una ruta de reciclaje temprano hacia la membrana plasmática. Por tanto, alteraciones en la activación de moesina explicarían la base molecular de enfermedades asociadas a una alteración de la internalización de receptores y reciclaje mediado por clatrina, como la progresión del cáncer, desordenes congénitos del sistema nervioso central e infecciones virales.

Por otra parte, nuestros resultados junto a los estudios de regulación de la infección por VIH-1 mediante la regulación de la dinámica de membrana, Arf6 dependiente y clatrina independiente (ANEXO 2, García-Expósito L., Barroso-González J., *et al*., MBoC 2011 ((Garcia-Exposito et al., 2011))), podemos proponer que la infección por VIH-1 no depende de la ruta endocítica de clatrina, pero que ésta, puede estar activa, vía moesina e inducida por el propio virus, para asegurar la captación de hierro por este sistema y la supervivencia celular durante las etapa

tempranas del ciclo viral del VIH-1. En consecuencia, la activación de moesina por el VIH-1 es crucial para asegurar la infección y la replicación viral.

4. El compuesto natural, derivado semisintético 30-oxo-calenduladiol es un nuevo y específico antagonista de CCR5, que bloquea la infección de cepas virales R5 trópicas del VIH-1, pudiendo ser un prometedor agente bioactivo (posible cabeza de serie) para el desarrollo de nuevos derivados eficaces para el tratamiento de la infección por el VIH-1, y contra desordenes biológicos relacionados con la migración celular mediada por CCR5, tales como por ejemplo la inflamación, respuesta inmune y migración de células tumorales.

6. BIBLIOGRAFÍA

Abbink, T.E., and B. Berkhout. 2008. HIV-1 reverse transcription initiation: a potential target for novel antivirals? *Virus Res*. 134:4-18.

Aghamohammadzadeh, S., and K.R. Ayscough. 2009. Differential requirements for actin during yeast and mammalian endocytosis. *Nat Cell Biol*. 11:1039-42.

Agrawal, L., X. Lu, Q. Jin, and G. Alkhatib. 2006. Anti-HIV therapy: Current and future directions. *Curr Pharm Des*. 12:2031-55.

Agrawal, L., X. Lu, J. Qingwen, Z. VanHorn-Ali, I.V. Nicolescu, D.H. McDermott, P.M. Murphy, and G. Alkhatib. 2004. Role for CCR5Delta32 protein in resistance to R5, R5X4, and X4 human immunodeficiency virus type 1 in primary CD4+ cells. *J Virol*. 78:2277-87.

Aiken, C., and C.H. Chen. 2005. Betulinic acid derivatives as HIV-1 antivirals. *Trends Mol Med*. 11:31-6.

Aiken, C., and D. Trono. 1995. Nef stimulates human immunodeficiency virus type 1 proviral DNA synthesis. *J Virol*. 69:5048-56.

Alexaki, A., Y. Liu, and B. Wigdahl. 2008. Cellular reservoirs of HIV-1 and their role in viral persistence. *Curr HIV Res*. 6:388-400.

Alfano, M., T. Pushkarsky, G. Poli, and M. Bukrinsky. 2000. The B-oligomer of pertussis toxin inhibits human immunodeficiency virus type 1 replication at multiple stages. *J Virol*. 74:8767-70.

Alfano, M., H. Schmidtmayerova, C.A. Amella, T. Pushkarsky, and M. Bukrinsky. 1999. The B-oligomer of pertussis toxin deactivates CC chemokine receptor 5 and blocks entry of M-tropic HIV-1 strains. *J Exp Med*. 190:597-605.

Alkhatib, G. 2009. The biology of CCR5 and CXCR4. *Curr Opin HIV AIDS*. 4:96-103.

Alkhatib, G., E.A. Berger, P.M. Murphy, and J.E. Pease. 1997a. Determinants of HIV-1 coreceptor function on CC chemokine receptor 3. Importance of both extracellular and transmembrane/cytoplasmic regions. *J Biol Chem*. 272:20420-6.

Alkhatib, G., C. Combadiere, C.C. Broder, Y. Feng, P.E. Kennedy, P.M. Murphy, and E.A. Berger. 1996. CC CKR5: a RANTES, MIP-1alpha, MIP-1beta receptor as a fusion cofactor for macrophage-tropic HIV-1. *Science*. 272:1955-8.

Alkhatib, G., M. Locati, P.E. Kennedy, P.M. Murphy, and E.A. Berger. 1997b. HIV-1 coreceptor activity of CCR5 and its inhibition by chemokines: independence from G protein signaling and importance of coreceptor downmodulation. *Virology*. 234:340-8.

Amara, A., S.L. Gall, O. Schwartz, J. Salamero, M. Montes, P. Loetscher, M. Baggiolini, J.L. Virelizier, and F. Arenzana-Seisdedos. 1997. HIV coreceptor downregulation as antiviral principle: SDF-1alpha-dependent internalization of the chemokine receptor CXCR4 contributes to inhibition of HIV replication. *J Exp Med*. 186:139-46.

Amara, A., A. Vidy, G. Boulla, K. Mollier, J. Garcia-Perez, J. Alcami, C. Blanpain, M. Parmentier, J.L. Virelizier, P. Charneau, and F. Arenzana-Seisdedos. 2003. G protein-dependent CCR5 signaling is not required for efficient infection of primary T lymphocytes and macrophages by R5 human immunodeficiency virus type 1 isolates. *J Virol*. 77:2550-8.

Anand, A.R., and R.K. Ganju. 2006. HIV-1 gp120-mediated apoptosis of T cells is regulated by the membrane tyrosine phosphatase CD45. *J Biol Chem*. 281:12289-99.

Appay, V., J.R. Almeida, D. Sauce, B. Autran, and L. Papagno. 2007. Accelerated immune senescence and HIV-1 infection. *Exp Gerontol*. 42:432-7.

Arai, H., and I.F. Charo. 1996. Differential regulation of G-protein-mediated signaling by chemokine receptors. *J Biol Chem*. 271:21814-9.

Aramori, I., S.S. Ferguson, P.D. Bieniasz, J. Zhang, B. Cullen, and M.G. Cullen. 1997. Molecular mechanism of desensitization of the chemokine receptor CCR-5:

receptor signaling and internalization are dissociable from its role as an HIV-1 co-receptor. *Embo J*. 16:4606-16.

Arber, S., F.A. Barbayannis, H. Hanser, C. Schneider, C.A. Stanyon, O. Bernard, and P. Caroni. 1998. Regulation of actin dynamics through phosphorylation of cofilin by LIM-kinase. *Nature*. 393:805-9.

Arhel, N.J., S. Souquere-Besse, S. Munier, P. Souque, S. Guadagnini, S. Rutherford, M.C. Prevost, T.D. Allen, and P. Charneau. 2007. HIV-1 DNA Flap formation promotes uncoating of the pre-integration complex at the nuclear pore. *Embo J*. 26:3025-37.

Arthos, J., C. Cicala, E. Martinelli, K. Macleod, D. Van Ryk, D. Wei, Z. Xiao, T.D. Veenstra, T.P. Conrad, R.A. Lempicki, S. McLaughlin, M. Pascuccio, R. Gopaul, J. McNally, C.C. Cruz, N. Censoplano, E. Chung, K.N. Reitano, S. Kottilil, D.J. Goode, and A.S. Fauci. 2008. HIV-1 envelope protein binds to and signals through integrin alpha4beta7, the gut mucosal homing receptor for peripheral T cells. *Nat Immunol*. 9:301-9.

Arthos, J., A. Rubbert, R.L. Rabin, C. Cicala, E. Machado, K. Wildt, M. Hanbach, T.D. Steenbeke, R. Swofford, J.M. Farber, and A.S. Fauci. 2000. CCR5 signal transduction in macrophages by human immunodeficiency virus and simian immunodeficiency virus envelopes. *J Virol*. 74:6418-24.

Atchison, R.E., J. Gosling, F.S. Monteclaro, C. Franci, L. Digilio, I.F. Charo, and M.A. Goldsmith. 1996. Multiple extracellular elements of CCR5 and HIV-1 entry: dissociation from response to chemokines. *Science*. 274:1924-6.

Azuma, T., K. Koths, L. Flanagan, and D. Kwiatkowski. 2000. Gelsolin in complex with phosphatidylinositol 4,5-bisphosphate inhibits caspase-3 and -9 to retard apoptotic progression. *J Biol Chem*. 275:3761-6.

Baba, M., O. Nishimura, N. Kanzaki, M. Okamoto, H. Sawada, Y. Iizawa, M. Shiraishi, Y. Aramaki, K. Okonogi, Y. Ogawa, K. Meguro, and M. Fujino. 1999. A small-molecule, nonpeptide CCR5 antagonist with highly potent and selective anti-HIV-1 activity. *Proc Natl Acad Sci U S A*. 96:5698-703.

Badr, G., G. Borhis, D. Treton, C. Moog, O. Garraud, and Y. Richard. 2005. HIV type 1 glycoprotein 120 inhibits human B cell chemotaxis to CXC chemokine ligand (CXCL) 12, CC chemokine ligand (CCL)20, and CCL21. *J Immunol*. 175:302-10.

Baggiolini, M., B. Dewald, and B. Moser. 1997. Human chemokines: an update. *Annu Rev Immunol*. 15:675-705.

Bailly, M., and J. Condeelis. 2002. Cell motility: insights from the backstage. *Nat Cell Biol*. 4:E292-4.

Balabanian, K., J. Harriague, C. Decrion, B. Lagane, S. Shorte, F. Baleux, J.L. Virelizier, F. Arenzana-Seisdedos, and L.A. Chakrabarti. 2004. CXCR4-tropic HIV-1 envelope glycoprotein functions as a viral chemokine in unstimulated primary CD4+ T lymphocytes. *J Immunol*. 173:7150-60.

Baleux, F., L. Loureiro-Morais, Y. Hersant, P. Clayette, F. Arenzana-Seisdedos, D. Bonnaffe, and H. Lortat-Jacob. 2009. A synthetic CD4-heparan sulfate glycoconjugate inhibits CCR5 and CXCR4 HIV-1 attachment and entry. *Nat Chem Biol*. 5:743-8.

Bamburg, J.R. 2011. Listeria monocytogenes cell invasion: a new role for cofilin in co-ordinating actin dynamics and membrane lipids. *Mol Microbiol*. 81:851-4.

Banda, N.K., J. Bernier, D.K. Kurahara, R. Kurrle, N. Haigwood, R.P. Sekaly, and T.H. Finkel. 1992. Crosslinking CD4 by human immunodeficiency virus gp120 primes T cells for activation-induced apoptosis. *J Exp Med*. 176:1099-106.

Barre-Sinoussi, F., J.C. Chermann, F. Rey, M.T. Nugeyre, S. Chamaret, J. Gruest, C. Dauguet, C. Axler-Blin, F. Vezinet-Brun, C. Rouzioux, W. Rozenbaum, and L. Montagnier. 1983. Isolation of a T-lymphotropic retrovirus from a patient at risk for acquired immune deficiency syndrome (AIDS). *Science*. 220:868-71.

Barroso-Gonzalez, J., L. Garcia-Exposito, I. Puigdomenech, L. de Armas-Rillo, J.D. Machado, J. Blanco, and A. Valenzuela-Fernandez. 2011. Viral infection: Moving through complex and dynamic cell-membrane structures. *Commun Integr Biol*. 4:398-408.

Baum, J., C.J. Tonkin, A.S. Paul, M. Rug, B.J. Smith, S.B. Gould, D. Richard, T.D. Pollard, and A.F. Cowman. 2008. A malaria parasite formin regulates actin polymerization and localizes to the parasite-erythrocyte moving junction during invasion. *Cell Host Microbe*. 3:188-98.

Beck, K.A., and J.H. Keen. 1991. Interaction of phosphoinositide cycle intermediates with the plasma membrane-associated clathrin assembly protein AP-2. *J Biol Chem*. 266:4442-7.

Becker, C., C. Taube, T. Bopp, C. Becker, K. Michel, J. Kubach, S. Reuter, N. Dehzad, M.F. Neurath, K. Reifenberg, F.J. Schneider, E. Schmitt, and H. Jonuleit. 2009. Protection from graft-versus-host disease by HIV-1 envelope protein gp120-mediated activation of human CD4+CD25+ regulatory T cells. *Blood*. 114:1263-9.

Benkirane, M., K.T. Jeang, and C. Devaux. 1994. The cytoplasmic domain of CD4 plays a critical role during the early stages of HIV infection in T-cells. *Embo J*. 13:5559-69.

Berger, E.A., P.M. Murphy, and J.M. Farber. 1999. Chemokine receptors as HIV-1 coreceptors: roles in viral entry, tropism, and disease. *Annu Rev Immunol*. 17:657-700.

Berson, J.F., and R.W. Doms. 1998. Structure-function studies of the HIV-1 coreceptors. *Semin Immunol*. 10:237-48.

Bhaskaran, K., O. Hamouda, M. Sannes, F. Boufassa, A.M. Johnson, P.C. Lambert, and K. Porter. 2008. Changes in the risk of death after HIV seroconversion compared with mortality in the general population. *Jama*. 300:51-9.

Bieniasz, P.D., and B.R. Cullen. 1998. Chemokine receptors and human immunodeficiency virus infection. *Front Biosci*. 3:d44-58.

Bieniasz, P.D., R.A. Fridell, I. Aramori, S.S. Ferguson, M.G. Caron, and B.R. Cullen. 1997. HIV-1-induced cell fusion is mediated by multiple regions within both the viral envelope and the CCR-5 co-receptor. *Embo J*. 16:2599-609.

Binley, J.M., P.J. Klasse, Y. Cao, I. Jones, M. Markowitz, D.D. Ho, and J.P. Moore. 1997. Differential regulation of the antibody responses to Gag and Env proteins of human immunodeficiency virus type 1. *J Virol*. 71:2799-809.

Blagoveshchenskaya, A.D., L. Thomas, S.F. Feliciangeli, C.H. Hung, and G. Thomas. 2002. HIV-1 Nef downregulates MHC-I by a PACS-1- and PI3K-regulated ARF6 endocytic pathway. *Cell*. 111:853-66.

Blanpain, C., B.J. Doranz, A. Bondue, C. Govaerts, A. De Leener, G. Vassart, R.W. Doms, A. Proudfoot, and M. Parmentier. 2003. The core domain of chemokines binds CCR5 extracellular domains while their amino terminus interacts with the transmembrane helix bundle. *J Biol Chem*. 278:5179-87.

Bleul, C.C., L. Wu, J.A. Hoxie, T.A. Springer, and C.R. Mackay. 1997. The HIV coreceptors CXCR4 and CCR5 are differentially expressed and regulated on human T lymphocytes. *Proc Natl Acad Sci U S A*. 94:1925-30.

Blue, C.E., O.B. Spiller, and D.J. Blackbourn. 2004. The relevance of complement to virus biology. *Virology*. 319:176-84.

Borrow, P., and N. Bhardwaj. 2008. Innate immune responses in primary HIV-1 infection. *Curr Opin HIV AIDS*. 3:36-44.

Botelho, R.J., M. Teruel, R. Dierckman, R. Anderson, A. Wells, J.D. York, T. Meyer, and S. Grinstein. 2000. Localized biphasic changes in phosphatidylinositol-4,5-bisphosphate at sites of phagocytosis. *J Cell Biol*. 151:1353-68.

Bour, S., R. Geleziunas, and M.A. Wainberg. 1995. The human immunodeficiency virus type 1 (HIV-1) CD4 receptor and its central role in promotion of HIV-1 infection. *Microbiol Rev*. 59:63-93.

Bowers, K., C. Pitcher, and M. Marsh. 1997. CD4: a co-receptor in the immune response and HIV infection. *Int J Biochem Cell Biol*. 29:871-5.

Brandt, S.M., R. Mariani, A.U. Holland, T.J. Hope, and N.R. Landau. 2002. Association of chemokine-mediated block to HIV entry with coreceptor internalization. *J Biol Chem*. 277:17291-9.

Brelot, A., N. Heveker, M. Montes, and M. Alizon. 2000. Identification of residues of CXCR4 critical for human immunodeficiency virus coreceptor and chemokine receptor activities. *J Biol Chem*. 275:23736-44.

Brelot, A., N. Heveker, O. Pleskoff, N. Sol, and M. Alizon. 1997. Role of the first and third extracellular domains of CXCR-4 in human immunodeficiency virus coreceptor activity. *J Virol*. 71:4744-51.

Brenchley, J.M., D.A. Price, T.W. Schacker, T.E. Asher, G. Silvestri, S. Rao, Z. Kazzaz, E. Bornstein, O. Lambotte, D. Altmann, B.R. Blazar, B. Rodriguez, L. Teixeira-Johnson, A. Landay, J.N. Martin, F.M. Hecht, L.J. Picker, M.M. Lederman, S.G. Deeks, and D.C. Douek. 2006. Microbial translocation is a cause of systemic immune activation in chronic HIV infection. *Nat Med*. 12:1365-71.

Brenchley, J.M., T.W. Schacker, L.E. Ruff, D.A. Price, J.H. Taylor, G.J. Beilman, P.L. Nguyen, A. Khoruts, M. Larson, A.T. Haase, and D.C. Douek. 2004. CD4+ T cell depletion during all stages of HIV disease occurs predominantly in the gastrointestinal tract. *J Exp Med*. 200:749-59.

Bretscher, A. 1999. Regulation of cortical structure by the ezrin-radixin-moesin protein family. *Curr Opin Cell Biol*. 11:109-16.

Briand, G., B. Barbeau, and M. Tremblay. 1997. Binding of HIV-1 to its receptor induces tyrosine phosphorylation of several CD4-associated proteins, including the phosphatidylinositol 3-kinase. *Virology*. 228:171-9.

Briant, L., V. Robert-Hebmann, V. Sivan, A. Brunet, J. Pouyssegur, and C. Devaux. 1998. Involvement of extracellular signal-regulated kinase module in HIV-mediated CD4 signals controlling activation of nuclear factor-kappa B and AP-1 transcription factors. *J Immunol*. 160:1875-85.

Briggs, J.A., and H.G. Krausslich. 2011. The molecular architecture of HIV. *J Mol Biol*. 410:491-500.

Brown, C., S.G. Morham, D. Walsh, and M.H. Naghavi. 2011. Focal adhesion proteins talin-1 and vinculin negatively affect paxillin phosphorylation and limit retroviral infection. *J Mol Biol*. 410:761-77.

Bukrinskaya, A., B. Brichacek, A. Mann, and M. Stevenson. 1998. Establishment of a functional human immunodeficiency virus type 1 (HIV-1) reverse transcription complex involves the cytoskeleton. *J Exp Med*. 188:2113-25.

Bukrinskaya, A.G. 2004. HIV-1 assembly and maturation. *Arch Virol*. 149:1067-82.

Burkhardt, J.K., E. Carrizosa, and M.H. Shaffer. 2008. The actin cytoskeleton in T cell activation. *Annu Rev Immunol*. 26:233-59.

Bushman, F.D., and R. Craigie. 1991. Activities of human immunodeficiency virus (HIV) integration protein in vitro: specific cleavage and integration of HIV DNA. *Proc Natl Acad Sci U S A*. 88:1339-43.

Cameron, P.U., S. Saleh, G. Sallmann, A. Solomon, F. Wightman, V.A. Evans, G. Boucher, E.K. Haddad, R.P. Sekaly, A.N. Harman, J.L. Anderson, K.L. Jones, J. Mak, A.L. Cunningham, A. Jaworowski, and S.R. Lewin. 2010. Establishment of HIV-1 latency in resting CD4+ T cells depends on chemokine-induced changes in the actin cytoskeleton. *Proc Natl Acad Sci U S A*. 107:16934-9.

Campbell, E.M., R. Nunez, and T.J. Hope. 2004. Disruption of the actin cytoskeleton can complement the ability of Nef to enhance human immunodeficiency virus type 1 infectivity. *J Virol*. 78:5745-55.

Cao, H., J.D. Orth, J. Chen, S.G. Weller, J.E. Heuser, and M.A. McNiven. 2003. Cortactin is a component of clathrin-coated pits and participates in receptor-mediated endocytosis. *Mol Cell Biol*. 23:2162-70.

Carr, A. 2003. Toxicity of antiretroviral therapy and implications for drug development. *Nat Rev Drug Discov*. 2:624-34.

Carrington, M., and S.J. O'Brien. 2003. The influence of HLA genotype on AIDS. *Annu Rev Med*. 54:535-51.

Carter, C.C., A. Onafuwa-Nuga, L.A. McNamara, J.t. Riddell, D. Bixby, M.R. Savona, and K.L. Collins. 2010. HIV-1 infects multipotent progenitor cells causing cell death and establishing latent cellular reservoirs. *Nat Med*. 16:446-51.

Cefai, D., P. Debre, M. Kaczorek, T. Idziorek, B. Autran, and G. Bismuth. 1990. Human immunodeficiency virus-1 glycoproteins gp120 and gp160 specifically inhibit the CD3/T cell-antigen receptor phosphoinositide transduction pathway. *J Clin Invest*. 86:2117-24.

Cicala, C., J. Arthos, N. Censoplano, C. Cruz, E. Chung, E. Martinelli, R.A. Lempicki, V. Natarajan, D. VanRyk, M. Daucher, and A.S. Fauci. 2006a. HIV-1 gp120 induces NFAT nuclear translocation in resting CD4+ T-cells. *Virology*. 345:105-14.

Cicala, C., J. Arthos, and A.S. Fauci. 2011. HIV-1 envelope, integrins and co-receptor use in mucosal transmission of HIV. *J Transl Med*. 9 Suppl 1:S2.

Cicala, C., J. Arthos, E. Martinelli, N. Censoplano, C.C. Cruz, E. Chung, S.M. Selig, D. Van Ryk, J. Yang, S. Jagannatha, T.W. Chun, P. Ren, R.A. Lempicki, and A.S. Fauci. 2006b. R5 and X4 HIV envelopes induce distinct gene expression profiles in primary peripheral blood mononuclear cells. *Proc Natl Acad Sci U S A*. 103:3746-51.

Cicala, C., J. Arthos, A. Rubbert, S. Selig, K. Wildt, O.J. Cohen, and A.S. Fauci. 2000. HIV-1 envelope induces activation of caspase-3 and cleavage of focal adhesion kinase in primary human CD4(+) T cells. *Proc Natl Acad Sci U S A*. 97:1178-83.

Cicala, C., J. Arthos, M. Ruiz, M. Vaccarezza, A. Rubbert, A. Riva, K. Wildt, O. Cohen, and A.S. Fauci. 1999. Induction of phosphorylation and intracellular association of CC chemokine receptor 5 and focal adhesion kinase in primary human CD4+ T cells by macrophage-tropic HIV envelope. *J Immunol*. 163:420-6.

Cicala, C., J. Arthos, S.M. Selig, G. Dennis, Jr., D.A. Hosack, D. Van Ryk, M.L. Spangler, T.D. Steenbeke, P. Khazanie, N. Gupta, J. Yang, M. Daucher, R.A. Lempicki, and A.S. Fauci. 2002. HIV envelope induces a cascade of cell signals in non-proliferating target cells that favor virus replication. *Proc Natl Acad Sci U S A*. 99:9380-5.

Cichewicz, R.H., and S.A. Kouzi. 2004. Chemistry, biological activity, and chemotherapeutic potential of betulinic acid for the prevention and treatment of cancer and HIV infection. *Med Res Rev*. 24:90-114.

Clercq, E.D. 2009. Anti-HIV drugs: 25 compounds approved within 25 years after the discovery of HIV. *International Journal of Antimicrobial Agents*.

Cluzel, C., F. Saltel, J. Lussi, F. Paulhe, B.A. Imhof, and B. Wehrle-Haller. 2005. The mechanisms and dynamics of (alpha)v(beta)3 integrin clustering in living cells. *J Cell Biol*. 171:383-92.

Cocchi, F., A.L. DeVico, A. Garzino-Demo, A. Cara, R.C. Gallo, and P. Lusso. 1996. The V3 domain of the HIV-1 gp120 envelope glycoprotein is critical for chemokine-mediated blockade of infection. *Nat Med*. 2:1244-7.

Coffin, J., A. Haase, J.A. Levy, L. Montagnier, S. Oroszlan, N. Teich, H. Temin, K. Toyoshima, H. Varmus, P. Vogt, and et al. 1986. Human immunodeficiency viruses. *Science*. 232:697.

Cohen, G.B., R.T. Gandhi, D.M. Davis, O. Mandelboim, B.K. Chen, J.L. Strominger, and D. Baltimore. 1999. The selective downregulation of class I major

histocompatibility complex proteins by HIV-1 protects HIV-infected cells from NK cells. *Immunity*. 10:661-71.

Connor, R.I., B.K. Chen, S. Choe, and N.R. Landau. 1995. Vpr is required for efficient replication of human immunodeficiency virus type-1 in mononuclear phagocytes. *Virology*. 206:935-44.

Conticello, S.G., R.S. Harris, and M.S. Neuberger. 2003. The Vif protein of HIV triggers degradation of the human antiretroviral DNA deaminase APOBEC3G. *Curr Biol*. 13:2009-13.

Corbeil, J., M. Tremblay, and D.D. Richman. 1996. HIV-induced apoptosis requires the CD4 receptor cytoplasmic tail and is accelerated by interaction of CD4 with p56lck. *J Exp Med*. 183:39-48.

Crowe, S.M., and S. Sonza. 2000. HIV-1 can be recovered from a variety of cells including peripheral blood monocytes of patients receiving highly active antiretroviral therapy: a further obstacle to eradication. *J Leukoc Biol*. 68:345-50.

Cha, B., M. Tse, C. Yun, O. Kovbasnjuk, S. Mohan, A. Hubbard, M. Arpin, and M. Donowitz. 2006. The NHE3 juxtamembrane cytoplasmic domain directly binds ezrin: dual role in NHE3 trafficking and mobility in the brush border. *Mol Biol Cell*. 17:2661-73.

Chakrabarti, L., M. Guyader, M. Alizon, M.D. Daniel, R.C. Desrosiers, P. Tiollais, and P. Sonigo. 1987. Sequence of simian immunodeficiency virus from macaque and its relationship to other human and simian retroviruses. *Nature*. 328:543-7.

Chan, D.C., and P.S. Kim. 1998. HIV entry and its inhibition. *Cell*. 93:681-4.

Chirivino, D., L. Del Maestro, E. Formstecher, P. Hupe, G. Raposo, D. Louvard, and M. Arpin. 2011. The ERM proteins interact with the HOPS complex to regulate the maturation of endosomes. *Mol Biol Cell*. 22:375-85.

Chirmule, N., A. Avots, S.M. LakshmiTamma, S. Pahwa, and E. Serfling. 1999. CD4-mediated signals induce T cell dysfunction in vivo. *J Immunol*. 163:644-9.

Chirmule, N., H. Goonewardena, S. Pahwa, R. Pasieka, V.S. Kalyanaraman, and S. Pahwa. 1995. HIV-1 envelope glycoproteins induce activation of activated protein-1 in CD4+ T cells. *J Biol Chem*. 270:19364-9.

Chishti, A.H., A.C. Kim, S.M. Marfatia, M. Lutchman, M. Hanspal, H. Jindal, S.C. Liu, P.S. Low, G.A. Rouleau, N. Mohandas, J.A. Chasis, J.G. Conboy, P. Gascard, Y. Takakuwa, S.C. Huang, E.J. Benz, Jr., A. Bretscher, R.G. Fehon, J.F. Gusella, V. Ramesh, F. Solomon, V.T. Marchesi, S. Tsukita, S. Tsukita, K.B. Hoover, and et al. 1998. The FERM domain: a unique module involved in the linkage of cytoplasmic proteins to the membrane. *Trends Biochem Sci*. 23:281-2.

Chiu, Y.L., and W.C. Greene. 2009. APOBEC3G: an intracellular centurion. *Philos Trans R Soc Lond B Biol Sci*. 364:689-703.

Choe, H., M. Farzan, Y. Sun, N. Sullivan, B. Rollins, P.D. Ponath, L. Wu, C.R. Mackay, G. LaRosa, W. Newman, N. Gerard, C. Gerard, and J. Sodroski. 1996. The beta-chemokine receptors CCR3 and CCR5 facilitate infection by primary HIV-1 isolates. *Cell*. 85:1135-48.

Chowers, M.Y., C.A. Spina, T.J. Kwoh, N.J. Fitch, D.D. Richman, and J.C. Guatelli. 1994. Optimal infectivity in vitro of human immunodeficiency virus type 1 requires an intact nef gene. *J Virol*. 68:2906-14.

Chukkapalli, V., I.B. Hogue, V. Boyko, W.S. Hu, and A. Ono. 2008. Interaction between the human immunodeficiency virus type 1 Gag matrix domain and phosphatidylinositol-(4,5)-bisphosphate is essential for efficient gag membrane binding. *J Virol*. 82:2405-17.

Chun, T.W., D.C. Nickle, J.S. Justement, D. Large, A. Semerjian, M.E. Curlin, M.A. O'Shea, C.W. Hallahan, M. Daucher, D.J. Ward, S. Moir, J.I. Mullins, C. Kovacs, and A.S. Fauci. 2005. HIV-infected individuals receiving effective

antiviral therapy for extended periods of time continually replenish their viral reservoir. *J Clin Invest*. 115:3250-5.

Chun, T.W., D.C. Nickle, J.S. Justement, J.H. Meyers, G. Roby, C.W. Hallahan, S. Kottilil, S. Moir, J.M. Mican, J.I. Mullins, D.J. Ward, J.A. Kovacs, P.J. Mannon, and A.S. Fauci. 2008. Persistence of HIV in gut-associated lymphoid tissue despite long-term antiretroviral therapy. *J Infect Dis*. 197:714-20.

Dalgleish, A.G., P.C. Beverley, P.R. Clapham, D.H. Crawford, M.F. Greaves, and R.A. Weiss. 1984. The CD4 (T4) antigen is an essential component of the receptor for the AIDS retrovirus. *Nature*. 312:763-7.

Davis, C.B., I. Dikic, D. Unutmaz, C.M. Hill, J. Arthos, M.A. Siani, D.A. Thompson, J. Schlessinger, and D.R. Littman. 1997. Signal transduction due to HIV-1 envelope interactions with chemokine receptors CXCR4 or CCR5. *J Exp Med*. 186:1793-8.

De Biasi, S.M.P., Milena Nasi, Lara Gibellini, Linda Bertoncelli, Serena Manzini, Cristina Mussini, Andrea Cossarizza. 2011. HIV-1 infection and the aging of the Immune system: Facts, Similarities and Perspectives. *Journal of Experimental and Clinical Medicine*.

Declaration, T.D. 2000. The Durban Declaration. *Nature*. 406:15-6.

Deeks, S.G. 2011. HIV infection, inflammation, immunosenescence, and aging. *Annu Rev Med*. 62:141-55.

Defacque, H., M. Egeberg, A. Habermann, M. Diakonova, C. Roy, P. Mangeat, W. Voelter, G. Marriott, J. Pfannstiel, H. Faulstich, and G. Griffiths. 2000. Involvement of ezrin/moesin in de novo actin assembly on phagosomal membranes. *Embo J*. 19:199-212.

Del Corno, M., Q.H. Liu, D. Schols, E. de Clercq, S. Gessani, B.D. Freedman, and R.G. Collman. 2001. HIV-1 gp120 and chemokine activation of Pyk2 and mitogen-activated protein kinases in primary macrophages mediated by calcium-dependent, pertussis toxin-insensitive chemokine receptor signaling. *Blood*. 98:2909-16.

del Real, G., S. Jimenez-Baranda, E. Mira, R.A. Lacalle, P. Lucas, C. Gomez-Mouton, M. Alegret, J.M. Pena, M. Rodriguez-Zapata, M. Alvarez-Mon, A.C. Martinez, and S. Manes. 2004. Statins inhibit HIV-1 infection by down-regulating Rho activity. *J Exp Med*. 200:541-7.

Deng, H., R. Liu, W. Ellmeier, S. Choe, D. Unutmaz, M. Burkhart, P. Di Marzio, S. Marmon, R.E. Sutton, C.M. Hill, C.B. Davis, S.C. Peiper, T.J. Schall, D.R. Littman, and N.R. Landau. 1996. Identification of a major co-receptor for primary isolates of HIV-1. *Nature*. 381:661-6.

Deniaud, A., C. Brenner, and G. Kroemer. 2004. Mitochondrial membrane permeabilization by HIV-1 Vpr. *Mitochondrion*. 4:223-33.

Desai, S., and A. Landay. 2010. Early immune senescence in HIV disease. *Curr HIV/AIDS Rep*. 7:4-10.

Dimitrov, D.S., X. Xiao, D.J. Chabot, and C.C. Broder. 1998. HIV coreceptors. *J Membr Biol*. 166:75-90.

Doms, R.W. 2000. Beyond receptor expression: the influence of receptor conformation, density, and affinity in HIV-1 infection. *Virology*. 276:229-37.

Doms, R.W., and D. Trono. 2000. The plasma membrane as a combat zone in the HIV battlefield. *Genes Dev*. 14:2677-88.

Dong, C., C. Kwas, and L. Wu. 2009. Transcriptional restriction of human immunodeficiency virus type 1 gene expression in undifferentiated primary monocytes. *J Virol*. 83:3518-27.

Doranz, B.J., J.F. Berson, J. Rucker, and R.W. Doms. 1997a. Chemokine receptors as fusion cofactors for human immunodeficiency virus type 1 (HIV-1). *Immunol Res*. 16:15-28.

Doranz, B.J., Z.H. Lu, J. Rucker, T.Y. Zhang, M. Sharron, Y.H. Cen, Z.X. Wang, H.H. Guo, J.G. Du, M.A. Accavitti, R.W. Doms, and S.C. Peiper. 1997b. Two distinct CCR5 domains can mediate coreceptor usage by human immunodeficiency virus type 1. *J Virol*. 71:6305-14.

Doranz, B.J., M.J. Orsini, J.D. Turner, T.L. Hoffman, J.F. Berson, J.A. Hoxie, S.C. Peiper, L.F. Brass, and R.W. Doms. 1999. Identification of CXCR4 domains that support coreceptor and chemokine receptor functions. *J Virol*. 73:2752-61.

Doranz, B.J., J. Rucker, Y. Yi, R.J. Smyth, M. Samson, S.C. Peiper, M. Parmentier, R.G. Collman, and R.W. Doms. 1996. A dual-tropic primary HIV-1 isolate that uses fusin and the beta-chemokine receptors CKR-5, CKR-3, and CKR-2b as fusion cofactors. *Cell*. 85:1149-58.

Dragic, T. 2001. An overview of the determinants of CCR5 and CXCR4 co-receptor function. *J Gen Virol*. 82:1807-14.

Dragic, T., V. Litwin, G.P. Allaway, S.R. Martin, Y. Huang, K.A. Nagashima, C. Cayanan, P.J. Maddon, R.A. Koup, J.P. Moore, and W.A. Paxton. 1996. HIV-1 entry into CD4+ cells is mediated by the chemokine receptor CC-CKR-5. *Nature*. 381:667-73.

Dragic, T., A. Trkola, S.W. Lin, K.A. Nagashima, F. Kajumo, L. Zhao, W.C. Olson, L. Wu, C.R. Mackay, G.P. Allaway, T.P. Sakmar, J.P. Moore, and P.J. Maddon. 1998. Amino-terminal substitutions in the CCR5 coreceptor impair gp120 binding and human immunodeficiency virus type 1 entry. *J Virol*. 72:279-85.

Eggena, M.P., B. Barugahare, N. Jones, M. Okello, S. Mutalya, C. Kityo, P. Mugyenyi, and H. Cao. 2005. Depletion of regulatory T cells in HIV infection is associated with immune activation. *J Immunol*. 174:4407-14.

Eitzen, G. 2003. Actin remodeling to facilitate membrane fusion. *Biochim Biophys Acta*. 1641:175-81.

Endres, M.J., P.R. Clapham, M. Marsh, M. Ahuja, J.D. Turner, A. McKnight, J.F. Thomas, B. Stoebenau-Haggarty, S. Choe, P.J. Vance, T.N. Wells, C.A. Power, S.S. Sutterwala, R.W. Doms, N.R. Landau, and J.A. Hoxie. 1996. CD4-independent infection by HIV-2 is mediated by fusin/CXCR4. *Cell*. 87:745-56.

Engqvist-Goldstein, A.E., and D.G. Drubin. 2003. Actin assembly and endocytosis: from yeast to mammals. *Annu Rev Cell Dev Biol*. 19:287-332.

Engqvist-Goldstein, A.E., R.A. Warren, M.M. Kessels, J.H. Keen, J. Heuser, and D.G. Drubin. 2001. The actin-binding protein Hip1R associates with clathrin during early stages of endocytosis and promotes clathrin assembly in vitro. *J Cell Biol*. 154:1209-23.

Este, J.A., and A. Telenti. 2007. HIV entry inhibitors. *Lancet*. 370:81-8.

Fackler, O.T., W. Luo, M. Geyer, A.S. Alberts, and B.M. Peterlin. 1999. Activation of Vav by Nef induces cytoskeletal rearrangements and downstream effector functions. *Mol Cell*. 3:729-39.

Fantini, J., D.G. Cook, N. Nathanson, S.L. Spitalnik, and F. Gonzalez-Scarano. 1993. Infection of colonic epithelial cell lines by type 1 human immunodeficiency virus is associated with cell surface expression of galactosylceramide, a potential alternative gp120 receptor. *Proc Natl Acad Sci U S A*. 90:2700-4.

Fantuzzi, L., I. Canini, F. Belardelli, and S. Gessani. 2001. HIV-1 gp120 stimulates the production of beta-chemokines in human peripheral blood monocytes through a CD4-independent mechanism. *J Immunol*. 166:5381-7.

Farnet, C.M., and W.A. Haseltine. 1991. Determination of viral proteins present in the human immunodeficiency virus type 1 preintegration complex. *J Virol*. 65:1910-5.

Farzan, M., H. Choe, K.A. Martin, Y. Sun, M. Sidelko, C.R. Mackay, N.P. Gerard, J. Sodroski, and C. Gerard. 1997. HIV-1 entry and macrophage inflammatory protein-1beta-mediated signaling are independent functions of the chemokine receptor CCR5. *J Biol Chem*. 272:6854-7.

Farzan, M., T. Mirzabekov, P. Kolchinsky, R. Wyatt, M. Cayabyab, N.P. Gerard, C. Gerard, J. Sodroski, and H. Choe. 1999. Tyrosine sulfation of the amino terminus of CCR5 facilitates HIV-1 entry. *Cell*. 96:667-76.

Fehon, R.G., A.I. McClatchey, and A. Bretscher. 2010. Organizing the cell cortex: the role of ERM proteins. *Nat Rev Mol Cell Biol*. 11:276-87.

Feng, Y., C.C. Broder, P.E. Kennedy, and E.A. Berger. 1996. HIV-1 entry cofactor: functional cDNA cloning of a seven-transmembrane, G protein-coupled receptor. *Science*. 272:872-7.

Fievet, B.T., A. Gautreau, C. Roy, L. Del Maestro, P. Mangeat, D. Louvard, and M. Arpin. 2004. Phosphoinositide binding and phosphorylation act sequentially in the activation mechanism of ezrin. *J Cell Biol*. 164:653-9.

Finzi, D., J. Blankson, J.D. Siliciano, J.B. Margolick, K. Chadwick, T. Pierson, K. Smith, J. Lisziewicz, F. Lori, C. Flexner, T.C. Quinn, R.E. Chaisson, E. Rosenberg, B. Walker, S. Gange, J. Gallant, and R.F. Siliciano. 1999. Latent infection of CD4+ T cells provides a mechanism for lifelong persistence of HIV-1, even in patients on effective combination therapy. *Nat Med*. 5:512-7.

Flexner, C. 1998. HIV-protease inhibitors. *N Engl J Med*. 338:1281-92.

Foti, M., M.A. Phelouzat, A. Holm, B.J. Rasmusson, and J.L. Carpentier. 2002. p56Lck anchors CD4 to distinct microdomains on microvilli. *Proc Natl Acad Sci U S A*. 99:2008-13.

Francois, F., and M.E. Klotman. 2003. Phosphatidylinositol 3-kinase regulates human immunodeficiency virus type 1 replication following viral entry in primary CD4+ T lymphocytes and macrophages. *J Virol*. 77:2539-49.

Fredericksen, B.L., B.L. Wei, J. Yao, T. Luo, and J.V. Garcia. 2002. Inhibition of endosomal/lysosomal degradation increases the infectivity of human immunodeficiency virus. *J Virol*. 76:11440-6.

Freed, E.O. 1998. HIV-1 gag proteins: diverse functions in the virus life cycle. *Virology*. 251:1-15.

Freed, E.O. 2001. HIV-1 replication. *Somat Cell Mol Genet*. 26:13-33.

Frey, S., M. Marsh, S. Gunther, A. Pelchen-Matthews, P. Stephens, S. Ortlepp, and T. Stegmann. 1995. Temperature dependence of cell-cell fusion induced by the envelope glycoprotein of human immunodeficiency virus type 1. *J Virol*. 69:1462-72.

Frischknecht, F., and M. Way. 2001. Surfing pathogens and the lessons learned for actin polymerization. *Trends Cell Biol*. 11:30-38.

Gallo, R.C., P.S. Sarin, E.P. Gelmann, M. Robert-Guroff, E. Richardson, V.S. Kalyanaraman, D. Mann, G.D. Sidhu, R.E. Stahl, S. Zolla-Pazner, J. Leibowitch, and M. Popovic. 1983. Isolation of human T-cell leukemia virus in acquired immune deficiency syndrome (AIDS). *Science*. 220:865-7.

Gallo, S.A., A. Puri, and R. Blumenthal. 2001. HIV-1 gp41 six-helix bundle formation occurs rapidly after the engagement of gp120 by CXCR4 in the HIV-1 Env-mediated fusion process. *Biochemistry*. 40:12231-6.

Ganser-Pornillos, B.K., M. Yeager, and W.I. Sundquist. 2008. The structural biology of HIV assembly. *Curr Opin Struct Biol*. 18:203-17.

Gao, X., G.W. Nelson, P. Karacki, M.P. Martin, J. Phair, R. Kaslow, J.J. Goedert, S. Buchbinder, K. Hoots, D. Vlahov, S.J. O'Brien, and M. Carrington. 2001. Effect of a single amino acid change in MHC class I molecules on the rate of progression to AIDS. *N Engl J Med*. 344:1668-75.

Garcia-Exposito, L., J. Barroso-Gonzalez, I. Puigdomenech, J.D. Machado, J. Blanco, and A. Valenzuela-Fernandez. 2011. HIV-1 requires Arf6-mediated membrane dynamics to efficiently enter and infect T lymphocytes. *Mol Biol Cell*. 22:1148-66.

Garcia-Perez, J., P. Rueda, J. Alcami, D. Rognan, F. Arenzana-Seisdedos, B. Lagane, and E. Kellenberger. 2011. Allosteric model of maraviroc binding to CC chemokine receptor 5 (CCR5). *J Biol Chem*. 286:33409-21.

Garron, M.L., J. Arthos, J.F. Guichou, J. McNally, C. Cicala, and S.T. Arold. 2008. Structural basis for the interaction between focal adhesion kinase and CD4. *J Mol Biol*. 375:1320-8.

Gaschen, B., J. Taylor, K. Yusim, B. Foley, F. Gao, D. Lang, V. Novitsky, B. Haynes, B.H. Hahn, T. Bhattacharya, and B. Korber. 2002. Diversity considerations in HIV-1 vaccine selection. *Science*. 296:2354-60.

Gazzard, B.G., J. Anderson, A. Babiker, M. Boffito, G. Brook, G. Brough, D. Churchill, B. Cromarty, S. Das, M. Fisher, A. Freedman, A.M. Geretti, M. Johnson, S. Khoo, C. Leen, D. Nair, B. Peters, A. Phillips, D. Pillay, A. Pozniak, J. Walsh, E. Wilkins, I. Williams, M. Williams, and M. Youle. 2008. British HIV Association Guidelines for the treatment of HIV-1-infected adults with antiretroviral therapy 2008. *HIV Med*. 9:563-608.

Geleziunas, R., S. Bour, and M.A. Wainberg. 1994. Cell surface down-modulation of CD4 after infection by HIV-1. *Faseb J*. 8:593-600.

Giguere, J.F., S. Bounou, J.S. Paquette, J. Madrenas, and M.J. Tremblay. 2004. Insertion of host-derived costimulatory molecules CD80 (B7.1) and CD86 (B7.2) into human immunodeficiency virus type 1 affects the virus life cycle. *J Virol*. 78:6222-32.

Giguere, J.F., J. Diou, J. Madrenas, and M.J. Tremblay. 2005. Virus attachment and replication are promoted after acquisition of host CD28 and CD152 by HIV-1. *J Infect Dis*. 192:1265-8.

Goldman, F., W.A. Jensen, G.L. Johnson, L. Heasley, and J.C. Cambier. 1994. gp120 ligation of CD4 induces p56lck activation and TCR desensitization independent of TCR tyrosine phosphorylation. *J Immunol*. 153:2905-17.

Goldstone, D.C., V. Ennis-Adeniran, J.J. Hedden, H.C. Groom, G.I. Rice, E. Christodoulou, P.A. Walker, G. Kelly, L.F. Haire, M.W. Yap, L.P. de Carvalho, J.P. Stoye, Y.J. Crow, I.A. Taylor, and M. Webb. 2011. HIV-1 restriction factor SAMHD1 is a deoxynucleoside triphosphate triphosphohydrolase. *Nature*.

Gordon-Alonso, M., M. Yanez-Mo, O. Barreiro, S. Alvarez, M.A. Munoz-Fernandez, A. Valenzuela-Fernandez, and F. Sanchez-Madrid. 2006. Tetraspanins CD9 and CD81 modulate HIV-1-induced membrane fusion. *J Immunol*. 177:5129-37.

Gorry, P.R., and P. Ancuta. 2011. Coreceptors and HIV-1 pathogenesis. *Curr HIV/AIDS Rep*. 8:45-53.

Gosling, J., F.S. Monteclaro, R.E. Atchison, H. Arai, C.L. Tsou, M.A. Goldsmith, and I.F. Charo. 1997. Molecular uncoupling of C-C chemokine receptor 5-induced chemotaxis and signal transduction from HIV-1 coreceptor activity. *Proc Natl Acad Sci U S A*. 94:5061-6.

Gottwein, E., S. Jager, A. Habermann, and H.G. Krausslich. 2006. Cumulative mutations of ubiquitin acceptor sites in human immunodeficiency virus type 1 gag cause a late budding defect. *J Virol*. 80:6267-75.

Gottwein, E., and H.G. Krausslich. 2005. Analysis of human immunodeficiency virus type 1 Gag ubiquitination. *J Virol*. 79:9134-44.

Graziani-Bowering, G., L.G. Filion, P. Thibault, and M. Kozlowski. 2002. CD4 is active as a signaling molecule on the human monocytic cell line Thp-1. *Exp Cell Res*. 279:141-52.

Groux, H., G. Torpier, D. Monte, Y. Mouton, A. Capron, and J.C. Ameisen. 1992. Activation-induced death by apoptosis in CD4+ T cells from human immunodeficiency virus-infected asymptomatic individuals. *J Exp Med*. 175:331-40.

Guillerm, C., N. Coudronniere, V. Robert-Hebmann, and C. Devaux. 1998. Delayed human immunodeficiency virus type 1-induced apoptosis in cells expressing truncated forms of CD4. *J Virol*. 72:1754-61.

Guntermann, C., B.J. Murphy, R. Zheng, A. Qureshi, P.A. Eagles, and K.E. Nye. 1999. Human immunodeficiency virus-1 infection requires pertussis toxin sensitive G-protein-coupled signalling and mediates cAMP downregulation. *Biochem Biophys Res Commun*. 256:429-35.

Ha-Lee, Y.M., Y. Lee, Y.K. Kim, and J. Sohn. 2000. Cross-linking of CD4 induces cytoskeletal association of CD4 and p56lck. *Exp Mol Med*. 32:18-22.

Haedicke, J., K. de Los Santos, S.P. Goff, and M.H. Naghavi. 2008. The Ezrin-radixin-moesin family member ezrin regulates stable microtubule formation and retroviral infection. *J Virol*. 82:4665-70.

Hall, R.A., R.T. Premont, and R.J. Lefkowitz. 1999. Heptahelical receptor signaling: beyond the G protein paradigm. *J Cell Biol*. 145:927-32.

Hamm, H.E. 1998. The many faces of G protein signaling. *J Biol Chem*. 273:669-72.

Hao, J.J., Y. Liu, M. Kruhlak, K.E. Debell, B.L. Rellahan, and S. Shaw. 2009. Phospholipase C-mediated hydrolysis of PIP2 releases ERM proteins from lymphocyte membrane. *J Cell Biol*. 184:451-62.

Harmon, B., N. Campbell, and L. Ratner. 2010. Role of Abl kinase and the Wave2 signaling complex in HIV-1 entry at a post-hemifusion step. *PLoS Pathog*. 6:e1000956.

Harmon, B., and L. Ratner. 2008. Induction of the Galpha(q) signaling cascade by the human immunodeficiency virus envelope is required for virus entry. *J Virol*. 82:9191-205.

Harouse, J.M., S. Bhat, S.L. Spitalnik, M. Laughlin, K. Stefano, D.H. Silberberg, and F. Gonzalez-Scarano. 1991. Inhibition of entry of HIV-1 in neural cell lines by antibodies against galactosyl ceramide. *Science*. 253:320-3.

Hecker, C., C. Weise, J. Schneider-Schaulies, H.C. Holmes, and V. ter Meulen. 1997. Specific binding of HIV-1 envelope protein gp120 to the structural membrane proteins ezrin and moesin. *Virus Res*. 49:215-23.

Hirao, M., N. Sato, T. Kondo, S. Yonemura, M. Monden, T. Sasaki, Y. Takai, S. Tsukita, and S. Tsukita. 1996. Regulation mechanism of ERM (ezrin/radixin/moesin) protein/plasma membrane association: possible involvement of phosphatidylinositol turnover and Rho-dependent signaling pathway. *J Cell Biol*. 135:37-51.

Horuk, R. 2009. Promiscuous drugs as therapeutics for chemokine receptors. *Expert Rev Mol Med*. 11:e1.

Hottiger, M., K. Gramatikoff, O. Georgiev, C. Chaponnier, W. Schaffner, and U. Hubscher. 1995. The large subunit of HIV-1 reverse transcriptase interacts with beta-actin. *Nucleic Acids Res*. 23:736-41.

Huang, C.C., M. Tang, M.Y. Zhang, S. Majeed, E. Montabana, R.L. Stanfield, D.S. Dimitrov, B. Korber, J. Sodroski, I.A. Wilson, R. Wyatt, and P.D. Kwong. 2005. Structure of a V3-containing HIV-1 gp120 core. *Science*. 310:1025-8.

Huang, J., F. Wang, E. Argyris, K. Chen, Z. Liang, H. Tian, W. Huang, K. Squires, G. Verlinghieri, and H. Zhang. 2007. Cellular microRNAs contribute to HIV-1 latency in resting primary CD4+ T lymphocytes. *Nat Med*. 13:1241-7.

Huang, Y.H., and K. Sauer. 2010. Lipid signaling in T-cell development and function. *Cold Spring Harb Perspect Biol*. 2:a002428.

Hubert, P., G. Bismuth, M. Korner, and P. Debre. 1995. HIV-1 glycoprotein gp120 disrupts CD4-p56lck/CD3-T cell receptor interactions and inhibits CD3 signaling. *Eur J Immunol*. 25:1417-25.

Hug, P., H.M. Lin, T. Korte, X. Xiao, D.S. Dimitrov, J.M. Wang, A. Puri, and R. Blumenthal. 2000. Glycosphingolipids promote entry of a broad range of human

immunodeficiency virus type 1 isolates into cell lines expressing CD4, CXCR4, and/or CCR5. *J Virol*. 74:6377-85.

Iyengar, S., J.E. Hildreth, and D.H. Schwartz. 1998. Actin-dependent receptor colocalization required for human immunodeficiency virus entry into host cells. *J Virol*. 72:5251-5.

Iyengar, S., D.H. Schwartz, and J.E. Hildreth. 1999. T cell-tropic HIV gp120 mediates CD4 and CD8 cell chemotaxis through CXCR4 independent of CD4: implications for HIV pathogenesis. *J Immunol*. 162:6263-7.

Ji, W.T., and H.J. Liu. 2008. PI3K-Akt signaling and viral infection. *Recent Pat Biotechnol*. 2:218-26.

Jimenez-Baranda, S., C. Gomez-Mouton, A. Rojas, L. Martinez-Prats, E. Mira, R. Ana Lacalle, A. Valencia, D.S. Dimitrov, A. Viola, R. Delgado, A.C. Martinez, and S. Manes. 2007. Filamin-A regulates actin-dependent clustering of HIV receptors. *Nat Cell Biol*. 9:838-46.

Jolly, C., K. Kashefi, M. Hollinshead, and Q.J. Sattentau. 2004. HIV-1 cell to cell transfer across an Env-induced, actin-dependent synapse. *J Exp Med*. 199:283-93.

Jolly, C., and Q.J. Sattentau. 2007. Human immunodeficiency virus type 1 assembly, budding, and cell-cell spread in T cells take place in tetraspanin-enriched plasma membrane domains. *J Virol*. 81:7873-84.

Judice, J.K., J.Y. Tom, W. Huang, T. Wrin, J. Vennari, C.J. Petropoulos, and R.S. McDowell. 1997. Inhibition of HIV type 1 infectivity by constrained alpha-helical peptides: implications for the viral fusion mechanism. *Proc Natl Acad Sci U S A*. 94:13426-30.

Juszczak, R.J., H. Turchin, A. Truneh, J. Culp, and S. Kassis. 1991. Effect of human immunodeficiency virus gp120 glycoprotein on the association of the protein tyrosine kinase p56lck with CD4 in human T lymphocytes. *J Biol Chem*. 266:11176-83.

Kanmogne, G.D., K. Schall, J. Leibhart, B. Knipe, H.E. Gendelman, and Y. Persidsky. 2007. HIV-1 gp120 compromises blood-brain barrier integrity and enhances monocyte migration across blood-brain barrier: implication for viral neuropathogenesis. *J Cereb Blood Flow Metab*. 27:123-34.

Keller, P.W., C.S. Adamson, J.B. Heymann, E.O. Freed, and A.C. Steven. 2011. HIV-1 maturation inhibitor bevirimat stabilizes the immature Gag lattice. *J Virol*. 85:1420-8.

Kelley, C.F., C.M. Kitchen, P.W. Hunt, B. Rodriguez, F.M. Hecht, M. Kitahata, H.M. Crane, J. Willig, M. Mugavero, M. Saag, J.N. Martin, and S.G. Deeks. 2009. Incomplete peripheral CD4+ cell count restoration in HIV-infected patients receiving long-term antiretroviral treatment. *Clin Infect Dis*. 48:787-94.

Kim, E.Y., T. Bhattacharya, K. Kunstman, P. Swantek, F.A. Koning, M.H. Malim, and S.M. Wolinsky. 2010. Human APOBEC3G-mediated editing can promote HIV-1 sequence diversification and accelerate adaptation to selective pressure. *J Virol*. 84:10402-5.

Kinch, M.S., J.L. Strominger, and C. Doyle. 1993. Cell adhesion mediated by CD4 and MHC class II proteins requires active cellular processes. *J Immunol*. 151:4552-61.

Kinet, S., F. Bernard, C. Mongellaz, M. Perreau, F.D. Goldman, and N. Taylor. 2002. gp120-mediated induction of the MAPK cascade is dependent on the activation state of CD4(+) lymphocytes. *Blood*. 100:2546-53.

Kinter, A., A. Catanzaro, J. Monaco, M. Ruiz, J. Justement, S. Moir, J. Arthos, A. Oliva, L. Ehler, S. Mizell, R. Jackson, M. Ostrowski, J. Hoxie, R. Offord, and A.S. Fauci. 1998. CC-chemokines enhance the replication of T-tropic strains of HIV-1 in CD4(+) T cells: role of signal transduction. *Proc Natl Acad Sci U S A*. 95:11880-5.

Kinter, A.L., C.A. Umscheid, J. Arthos, C. Cicala, Y. Lin, R. Jackson, E. Donoghue, L. Ehler, J. Adelsberger, R.L. Rabin, and A.S. Fauci. 2003. HIV envelope induces virus expression from resting CD4+ T cells isolated from HIV-infected individuals in the absence of markers of cellular activation or apoptosis. *J Immunol*. 170:2449-55.

Klatzmann, D., E. Champagne, S. Chamaret, J. Gruest, D. Guetard, T. Hercend, J.C. Gluckman, and L. Montagnier. 1984. T-lymphocyte T4 molecule behaves as the receptor for human retrovirus LAV. *Nature*. 312:767-8.

Koot, M., I.P. Keet, A.H. Vos, R.E. de Goede, M.T. Roos, R.A. Coutinho, F. Miedema, P.T. Schellekens, and M. Tersmette. 1993. Prognostic value of HIV-1 syncytium-inducing phenotype for rate of CD4+ cell depletion and progression to AIDS. *Ann Intern Med*. 118:681-8.

Kozak, S.L., J.M. Heard, and D. Kabat. 2002. Segregation of CD4 and CXCR4 into distinct lipid microdomains in T lymphocytes suggests a mechanism for membrane destabilization by human immunodeficiency virus. *J Virol*. 76:1802-15.

Krementsov, D.N., J. Weng, M. Lambele, N.H. Roy, and M. Thali. 2009. Tetraspanins regulate cell-to-cell transmission of HIV-1. *Retrovirology*. 6:64.

Kubo, Y., H. Yoshii, H. Kamiyama, C. Tominaga, Y. Tanaka, H. Sato, and N. Yamamoto. 2008. Ezrin, Radixin, and Moesin (ERM) proteins function as pleiotropic regulators of human immunodeficiency virus type 1 infection. *Virology*. 375:130-40.

Kuhmann, S.E., E.J. Platt, S.L. Kozak, and D. Kabat. 2000. Cooperation of multiple CCR5 coreceptors is required for infections by human immunodeficiency virus type 1. *J Virol*. 74:7005-15.

Kurisu, S., and T. Takenawa. 2010. WASP and WAVE family proteins: friends or foes in cancer invasion? *Cancer Sci*. 101:2093-104.

Kwiatkowska, K. 2010. One lipid, multiple functions: how various pools of PI(4,5)P(2) are created in the plasma membrane. *Cell Mol Life Sci*. 67:3927-46.

Lai, W., L. Huang, P. Ho, Z. Li, D. Montefiori, and C.H. Chen. 2008. Betulinic acid derivatives that target gp120 and inhibit multiple genetic subtypes of human immunodeficiency virus type 1. *Antimicrob Agents Chemother*. 52:128-36.

Lapham, C.K., J. Ouyang, B. Chandrasekhar, N.Y. Nguyen, D.S. Dimitrov, and H. Golding. 1996. Evidence for cell-surface association between fusin and the CD4-gp120 complex in human cell lines. *Science*. 274:602-5.

Lapham, C.K., M.B. Zaitseva, S. Lee, T. Romanstseva, and H. Golding. 1999. Fusion of monocytes and macrophages with HIV-1 correlates with biochemical properties of CXCR4 and CCR5. *Nat Med*. 5:303-8.

Lappalainen, P., and D.G. Drubin. 1997. Cofilin promotes rapid actin filament turnover in vivo. *Nature*. 388:78-82.

Layne, S.P., M.J. Merges, M. Dembo, J.L. Spouge, and P.L. Nara. 1990. HIV requires multiple gp120 molecules for CD4-mediated infection. *Nature*. 346:277-9.

Le Gall, S., L. Erdtmann, S. Benichou, C. Berlioz-Torrent, L. Liu, R. Benarous, J.M. Heard, and O. Schwartz. 1998. Nef interacts with the mu subunit of clathrin adaptor complexes and reveals a cryptic sorting signal in MHC I molecules. *Immunity*. 8:483-95.

Lee, B., M. Sharron, C. Blanpain, B.J. Doranz, J. Vakili, P. Setoh, E. Berg, G. Liu, H.R. Guy, S.R. Durell, M. Parmentier, C.N. Chang, K. Price, M. Tsang, and R.W. Doms. 1999. Epitope mapping of CCR5 reveals multiple conformational states and distinct but overlapping structures involved in chemokine and coreceptor function. *J Biol Chem*. 274:9617-26.

Lee, C., Q.H. Liu, B. Tomkowicz, Y. Yi, B.D. Freedman, and R.G. Collman. 2003. Macrophage activation through CCR5- and CXCR4-mediated gp120-elicited signaling pathways. *J Leukoc Biol*. 74:676-82.

Lee, S., C.K. Lapham, H. Chen, L. King, J. Manischewitz, T. Romantseva, H. Mostowski, T.S. Stantchev, C.C. Broder, and H. Golding. 2000. Coreceptor competition for association with CD4 may change the susceptibility of human cells to infection with T-tropic and macrophagetropic isolates of human immunodeficiency virus type 1. *J Virol*. 74:5016-23.

Lehmann, M.J., N.M. Sherer, C.B. Marks, M. Pypaert, and W. Mothes. 2005. Actin- and myosin-driven movement of viruses along filopodia precedes their entry into cells. *J Cell Biol*. 170:317-25.

Levkau, B., B. Herren, H. Koyama, R. Ross, and E.W. Raines. 1998. Caspase-mediated cleavage of focal adhesion kinase pp125FAK and disassembly of focal adhesions in human endothelial cell apoptosis. *J Exp Med*. 187:579-86.

Levy, J.A. 2003. The search for the CD8+ cell anti-HIV factor (CAF). *Trends Immunol*. 24:628-32.

Levy, J.A. 2009. HIV pathogenesis: 25 years of progress and persistent challenges. *Aids*. 23:147-60.

Li, F., R. Goila-Gaur, K. Salzwedel, N.R. Kilgore, M. Reddick, C. Matallana, A. Castillo, D. Zoumplis, D.E. Martin, J.M. Orenstein, G.P. Allaway, E.O. Freed, and C.T. Wild. 2003. PA-457: a potent HIV inhibitor that disrupts core condensation by targeting a late step in Gag processing. *Proc Natl Acad Sci U S A*. 100:13555-60.

Li, J.G., C. Chen, and L.Y. Liu-Chen. 2002. Ezrin-radixin-moesin-binding phosphoprotein-50/Na+/H+ exchanger regulatory factor (EBP50/NHERF) blocks U50,488H-induced down-regulation of the human kappa opioid receptor by enhancing its recycling rate. *J Biol Chem*. 277:27545-52.

Lim, J.K., W.G. Glass, D.H. McDermott, and P.M. Murphy. 2006. CCR5: no longer a "good for nothing" gene--chemokine control of West Nile virus infection. *Trends Immunol*. 27:308-12.

Lin, C.L., A.K. Sewell, G.F. Gao, K.T. Whelan, R.E. Phillips, and J.M. Austyn. 2000. Macrophage-tropic HIV induces and exploits dendritic cell chemotaxis. *J Exp Med*. 192:587-94.

Lin, Y.L., C. Mettling, P. Portales, B. Reant, J. Clot, and P. Corbeau. 2005. G-protein signaling triggered by R5 human immunodeficiency virus type 1 increases virus replication efficiency in primary T lymphocytes. *J Virol*. 79:7938-41.

Ling, K., N.J. Schill, M.P. Wagoner, Y. Sun, and R.A. Anderson. 2006. Movin' on up: the role of PtdIns(4,5)P(2) in cell migration. *Trends Cell Biol*. 16:276-84.

Liu, Q.H., D.A. Williams, C. McManus, F. Baribaud, R.W. Doms, D. Schols, E. De Clercq, M.I. Kotlikoff, R.G. Collman, and B.D. Freedman. 2000. HIV-1 gp120 and chemokines activate ion channels in primary macrophages through CCR5 and CXCR4 stimulation. *Proc Natl Acad Sci U S A*. 97:4832-7.

Liu, R., W.A. Paxton, S. Choe, D. Ceradini, S.R. Martin, R. Horuk, M.E. MacDonald, H. Stuhlmann, R.A. Koup, and N.R. Landau. 1996. Homozygous defect in HIV-1 coreceptor accounts for resistance of some multiply-exposed individuals to HIV-1 infection. *Cell*. 86:367-77.

Liu, Y., N.V. Belkina, and S. Shaw. 2009. HIV infection of T cells: actin-in and actin-out. *Sci Signal*. 2:pe23.

Lore, K., A. Smed-Sorensen, J. Vasudevan, J.R. Mascola, and R.A. Koup. 2005. Myeloid and plasmacytoid dendritic cells transfer HIV-1 preferentially to antigen-specific CD4+ T cells. *J Exp Med*. 201:2023-33.

Louvet-Vallee, S. 2000. ERM proteins: from cellular architecture to cell signaling. *Biol Cell*. 92:305-16.

Lu, Z., J.F. Berson, Y. Chen, J.D. Turner, T. Zhang, M. Sharron, M.H. Jenks, Z. Wang, J. Kim, J. Rucker, J.A. Hoxie, S.C. Peiper, and R.W. Doms. 1997. Evolution of HIV-1 coreceptor usage through interactions with distinct CCR5 and CXCR4 domains. *Proc Natl Acad Sci U S A*. 94:6426-31.

Lundgren, J.D., M. Battegay, G. Behrens, S. De Wit, G. Guaraldi, C. Katlama, E. Martinez, D. Nair, W.G. Powderly, P. Reiss, J. Sutinen, and A. Vigano. 2008. European AIDS Clinical Society (EACS) guidelines on the prevention and management of metabolic diseases in HIV. *HIV Med*. 9:72-81.

Lusso, P. 2006. HIV and the chemokine system: 10 years later. *Embo J*. 25:447-56.

Luster, A.D. 1998. Chemokines--chemotactic cytokines that mediate inflammation. *N Engl J Med*. 338:436-45.

Maddon, P.J., J.S. McDougal, P.R. Clapham, A.G. Dalgleish, S. Jamal, R.A. Weiss, and R. Axel. 1988. HIV infection does not require endocytosis of its receptor, CD4. *Cell*. 54:865-74.

Magadan, J.G., F.J. Perez-Victoria, R. Sougrat, Y. Ye, K. Strebel, and J.S. Bonifacino. 2010. Multilayered mechanism of CD4 downregulation by HIV-1 Vpu involving distinct ER retention and ERAD targeting steps. *PLoS Pathog*. 6:e1000869.

Malinowsky, K., J. Luksza, and M.T. Dittmar. 2008. Susceptibility to virus-cell fusion at the plasma membrane is reduced through expression of HIV gp41 cytoplasmic domains. *Virology*. 376:69-78.

Manches, O., D. Munn, A. Fallahi, J. Lifson, L. Chaperot, J. Plumas, and N. Bhardwaj. 2008. HIV-activated human plasmacytoid DCs induce Tregs through an indoleamine 2,3-dioxygenase-dependent mechanism. *J Clin Invest*. 118:3431-9.

Manes, S., G. del Real, R.A. Lacalle, P. Lucas, C. Gomez-Mouton, S. Sanchez-Palomino, R. Delgado, J. Alcami, E. Mira, and A.C. Martinez. 2000. Membrane raft microdomains mediate lateral assemblies required for HIV-1 infection. *EMBO Rep*. 1:190-6.

Mangeat, P., C. Roy, and M. Martin. 1999. ERM proteins in cell adhesion and membrane dynamics. *Trends Cell Biol*. 9:187-92.

Manninen, A., M. Hiipakka, M. Vihinen, W. Lu, B.J. Mayer, and K. Saksela. 1998. SH3-Domain binding function of HIV-1 Nef is required for association with a PAK-related kinase. *Virology*. 250:273-82.

Mao, Y.S., and H.L. Yin. 2007. Regulation of the actin cytoskeleton by phosphatidylinositol 4-phosphate 5 kinases. *Pflugers Arch*. 455:5-18.

Marsh, M., and A. Helenius. 2006. Virus entry: open sesame. *Cell*. 124:729-40.

Masci, A.M., M. Galgani, S. Cassano, S. De Simone, A. Gallo, V. De Rosa, S. Zappacosta, and L. Racioppi. 2003. HIV-1 gp120 induces anergy in naive T lymphocytes through CD4-independent protein kinase-A-mediated signaling. *J Leukoc Biol*. 74:1117-24.

Matsuyama, A., T. Shimazu, Y. Sumida, A. Saito, Y. Yoshimatsu, D. Seigneurin-Berny, H. Osada, Y. Komatsu, N. Nishino, S. Khochbin, S. Horinouchi, and M. Yoshida. 2002. In vivo destabilization of dynamic microtubules by HDAC6-mediated deacetylation. *Embo J*. 21:6820-31.

McClure, M.O., M. Marsh, and R.A. Weiss. 1988. Human immunodeficiency virus infection of CD4-bearing cells occurs by a pH-independent mechanism. *Embo J*. 7:513-8.

McCutchan, F.E. 2000. Understanding the genetic diversity of HIV-1. *Aids*. 14 Suppl 3:S31-44.

McDonald, D., M.A. Vodicka, G. Lucero, T.M. Svitkina, G.G. Borisy, M. Emerman, and T.J. Hope. 2002. Visualization of the intracellular behavior of HIV in living cells. *J Cell Biol*. 159:441-52.

McMahon, H.T., and E. Boucrot. 2011. Molecular mechanism and physiological functions of clathrin-mediated endocytosis. *Nat Rev Mol Cell Biol*. 12:517-33.

McMichael, A.J., P. Borrow, G.D. Tomaras, N. Goonetilleke, and B.F. Haynes. 2010. The immune response during acute HIV-1 infection: clues for vaccine development. *Nat Rev Immunol*. 10:11-23.

Melar, M., D.E. Ott, and T.J. Hope. 2007. Physiological levels of virion-associated human immunodeficiency virus type 1 envelope induce coreceptor-dependent calcium flux. *J Virol*. 81:1773-85.

Melikyan, G.B., R.M. Markosyan, H. Hemmati, M.K. Delmedico, D.M. Lambert, and F.S. Cohen. 2000. Evidence that the transition of HIV-1 gp41 into a six-helix bundle, not the bundle configuration, induces membrane fusion. *J Cell Biol*. 151:413-23.

Mercenne, G., S. Bernacchi, D. Richer, G. Bec, S. Henriet, J.C. Paillart, and R. Marquet. 2010. HIV-1 Vif binds to APOBEC3G mRNA and inhibits its translation. *Nucleic Acids Res*. 38:633-46.

Merrifield, C.J. 2004. Seeing is believing: imaging actin dynamics at single sites of endocytosis. *Trends Cell Biol*. 14:352-8.

Merrifield, C.J., M.E. Feldman, L. Wan, and W. Almers. 2002. Imaging actin and dynamin recruitment during invagination of single clathrin-coated pits. *Nat Cell Biol*. 4:691-8.

Merrifield, C.J., D. Perrais, and D. Zenisek. 2005. Coupling between clathrin-coated-pit invagination, cortactin recruitment, and membrane scission observed in live cells. *Cell*. 121:593-606.

Meyerhans A, B.T., Vartanian J, Wain-Hobson S. 2003. Forms and functions of intracellular HIV DNA. *Theoretical Biology and Biophysics*.

Miller, M.D., M.T. Warmerdam, K.A. Page, M.B. Feinberg, and W.C. Greene. 1995. Expression of the human immunodeficiency virus type 1 (HIV-1) nef gene during HIV-1 production increases progeny particle infectivity independently of gp160 or viral entry. *J Virol*. 69:579-84.

Misse, D., M. Cerutti, N. Noraz, P. Jourdan, J. Favero, G. Devauchelle, H. Yssel, N. Taylor, and F. Veas. 1999. A CD4-independent interaction of human immunodeficiency virus-1 gp120 with CXCR4 induces their cointernalization, cell signaling, and T-cell chemotaxis. *Blood*. 93:2454-62.

Misse, D., P.O. Esteve, B. Renneboog, M. Vidal, M. Cerutti, Y. St Pierre, H. Yssel, M. Parmentier, and F. Veas. 2001. HIV-1 glycoprotein 120 induces the MMP-9 cytopathogenic factor production that is abolished by inhibition of the p38 mitogen-activated protein kinase signaling pathway. *Blood*. 98:541-7.

Mitsuya, H., K.J. Weinhold, P.A. Furman, M.H. St Clair, S.N. Lehrman, R.C. Gallo, D. Bolognesi, D.W. Barry, and S. Broder. 1985. 3'-Azido-3'-deoxythymidine (BW A509U): an antiviral agent that inhibits the infectivity and cytopathic effect of human T-lymphotropic virus type III/lymphadenopathy-associated virus in vitro. *Proc Natl Acad Sci U S A*. 82:7096-100.

Miyauchi, K., Y. Kim, O. Latinovic, V. Morozov, and G.B. Melikyan. 2009. HIV enters cells via endocytosis and dynamin-dependent fusion with endosomes. *Cell*. 137:433-44.

Moon, H.S., and J.S. Yang. 2006. Role of HIV Vpr as a regulator of apoptosis and an effector on bystander cells. *Mol Cells*. 21:7-20.

Moore, J.P., and R.W. Doms. 2003. The entry of entry inhibitors: a fusion of science and medicine. *Proc Natl Acad Sci U S A*. 100:10598-602.

Moore, J.P., J.A. McKeating, W.A. Norton, and Q.J. Sattentau. 1991. Direct measurement of soluble CD4 binding to human immunodeficiency virus type 1 virions: gp120 dissociation and its implications for virus-cell binding and fusion reactions and their neutralization by soluble CD4. *J Virol*. 65:1133-40.

Moore, J.P., A. Trkola, and T. Dragic. 1997. Co-receptors for HIV-1 entry. *Curr Opin Immunol*. 9:551-62.

Morel, E., R.G. Parton, and J. Gruenberg. 2009. Annexin A2-dependent polymerization of actin mediates endosome biogenesis. *Dev Cell*. 16:445-57.

Morita, E., and W.I. Sundquist. 2004. Retrovirus budding. *Annu Rev Cell Dev Biol*. 20:395-425.

Moutouh, L., J. Estaquier, D.D. Richman, and J. Corbeil. 1998. Molecular and cellular analysis of human immunodeficiency virus-induced apoptosis in lymphoblastoid T-cell-line-expressing wild-type and mutated CD4 receptors. *J Virol*. 72:8061-72.

Murphy, P.M., M. Baggiolini, I.F. Charo, C.A. Hebert, R. Horuk, K. Matsushima, L.H. Miller, J.J. Oppenheim, and C.A. Power. 2000. International union of pharmacology. XXII. Nomenclature for chemokine receptors. *Pharmacol Rev*. 52:145-76.

Naeger, D.M., J.N. Martin, E. Sinclair, P.W. Hunt, D.R. Bangsberg, F. Hecht, P. Hsue, J.M. McCune, and S.G. Deeks. 2010. Cytomegalovirus-specific T cells persist at very high levels during long-term antiretroviral treatment of HIV disease. *PLoS One*. 5:e8886.

Naghavi, M.H., S. Valente, T. Hatziioannou, K. de Los Santos, Y. Wen, C. Mott, G.G. Gundersen, and S.P. Goff. 2007. Moesin regulates stable microtubule formation and limits retroviral infection in cultured cells. *Embo J*. 26:41-52.

Nakamura, F., L. Huang, K. Pestonjamasp, E.J. Luna, and H. Furthmayr. 1999. Regulation of F-actin binding to platelet moesin in vitro by both phosphorylation of threonine 558 and polyphosphatidylinositides. *Mol Biol Cell*. 10:2669-85.

Neisch, A.L., and R.G. Fehon. 2011. Ezrin, Radixin and Moesin: key regulators of membrane-cortex interactions and signaling. *Curr Opin Cell Biol*. 23:377-82.

Nethe, M., B. Berkhout, and A.C. van der Kuyl. 2005. Retroviral superinfection resistance. *Retrovirology*. 2:52.

Nguyen, D.H., and J.E. Hildreth. 2000. Evidence for budding of human immunodeficiency virus type 1 selectively from glycolipid-enriched membrane lipid rafts. *J Virol*. 74:3264-72.

Nguyen, D.H., and D. Taub. 2002. CXCR4 function requires membrane cholesterol: implications for HIV infection. *J Immunol*. 168:4121-6.

Niggli, V. 2005. Regulation of protein activities by phosphoinositide phosphates. *Annu Rev Cell Dev Biol*. 21:57-79.

Oberlin, E., A. Amara, F. Bachelerie, C. Bessia, J.L. Virelizier, F. Arenzana-Seisdedos, O. Schwartz, J.M. Heard, I. Clark-Lewis, D.F. Legler, M. Loetscher, M. Baggiolini, and B. Moser. 1996. The CXC chemokine SDF-1 is the ligand for LESTR/fusin and prevents infection by T-cell-line-adapted HIV-1. *Nature*. 382:833-5.

Ohnimus, H., M. Heinkelein, and C. Jassoy. 1997. Apoptotic cell death upon contact of CD4+ T lymphocytes with HIV glycoprotein-expressing cells is mediated by caspases but bypasses CD95 (Fas/Apo-1) and TNF receptor 1. *J Immunol*. 159:5246-52.

Ono, A., S.D. Ablan, S.J. Lockett, K. Nagashima, and E.O. Freed. 2004. Phosphatidylinositol (4,5) bisphosphate regulates HIV-1 Gag targeting to the plasma membrane. *Proc Natl Acad Sci U S A*. 101:14889-94.

Ott, D.E. 2008. Cellular proteins detected in HIV-1. *Rev Med Virol*. 18:159-75.

Ott, D.E., L.V. Coren, B.P. Kane, L.K. Busch, D.G. Johnson, R.C. Sowder, 2nd, E.N. Chertova, L.O. Arthur, and L.E. Henderson. 1996. Cytoskeletal proteins inside human immunodeficiency virus type 1 virions. *J Virol*. 70:7734-43.

Oude Weernink, P.A., M. Schmidt, and K.H. Jakobs. 2004. Regulation and cellular roles of phosphoinositide 5-kinases. *Eur J Pharmacol*. 500:87-99.

Oyaizu, N., N. Chirmule, Y. Ohnishi, V.S. Kalyanaraman, and S. Pahwa. 1991. Human immunodeficiency virus type 1 envelope glycoproteins gp120 and gp160 induce interleukin-6 production in CD4+ T-cell clones. *J Virol*. 65:6277-82.

Oyaizu, N., T.W. McCloskey, S. Than, R. Hu, V.S. Kalyanaraman, and S. Pahwa. 1994. Cross-linking of CD4 molecules upregulates Fas antigen expression in lymphocytes by inducing interferon-gamma and tumor necrosis factor-alpha secretion. *Blood*. 84:2622-31.

Paxton, W., R.I. Connor, and N.R. Landau. 1993. Incorporation of Vpr into human immunodeficiency virus type 1 virions: requirement for the p6 region of gag and mutational analysis. *J Virol*. 67:7229-37.

Pelchen-Matthews, A., J.E. Armes, G. Griffiths, and M. Marsh. 1991. Differential endocytosis of CD4 in lymphocytic and nonlymphocytic cells. *J Exp Med*. 173:575-87.

Pelchen-Matthews, A., P. Clapham, and M. Marsh. 1995. Role of CD4 endocytosis in human immunodeficiency virus infection. *J Virol*. 69:8164-8.

Perlman, J.H., W. Wang, D.R. Nussenzveig, and M.C. Gershengorn. 1995. A disulfide bond between conserved extracellular cysteines in the thyrotropin-releasing hormone receptor is critical for binding. *J Biol Chem*. 270:24682-5.

Picard, L., G. Simmons, C.A. Power, A. Meyer, R.A. Weiss, and P.R. Clapham. 1997a. Multiple extracellular domains of CCR-5 contribute to human immunodeficiency virus type 1 entry and fusion. *J Virol*. 71:5003-11.

Picard, L., D.A. Wilkinson, A. McKnight, P.W. Gray, J.A. Hoxie, P.R. Clapham, and R.A. Weiss. 1997b. Role of the amino-terminal extracellular domain of CXCR-4 in human immunodeficiency virus type 1 entry. *Virology*. 231:105-11.

Pierson, T., T.L. Hoffman, J. Blankson, D. Finzi, K. Chadwick, J.B. Margolick, C. Buck, J.D. Siliciano, R.W. Doms, and R.F. Siliciano. 2000. Characterization of chemokine receptor utilization of viruses in the latent reservoir for human immunodeficiency virus type 1. *J Virol*. 74:7824-33.

Piguet, V., and Q. Sattentau. 2004. Dangerous liaisons at the virological synapse. *J Clin Invest*. 114:605-10.

Piller, S.C., G.D. Ewart, D.A. Jans, P.W. Gage, and G.B. Cox. 1999. The amino-terminal region of Vpr from human immunodeficiency virus type 1 forms ion channels and kills neurons. *J Virol*. 73:4230-8.

Poignard, P., E.O. Saphire, P.W. Parren, and D.R. Burton. 2001. gp120: Biologic aspects of structural features. *Annu Rev Immunol*. 19:253-74.

Pollard, T.D., and G.G. Borisy. 2003. Cellular motility driven by assembly and disassembly of actin filaments. *Cell*. 112:453-65.

Pontow, S., B. Harmon, N. Campbell, and L. Ratner. 2007. Antiviral activity of a Rac GEF inhibitor characterized with a sensitive HIV/SIV fusion assay. *Virology*. 368:1-6.

Pontow, S.E., N.V. Heyden, S. Wei, and L. Ratner. 2004. Actin cytoskeletal reorganizations and coreceptor-mediated activation of rac during human immunodeficiency virus-induced cell fusion. *J Virol*. 78:7138-47.

Popik, W., T.M. Alce, and W.C. Au. 2002. Human immunodeficiency virus type 1 uses lipid raft-colocalized CD4 and chemokine receptors for productive entry into CD4(+) T cells. *J Virol*. 76:4709-22.

Popik, W., J.E. Hesselgesser, and P.M. Pitha. 1998. Binding of human immunodeficiency virus type 1 to CD4 and CXCR4 receptors differentially regulates expression of inflammatory genes and activates the MEK/ERK signaling pathway. *J Virol*. 72:6406-13.

Popik, W., and P.M. Pitha. 1996. Binding of human immunodeficiency virus type 1 to CD4 induces association of Lck and Raf-1 and activates Raf-1 by a Ras-independent pathway. *Mol Cell Biol*. 16:6532-41.

Popik, W., and P.M. Pitha. 1998. Early activation of mitogen-activated protein kinase kinase, extracellular signal-regulated kinase, p38 mitogen-activated protein kinase, and c-Jun N-terminal kinase in response to binding of simian immunodeficiency virus to Jurkat T cells expressing CCR5 receptor. *Virology*. 252:210-7.

Popik, W., and P.M. Pitha. 2000. Exploitation of cellular signaling by HIV-1: unwelcome guests with master keys that signal their entry. *Virology*. 276:1-6.

Poullet, P., A. Gautreau, G. Kadare, J.A. Girault, D. Louvard, and M. Arpin. 2001. Ezrin interacts with focal adhesion kinase and induces its activation independently of cell-matrix adhesion. *J Biol Chem*. 276:37686-91.

Poupon, V., A. Stewart, S.R. Gray, R.C. Piper, and J.P. Luzio. 2003. The role of mVps18p in clustering, fusion, and intracellular localization of late endocytic organelles. *Mol Biol Cell*. 14:4015-27.

Powell, R.D., P.J. Holland, T. Hollis, and F.W. Perrino. 2011. The Aicardi-Goutieres syndrome gene and HIV-1 restriction factor SAMHD1 is a dGTP-regulated deoxynucleotide triphosphohydrolase. *J Biol Chem*.

Prasad, K.V., R. Kapeller, O. Janssen, H. Repke, J.S. Duke-Cohan, L.C. Cantley, and C.E. Rudd. 1993. Phosphatidylinositol (PI) 3-kinase and PI 4-kinase binding to the CD4-p56lck complex: the p56lck SH3 domain binds to PI 3-kinase but not PI 4-kinase. *Mol Cell Biol*. 13:7708-17.

Princen, K., and D. Schols. 2005. HIV chemokine receptor inhibitors as novel anti-HIV drugs. *Cytokine Growth Factor Rev*. 16:659-77.

Purcell, D.F., and M.A. Martin. 1993. Alternative splicing of human immunodeficiency virus type 1 mRNA modulates viral protein expression, replication, and infectivity. *J Virol*. 67:6365-78.

Quakkelaar, E.D., T. Beaumont, A.C. van Nuenen, F.P. van Alphen, B.D. Boeser-Nunnink, A.B. van 't Wout, and H. Schuitemaker. 2007. T cell line passage can select for pre-existing neutralization-sensitive variants from the quasispecies of primary human immunodeficiency virus type-1 isolates. *Virology*. 359:92-104.

Quirk, E., H. McLeod, and W. Powderly. 2004. The pharmacogenetics of antiretroviral therapy: a review of studies to date. *Clin Infect Dis*. 39:98-106.

Rabinovitch, M. 1995. Professional and non-professional phagocytes: an introduction. *Trends Cell Biol*. 5:85-7.

Rabut, G.E., J.A. Konner, F. Kajumo, J.P. Moore, and T. Dragic. 1998. Alanine substitutions of polar and nonpolar residues in the amino-terminal domain of CCR5 differently impair entry of macrophage- and dualtropic isolates of human immunodeficiency virus type 1. *J Virol*. 72:3464-8.

Raucher, D., T. Stauffer, W. Chen, K. Shen, S. Guo, J.D. York, M.P. Sheetz, and T. Meyer. 2000. Phosphatidylinositol 4,5-bisphosphate functions as a second messenger that regulates cytoskeleton-plasma membrane adhesion. *Cell*. 100:221-8.

Reitter, J.N., R.E. Means, and R.C. Desrosiers. 1998. A role for carbohydrates in immune evasion in AIDS. *Nat Med*. 4:679-84.

Renkema, G.H., A. Manninen, and K. Saksela. 2001. Human immunodeficiency virus type 1 Nef selectively associates with a catalytically active subpopulation of p21-activated kinase 2 (PAK2) independently of PAK2 binding to Nck or beta-PIX. *J Virol*. 75:2154-60.

Rey, M., A. Valenzuela-Fernandez, A. Urzainqui, M. Yanez-Mo, M. Perez-Martinez, P. Penela, F. Mayor, Jr., and F. Sanchez-Madrid. 2007. Myosin IIA is involved in the endocytosis of CXCR4 induced by SDF-1alpha. *J Cell Sci*. 120:1126-33.

Rey, M., M. Vicente-Manzanares, F. Viedma, M. Yanez-Mo, A. Urzainqui, O. Barreiro, J. Vazquez, and F. Sanchez-Madrid. 2002. Cutting edge: association of the motor protein nonmuscle myosin heavy chain-IIA with the C terminus of the chemokine receptor CXCR4 in T lymphocytes. *J Immunol*. 169:5410-4.

Richman, D.D., T. Wrin, S.J. Little, and C.J. Petropoulos. 2003. Rapid evolution of the neutralizing antibody response to HIV type 1 infection. *Proc Natl Acad Sci U S A*. 100:4144-9.

Ridley, A.J., and A. Hall. 1992. The small GTP-binding protein rho regulates the assembly of focal adhesions and actin stress fibers in response to growth factors. *Cell*. 70:389-99.

Ridley, A.J., H.F. Paterson, C.L. Johnston, D. Diekmann, and A. Hall. 1992. The small GTP-binding protein rac regulates growth factor-induced membrane ruffling. *Cell*. 70:401-10.

Rink, J., E. Ghigo, Y. Kalaidzidis, and M. Zerial. 2005. Rab conversion as a mechanism of progression from early to late endosomes. *Cell*. 122:735-49.

Rizzuto, C.D., R. Wyatt, N. Hernandez-Ramos, Y. Sun, P.D. Kwong, W.A. Hendrickson, and J. Sodroski. 1998. A conserved HIV gp120 glycoprotein structure involved in chemokine receptor binding. *Science*. 280:1949-53.

Robertson, D.L., J.P. Anderson, J.A. Bradac, J.K. Carr, B. Foley, R.K. Funkhouser, F. Gao, B.H. Hahn, M.L. Kalish, C. Kuiken, G.H. Learn, T. Leitner, F. McCutchan, S. Osmanov, M. Peeters, D. Pieniazek, M. Salminen, P.M. Sharp, S. Wolinsky, and B. Korber. 2000. HIV-1 nomenclature proposal. *Science*. 288:55-6.

Roderiquez, G., T. Oravecz, M. Yanagishita, D.C. Bou-Habib, H. Mostowski, and M.A. Norcross. 1995. Mediation of human immunodeficiency virus type 1 binding by interaction of cell surface heparan sulfate proteoglycans with the V3 region of envelope gp120-gp41. *J Virol*. 69:2233-9.

Roy, J., G. Martin, J.F. Giguere, D. Belanger, M. Petrin, and M.J. Tremblay. 2005. HIV type 1 can act as an APC upon acquisition from the host cell of peptide-loaded HLA-DR and CD86 molecules. *J Immunol*. 174:4779-88.

Ruben, S., A. Perkins, R. Purcell, K. Joung, R. Sia, R. Burghoff, W.A. Haseltine, and C.A. Rosen. 1989. Structural and functional characterization of human immunodeficiency virus tat protein. *J Virol*. 63:1-8.

Rucker, J., M. Samson, B.J. Doranz, F. Libert, J.F. Berson, Y. Yi, R.J. Smyth, R.G. Collman, C.C. Broder, G. Vassart, R.W. Doms, and M. Parmentier. 1996. Regions in beta-chemokine receptors CCR5 and CCR2b that determine HIV-1 cofactor specificity. *Cell*. 87:437-46.

Russell, J.H., and T.J. Ley. 2002. Lymphocyte-mediated cytotoxicity. *Annu Rev Immunol*. 20:323-70.

Saarikangas, J., H. Zhao, and P. Lappalainen. 2010. Regulation of the actin cytoskeleton-plasma membrane interplay by phosphoinositides. *Physiol Rev*. 90:259-89.

Saez-Cirion, A., G. Pancino, M. Sinet, A. Venet, and O. Lambotte. 2007. HIV controllers: how do they tame the virus? *Trends Immunol*. 28:532-40.

Saifuddin, M., C.J. Parker, M.E. Peeples, M.K. Gorny, S. Zolla-Pazner, M. Ghassemi, I.A. Rooney, J.P. Atkinson, and G.T. Spear. 1995. Role of virion-associated glycosylphosphatidylinositol-linked proteins CD55 and CD59 in complement resistance of cell line-derived and primary isolates of HIV-1. *J Exp Med*. 182:501-9.

Saleh, S., A. Solomon, F. Wightman, M. Xhilaga, P.U. Cameron, and S.R. Lewin. 2007. CCR7 ligands CCL19 and CCL21 increase permissiveness of resting memory CD4+ T cells to HIV-1 infection: a novel model of HIV-1 latency. *Blood*. 110:4161-4.

Salzwedel, K., E.D. Smith, B. Dey, and E.A. Berger. 2000. Sequential CD4-coreceptor interactions in human immunodeficiency virus type 1 Env function: soluble CD4 activates Env for coreceptor-dependent fusion and reveals blocking activities of antibodies against cryptic conserved epitopes on gp120. *J Virol*. 74:326-33.

Samson, M., F. Libert, B.J. Doranz, J. Rucker, C. Liesnard, C.M. Farber, S. Saragosti, C. Lapoumeroulie, J. Cognaux, C. Forceille, G. Muyldermans, C. Verhofstede, G. Burtonboy, M. Georges, T. Imai, S. Rana, Y. Yi, R.J. Smyth, R.G. Collman, R.W. Doms, G. Vassart, and M. Parmentier. 1996. Resistance to HIV-1 infection in caucasian individuals bearing mutant alleles of the CCR-5 chemokine receptor gene. *Nature*. 382:722-5.

Scarlatti, G. 2004. Mother-to-child transmission of HIV-1: advances and controversies of the twentieth centuries. *AIDS Rev*. 6:67-78.

Schafer, D.A. 2002. Coupling actin dynamics and membrane dynamics during endocytosis. *Curr Opin Cell Biol*. 14:76-81.

Schmid-Antomarchi, H., M. Benkirane, V. Breittmayer, H. Husson, M. Ticchioni, C. Devaux, and B. Rossi. 1996. HIV induces activation of phosphatidylinositol 4-kinase and mitogen-activated protein kinase by interacting with T cell CD4 surface molecules. *Eur J Immunol*. 26:717-20.

Schmid, E.M., M.G. Ford, A. Burtey, G.J. Praefcke, S.Y. Peak-Chew, I.G. Mills, A. Benmerah, and H.T. McMahon. 2006. Role of the AP2 beta-appendage hub in recruiting partners for clathrin-coated vesicle assembly. *PLoS Biol*. 4:e262.

Schroder, A.R., P. Shinn, H. Chen, C. Berry, J.R. Ecker, and F. Bushman. 2002. HIV-1 integration in the human genome favors active genes and local hotspots. *Cell*. 110:521-9.

Schubert, U., D.E. Ott, E.N. Chertova, R. Welker, U. Tessmer, M.F. Princiotta, J.R. Bennink, H.G. Krausslich, and J.W. Yewdell. 2000. Proteasome inhibition interferes with gag polyprotein processing, release, and maturation of HIV-1 and HIV-2. *Proc Natl Acad Sci U S A*. 97:13057-62.

Schuitemaker, H., M. Koot, N.A. Kootstra, M.W. Dercksen, R.E. de Goede, R.P. van Steenwijk, J.M. Lange, J.K. Schattenkerk, F. Miedema, and M. Tersmette. 1992. Biological phenotype of human immunodeficiency virus type 1 clones at different stages of infection: progression of disease is associated with a shift from monocytotropic to T-cell-tropic virus population. *J Virol*. 66:1354-60.

Schuitemaker, H., A.B. van 't Wout, and P. Lusso. 2011. Clinical significance of HIV-1 coreceptor usage. *J Transl Med*. 9 Suppl 1:S5.

Schwartz, O., V. Marechal, O. Danos, and J.M. Heard. 1995. Human immunodeficiency virus type 1 Nef increases the efficiency of reverse transcription in the infected cell. *J Virol*. 69:4053-9.

Seto, M., K. Aikawa, N. Miyamoto, Y. Aramaki, N. Kanzaki, K. Takashima, Y. Kuze, Y. Iizawa, M. Baba, and M. Shiraishi. 2006. Highly potent and orally active CCR5 antagonists as anti-HIV-1 agents: synthesis and biological activities of 1-benzazocine derivatives containing a sulfoxide moiety. *J Med Chem*. 49:2037-48.

Shankarappa, R., J.B. Margolick, S.J. Gange, A.G. Rodrigo, D. Upchurch, H. Farzadegan, P. Gupta, C.R. Rinaldo, G.H. Learn, X. He, X.L. Huang, and J.I. Mullins. 1999. Consistent viral evolutionary changes associated with the progression of human immunodeficiency virus type 1 infection. *J Virol*. 73:10489-502.

Shcherbina, A., A. Bretscher, D.M. Kenney, and E. Remold-O'Donnell. 1999. Moesin, the major ERM protein of lymphocytes and platelets, differs from ezrin in its insensitivity to calpain. *FEBS Lett*. 443:31-6.

Siegal, F.P., N. Kadowaki, M. Shodell, P.A. Fitzgerald-Bocarsly, K. Shah, S. Ho, S. Antonenko, and Y.J. Liu. 1999. The nature of the principal type 1 interferon-producing cells in human blood. *Science*. 284:1835-7.

Siliciano, J.D., and R.F. Siliciano. 2000. Latency and viral persistence in HIV-1 infection. *J Clin Invest*. 106:823-5.

Simon, M.I., M.P. Strathmann, and N. Gautam. 1991. Diversity of G proteins in signal transduction. *Science*. 252:802-8.

Simon, V., D.D. Ho, and Q. Abdool Karim. 2006. HIV/AIDS epidemiology, pathogenesis, prevention, and treatment. *Lancet*. 368:489-504.

Simons, P.C., S.F. Pietromonaco, D. Reczek, A. Bretscher, and L. Elias. 1998. C-terminal threonine phosphorylation activates ERM proteins to link the cell's cortical lipid bilayer to the cytoskeleton. *Biochem Biophys Res Commun*. 253:561-5.

Singer, II, S. Scott, D.W. Kawka, J. Chin, B.L. Daugherty, J.A. DeMartino, J. DiSalvo, S.L. Gould, J.E. Lineberger, L. Malkowitz, M.D. Miller, L. Mitnaul, S.J. Siciliano,

M.J. Staruch, H.R. Williams, H.J. Zweerink, and M.S. Springer. 2001. CCR5, CXCR4, and CD4 are clustered and closely apposed on microvilli of human macrophages and T cells. *J Virol*. 75:3779-90.

Singh, A., and R.G. Collman. 2000. Heterogeneous spectrum of coreceptor usage among variants within a dualtropic human immunodeficiency virus type 1 primary-isolate quasispecies. *J Virol*. 74:10229-35.

Smith, D.M., D.D. Richman, and S.J. Little. 2005. HIV superinfection. *J Infect Dis*. 192:438-44.

Soler, F., C. Poujade, M. Evers, J.C. Carry, Y. Henin, A. Bousseau, T. Huet, R. Pauwels, E. De Clercq, J.F. Mayaux, J.B. Le Pecq, and N. Dereu. 1996. Betulinic acid derivatives: a new class of specific inhibitors of human immunodeficiency virus type 1 entry. *J Med Chem*. 39:1069-83.

Sougrat, R., A. Bartesaghi, J.D. Lifson, A.E. Bennett, J.W. Bess, D.J. Zabransky, and S. Subramaniam. 2007. Electron tomography of the contact between T cells and SIV/HIV-1: implications for viral entry. *PLoS Pathog*. 3:e63.

Soumelis, V., I. Scott, F. Gheyas, D. Bouhour, G. Cozon, L. Cotte, L. Huang, J.A. Levy, and Y.J. Liu. 2001. Depletion of circulating natural type 1 interferon-producing cells in HIV-infected AIDS patients. *Blood*. 98:906-12.

Spina, C.A., T.J. Kwoh, M.Y. Chowers, J.C. Guatelli, and D.D. Richman. 1994. The importance of nef in the induction of human immunodeficiency virus type 1 replication from primary quiescent CD4 lymphocytes. *J Exp Med*. 179:115-23.

Stanasila, L., L. Abuin, D. Diviani, and S. Cotecchia. 2006. Ezrin directly interacts with the alpha1b-adrenergic receptor and plays a role in receptor recycling. *J Biol Chem*. 281:4354-63.

Stantchev, T.S., and C.C. Broder. 2001. Human immunodeficiency virus type-1 and chemokines: beyond competition for common cellular receptors. *Cytokine Growth Factor Rev*. 12:219-43.

Steffens, C.M., and T.J. Hope. 2003. Localization of CD4 and CCR5 in living cells. *J Virol*. 77:4985-91.

Stein, B.S., S.D. Gowda, J.D. Lifson, R.C. Penhallow, K.G. Bensch, and E.G. Engleman. 1987. pH-independent HIV entry into CD4-positive T cells via virus envelope fusion to the plasma membrane. *Cell*. 49:659-68.

Stevens, M., E. De Clercq, and J. Balzarini. 2006. The regulation of HIV-1 transcription: molecular targets for chemotherapeutic intervention. *Med Res Rev*. 26:595-625.

Stolp, B., M. Reichman-Fried, L. Abraham, X. Pan, S.I. Giese, S. Hannemann, P. Goulimari, E. Raz, R. Grosse, and O.T. Fackler. 2009. HIV-1 Nef interferes with host cell motility by deregulation of Cofilin. *Cell Host Microbe*. 6:174-86.

Stopak, K., C. de Noronha, W. Yonemoto, and W.C. Greene. 2003. HIV-1 Vif blocks the antiviral activity of APOBEC3G by impairing both its translation and intracellular stability. *Mol Cell*. 12:591-601.

Su, S.B., W. Gong, M. Grimm, I. Utsunomiya, R. Sargeant, J.J. Oppenheim, and J. Ming Wang. 1999. Inhibition of tyrosine kinase activation blocks the down-regulation of CXC chemokine receptor 4 by HIV-1 gp120 in CD4+ T cells. *J Immunol*. 162:7128-32.

Tamma, S.M., N. Chirmule, H. Yagura, N. Oyaizu, V. Kalyanaraman, and S. Pahwa. 1997. CD4 cross-linking (CD4XL) induces RAS activation and tumor necrosis factor-alpha secretion in CD4+ T cells. *Blood*. 90:1588-93.

Taylor, M.P., O.O. Koyuncu, and L.W. Enquist. 2011. Subversion of the actin cytoskeleton during viral infection. *Nat Rev Microbiol*. 9:427-39.

Thoulouze, M.I., N. Sol-Foulon, F. Blanchet, A. Dautry-Varsat, O. Schwartz, and A. Alcover. 2006. Human immunodeficiency virus type-1 infection impairs the formation of the immunological synapse. *Immunity*. 24:547-61.

Tokunaga, K., M.L. Greenberg, M.A. Morse, R.I. Cumming, H.K. Lyerly, and B.R. Cullen. 2001. Molecular basis for cell tropism of CXCR4-dependent human immunodeficiency virus type 1 isolates. *J Virol*. 75:6776-85.

Trkola, A., T. Dragic, J. Arthos, J.M. Binley, W.C. Olson, G.P. Allaway, C. Cheng-Mayer, J. Robinson, P.J. Maddon, and J.P. Moore. 1996. CD4-dependent, antibody-sensitive interactions between HIV-1 and its co-receptor CCR-5. *Nature*. 384:184-7.

Trono, D. 1995. HIV accessory proteins: leading roles for the supporting cast. *Cell*. 82:189-92.

Trushin, S.A., G.D. Bren, and A.D. Badley. 2010. CXCR4 Tropic HIV-1 gp120 Inhibition of SDF-1alpha-Induced Chemotaxis Requires Lck and is Associated with Cofilin Phosphorylation. *Open Virol J*. 4:157-62.

Turlure, F., E. Devroe, P.A. Silver, and A. Engelman. 2004. Human cell proteins and human immunodeficiency virus DNA integration. *Front Biosci*. 9:3187-208.

Turner, B.G., and M.F. Summers. 1999. Structural biology of HIV. *J Mol Biol*. 285:1-32.

Ugolini, S., M. Moulard, I. Mondor, N. Barois, D. Demandolx, J. Hoxie, A. Brelot, M. Alizon, J. Davoust, and Q.J. Sattentau. 1997. HIV-1 gp120 induces an association between CD4 and the chemokine receptor CXCR4. *J Immunol*. 159:3000-8.

Valenzuela-Fernandez, A., S. Alvarez, M. Gordon-Alonso, M. Barrero, A. Ursa, J.R. Cabrero, G. Fernandez, S. Naranjo-Suarez, M. Yanez-Mo, J.M. Serrador, M.A. Munoz-Fernandez, and F. Sanchez-Madrid. 2005. Histone deacetylase 6 regulates human immunodeficiency virus type 1 infection. *Mol Biol Cell*. 16:5445-54.

Valenzuela-Fernandez, A., T. Planchenault, F. Baleux, I. Staropoli, K. Le-Barillec, D. Leduc, T. Delaunay, F. Lazarini, J.L. Virelizier, M. Chignard, D. Pidard, and F. Arenzana-Seisdedos. 2002. Leukocyte elastase negatively regulates Stromal cell-derived factor-1 (SDF-1)/CXCR4 binding and functions by amino-terminal processing of SDF-1 and CXCR4. *J Biol Chem*. 277:15677-89.

Valenzuela, A., J. Blanco, B. Krust, R. Franco, and A.G. Hovanessian. 1997. Neutralizing antibodies against the V3 loop of human immunodeficiency virus type 1 gp120 block the CD4-dependent and -independent binding of virus to cells. *J Virol*. 71:8289-98.

van Deventer, H.W., Q.P. Wu, D.T. Bergstralh, B.K. Davis, B.P. O'Connor, J.P. Ting, and J.S. Serody. 2008. C-C chemokine receptor 5 on pulmonary fibrocytes facilitates migration and promotes metastasis via matrix metalloproteinase 9. *Am J Pathol*. 173:253-64.

van Rheenen, J., X. Song, W. van Roosmalen, M. Cammer, X. Chen, V. Desmarais, S.C. Yip, J.M. Backer, R.J. Eddy, and J.S. Condeelis. 2007. EGF-induced PIP2 hydrolysis releases and activates cofilin locally in carcinoma cells. *J Cell Biol*. 179:1247-59.

Vasiliver-Shamis, G., M. Tuen, T.W. Wu, T. Starr, T.O. Cameron, R. Thomson, G. Kaur, J. Liu, M.L. Visciano, H. Li, R. Kumar, R. Ansari, D.P. Han, M.W. Cho, M.L. Dustin, and C.E. Hioe. 2008. Human immunodeficiency virus type 1 envelope gp120 induces a stop signal and virological synapse formation in noninfected CD4+ T cells. *J Virol*. 82:9445-57.

Veazey, R.S., M. DeMaria, L.V. Chalifoux, D.E. Shvetz, D.R. Pauley, H.L. Knight, M. Rosenzweig, R.P. Johnson, R.C. Desrosiers, and A.A. Lackner. 1998. Gastrointestinal tract as a major site of CD4+ T cell depletion and viral replication in SIV infection. *Science*. 280:427-31.

Viard, M., I. Parolini, M. Sargiacomo, K. Fecchi, C. Ramoni, S. Ablan, F.W. Ruscetti, J.M. Wang, and R. Blumenthal. 2002. Role of cholesterol in human immunodeficiency virus type 1 envelope protein-mediated fusion with host cells. *J Virol*. 76:11584-95.

Vorster, P.J., J. Guo, A. Yoder, W. Wang, Y. Zheng, X. Xu, D. Yu, M. Spear, and Y. Wu. 2011. LIM kinase 1 modulates cortical actin and CXCR4 cycling and is activated by HIV-1 to initiate viral infection. *J Biol Chem*. 286:12554-64.

Wang, J., R. Alvarez, G. Roderiquez, E. Guan, and M.A. Norcross. 2004. Constitutive association of cell surface CCR5 and CXCR4 in the presence of CD4. *J Cell Biochem*. 93:753-60.

Wang, J.M., H. Ueda, O.M. Howard, M.C. Grimm, O. Chertov, X. Gong, W. Gong, J.H. Resau, C.C. Broder, G. Evans, L.O. Arthur, F.W. Ruscetti, and J.J. Oppenheim. 1998. HIV-1 envelope gp120 inhibits the monocyte response to chemokines through CD4 signal-dependent chemokine receptor down-regulation. *J Immunol*. 161:4309-17.

Wang, L., H. Zhang, P.A. Solski, M.J. Hart, C.J. Der, and L. Su. 2000. Modulation of HIV-1 replication by a novel RhoA effector activity. *J Immunol*. 164:5369-74.

Wei, B.L., P.W. Denton, E. O'Neill, T. Luo, J.L. Foster, and J.V. Garcia. 2005. Inhibition of lysosome and proteasome function enhances human immunodeficiency virus type 1 infection. *J Virol*. 79:5705-12.

Weinman, E.J., R.A. Hall, P.A. Friedman, L.Y. Liu-Chen, and S. Shenolikar. 2006. The association of NHERF adaptor proteins with g protein-coupled receptors and receptor tyrosine kinases. *Annu Rev Physiol*. 68:491-505.

Wen, W., S. Chen, Y. Cao, Y. Zhu, and Y. Yamamoto. 2005. HIV-1 infection initiates changes in the expression of a wide array of genes in U937 promonocytes and HUT78 T cells. *Virus Res*. 113:26-35.

Weng, J., D.N. Krementsov, S. Khurana, N.H. Roy, and M. Thali. 2009. Formation of syncytia is repressed by tetraspanins in human immunodeficiency virus type 1-producing cells. *J Virol*. 83:7467-74.

Wild, C.T., D.C. Shugars, T.K. Greenwell, C.B. McDanal, and T.J. Matthews. 1994. Peptides corresponding to a predictive alpha-helical domain of human immunodeficiency virus type 1 gp41 are potent inhibitors of virus infection. *Proc Natl Acad Sci U S A*. 91:9770-4.

Wilk, T., B. Gowen, and S.D. Fuller. 1999. Actin associates with the nucleocapsid domain of the human immunodeficiency virus Gag polyprotein. *J Virol*. 73:1931-40.

Willey, R.L., F. Maldarelli, M.A. Martin, and K. Strebel. 1992. Human immunodeficiency virus type 1 Vpu protein induces rapid degradation of CD4. *J Virol*. 66:7193-200.

Wong, J.K., M. Hezareh, H.F. Gunthard, D.V. Havlir, C.C. Ignacio, C.A. Spina, and D.D. Richman. 1997. Recovery of replication-competent HIV despite prolonged suppression of plasma viremia. *Science*. 278:1291-5.

Wu, L., N.P. Gerard, R. Wyatt, H. Choe, C. Parolin, N. Ruffing, A. Borsetti, A.A. Cardoso, E. Desjardin, W. Newman, C. Gerard, and J. Sodroski. 1996. CD4-induced interaction of primary HIV-1 gp120 glycoproteins with the chemokine receptor CCR-5. *Nature*. 384:179-83.

Wu, L., W.A. Paxton, N. Kassam, N. Ruffing, J.B. Rottman, N. Sullivan, H. Choe, J. Sodroski, W. Newman, R.A. Koup, and C.R. Mackay. 1997. CCR5 levels and expression pattern correlate with infectability by macrophage-tropic HIV-1, in vitro. *J Exp Med*. 185:1681-91.

Wu, Y., and A. Yoder. 2009. Chemokine coreceptor signaling in HIV-1 infection and pathogenesis. *PLoS Pathog*. 5:e1000520.

Wyatt, R., and J. Sodroski. 1998. The HIV-1 envelope glycoproteins: fusogens, antigens, and immunogens. *Science*. 280:1884-8.

Xiao, X., L. Wu, T.S. Stantchev, Y.R. Feng, S. Ugolini, H. Chen, Z. Shen, J.L. Riley, C.C. Broder, Q.J. Sattentau, and D.S. Dimitrov. 1999. Constitutive cell surface association between CD4 and CCR5. *Proc Natl Acad Sci U S A*. 96:7496-501.

Xiong, W., and J.T. Parsons. 1997. Induction of apoptosis after expression of PYK2, a tyrosine kinase structurally related to focal adhesion kinase. *J Cell Biol*. 139:529-39.

Yamada, H., T. Abe, S.A. Li, Y. Masuoka, M. Isoda, M. Watanabe, Y. Nasu, H. Kumon, A. Asai, and K. Takei. 2009. Dynasore, a dynamin inhibitor, suppresses lamellipodia formation and cancer cell invasion by destabilizing actin filaments. *Biochem Biophys Res Commun*. 390:1142-8.

Yang, N., O. Higuchi, K. Ohashi, K. Nagata, A. Wada, K. Kangawa, E. Nishida, and K. Mizuno. 1998. Cofilin phosphorylation by LIM-kinase 1 and its role in Rac-mediated actin reorganization. *Nature*. 393:809-12.

Yankulov, K., J. Blau, T. Purton, S. Roberts, and D.L. Bentley. 1994. Transcriptional elongation by RNA polymerase II is stimulated by transactivators. *Cell*. 77:749-59.

Yarar, D., C.M. Waterman-Storer, and S.L. Schmid. 2005. A dynamic actin cytoskeleton functions at multiple stages of clathrin-mediated endocytosis. *Mol Biol Cell*. 16:964-75.

Yin, H.L., and P.A. Janmey. 2003. Phosphoinositide regulation of the actin cytoskeleton. *Annu Rev Physiol*. 65:761-89.

Yoder, A., D. Yu, L. Dong, S.R. Iyer, X. Xu, J. Kelly, J. Liu, W. Wang, P.J. Vorster, L. Agulto, D.A. Stephany, J.N. Cooper, J.W. Marsh, and Y. Wu. 2008. HIV envelope-CXCR4 signaling activates cofilin to overcome cortical actin restriction in resting CD4 T cells. *Cell*. 134:782-92.

Yonemura, S., S. Tsukita, and S. Tsukita. 1999. Direct involvement of ezrin/radixin/moesin (ERM)-binding membrane proteins in the organization of microvilli in collaboration with activated ERM proteins. *J Cell Biol*. 145:1497-509.

Yonezawa, A., M. Cavrois, and W.C. Greene. 2005. Studies of ebola virus glycoprotein-mediated entry and fusion by using pseudotyped human immunodeficiency virus type 1 virions: involvement of cytoskeletal proteins and enhancement by tumor necrosis factor alpha. *J Virol*. 79:918-26.

Yoshida, H., Y. Koga, Y. Moroi, G. Kimura, and K. Nomoto. 1992. The effect of p56lck, a lymphocyte specific protein tyrosine kinase, on the syncytium formation induced by human immunodeficiency virus envelope glycoprotein. *Int Immunol*. 4:233-42.

Yoshida, S., S. Bartolini, and D. Pellman. 2009. Mechanisms for concentrating Rho1 during cytokinesis. *Genes Dev*. 23:810-23.

Yu, D., W. Wang, A. Yoder, M. Spear, and Y. Wu. 2009. The HIV envelope but not VSV glycoprotein is capable of mediating HIV latent infection of resting CD4 T cells. *PLoS Pathog*. 5:e1000633.

Zennou, V., C. Petit, D. Guetard, U. Nerhbass, L. Montagnier, and P. Charneau. 2000. HIV-1 genome nuclear import is mediated by a central DNA flap. *Cell*. 101:173-85.

Zhang, L., X. Jia, X. Zhang, J. Sun, X. Peng, T. Qi, F. Ma, L. Yin, Y. Yao, C. Qiu, and H. Lu. 2010. Proteomic analysis of PBMCs: characterization of potential HIV-associated proteins. *Proteome Sci*. 8:12.

Zhao, H., H. Shiue, S. Palkon, Y. Wang, P. Cullinan, J.K. Burkhardt, M.W. Musch, E.B. Chang, and J.R. Turner. 2004. Ezrin regulates NHE3 translocation and activation after Na+-glucose cotransport. *Proc Natl Acad Sci U S A*. 101:9485-90.

Zhou, J., X. Yuan, D. Dismuke, B.M. Forshey, C. Lundquist, K.H. Lee, C. Aiken, and C.H. Chen. 2004. Small-molecule inhibition of human immunodeficiency virus type 1 replication by specific targeting of the final step of virion maturation. *J Virol*. 78:922-9.

Zhou, M., M.A. Halanski, M.F. Radonovich, F. Kashanchi, J. Peng, D.H. Price, and J.N. Brady. 2000. Tat modifies the activity of CDK9 to phosphorylate serine 5 of the RNA polymerase II carboxyl-terminal domain during human immunodeficiency virus type 1 transcription. *Mol Cell Biol*. 20:5077-86.

Zhou, R., L. Zhu, A. Kodani, P. Hauser, X. Yao, and J.G. Forte. 2005. Phosphorylation of ezrin on threonine 567 produces a change in secretory phenotype and repolarizes the gastric parietal cell. *J Cell Sci*. 118:4381-91.

Zoncu, R., R.M. Perera, R. Sebastian, F. Nakatsu, H. Chen, T. Balla, G. Ayala, D. Toomre, and P.V. De Camilli. 2007. Loss of endocytic clathrin-coated pits upon acute depletion of phosphatidylinositol 4,5-bisphosphate. *Proc Natl Acad Sci U S A*. 104:3793-8.

7. ANEXOS

ANEXO 1:

La actividad productora de PIP_2 por la quinasa PI4P5-K Iα, inducida por la proteína de la envuelta viral gp120 del VIH-1, activa moesina aumentando su nivel de fosforilación.

Como se ha descrito durante esta Tesis Doctoral, el VIH-1, a través de la activación de la quinasa PI4P5-K Iα, estimula la producción localizada de PIP_2 en las zonas de contacto virus-célula. Además, mostramos que en esa misma zona tiene lugar el reclutamiento y activación, por fosforilación, de la proteína adaptadora de F-actina moesina, quien posteriormente se encarga del agrupamiento e interacción entre CD4 y CXCR4 de manera dependiente del citoesqueleto de actina en las zonas de contacto virus-célula, favoreciendo la fusión, entrada e infección por el VIH-1. Como el PIP_2 es una de las moléculas clave en la activación de las proteínas de la familia de las ERM (revisado en (Fehon et al., 2010)), estudiamos el efecto de la sobreexpresión de una construcción funcional (wt) y un dominante inactivo (D/A) de la quinasa PI4P5-K Iα sobre la activación y el estado de forforilación de moesina y ezrina inducido por la envuelta gp120 del VIH-1. Nuestros resultados muestras que la expresión en linfocitos T $CD4^+$ de una construcción funcional de la quinasa PI4P5-K Iα (Anexo 1A, wt-PI4P5-K Iα) potencia la activación de moesina inducida por la proteína gp120, como se observa por los niveles tan bajos o casi indetectables de fosforilación de las ERM (Anexo 1B, (-/+) gp120 en wt-PI4P5-K Iα), mientras que la expresión de un dominante inactivo de la quinasa (Anexo 1A, D/A-PI4P5-K Iα) inhibe la activación de moesina por gp120 (Anexo 1B, condición (-/+) gp120 en D/A-PI4P5-K Iα). Con estos resultados, podemos concluir que la activación de la quinasa PI4P5-K Iα por el VIH-1, y la consiguiente producción de PIP_2, representa un requisito fundamental para la activación de moesina y su implicación funcional durante la fusión, entrada e infección viral productiva por el VIH-1. Por tanto, moesina se activa por PIP_2, producción dependiente de PI4P5-K Iα y gracias a la acción del VIH-1 durante los primeros estadios de infección, siendo la fosforilación de moesina un “readout” del nivel de activación de esta ERM.

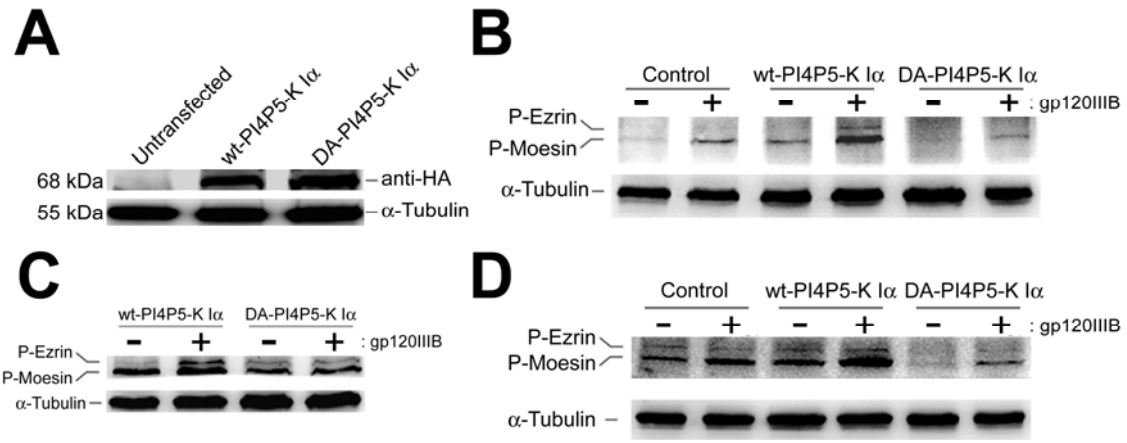

Anexo 1: La sobreexpresión de la quinasa funcional PI4P5-K Iα potencia la fosforilación de moesina en respuesta a la proteína de la envuelta viral gp120, mientras que la expresión de un dominante inactivo de la quinasa, D/A-PI4P5-K Iα, bloquea la activación de moesina por el VIH-1. A) "*Western blot*" representativo del nivel de expresión de las construcciones funcional (wt) y dominante inactivo (D/A) de la quinasa PI4P5-K Iα en linfocitos T $CD4^+$. B) Efecto de la sobreexpresión de la quinasa wt-PI4P5-K Iα y un dominante inactivo de la quinasa (D/A-PI4P5-K Iα) sobre la fosforilación de las proteínas ezrina y moesina inducida por la proteína de la envuelta del VIH-1 gp120. C y D) Repeticiones de los experimentos mostrados en B.

ANEXO 2:

HIV-1 requires Arf6-mediated membrane dynamics to efficiently enter and infect T lymphocytes

Laura García-Expósito[a,*], Jonathan Barroso-González[a,*], Isabel Puigdomènech[b], José-David Machado[a], Julià Blanco[b], and Agustín Valenzuela-Fernández[a]

[a]Laboratorio de Inmunología Celular y Viral, Laboratorio de Neurosecreción, Unidad de Farmacología, Departamento de Medicina Física y Farmacología, Facultad de Medicina, Instituto de Tecnologías Biomédicas, Universidad de La Laguna, Campus de Ofra s/n, Tenerife 38071, Spain; [b]Fundació irsiCaixa-HIVACAT, Institut de Recerca en Ciències de la Salut Germans Trias i Pujol, Hospital Germans Trias i Pujol, Universitat Autònoma de Barcelona, Badalona 08916, Barcelona, Catalonia, Spain

ABSTRACT As the initial barrier to viral entry, the plasma membrane along with the membrane trafficking machinery and cytoskeleton are of fundamental importance in the viral cycle. However, little is known about the contribution of plasma membrane dynamics during early human immunodeficiency virus type 1 (HIV-1) infection. Considering that ADP ribosylation factor 6 (Arf6) regulates cellular invasion via several microorganisms by coordinating membrane trafficking, our aim was to study the function of Arf6-mediated membrane dynamics on HIV-1 entry and infection of T lymphocytes. We observed that an alteration of the Arf6–guanosine 5′-diphosphate/guanosine 5′-triphosphate (GTP/GDP) cycle, by GDP-bound or GTP-bound inactive mutants or by specific Arf6 silencing, inhibited HIV-1 envelope–induced membrane fusion, entry, and infection of T lymphocytes and permissive cells, regardless of viral tropism. Furthermore, cell-to-cell HIV-1 transmission of primary human CD4+ T lymphocytes was inhibited by Arf6 knockdown. Total internal reflection fluorescence microscopy showed that Arf6 mutants provoked the accumulation of phosphatidylinositol-(4,5)-biphosphate–associated structures on the plasma membrane of permissive cells, without affecting CD4-viral attachment but impeding CD4-dependent HIV-1 entry. Arf6 silencing or its mutants did not affect fusion, entry, and infection of vesicular stomatitis virus G–pseudotyped viruses or ligand-induced CXCR4 or CCR5 endocytosis, both clathrin-dependent processes. Therefore we propose that efficient early HIV-1 infection of CD4+ T lymphocytes requires Arf6-coordinated plasma membrane dynamics that promote viral fusion and entry.

Monitoring Editor
Jean E. Gruenberg
University of Geneva

Received: Aug 25, 2010
Revised: Feb 1, 2011
Accepted: Feb 10, 2011

This article was published online ahead of print in MBoC in Press (http://www.molbiolcell.org/cgi/doi/10.1091/mbc.E10-08-0722) on February 23, 2011.

*These authors contributed equally to this work.

The authors declare that they have no conflicting financial interests.

Address correspondence to: Agustín Valenzuela-Fernández (avalenzu@ull.es).

Abbreviations used: Arf6, ADP ribosylation factor 6; BSA, bovine serum albumin; CCP, clathrin-coated pit; CCS, clathrin-coated structure; CCV, clathrin-coated vesicle; DIC, differential interference contrast; ECFP, enhanced cyan fluorescent protein; EF, evanescent field; EGFP, enhanced green fluorescent protein; FCS, fetal calf serum; GDP, guanosine 5′-diphosphate; GTP, guanosine 5′-triphosphate; GTPase, guanosine 5′-triphosphatase; HA, hemagglutinin; HIV-1, human immunodeficiency virus type 1; HLA, human leukocyte antigen; HSV-1, herpes simplex virus 1; IgG, immunoglobulin G; LTR, long terminal repeat; mAb, monoclonal antibody; MHC, major histocompatibility complex; NA, numerical aperture; pAb, polyclonal antibody; PBS, phosphate-buffered saline; PE, phycoerythrin; PH, pleckstrin homology; PIP_2, phosphatidylinositol-(4,5)-biphosphate; PI4P5-K Iα, phosphatidylinositol-4-phosphate 5-kinase Iα; $PLC\delta_1$, phospholipase C δ_1; PLD, phospholipase D; RANTES, regulated on activation, normal T expressed and secreted; RNAi, RNA interference; SDF, stromal cell–derived factor; SEM, standard error of the mean; siRNA, small interfering RNA; TIRFM, total internal reflection fluorescence microscopy; VSV-G, vesicular stomatitis virus G; WT, wild-type.

INTRODUCTION

There is increasing evidence suggesting that membrane dynamics, like the traffic of vesicles and their spatial reorganization, is required for several biological functions such as cytokinesis (Albertson *et al.*, 2005), cellular migration (Sabe, 2003; Schmoranzer *et al.*, 2003; Letinic *et al.*, 2009), regulation of plasma membrane morphology

and polarization (Mellman and Warren, 2000; Folsch *et al.*, 2009), and phagocytosis (Faurschou and Borregaard, 2003; Nordenfelt *et al.*, 2009). Furthermore, some bacteria and viruses regulate membrane traffic in target cells to generate compartments to accomplish their replication process, which in many cases is regulated by Rab and ADP ribosylation factor (Arf) guanosine 5′-triphosphatases (GTPases) (Belov and Ehrenfeld, 2007; Pierini *et al.*, 2009).

As the initial barrier to viral entry, the plasma membrane along with membrane-trafficking machinery is also of fundamental importance in the first stages of the viral cycle (Marsh and Helenius, 2006; Mudhakir and Harashima, 2009). It is thought that certain enveloped viruses such as herpes simplex virus 1 (HSV-1), Sendai virus, human immunodeficiency virus type 1 (HIV-1), and many retroviruses have pH-independent viral fusion proteins that allow the virus to penetrate into cells by fusing directly with the plasma membrane (Stein *et al.*, 1987; Earp *et al.*, 2005; Kielian and Rey, 2006; Marsh and Helenius, 2006). HIV-1 interacts with target cells through cell-surface CD4 and CXCR4 or CCR5 coreceptors, a process that is cooperative and requires cell signaling such as actin polymerization, reorganization (Iyengar *et al.*, 1998; Jimenez-Baranda *et al.*, 2007; Yoder *et al.*, 2008; Barrero-Villar *et al.*, 2009; Liu *et al.*, 2009), and stabilization of microtubules (Valenzuela-Fernandez *et al.*, 2005; Malinowsky *et al.*, 2008) to achieve pore fusion formation. Although cytoskeleton reorganization and dynamics have well-documented roles in HIV-1 fusion and entry events, the contribution of plasma membrane dynamics is less clear during these early viral infection steps. It has been reported that HIV-1 fusion and entry could occur in micropinosomes and endosomes (Pauza and Price, 1988; Marechal *et al.*, 2001), a process described as being clathrin dependent (Daecke *et al.*, 2005), pH independent, and dynamin dependent (Miyauchi *et al.*, 2009). On the other hand, HIV-1 internalization and infection in polarized trophoblasts appear to be pH-dependent processes (Vidricaire and Tremblay, 2005) that are driven by a clathrin-, caveolae-, and dynamin-independent endocytic pathway and require free membrane cholesterol (Vidricaire and Tremblay, 2007). Therefore HIV-1 entry and infection are orchestrated by viral and cellular membrane interaction, which appears to occur through complexes and associated membrane traffic events.

We have recently reported that the fluidity of plasma membrane, regulated by phosphatidylinositol-4-phosphate 5-kinase Iα (PI4P5-K Iα)–mediated phosphatidylinositol-(4,5)-biphosphate (PIP_2) production, is crucial for HIV-1 entry and the early steps of infection in permissive lymphocytes (Barrero-Villar *et al.*, 2008). Interestingly, plasma membrane morphology and dynamics are also regulated by the traffic of PIP_2-associated membranes from the cell surface to a nonclathrin intracellular compartment, which in turn relies on the membrane transport activity of ADP ribosylation factor 6 (Arf6) (Radhakrishna and Donaldson, 1997; Franco *et al.*, 1999; Donaldson, 2003; Naslavsky *et al.*, 2003; Aikawa and Martin, 2005; Donaldson and Honda, 2005). In fact, Arf6 is the only member of the Ras-related Arf family of small GTPases that affects cell-surface dynamics, thereby regulating plasma membrane/endosome trafficking and cortical actin reorganization (D'Souza-Schorey *et al.*, 1995; Radhakrishna and Donaldson, 1997; Franco *et al.*, 1999; Al-Awar *et al.*, 2000; Donaldson, 2003; Naslavsky *et al.*, 2003; Donaldson and Honda, 2005). Arf6 appears to be associated with a tubular endosomal compartment in its inactive GDP-bound form and with the plasma membrane in its active GTP-bound form, thereby regulating membrane movement between these two compartments through its GTPase cycle (D'Souza-Schorey *et al.*, 1995, 1998; Radhakrishna and Donaldson, 1997). On the other hand, it seems that the GDP/GTP cycle of Arf6 occurs mainly at the plasma membrane (Pasqualato *et al.*, 2001), suggesting that Arf6 coordinates membrane dynamics on the cell surface (Macia *et al.*, 2004). Therefore Arf6-dependent membrane movement is a complex process that has still not been elucidated.

Considering that Arf6 is key to coordinating plasma membrane dynamics and has functional implications for cellular invasion by several microorganisms (Criss *et al.*, 2001; Nishi and Saigo, 2007; Laakkonen *et al.*, 2009; Marchant *et al.*, 2009), we decided to study the role of Arf6-mediated membrane dynamics during early HIV-1 entry and infection of T lymphocytes. In the present work, we observed that perturbation of Arf6-driven PIP_2-associated membrane movement inhibits HIV-1 fusion, entry, and infection of permissive cells, regardless of the viral tropism. Therefore it appears that efficient early HIV-1 infection of $CD4^+$ T lymphocytes requires Arf6-mediated plasma membrane dynamics.

RESULTS

Alteration of Arf6-dependent membrane trafficking impairs HIV-1 infection in permissive lymphocytes

We used the Arf6 wild-type construct (WT Arf6), which could cycle between its GDP-bound inactive and GTP-bound active forms, and the Arf6 mutants Q67L and T44N (Arf6-Q67L and Arf6-T44N), which are respectively locked in their GTP- and GDP-bound conformations (D'Souza-Schorey *et al.*, 1995; Donaldson, 2003; Macia *et al.*, 2004), in order to explore the functional role of Arf6-mediated membrane dynamics in HIV-1 entry and infection of permissive lymphocytes. These Arf6 mutants, defective in GTP-bound (T44N) and GTP hydrolysis (Q67L), have been used to identify Arf6's cellular locations and to define its cellular functions (Radhakrishna *et al.*, 1996; Al-Awar *et al.*, 2000; Donaldson, 2003).

We used C-terminal hemagglutinin (HA)– and enhanced green fluorescent protein (EGFP)–tagged WT Arf6 or mutant constructs to explore the functional involvement of Arf6 in HIV-1 entry and infection. First, we analyzed the endogenous level of Arf6 expression and the different C-terminal EGFP-tagged Arf6 constructs by Western blot (Figure 1A), transiently expressed in the permissive CEM-CCR5 cell line. Furthermore, we studied the cellular localization of these EGFP-labeled Arf6 constructs in these permissive cells (Figure 1B). We observed that WT Arf6–EGFP localized mainly at the plasma membrane. The Arf6-Q67L–EGFP and Arf6-T44N–EGFP mutants were localized at the plasma membrane and cytoplasm of permissive T-cells (Figure 1B, EGFP images). These Arf6 constructs colocalized with PIP_2-associated structures (Figure 1B, PH-ECFP and merged images), as monitored by the pleckstrin homology–enhanced cyan fluorescent protein (PH-ECFP) probe, previously described in Barrero-Villar *et al.* (2008). As a control, we transfected a construct codifying the EGFP protein, which presented a clear-cut cytoplasmic distribution pattern, excluded from plasma membrane as monitored by cortical F-actin localization (Figure 1B, pEGFP-N1 images).

It is thought that Arf6 localizes at the plasma membrane and in endosome-associated membranes in many cells (Cavenagh *et al.*, 1996; D'Souza-Schorey *et al.*, 1998; Donaldson, 2003), as it is involved in membrane/vesicle trafficking from the plasma membrane (D'Souza-Schorey *et al.*, 1998; Donaldson, 2003; D'Souza-Schorey and Chavrier, 2006). The Arf6-Q67L mutant has been reported to impede recycling of the internalized vesicles, provoking the accumulation of PIP_2- and F-actin–coated membrane structures (Donaldson, 2003; Naslavsky *et al.*, 2003). Furthermore, the inactive GDP-bound Arf6-T44N mutant distributed with F-actin in many cell-surface structures, such as large membrane folds and small membrane extensions, where it codistributed with PIP_2, as monitored by the PH

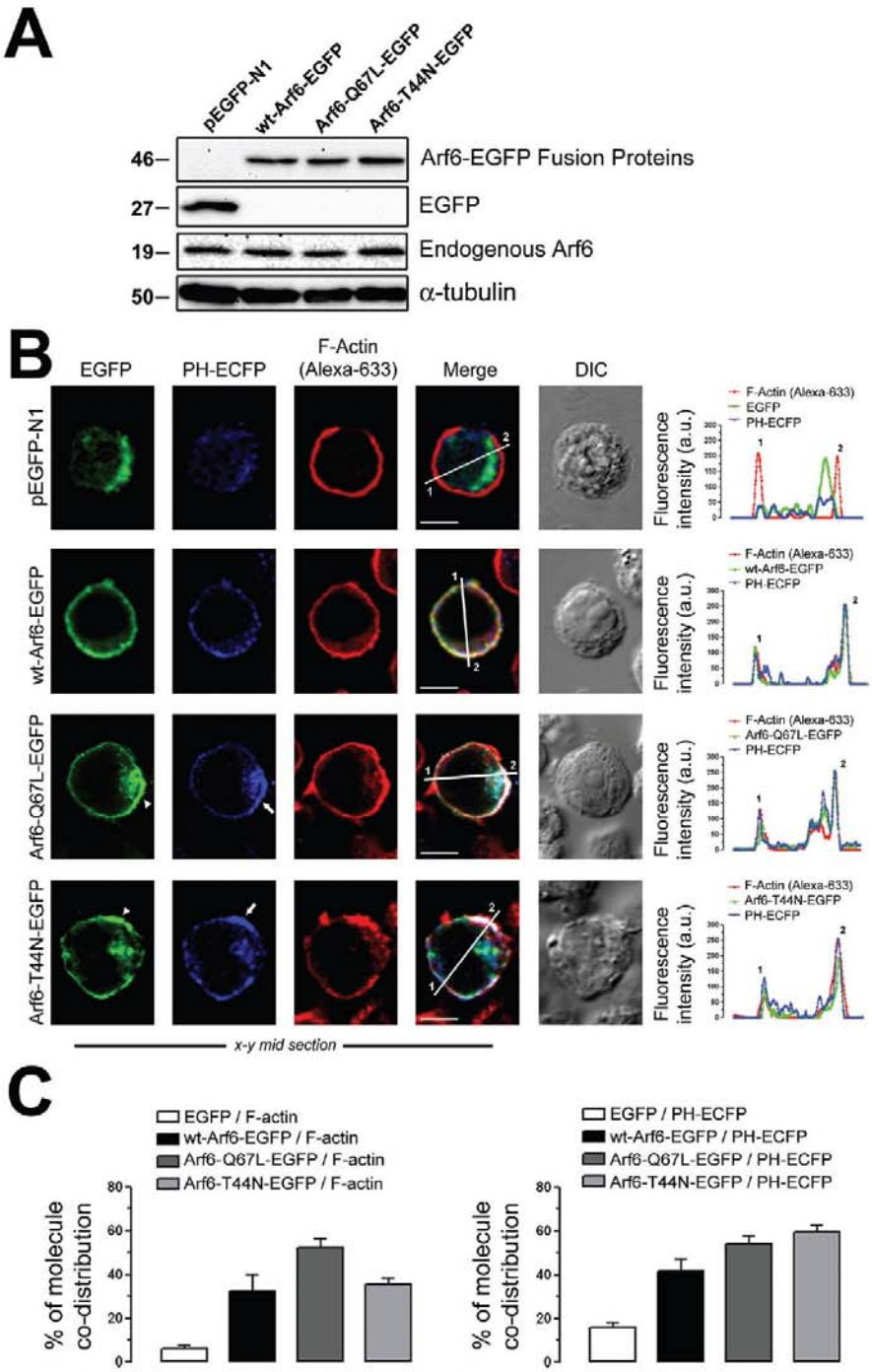

FIGURE 1: Pattern of expression of endogenous Arf6 and Arf6-EGFP constructs on permissive lymphocytes. (A) Western blot analysis of endogenous Arf6, WT Arf6–, Arf6-Q67L–, and Arf6-T44N–EGFP expression in CEM-CCR5 cells. α-Tubulin and pEGFP-N1 are the controls for total protein and EGFP expression, respectively. (B) Left, a series of confocal images, *x*–*y* midsections, show the expression pattern for WT Arf6–, Arf6-Q67L–, and Arf6-T44N–EGFP molecules in CEM-CCR5 cells. PIP_2 (PH-ECFP probe), F-actin (Alexa 633–labeled phalloidin), free EGFP distribution, and merged and differential interference contrast (DIC) images are shown. White arrowheads and arrows indicate Arf6 mutants and PH-ECFP plasma-membrane localization, respectively. Bar, 5 μm. Right, Arf6-EGFP constructs, F-actin, and PH-ECFP distribution were quantified along lines drawn through the diameter of the cells (1 and 2 indicate measurement points in merged pictures). (C) Codistribution quantification for each Arf6-EGFP construct or EGFP with F-actin (left) or with the PH-ECFP probe (right) in whole cells. Data are mean ± standard error of the mean (SEM) (n = 15 different cells).

domain of the phospholipase C δ_1 ($PLC\delta_1$) (Macia *et al.*, 2004). Similarly, we observed that the Arf6-Q67L– and Arf6-T44N–EGFP mutants provoked accumulation of PIP_2-associated structures (Figure 1B, PH-ECFP and merged images in Arf6-mutant-EGFP and line scans at right), which did not occur with control or WT Arf6–transfected cells (Figure 1B, pEGFP-N1 or WT Arf6–EGFP images and line scans at right). Moreover we also observed a plasma membrane ruffling effect in permissive lymphocytes overexpressing the Arf6-EGFP mutants, as is shown by the cortical F-actin protrusive distribution (Figure 1B, F-actin images in Arf6-Q67L– and Arf6-T44N–EGFP conditions), when compared with control-, WT Arf6–EGFP–, and EGFP-transfected lymphocytes (Figure 1B, F-actin images in pEGFP-N1 and WT Arf6–EGFP conditions). Qualitative and quantitative analyses revealed the specific codistribution of WT and mutant Arf6 molecules with F-actin and the PH-ECFP probe. Codistribution was absent for free EGFP and appeared to be slightly higher for the Arf6 mutants (Figure 1, B, line scans at right, and C). These data indicate that Arf6 mutants negatively affect PIP_2-associated membrane trafficking in permissive lymphocytes.

To further characterize these Arf6 constructs, we analyzed their distribution with class I molecules of the major histocompatibility complex (MHC-I), which is thought to traffic and recycle to plasma membrane from an Arf6-tubulovesicular network (Blagoveshchenskaya *et al.*, 2002; Caplan *et al.*, 2002; Larsen *et al.*, 2004; Massol *et al.*, 2005; Barral *et al.*, 2008; Yi *et al.*, 2010). We first analyzed cell-surface expression of human leukocyte antigen (HLA)-A/B/C in nonpermeabilized CEM-CCR5 cells expressing Arf6-EGFP constructs. We observed a dotted, cell-surface pattern of expression for HLA-A/B/C molecules, with some degree of codistribution with Arf6-EGFP constructs (Figure 2A, left). Arf6-Q67L– and Arf6-T44N–associated structures accumulated in cytoplasm, whereas WT Arf6–EGFP localized mainly at the cell surface, as we observed earlier. Flow cytometry analysis indicated that Arf6-EGFP constructs did not alter cell-surface expression of HLA-A/B/C molecules, compared with free EGFP-transfected cells (Figure 2A, right). In permeabilized CEM-CCR5 cells, we observed cell-surface and cytoplasmic codistribution of endogenous HLA-A/B/C molecules with overexpressed Arf6-EGFP constructs (Figure 2B). These results agree with reported data indicating that Arf6 constructs did not induce per se down-regulation of cell-surface MHC-I molecules (Blagoveshchenskaya

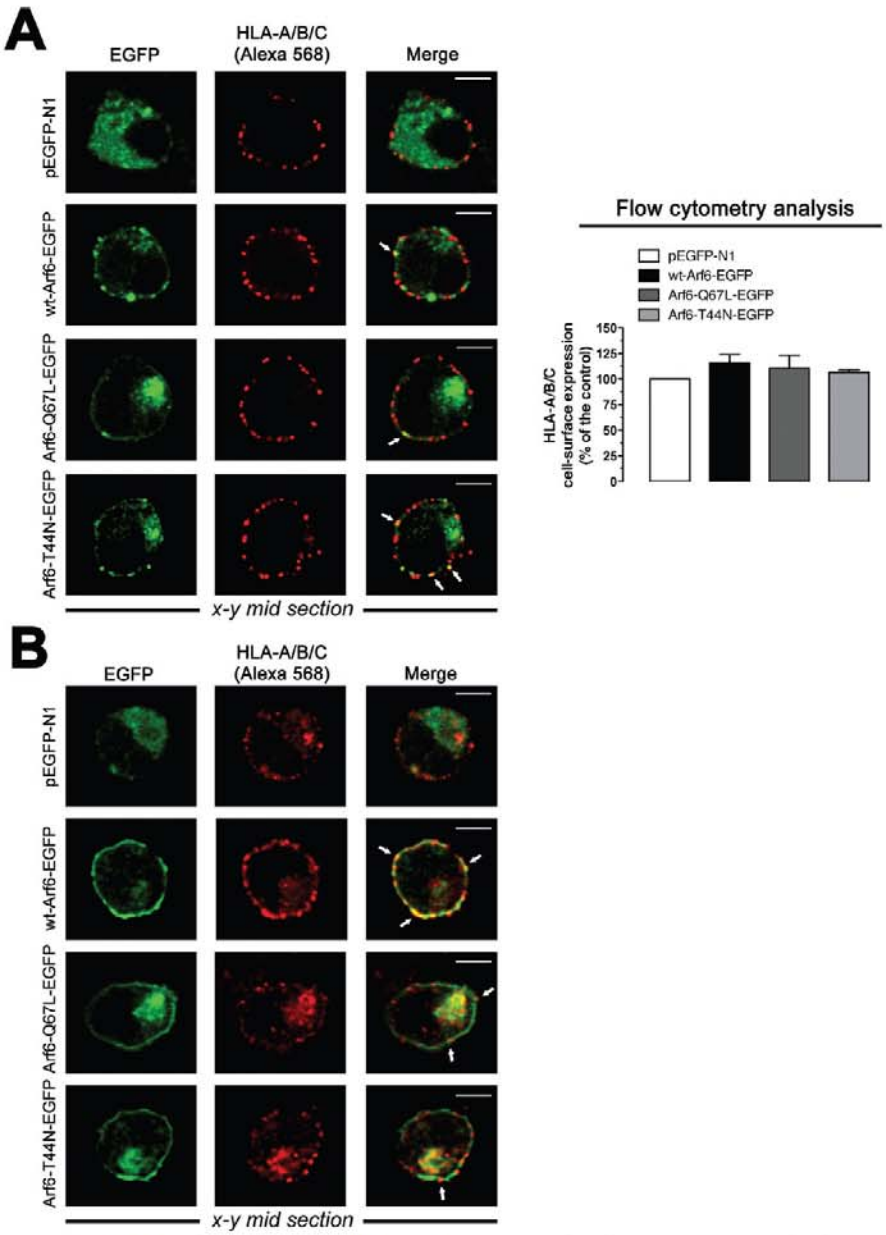

FIGURE 2: Pattern of expression of Arf6-EGFP constructs and endogenous MHC-I molecules on permissive lymphocytes. (A) Left, a series of confocal images, *x–y* midsections, show the expression pattern for endogenous HLA-A/B/C molecules and overexpressed WT Arf6–, Arf6-Q67L–, and Arf6-T44N–EGFP constructs in nonpermeabilized CEM-CCR5 cells. Free EGFP distribution and merged images are shown. White arrows indicate Arf6-EGFP constructs and HLA-A/B/C codistribution at cell surface. Bar, 5 μm. Right, flow cytometry analysis of HLA-A/B/C cell-surface expression in Arf6-EGFP–transfected cells (control, 100% HLA-A/B/C expression in pEGFP-N1–transfected cells). Data are mean ± SEM, n = 9. (B) A series of confocal images, *x–y* midsections, show the expression pattern for endogenous HLA-A/B/C and overexpressed WT Arf6–, Arf6-Q67L–, and Arf6-T44N–EGFP constructs in permeabilized CEM-CCR5 cells. Free EGFP distribution and merged images are shown. Bar, 5 μm.

et al., 2002; Larsen *et al.*, 2004; Yi *et al.*, 2010) and that MHC-I recycles to plasma membrane from Arf6 intracellular compartments (Blagoveshchenskaya *et al.*, 2002; Caplan *et al.*, 2002; Naslavsky *et al.*, 2003; Larsen *et al.*, 2004; Massol *et al.*, 2005; Barral *et al.*, 2008; Yi *et al.*, 2010). Although the role of Arf6 activity on Nef-mediated MHC-I down-regulation and recycling has been extensively studied in Nef-expressing cells (Blagoveshchenskaya *et al.*, 2002; Larsen *et al.*, 2004; Massol *et al.*, 2005; Barral *et al.*, 2008; Yi *et al.*, 2010), the present work focuses on the role played by Arf6-mediated membrane dynamics during early HIV-1 infection and therefore in Nef-negative uninfected cells.

We conducted HIV-1 infection experiments, under these experimental conditions, with single-cycle viruses bearing the *Luc*-reporter gene, which allows the monitoring and quantifying of HIV-1 entry and infection (Barrero-Villar *et al.*, 2008, 2009; Barroso-Gonzalez *et al.*, 2009a). We first observed that overexpression of C-terminal HA-tagged WT Arf6, Q67L, or T44N constructs (Figure 3A) did not affect the cell-surface level of expression of CD4, CXCR4, and CCR5 molecules, the receptors for HIV-1 infection, in permissive lymphocytes (Figure 3B). Nonreplicative X4- or R5-tropic HIV-1 viral particles were then incubated with CEM-CCR5 permissive cells overexpressing either WT Arf6–, Arf6-Q67L–, or Arf6-T44N–HA mutant. HIV-1 entry and infection were impaired in cells overexpressing the Arf6-Q67L or Arf6-T44N mutant (Figure 3, C and D). Data obtained for these events were similar when using either X4- or R5-tropic HIV-1 viral strains (Figure 3, C and D; 40% or 52% of inhibition by Arf6-Q67L or Arf6-T44N, and 59% or 61% of inhibition by Arf6-Q67L or Arf6-T44N, respectively), indicating that alteration of Arf6-mediated membrane dynamics affects HIV-1 entry and infection regardless of viral tropism.

We also assayed the effect of Arf6-N48I/Q67L– and Arf6-T27N–HA constructs, two mutants for the Arf6-GTP/GDP cycling activity, on HIV-1 entry and infection (Figure 4, A and B). There are two possible explanations of why cytoplasmic Arf6-T27N is defective in GTP loading acting as a cytoplasmic dominant-negative protein: 1) It is thought to be locked in the GDP-bound state, where it interferes with the traffic through the intracellular vesiculotubular Arf6 network (Radhakrishna and Donaldson, 1997), or 2) it does not mimic a GDP-bound form, thereby affecting the binding of both GTP and GDP nucleotides (Macia *et al.*, 2004). The Arf6-N48I/Q67L double mutant persists in the active GTP-bound state (Q67L mutation) and fails to activate the Arf6-downstream phospholipase D (PLD) (N48I mutation) (Vitale *et al.*, 2002). Overexpression of these two mutants (Figure 4A) also inhibited X4- and R5-tropic HIV-1 entry and infection (Figure 4B). The results obtained with Arf6-Q67L, Arf6-T44N, and Arf6-T27N mutants together with the fact that the Arf6-N48I/Q67L construct bears the Q67L mutation, acting as Arf6-Q67L, reinforce the role of the Arf6 GTP/GDP cycle in early HIV-1 infection and suggest that the Arf6-mediated PLD signal is not involved during the first

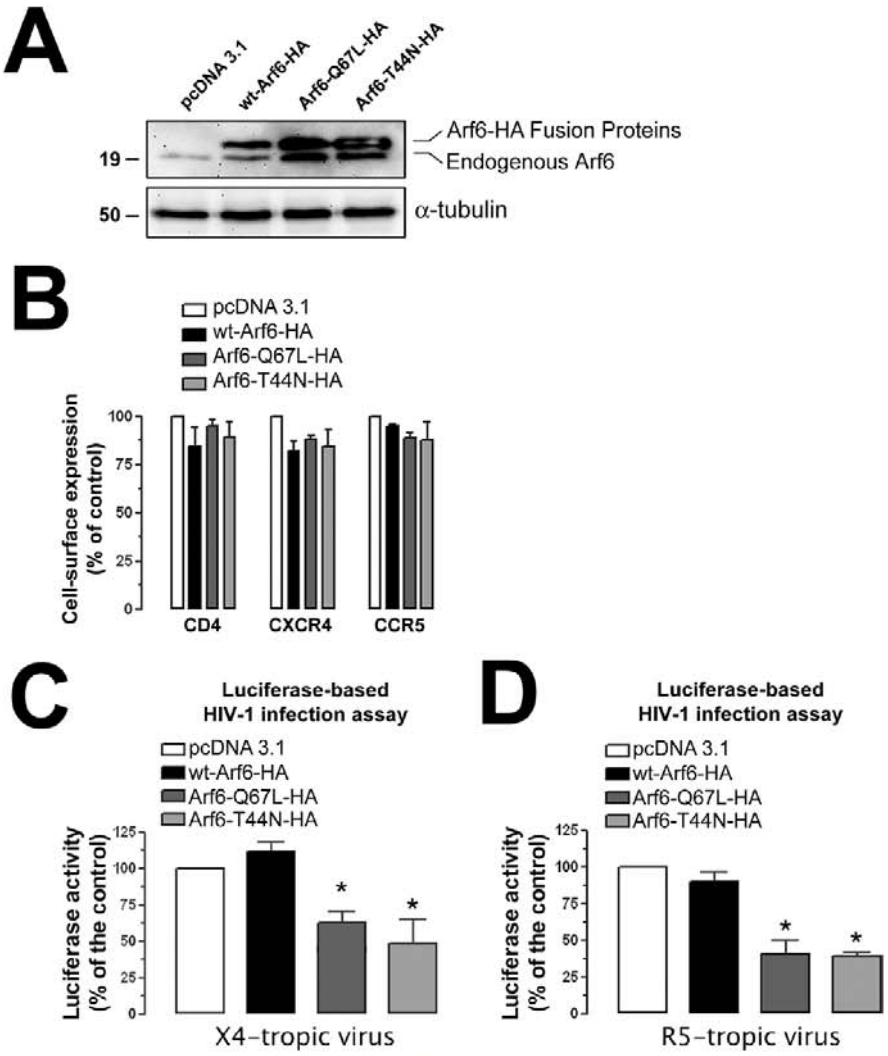

FIGURE 3: Effect of the Arf6 constructs on HIV-1 entry and infection in permissive lymphocytes. (A) Western blot analysis of endogenous Arf6, WT Arf6–, Arf6-Q67L–, and Arf6-T44N–HA expression in CEM-CCR5 cells. α-Tubulin and pcDNA 3.1 are the controls for total protein and transfected cells, respectively. A representative experiment of the three is shown. (B) Flow cytometry analysis of CD4, CXCR4, and CCR5 cell-surface expression in Arf6-HA–transfected cells. Data are mean ± SEM, n = 9. (C and D) Luciferase-based assay of viral entry and infection by nonreplicative X4- and R5-tropic HIV-1 viral particles, respectively, in Arf6-HA–transfected CEM-CCR5 cells (control, 100% viral entry and infection in pcDNA3.1-transfected cells). Data are mean ± SEM of three independent experiments carried out in triplicate. Asterisk indicates $p < 0.05$, *t* test.

steps of viral infection. It is noteworthy that Arf6-induced PLD activity acts in exocytic events as reported with Arf6-N48I/Q67L and Arf6-N48I mutants (Vitale *et al.*, 2002; Begle *et al.*, 2009). More work needs to be performed to determine whether this downstream Arf6-effector is involved in early HIV-1 infection.

Overexpression of WT Arf6 did not enhance HIV-1 entry and infection (Figure 3, C, 12% enhancement by WT Arf6 with respect to the control, and D), even in the presence of the cotransfected guanine nucleotide exchange factor EFA6 (Figure 4, C and D), described as being specific for Arf6 (Franco *et al.*, 1999). Overexpression of EFA6 alone (Figure 4C) did not significantly enhance viral entry and infection, regardless of viral tropism (Figure 4D). In general, Arf6 functions have been determined by using their related Arf6 mutants, owing to the lack of functional effect of WT Arf6 overexpression (Blagoveshchenskaya *et al.*, 2002; Donaldson, 2003; Larsen *et al.*, 2004).

Although Arf6 activates PLD and PI4P5-K effectors (Brown *et al.*, 2001; Vitale *et al.*, 2002; D'Souza-Schorey and Chavrier, 2006; Gillingham and Munro, 2007), and overexpression of PI4P5-K Iα enhances HIV-1 viral fusion and infection (Barrero-Villar *et al.*, 2008), the results we obtained with Arf6/EFA6 (Figure 4, C and D), single Arf6-GTP/GDP cycle mutants, and the Arf6-N48I/Q67L mutant (Figures 3 and 4, A and B, Figures 8 and 10 later in this paper, and Supplemental Figure 3), which fails to activate PLD, suggest that WT Arf6/EFA6 overexpression does not activate PI4P5-K Iα and that PLD activity is not directly involved in the regulation of viral fusion and entry. Therefore we propose that HIV-1 takes advantage of Arf6-coordinated plasma membrane movements, a dynamic process inhibited by Arf6-GTPase knockdown or Arf6 mutants, to efficiently fuse, enter, and infect $CD4^+$ lymphocytes.

Specific RNA interference (RNAi) of endogenous Arf6 inhibits HIV-1 infection in permissive T-cells

To further confirm the functional involvement of Arf6 during early HIV-1 infection, we infected permissive lymphocytes in which endogenous Arf6 protein expression was previously silenced by specific small interfering RNA (siRNA) (Figure 5A, siRNA-Arf6 band), without affecting cell-surface expression of HIV-1 receptors (Figure 5B). We observed that endogenous Arf6 knockdown negatively affected luciferase–HIV-1 entry and infection, as opposed to control scrambled-transfected cells. The extent of this blockade was similar to the level of Arf6 silencing achieved (Figure 5, C and D; 50% and 56% of inhibition, respectively). The inhibition of HIV-1 entry and infection again appeared to be independent of the viral tropism (Figure 5, C and D).

Therefore all these data suggest that efficient HIV-1 entry and infection require functional Arf6.

Specific silencing of endogenous Arf6 inhibits HIV-1 spreading and the infection of primary $CD4^+$ T-cells

We also addressed the role of Arf6 in HIV-1 infection of primary cells. Preliminary work using stimulated primary lymphocytes showed long-term toxicity with Arf6 mutants or Arf6 silencing that hampered not only the maintenance of the siRNA silencing but also the analysis of cell-free HIV-1 infections over 4 d (unpublished data). Therefore to avoid long-term cultures of previously Arf6-transfected or Arf6-silenced HIV-1–infected and stimulated $CD4^+$ T-cells, we analyzed the effect of endogenous Arf6 silencing on target nonactivated primary $CD4^+$ T-cells during cell-mediated HIV-1 transmission, which is a fast and highly efficient mechanism of viral spread (Blanco *et al.*, 2004; Jolly *et al.*, 2004; Chen *et al.*, 2007; Puigdomenech *et al.*, 2008) that accounts for more than

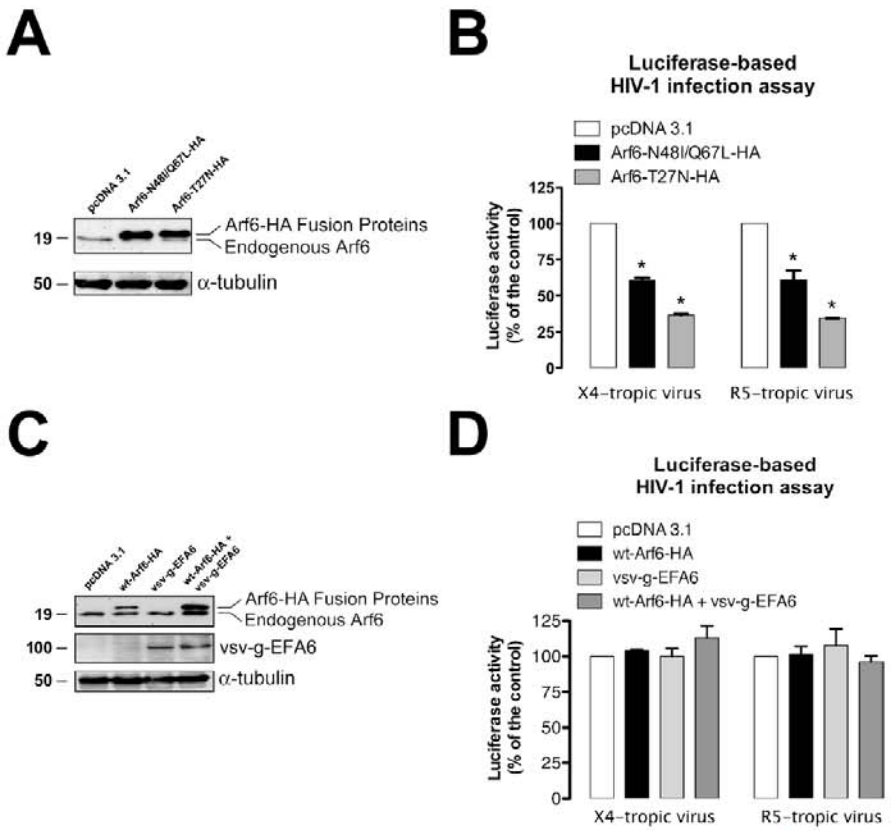

FIGURE 4: Effect of different Arf6 constructs and the EFA6 factor on HIV-1 entry and infection in permissive lymphocytes. (A) Western blot analysis of endogenous Arf6, Arf6-N48I/Q67L–, and Arf6-T27N–HA expression in CEM-CCR5 cells. α-Tubulin and pcDNA 3.1 are the controls for total protein and transfected cells, respectively. A representative experiment of the three is shown. (B) Luciferase-based assay of viral entry and infection by nonreplicative X4- and R5-tropic HIV-1 viral particles, respectively, in Arf6-N48I/Q67L– and Arf6-T27N–HA–transfected CEM-CCR5 cells (control, 100% viral entry and infection in pcDNA3.1-transfected cells). Data are mean ± SEM of three independent experiments carried out in triplicate. Asterisk indicates $p < 0.05$, *t* test. (C) Western blot analysis of endogenous Arf6, WT Arf6–HA, and vsv-g-EFA6 expression in CEM-CCR5 cells. α-Tubulin and pcDNA 3.1 are the controls for total protein and transfected cells, respectively. A representative experiment of the three is shown. (D) Luciferase-based assay of viral entry and infection by nonreplicative X4- and R5-tropic HIV-1 viral particles, respectively, in WT Arf6–HA, vsv-g-EFA6, and double WT Arf6–HA/vsv-g-EFA6–transfected CEM-CCR5 cells (control, 100% viral entry and infection in pcDNA3.1-transfected cells). Data are mean ± SEM of three independent experiments carried out in triplicate.

90% of new CD4+ T-cell infections in vivo (Dixit and Perelson, 2004).

To do this, MOLT/CCR5 cells chronically infected with X4 or R5 viral isolates, $MOLT_{NL4-3}$ or $MOLT_{BaL}$, respectively, were used as effector cells and cocultured with unstimulated primary CD4+ T-cells, which were previously nucleofected with scrambled or specific siRNA for Arf6 silencing (Figure 6A). In addition, in this set of experiments, an siRNA directed against CD4 was used as a control of inhibition of HIV-1 transmission. After silencing, a reduction in the levels of Arf6 and CD4 expression was observed by Western blot as compared with the scrambled control (Figure 6, A and B). Specific Arf6 silencing did not affect CD4, CXCR4, and CCR5 cell-surface expression (unpublished data). Proviral HIV-1 DNA was measured after 24 h of coculture by quantitative PCR using primers to amplify the viral long terminal repeats (LTRs). It is worth mentioning that both Arf6 and CD4 knockdown partially but significantly inhibited cell-mediated HIV-1 transmission, irrespective of the viral tropism (Figure 6, C and D). Complete inhibition of viral transmission, which yielded background HIV DNA levels in MOLT/CCR5 cells, was achieved in C34 (anti-fusogenic peptide)–treated cultures (Figure 6, C and D, dashed line).

Taken together these data suggest that Arf6-mediated membrane dynamics are involved in efficient cell-to-cell HIV-1 transmission to primary CD4+ T lymphocytes.

Arf6-mediated membrane dynamics regulate HIV-1 fusion, entry, and infection in permissive cells

Arf6-mediated membrane trafficking and its cellular characterization have been extensively described in HeLa cells (Radhakrishna and Donaldson, 1997; Donaldson, 2003). It appears that the Arf6-mediated membrane recycling system is different from the transferrin receptor recycling pathway and from its actin reorganization activity (Radhakrishna and Donaldson, 1997; Al-Awar *et al.*, 2000; Donaldson, 2003). Permissive CXCR4+/CCR5+/CD4+-HeLa cells, such as HeLa-P5 and TZMbl cells, have been used to study and image HIV-1 infection, as envelope-mediated membrane fusion, entry, and viral egress events (Pleskoff *et al.*, 1997; Valenzuela-Fernandez *et al.*, 2005; Jouvenet *et al.*, 2008; Barrero-Villar *et al.*, 2009; Barroso-Gonzalez *et al.*, 2009a; Ivanchenko *et al.*, 2009; Miyauchi *et al.*, 2009). Therefore we studied Arf6 cellular location and the functional consequences of Arf6 mutants and Arf6 silencing on Arf6-mediated membrane dynamics during early HIV-1 infection in permissive HeLa cells.

We further validated the data obtained in CD4+ T lymphocytes by first analyzing the expression pattern of C-terminal EGFP- or ECFP-tagged WT Arf6, Arf6 Q67L, and Arf6 T44N (mutants for the GTP/GDP cycle able to localize at the cell surface) constructs, transiently transfected in permissive TZMbl cells (Figure 7 and Supplemental Figure 1), and compared them with the distribution of cellular PIP_2-associated structures and free or HIV-1–bound CD4 viral receptor. Fluorescence confocal microscopy showed that WT Arf6–EGFP was homogeneously localized on the plasma membrane as well as on cytoplasm in permissive TZMbl cells without promoting the accumulation of large PIP_2-associated structures (Supplemental Figure 1, WT Arf6–EGFP and related PH-ECFP and merged images). We observed accumulation of PIP_2-associated structures in cells overexpressing Arf6-Q67L– and Arf6-T44N–EGFP (Supplemental Figure 1, see arrowheads in Arf6 mutants and arrows in related PH-ECFP and merged images). We also observed colocalization of Arf6 constructs with F-actin (Supplemental Figure 1, see F-actin in related Arf6 images). The quantification of the codistribution pattern of each EGFP-labeled Arf6 construct or the free EGFP protein with the PH-ECFP probe or F-actin is shown in line scans (Supplemental Figure 1).

Furthermore, we analyzed the distribution of the different Arf6-EGFP constructs together with the PH-ECFP probe at the plasma

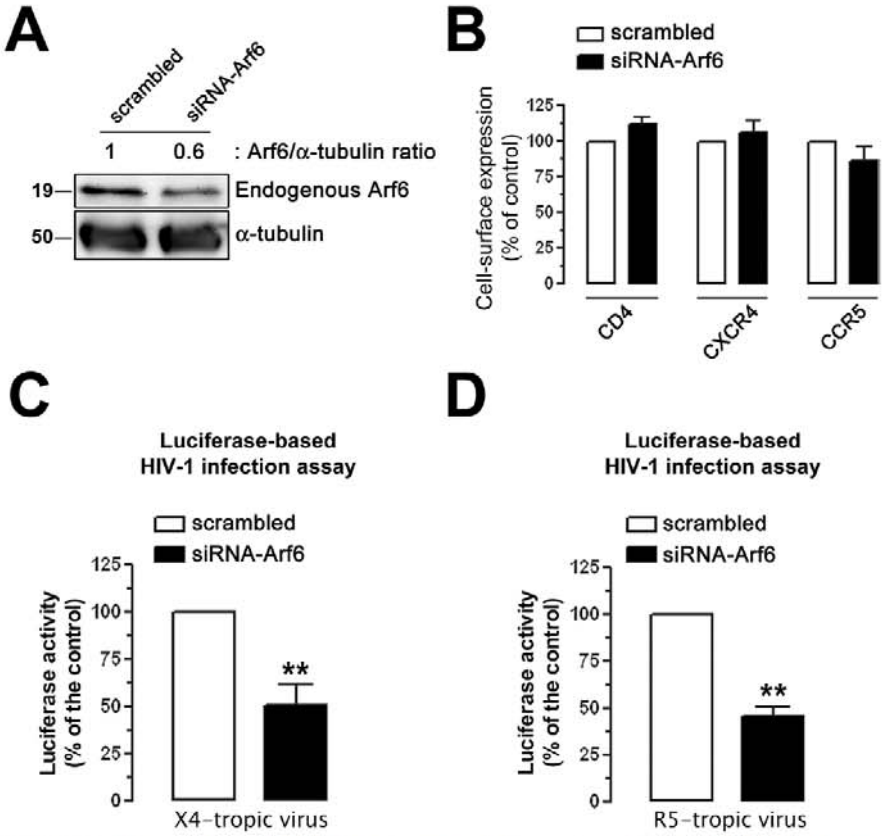

FIGURE 5: Effect of knockdown of the endogenous Arf6 protein on HIV-1 entry and infection in permissive lymphocytes. (A) Western blot analysis of endogenous Arf6 knockdown in siRNA-Arf6–treated CEM-CCR5 cells, quantified as the band intensity ratios to α-tubulin. A representative experiment of three is shown. (B) Flow cytometry analysis of CD4, CXCR4, and CCR5 cell-surface expression in scrambled- or siRNA-Arf6–treated CEM-CCR5 cells. Data are the mean ± SEM of three independent experiments carried out in triplicate. (C and D) Luciferase-based assay of viral entry and infection by nonreplicative X4- and R5-tropic HIV-1 viral strains, respectively, in siRNA-Arf6–silenced CEM-CCR5 cells (control, 100% viral entry in scrambled-treated cells). Data are mean ± SEM of three independent experiments carried out in triplicate. Asterisks indicate $p < 0.01$, *t* test.

membrane of these permissive cells using TIRFM. We observed that TZMbl cells expressing Arf6-Q67L– and Arf6-T44N–EGFP (Figure 7, A and B) presented accumulation of PIP_2-associated structures on plasma membranes, as observed in the evanescent field (EF) (Figure 7B, see arrows in PH-ECFP images), where these mutants colocalized (Figure 7B, see arrowheads in Arf6-Q67L– and Arf6-T44N–EGFP images). In general, we observed that the Arf6-Q67L mutant induced a more extensive accumulation of PIP_2-associated structures either on cytoplasm or on plasma membrane, compared with the effect exerted by the Arf6-T44N mutant (Figure 7, B and C, and Supplemental Figures 1 and 5; see related PH-ECFP or merged images). In this regard, we even observed the accumulation of PIP_2-associated vacuole-like structures near the plasma membrane in some cells overexpressing the Arf6-Q67L–HA mutant (Supplemental Figure 2). This fact has also been previously reported in cells transfected with the GTP-bound Arf6-Q67L mutant (Naslavsky *et al.*, 2003; Aikawa and Martin, 2005; Cohen *et al.*, 2007). The quantification of the codistribution of each EGFP-labeled Arf6 construct or the free EGFP protein with the PH-ECFP probe on plasma membrane observed by TIRFM indicated that all Arf6 molecules similarly codistributed with PIP_2-associated plasma membrane domains (Figure 7C, top). The quantification of the codistribution of the PH-ECFP probe with each EGFP-labeled Arf6 construct or the free EGFP protein on plasma membrane clearly indicated that Arf6 mutants provoked the accumulation of PIP_2-associated membrane domains on cell-surface regions where the mutants are localized (Figure 7C, bottom). Therefore inhibition of the Arf6-GTP/GDP cycle seems to perturb the movement of PIP_2-associated structures, provoking its accumulation on plasma membrane of Arf6-Q67L– or Arf6-T44N–treated cells.

TIRFM studies indicate that WT Arf6–, Arf6-Q67L–, and Arf6-T44N–ECFP constructs did not colocalize with cell-surface CD4-DsRed (Figure 7D). HIV-1 binding to CD4 did not promote codistribution of virus-bound or free CD4 with Arf6 constructs, and Arf6 constructs did not affect the first CD4/HIV-1 interaction (Figure 7D). We observed that free or HIV-1–bound CD4-DsRed molecules did not distribute with Arf6 structures (Figure 7D, line scans). This fact suggests that CD4 molecules do not internalize to or recycle from Arf6 compartments. Therefore the results obtained with Arf6-EGFP and Arf6-ECFP constructs point to the coordination of PIP_2-associated membrane dynamics exerted by Arf6 on plasma membrane, which is perturbed by the Arf6-Q67L and Arf6-T44N mutants, without affecting CD4 cell-surface expression and the first HIV-1/CD4 interactions.

TIRFM studies indicate that functional Arf6 is required for efficient HIV-1 entry

We studied the ability of the CD4-bound HIV-1 virus to enter target cells with a perturbed Arf6-GTP/GDP cycle and, therefore, with accumulated PIP_2-associated structures at the cell surface. TIRFM can dynamically study, at the plasma membrane, the fate of internalization or export of different cargos or cell-surface molecules (Barroso-Gonzalez *et al.*, 2009a, 2009b). Furthermore, it has also been applied to the study of HIV-1 fusion and entry, viral assembly, and release (Jouvenet *et al.*, 2006; Ivanchenko *et al.*, 2009). In this regard, we performed TIRFM studies of the CD4-dependent HIV-1 uptake process by using nonreplicative, fluorescent HIV-1–Gag-EGFP viral particles in nonlymphoid permissive TZMbl ($CD4^+$/$CXCR4^+$/$CCR5^+$) cells (see *Materials and Methods*) transiently expressing the fluorescent CD4-DsRed molecule together with one of the different Arf6-HA constructs and the PH-ECFP probe. This probe allowed us to monitor accumulated PIP_2-associated structures at the EF of permissive cells and provided a clear-cut readout for effective Arf6 mutant–mediated inhibition of endogenous Arf6-coordinated PIP_2-membrane traffic (Figure 8, PH-ECFP images). The study of CD4-dependent HIV-1 entry in cells presenting accumulation of PIP_2-associated structures, provoked by Arf6 mutants that also codistributed with Arf6 mutants (Figures 1, 7, and 8 and Supplemental Figures 1, 2, and 5), gives a better guaranty of selecting cells where Arf6-dependent membrane dynamics have

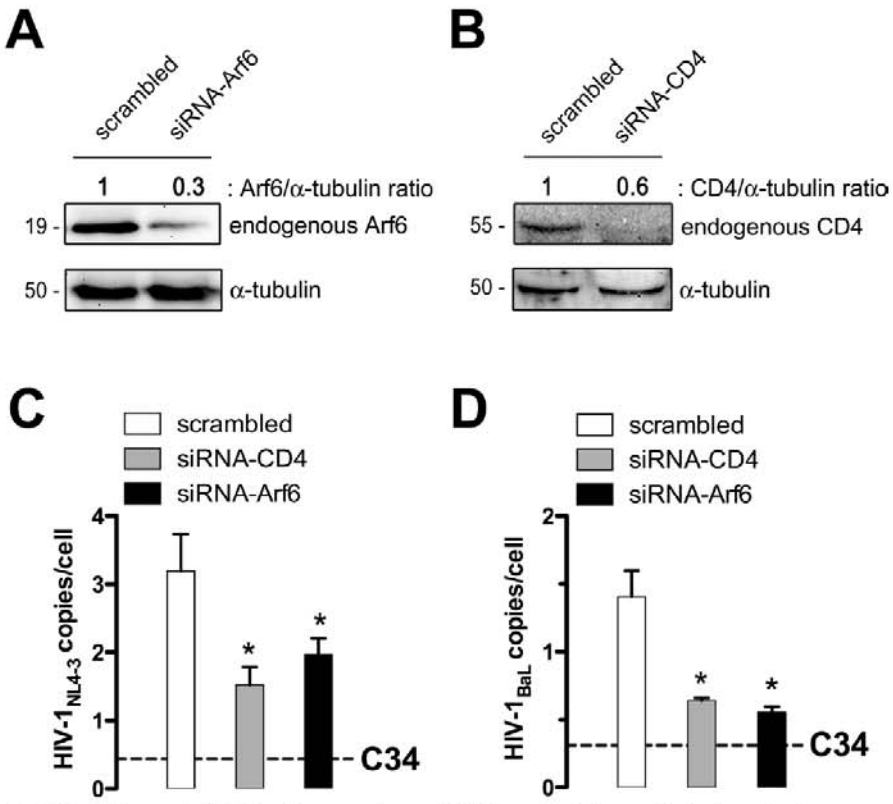

FIGURE 6: Effect of Arf6 silencing on cell-to-cell HIV-1 transmission and infection of primary CD4+ T-cells. (A and B) Western blot analysis of Arf6 and CD4 knockdown in specific siRNA- or scrambled-nucleofected human primary CD4+ T-cells, 24 h after nucleofection, quantified as the band intensity ratios to α-tubulin. A representative experiment of three is shown. (C and D) After 24 h, nucleofected unstimulated primary CD4+ T-cells were cocultured with (C) $MOLT_{NL4-3}$ or (D) $MOLT_{BaL}$ cells. Cell-to-cell HIV-1 transmission was analyzed at 24 h postcoculture by real-time PCR using a standard curve of a known number of HIV and CCR5 copies. Data represented HIV-1 DNA copies per cell, as values were normalized to the copy number of CCR5. Dashed lines represent the background levels of HIV-1 DNA in MOLT cells as determined in control cocultures in the presence of the fusion inhibitor peptide C34. Data are mean ± SD of three independent experiments. Asterisks indicate $p < 0.05$, *t* test.

been altered, thereby avoiding a possible incorrect selection of cells for analysis of viral uptake based on Arf6 detection, which could lead to the selection of cells expressing critical levels of Arf6-fluorescent constructs without perturbing Arf6/PIP_2-coordinated membrane dynamics.

We first assayed luciferase-based HIV-1 entry and infection experiments on HeLa-P5 cells, transfected with the different Arf6-HA constructs or siRNA-Arf6 oligonucleotides (Supplemental Figures 3A and 4A, respectively), in order to confirm that Arf6-HA mutants and siRNA-Arf6 treatment affect early HIV-1 infection in HeLa permissive cells. CD4, CXCR4, and CCR5 cell-surface expression was not affected by the expression of any Arf6-HA construct used (Supplemental Figure 3B). Furthermore, X4- and R5-tropic HIV-1 entry and infection appeared to be impaired by Arf6-GTP/GDP cycling mutants (Supplemental Figure 3, C and D, 40% and 42% inhibition by Arf6-Q67L and Arf6-T44N and 50% and 43% inhibition by Arf6-Q67L and Arf6-T44N, respectively). Similar inhibitory effects on viral infection were observed by the anti-fusogenic T-20 peptide (Supplemental Figure 3, C and D, T-20 bars in cells transfected with pcDNA3.1). However, Arf6 mutants did not affect cell infection by HIV-1 vectors pseudotyped with the vesicular stomatitis virus G (VSV-G) protein (Supplemental Figure 3E), an envelope protein that drives the entry and infection process in a clathrin-dependent endocytic manner (Matlin *et al.*, 1982; Sun *et al.*, 2005). Similarly, nonfunctional Arf6 mutants impaired HIV-1 envelope–mediated cell-to-cell fusion, independently of envelope-viral tropism (Supplemental Figure 3, F and G, 40% and 48% inhibition by Arf6-Q67L and Arf6-T44N and 39% and 42% inhibition by Arf6-Q67L and Arf6-T44N, respectively), when quantified by a β-galactosidase-based cellular model for membrane fusion as previously described (Pleskoff *et al.*, 1997; Valenzuela-Fernandez *et al.*, 2005; Barrero-Villar *et al.*, 2009; Barroso-Gonzalez *et al.*, 2009a). Furthermore, endogenous Arf6 knockdown (Supplemental Figure 4A), which did not affect cell-surface expression of CD4, CXCR4, or CCR5 viral receptors (Supplemental Figure 4B), negatively affected X4- and R5-tropic luciferase-based HIV-1 infection (Supplemental Figure 4, C and D, ~50% inhibition). However, Arf6 knockdown did not affect cell infection by HIV-1 vectors pseudotyped with the VSV-G protein (Supplemental Figure 4E). Altogether these data lead us to suggest that Arf6-HA constructs and specific Arf6 silencing affect viral entry and infection in HeLa permissive cells, as observed in CD4+ lymphocytes, thus confirming the inhibitory effect of Arf6-HA mutants on HIV-1 entry and infection used in the following TIRFM studies.

Our results suggest that the Arf6-mediated effect on HIV-1 entry is independent of the viral tropism. Thus we present CD4-dependent viral uptake experiments performed by using X4-tropic HIV-1–Gag-EGFP virions in this section. Cell-surface CD4-DsRed molecules can monitor CD4-dependent HIV-1 uptake, whereas the PH-ECFP probe serves as a readout for the accumulation of PIP_2-associated structures at the plasma membrane of cells expressing the GTP/GDP cycling Arf6-HA mutants (Figure 8, A–D). Of note, overexpression of each Arf6-HA construct did not affect the initial CD4/HIV-1 interaction (Figure 8, A–D, cell-surface CD4-DsRed/HIV-1–Gag-EGFP codistribution in merged images). Interestingly, PIP_2 accumulation was clearly observed in the EF of cells transfected with either Arf6-Q67L–HA or Arf6-T44N–HA (Figure 8, C and D, PH-ECFP images), thereby representing an alteration of Arf6-coordinated plasma membrane dynamics. On the contrary, overexpression of the WT Arf6–HA construct did not provoke the accumulation of large PIP_2-associated structures (Figure 8, A and B, PH-ECFP images), which could be indicative of normal membrane dynamics.

HIV-1 uptake was studied under each experimental condition as described in *Materials and Methods*. CD4-dependent viral uptake was clearly observed in control and WT Arf6–nucleofected cells (Figure 8A and quantified in E as 57% of CD4-dependent viral uptake), as monitored by the coordinated dimming of the intensity of fluorescence for the DsRed and EGFP fluorophores, respectively, associated with CD4 and viral particles (Figure 8A, fluorescence intensity curves and time lapse images from zoom area for CD4-DsRed and

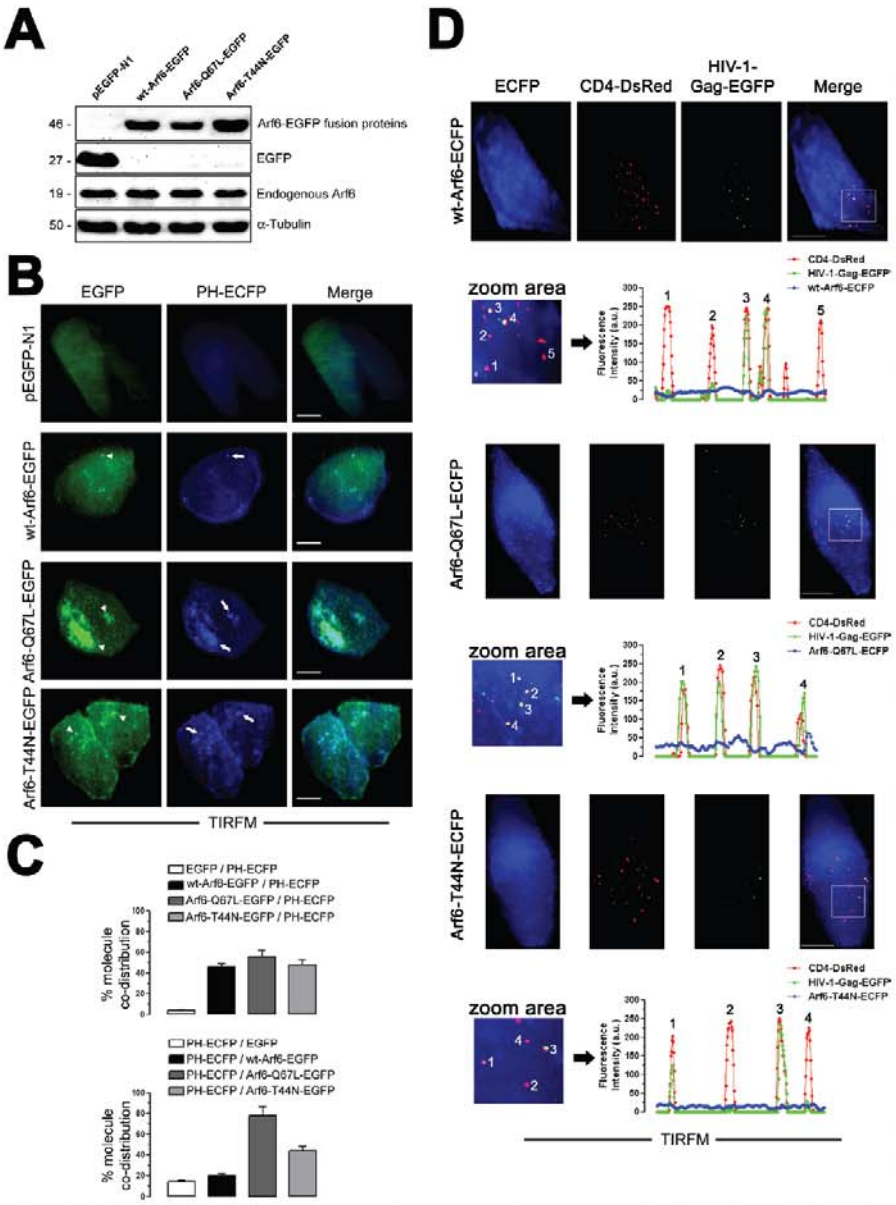

FIGURE 7: TIRFM analysis for plasma membrane expression pattern of Arf6-EGFP or Arf6-ECFP constructs, and free or HIV-1–bound CD4-DsRed molecules on permissive HeLa cells. (A) Western blot analysis of endogenous Arf6, WT Arf6–, Arf6-Q67L–, and Arf6-T44N–EGFP expression in permissive TZMbl cells. α-Tubulin is the control for total protein. Free EGFP protein expression in pEGFP-N1–transfected cells. A representative experiment of the three is shown. (B) TIRFM analysis for the plasma membrane expression pattern of each Arf6-EGFP and the PH-ECFP probe. Merged images are shown. A representative experiment of the three is shown. Bar, 5 μm. White arrowheads or arrows indicate the distribution of Arf6 mutant or accumulation of PIP_2-associated structures, respectively. (C) Quantification of the codistribution of each Arf6-EGFP or free EGFP molecule with PIP_2 (PH-ECFP)–associated plasma membrane structures (top) or PIP_2 (PH-ECFP) with each Arf6-EGFP or free EGFP molecule (bottom) from TIRFM images, as shown in (B). A representative experiment of three is shown. (D) A series of TIRFM images representing the expression pattern of cell-surface CD4-DsRed, HIV-1–Gag-EGFP virions, CD4-attached HIV-1–Gag-EGFP virions (merge), and WT Arf6–, Arf6-Q67L–, or Arf6-T44N–ECFP constructs, respectively, at the EF of TZMbl cells. The quantification of the pattern of distribution of free or HIV-1–Gag-EGFP–bound CD4-DsRed or Arf6-ECFP constructs is shown by line scan quantification, after background remove, through regions 1–4 or 5 indicated in zoom areas. Bar, 5 μm.

bound HIV-1–Gag-EGFP, and Supplemental Video 1). We performed CD4-dependent HIV-1–Gag-EGFP uptake experiments in cells overexpressing WT Arf6–HA in the presence of the anti-fusogenic peptide T-20 to analyze CD4-dependent productive viral entry. We observed an important inhibition of CD4-dependent viral uptake (Figure 8, B and quantified in E as only 11.4% of CD4-dependent viral uptake). Therefore the CD4-dependent viral uptake observed in the presence of T-20 could correspond to nonproductive viral entry, considering that CD4-dependent fusogenic entry is blocked by T-20 (Figure 8B, fluorescence intensity curves and time lapse images from zoom area for CD4-DsRed and bound HIV-1–Gag-EGFP, and Supplemental Video 2).

Our results obtained in permissive cells overexpressing Arf6-Q67L–HA or Arf6-T44N–HA mutants indicated that alteration of Arf6-mediated PIP_2-membrane dynamics prevented CD4-dependent HIV-1 uptake (Figure 8, C or D and quantified in E as 12.5% and 15% of CD4-dependent viral uptake, respectively). Given all the data presented concerning the inhibitory effect of each Arf6 mutant on HIV-1 viral entry and infection, and the blockade of CD4-dependent viral uptake by T-20, it is conceivable that Arf6 mutants inhibited CD4-dependent productive viral entry as observed by TIRFM (Figure 8, C and D, fluorescence intensity curves and time lapse images from zoom area for CD4-DsRed and bound HIV-1–Gag-EGFP, and Supplemental Videos 3 and 4).

We performed similar experiments on TZMbl cells, transiently expressing CD4-DsRed, where endogenous Arf6 protein expression was previously silenced to further confirm the role of Arf6 function during HIV-1 entry (Figure 9). We used fluorescent siRNA-Arf6 oligonucleotides to select cells to be studied by TIRFM for this purpose. We first confirmed that fluorescent siRNA-Arf6 oligonucleotides silenced the expression of the endogenous Arf6 protein (Figure 9A), as did the nonfluorescent oligonucleotides (Figures 5A, 6A, and 10A and Supplemental Figure 4A). The presence of the fluorescent scrambled or siRNA-Arf6 oligonucleotides inside the cells was monitored by epifluorescence (Figure 9, B and C, epifluorescence images) during TIRFM-based CD4-dependent HIV-1 uptake experiments. Our results indicated that endogenous Arf6 knockdown did not affect the first CD4-DsRed/HIV-1–Gag-EGFP interaction (Figure 9, B and C, merged images) but prevented CD4-dependent viral uptake, compared with control and scrambled-treated cells (Figure 9D, 63% and 10.7% of CD4-dependent viral uptake for scrambled and siRNA-Arf6, respectively). Given the observed inhibitory effect of Arf6 knockdown on HIV-1 viral entry and infection (Figures 5 and 6 and Supplemental Figure 4), it is

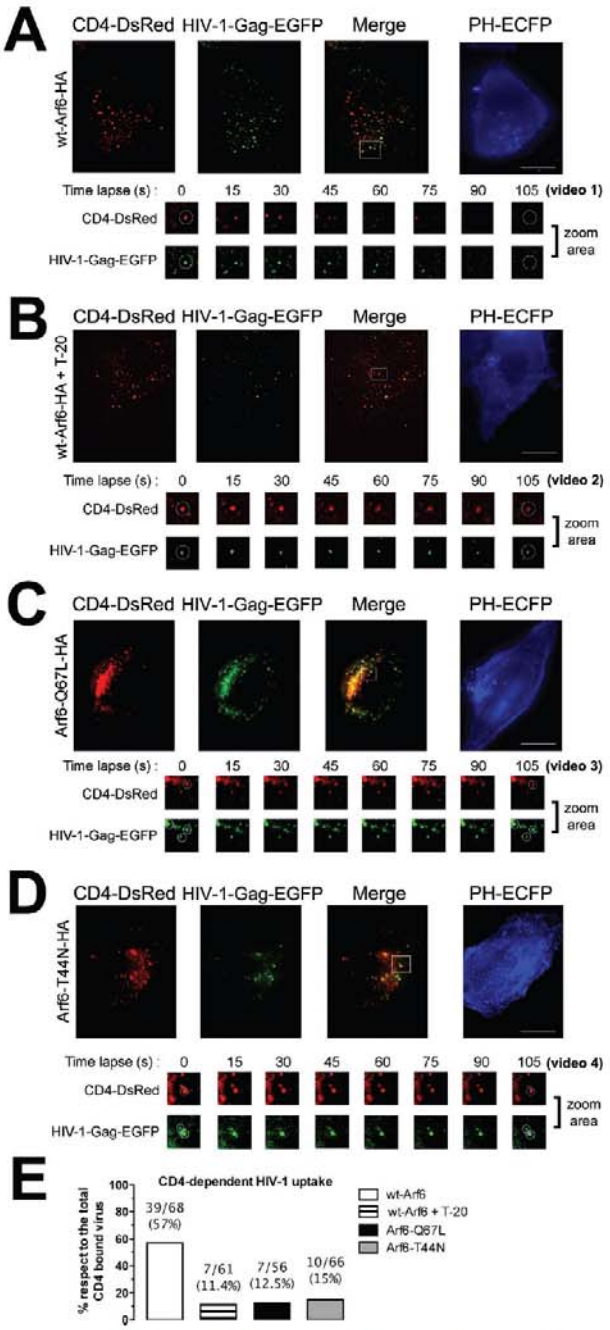

FIGURE 8: Effects of the different Arf6-HA constructs on PIP_2–plasma membrane distribution and HIV-1 entry analyzed by TIRFM. (A–D) A series of TIRFM images representing the expression pattern of cell-surface CD4-DsRed, HIV-1–Gag-EGFP virions, CD4-attached HIV-1–Gag-EGFP virions (merge), and the PH-ECFP probe (readout for PIP_2) at the EF of TZMbl cells, under any experimental condition. T-20 treatment represents a control for the blockade of CD4-dependent fusogenic viral entry. White squares in merged images show a representative area (zoom area) where CD4-dependent HIV-1 uptake or blockade was observed, corresponding to Supplemental Videos 1–4, and a time lapse series of images (105 s, zoom area), under any experimental condition. White open circles, in a time lapse series of images, show representative events for CD4-dependent viral uptake or inhibition analyzed by time for their fluorescence intensities (right curves). Bar, 5 μm. (E) Histograms show the percentage of bound HIV-1–Gag-EGFP particles to CD4-DsRed that entered seven cells (ratio of CD4-dependent viral uptake events to the total number of CD4/HIV-1 interactions analyzed appears above the histograms), under any experimental condition.

conceivable that siRNA-Arf6 inhibited CD4-dependent productive viral entry, as was observed by TIRFM (Figure 9, B and C, fluorescence intensity curves and time lapse images from zoom area for CD4-DsRed and bound HIV-1–Gag-EGFP, and Supplemental Videos 5 and 6).

Arf6 regulates HIV-1 viral fusion and entry steps of the viral cycle

We performed viral fusion and entry experiments by using R5- and X4-tropic HIV-1 viral particles containing the BlaM-Vpr chimera in Arf6-silenced CD4+ T lymphocytes (Figure 10A) to ascertain the mechanism involved in Arf6-dependent efficient early HIV-1 infection. These chimera virions were designed specifically to study the first steps of viral infection (Cavrois *et al.*, 2002) because β-lactamase activity directly correlates with viral fusion and entry (Cavrois *et al.*, 2002; Barrero-Villar *et al.*, 2008, 2009). Control (scrambled)– or siRNA-Arf6–treated CEM-CCR5 cells were incubated (3 h) with equivalent viral inputs of X4-tropic or R5-tropic virions containing the BlaM-Vpr fusion protein. Concurring with all the results presented earlier in this article and as observed by TIRFM (Figure 9), specific Arf6 silencing significantly inhibited viral fusion and entry, regardless of viral tropism, compared with the more susceptible scrambled-treated cells to viral fusion and entry (Figure 10B). Therefore it seems that Arf6 knockdown interfered with Arf6-mediated plasma membrane dynamics during the virus–cell fusion process.

It has been recently reported that HIV-1 enters cells in mainly a clathrin-dependent, endocytic pathway (Miyauchi *et al.*, 2009). We used BlaM-Vpr virions pseudotyped with the VSV-G envelope protein as a control of the specificity of Arf6 knockdown regulation of HIV-1–induced membrane fusion to explore the Arf6 role on clathrin-dependent viral fusion and entry process. These pseudotyped viruses enter target cells using the clathrin-endocytic lower pH pathway due to the VSV-G envelope (Matlin *et al.*, 1982; Sun *et al.*, 2005). As observed above, VSV-G–mediated viral fusion and entry were independent of Arf6 activity (Figure 10B), thereby suggesting that Arf6 activity did not affect clathrin-mediated vesicle trafficking from the cell surface.

We next analyzed the possibility that Arf6 silencing or Arf6-GTP/GDP cycle mutants may affect the function of CXCR4 and CCR5, the main HIV-1 coreceptors, which may result in viral fusion, entry, and infection inhibition. For this purpose, we first assayed ligand-induced CXCR4 and CCR5 internalization in CD4+ lymphocytes, transiently transfected with control or siRNA-Arf6–pEGFP-N2-RNAi plasmids. Cells transfected with these vectors express both control and siRNA-Arf6 oligonucleotides, for Arf6 knockdown, and the EGFP protein (Figure 10C), which allows us to identify control and Arf6-silenced cells by

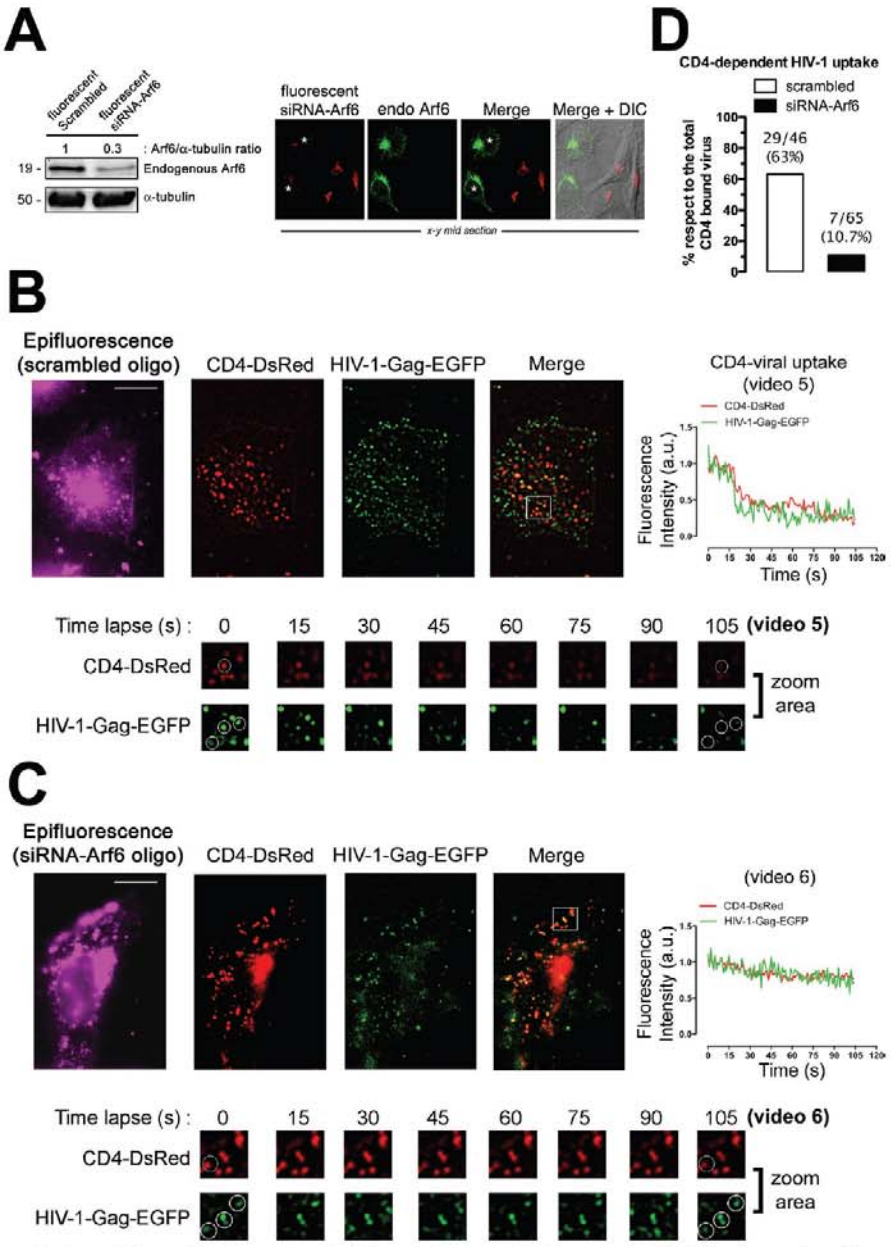

FIGURE 9: Effect of endogenous Arf6 knockdown on HIV-1 entry in TZMbl cells analyzed by TIRFM. (A) Left, Western blot analysis of endogenous Arf6 knockdown, 24 h after fluorescent-siRNA nucleofection of TZMbl cells, quantified as the band intensity ratios to α-tubulin. Fluorescent scrambled oligonucleotides represent the negative control for RNAi. A representative experiment of three is shown. Right, a series of *x*–*y* midsection images showing the specific silencing of endogenous Arf6 (green) by fluorescent siRNA-Arf6 oligonucleotides (red). Asterisks indicate cells where Arf6 was not silenced. Merge and merge/DIC images are shown from a representative experiment. (B and C) A series of TIRFM images indicating cell-surface CD4-DsRed, HIV-1–Gag-EGFP virions, and CD4-attached HIV-1–Gag-EGFP virions (merge) at the EF of TZMbl, both in scrambled- or siRNA-Arf6–transfected cells. Fluorescent scrambled or siRNA-Arf6 oligonucleotides are monitored by epifluorescence. White squares in the merged images show a representative area (zoom area) where CD4-dependent HIV-1 uptake or blockade was observed, corresponding to Supplemental Videos 5 and 6, and a time lapse series of images (105 s, zoom area). Bar 5 μm. White open circles, in a time lapse series of images, show representative events for CD4-dependent viral uptake or inhibition, analyzed by time for their fluorescence intensities (right curves). (D) Histograms show the percentage of bound HIV-1–Gag-EGFP particles to CD4-DsRed that entered seven cells (ratio of CD4-dependent viral uptake events to the total number of CD4/HIV-1 interactions analyzed appears above the histograms), under any experimental condition.

EGFP-associated fluorescence. Ligand-induced endocytosis of viral coreceptors was then performed and analyzed by flow cytometry in EGFP-positive cells under any experimental condition. Arf6 knockdown by this plasmid did not affect CXCR4 or CCR5 cell–surface expression (Figure 10D), as presented for Arf6-silenced cells (Figure 5B and Supplemental Figure 4B). It is noteworthy that Arf6 silencing did not affect SDF-1α (CXCL12)– or RANTES (regulated on activation, normal T expressed and secreted) (CCL5)–mediated CXCR4 or CCR5 internalization, respectively, compared with control cells (Figure 10D). Similarly, overexpression of Arf6-Q67L– or Arf6-T44N–EGFP mutants (Figure 10E) neither affected cell–surface expression of CXCR4 and CCR5 nor prevented its ligand-induced internalization, compared with WT Arf6–EGFP–transfected cells (Figure 10F). These data were obtained by flow cytometry analysis of EGFP-positive cells expressing Arf6-EGFP constructs. Therefore ligand-induced CXCR4 and CCR5 internalization, a clathrin-dependent endocytic process (Borroni *et al.*, 2010), does not seem to be affected by Arf6 activity (Figure 10, C–F). CXCR4 and CCR5 viral coreceptors appear to be functional under our experimental conditions.

Taken together these results prompted us to suggest that Arf6-coordianted PIP_2-associated plasma membrane dynamics are required for efficient HIV-1 fusion and entry events, regardless of the viral tropism and without affecting CD4 expression and trafficking, HIV-1/CD4 interaction, and CXCR4 or CCR5 function. Arf6 activity does not seem to be involved in VSV-G–mediated fusion, entry, and infection or ligand-mediated viral coreceptor endocytosis; both are clathrin-dependent processes.

Arf6-dependent and clathrin/transferrin-dependent endocytic pathways have been reported to coexist as two separately trafficking routes from plasma membrane in HeLa cells and other cell types (Radhakrishna and Donaldson, 1997; Nichols and Lippincott-Schwartz, 2001; Donaldson, 2003; Naslavsky *et al.*, 2003; Donaldson *et al.*, 2009). We observed, using TIRFM, the distribution of clathrin-coated structures (CCS; i.e., clathrin-coated pits [CCP] and vesicles [CCV]) at the plasma membrane, under any experimental condition and as described in Barroso-Gonzalez *et al.* (2009b). It appears that neither CCP nor CCV formation at the plasma membrane was affected by an alteration of Arf6 activity, after overexpressing each Arf6 mutant, when compared with control conditions (Supplemental Figure 5, CCS-mLCa-DsRed images). In addition, we observed

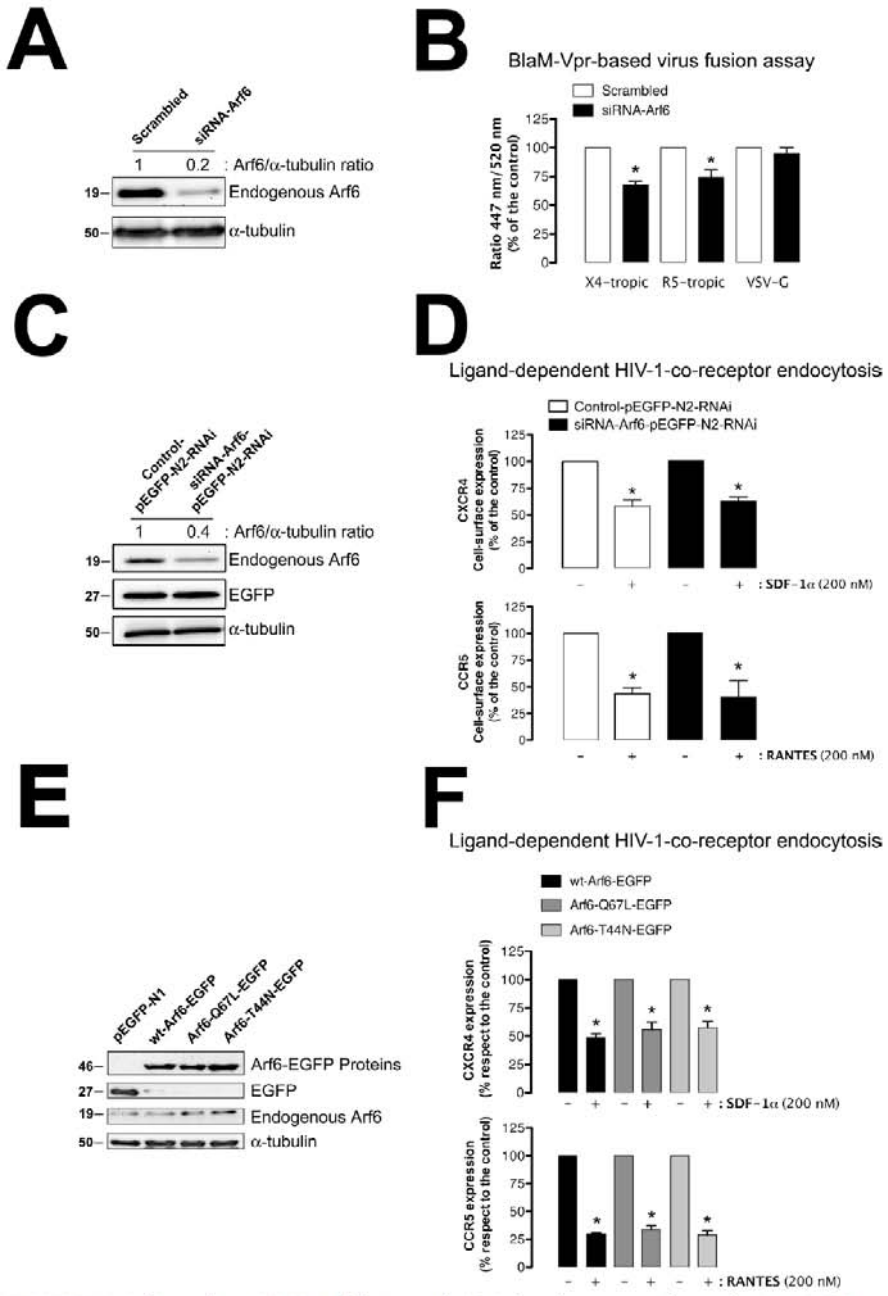

FIGURE 10: Arf6 regulates HIV-1 viral fusion with CD4+ lymphocytes, without affecting CCR5 and CXCR4 internalization. (A) Western blot analysis of endogenous Arf6 knockdown 24 h after siRNA nucleofection of CEM-CCR5 cells, quantified as the band intensity ratios to α-tubulin. Scrambled oligonucleotides represent the negative control for RNAi. A representative experiment of three is shown. (B) Specific silencing of endogenous Arf6 specifically affects the early steps of viral infection. Control (scrambled)– or siRNA-Arf6–treated CEM-CCR5 cells were incubated for 3 h with equivalent viral inputs (determined by standard p24-ELISA) of X4-tropic or R5-tropic pNL4-3.Luc.R-E- virions containing the BlaM-Vpr fusion protein. After adsorption for 3 h, cells were treated with CCF2-AM and analyzed by fluorescence spectrophotometry after 16 h. VSV-G virions containing the BlaM-Vpr fusion protein were used to control the specificity of Arf6-mediated effects on HIV-1 viral fusion. The percentages of HIV-1–fused cells were determined by measuring the ratio of blue (447 nm; cleaved CCF2) to green (520 nm; intact CCF2) fluorescence signals in target cells. Each assay was done in triplicate, and results are representative of three independent experiments. (C) Western blot analysis of endogenous Arf6 knockdown, 24 h after control- or siRNA-Arf6–pEGFP-N2-RNAi nucleofection of CEM-CCR5 cells, quantified as the band intensity ratios to α-tubulin. Control and siRNA oligonucleotides were transfected using the pEGFP-N2-RNAi plasmid; therefore treated cells expressed the EGFP protein, which serves as a control of cell treatment. A representative experiment of three is shown. (D) Effect of Arf6 knockdown on ligand-induced CXCR4 (SDF-1α) and CCR5 (RANTES) endocytosis in CEM-CCR5 cells. Control or siRNA-Arf6–pEGFP-N2-RNAi–treated cells were exposed to SDF-1α (200 nM) or RANTES (200 nM) for 1 h at 37°C. Then CXCR4 or CCR5 expression was analyzed by flow cytometry in control/EGFP+ and siRNA-Arf6/EGFP+ cells using PE-conjugated specific mAbs against cell-surface CXCR4 or CCR5. Data are mean ± SEM of three independent experiments carried out in triplicate and refer to CXCR4 or CCR5 expression in the absence of SDF-1α or RANTES, respectively, taken as 100%. Asterisk indicates $p < 0.05$, *t* test. (E) Western blot analysis of endogenous Arf6, WT Arf6–, Arf6-Q67L–, and Arf6-T44N–EGFP expression in CEM-CCR5 cells. α-Tubulin and pEGFP-N1 are the controls for total protein and intact Arf6-EGFP expression, respectively. (F). Effect of different Arf6-EGFP constructs on ligand-induced CXCR4 (SDF-1α) and CCR5 (RANTES) endocytosis in CEM-CCR5 cells. The experiments were carried out as indicated in (D) but in cells overexpressing each Arf6-EGFP construct. Data are mean ± SEM of three independent experiments carried out in triplicate and refer to cell-surface CXCR4 or CCR5 expression in WT Arf6–EGFP–transfected cells in the absence of SDF-1α or RANTES, respectively, taken as 100%. Asterisk indicates $p < 0.05$, *t* test.

that each Arf6 mutant colocalized with and provoked the accumulation of PIP_2-associated structures at the plasma membrane in nonclathrin plasma membrane regions (Supplemental Figure 5, EGFP, PH-ECFP, and merged images). Therefore it seems that Arf6 did not alter CCS at the plasma membrane; VSV-G-mediated virus fusion, entry, and infection; and ligand-induced endocytosis of HIV-1 main coreceptors.

Taking all the presented results together, we propose that efficient HIV-1 fusion, entry, and infection require Arf6-coordinated PIP_2-associated membrane dynamics. This process depends on Arf6-GTP/GDP activity to promote viral fusion (i.e., pore fusion formation) at the cell surface of target cells and appears to be clathrin independent.

DISCUSSION

We have shown here that early HIV-1 infection of permissive CD4+ T lymphocytes was impaired by the modification of Arf6-dependent membrane dynamics, either by specific RNAi or by overexpressing GTP-bound or GDP-bound inactive mutants of Arf6. Arf6-Q67L and Arf6-T44N mutants induced the accumulation of PIP_2-associated structures at the plasma membrane of permissive cells,

as monitored by the PH-ECFP probe. This fact is indicative of a perturbed PIP_2-associated membrane trafficking from the cell surface. Arf6-Q67L, Arf6-T44N, Arf6-T27N, and Arf6-N48I/Q67L mutants inhibited early viral infection, indicating that the Arf6-GTP/GDP cycle regulates efficient HIV-1 entry and infection.

Alteration of the GTPase cycle of Arf6 had no effect on the cell-surface level of expression and function of CD4, CCR5, and CXCR4 receptors for HIV-1. TIRFM studies for CD4-dependent HIV-1 uptake, in nonlymphoid permissive HeLa-derived cells expressing CD4, CCR5, and CXCR4 viral receptors, showed that the first virus/CD4 interactions are not affected by the inhibition of Arf6-coordinated plasma membrane dynamics. Arf6 mutants or specific Arf6 silencing inhibits viral entry and infection independently of viral tropism, suggesting that viral receptors are not affected or negatively involved in this process. Free or virus-bound CD4 does not distribute or localize with Arf6 constructs, suggesting that CD4 neither traffics from nor recycles to plasma membrane Arf6 dependently. Arf6 mutants or silencing do not appear to affect ligand-induced CXCR4 or CCR5 endocytosis, a clathrin-dependent process (Borroni *et al.*, 2010).

Regulation of early HIV-1 infection by Arf6 activity seems to be related to fusion and entry steps of the viral cycle. We observed that either Arf6 mutants or specific Arf6 silencing inhibited HIV-1 Env–mediated membrane fusion, viral entry, and infection regardless of viral tropism. We observed, by TIRFM, that CD4-DsRed–preattached HIV-1–Gag-EGFP viral input internalized together with the associated cell-surface CD4 receptor in cells transfected by WT Arf6–HA. In fact, their respective intensity of fluorescence dimmed in the EF, representing CD4-dependent viral uptake. On the contrary, PIP_2-associated plasma membrane structures accumulated in cells overexpressing each Arf6-HA mutant, rendering them refractory to CD4-dependent HIV-1 uptake. Comparable inhibition was observed in cells transfected by WT Arf6–HA pretreated by T-20, which prevents CD4-dependent HIV-1 fusion and productive entry. Transiently expressed CD4-DsRed attached HIV-1–Gag-EGFP virions under any experimental condition. This fact indicates that Arf6-mediated plasma membrane trafficking is required for efficient CD4-dependent HIV-1 entry, without affecting CD4/virus interaction. Blockade of Arf6-GTP/GDP activity by siRNA silencing inhibits efficient X4- or R5-tropic HIV-1 fusion and entry (i.e., pore fusion formation) of viruses containing the BlaM-Vpr chimera in $CD4^+$ lymphocytes, without affecting ligand-induced CXCR4 or CCR5 endocytosis, and VSV-G-mediated fusion, entry, and infection, both clathrin-dependent processes. Therefore Arf6 knockdown appears to interfere with Arf6-mediated plasma membrane dynamics.

In general, viruses, including HIV, can disseminate within an infected host by cell-free viruses and via direct cell-to-cell transmission (Phillips, 1994; Johnson and Huber, 2002; McDonald *et al.*, 2003; Gousset *et al.*, 2008). The relative contribution of these modes of HIV-1 dissemination in vivo is not well established, but cell-to-cell spread probably occurs mainly in tissues densely populated with target cells, such as $CD4^+$ T-cells in lymph nodes (Haase, 1999; McDonald *et al.*, 2003). Our results indicate that efficient cell–HIV-1 transmission and infection of human primary $CD4^+$ T-cells requires Arf6 activity in target lymphocytes because it is inhibited by Arf6-GTPase silencing independently of viral tropism. These data agree with Arf6 silencing–mediated inhibition of HIV-1 fusion, entry, and infection with luciferase- and BlaM-Vpr–bearing virions. BlaM-Vpr–based experiments are sensitive and specific to the detection of viral entry due to the quantitative measurement of the incorporated BlaM-Vpr chimeric virions present at cytoplasm after viral fusion (Cavrois *et al.*, 2002), avoiding interference with viruses captured in vesicular compartments, which may account for 60–90% of total viral uptake (Marechal *et al.*, 1998, 2001). Cellular signaling in target $CD4^+$ T-cells, such as cell-surface receptors and actin cytoskeleton reorganization, occurred equally during early HIV-1 infection, both in cell-to-cell transmission (i.e., the virological synapse) and free HIV-1 particle models (Jolly *et al.*, 2004; Jolly and Sattentau, 2004; Jimenez-Baranda *et al.*, 2007; Yoder *et al.*, 2008; Barrero-Villar *et al.*, 2009; Liu *et al.*, 2009). This finding is consistent with the fact that, at the virological synapse, HIV first buds from the infected donor cell and then binds to and fuses with the recipient cell, as in a free virus system (Blanco *et al.*, 2004; Puigdomenech *et al.*, 2009). Our results, obtained by using these two working models, indicate that Arf6-mediated membrane dynamics are required for efficient cell-viral transmission, HIV-1 fusion, entry, and infection of $CD4^+$ T lymphocytes.

There are divergent data regarding the functional implication of Arf6 activity in different aspects of HIV-1 cell biology. Thus HIV-1 infection in polarized trophoblasts, which are thought to play a determinant role in HIV-1 transmission in utero, seems to rely on Rab5 and Rab7 without the contribution of Arf6 or Rab11. This process is an unusual clathrin/caveolae-independent endocytic pathway, independent of the HIV-1 envelope complex (Vidricaire and Tremblay, 2005, 2007). HIV-1 eludes its specific immune recognition by down-regulating the expression of MHC-I at the cell surface of infected cells (Schwartz *et al.*, 1996). Arf6-activity, using the Arf6-Q67L mutant, is involved in this Nef-induced MHC-I internalization process (Blagoveshchenskaya *et al.*, 2002). However, other authors indicate that Arf6 activity is not involved in Nef-mediated down-modulation of MHC-I (Larsen *et al.*, 2004). Overexpression of WT Arf6 did not enhance or substitute the effects of Nef on MHC-I internalization (Blagoveshchenskaya *et al.*, 2002; Larsen *et al.*, 2004). We have not observed any functional effect for WT Arf6, EFA6, or WT Arf6/EFA6 overexpression on HIV-1 fusion, entry, and infection in permissive cells, indicating that Arf6-dependent signaling is not involved in this process. This lack of activity for full-length Arf6 has been described in several cellular processes, in which Arf6 implication was determined by using its different mutants (Blagoveshchenskaya *et al.*, 2002; Donaldson, 2003; Larsen *et al.*, 2004). Although Arf6 activates PLD and PI4P5-K effectors (Brown *et al.*, 2001; Vitale *et al.*, 2002; D'Souza-Schorey and Chavrier, 2006; Gillingham and Munro, 2007), and considering that overexpression of PI4P5-K Iα enhances HIV-1 viral fusion and infection (Barrero-Villar *et al.*, 2008), our results with Arf6/EFA6, single Arf6-GTP/GDP cycle mutants, and the Arf6-N48I/Q67L mutant, which bears the Q67L mutation and fails to activate PLD, suggest that WT Arf6/EFA6 overexpression does not activate PI4P5-K Iα and that PLD activity is not directly involved in the regulation of viral fusion and entry.

It has been reported that HIV-1 fuses with and enters cells via endocytosis in a dynamin- and clathrin-dependent manner in HeLa permissive cells (Miyauchi *et al.*, 2009). Arf6- and clathrin/transferrin-dependent endocytic pathways have been reported to coexist as two separately trafficking routes from plasma membrane in HeLa and other cell types (Radhakrishna and Donaldson, 1997; Nichols and Lippincott-Schwartz, 2001; Donaldson, 2003, Naslavsky *et al.*, 2003; Donaldson *et al.*, 2009). Our TIRFM studies indicate that Arf6 inhibition did not affect CCS formation at plasma membrane. Moreover, Arf6 mutants or specific Arf6 silencing did not inhibit cell infection by HIV-1 vectors pseudotyped with the VSV-G protein. Considering all the exposed data and discussion, we propose that Arf6-GTP/GDP activity has synergy with the key first HIV-1/receptors interactions by maintaining PIP_2-associated membrane dynamics to promote efficient viral fusion and entry in a clathrin-independent manner.

Therefore efficient early HIV-1 infection of permissive CD4+ T lymphocytes requires Arf6-coordinated plasma membrane dynamics.

MATERIALS AND METHODS

Antibodies and reagents

The monoclonal antibody (mAb) RPA-T4 (clone) is directed against CD4, and the CD184 (clone 12G5) and CD195 (clone 2D7/CCR5), used as phycoerythrin (PE) conjugates (BD Bioscience/BD PharMingen, San Jose, CA), are directed against the second extracellular loop of CXCR4 or CCR5, respectively. The mAb L3T4 is a neutralizing antibody against CD4 (eBioscience, San Diego, CA). The anti-CD4 mAb Leu3a was from Becton Dickinson (Franklin Lakes, NJ). C34 is a fusion inhibitor covering the 628–661 amino-acid sequence of gp41 viral protein, similar to T-1249 (residues 628–663) and to T-20 (residues 638–673). Mouse mAb (8A6-4) against Arf6 (Londono *et al.*, 1999) was kindly provided by Sylvain Bourgoin (Center de Recherche du CHUQ, pavillon CHUL, Rheumatologie et Immunologie, Ste-Foy, QC, Canada). The mAb recognizing Arf6 (ARF6 [3A-1]: sc-7971), anti-EGFP rabbit polyclonal antibody (pAb) (sc-8334), anti-HA mAb (sc-7392), anti–HLA-A/B/C mAb (3F10; sc-65288), and PE-conjugated goat anti-mouse immunoglobulin (Ig) G (sc-3738) came from Santa Cruz Biotechnology (Santa Cruz, CA). Anti–VSV-G tag (ab3861) goat pAb to detect vsv-g-EFA6 was from Abcam (Cambridge, UK). Anti–α-tubulin mAb was from Sigma-Aldrich (St. Louis, MO). Secondary horseradish peroxidase–conjugated anti-mAb was from ImmunoTools (Friesoythe, Germany), and secondary horseradish peroxidase–conjugated anti–rabbit and anti–goat antibody were from Dako (Glostrup, Denmark). Alexa Fluor 633 phalloidin and Alexa Fluor 568–goat anti-mouse were from Molecular Probes (Eugene, OR). Stromal cell–derived factor (SDF) 1α (CXCL12) was kindly synthesized and provided by Françoise Baleux (Institut Pasteur, Paris, France) (Valenzuela-Fernandez *et al.*, 2001, 2002). RANTES (CCL5) was from R&D Systems (Minneapolis, MN).

Cells

The human CEM.NKR-CCR5 (CEM-CCR5) permissive cell line (catalogue no. 4376, NIH AIDS Research and Reference Reagent Program, Division of AIDS, National Institute of Allergy and Infectious Diseases [NIAID], National Institutes of Health [NIH]) was grown at 37°C in a humidified atmosphere with 5% CO_2 in RPMI 1640 medium (Lonza, Verviers, Belgium) supplemented with 10% fetal calf serum (FCS) (Lonza), 1% L-glutamine, and 1% penicillin-streptomycin antibiotics. Cells were regularly passaged every 3 d. The 293T cell line was similarly cultured in supplemented DMEM (Lonza) and was regularly passaged every 2–3 d. Cells were harvested and resuspended at a density of 50–70% in fresh supplemented DMEM 24 h before cell transfection with viral DNA constructs. HeLa-P5 cells, stably transfected with human CD4 and C-terminal EGFP-tagged CCR5 cDNAs and with an HIV-LTR–driven β-galactosidase (β-Gal) reporter gene, were provided by M. Alizon (Hôpital Cochin, Paris, France) (Valenzuela-Fernandez *et al.*, 2005; Barrero-Villar *et al.*, 2009; Barroso-Gonzalez *et al.*, 2009a). TZMbl (HeLa) cells are similar to HeLa-P5 cells but express nonfluorescent human CCR5 and contain integrated HIV-LTR–driven β-Gal and firefly luciferase reporter genes (TZMbl, catalogue no. 8129, NIH AIDS Research and Reference Reagent Program). HeLa 243 and HeLa ADA cells coexpressing the Tat and HIV-1 Env proteins were also provided by M. Alizon (Pleskoff *et al.*, 1997; Valenzuela-Fernandez *et al.*, 2005; Barrero-Villar *et al.*, 2009; Barroso-Gonzalez *et al.*, 2009a). Peripheral blood mononuclear cells were obtained by Ficoll density gradient of blood cells provided by the local blood bank and immediately used to purify CD4 T-cells (>95%) by immunomagnetic negative selection (Miltenyi Biotec, Bergisch Gladbach, Germany). MOLT-4/CCR5 (MOLT/CCR5) cells, which are highly permissive for R5-tropic HIV-1 infection either uninfected or chronically infected with the HIV-1_{NL4-3} and HIV-1_{BaL} isolates (>90% producing HIV-1 particles) have been previously described (Blanco *et al.*, 2004; Puigdomenech *et al.*, 2008). Cells were maintained in RPMI 1640 (Life Technologies-BRL, Grand Island, NY) supplemented with 10% FCS (Life Technologies) and used without stimulation.

Human DNA constructs

Human cDNAs of the C-terminal HA-tagged WT Arf6–, Arf6-Q67L–, and Arf6-T27N–HA were kindly provided by Julie Donaldson (Laboratory of Cell Biology, National Heart, Lung, and Blood Institute, Bethesda, MD). Arf6-T44N–HA mutant and vsv-g–tagged EFA6 factor were gifts from Michel Franco (Institut de Pharmacologie Moléculaire et Cellulaire, Centre National de la Recherche Scientifique [CNRS] Unité Mixte de Recherche 6097, Valbonne Sophia-Antipolis, France). Arf6-N48I/Q67L–HA, control- and siRNA-Arf6–pEGFP-N2-RNAi plasmids were gifts from Nicolas Vitale (Institut des Neurosciences Cellulaires et Intégratives, CNRS, Strasbourg, France) (Vitale *et al.*, 2002; Begle *et al.*, 2009). Arf6-EGFP or Arf6-ECFP constructs were generated by PCR using each Arf6-HA construct as template and CGCTCGAGGCCACCATGGGGAAGGTGCTATC (sense) and CGGAATTCCAGATTTGTAGTTAGAGG (antisense) as 5′ and 3′ primers, respectively. The amplified products were respectively subcloned into pEGFP-N1 or pECFP-N1 (Clontech, Palo Alto, CA) after restriction with *Xho*I and *Eco*RI. For CD4-DsRed expression, total RNA from CEM.NKR-CCR5 T-cells was extracted, and first-strand cDNA was made using reverse transcriptase and random hexamers as primers. Thus the CD4 construct lacking the stop codon was generated by Expand High Fidelity PCR using cDNA as template and CTTCGAATTCGCCACCATGAACCGGGGAGTCCCTTTTAGGC (sense) and GCGGGGTACCACAATGGGGCTACATGTCTTCTGAAACC (antisense) as 5′ and 3′ primers, respectively. The amplified product was subcloned into pDsRed-NI (Clontech) after restriction with *Eco*RI and *Kpn*I restriction enzymes.

The C-terminal ECFP-tagged PH domain of the PLCδ_1 (PH-ECFP) was provided by Senena Corbalán-García (Universidad de Murcia, Spain) and was used as a PIP_2 biosensor in the plasma membrane as described (Marin-Vicente *et al.*, 2005; Barrero-Villar *et al.*, 2008; Barroso-Gonzalez *et al.*, 2009b). mLCa-DsRed was provided by Wolfhard Almers (Vollum Institute, Oregon Health and Science University, Portland, OR) and was used as described (Barroso-Gonzalez *et al.*, 2009b). All constructs were verified by digestion with restriction enzymes.

Messenger RNA silencing

We have designed the following specific short interference oligonucleotides against the following mRNA (siRNA) sequence of Arf6: siRNA-Arf6 1 (position 699–622; sense: 5′-gacaacaauccuguacaag-3′-dTdT; antisense: 5′-guuguacaggauuguuguc-3′dTdT) and siRNA-Arf6 2 (position 930–622; sense: 5′-gcaccgcauuaucaaugaccg-3′-dTdT; antisense: 5′-cggugauugauaaugcggugc-3′-dTdT). We used a mix of these two oligonucleotides to induce specific siRNA-mediated silencing of the endogenous expression of the Arf6 protein, which is called siRNA-Arf6 in the present work. We have also designed the following siRNA oligonucleotides against human CD4 mRNA: siRNA-CD4 (position 769–787: sense: 5′-gaacaaggaaguucugua-3′-dTdT; antisense: 5′-uacagacacuuccuuguuc-3′-dTdT). Alexa 546–conjugated or nonfluorescence siRNA oligonucleotides, irrelevant scrambled siRNA (control), or siRNA-Arf6 oligonucleotides were from

Sigma-Aldrich. cDNA fragments, kindly provided by Nicolas Vitale (Strasbourg, France), encoding 19-nucleotide siRNA sequence (GCTGCACCGCATTATCAAT) derived from the target transcript and separated from its reverse 19-nucleotide complement by a short spacer, were annealed and cloned in the *Bgl*II and *Hind*III sites in front of the H1 promoter of the pEGFP-N2-RNAi plasmid, as previously described (Begle *et al.*, 2009) for siRNA targeting of human Arf6 by plasmids. Cells treated with control or siRNA-Arf6–pEGFP-N2-RNAi plasmid express free EGFP. The siRNAs for Arf6 and CD4 sustained specific interference of protein expression for at least 72 h, as monitored by Western blot (unpublished data).

Cellular transfection

All human permissive HeLa cell lines were grown at 37°C in a humidified atmosphere with 5% CO_2 in DMEM (Lonza) supplemented with 10% FCS (Lonza), 1% L-glutamine, and 1% penicillin-streptomycin antibiotics. Cells were harvested and resuspended at a density of 50–70% in fresh supplemented DMEM 24 h before cell transfection with siRNA and/or DNA constructs. Specific Amaxa kits (Amaxa, Köln, Germany) were used for delivery of DNA constructs and/or siRNA into HeLa cells. Similarly, permissive T lymphocytes and human primary $CD4^+$ T-cells were nucleofected according to the manufacturer's instructions (Amaxa), as previously described (Barrero-Villar *et al.*, 2008, 2009; Barroso-Gonzalez *et al.*, 2009a), with 1 μM siRNA and/or 1 μg of each DNA construct used and assayed no more than 24 or 48 h later.

Western blotting

The extent of protein expression or gene silencing was assessed by Western blot of cell lysates. Cells nucleofected with scrambled or specific siRNA oligonucleotides against Arf6 or CD4, or with the different DNA constructs, were lysed 24 h later for 30 min at 4°C in 1% Triton X-100, 50 mM Tris HCl, and 150 mM NaCl with a protease and phosphatase inhibitor mixture (Roche Diagnostics, Mannheim, Germany) and centrifuged at 4°C, 13,000 rpm, for 15 min. Equivalent amounts of proteins, measured using the bicinchoninic acid method (BCA protein assay kit from Pierce, Rockford, IL), were separated by SDS–PAGE using 12% gradient gels and electroblotted onto 0.45 μm polyvinylidene difluoride membranes (Millipore Corporation, Billerica, MA). Cell lysates were immunoblotted with specific antibodies, protein bands were detected by luminescence using an ECL System (Pierce), and protein bands were analyzed using a VersaDoc device and Quantity One 4.6.7 software (Bio-Rad, Hercules, CA).

Viral DNA constructs

The pNL4-3.Luc.R-E- provirus (catalogue no. 6070013), HXB2-env (catalogue no. 5040154), and pCAGGSSF162-gp160-env (catalogue no. 3041817) glycoprotein vectors for X4- and R5-tropic viral envelopes, and the pGag-EGFP (catalogue no. 11468; from Marilyn Resh) vector, allowing imaging of intracellular Gag trafficking and localization in live cells, which directs Rev-independent expression of an HIV-1–Gag-EGFP fusion protein (Schwartz *et al.*, 1992), were obtained through the NIH AIDS Research and Reference Reagent Program. The pCMV-BlaM-Vpr vector was kindly provided by Warner C. Greene (University of California, San Francisco).

Production of viral particles

Replication-deficient luciferase–HIV-1 viral particles were obtained as previously described (Barrero-Villar *et al.*, 2008, 2009; Barroso-Gonzalez *et al.*, 2009a). Briefly, replication-deficient viral particles were derived by the luciferase-expressing reporter virus HIV/Δ*nef*/Δ*env*/*luc*$^+$ (which bears the luciferase gene inserted into the *nef* ORF and does not express envelope glycoprotein) with an X4-tropic (Lai) or R5-tropic (SF162) envelope glycoprotein. X4- or R5-tropic HIV-1 viral particles were produced by cotransfecting 293T cells (70% of confluence) in 10-cm^2 dishes with pNL4-3.Luc.R-E- (10 μg) and X4-tropic (HXB2-env) or R5-tropic (pCAGGS SF162 gp160) envelope glycoprotein (10 μg) vector, as previously described (Barrero-Villar *et al.*, 2008, 2009; Barroso-Gonzalez *et al.*, 2009a). Viral plasmids were transduced in 293T cells by using linear polyethylenimine, with an average molecular mass of 25 kDa (PEI25k) (Polyscience, Warrington, PA). Viral plasmids were first dissolved in 1/20th of the final tissue culture volume of DMEM in 150 mM NaCl. The PEI25k was prepared as a 1 mg/ml solution in water and adjusted to neutral pH. After the addition of PEI25k, previously dissolved in 150 mM NaCl, to the viral plasmids (at a plasmids:PEI25k ratio of 1:3 [wt/wt]), the solution was mixed by vortexing, incubated for 20–30 min at room temperature, and then added to 293T cells in culture. After 6 h the medium was changed to RPMI 1640 and supplemented with 10% FCS and antibiotics, and the cells were cultivated for 48 h to allow viral production. Viruses were harvested 48 h posttransfection. The supernatant was clarified by centrifugation at 3000 × *g* for 30 min, filtered by 0.45 μm, and concentered by Amicon Ultra-4 Centrifugal filter devices (Millipore). Virions were then stored at −80°C. Viral stocks were normalized by p24-Gag content measured with an enzyme-linked immunosorbent assay test (Innogenetics, Gent, Belgium). HIV-1–Gag-EGFP virions were similarly obtained after cotransduction of the pGag-EGFP vector (5 μg) with Env vectors (10 μg). Therefore we used this pGag-EGFP vector to produce fluorescent viruslike particles with an efficiency equivalent to that of Gag (Schwartz *et al.*, 1992), which allowed us to image HIV-1 entry by TIRFM. Nonreplicative viral particles, containing the BlaM-Vpr chimera, were similarly produced after cotransduction of the pCMV-BlaM-Vpr vector (5 μg) with pNL4-3.Luc.R-E- (10 μg) and Env vectors (10 μg), as described (Barrero-Villar *et al.*, 2008, 2009).

Luciferase viral entry and infection assay

Untreated or nucleofected CEM-CCR5 cells (100,000 cells in 96-well plates) and untreated or nucleofected HeLa-P5 cells (20,000 cells in 96-well plates) were infected with a synchronous dose of luciferase-based X4- or R5-tropic HIV-1 viral inputs (500 ng of p24), in 200 μl RPMI 1640 medium for 2 h, as described (Barrero-Villar *et al.*, 2008, 2009; Barroso-Gonzalez *et al.*, 2009a). Virus was removed by washing infected cells. After 48 h of infection, luciferase activity was determined by using a luciferase assay kit (Biotium, Hayward, CA) with a microplate reader (VictorTM X5, PerkinElmer, Waltham, MA). When indicated T-20 (5 μM) was used as a control for the blockage of viral–cell fusion, preincubated in cells for 30 min at 37°C before infection. Data were analyzed using GraphPad Prism 5.0 software (GraphPad Software, San Diego, CA).

Virion-based fusion assay

The 0.5 × 10^6 CEM-CCR5 permissive cells (scrambled or siRNA-Arf6 treated) were incubated for 3 h with equivalent viral inputs of BlaM-Vpr–containing virions (500 ng p24) in 500 μl RPMI-1640 medium. Cells were then extensively washed to remove free virions and incubated (1 h, room temperature) with CCF2-AM loading mix, as recommended by the manufacturer (GeneBLAzer detection kit; Invitrogen, Carlsbad, CA), as previously described (Barrero-Villar *et al.*, 2008, 2009). Next excess dye was washed off and cells were incubated for 16 h at room temperature before

fixation with 1.2% paraformaldehyde. The percentages of CCF2-loaded target-infected cells, fused with BlaM-Vpr–containing virions, were determined by measuring the fluorescence intensities of the intact and cleaved CCF2 probe in a fluorescence spectrophotometer (Cary Eclipse, Varian, Melbourne, Australia), as described (Barrero-Villar *et al.*, 2009). Thus the percentage of 100% of infection was determined by measuring the fluorescence intensities of the intact and cleaved CCF2 probe in control infected cells (scrambled treated cells) and subtracting the background blue and green fluorescence ratio determined in noninfected cells (without β-lactamase activity), as proposed by the manufacturer (GeneBLAzer detection kit, Invitrogen). In siRNA-Arf6–treated cells, a decrease in the ratio of blue (447 nm; cleaved CCF2) to green (520 nm; intact CCF2) fluorescence signals compared with control (scrambled) cells indicates fewer virions fused to target cells. The background blue and green fluorescence was determined in noninfected CCF2-loaded cells (without β-lactamase activity), under any experimental condition.

HIV-1 Env–mediated cell-to-cell fusion assay

A β-Gal cell fusion assay was performed as previously described (Barrero-Villar *et al.*, 2008, 2009; Barroso-Gonzalez *et al.*, 2009a). Briefly, HeLa-243 or HeLa-ADA cells were mixed with HeLa-P5 cells or control, or previously transfected with Arf6 constructs, in 96-well plates in a 1:1 ratio (20,000 total cells). These cocultures were kept at fusion for 16 h at 37°C. The fused cells were washed with Hanks' balanced salt solution and lysed, and the enzymatic activity was evaluated by chemiluminescence (β-Gal reporter gene assay, Roche Diagnostics). Anti-CD4 neutralizing mAb L3T4 was used as a control for the blockage of cell fusion (5 µg/ml was preincubated in HeLa-P5 cells for 30 min at 37°C before coculture with Env$^+$-HeLa cells).

Cocultures of HIV-1–infected MOLT/CCR5 cells with primary CD4$^+$ T-cells

Chronically infected MOLT/CCR5 cells (500,000 cells/well) were preincubated in 96-well plates, either alone (control) or with the fusion inhibitor peptide C34 (5 µg/ml) for 1 h at 37°C, before adding 500,000 primary nonactivated, scrambled-, or siRNA-Arf6–treated CD4$^+$ T-cells. C34 inhibitor concentrations were selected on the basis of complete inhibition of cell-to-cell HIV-1 transmission and infection. DNA was extracted after 24 h using the QIAmp DNA Blood Mini Kit (Qiagen, Hilden, Germany) and amplified in duplicate using a TaqMan universal PCR Master Mix, primers and probes for HIV-1 LTR, and human CCR5 genes (Applied Biosystems, Foster City, CA). Reactions (40 cycles of 15 s at 95°C for melting and 1 min at 60°C for annealing/extending) were conducted in an ABI 7000 Sequence Detection System (Applied Biosystems). HIV-1 infection was quantified by qPCR in which the relative proviral DNA synthesis was calculated using a standard curve generated with a plasmid that harbors the sequence of the HIV-1 LTR and the CCR5 gene. Copy numbers obtained for each sample were extrapolated to the standard equation as described (Buzon *et al.*, 2010). The concentrations obtained for LTR amplifications were then normalized to the CCR5 gene copy number as a measure of the number of cells present in each sample. The level of HIV-1 DNA into MOLT-infected cells was calculated from C34-containing cocultures.

Flow cytometry analysis

Permissive cells (CEM.NKR-CCR5 cells, primary CD4$^+$ lymphocytes, or phosphate-buffered saline [PBS]/EDTA–detached permissive HeLa cells) were incubated with PE-labeled specific antibodies against HLA-A/B/C (previously incubated with a specific primary mAb) and CD4, CXCR4, or CCR5 in control cells or cells transfected with Arf6 constructs or siRNA oligonucleotides. Cells were then washed by ice-cold PBS, fixed in PBS with 1% paraformaldehyde, and analyzed by flow cytometry (XL-MCL system; Beckman-Coulter, CA), as described (Valenzuela-Fernandez *et al.*, 2005; Barrero-Villar *et al.*, 2008, 2009; Barroso-Gonzalez *et al.*, 2009a).

Ligand-induced CXCR4 and CCR5 endocytosis

CEM-CCR5 cells (0.5×10^6 cells/ml) were incubated with 200 nM of SDF-1α or RANTES for 1 h at 37°C in free-serum RPMI 1640 medium, as described (Valenzuela-Fernandez *et al.*, 2002; Barroso-Gonzalez *et al.*, 2009a). Cells were then incubated for 3 min at 4°C in an acidic buffer (50 mM glycine, pH 3) that stops receptor endocytosis and removes CXCR4-bound SDF-1α or CCR5-bound RANTES molecules that would mask cell-surface receptors recognition by specific mAbs. Cells were washed twice with ice-cold PBS and 0.1% bovine serum albumin (BSA), before incubation with specific anti-receptor PE-conjugated mAbs (1:50) for 1 h at 4°C, and then fixed in 1% paraformaldehyde in PBS. Samples were analyzed on a flow cytometer (XL-MCL system) by measuring cell-surface receptor labeling on EGFP$^+$ cells, which express either Arf6-EGFP constructs or control- or siRNA-Arf6–pEGFP-N2-RNAi plasmids. Basal cell fluorescence intensity for cell-surface CXCR4 and CCR5 was determined using cells stained with a PE-conjugated IgG2a isotype control alone.

Immunofluorescence

Immunofluorescent lymphocytes or permissive HeLa cells (grown on glass coverslips, ~50% confluent) were washed three times with PBS and fixed for 20 min in 2% paraformaldehyde with 1% sucrose in PBS. Cells were washed three times with PBS after fixation and, when indicated, permeabilized with 0.1% Triton X-100 in PBS. The cells were then washed with PBS after permeabilization and immunostained for 1 h at room temperature by Alexa 633–labeled phalloidin or Alexa 568–labeled goat anti–mouse against HLA-A/B/C previously incubated with a specific mAb and diluted in PBS with 0.1% BSA. For Arf6 silencing, cells were nucleofected with fluorescent siRNA-Arf6 oligonucleotides and analyzed for endogenous Arf6 knockdown by using specific primary antibody against Arf6 before incubation with Alexa 488 secondary antibody species specific, at 24 h posttransfection in permeabilized cells, as described earlier in this article. Coverslips were mounted in Mowiol-antifade (Dako) and imaged in *x–y* midsections in a FluoView FV1000 confocal microscope through a 1.35 numerical aperture (NA) objective (60×) (Olympus, Center Valley, PA) for high-resolution imaging of fixed cells. The final images and molecule codistributions were analyzed and quantified with MetaMorph software (Universal Imaging, Downington, PA).

Total internal reflection fluorescence microscopy and analysis of HIV-1 entry

We performed total internal reflection fluorescence microscopy (TIRFM) experiments in adherent, nonlymphoid permissive HeLa-derived cells stably expressing CD4, CCR5, and CXCR4 viral receptors, owing to the intrinsic difficulties of the EF microscopy approach in lymphoid cells. Permissive TZMbl cells, transiently expressing the different Arf6-HA or Arf6-EGFP constructs or fluorescent siRNA oligonucleotides (λ_{Em} 680 nm) together with PH-ECFP and CD4-DsRed molecules, or Arf6-ECFP constructs with CD4-DsRed, were imaged with an inverted microscope Zeiss 200M

(Zeiss, Jena, Germany) through a 1.45 NA objective (αFluar, 100×, Zeiss), as described (Barroso-Gonzalez *et al.*, 2009a, 2009b). Experiments were performed and imaged with cells in a Krebs-HEPES buffer containing 2 mM Ca^{2+} at 37°C. After transfection, TZMbl cells (1×10^5 cells/well) were grown overnight on coverslips placed on 12-well plates. Synchronous doses (multiplicity of infection 1.0) of nonreplicative HIV-1–Gag-EGFP virions were preincubated with permissive cells for 30 min at 4°C to allow virus/CD4 binding and to prevent viral uptake. Cells were then washed with cold Krebs-HEPES buffer to remove unbound viral particles, and CD4-dependent HIV-1 uptake was studied at 37°C by TIRFM. When T-20 (5 μM) was used, the anti-fusogenic peptide was added to all buffers and steps during all processes. The objective was coupled to the coverslip using an immersion fluid (n488 = 1.518, Zeiss). The expanded beam of an argon ion laser (LASOS Lasertechnik, Jena, Germany) was band-pass filtered and used to selectively excite different fluorescent proteins. The excitation light (around 488 nm) was directed to the objective by a dichroic mirror (500 nm) for EF illumination, and this was used to excite both the green fluorescent HIV-1–Gag-EGFP virions and the CD4-DsRed molecules at the plasma membrane. Green and red fluorescence was viewed through a DV2 image system (Photometrics, Tucson, AZ) that split red and green components of the image with a 565-nm dichroic mirror (565DCRX) and filtered them through D630/50-nm and D520/30 band-pass filters, respectively. The images were then projected side by side onto an EM-CCD digital camera (C9100-13, Hamamatsu Photonics, Hamamatsu City, Japan). The beam was focused on an off-axis position in the back focal plane of the objective. Light, after entering the coverslip, underwent total internal reflection as it struck the interface between the glass and the solution or cell at a glancing angle. Total internal reflection generates an EF that declines exponentially with increasing distance from the interface, depending on the angle at which light strikes the interface. The angle was measured using a hemicylinder, as described previously (Barroso-Gonzalez *et al.*, 2009a, 2009b). Each cell was imaged using HC Image acquisition software (Hamamatsu Photonics) for up to 3 min with 0.25-s exposures at 1 Hz when illuminated under the EF. At the beginning of each cell acquisition, we took epifluorescence images using a Hg lamp that were projected onto a back-illuminated CCD camera (AxioCam MRm, Zeiss) through a dichroic and specific band-pass filter for fluorescent siRNA oligonucleotides. The splitter DV2 system was aligned in each recording session, and to do this we took an alignment image showing densely scattered 0.2-μm fluorescein isothiocyanate–conjugated beads (Molecular Probes). They were visible in both the green and red channels and thus provided markers in the *x*–*y* plane.

To determinate the overlap between HIV-1–Gag-EGFP and CD4-DsRed, EF images were taken. The EF images were background subtracted using MetaMorph. We plotted a small circle of 0.9-μm diameter and a big circle of 1.8-μm diameter around each structure expressing HIV-1–Gag-EGFP. The big circle was used to calculate the local background. The circles in the green image were transferred to the red image. Colocalization was scored positive when the fluorescence in the green channel was at least 10% of the local background. To study the entry of HIV-1–Gag-EGFP, we used only the ones that overlapped with CD4-DsRed and seemed likely to represent a single structure. Those structures that were >0.5 μm or showed extensive lateral movement were excluded from the analysis. To analyze entry events, EF stacks were searched for candidate HIV-1–Gag-EGFP spots that disappeared and seemed likely to represent single CD4-DsRed in that they were circular and of diffraction-limited size, as described (Merrifield *et al.*, 2002; Barroso-Gonzalez *et al.*, 2009b). A circle of 0.9-μm diameter was drawn around the center of each region, both in the red and green channels, and the average fluorescence intensity therein was calculated. The local background was the average fluorescence outside the region after excluding small regions where the intensity exceeded a threshold set by the user, one each for red and green channels. Time lapses showing CD4-DsRed–dependent HIV-1–Gag-EGFP entry or blockade were recorded under these technical conditions. Representative videos, shown in Supplemental Videos 1–6, were rated to 7 s, containing 15 frames/s. Total elapsed time is 105 s from the original stack.

Statistics

Data were compared using Student's *t* test. One and two asterisks indicate $p < 0.05$ and $p < 0.01$, respectively.

ACKNOWLEDGMENTS

This work and A.V.-F. are supported by SAF2008-01729 (Ministerio de Ciencia e Innovación, Spain), the European Regional Development Fund, 24661/07 and 24-0740-09 (Fundación para la Investigación y la Prevención del SIDA en España [FIPSE]), the HIVACAT Program, the FIS project PI08/1306, and the Spanish AIDS network (RD06/0006). L.G.-E. and J.B.-G. are supported by SAF2008-01729– and FIPSE-24-0740-09–associated fellowships, respectively. J.D.M. is supported by CONSOLIDER grant CSD-000005 and PI2007/017 (Gobierno de Canarias). J.B. is supported by the Instituto de Salud Carlos III and the Health Department (Generalitat de Catalunya). I.P. is supported by a predoctoral grant (Generalitat de Catalunya) and the European Social Fund. We thank the National Institutes of Health AIDS Research and Reference Reagent Program for providing HIV-1 plasmids and cells. The authors also thank María del Valle Croissier-Elías for critical reading of the manuscript and Patrick Dennis for his help in revising and editing the English content of the manuscript.

REFERENCES

Aikawa Y, Martin TF (2005). ADP-ribosylation factor 6 regulation of phosphatidylinositol-4,5-bisphosphate synthesis, endocytosis, and exocytosis. Methods Enzymol 404, 422–431.

Al-Awar O, Radhakrishna H, Powell NN, Donaldson JG (2000). Separation of membrane trafficking and actin remodeling functions of ARF6 with an effector domain mutant. Mol Cell Biol 20, 5998–6007.

Albertson R, Riggs B, Sullivan W (2005). Membrane traffic: a driving force in cytokinesis. Trends Cell Biol 15, 92–101.

Barral DC, Cavallari M, McCormick PJ, Garg S, Magee AI, Bonifacino JS, De Libero G, Brenner MB (2008). CD1a and MHC class I follow a similar endocytic recycling pathway. Traffic 9, 1446–1457.

Barrero-Villar M, Barroso-Gonzalez J, Cabrero JR, Gordon-Alonso M, Alvarez-Losada S, Munoz-Fernandez MA, Sanchez-Madrid F, Valenzuela-Fernandez A (2008). PI4P5-kinase Iα is required for efficient HIV-1 entry and infection of T-cells. J Immunol 181, 6882–6888.

Barrero-Villar M, Cabrero JR, Gordon-Alonso M, Barroso-Gonzalez J, Alvarez-Losada S, Munoz-Fernandez MA, Sanchez-Madrid F, Valenzuela-Fernandez A (2009). Moesin is required for HIV-1-induced CD4-CXCR4 interaction, F-actin redistribution, membrane fusion and viral infection in lymphocytes. J Cell Sci 122, 103–113.

Barroso-Gonzalez J, El Jaber-Vazdekis N, Garcia-Exposito L, Machado JD, Zarate R, Ravelo AG, Estevez-Braun A, Valenzuela-Fernandez A (2009a). The lupane-type triterpene 30-oxo-calenduladiol is a CCR5 antagonist with anti-HIV-1 and anti-chemotactic activities. J Biol Chem 284, 16609–16620.

Barroso-Gonzalez J, Machado JD, Garcia-Exposito L, Valenzuela-Fernandez A (2009b). Moesin regulates the trafficking of nascent clathrin-coated vesicles. J Biol Chem 284, 2419–2434.

Begle A, Tryoen-Toth P, de Barry J, Bader MF, Vitale N (2009). ARF6 regulates the synthesis of fusogenic lipids for calcium-regulated exocytosis in neuroendocrine cells. J Biol Chem 284, 4836–4845.

Belov GA, Ehrenfeld E (2007). Involvement of cellular membrane traffic proteins in poliovirus replication. Cell Cycle 6, 36–38.
Blagoveshchenskaya AD, Thomas L, Feliciangeli SF, Hung CH, Thomas G (2002). HIV-1 Nef downregulates MHC-I by a PACS-1- and PI3K-regulated ARF6 endocytic pathway. Cell 111, 853–866.
Blanco J, Bosch B, Fernandez-Figueras MT, Barretina J, Clotet B, Este JA (2004). High level of coreceptor-independent HIV transfer induced by contacts between primary CD4 T-cells. J Biol Chem 279, 51305–51314.
Borroni EM, Mantovani A, Locati M, Bonecchi R (2010). Chemokine receptors intracellular trafficking. Pharmacol Ther 127, 1–8.
Brown FD, Rozelle AL, Yin HL, Balla T, Donaldson JG (2001). Phosphatidylinositol 4,5-bisphosphate and Arf6-regulated membrane traffic. J Cell Biol 154, 1007–1017.
Buzon MJ *et al.* (2010). HIV-1 replication and immune dynamics are affected by raltegravir intensification of HAART-suppressed subjects. Nat Med 16, 460–465.
Caplan S, Naslavsky N, Hartnell LM, Lodge R, Polishchuk RS, Donaldson JG, Bonifacino JS (2002). A tubular EHD1-containing compartment involved in the recycling of major histocompatibility complex class I molecules to the plasma membrane. EMBO J 21, 2557–2567.
Cavenagh MM, Whitney JA, Carroll K, Zhang C, Boman AL, Rosenwald AG, Mellman I, Kahn RA (1996). Intracellular distribution of Arf proteins in mammalian cells. Arf6 is uniquely localized to the plasma membrane. J Biol Chem 271, 21767–21774.
Cavrois M, De Noronha C, Greene WC (2002). A sensitive and specific enzyme-based assay detecting HIV-1 virion fusion in primary T lymphocytes. Nat Biotechnol 20, 1151–1154.
Chen P, Hubner W, Spinelli MA, Chen BK (2007). Predominant mode of human immunodeficiency virus transfer between T-cells is mediated by sustained Env-dependent neutralization-resistant virological synapses. J Virol 81, 12582–12595.
Cohen LA, Honda A, Varnai P, Brown FD, Balla T, Donaldson JG (2007). Active Arf6 recruits ARNO/cytohesin GEFs to the PM by binding their PH domains. Mol Biol Cell 18, 2244–2253.
Criss AK, Silva M, Casanova JE, McCormick BA (2001). Regulation of *Salmonella*-induced neutrophil transmigration by epithelial ADP-ribosylation factor 6. J Biol Chem 276, 48431–48439.
Daecke J, Fackler OT, Dittmar MT, Krausslich HG (2005). Involvement of clathrin-mediated endocytosis in human immunodeficiency virus type 1 entry. J Virol 79, 1581–1594.
Dixit NM, Perelson AS (2004). Multiplicity of human immunodeficiency virus infections in lymphoid tissue. J Virol 78, 8942–8945.
Donaldson JG (2003). Multiple roles for Arf6: sorting, structuring, and signaling at the plasma membrane. J Biol Chem 278, 41573–41576.
Donaldson JG, Honda A (2005). Localization and function of Arf family GTPases. Biochem Soc Trans 33, 639–642.
Donaldson JG, Porat-Shliom N, Cohen LA (2009). Clathrin-independent endocytosis: a unique platform for cell signaling and PM remodeling. Cell Signal 21, 1–6.
D'Souza-Schorey C, Chavrier P (2006). ARF proteins: roles in membrane traffic and beyond. Nat Rev Mol Cell Biol 7, 347–358.
D'Souza-Schorey C, Li G, Colombo MI, Stahl PD (1995). A regulatory role for ARF6 in receptor-mediated endocytosis. Science 267, 1175–1178.
D'Souza-Schorey C, van Donselaar E, Hsu VW, Yang C, Stahl PD, Peters PJ (1998). ARF6 targets recycling vesicles to the plasma membrane: insights from an ultrastructural investigation. J Cell Biol 140, 603–616.
Earp LJ, Delos SE, Park HE, White JM (2005). The many mechanisms of viral membrane fusion proteins. Curr Top Microbiol Immunol 285, 25–66.
Faurschou M, Borregaard N (2003). Neutrophil granules and secretory vesicles in inflammation. Microbes Infect 5, 1317–1327.
Folsch H, Mattila PE, Weisz OA (2009). Taking the scenic route: biosynthetic traffic to the plasma membrane in polarized epithelial cells. Traffic 10, 972–981.
Franco M, Peters PJ, Boretto J, van Donselaar E, Neri A, D'Souza-Schorey C, Chavrier P (1999). EFA6, a sec7 domain-containing exchange factor for ARF6, coordinates membrane recycling and actin cytoskeleton organization. EMBO J 18, 1480–1491.
Gillingham AK, Munro S (2007). The small G proteins of the Arf family and their regulators. Annu Rev Cell Dev Biol 23, 579–611.
Gousset K, Ablan SD, Coren LV, Ono A, Soheilian F, Nagashima K, Ott DE, Freed EO (2008). Real-time visualization of HIV-1 GAG trafficking in infected macrophages. PLoS Pathog 4, e1000015.
Haase AT (1999). Population biology of HIV-1 infection: viral and CD4$^+$ T-cell demographics and dynamics in lymphatic tissues. Annu Rev Immunol 17, 625–656.
Ivanchenko S, Godinez WJ, Lampe M, Krausslich HG, Eils R, Rohr K, Brauchle C, Muller B, Lamb DC (2009). Dynamics of HIV-1 assembly and release. PLoS Pathog 5, e1000652.
Iyengar S, Hildreth JE, Schwartz DH (1998). Actin-dependent receptor colocalization required for human immunodeficiency virus entry into host cells. J Virol 72, 5251–5255.
Jimenez-Baranda S *et al.* (2007). Filamin-A regulates actin-dependent clustering of HIV receptors. Nat Cell Biol 9, 838–846.
Johnson DC, Huber MT (2002). Directed egress of animal viruses promotes cell-to-cell spread. J Virol 76, 1–8.
Jolly C, Kashefi K, Hollinshead M, Sattentau QJ (2004). HIV-1 cell to cell transfer across an Env-induced, actin-dependent synapse. J Exp Med 199, 283–293.
Jolly C, Sattentau QJ (2004). Retroviral spread by induction of virological synapses. Traffic 5, 643–650.
Jouvenet N, Bieniasz PD, Simon SM (2008). Imaging the biogenesis of individual HIV-1 virions in live cells. Nature 454, 236–240.
Jouvenet N, Neil SJ, Bess C, Johnson MC, Virgen CA, Simon SM, Bieniasz PD (2006). Plasma membrane is the site of productive HIV-1 particle assembly. PLoS Biol 4, e435.
Kielian M, Rey FA (2006). Virus membrane-fusion proteins: more than one way to make a hairpin. Nat Rev Microbiol 4, 67–76.
Laakkonen JP *et al.* (2009). Clathrin-independent entry of baculovirus triggers uptake of *E. coli* in nonphagocytic human cells. PLoS One 4, e5093.
Larsen JE, Massol RH, Nieland TJ, Kirchhausen T (2004). HIV Nef-mediated major histocompatibility complex class I down-modulation is independent of Arf6 activity. Mol Biol Cell 15, 323–331.
Letinic K, Sebastian R, Toomre D, Rakic P (2009). Exocyst is involved in polarized cell migration and cerebral cortical development. Proc Natl Acad Sci USA 106, 11342–11347.
Liu Y, Belkina NV, Shaw S (2009). HIV infection of T-cells: actin-in and actin-out. Sci Signal 2, pe23.
Londono I, Marshansky V, Bourgoin S, Vinay P, Bendayan M (1999). Expression and distribution of adenosine diphosphate-ribosylation factors in the rat kidney. Kidney Int 55, 1407–1416.
Macia E, Luton F, Partisani M, Cherfils J, Chardin P, Franco M (2004). The GDP-bound form of Arf6 is located at the plasma membrane. J Cell Sci 117, 2389–2398.
Malinowsky K, Luksza J, Dittmar MT (2008). Susceptibility to virus-cell fusion at the plasma membrane is reduced through expression of HIV gp41 cytoplasmic domains. Virology 376, 69–78.
Marchant D, Sall A, Si X, Abraham T, Wu W, Luo Z, Petersen T, Hegele RG, McManus BM (2009). ERK MAP kinase-activated Arf6 trafficking directs coxsackievirus type B3 into an unproductive compartment during virus host-cell entry. J Gen Virol 90, 854–862.
Marechal V, Clavel F, Heard JM, Schwartz O (1998). Cytosolic Gag p24 as an index of productive entry of human immunodeficiency virus type 1. J Virol 72, 2208–2212.
Marechal V, Prevost MC, Petit C, Perret E, Heard JM, Schwartz O (2001). Human immunodeficiency virus type 1 entry into macrophages mediated by macropinocytosis. J Virol 75, 11166–11177.
Marin-Vicente C, Gomez-Fernandez JC, Corbalan-Garcia S (2005). The ATP-dependent membrane localization of protein kinase Cα is regulated by $Ca2^+$ influx and phosphatidylinositol 4,5-bisphosphate in differentiated PC12 cells. Mol Biol Cell 16, 2848–2861.
Marsh M, Helenius A (2006). Virus entry: open sesame. Cell 124, 729–740.
Massol RH, Larsen JE, Kirchhausen T (2005). Possible role of deep tubular invaginations of the plasma membrane in MHC-I trafficking. Exp Cell Res 306, 142–149.
Matlin KS, Reggio H, Helenius A, Simons K (1982). Pathway of vesicular stomatitis virus entry leading to infection. J Mol Biol 156, 609–631.
McDonald D, Wu L, Bohks SM, KewalRamani VN, Unutmaz D, Hope TJ (2003). Recruitment of HIV and its receptors to dendritic cell–T cell junctions. Science 300, 1295–1297.
Mellman I, Warren G (2000). The road taken: past and future foundations of membrane traffic. Cell 100, 99–112.
Merrifield CJ, Feldman ME, Wan L, Almers W (2002). Imaging actin and dynamin recruitment during invagination of single clathrin-coated pits. Nat Cell Biol 4, 691–698.
Miyauchi K, Kim Y, Latinovic O, Morozov V, Melikyan GB (2009). HIV enters cells via endocytosis and dynamin-dependent fusion with endosomes. Cell 137, 433–444.
Mudhakir D, Harashima H (2009). Learning from the viral journey: how to enter cells and how to overcome intracellular barriers to reach the nucleus. AAPS J 11, 65–77.

Naslavsky N, Weigert R, Donaldson JG (2003). Convergence of nonclathrin- and clathrin-derived endosomes involves Arf6 inactivation and changes in phosphoinositides. Mol Biol Cell 14, 417–431.
Nichols BJ, Lippincott-Schwartz J (2001). Endocytosis without clathrin coats. Trends Cell Biol 11, 406–412.
Nishi K, Saigo K (2007). Cellular internalization of green fluorescent protein fused with herpes simplex virus protein VP22 via a lipid raft-mediated endocytic pathway independent of caveolae and Rho family GTPases but dependent on dynamin and Arf6. J Biol Chem 282, 27503–27517.
Nordenfelt P, Winberg ME, Lonnbro P, Rasmusson B, Tapper H (2009). Different requirements for early and late phases of azurophilic granule-phagosome fusion. Traffic 10, 1881–1893.
Pasqualato S, Menetrey J, Franco M, Cherfils J (2001). The structural GDP/GTP cycle of human Arf6. EMBO Rep 2, 234–238.
Pauza CD, Price TM (1988). Human immunodeficiency virus infection of T-cells and monocytes proceeds via receptor-mediated endocytosis. J Cell Biol 107, 959–968.
Phillips DM (1994). The role of cell-to-cell transmission in HIV infection. Aids 8, 719–731.
Pierini R, Cottam E, Roberts R, Wileman T (2009). Modulation of membrane traffic between endoplasmic reticulum, ERGIC and Golgi to generate compartments for the replication of bacteria and viruses. Semin Cell Dev Biol 20, 828–833.
Pleskoff O, Treboute C, Brelot A, Heveker N, Seman M, Alizon M (1997). Identification of a chemokine receptor encoded by human cytomegalovirus as a cofactor for HIV-1 entry. Science 276, 1874–1878.
Puigdomenech I, Massanella M, Cabrera C, Clotet B, Blanco J (2009). On the steps of cell-to-cell HIV transmission between CD4 T-cells. Retrovirology 6, 89.
Puigdomenech I, Massanella M, Izquierdo-Useros N, Ruiz-Hernandez R, Curriu M, Bofill M, Martinez-Picado J, Juan M, Clotet B, Blanco J (2008). HIV transfer between CD4 T-cells does not require LFA-1 binding to ICAM-1 and is governed by the interaction of HIV envelope glycoprotein with CD4. Retrovirology 5, 32.
Radhakrishna H, Donaldson JG (1997). ADP-ribosylation factor 6 regulates a novel plasma membrane recycling pathway. J Cell Biol 139, 49–61.
Radhakrishna H, Klausner RD, Donaldson JG (1996). Aluminum fluoride stimulates surface protrusions in cells overexpressing the ARF6 GTPase. J Cell Biol 134, 935–947.
Sabe H (2003). Requirement for Arf6 in cell adhesion, migration, and cancer cell invasion. J Biochem 134, 485–489.
Schmoranzer J, Kreitzer G, Simon SM (2003). Migrating fibroblasts perform polarized, microtubule-dependent exocytosis towards the leading edge. J Cell Sci 116, 4513–4519.
Schwartz O, Marechal V, Le Gall S, Lemonnier F, Heard JM (1996). Endocytosis of major histocompatibility complex class I molecules is induced by the HIV-1 Nef protein. Nat Med 2, 338–342.
Schwartz S, Campbell M, Nasioulas G, Harrison J, Felber BK, Pavlakis GN (1992). Mutational inactivation of an inhibitory sequence in human immunodeficiency virus type 1 results in Rev-independent gag expression. J Virol 66, 7176–7182.
Stein BS, Gowda SD, Lifson JD, Penhallow RC, Bensch KG, Engleman EG (1987). pH-independent HIV entry into CD4-positive T-cells via virus envelope fusion to the plasma membrane. Cell 49, 659–668.
Sun X, Yau VK, Briggs BJ, Whittaker GR (2005). Role of clathrin-mediated endocytosis during vesicular stomatitis virus entry into host cells. Virology 338, 53–60.
Valenzuela-Fernandez A *et al.* (2005). Histone deacetylase 6 regulates human immunodeficiency virus type 1 infection. Mol Biol Cell 16, 5445–5454.
Valenzuela-Fernandez A, Palanche T, Amara A, Magerus A, Altmeyer R, Delaunay T, Virelizier JL, Baleux F, Galzi JL, Arenzana-Seisdedos F (2001). Optimal inhibition of X4 HIV isolates by the CXC chemokine stromal cell-derived factor 1 alpha requires interaction with cell surface heparan sulfate proteoglycans. J Biol Chem 276, 26550–26558.
Valenzuela-Fernandez A *et al.* (2002). Leukocyte elastase negatively regulates Stromal cell-derived factor-1 (SDF-1)/CXCR4 binding and functions by amino-terminal processing of SDF-1 and CXCR4. J Biol Chem 277, 15677–15689.
Vidricaire G, Tremblay MJ (2005). Rab5 and Rab7, but not ARF6, govern the early events of HIV-1 infection in polarized human placental cells. J Immunol 175, 6517–6530.
Vidricaire G, Tremblay MJ (2007). A clathrin, caveolae, and dynamin-independent endocytic pathway requiring free membrane cholesterol drives HIV-1 internalization and infection in polarized trophoblastic cells. J Mol Biol 368, 1267–1283.
Vitale N, Chasserot-Golaz S, Bailly Y, Morinaga N, Frohman MA, Bader MF (2002). Calcium-regulated exocytosis of dense-core vesicles requires the activation of ADP-ribosylation factor (ARF)6 by ARF nucleotide binding site opener at the plasma membrane. J Cell Biol 159, 79–89.
Yi L, Rosales T, Rose JJ, Chowdhury B, Knutson JR, Venkatesan S (2010). HIV-1 Nef binds a subpopulation of MHC-I throughout its trafficking itinerary and down-regulates MHC-I by perturbing both anterograde and retrograde trafficking. J Biol Chem 285, 30884–30905.
Yoder A *et al.* (2008). HIV envelope-CXCR4 signaling activates cofilin to overcome cortical actin restriction in resting CD4 T-cells. Cell 134, 782–792.

Communicative & Integrative Biology 4:4, 398-408; July/August 2011; ©2011 Landes Bioscience

ANEXO 3:

Viral infection

Moving through complex and dynamic cell-membrane structures

Jonathan Barroso-González,[1,†] Laura García-Expósito,[1,†] Isabel Puigdomènech,[2] Laura de Armas-Rillo,[1] José-David Machado,[1] Julià Blanco[2,†] and Agustín Valenzuela-Fernández[1,†,*]

[1]Laboratorio de Inmunología Celular y Viral; Laboratorio de Neurosecreción; Unidad de Farmacología; Departamento de Medicina Física y Farmacología; Facultad de Medicina; Instituto de Tecnologías Biomédicas (ITB); Universidad de La Laguna (ULL); [2]Fundació irsiCaixa-HIVACAT; Institut de Recerca en Ciències de la Salut Germans Trias i Pujol (IGTP); Hospital Germans Trias i Pujol; Universitat Autònoma de Barcelona; Barcelona, Catalonia Spain

[†]These authors contributed equally to this work.

Key words: membrane dynamics, viral fusion and entry, membrane-associated viral factories, viral budding, viral synapse and spreading, exosomes and trogocytosis

Viruses have developed different survival strategies in host cells by crossing cell-membrane compartments, during different steps of their viral life cycle. In fact, the non-regenerative viral membrane of enveloped viruses needs to encounter the dynamic cell-host membrane, during early steps of the infection process, in which both membranes fuse, either at cell-surface or in an endocytic compartment, to promote viral entry and infection. Once inside the cell, many viruses accomplish their replication process through exploiting or modulating membrane traffic, and generating specialized compartments to assure viral replication, viral budding and spreading, which also serve to evade the immune responses against the pathogen. In this review, we have attempted to present some data that highlight the importance of membrane dynamics during viral entry and replicative processes, in order to understand how viruses use and move through different complex and dynamic cell-membrane structures and how they use them to persist.

Viruses are small structures lacking intravital metabolic pathways and mechanisms to assure their own survival and therefore, depend a fortiori on host-cell machinery to replicate their DNA or RNA genome, and to spread their infectious progeny. Hence, many viruses have developed different survival strategies to enter and infect cells, or to accomplish their replication process through exploiting or modulating membrane traffic and generating specialized compartments[1-3] (**Figs. 1–3**), which also serve to evade the immune responses. In turn, increasing evidence points to that membrane dynamics, like the traffic of vesicles and their spatial reorganization, is key to cell defense against pathogen infections, as in the case of neutrophil-mediated phagocytosis, where orchestrated secretion of granules and vesicles allows cells to locate and destroy invading microorganisms in a controlled manner.[4-7] Viruses use structural or non-structural proteins to exploit the major cellular trafficking pathways to navigate across their target cells by recruiting clathrin, coatomer protein complex (COPI) I and II or endosomal sorting complex required for transport (ESCRT) and their accessory proteins, in a non-structural or structural viral proteins-dependent manner (excellently reviewed in ref. 2, 3 and 8–10). In addition, many of the cellular proteins recruited by the virus to accomplish its viral cycle are small GTPases that are able to generate, move and/or fuse different endosomes or vesicular compartments.[1-3,9]

This work is not a comprehensive review of all membrane dynamics events reported to occur during the cycle of infection of different viruses. Instead, we have attempted to present some data that highlight the importance of the constant flux of membrane structures during early viral entry and replication processes, in order to understand how viruses move through the different complex and dynamic cell-membrane compartments to survive.

*Correspondence to: Agustín Valenzuela-Fernández; Email: avalenzu@ull.es
Submitted: 05/31/11; Accepted: 05/31/11
DOI: 10.4161/cib.4.4.16716

Viral Entry and Membrane Dynamics

As the initial barrier to viral entry, the plasma membrane together with membrane-trafficking machinery is also of fundamental importance in the first stages of the viral cycle.[2,11-14] Although the mechanisms of viral entry for non-enveloped virus are poorly characterized, the molecular mechanism involved in viral fusion and entry for enveloped virus begins to be more clearly understood.[2] It is thought that certain enveloped viruses such as human immunodeficiency virus type 1 (HIV-1), herpes simplex virus 1 (HSV-1), Sendai virus and many other retroviruses have pH-independent viral fusion proteins which allow the virus to penetrate into cells by fusing directly with the plasma membrane[2,13,15-20] (**Fig. 1**; Viral fusion and entry and Viral endocytosis schemes).

Plasma membrane morphology and polarization appears to be regulated by cell cytoskeleton reorganization and direct association with the different components of cellular cortex,[21-26] and by

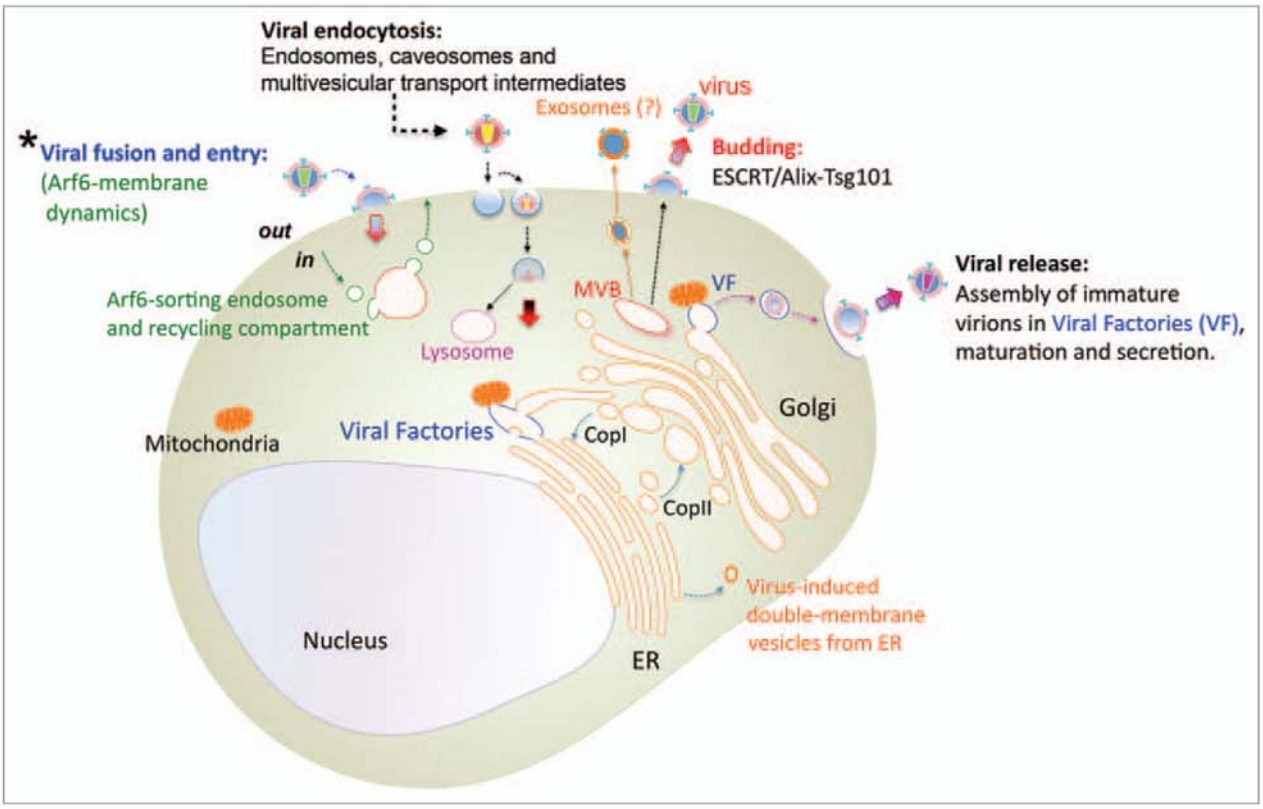

Figure 1. Membrane dynamics processes in host cells that are involved in the life cycle of viral infection. The schematic representation of a cell and the different intracellular membrane-compartments, constitutive or putative sites formed by viruses to accomplish their infection processes, are shown. The non-regenerative viral membrane of enveloped viruses and the dynamics cell-host membranes play an important role during early infection process, since these two opposed membranes need to fuse, either at cell-surface or in an endocytic route (clathrin-, caveolae- or pinocytosis-dependent), to promote viral entry and infection. Endocytosis is initiated at the plasma membrane and progress through early and late endosomes, where some viruses replicate and are recycled back to the plasma membrane or transported to lysosomes to complete the life cycle. In the case of HIV-1, this enveloped virus requires Arf6-membrane dynamics to efficiently fuse with plasma membrane and promote entry and infection of $CD4^+$ T lymphocytes (Asterisk scheme and **Fig. 2**). The non-endocytic route followed by HIV-1 during early infection is decisive to establish viral latent infection. Once inside the cell, many viruses accomplish their replication process through exploiting or modulating membrane traffic, and generating specialized compartments to assure viral survival, such as Viral Factories (VF), multivesicular bodies (MVB), double-membrane compartments, budding on plasma membrane and exosomes (it is conceivable that some viruses may actually be released as exosomes). These membrane structures, cell-constitutive or arranged by the different viral proteins, are required for viral-gene replication, morphogenesis, export, viral maturation and release from cell-surface, and also serve to evade the immune responses against viral genomes. Viral proteins could enter the secretory pathway by co-translational translocation into the endoplasmic reticulum (ER; only a part of the perinuclear ER is shown), to be further transported from the ER to the Golgi complex in vesicles and in a coatomer protein complex (COP) II-dependent manner. Viral complexes formed inside MVBs, in communication with vesicles, mitochondria, Golgi cisternae and ER-membranes, could be transported through the Golgi network to the plasma membrane to be released as viral particles. Viral budding of enveloped viruses is mainly under the control of the activity of ESCRT-III complexes that are recruited to the site of viral release by ESCRT-I or Alix proteins that interacts with matrix viral proteins located on cell-surface.

the insertion and uptake of membrane structures at cell-surface that regulates plasma membrane dynamics.[27-31] Although cytoskeleton reorganization and dynamics have well-documented roles in HIV-1 fusion and entry events, the contribution of plasma membrane dynamics is less clear during these early viral infection steps. HIV-1 interacts with target cells through cell-surface CD4 and CXCR4 or CCR5 viral co-receptor, a process that is cooperative and requires cell signaling, actin polymerization and reorganization[32-41] and stabilization of microtubules,[22,42,43] in order to achieve pore fusion formation throughout which viruses reach the inner cell. In this concern, it has been reported that HIV-1 fusion and entry could occur in micropinosomes and endosomes,[44,45] a process that has been proposed to be clathrin-dependent,[46] pH-independent and dynamin-dependent.[47,48] In fact, dynamin- and endosome-dependent HIV-1 entry and infection have been recently controverted.[49-51]

In this regard, it has been reported that HIV-1 internalization and infection in polarized trophoblasts is a pH-dependent process,[52,53] which is driven by a clathrin-, caveolae- and dynamin-independent endocytic pathway, and requires free membrane cholesterol.[54] A recent work from our group suggested that the fluidity of plasma membrane, regulated by the phosphatidyl-inositol-4-phosphate-5-kinase Iα (PI4P5-K Iα) and subsequent phosphatidylinositol-4,5-biphosphate (PIP_2) production,

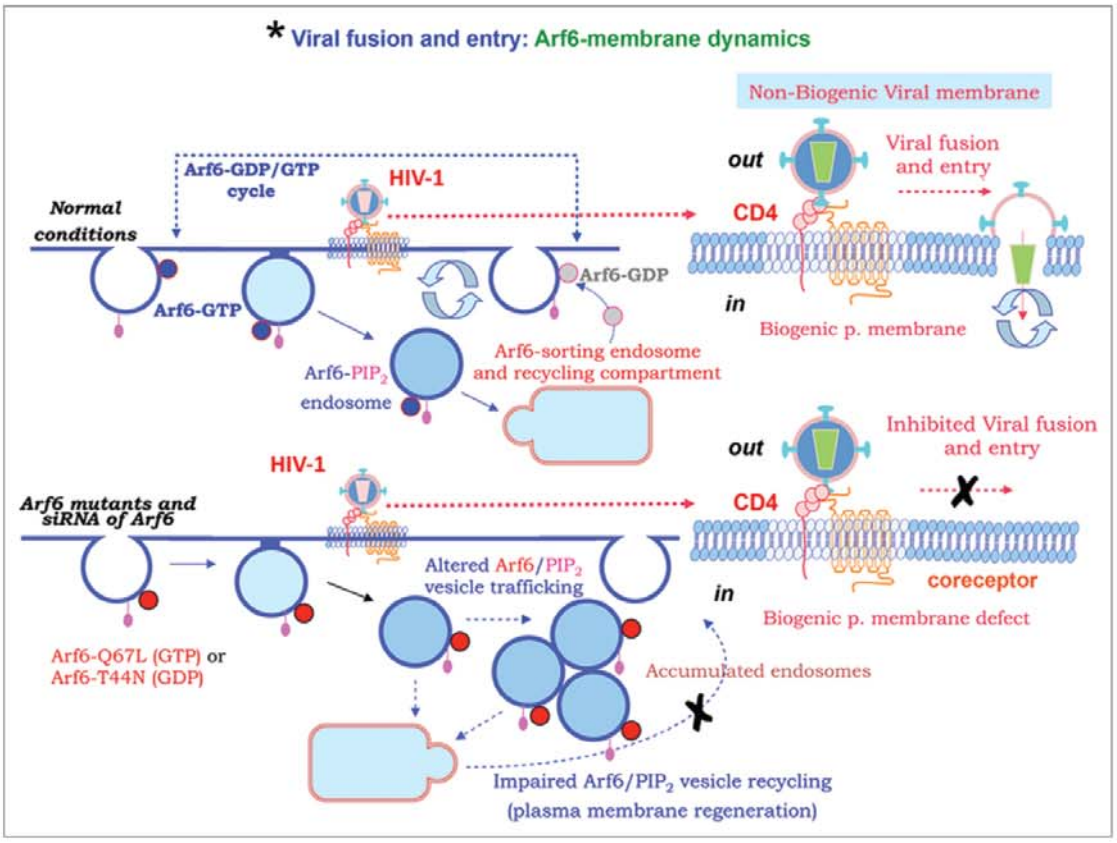

Figure 2. Arf6-membrane dynamics regulates efficient HIV-1 infection. HIV-1 requires Arf6-coordinated membrane dynamics to efficiently fuse with plasma membrane and promote entry and infection of CD4+ T lymphocytes. In fact, movement of PIP_2-associated membrane structures, driven by the Arf6-GTP/GDP cycle activity on plasma membrane from a sorting and recycling endosomal compartment, assures the regeneration of cell-surface membrane by coordinating the turnover of these PIP_2-associated vesicles. This membrane traffic has synergy with the key first HIV-1/receptors interactions to promote pore fusion formation, between the non-regenerative HIV-1 viral membrane and the dynamic cell-surface, thereby favouring efficient virus-cell fusion, entry and infection (scheme corresponding to early fusion and entry steps of the HIV-1 infection process, also indicated in **Fig. 1** by an asterisk). The alteration of the Arf6-GTP/GDP cycle, by GDP-bound or GTP-bound mutants provokes an accumulation of Arf6/PIP_2-membrane structures on the plasma membrane. Specific Arf6 silencing also inhibits HIV-1-envelope-induced membrane fusion, entry and infection of T lymphocytes and permissive cells, regardless of viral tropism.

is crucial for HIV-1 entry and the early steps of infection in permissive lymphocytes.[39] PIP_2 and the PI4P5-K Iα are functionally linked to the small GTPase, ADP-ribosylation factor 6 (Arf6), which regulates membrane trafficking and regeneration of plasma membrane.[55-58] Furthermore, efficient early HIV-1 fusion, entry and infection require both an Arf6-dependent dynamic and regenerative plasma membrane at the virus/cell-surface interacting regions,[51] and a correct cell-surface localization of viral receptors (**Fig. 1** and Viral fusion and entry scheme, and associated **Fig. 2**). Thus, movement of PIP_2-associated membrane structures, driven by the Arf6-GTP/GDP cycle activity on plasma membrane, assures the regeneration of cell-surface membrane by coordinating the turnover of these PIP_2-associated vesicles, which has synergy with the key first HIV-1/receptors interactions.[37,40] Altogether, this process promotes pore fusion formation, between the non-regenerative HIV-1 viral membrane and the dynamic cell-surface, thereby favoring efficient cell-to-cell viral transmission, entry and infection[51] (**Fig. 2**). The alteration of the Arf6-GTP/GDP cycle either by using GDP-bound or GTP-bound inactive mutants, which provokes the accumulation of Arf6/PIP_2-associated membrane structures on cell-surface, or by specific Arf6 silencing inhibits HIV-1-envelope-induced membrane fusion, entry and infection of T lymphocytes and permissive cells, regardless of viral tropism. Conversely, Arf6 silencing or its dominant mutants did not affect fusion, entry and infection of viruses pseudotyped with the envelope-G protein of the vesicular stomatitis virus (VSV-G), or ligand-induced CXCR4 or CCR5 endocytosis, both clathrin-dependent processes. These results confirmed that early HIV-1 infection of CD4+ T lymphocytes requires Arf6-coordinated plasma membrane dynamics in order to promotes viral fusion and entry. The non-endocytic route followed by HIV-1 during early infection seems to be decisive to establish viral latent infection,[49] thus Arf6-regulated HIV-1 pathway of infection could be key for HIV-1 infection and pathogenesis.

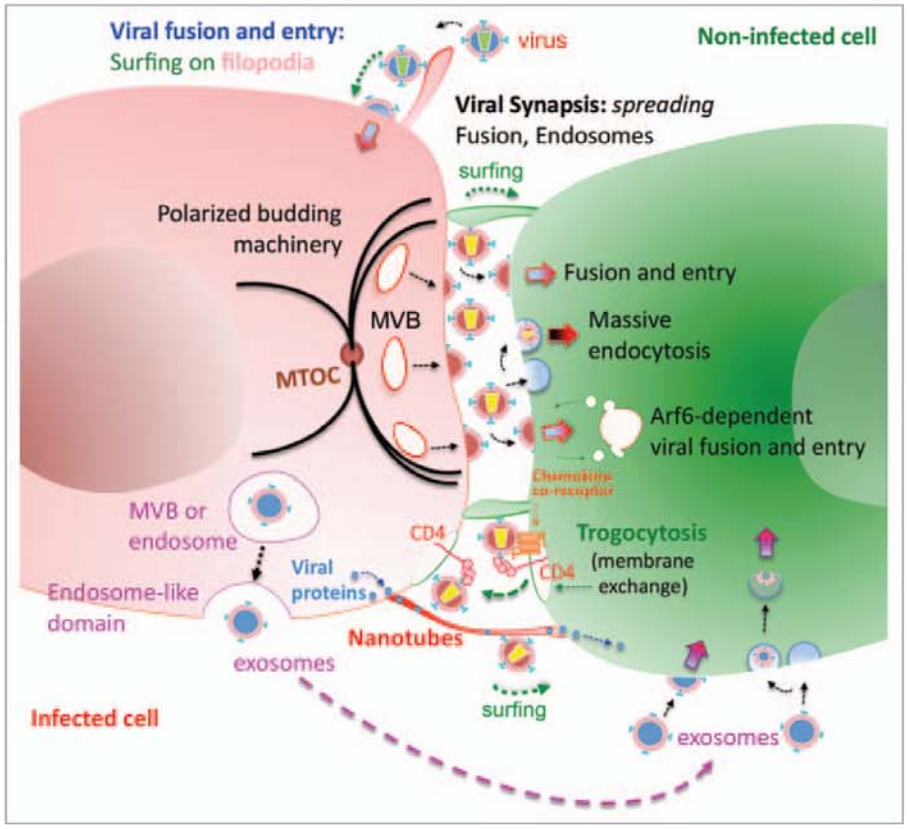

Figure 3. Membrane dynamics at the virological synapse. At the virological synapse (VS), some viruses either attach to the plasma membrane or surf along the filopodia and finally bind to specific receptors on the target cell. Viruses can also directly fuse with the plasma membrane, as in the case of HIV-1. Cell-to-cell transfer of HIV-1 takes place in an Arf6-membrane dynamics-dependent manner, which hijack endocytic pathways, including clathrin-dependent, caveolin-dependent or both independent pathways for viral internalization. The VS represents an efficient environment for viral budding, where the membrane of the infected cell is polarized towards the synaptic junction by the movement for of vesicles or MVBs coordinated by the translocation of the microtubule organizing centre (MTOC). This scaffolding allows for a subsequent viral infection and spread, that favours viral fusion and entry, viral endocytosis and viral protein/gene transfer from the infected to the close non-infected cell. Besides, long membrane nanotubes may also be formed between neighboring cells, which promote viral protein traffic and also HIV surfing and infection, from infected cell to non-infected cell. Other membrane dynamics events involved or occurred during viral infection and spreading are Trogocytosis and exosomal transport. Trogocytosis of cell-surface patches, containing CD4/HIV-1-bound molecules, occurs from non-infected to infected cells in a gp120/CD4-dependent manner. Exosomes are membrane vesicles, formed from MVB that could account for viral infection and spreading within membrane structures that are protected from immune responses.

In this concern, a new broad-spectrum antiviral agent, acting only against enveloped viruses (e.g., HIV-1, VSV, Ebola, Marburg, influenza, hepatitis C (HCV) and West Nile viruses), inhibited free virus-cell fusion and infection by perturbing non-regenerative viral membranes, without affecting non-enveloped viruses in vitro (e.g., adenovirus, coxsackievirus and reovirus). However, this molecule failed to block cell-to-cell fusion and infection due to its inactivity on dynamic, regenerative plasma membranes.[59] Considering that Arf6 is key to coordinate plasma membrane dynamics, and its functional implication on cellular invasion by HIV-1 and several microorganisms,[51,60-66] it is therefore plausible that different enveloped viruses may also benefit from Arf6-coordinated plasma membrane traffic to promote entry and infection processes. Arf6 is the only member of the Ras-related Arf-family of small GTPases that affects cell-surface dynamics, thereby regulating plasma membrane/endosome trafficking and cortical actin reorganization.[58,67-73] Remarkably, plasma membrane morphology and dynamics is also regulated by the traffic of PIP_2-associated membranes from plasma membrane to a non-clathrin intracellular compartment,[67,68,74-78] which in turn relies on the membrane transport activity of Arf6.[21,56-58,67-69,79] Therefore, it is also conceivable that Arf6-coordinated membrane movements might control entry and infection processes of some non-enveloped viruses, such as coxsackievirus.[80]

In the case of the VSV virus, which has had an important role in our increasing understanding of both innate and acquired immunity, as well as virology in general,[81] the viral-envelope glycoprotein G binds to phosphatidylserine, a near-universal component of cell-surface membranes, enabling VSV to infect virtually all animal cells. Although phosphatidylserine had been proposed to serve as VSV receptor,[82] this conviction has been recently challenged.[83] Following attachment to the cell surface, the virus enters by endocytosis and, after a subsequent drop in endosomal pH, the glycoprotein catalyzes the fusion of viral and cellular membranes, releasing the viral ribonucleoprotein (RNP) into the cytoplasm. In fact, VSV fusion occurs in multivesicular transport intermediates, formed between early and late endosome, and not in late endosomes,[84,85] where finally viral nucleocapsid is delivered to the cytoplasm (**Fig. 1** and Viral endocytosis scheme). Of note, the extensive tissue tropism of VSV enables this virus to be therefore used as an anti-cancer agent in all types of tumors.[81]

Other viruses could enter cells by more than one mechanism that implies the passage from cell-surface through different membrane structures (**Fig. 1** and Viral endocytosis scheme). The enveloped influenza retrovirus mainly enters cells by clathrin-mediated endocytosis, but it can also follow a clathrin-independent pathway,[86] which appears to be regulated by Epsin 1.[87]

Moreover, simian virus 40 (SV40) is alternatively internalized either via caveolae[88] or a CLICs/GEECs (clathrin-independent carriers/glycosylphosphatidylinositol-anchored proteins and enriched early endosomal compartments)-driven pathway.[3,89,90] The capsid of the non-enveloped DNA SV40 virus is composed of VP1 homopentamers, which resemble cholera toxin B pentamers, and like the cholera toxin B subunit, SV40 binds gangliosides on the cell surface and enters via a raft/caveolar pathway.[2,81,90,91] Echovirus 1, a picornavirus that binds to integrins, follows a caveolar/raft uptake process that involves protein kinase C, and penetration seems to occur in caveosomes without the involvement of the endoplasmic reticulum (ER).[2,92,93] For some viruses, such as for Ebola virus, SARS coronavirus (that causes severe acute respiratory syndrome [SARS]), and the non-enveloped mammalian reoviruses, an acidic pH alone is not sufficient to induce virus-endosome fusion and entry, thus participation of cathepsins L and B acid-dependent endosomal proteases are required to acquire the penetration-competent state of viral proteins.[94-96]

It has been described for certain viruses, such as HIV-1, VSV, murine leukemia virus, human papillomavirus type 16 and the DNA-enveloped vaccinia virus, that before entry into their target cells these viruses interact with and surf upon cell-surface filopodia toward the base of the filopodia,[97-99] where certain virus enter cells by macropinocytosis, as echovirus 1 and adenovirus serotype 3,[100-102] or by triggering the formation of transient membrane blebs[99] (**Fig. 3** and Surfing on filopodia in Viral fusion and entry scheme, and surfing in viral synapse).

Altogether, the viral endocytic route could represent an easy way to overcome the barrier that cortical cytoskeleton imposes to the virus during early entry and infection processes, being also of importance to evade the immune responses against viruses.[2,3,81]

Viral Replication and Membrane Dynamics

Intracellular membrane dynamics is not only essential during the first stages of viral fusion and subsequent entry but also to accomplish the viral replicative process. Replication of many viruses is associated with specific intracellular compartments so-called viral factories (VF; see VF schemes in **Fig. 1**). These are thought to provide a physical scaffold to concentrate viral components for genome replication and morphogenesis.[8,103,104] The formation of VF often results in rearrangement of cellular membranes, reorganization of the cytoskeleton and recruitment of mitochondria.[105,106] One of the early events in factory formation is the assembly of replication complexes (RCs) that associates with membranes derived from the ER, as observed in the case of flaviviruses, hepaciviruses, coronaviruses, arteriviruses and picornaviruses (**Fig. 1** and VF schemes). On the other hand, RC of Togaviruses associate with membranes of endocytic origin, whereas RC of nodaviruses associate with mitochondrial membranes (reviewed in ref. 8). In fact, RNA viruses modify specific membranes of the factory to concentrate viral replicases and necessary cofactors for a more efficient replication of the viral genome.[107-113] In this regard, rubella virus (RUBV), an important human teratogenic virus and the only member of the genus Rubivirus in the Togaviridae family,[114] and Semliki Forest virus (SFV),[115] anchors its RNA synthesis in membranes of a cell organelle known as the cytopathic vacuole (CPV),[116-118] which derives from modified endosomes and lysosomes.[109,117,119] In fact, ER cisternae, mitochondria and Golgi stacks are recruited around CPVs to build RUBV factories[106] (**Fig. 1** and VF schemes), which help the virus to evade host cell defense responses as well as connecting viral replication with assembly and maturation of new viral particles in recruited Golgi membranes.[120] The Golgi apparatus is a highly dynamic organelle with functional and sustained membrane and protein flow[121] and serves as a morphogenic mold for rubiviruses and other viruses, such as coronaviruses, arteriviruses and Bunyaviruses.[8,105,106,120,122,123] The surface of CPVs consists of small vesicular invaginations or spherules (the sites of viral RNA replication) that line the vacuole membrane at regular intervals.[109,117-119,124] These CPV structures also exhibit a variety of complex contacts with the endocytic pathway through its internal membranes that are interconnected with different transport vesicles.[106] A remarkably case of VF occurs with the poxvirus vaccinia virus, an example of DNA-virus that does not replicate inside the nucleus of host cells. Thus, discrete cisternae derived from the rough ER enclose the cytoplasmic site of viral-DNA replication and it is thought to eventually resemble a cytoplasmic mini-nucleus for viral replication.[125-127]

Other RNA$^+$ viruses that belong to the Flaviviridae family and the Nidovirales order induce the formation of spherical, double-membrane vesicles (DMVs) to replicate[128-130] (**Fig. 1** and double-membrane vesicles scheme), while polioviruses-RNA polymerase molecules can also assemble bidimensional arrays.[110,131] In fact, one of the best-studied viruses that induce membrane rearrangements is the human pathogen poliovirus, a member of the Picornaviridae family that causes poliomyelitis. Thus the trafficking and alteration of intracellular membrane structures regulate poliovirus infection, where all cellular organelles except mitochondria are virtually converted into virus replication vesicles.[132-136] Indeed, endosomes and lysosomes (Togaviruses), peroxisomes and chloroplasts (members of the genus Tombusvirus) and mitochondria (nodaviruses) represents protective environments used as sites for RNA replication, while all plus-strand RNA viruses replicate in association with cytoplasmic membranes of infected cells.[107] Some data about the antiviral effect of brefeldin A (BFA) suggest the functional involvement of membrane trafficking proteins on virus replication of Enteroviruses, such as for the picornaviruses poliovirus and coxsackievirus.[137] BFA inhibits Arf-GTP exchange proteins (Arf-GEFS), reduces the Arf1-GTP needed to generate COPI coats in the Golgi and blocks the recruitment of membranes into replication compartments.[133] Thus sequestration of Arf-1 into the replication complex would also explain the block in secretion seen in infected cells.[138] However, BFA does not prevent formation of densely packed vesicles by poliovirus, so vesicle formation does not require activated Arf-GEF proteins.[136] Several picornaviruses are resistant to BFA, and their 3A proteins do not slow ER to Golgi transport as occurred with foot-and-mouth disease virus.[139-141] For these viruses COPII coated vesicles may provide membranes for replication,[142-145] while other studies implicate a role for autophagosomes.[146]

The induction of coated-pit formation has also been observed for reovirus and SFV.[2,147] Internalized SFV early recruits the intermediate-endosome Rab7-small GTPase[148] to later induce the formation of CPVs, important for viral RNA synthesis,[118] which are derived from late endocytic compartments. In the case of HCV virus, it seems that recruitment of membrane trafficking proteins to ER-derived membrane scaffolds is key for viral replication. Hence, the NS5A protein is anchored to the cytoplasmic face of this membrane web to recruit the RNA-dependent RNA polymerase, NS5B. Both NS5A and NS5B bind VAMP associated proteins (VAPs) [149,150] and recruit Rab1, Rab5 and Rab7 small GTPases that could direct the transport of vesicles to fuse with or enlarge this viral replicative membrane-web compartment.[9,151-153] It is conceivable that other RNA$^+$ viruses such as Norwalk virus take advantage of the formation of ER-derived membrane scaffolds to replicate, as observed with the membrane-bound nsp48 protein that also binds VAP-A.[9,154]

The cell-host plasma membrane undergoes an immense rearrangement and a deformability process during viral budding, a key event of the life cycle of enveloped viruses, thereby determining viral morphology and infectiveness (reviewed in ref. 10) (**Figs. 1 and 3**, Budding schemes). The majority of studied enveloped viruses bud from cells by co-opting the host ESCRT machinery,[155-159] critical for budding of vesicles in multivesicular bodies (MVBs) that are important intermediates in endolysosomal transport.[10,160,161] The HIV-1 viral polyprotein Gag binds, through its C-terminal region, both to cellular ESCRT-I complex and to ALIX protein, which both recruit ESCRT-III complex to the budding site to catalyze the scission of nascent virions, an event that it is thought to be carried out by the same process as for cleavage of intralumenal vesicles in MVBs.[10,162]

Furthermore, the tumor susceptibility gene 101 (Tsg101) subunit of the ESCRT-I complex, which mediates receptor sorting into MVBs,[163,164] appears to be dispensable for viral envelope fusion with endosomal membranes and viral RNA transport to late endosomes, but is necessary for infection and RNA release.[85] These data indicate that Tsg101, in addition to its role in receptor sorting into MVBs, may well play a direct role in the release of nucleocapsids from within MVBs to the cytoplasm by controlling the back-fusion process. However, several recently reported data indicate that the interaction of Gag viral protein with the ESCRT machinery is dispensable for HIV-1 viral budding and infectiveness.[165-167] In this regard, the matrix protein of the enveloped influenza virus lacks an ESCRT binding domain, thus it buds in an ESCRT-independent manner.[168,169]

In turn, the HIV-1 Gag localizes on PIP_2-enriched plasma membrane regions, where PIP_2 plays a critical role in HIV-1 particle assembly.[170,171] Overexpression of polyphosphoinositide-5-phosphatase IV (5ptaseIV), which hydrolyzes the phosphate at the D5 position and reduces plasma membrane PIP_2 levels,[172] drastically impairs HIV-1 release by relocalizing the viral polypeptide Gag from the plasma membrane to CD63-positive intracellular compartments.[171] Indeed, disrupting PIP_2 levels and localization by expression of Arf6/Q67L, a GTP-bound mutant of Arf6, reduces virus release by retargeting Gag to newly formed PIP_2-enriched endosomal vesicles.[171]

Finally, other viruses bud from plasma membrane of host cells through their matrix viral protein. This is the case of Newcastle disease virus (a Paramyxovirus) and VSV virus, where bud formation and scission from membranes are both matrix-dependent processes.[173-175]

Viral Spread: Membrane Dynamics at the Virological Synapse

There is growing evidence that a number of different viruses can exploit pre-existing mechanisms of physiological communication between cells to facilitate direct cell-cell viral spread.[38] Studies revealing the co-clustering of viral egress machinery and viral receptors at the interface between conjugates of infected and uninfected cells respectively, have led to the definition of this structure as virological synapse (VS) [176,177] (**Fig. 3** and Viral synapse scheme). The first detailed description of VS was reported for the human T cell leukemia virus type 1 (HTLV-1),[178] and was then translated to the HIV field.[179] The cell-free form of HTLV-1 is very inefficient at infecting T cells and is spread between, and within individuals by strictly dependent cell-to-cell transmission mechanisms. Noteworthy, cell-to-cell viral spread presents numerous advantages for the virus as compared to cell-free virus infections, which could be summarized as follows:

- A more rapid replication kinetics is obtained when viruses are transmitted across VS due to the higher concentration of viral particles released at the point of contact between the cell partners thus obviating the rate-limiting step of fluid-phase diffusion of free viral particles.[180]
- Infected cells entering a new host could adhere to, and cross by transmigration, a mucosal epithelial barrier that would otherwise be impermeable to cell free virions.[38]
- The formation of stable junctions whereby viruses traffic, shields the virus from immune response or drugs both sterically and kinetically in terms of exposure time although it is still unclear whether this is also the case for HIV.[181,182]

At the molecular level, VS synchronize both viral egress and entry processes in the synaptic cleft. Most recent literature suggests that HIV-1 cell-to-cell transmission results from microtubules-mediated polarized and massive HIV budding and subsequent entry of viral particles into target cells[182,183] (**Fig. 3** and Viral synapse scheme). Therefore, most of the mechanisms that regulate cell-free virus entry by perturbing membrane dynamics also apply for cell-to-cell virus transmission. Indeed, it is known that membrane-cholesterol sequestering agents[184] and inhibitors of cytoskeleton motility[185] interfere with retroviral transmission between infected and uninfected cells. Similarly, the blockade of Arf6-coordinated plasma membrane dynamics by siRNA-Arf6 silencing or expression of dominant mutants has detrimental effects on cell-to-cell HIV-1 transmission[51] (**Fig. 3** and Arf6-dependent viral fusion and entry scheme).

Despite these similarities, some specific events of synaptic contacts that involve membrane dynamics should be also considered. It is well known that massive viral endocytosis accompanies viral entry during cell-to-cell HIV transmission[186] (**Fig. 3**). In contrast, HTLV-1 appears to be transmitted from biofilm-like

structures that accumulate viral particles on the surface of infected cells.[187] Other viruses have developed alternative strategies, pseudo-rabies virus transferred from cellular projections, HSV are transported within long membrane protrusions towards adjacent cells, and murine leukaemia virus moves along the surface of filopodia before viral entry at the cell body of fibroblasts[188] (**Fig. 3** and surfing scheme at Viral synapse). Such filopodia that also participate in HIV transmission extend through receptor-mediated mechanisms from uninfected towards the infected cell.[188] A similar retroviral surfing has been described over narrower membranous structures called nanotubes that can connect cells separated by up to 100 mm,[189] which also transfer viral proteins at the inner inside. In this case, receptor specificity seems to play a minor role, as these actin-driven structures seems to extend from HIV infected cells in the absence of receptor-envelope interactions (**Fig. 3** and Nanotubes scheme).

The formation of different bridging tubular structures within the synapses, usually involve huge membrane invaginations engulfing cellular fragments,[183] which may lead to the exchange of membranes between counteracting cells, a synapse-specific event that is known as trogocytosis.[190] Trogocytic exchange of membrane patches, initially described during cellular contacts among cells of the immune system, has been proposed as a possible mechanism to control the length and the stability of the synapse and therefore regulate its outcome.[190] Recently, trogocytosis has been reported to occur at the HIV induced VS, a process dependent on gp120 binding to CD4. Interestingly, HIV particles as well as membrane components (such as CD4 molecules) were transferred in an unidirectional way from the uninfected towards the infected cells[182] (**Fig. 3** and Trogocytosis scheme). This mechanism could have a huge impact rendering cells permissive to HIV infection as suggested in a recent study.[191]

Besides the direct transfer from infected to uninfected cells, several pathogens take advantage of other mechanisms of immune communication between antigen presenting cells, mainly dendritic cells (DCs) and T cells. As DCs are professional pathogen hunters, several viruses, such as HIV or cytomegalovirus (CMV), have developed strategies to stably associate in an infectious state to these cells and infect lymphocytes during antigen presentation.[192,193] HIV has been shown to reside in CD81 enriched salk-like structures inside DC that are released at the synaptic space during T cell scanning or antigen presentation.[193] Interestingly, the journey of HIV in DCs appears to be reminiscent of the exosomal pathway of antigen presentation (**Figs. 1 and 3**, Exosome schemes), suggesting that HIV hijacks this cellular mechanism in its own benefit and highlighting the similarities between retroviruses and exosomes.[194] Importantly, multiple pathogens, including some bacteria and other parasites, hijack the complex mechanisms of recognition and capture by DC to increase their spread efficiency in the infected hosts.[195]

Conclusions and Perspectives

This article attempt a non-comprehensive review about the journey that different viruses accomplish to successfully infect their target cells, describing viral entry pathways and intracellular trafficking, from cell-surface and through complex and dynamic cell-membrane structures, which often are newly organized by the viruses in order to replicate. The different host intracellular compartments, such as ER, endosomes, lysosomes or mitochondria, serve as an adaptable membrane source to form viral replication factories and allow viruses to adopt their own functional morphology with the appropriated lipid composition. Indeed, it is conceivable that these membrane structures help to confine the process of RNA replication to a specific cytoplasmic location, just preventing the activation of certain host defense mechanisms that can be triggered by the viral genome during unwinding and replication.

Although several data have been reported about the functional role of membrane dynamics during viral infection, many related questions remain to be addressed. For example, how could different viral proteins, from divergent viruses and host cells, gain the ability to modify the same intracellular membrane compartments to assure viral replication, without critically affecting important cellular processes? In turn, why viruses choose different subcellular-membrane compartments for their replication? And, how viral proteins are targeted to and moving across those membranes and what host factors are recruited or involved in these events? The answer of these questions will surely contribute to our understanding of some of the basic mechanisms that control membrane dynamics, both in cellular functions and viral infection cycle. This may open the door to the design of new antiviral strategies aimed at effectively target the dynamic of viral-cell interactions, which hopefully would lead to new therapies for combat viral infections, such as HIV-1 infection and Acquired Immunodeficiency Disease Syndrome (AIDS). Moreover, it may also provide new rational designs by which non-viral gene delivery systems can be improved and therapeutically used in different gene-originated tumor and immune diseases.

Finally, the two- and three-dimensional study of viral fusion, entry and trafficking at the level of cells and virus particles will bring the technical development of new and more powerful microscopy devices, from fluorescent and high-end light microscopy and total internal reflection fluorescence microscopy (TIRFM) to transmission electron microscopy (TEM) with cellular electron tomography (ET),[51,106,196-199] which allow to analyze these events with increased spatial and temporal resolution, in order to understand how viruses move through the different complex and dynamic cell-membrane structures to infect and survive.

Acknowledgments

This work and A.V.F. are supported by SAF2008-01729 (MICINN, Spain), European Regional Development Fund (ERDF), 24661/07 and 24-0740-09 (Fundacion Investigacion y Prevencion del SIDA en España), and ProID20100020 (Agencia Canaria de Investigación, Innovación y Soc. Información; Gobierno de Canarias) grants. The HIVACAT Program, the FIS project PI08/1306 and the Spanish AIDS network (RD06/0006). J.B.G., L.G.E. and L. de A.R. are supported by FIPSE-24-0740-09, SAF2008-01729 and ProID20100020

associated fellowships, respectively. J.D.M. is supported by the Ramón y Cajal program (R&C-2010-06256, MICINN). J.B. is supported by the ISCIII and Health Department (Generalitat de Catalunya). The authors declare that they have no conflicting financial interests. We specially thank to Prof. Manuel Feria for critical reading of the manuscript and for his continuous and generous support. We apologize for all research works and reviews that we have not reported or considered in this mini-review, where we have tried to avoid omissions by our unpremeditated unknowledge.

References

1. Greber UF, Way M. A superhighway to virus infection. Cell 2006; 124:741-54.
2. Marsh M, Helenius A. Virus entry: open sesame. Cell 2006; 124:729-40.
3. Gruenberg J. Viruses and endosome membrane dynamics. Curr Opin Cell Biol 2009; 21:582-8.
4. Bajno L, Peng XR, Schreiber AD, Moore HP, Trimble WS, Grinstein S. Focal exocytosis of VAMP3-containing vesicles at sites of phagosome formation. J Cell Biol 2000; 149:697-706.
5. Nordenfelt P, Winberg ME, Lonnbro P, Rasmusson B, Tapper H. Different requirements for early and late phases of azurophilic granule-phagosome fusion. Traffic 2009; 10:1881-93.
6. Faurschou M, Borregaard N. Neutrophil granules and secretory vesicles in inflammation. Microbes Infect 2003; 5:1317-27.
7. Maganto-Garcia E, Punzon C, Terhorst C, Fresno M. Rab5 activation by Toll-like receptor 2 is required for *Trypanosoma cruzi* internalization and replication in macrophages. Traffic 2008; 9:1299-315.
8. Miller S, Krijnse-Locker J. Modification of intracellular membrane structures for virus replication. Nat Rev Microbiol 2008; 6:363-74.
9. Pierini R, Cottam E, Roberts R, Wileman T. Modulation of membrane traffic between endoplasmic reticulum, ERGIC and Golgi to generate compartments for the replication of bacteria and viruses. Semin Cell Dev Biol 2009; 20:828-33.
10. Hurley JH, Boura E, Carlson LA, Rozycki B. Membrane budding. Cell 2010; 143:875-87.
11. Mudhakir D, Harashima H. Learning from the viral journey: how to enter cells and how to overcome intracellular barriers to reach the nucleus. Aaps J 2009; 11:65-77.
12. Sodeik B. Mechanisms of viral transport in the cytoplasm. Trends Microbiol 2000; 8:465-72.
13. Doms RW, Trono D. The plasma membrane as a combat zone in the HIV battlefield. Genes Dev 2000; 14:2677-88.
14. Waheed AA, Freed EO. Lipids and membrane microdomains in HIV-1 replication. Virus Res 2009; 143:162-76.
15. Stein BS, Gowda SD, Lifson JD, Penhallow RC, Bensch KG, Engleman EG. pH-independent HIV entry into CD4-positive T cells via virus envelope fusion to the plasma membrane. Cell 1987; 49:659-68.
16. Stein BS, Engleman EG. Mechanism of HIV-1 entry into CD4+ T cells. Adv Exp Med Biol 1991; 300:71-86.
17. Pelchen-Matthews A, Clapham P, Marsh M. Role of CD4 endocytosis in human immunodeficiency virus infection. J Virol 1995; 69:8164-8.
18. Wyatt R, Sodroski J. The HIV-1 envelope glycoproteins: fusogens, antigens and immunogens. Science 1998; 280:1884-8.
19. Earp LJ, Delos SE, Park HE, White JM. The many mechanisms of viral membrane fusion proteins. Curr Top Microbiol Immunol 2005; 285:25-66.
20. Harrison SC. Mechanism of membrane fusion by viral envelope proteins. Adv Virus Res 2005; 64:231-61.
21. Behnia R, Munro S. Organelle identity and the signposts for membrane traffic. Nature 2005; 438:597-604.
22. Valenzuela-Fernandez A, Cabrero JR, Serrador JM, Sanchez-Madrid F. HDAC6: a key regulator of cytoskeleton, cell migration and cell-cell interactions. Trends Cell Biol 2008; 18:291-7.
23. Albiges-Rizo C, Destaing O, Fourcade B, Planus E, Block MR. Actin machinery and mechanosensitivity in invadopodia, podosomes and focal adhesions. J Cell Sci 2009; 122:3037-49.
24. Mogilner A, Keren K. The shape of motile cells. Curr Biol 2009; 19:762-71.
25. Pollard TD, Cooper JA. Actin, a central player in cell shape and movement. Science 2009; 326:1208-12.
26. Saarikangas J, Zhao H, Lappalainen P. Regulation of the actin cytoskeleton-plasma membrane interplay by phosphoinositides. Physiol Rev 2010; 90:259-89.
27. Mellman I. Quo vadis: polarized membrane recycling in motility and phagocytosis. J Cell Biol 2000; 149:529-30.
28. Mellman I, Warren G. The road taken: past and future foundations of membrane traffic. Cell 2000; 100:99-112.
29. Heck JN, Mellman DL, Ling K, Sun Y, Wagoner MP, Schill NJ, et al. A conspicuous connection: structure defines function for the phosphatidylinositol-phosphate kinase family. Crit Rev Biochem Mol Biol 2007; 42:15-39.
30. Folsch H, Mattila PE, Weisz OA. Taking the scenic route: biosynthetic traffic to the plasma membrane in polarized epithelial cells. Traffic 2009; 10:972-81.
31. Shibata Y, Hu J, Kozlov MM, Rapoport TA. Mechanisms shaping the membranes of cellular organelles. Annu Rev Cell Dev Biol 2009; 25:329-54.
32. Iyengar S, Hildreth JE, Schwartz DH. Actin-dependent receptor colocalization required for human immunodeficiency virus entry into host cells. J Virol 1998; 72:5251-5.
33. Doms RW. Beyond receptor expression: the influence of receptor conformation, density and affinity in HIV-1 infection. Virology 2000; 276:229-37.
34. Kuhmann SE, Platt EJ, Kozak SL, Kabat D. Cooperation of multiple CCR5 coreceptors is required for infections by human immunodeficiency virus type 1. J Virol 2000; 74:7005-15.
35. Jimenez-Baranda S, Gomez-Mouton C, Rojas A, et al. Filamin-A regulates actin-dependent clustering of HIV receptors. Nat Cell Biol 2007; 9:838-46.
36. Yoder A, Yu D, Dong L, Iyer SR, Xu X, Kelly J, et al. HIV envelope-CXCR4 signaling activates cofilin to overcome cortical actin restriction in resting CD4 T cells. Cell 2008; 134:782-92.
37. Barrero-Villar M, Cabrero JR, Gordón-Alonso M, Barroso-González J, Alvarez-Losada S, Muñoz-Fernández MA, et al. Moesin is required for HIV-1-induced CD4-CXCR4 interaction, F-actin redistribution, membrane fusion and viral infection in lymphocytes. J Cell Sci 2009; 122:103-13.
38. Sattentau Q. Avoiding the void: cell-to-cell spread of human viruses. Nat Rev Microbiol 2008; 6:815-26.
39. Barrero-Villar M, Barroso-González J, Cabrero JR, Gordón-Alonso M, Alvarez-Losada S, Muñoz-Fernández MA, et al. PI4P5-kinase Ialpha is required for efficient HIV-1 entry and infection of T cells. J Immunol 2008; 181:6882-8.
40. Liu Y, Belkina NV, Shaw S. HIV infection of T cells: actin-in and actin-out. Sci Signal 2009; 2:23.
41. Vorster PJ, Guo J, Yoder A, Wang W, Zheng Y, Xu X, et al. LIM kinase 1 modulates cortical actin and CXCR4 cycling and is activated by HIV-1 to initiate viral infection. J Biol Chem 2011; 286:12554-64.
42. Valenzuela-Fernández A, Alvarez S, Gordon-Alonso M, Barrero M, Ursa A, Cabrero JR, et al. Histone deacetylase 6 regulates human immunodeficiency virus type 1 infection. Mol Biol Cell 2005; 16:5445-54.
43. Malinowsky K, Luksza J, Dittmar MT. Susceptibility to virus-cell fusion at the plasma membrane is reduced through expression of HIV gp41 cytoplasmic domains. Virology 2008; 376:69-78.
44. Pauza CD, Price TM. Human immunodeficiency virus infection of T cells and monocytes proceeds via receptor-mediated endocytosis. J Cell Biol 1988; 107:959-68.
45. Marechal V, Prevost MC, Petit C, Perret E, Heard JM, Schwartz O. Human immunodeficiency virus type 1 entry into macrophages mediated by macropinocytosis. J Virol 2001; 75:11166-77.
46. Daecke J, Fackler OT, Dittmar MT, Krausslich HG. Involvement of clathrin-mediated endocytosis in human immunodeficiency virus type 1 entry. J Virol 2005; 79:1581-94.
47. Miyauchi K, Kim Y, Latinovic O, Morozov V, Melikyan GB. HIV enters cells via endocytosis and dynamin-dependent fusion with endosomes. Cell 2009; 137:433-44.
48. Carter GC, Bernstone L, Baskaran D, James W. HIV-1 infects macrophages by exploiting an endocytic route dependent on dynamin, Rac1 and Pak1. Virology 2011; 409:234-50.
49. Yu D, Wang W, Yoder A, Spear M, Wu Y. The HIV envelope but not VSV glycoprotein is capable of mediating HIV latent infection of resting CD4 T cells. PLoS Pathog 2009; 5:1000633.
50. Harmon B, Campbell N, Ratner L. Role of Abl kinase and the Wave2 signaling complex in HIV-1 entry at a post-hemifusion step. PLoS Pathog 2010; 6:1000956.
51. Garcia-Exposito L, Barroso-Gonzalez J, Puigdomenech I, Machado JD, Blanco J, Valenzuela-Fernandez A. HIV-1 requires Arf6-mediated membrane dynamics to efficiently enter and infect T lymphocytes. Mol Biol Cell 2011; 22:1148-66.
52. Vidricaire G, Imbeault M, Tremblay MJ. Endocytic host cell machinery plays a dominant role in intracellular trafficking of incoming human immunodeficiency virus type 1 in human placental trophoblasts. J Virol 2004; 78:11904-15.
53. Vidricaire G, Tremblay MJ. Rab5 and Rab7, but not ARF6, govern the early events of HIV-1 infection in polarized human placental cells. J Immunol 2005; 175:6517-30.
54. Vidricaire G, Tremblay MJ. A clathrin, caveolae and dynamin-independent endocytic pathway requiring free membrane cholesterol drives HIV-1 internalization and infection in polarized trophoblastic cells. J Mol Biol 2007; 368:1267-83.
55. Honda A, Nogami M, Yokozeki T, Yamazaki M, Nakamura H, Watanabe H, et al. Phosphatidylinositol-4-phosphate-5-kinase alpha is a downstream effector of the small G protein ARF6 in membrane ruffle formation. Cell 1999; 99:521-32.
56. Aikawa Y, Martin TF. ADP-ribosylation factor 6 regulation of phosphatidylinositol-4,5-bisphosphate synthesis, endocytosis and exocytosis. Methods Enzymol 2005; 404:422-31.
57. Brown FD, Rozelle AL, Yin HL, Balla T, Donaldson JG. Phosphatidylinositol-4,5-bisphosphate and Arf6-regulated membrane traffic. J Cell Biol 2001; 154:1007-17.
58. Donaldson JG. Multiple roles for Arf6: sorting, structuring and signaling at the plasma membrane. J Biol Chem 2003; 278:41573-6.

59. Wolf MC, Freiberg AN, Zhang T, Akyol-Ataman Z, Grock A, Hong PW, et al. A broad-spectrum antiviral targeting entry of enveloped viruses. Proc Natl Acad Sci USA 2010; 107:3157-62.
60. Criss AK, Silva M, Casanova JE, McCormick BA. Regulation of Salmonella-induced neutrophil transmigration by epithelial ADP-ribosylation factor 6. J Biol Chem 2001; 276:48431-9.
61. Smith AC, Cirulis JT, Casanova JE, Scidmore MA, Brumell JH. Interaction of the Salmonella-containing vacuole with the endocytic recycling system. J Biol Chem 2005; 280:24634-41.
62. Lodge R, Descoteaux A. Phagocytosis of *Leishmania donovani* amastigotes is Rac1 dependent and occurs in the absence of NADPH oxidase activation. Eur J Immunol 2006; 36:2735-44.
63. Nishi K, Saigo K. Cellular internalization of green fluorescent protein fused with herpes simplex virus protein VP22 via a lipid raft-mediated endocytic pathway independent of caveolae and Rho family GTPases but dependent on dynamin and Arf6. J Biol Chem 2007; 282:27503-17.
64. Muschiol S, Normark S, Henriques-Normark B, Subtil A. Small molecule inhibitors of the Yersinia type III secretion system impair the development of Chlamydia after entry into host cells. BMC Microbiol 2009; 9:75.
65. Marchant D, Sall A, Si X, Abraham T, Wu W, Luo Z, et al. ERK MAP kinase-activated Arf6 trafficking directs coxsackievirus type B3 into an unproductive compartment during virus host-cell entry. J Gen Virol 2009; 90:854-62.
66. Laakkonen JP, Mäkelä AR, Kakkonen E, Turkki P, Kukkonen S, Peränen J, et al. Clathrin-independent entry of baculovirus triggers uptake of *E. coli* in non-phagocytic human cells. PLoS One 2009; 4:5093.
67. Radhakrishna H, Donaldson JG. ADP-ribosylation factor 6 regulates a novel plasma membrane recycling pathway. J Cell Biol 1997; 139:49-61.
68. Donaldson JG, Honda A. Localization and function of Arf family GTPases. Biochem Soc Trans 2005; 33:639-42.
69. Naslavsky N, Weigert R, Donaldson JG. Convergence of non-clathrin- and clathrin-derived endosomes involves Arf6 inactivation and changes in phosphoinositides. Mol Biol Cell 2003; 14:417-31.
70. D'Souza-Schorey C, Li G, Colombo MI, Stahl PD. A regulatory role for ARF6 in receptor-mediated endocytosis. Science 1995; 267:1175-8.
71. Chavrier P, Goud B. The role of ARF and Rab GTPases in membrane transport. Curr Opin Cell Biol 1999; 11:466-75.
72. Al-Awar O, Radhakrishna H, Powell NN, Donaldson JG. Separation of membrane trafficking and actin remodeling functions of ARF6 with an effector domain mutant. Mol Cell Biol 2000; 20:5998-6007.
73. D'Souza-Schorey C, Chavrier P. ARF proteins: roles in membrane traffic and beyond. Nat Rev Mol Cell Biol 2006; 7:347-58.
74. Song J, Khachikian Z, Radhakrishna H, Donaldson JG. Localization of endogenous ARF6 to sites of cortical actin rearrangement and involvement of ARF6 in cell spreading. J Cell Sci 1998; 111:2257.
75. Martin TF. PI(4,5)P(2) regulation of surface membrane traffic. Curr Opin Cell Biol 2001; 13:493-9.
76. Luton F, Klein S, Chauvin JP, Le Bivic A, Bourgoin S, Franco M, et al. EFA6, exchange factor for ARF6, regulates the actin cytoskeleton and associated tight junction in response to E-cadherin engagement. Mol Biol Cell 2004; 15:1134-45.
77. Donaldson JG. Arf6 and its role in cytoskeletal modulation. Methods Mol Biol 2002; 189:191-8.
78. Hernandez-Deviez DJ, Roth MG, Casanova JE, Wilson JM. ARNO and ARF6 regulate axonal elongation and branching through downstream activation of phosphatidylinositol-4-phosphate-5-kinase alpha. Mol Biol Cell 2004; 15:111-20.
79. Franco M, Peters PJ, Boretto J, van Donselaar E, Neri A, D'Souza-Schorey C, et al. EFA6, a sec7 domain-containing exchange factor for ARF6, coordinates membrane recycling and actin cytoskeleton organization. EMBO J 1999; 18:1480-91.
80. Heikkilä O, Susi P, Tevaluoto T, Härmä H, Marjomäki V, Hyypiä T, et al. Internalization of coxsackievirus A9 is mediated by {beta}2-microglobulin, dynamin and Arf6 but not by caveolin-1 or clathrin. J Virol 2010; 84:3666-81.
81. Lichty BD, Power AT, Stojdl DF, Bell JC. Vesicular stomatitis virus: re-inventing the bullet. Trends Mol Med 2004; 10:210-6.
82. Schlegel R, Tralka TS, Willingham MC, Pastan I. Inhibition of VSV binding and infectivity by phosphatidylserine: is phosphatidylserine a VSV-binding site? Cell 1983; 32:639-46.
83. Coil DA, Miller AD. Phosphatidylserine is not the cell surface receptor for vesicular stomatitis virus. J Virol 2004; 78:10920-6.
84. Le Blanc I, Luyet PP, Pons V, Ferguson C, Emans N, Petiot A, et al. Endosome-to-cytosol transport of viral nucleocapsids. Nat Cell Biol 2005; 7:653-64.
85. Luyet PP, Falguieres T, Pons V, Pattnaik AK, Gruenberg J. The ESCRT-I subunit TSG101 controls endosome-to-cytosol release of viral RNA. Traffic 2008; 9:2279-90.
86. Rust MJ, Lakadamyali M, Zhang F, Zhuang X. Assembly of endocytic machinery around individual influenza viruses during viral entry. Nat Struct Mol Biol 2004; 11:567-73.
87. Chen C, Zhuang X. Epsin 1 is a cargo-specific adaptor for the clathrin-mediated endocytosis of the influenza virus. Proc Natl Acad Sci USA 2008; 105:11790-5.
88. Pelkmans L, Kartenbeck J, Helenius A. Caveolar endocytosis of simian virus 40 reveals a new two-step vesicular-transport pathway to the ER. Nat Cell Biol 2001; 3:473-83.
89. Damm EM, Pelkmans L, Kartenbeck J, Mezzacasa A, Kurzchalia T, Helenius A. Clathrin- and caveolin-1-independent endocytosis: entry of simian virus 40 into cells devoid of caveolae. J Cell Biol 2005; 168:477-88.
90. Mayor S, Pagano RE. Pathways of clathrin-independent endocytosis. Nat Rev Mol Cell Biol 2007; 8:603-12.
91. Neu U, Woellner K, Gauglitz G, Stehle T. Structural basis of GM1 ganglioside recognition by simian virus 40. Proc Natl Acad Sci USA 2008; 105:5219-24.
92. Pietiainen V, Marjomaki V, Upla P, Pelkmans L, Helenius A, Hyypia T. Echovirus 1 endocytosis into caveosomes requires lipid rafts, dynamin II and signaling events. Mol Biol Cell 2004; 15:4911-25.
93. Upla P, Marjomäki V, Kankaanpää P, Ivaska J, Hyypiä T, Van Der Goot FG, et al. Clustering induces a lateral redistribution of alpha2beta1 integrin from membrane rafts to caveolae and subsequent protein kinase C-dependent internalization. Mol Biol Cell 2004; 15:625-36.
94. Chandran K, Sullivan NJ, Felbor U, Whelan SP, Cunningham JM. Endosomal proteolysis of the Ebola virus glycoprotein is necessary for infection. Science 2005; 308:1643-5.
95. Ebert DH, Deussing J, Peters C, Dermody TS. Cathepsin L and cathepsin B mediate reovirus disassembly in murine fibroblast cells. J Biol Chem 2002; 277:24609-17.
96. Simmons G, Gosalia DN, Rennekamp AJ, Reeves JD, Diamond SL, Bates P. Inhibitors of cathepsin L prevent severe acute respiratory syndrome coronavirus entry. Proc Natl Acad Sci USA 2005; 102:11876-81.
97. Lehmann MJ, Sherer NM, Marks CB, Pypaert M, Mothes W. Actin- and myosin-driven movement of viruses along filopodia precedes their entry into cells. J Cell Biol 2005; 170:317-25.
98. Schelhaas M, Ewers H, Rajamaki ML, Day PM, Schiller JT, Helenius A. Human papillomavirus type 16 entry: retrograde cell surface transport along actin-rich protrusions. PLoS Pathog 2008; 4:1000148.
99. Mercer J, Helenius A. Vaccinia virus uses macropinocytosis and apoptotic mimicry to enter host cells. Science 2008; 320:531-5.
100. Karjalainen M, Kakkonen E, Upla P, Paloranta H, Kankaanpää P, Liberali P, et al. A Raft-derived, Pak1-regulated entry participates in alpha2beta1 integrin-dependent sorting to caveosomes. Mol Biol Cell 2008; 19:2857-69.
101. Liberali P, Kakkonen E, Turacchio G, Valente C, Spaar A, Perinetti G, et al. The closure of Pak1-dependent macropinosomes requires the phosphorylation of CtBP1/BARS. EMBO J 2008; 27:970-81.
102. Amstutz B, Gastaldelli M, Kälin S, Imelli N, Boucke K, Wandeler E, et al. Subversion of CtBP1-controlled macropinocytosis by human adenovirus serotype 3. EMBO J 2008; 27:956-69.
103. Netherton C, Moffat K, Brooks E, Wileman T. A guide to viral inclusions, membrane rearrangements, factories and viroplasm produced during virus replication. Adv Virus Res 2007; 70:101-82.
104. Novoa RR, Calderita G, Arranz R, Fontana J, Granzow H, Risco C. Virus factories: associations of cell organelles for viral replication and morphogenesis. Biol Cell 2005; 97:147-72.
105. Fontana J, Lopez-Montero N, Elliott RM, Fernandez JJ, Risco C. The unique architecture of Bunyamwera virus factories around the Golgi complex. Cell Microbiol 2008; 10:2012-28.
106. Fontana J, Lopez-Iglesias C, Tzeng WP, Frey TK, Fernandez JJ, Risco C. Three-dimensional structure of Rubella virus factories. Virology 2010; 405:579-91.
107. Salonen A, Ahola T, Kaariainen L. Viral RNA replication in association with cellular membranes. Curr Top Microbiol Immunol 2005; 285:139-73.
108. Dye BT, Miller DJ, Ahlquist P. In vivo self-interaction of nodavirus RNA replicase protein a revealed by fluorescence resonance energy transfer. J Virol 2005; 79:8909-19.
109. Fontana J, Tzeng WP, Calderita G, Fraile-Ramos A, Frey TK, Risco C. Novel replication complex architecture in rubella replicon-transfected cells. Cell Microbiol 2007; 9:875-90.
110. Lyle JM, Bullitt E, Bienz K, Kirkegaard K. Visualization and functional analysis of RNA-dependent RNA polymerase lattices. Science 2002; 296:2218-22.
111. Mackenzie J. Wrapping things up about virus RNA replication. Traffic 2005; 6:967-77.
112. Spagnolo JF, Rossignol E, Bullitt E, Kirkegaard K. Enzymatic and nonenzymatic functions of viral RNA-dependent RNA polymerases within oligomeric arrays. RNA 2010; 16:382-93.
113. Wang QM, Hockman MA, Staschke K, Johnson RB, Case KA, Lu J, et al. Oligomerization and cooperative RNA synthesis activity of hepatitis C virus RNA-dependent RNA polymerase. J Virol 2002; 76:3865-72.
114. Frey TK. Molecular biology of rubella virus. Adv Virus Res 1994; 44:69-160.
115. Kujala P, Ikaheimonen A, Ehsani N, Vihinen H, Auvinen P, Kaariainen L. Biogenesis of the Semliki Forest virus RNA replication complex. J Virol 2001; 75:3873-84.
116. Kujala P, Ahola T, Ehsani N, Auvinen P, Vihinen H, Kaariainen L. Intracellular distribution of rubella virus nonstructural protein P150. J Virol 1999; 73:7805-11.
117. Lee JY, Marshall JA, Bowden DS. Characterization of rubella virus replication complexes using antibodies to double-stranded RNA. Virology 1994; 200:307-12.
118. Froshauer S, Kartenbeck J, Helenius A. Alphavirus RNA replicase is located on the cytoplasmic surface of endosomes and lysosomes. J Cell Biol 1988; 107:2075-86.
119. Magliano D, Marshall JA, Bowden DS, Vardaxis N, Meanger J, Lee JY. Rubella virus replication complexes are virus-modified lysosomes. Virology 1998; 240:57-63.

120. Risco C, Carrascosa JL, Frey TK. Structural maturation of rubella virus in the Golgi complex. Virology 2003; 312:261-9.
121. James Morre D, Mollenhauer HH. Microscopic morphology and the origins of the membrane maturation model of Golgi apparatus function. Int Rev Cytol 2007; 262:191-218.
122. Salanueva IJ, Novoa RR, Cabezas P, López-Iglesias C, Carrascosa JL, Elliott RM, et al. Polymorphism and structural maturation of bunyamwera virus in Golgi and post-Golgi compartments. J Virol 2003; 77:1368-81.
123. Novoa RR, Calderita G, Cabezas P, Elliott RM, Risco C. Key Golgi factors for structural and functional maturation of bunyamwera virus. J Virol 2005; 79:10852-63.
124. Grimley PM, Levin JG, Berezesky IK, Friedman RM. Specific membranous structures associated with the replication of group A arboviruses. J Virol 1972; 10:492-503.
125. Cairns J. The initiation of vaccinia infection. Virology 1960; 11:603-23.
126. Kit S, Dubbs DR, Hsu TC. Biochemistry of vaccinia-infected mouse fibroblasts (strain L-M). III. Radioautographic and biochemical studies of thymidine-H3 uptake into DNA of L-M cells and rabbit cells in primary culture. Virology 1963; 19:13-22.
127. Tolonen N, Doglio L, Schleich S, Krijnse Locker J. Vaccinia virus DNA replication occurs in endoplasmic reticulum-enclosed cytoplasmic mini-nuclei. Mol Biol Cell 2001; 12:2031-46.
128. Hall RA, Scherret JH, Mackenzie JS. Kunjin virus: an Australian variant of West Nile? Ann NY Acad Sci 2001; 951:153-60.
129. Pedersen KW, van der Meer Y, Roos N, Snijder EJ. Open reading frame 1a-encoded subunits of the arterivirus replicase induce endoplasmic reticulum-derived double-membrane vesicles which carry the viral replication complex. J Virol 1999; 73:2016-26.
130. van der Meer Y, van Tol H, Locker JK, Snijder EJ. ORF1a-encoded replicase subunits are involved in the membrane association of the arterivirus replication complex. J Virol 1998; 72:6689-98.
131. Hobson SD, Rosenblum ES, Richards OC, Richmond K, Kirkegaard K, Schultz SC. Oligomeric structures of poliovirus polymerase are important for function. EMBO J 2001; 20:1153-63.
132. Cherry S, Kunte A, Wang H, Coyne C, Rawson RB, Perrimon N. COPI activity coupled with fatty acid biosynthesis is required for viral replication. PLoS Pathog 2006; 2:102.
133. Belov GA, Ehrenfeld E. Involvement of cellular membrane traffic proteins in poliovirus replication. Cell Cycle 2007; 6:36-8.
134. Hogle JM. Poliovirus cell entry: common structural themes in viral cell entry pathways. Annu Rev Microbiol 2002; 56:677-702.
135. Bubeck D, Filman DJ, Hogle JM. Cryo-electron microscopy reconstruction of a poliovirus-receptor-membrane complex. Nat Struct Mol Biol 2005; 12:615-8.
136. Belov GA, Feng Q, Nikovics K, Jackson CL, Ehrenfeld E. A critical role of a cellular membrane traffic protein in poliovirus RNA replication. PLoS Pathog 2008; 4:1000216.
137. Maynell LA, Kirkegaard K, Klymkowsky MW. Inhibition of poliovirus RNA synthesis by brefeldin A. J Virol 1992; 66:1985-94.
138. Doedens JR, Kirkegaard K. Inhibition of cellular protein secretion by poliovirus proteins 2B and 3A. EMBO J 1995; 14:894-907.
139. Wessels E, Duijsings D, Lanke KH, van Dooren SH, Jackson CL, Melchers WJ, et al. Effects of picornavirus 3A Proteins on Protein Transport and GBF1-dependent COP-I recruitment. J Virol 2006; 80:11852-60.
140. Choe SS, Dodd DA, Kirkegaard K. Inhibition of cellular protein secretion by picornaviral 3A proteins. Virology 2005; 337:18-29.
141. Moffat K, Howell G, Knox C, Belsham GJ, Monaghan P, Ryan MD, et al. Effects of foot-and-mouth disease virus nonstructural proteins on the structure and function of the early secretory pathway: 2BC but not 3A blocks endoplasmic reticulum-to-Golgi transport. J Virol 2005; 79:4382-95.
142. Gazina EV, Mackenzie JM, Gorrell RJ, Anderson DA. Differential requirements for COPI coats in formation of replication complexes among three genera of Picornaviridae. J Virol 2002; 76:11113-22.
143. Rust RC, Landmann L, Gosert R, Tang BL, Hong W, Hauri HP, et al. Cellular COPII proteins are involved in production of the vesicles that form the poliovirus replication complex. J Virol 2001; 75:9808-18.
144. Egger D, Bienz K. Intracellular location and translocation of silent and active poliovirus replication complexes. J Gen Virol 2005; 86:707-18.
145. Wei T, Wang A. Biogenesis of cytoplasmic membranous vesicles for plant potyvirus replication occurs at endoplasmic reticulum exit sites in a COPI- and COPII-dependent manner. J Virol 2008; 82:12252-64.
146. Jackson WT, Giddings TH Jr, Taylor MP, Mulinyawe S, Rabinovitch M, Kopito RR, et al. Subversion of cellular autophagosomal machinery by RNA viruses. PLoS Biol 2005; 3:156.
147. Ehrlich M, Boll W, Van Oijen A, Hariharan R, Chandran K, Nibert ML, et al. Endocytosis by random initiation and stabilization of clathrin-coated pits. Cell 2004; 118:591-605.
148. Vonderheit A, Helenius A. Rab7 associates with early endosomes to mediate sorting and transport of Semliki forest virus to late endosomes. PLoS Biol 2005; 3:233.
149. Tu H, Gao L, Shi ST, Taylor DR, Yang T, Mircheff AK, et al. Hepatitis C virus RNA polymerase and NS5A complex with a SNARE-like protein. Virology 1999; 263:30-41.
150. Hamamoto I, Nishimura Y, Okamoto T, Aizaki H, Liu M, Mori Y, et al. Human VAP-B is involved in hepatitis C virus replication through interaction with NS5A and NS5B. J Virol 2005; 79:13473-82.
151. Sklan EH, Serrano RL, Einav S, Pfeffer SR, Lambright DG, Glenn JS. TBC1D20 is a Rab1 GTPase-activating protein that mediates hepatitis C virus replication. J Biol Chem 2007; 282:36354-61.
152. Stone M, Jia S, Heo WD, Meyer T, Konan KV. Participation of rab5, an early endosome protein, in hepatitis C virus RNA replication machinery. J Virol 2007; 81:4551-63.
153. Manna D, Aligo J, Xu C, Park WS, Koc H, Heo WD, et al. Endocytic Rab proteins are required for hepatitis C virus replication complex formation. Virology 398:21-37.
154. Ettayebi K, Hardy ME. Norwalk virus nonstructural protein p48 forms a complex with the SNARE regulator VAP-A and prevents cell surface expression of vesicular stomatitis virus G protein. J Virol 2003; 77:11790-7.
155. Chen BJ, Lamb RA. Mechanisms for enveloped virus budding: can some viruses do without an ESCRT? Virology 2008; 372:221-32.
156. Welsch S, Muller B, Krausslich HG. More than one door—Budding of enveloped viruses through cellular membranes. FEBS Lett 2007; 581:2089-97.
157. Bieniasz PD. Late budding domains and host proteins in enveloped virus release. Virology 2006; 344:55-63.
158. Morita E, Sundquist WI. Retrovirus budding. Annu Rev Cell Dev Biol 2004; 20:395-425.
159. Freed EO. Viral late domains. J Virol 2002; 76:4679-87.
160. Gruenberg J, Stenmark H. The biogenesis of multivesicular endosomes. Nat Rev Mol Cell Biol 2004; 5:317-23.
161. Piper RC, Katzmann DJ. Biogenesis and function of multivesicular bodies. Annu Rev Cell Dev Biol 2007; 23:519-47.
162. Hurley JH, Hanson PI. Membrane budding and scission by the ESCRT machinery: it's all in the neck. Nat Rev Mol Cell Biol 2010; 11:556-66.
163. Saksena S, Emr SD. ESCRTs and human disease. Biochem Soc Trans 2009; 37:167-72.
164. Rodahl LM, Stuffers S, Lobert VH, Stenmark H. The role of ESCRT proteins in attenuation of cell signaling. Biochem Soc Trans 2009; 37:137-42.
165. Fujii K, Munshi UM, Ablan SD, Demirov DG, Soheilian F, Nagashima K, et al. Functional role of Alix in HIV-1 replication. Virology 2009; 391:284-92.
166. Zhang Y, Qian H, Love Z, Barklis E. Analysis of the assembly function of the human immunodeficiency virus type 1 gag protein nucleocapsid domain. J Virol 1998; 72:1782-9.
167. Popova E, Popov S, Gottlinger HG. Human immunodeficiency virus type 1 nucleocapsid p1 confers ESCRT pathway dependence. J Virol 2010; 84:6590-7.
168. Bruce EA, Medcalf L, Crump CM, Noton SL, Stuart AD, Wise HM, et al. Budding of filamentous and non-filamentous influenza A virus occurs via a VPS4 and VPS28-independent pathway. Virology 2009; 390:268-78.
169. Chen BJ, Leser GP, Morita E, Lamb RA. Influenza virus hemagglutinin and neuraminidase, but not the matrix protein, are required for assembly and budding of plasmid-derived virus-like particles. J Virol 2007; 81:7111-23.
170. Chukkapalli V, Hogue IB, Boyko V, Hu WS, Ono A. Interaction between the human immunodeficiency virus type 1 Gag matrix domain and phosphatidylinositol-(4,5)-bisphosphate is essential for efficient gag membrane binding. J Virol 2008; 82:2405-17.
171. Ono A, Ablan SD, Lockett SJ, Nagashima K, Freed EO. Phosphatidylinositol-(4,5)-bisphosphate regulates HIV-1 Gag targeting to the plasma membrane. Proc Natl Acad Sci USA 2004; 101:14889-94.
172. Kisseleva MV, Wilson MP, Majerus PW. The isolation and characterization of a cDNA encoding phospholipid-specific inositol polyphosphate-5-phosphatase. J Biol Chem 2000; 275:20110-6.
173. Shnyrova AV, Ayllon J, Mikhalyov II, Villar E, Zimmerberg J, Frolov VA. Vesicle formation by self-assembly of membrane-bound matrix proteins into a fluidlike budding domain. J Cell Biol 2007; 179:627-33.
174. Solon J, Gareil O, Bassereau P, Gaudin Y. Membrane deformations induced by the matrix protein of vesicular stomatitis virus in a minimal system. J Gen Virol 2005; 86:3357-63.
175. Irie T, Licata JM, Jayakar HR, Whitt MA, Bell P, Harty RN. Functional analysis of late-budding domain activity associated with the PSAP motif within the vesicular stomatitis virus M protein. J Virol 2004; 78:7823-7.
176. Piguet V, Sattentau Q. Dangerous liaisons at the virological synapse. J Clin Invest 2004; 114:605-10.
177. Jolly C, Sattentau QJ. Retroviral spread by induction of virological synapses. Traffic 2004; 5:643-50.
178. Igakura T, Stinchcombe JC, Goon PK, Taylor GP, Weber JN, Griffiths GM, et al. Spread of HTLV-I between lymphocytes by virus-induced polarization of the cytoskeleton. Science 2003; 299:1713-6.
179. Jolly C, Kashefi K, Hollinshead M, Sattentau QJ. HIV-1 cell to cell transfer across an Env-induced, actin-dependent synapse. J Exp Med 2004; 199:283-93.
180. Dimitrov DS, Willey RL, Sato H, Chang LJ, Blumenthal R, Martin MA. Quantitation of human immunodeficiency virus type 1 infection kinetics. J Virol 1993; 67:2182-90.
181. Martin N, Sattentau Q. Cell-to-cell HIV-1 spread and its implications for immune evasion. Curr Opin HIV AIDS 2009; 4:143-9.

182. Massanella M, Puigdomènech I, Cabrera C, Fernandez-Figueras MT, Aucher A, Gaibelet G, et al. Antigp41 antibodies fail to block early events of virological synapses but inhibit HIV spread between T cells. Aids 2009; 23:183-8.
183. Martin N, Welsch S, Jolly C, Briggs JA, Vaux D, Sattentau QJ. Virological synapse-mediated spread of human immunodeficiency virus type 1 between T cells is sensitive to entry inhibition. J Virol 2010; 84:3516-27.
184. Jolly C, Sattentau QJ. Human immunodeficiency virus type 1 virological synapse formation in T cells requires lipid raft integrity. J Virol 2005; 79:12088-94.
185. Jolly C, Mitar I, Sattentau QJ. Requirement for an intact T-cell actin and tubulin cytoskeleton for efficient assembly and spread of human immunodeficiency virus type 1. J Virol 2007; 81:5547-60.
186. Puigdomenech I, Massanella M, Cabrera C, Clotet B, Blanco J. On the steps of cell-to-cell HIV transmission between CD4 T cells. Retrovirology 2009; 6:89.
187. Pais-Correia AM, Sachse M, Guadagnini S, Robbiati V, Lasserre R, Gessain A, et al. Biofilm-like extracellular viral assemblies mediate HTLV-1 cell-to-cell transmission at virological synapses. Nat Med 2010; 16:83-9.
188. Sherer NM, Lehmann MJ, Jimenez-Soto LF, Horensavitz C, Pypaert M, Mothes W. Retroviruses can establish filopodial bridges for efficient cell-to-cell transmission. Nat Cell Biol 2007; 9:310-5.
189. Sowinski S, Jolly C, Berninghausen O, Purbhoo MA, Chauveau A, Köhler K, et al. Membrane nanotubes physically connect T cells over long distances presenting a novel route for HIV-1 transmission. Nat Cell Biol 2008; 10:211-9.
190. Joly E, Hudrisier D. What is trogocytosis and what is its purpose? Nat Immunol 2003; 4:815.
191. Aucher A, Puigdomenech I, Joly E, Clotet B, Hudrisier D, Blanco J. Could CD4 capture by $CD8^+$ T cells play a role in HIV spreading? J Biomed Biotechnol 2010; 2010:907371.
192. Halary F, Amara A, Lortat-Jacob H, Messerle M, Delaunay T, Houlès C, et al. Human cytomegalovirus binding to DC-SIGN is required for dendritic cell infection and target cell trans-infection. Immunity 2002; 17:653-64.
193. Izquierdo-Useros N, Naranjo-Gómez M, Erkizia I, Puertas MC, Borràs FE, Blanco J, et al. HIV and mature dendritic cells: Trojan exosomes riding the Trojan horse? PLoS Pathog 2010; 6:1000740.
194. Izquierdo-Useros N, Puertas MC, Borras FE, Blanco J, Martinez-Picado J. Exosomes and retroviruses: the chicken or the egg? Cell Microbiol 2011; 13:10-7.
195. van Kooyk Y, Geijtenbeek TB. DC-SIGN: escape mechanism for pathogens. Nat Rev Immunol 2003; 3:697-709.
196. Brandenburg B, Zhuang X. Virus trafficking—learning from single-virus tracking. Nat Rev Microbiol 2007; 5:197-208.
197. McIntosh R, Nicastro D, Mastronarde D. New views of cells in 3D: an introduction to electron tomography. Trends Cell Biol 2005; 15:43-51.
198. Kopek BG, Perkins G, Miller DJ, Ellisman MH, Ahlquist P. Three-dimensional analysis of a viral RNA replication complex reveals a virus-induced mini-organelle. PLoS Biol 2007; 5:220.
199. Diestra E, Fontana J, Guichard P, Marco S, Risco C. Visualization of proteins in intact cells with a clonable tag for electron microscopy. J Struct Biol 2009; 165:157-68.